Universidad de Valladolid

ioba
Instituto Universitario de Oftalmobiología Aplicada

UNIVERSIDAD DE VALLADOLID
INSTITUTO UNIVERSITARIO DE OFTALMOBIOLOGÍA APLICADA

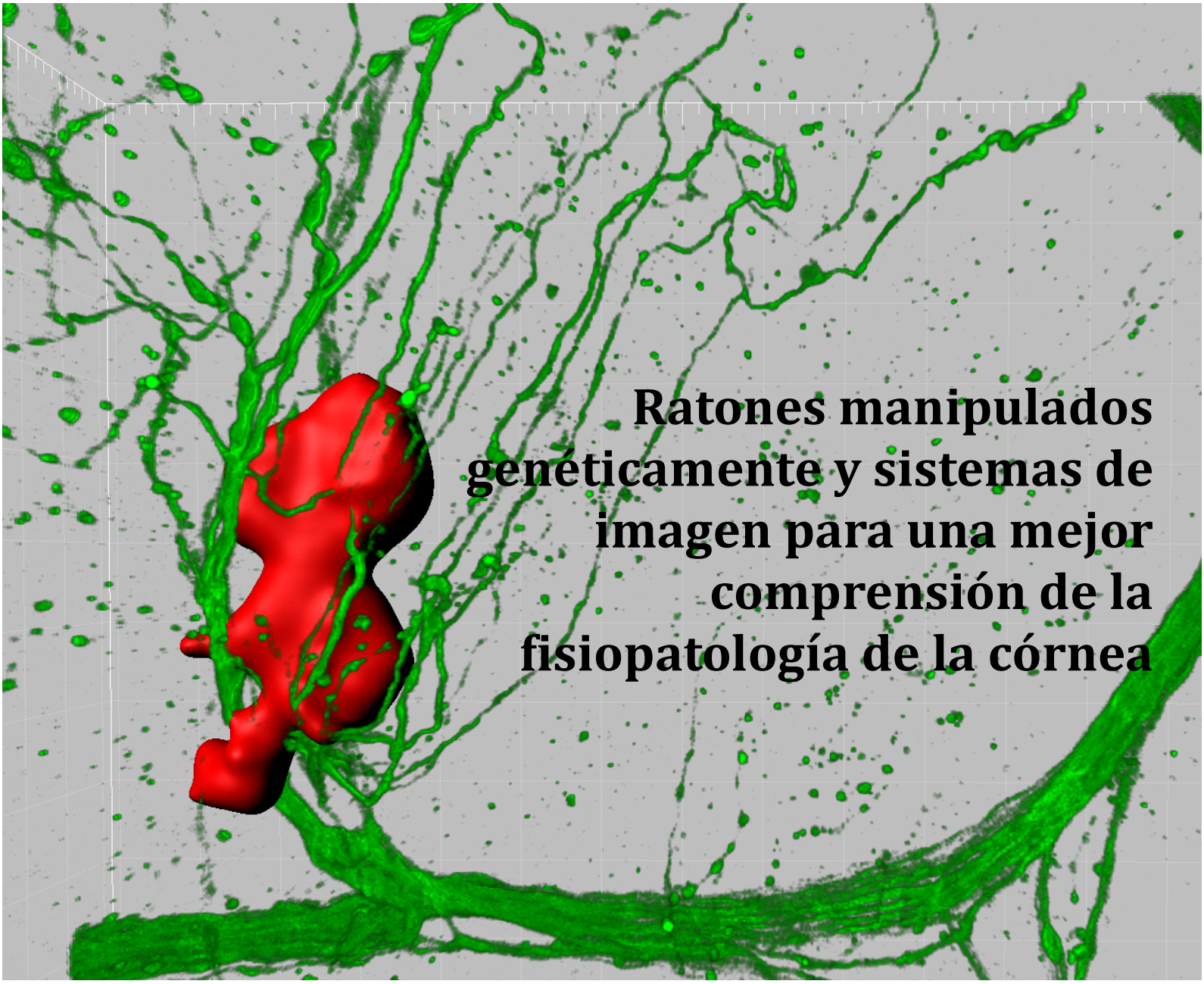

Ratones manipulados genéticamente y sistemas de imagen para una mejor comprensión de la fisiopatología de la córnea

José Tomás Blanco Mezquita

2015

Universidad de Valladolid

UNIVERSIDAD DE VALLADOLID

INSTITUTO UNIVERSITARIO DE OFTALMOBIOLOGÍA APLICADA

TESIS DOCTORAL:

RATONES MANIPULADOS GENÉTICAMENTE Y SISTEMAS DE IMAGEN PARA UNA MEJOR COMPRENSIÓN DE LA FISIOPATOLOGÍA DE LA CÓRNEA

"The use of genetically engineered mice and imaging systems for understanding the pathophysiology of the cornea"

Presentada por **José Tomás Blanco Mezquita** para optar al grado de Doctor por la Universidad de Valladolid

Dirigida por:

Dr. Daniel R. Saban

2015

Universidad de Valladolid

Impreso 2T
English

AUTORIZACIÓN DEL DIRECTOR DE TESIS
THESIS DIRECTOR AUTHORIZATION

(Art. 2.1. c de la Normativa para la presentación y defensa de la Tesis Doctoral en la UVa)

DANIEL R. SABAN, Ph.D.,

Passport n# 489516330	
Position: Assistant professor, Departments of Ophthalmology and Immunology	
University/ Research Institute/ Entity	Duke University School of Medicine
Mailing Address	2351 Erwin Rd, Wadsworth Rm 134, Durham, NC 27705
Email Address daniel.saban@duke.edu	Telephone 919-660-0404

As a Supervisor of the Ph.D. Candidate:

Ph.D. Candidate	JOSÉ TOMÁS BLANCO MEZQUITA
Doctoral Thesis's Title	The use of genetically engineered mice and imaging systems for understanding the pathophysiology of the cornea. *Ratones manipulados genéticamente y sistemas de imagen para una mejor comprensión de la fisiopatología de la córnea.*
Ph.D. Program	Vision Sciences / *Ciencias de la Visión*
Ph.D. Program Coordinators	Institute of Applied OphthamoBiology / *Instituto de Oftalmobiología Aplicada (IOBA)*

I consider the aforementioned Thesis is suitable for presentation, according to the regulations of the University of Valladolid, and therefore I authorize its deposit

Dr. DANIEL R. SABAN,

Signature: .....

Place and date..... USA 6/18/15 .....

SR. PRESIDENTE DE LA COMISIÓN DE DOCTORADO / *Doctoral Committee Chair*

Schepens Eye Research Institute
Massachusetts Eye and Ear

James D. Zieske, Ph.D.
Senior Scientist, Schepens Eye Research Institute
Associate Professor of Ophthalmology,
Harvard Medical School
20 Staniford Street • Boston, MA 02114
617.912.0282 • FAX: 617.912.0107
james_zieske@meei.harvard.edu

CERTIFICADO DE ESTANCIA EN UNA INSTITUCIÓN EXTRANJERA
CERTIFICATE OF STAY IN A FOREIGN INSTITUTION

BENEFICIARIO / *APPLICANT*

Nombre y apellidos/ *Name*: José Tomás Blanco Mezquita
D.N.I./ *National identity Card:* 11971888-C
Centro de partida/ *Home Institution:* Instituto de Oftalmobiología Aplicada (IOBA), Universidad de Valladolid, Valladolid, Spain

CENTRO EN EL QUE SE HA REALIZADO LA ESTANCIA / *HOST INSTITUTION*

Nombre/ *Name*: Schepens Eye Research Institute/MEE and Harvard Medical School
Localidad/ *Country*: Boston, MA, USA
Dirección/ *Address*: 20 Staniford Street

Investigador responsable en el centro de la estancia/ *Host Institution Supervisor*: James D. Zieske, PhD
Cargo/ *Faculty Position*: Senior Scientist, Schepens Eye Research Institute,
Associate Professor of Ophthalmology, Harvard Medical School

CERTIFICO:
que la persona arriba mencionada ha realizado una estancia en este centro en las siguientes fechas:
desde 15 / Mayo / 2008 hasta 14 / Mayo / 2011

THIS IS TO CERTIFY:
that the above mentioned person has performed a stay in this Institution in the following dates:
From: May / 15 / 2008 *To: May / 14 / 2011*

Lugar y fecha / *City and date*:
Boston, MA, USA
06/22/15

Firma y Sello/ *Signature & Stamp*

James D Zieske

James D. Zieske, Ph.D.
Senior Scientist
Schepens Eye Research Institute
Associate Professor
Department of Ophthalmology
Harvard Medical School

Harvard Medical School Affiliate

A mis padres

PRÓLOGO

Al Profesor Pastor:

Ha llovido mucho desde el verano del 2002 cuando llegué por primera vez al IOBA. Fue una etapa dura en la que había que ganarse la plata de obrero de la construcción y vocalista de orquesta. Como paleto de provincias, recuerdo que arribé en el "IOVA" suponiendo que VA era como la matrícula de Valladolid. No he dejado de ser un paleto de provincia, ni quiero dejar de serlo, pero creo, que en todos estos años he aprendido mucho; y si bien, éste es el fin de un capítulo, quería escribir su prólogo.

En mis principios en el IOBA, cuando ya supe que la "B" y la "A" tenían otro significado, no estaba en el programa ni en mi programa semejante hoja de ruta para llegar hasta aquí. Recuerdo que en la tercera planta de la Facultad de Medicina, en el antiguo edificio del IOBA, en la puerta de un despacho, una vieja y amarillenta hoja de papel decía "Never stop dreaming. What seemed impossible yesterday can become a reality tomorrow" Charles L. Schepens. Más tarde supe que ése era el despacho del Profesor Pastor y mucho más tarde, que el Profesor además era el Jefe del IOBA.

A estas alturas uno ya no tiene que recurrir a escribir alabanzas con premeditación y sabe el Profesor Pastor que no soy dado a masticar pastillas y mucho menos a darlas. Uno que sueña más despierto que dormido, unos años más tarde, tuvo la oportunidad de trabajar en el Instituto creado por el autor de la frase arriba mencionada ¿Tal vez fue impronta? ¿tal vez un sueño? Tal vez, pero si sé que no lo soñé y que lo viví y como en la jota castellana, que me quiten el baile "echao". También sé que no soñé, que no ha sido fácil, no, no lo ha sido y ni espero ni quiero, que pueda llegar a serlo algún día.

Si el Profesor Pastor consiguió su sueño y el IOBA hoy en día es una realidad, no fue porque él tuviese un sueño imposible que se hizo realidad como crisálida que se convierte en mariposa. Se hizo realidad porque tanto él como todos los que soñaron con él, lo hicieron posible.

La impronta del IOBA se lleva de por vida y más cuando al pasar por otros lugares, uno se da cuenta de lo que dejó atrás, pero a la vez, con el convencimiento de que nunca se fue y el conocimiento de que es, a la vez, tu casa para siempre. Me imagino que todo esto es una amalgama, en la que los matices podrían desbordar el factorial de los siete colores básicos del arco iris. Sería un error darle todo el mérito al Profesor, pero si estoy seguro, que en parte, él es culpable exponencial por soñar… y por lo que es más importante para mi: haber formado y formar yo, parte de su sueño.

Gracias Profesor por despertarme y enseñarme a soñar

AGRADECIMIENTOS

Si bien esta tesis doctoral es el resultado formal de un trabajo reciente, ni quiero, ni puedo ni debo olvidar que éste, es a la vez resultado de un trabajo anterior.

Por ello es mi deber agradecer a todas las personas con las que inicié esta andadura y si bien es imposible nombrar a todos y cada uno, me gustaría agradecer al antiguo Grupo de Cirugía Refractiva del IOBA: Guadalupe, Nuria, Rodrigo, Patricia, Larisa, Roberto, Marta, Lucía, Susana, Patricia, Carmen, Vicky…

De la misma manera no hubiese llegado hasta aquí sin lo aprendido en el Departamento de Biología Celular de la Facultad de Medicina de Valladolid y quiero dar las gracias: al Profesor Gayoso, Carmen Martínez, Luis, Olga, Nacho, Alí, Javier, Luis Bejarano…

Al Grupo de Óptica del CSIC en Madrid: Susana Marcos, Carlos, Pablo, Lurdes, Carlos, Jose.

También quiero agradecer a Ruiz Proença, Pedro, Ana Paula y Aldina Reis del IBILI en Coimbra, Portugal; a José Ramón Alonso y Azucena del Departamento de Biología Celular de la Universidad de Salamanca.

Así mismo mi más sincero agradecimiento a una de las personas con la que más he aprendido de la córnea y con quien fue un verdadero placer y orgullo trabajar mano a mano en el trabajo de campo: Gracias Profesor Santiago Mar.

Gracias a toda la familia del IOBA a todos y cada uno, pero por alguna razón mi agradecimiento especial a Mori, Maite, Miguelón, Pepe, Nieves, Berta, MariPaz, Rosi, Ana, Iván, Janneth, Jimena, Agustín, Hernán, Marga, Amalia, Chema, Mari-Ángeles, Paco Blázquez y sus duendes…

No puedo terminar esta primera parte, sin agradecer a Jesús Merayo de quien aprendí las lecciones más importantes que uno puede aprender en la vida. Gracias Jesús.

Sin embargo, este nuevo trabajo que se presenta no hubiese sido posible sin la colaboración de muchas otras personas a ambos lados del Océano:

Quiero agradecer a todo Grupo de investigación de Jim Zieske en el SERI de la Universidad de Harvard y especialmente a Audrey Hutcheon ("lab manager"), Donald Pottle (microscopía), Bianai Fan (laboratorio de histología), Patricia Pearson (microscopía electrónica) así como a Frances Ng (administración). Dar las gracias a Mary Ann Stepp del Departamento de Anatomía y Biología Regenerativa de la Universidad George Washington por sus magistrales consejos y puntualizaciones en el ámbito de la investigación de las integrinas de membrana en la córnea.

Muchas gracias a Darlene Dart, "believe or not, this Thesis started in your lab, where I attempted *intravital* imaging for first time".

Igualmente agradecer a todo el grupo de Reza Dana en el SERI donde entré en contacto con la inflamación ocular y sus aspectos clínicos

Sin duda esta tesis no se hubiese llevado a cabo sin el esfuerzo me muchas personas en el "Duke Eye Center" de la Universidad de Duke. En primer lugar el grupo al completo de Daniel Saban: Rose, Nancy, Rachel, Sarah, Joan and Emily… thank you all! Peter Salupis, Grazzia Spiga, Paloma Liton, Rupa, Padhu, Mikael … ¡gracias!

Especial agradecimiento para Sam Johnson, Benjamin Carlson y Yasheng Gao del centro de microscopía avanzada de la Universidad de Duke.

Mis ratoncitos y el cuidado especial de Cheryl Mills quien no sólo los cuidó, sino que los mimó con la delicadeza que tan delicados animales requieren

Michael Gunn del Departamento de Inmunología, Brigid Hogan del Departamento de Biología Celular, Henry Tseng y Scott Cousins del Departamento

de Oftalmología. Ladan Espandar, Anthony Kuo, Molly Walsh, Dan Stramer y Li Quorong del Duke Eye Center

Gracias a Laura Contreras y Laura García por el último empujón

Un agradecimiento muy especial a Lourdes Pérez Velesar a quien sólo puedo decirle: ¡muchas gracias Lur! y ojalá hubiese más como tú.

Muy poco hubiese sido de este maratón sin la ayuda de Yolanda Diebold Luque a quien, por razones de forma, sólo puedo darle las gracias en general y no por todas y cada una de las particularidades, que han sido muchas *"sine qua non"* escribiría éstas letras finales. Gracias Yolanda

"Finally, I wish to truly say thanks to Jim Zieske, my supervisor at Harvard University, and Daniel Saban my supervisor at Duke University and Director of this Thesis. It sounds ironic and convoluted but it is what it is and anything, written above and below, would not have been possible without both of you". Gracias Jim, muchas gracias Danny.

!Gracias a todos

"...que ser valiente no salga tan caro,
que ser cobarde no valga la pena"

Joaquín Sabina

Financiación

Este trabajo de investigación ha sido posible gracias al apoyo económico recibido de diferentes organismos públicos y privados de EE.UU. y de España que han financiado los siguientes proyectos de investigación, en los que he participado como personal investigador:

1. "National Institutes of Health/National Eye Institute Grants" **EY005665 (JDZ), EY05665-25S1 (JDZ),** and **EY03790 (Core-JDZ)**, James D. Zieske Lab, Schepens Eye Research Institute & Massachusetts Eye and Ear, Harvard Medical School, Boston, MA, USA.

2. "Research to Prevent Blindness, Career Development Award (D.R.S). Grant Number: **R01EY021798,** Daniel R. Saban Lab, Schepens Eye Research Institute & Massachusetts Eye and Ear, Harvard Medical School, Boston, MA, USA and Duke Eye Center, Duke School of Medicine"

3. Ayuda para la realización de estancias, financiada por **Ferrara e Hijos S.L.** Parque Tecnológico de Boecillo. Edificio de Usos Comunes, Boecillo, 47151, Valladolid. Estancia realizada en el "Schepens Eye Research Institute & Massachusetts Eye and Ear, Harvard Medical School, Boston, MA, USA". Periodo de la ayuda: 15/05/2008-31/03/2009

Breve Curriculum Vitae

1. Licenciatura en Ciencias Biológicas, Universidad de Salamanca.

2. Diploma de estudios avanzados (DEA) en Ciencias de la Visión, IOBA, Universidad de Valladolid, homologado en EE.UU. como "Master in Visual Sciences".

3. Estancias externas: "Schepens Eye Research Institute & Mass Eye and Ear" (SERI&MEEI), Universidad de Harvard, Boston, EE.UU (4 años); "Duke Eye Center" Universidad de Duke. Durham, EE.UU. (3 años); IBILI, Universidad de Coímbra (6 meses); INCYL, Universidad de Salamanca (2 meses).

4. Publicaciones: 17 artículos científicos en revistas de divulgación con índice de impacto, 6 relacionados con la temática de la tesis de los cuales 3 han sido incluidos en esta memoria.

5. Comunicaciones: 75 comunicaciones en congresos nacionales e internacionales de las que destacan para esta tesis: 3 comunicaciones orales en ARVO ("Association for Research in Vision and Ophthalmology") (2011, 2013, 2104), 2 en Keystone (2013, 2014) y otra en ESCRS ("European Society of Cataract and Refractive Surgeons") (2011).

6. Participación en gran número de conferencias, seminarios y simposios de los que se destaca: 3 presentaciones en la "Biennial Cornea Conference" (SERI&MEEI) así como todos los seminarios regulares tanto del IOBA en la Universidad de Valladolid, SERI&MEEI en la Universidad de Harvard, "Duke Eye Center" y Departamento de Inmunología de la Universidad de Duke.

7. Premios relevantes: Beca estancia internacional (Ferrara Ring, 2008-2009), "ARVO travel grant" (NEI, 2011) y Beca de estancia ("Cornea Conference, Ophthalmology Department, Harvard Medical School" (2012)).

8. Experiencia docente destacable: Colaborador honorífico en los Departamentos de Oftalmología y Biología Celular de la Universidad de Valladolid (2003-2008).

9. Revisor de las revistas de divulgación científica: IOVS, "Clinical and Experimental Ophthalmology", DOVE y "Biomarker Insights".

10. Campo de investigación: córnea (2002-actualidad).

11. Idiomas: castellano, inglés y portugués.

A Natalia

INDICE

RESUMEN

Esa tesis doctoral se presenta como una evolución en la metodología utilizada para el estudio de la córnea. Esta evolución se puede observar cronológicamente en los capítulos, pero en general representa una innovación significativa respecto a la metodología usada hasta ahora por otros grupos de investigación.

En el primer capítulo, se observó que la deficiencia de la integrina αVβ6 causa problemas en la cicatrización corneal. Usando ratones carentes de la subunidad β6 ($\beta6^{-/-}$), se observó que éstos no recuperan la membrana basal ni los hemidesmosomas que anclan el epitelio al estroma, después de una lesión corneal. Las córneas muestran ampollas sub-epiteliales similares a las que muestran pacientes con queratopatía bullosa o distrofia de la membrana basal.

Posteriormente (capítulo 2), se usó un ratón deficiente en trombospondina-1 (THSB1) para estudiar el proceso de reparación de la córnea después de una incisión corneal penetrante. Se observó que la THBS1 es fundamental en el mecanismo de cicatrización general y para el proceso de reparación del estroma y la regeneración del endotelio en concreto. Las córneas de los ratones carentes de THBS1 presentan fallo general desarrollando edema crónico. En este trabajo de utilizó por primera vez un sistema de microscopía confocal *"in vivo"* para evaluar el proceso de cicatrización sin sacrificar el ratón.

Usando el mismo sistema de microscopía confocal *"in vivo"*, se procedió al estudio de la inflamación de la superficie ocular en un modelo de conjuntivitis alérgica en ratón (capítulo 3). Se observó el proceso de infiltración celular en la superficie ocular a tiempo real. Como novedad, se detectó que la córnea sufre un proceso inflamatorio (infiltración celular) mucho antes de que sea detectado con la lámpara de hendidura. El número de células así como la distribución espaciotemporal de éstas en la córnea, está en relación con la progresión de los síntomas clínicos de la alergia observados con la lámpara de

hendidura. A su vez se confirmó la naturaleza inflamatoria de las células, mediante citometría de flujo e inmunofluorescencia.

En este punto se incorporó un sistema de microscopía multifotónica *"intravital"* y cepas de ratones que expresan fluorescencia en las células de origen mieloide o en los nervios. Con esta tecnología se visualizó, a nivel celular y de forma no invasiva, la córnea en el ratón vivo. Se mapeó la población inmunitaria residente de la córnea con alta resolución y definición tridimensional (capítulo 4). Además se generaron nuevos ratones quiméricos mediante irradiación letal y trasplante de la médula ósea. En estos ratones se observó *"in vivo"* el proceso de recambio de la población mieloide de la córnea. También se realizó un estudio de "fate mapping" de dicha población residente. Se comprobó que esta población tiene un origen embrionario en lugar de hematopoyético.

Por otro lado, se visualizó de forma *"intravital"* los nervios corneales en el ratón (capítulo 5). Se muestra por primera vez el mapeado completo usando un sistema multifotónico y además éste es expuesto con alta resolución y presentación tridimensional. También se observó la existencia de haces radiales estromales profundos (no descritos anteriormente en el ratón) que complementan la inervación radial periférica del plexo sub-basal. Así mismo, se detalla la existencia de bifurcaciones nerviosas en 180° (no descritas) inervando el plexo en ambas direcciones: centrípeta y centrífuga.

La interacción física de ambos sistemas inmunitario y nervioso se muestra en el capítulo 6. La relevancia de esta interacción, si bien se intuye en el ojo seco y se cree muy relevante en el rechazo al trasplante de córnea, no se ha descrito anteriormente en la córnea. De esta manera, se presenta la córnea como un órgano mucho más complejo, de lo que se ha descrito, donde dos "supersistemas" (nervioso y periférico) interactúan de forma estocástica para mantener su homeostasis. Esto se comprobó generando una quimera mediante irradiación de un ratón receptor que expresa neurofluorescencia y posterior trasplante de medula ósea de un donante que expresa fluorescencia de origen mieloide. A los tres meses ambos "supersistemas" se observaron interconectados físicamente. Este modelo pone de manifiesto la relevancia de la interacción neuro-inmune

en la córnea y puede ser utilizado en el futuro para estudios de patologías como el ojo seco, el queratocono y otras patologías de la córnea.

Por último, se muestran algunas aplicaciones de la microscopía multifotónica *"intravital"*. En primer lugar, se hizo un seguimiento *"in vivo"* y a tiempo real de células madre del tejido adiposo trasplantadas en la córnea. Se observó su comportamiento durante 4 semanas. Por otro lado se detectó la presencia en la cámara anterior, malla trabecular y canal de Schlemm de sistemas de liberación de fármacos como nanopartículas, liposomas o proteínas de unión al colágeno sin necesidad de sacrificar al ratón. Además se observó un sistema de infección de las células endoteliales mediante inyección de adenovirus. Cuando el virus infecta la célula, ésta emite fluorescencia que puede ser detectada *"in vivo"*. Por último se evaluó la tasa de recambio de células dendríticas CD11c tras ser selectivamente eliminadas con toxina diftérica.

ORGANIZACIÓN DE LA TESIS

Esta memoria de tesis se presenta en la modalidad de compendio de publicaciones y opta a la Mención Internacional en el título de Doctor. Por lo tanto, su organización se ajusta a lo requerido por la Comisión de Doctorado de la Universidad de Valladolid, con una síntesis general en ambos idiomas (Castellano e Inglés), donde se justifica la unidad temática del trabajo y se presentan los objetivos perseguidos, la metodología empleada, los resultados con discusión y las conclusiones alcanzadas. Se presentan tres artículos aceptados en revistas científicas con factor de impacto (Capítulos 1, 2 y 6). Adicionalmente se ha incluido otros 2 artículos que se encuentran en fase de revisión (Capítulos 3 y 5) y otro en periodo de preparación (Capítulo 5). Además, se ha complementado con abundante material suplementario al artículo publicado en el capítulo 6. Por último se ha incorporado un apartado final (Capítulo 7) mostrando posibilidades futuras de parte metodológica utilizada en esta tesis.

Tras la síntesis general, la memoria de esta tesis doctoral se ha organizado en ocho capítulos, correspondientes a los seis artículos (publicados, en revisión o en fase de preparación) más el correspondiente a aplicaciones futuras, que recogen los distintos bloques de experimentos realizados. Los capítulos no se han ordenado de forma cronológica, sino de una forma tal que facilite la comprensión de la evolución en la metodología empleada.

También se ha incluido un capítulo introductorio íntegramente en castellano y en inglés (**Capítulo 0**). De esta manera se elimina la introducción general, por la diversidad en los contenidos, y se revisa el estado actual del arte en la córnea como órgano así como las patologías más importantes. Además se describe, en parte, la parte experimental más novedosa de tal forma que se favorece la lectura e interpretación de los capítulos posteriores. En este capítulo se describe la relevancia del uso de ratones manipulados genéticamente así como la importancia de incorporar nuevos sistemas de imagen que

permitan una mejor comprensión de la fisiología y de las múltiples patologías que afectan a la córnea.

El primer paso experimental de este proyecto de tesis fue desarrollar un modelo animal en ratones carentes de la integrina β6 ($\beta6^{-/-}$) para estudiar la función de la integrina αVβ6 en el proceso de reparación corneal. Este trabajo está reflejado en el **Capítulo 1:** "***αVβ6 integrin promotes corneal wound healing***" **(**Blanco-Mezquita J.T. et al. "Investigative Ophthalmology & Visual Science") [1]. En este modelo se constató que la falta de la integrina αVβ6 causa problemas en la cicatrización del epitelio cuando se daña la membrana basal. El modelo reproduce patologías de la membrana basal como las ampollas sub-epiteliales, fácilmente observables con la lámpara de hendidura. Además se confirmó que la ausencia de la integrina αVβ6 no tiene consecuencias observables en el estroma o en el endotelio de la córnea.

A continuación, se diseño un modelo animal en ratones carentes de trombospondina-1 (THBS1) ($Thbs1^{-/-}$) para investigar la función de la THBS1 en el proceso de reparación corneal después de una lesión integral de todas las capas de la córnea. Este trabajo está reflejado en el **Capítulo 2**: "***Role of Thrombospondin-1 in Repair of Penetrating Corneal Wounds***" (Blanco-Mezquita J.T. et al. ""Investigative Ophthalmology & Visual Science") [2]. En este modelo se hizo un seguimiento de la cicatrización corneal constatándose que la THBS1 es fundamental para dicho proceso, especialmente en el estroma y en el endotelio. Además de la lámpara de hendidura, se incorporó por primera vez el uso del microscopio confocal "*in vivo*" (IVCM "*in vivo* confocal microscopy") (HRT3-RCM), como sistema adicional de imagen "*intravital*". Con el uso de este sistema se evaluó el proceso de cicatrización en todas las capas de la córnea, usando el mismo ratón en diferentes intervalos de tiempo sin necesidad de sacrificarlo.

Sin duda, el microscopio confocal "*in vivo*" supuso un avance considerable en la

forma de evaluar a tiempo real los cambios a nivel celular y tisular ocurridos en la superficie ocular. Por ello se procedió al estudio del proceso de infiltración celular en la superficie ocular, en un modelo de alergia ocular en ratón. Este trabajo está reflejado en el **Capítulo 3**: ***"Intravital Confocal Microscopy Reveals Corneal Involvement in an Allergic Eye Disease Mouse Model: an in vivo Study"*** (Blanco T. et al. Investigative Ophthalmology & Visual Science 2015, en fase de revisión. Este trabajo ha sido presentado, en parte, en ARVO 2012 ("*Corneal Inflammatory Cell (IC) Recruitment in Murine Allergic Conjunctivitis (AC): An Intravital Confocal Microscopy Study"* Tomas Blanco, Hyun Soo Lee, Daniel R. Saban. Ophthalmology Department, Schepens Eye Res Inst, MEE, Harvard Medical School, Boston, MA) y 2014 ("*Novel Mouse Model of Severe Ocular Allergy Reveals a Key Role for Pathogenic Th17 Cells*", Nancy Reyes; Tomas Blanco; Rose Mathew; Daniel R. Saban, Ophthalmology, Duke University, School of Medicine, Durham, NC, United States). En este trabajo se observó de forma *"intravital"* y a tiempo real el proceso de infiltración celular inflamatorio en la superficie ocular en un modelo de alergia ocular. La relevancia de este trabajo fue observar un proceso de infiltración celular en la córnea asociado con la progresión de los síntomas de la conjuntivitis alérgica. Este proceso de infiltración no es detectable con la lámpara de hendidura pero se contrastó con análisis de citometría de flujo e inmunofluorescencia. Estos resultados indican un componente inflamatorio en la córnea del ratón, no descrito anteriormente, durante la progresión de la inflamación conjuntival alérgica.

Debido a las observaciones anteriores, el trabajo tomó una dirección diferente. Por un lado se inició un estudio clínico para estudiar el proceso de infiltración celular en la córnea en voluntarios con conjuntivitis alérgica (proyecto en curso y no descrito en esta memoria, "IRB approved project # Pro00042819 Study Title: Corneal Involvement in Allergic Conjunctivitis, Investigator: Daniel Saban, PhD, Duke Eye Center"), y por otro lado, el sistema IVCM se sustituyó definitivamente por un microscopio multifotónico. Este sistema permitió, por primera vez, el estudio *"intravital"* y a nivel celular de la

córnea. Además se incorporaron diferentes cepas de ratones transgénicos que expresan proteínas fluorescentes y se generaron ratones quiméricos. Finalmente se usó un software de análisis de imagen proporcionando fotografías y animaciones reales en tres dimensiones para una mejor interpretación y comprensión de los resultados. Los dos capítulos siguientes forman parte de un trabajo más amplio en fase de revisión: ***"Mononuclear phagocytes in vivo form vast networks of membrane nanotubes that contact and track along peripheral nerves"***) (Blanco et al. Nature Medicine). En este trabajo, la córnea se tomó como modelo, pero el trabajo completo en si, no guarda relación con la temática de esta tesis. Por ello se utilizó parte de la metodología y de resultados relacionados con la córnea, pero no incluidos en el manuscrito anteriormente mencionado. De esta manera se complementó con material adicional los capítulos 4 y 5 que sirven de enlace con el capitulo 6. Estos dos capítulos están en fase de preparación (4) y revisión (5) para publicación independiente de el anteriormente mencionado trabajo.

En primer lugar se procedió a la visualización y mapeado *"in vivo"* de la población inmunitaria residente en la córnea. Se utilizaron ratones transgénicos con diferentes marcadores fluorescentes. Este trabajo está reflejado en el **Capítulo 4**: ***"Cutting Edge in vivo Imaging I: Multi-Photon intravital Microscopy to Visualize the Resident Myeloid-Derived Population in the Mouse Cornea"***, (Blanco et al. en preparación. Presentado en dos comunicaciones orales ARVO 2013 ("*Cornea Intravital Multiphoton Visualization of the Resident Mononuclear Phagocyte Network in Allergy*", Tomas Blanco; Matthew Kan; Michael Gunn; Daniel R. Saban; Ophthalmology, Duke University, School of Medicine, Durham, NC, United States) y 2014 (*"Intravital multiphoton visualization identifies inter-networking between nerves and bone marrow derived cells of the mouse cornea",* Tomas Blanco; Daniel R. Saban, Ophthalmology, Duke University, School of Medicine, Durham, NC, United States). En este trabajo se visualizó y mapeó por primera *"in vivo"* la población inmunitaria de la córnea usando un microscopio multifotónico. Para ello se detectó la expresión de proteínas fluorescentes (GFP, YFP y td/Tomato(RFP)) bajo el

control del promotor del gen Cx3cr1. Además se generaron ratones quiméricos (irradiación letal y trasplante de médula ósea) y se usó un sistema de expresión inducible de fluorescencia mediante inyección de tamoxifeno para constatar *"in vivo"* el proceso de recambio de las células inmunitarias corneales. Entre otras características, este sistema permite una resolución de imagen, *"in vivo"*, similar a la obtenida en *"explantes"* de tejido, pero de forma no invasiva y sin necesidad de sacrificar el animal. Además se constató que la población mieloide residente en la córnea, tiene un origen embrionario en lugar de hematopoyético. Tanto la introducción como la discusión de este capítulo se muestran en versión extendida.

A continuación, se realizó un mapeado de alta resolución de los nervios de la córnea, por primera vez, en un ratón vivo. Para ello se utilizó el sistema multifotónico anterior y un ratón transgénico que expresa YFP en el promotor del gen Thy1. Este trabajo está reflejado en el **Capítulo 5:** "***Cutting Edge in vivo Imaging II: Multi-Photon intravital Microscopy to Visualize Transgenic Neurofluorescence in a Thy1-YFP Mouse Cornea***" (Blanco T. et al. "Investigative Ophthalmology & Visual Science" 2015, en fase de revisión. Presentado en dos comunicaciones orales en ARVO 2013 (*"Cornea Intravital Multiphoton Visualization of the Resident Mononuclear Phagocyte Network in Allergy"*, Tomas Blanco; Matthew Kan; Michael Gunn; Daniel R. Saban; Ophthalmology, Duke University, School of Medicine, Durham, NC, United States) y 2014 (*"Intravital multiphoton visualization identifies inter-networking between nerves and bone marrow derived cells of the mouse cornea",* Tomas Blanco; Daniel R. Saban, Ophthalmology, Duke University, School of Medicine, Durham, NC, United States). Este modelo permitió escanear la anatomía completa de los nervios corneales del ratón sin necesidad de sacrificar al animal. Por otro lado, se describen algunos detalles de la anatomía de la córnea del ratón no descritos anteriormente. Se muestra la presencia de haces nerviosos estromales profundos que inervan el centro de la córnea, así como bifurcaciones de los grupos axonales en 180° en el plexo basal. La anatomía de los

nervios corneales se muestra de forma interactiva en tres dimensiones y con resolución micrométrica tanto en imagen *"in vivo"* como *"ex vivo"*

El hecho de poder evaluar in vivo, por un lado la estratificación de la población inmunitaria de la córnea y por otro la anatomía de los nervios, nos llevó al siguiente paso: la interacción de ambos sistemas. Este trabajo está reflejado en el **Capítulo 6** ***"The cornea has "the nerve" to encourage immune rejection"*** (Blanco et al. American Journal of Transplantation, 2015) [3]. Éste es un artículo de apoyo al trabajo titulado "*Severing Corneal Nerves in One Eye Induces Sympathetic Loss of Immune Privilege and Promotes Rejection of Future Corneal Allografts Placed in Either Eye*" Paunicka et al., "American Journal of Transplantion [4]; en el cual se muestra la interacción de los nervios con las células inmunitarias de la córnea y su posible relación con el rechazo al trasplante corneal. Es por ello que se incluye material adicional, que si bien no publicado todavía, condujo a los resultados que forman parte de la publicación mencionada anteriormente. En la versión extendida, se muestra la córnea como un órgano en el cual dos "supersistemas" (nervioso e inmunitario) están físicamente interconectados. Además se creó un ratón quimérico en el cual se puede estudiar "*in vivo*" la interacción de éstos.

Por último se incluye un apartado adicional (**Capítulo 7**) donde se muestra el uso del microscopio multifotónico *"in vivo"* para otras aplicaciones con grandes expectativas para el futuro:

1. Terapia celular: implantación de células madre de la grasa en un modelo de herida corneal en el ratón. En este modelo, se hizo un seguimiento durante varias semanas, del proceso de implantación y diferenciación de dichas células marcadas con GFP, tras varias lesiones corneales
2. Sistemas de liberación de fármacos para el tratamiento del glaucoma. En este estudio se usaron ratones albinos Balb/c en los cuales se inyectó diferentes sistemas de liberación de fármacos (nanoesferas, partículas de colágeno,

partículas de adhesión endotelial y liposomas) marcados con GFP en la cámara anterior. Estos sistemas se detectaron *"in vivo"* en el endotelio, en el canal de Schlemm y en la malla trabecular.

3. Evaluación *"in vivo"* de la capacidad infectiva de adenovirus en las células del endotelio.
4. Seguimiento de la repoblación de la córnea, por una población específica de células dendríticas CD11c, después de ser eliminada con toxina diftérica aplicada de forma tópicamente.

El objetivo general de este capitulo es mostrar la potencialidad de la microscopía *"in vivo"*. Es por ello que sólo se muestran los resultados con una breve descripción metodológica. No se presenta parte introductoria ni tampoco discusión.

Citaciones

1. Blanco-Mezquita, J.T., A.E. Hutcheon, M.A. Stepp and J.D. Zieske, *αVβ6 integrin promotes corneal wound healing.* Investigative ophthalmology & visual science, 2011. **52**(11): p. 8505-8513.
2. Blanco-Mezquita, J.T., A.E. Hutcheon and J.D. Zieske, *Role of thrombospondin-1 in repair of penetrating corneal wounds.* Invest Ophthalmol Vis Sci, 2013. **54**(9): p. 6262-8.
3. Blanco, T. and D.R. Saban, *The Cornea Has "the Nerve" to Encourage Immune Rejection.* Am J Transplant, 2015.
4. Paunicka, K.J., J. Mellon, D. Robertson, M. Petroll, J.R. Brown and J.Y. Niederkorn, *Severing corneal nerves in one eye induces sympathetic loss of immune privilege and promotes rejection of future corneal allografts placed in either eye.* Am J Transplant, 2015. **15**(6): p. 1490-501.

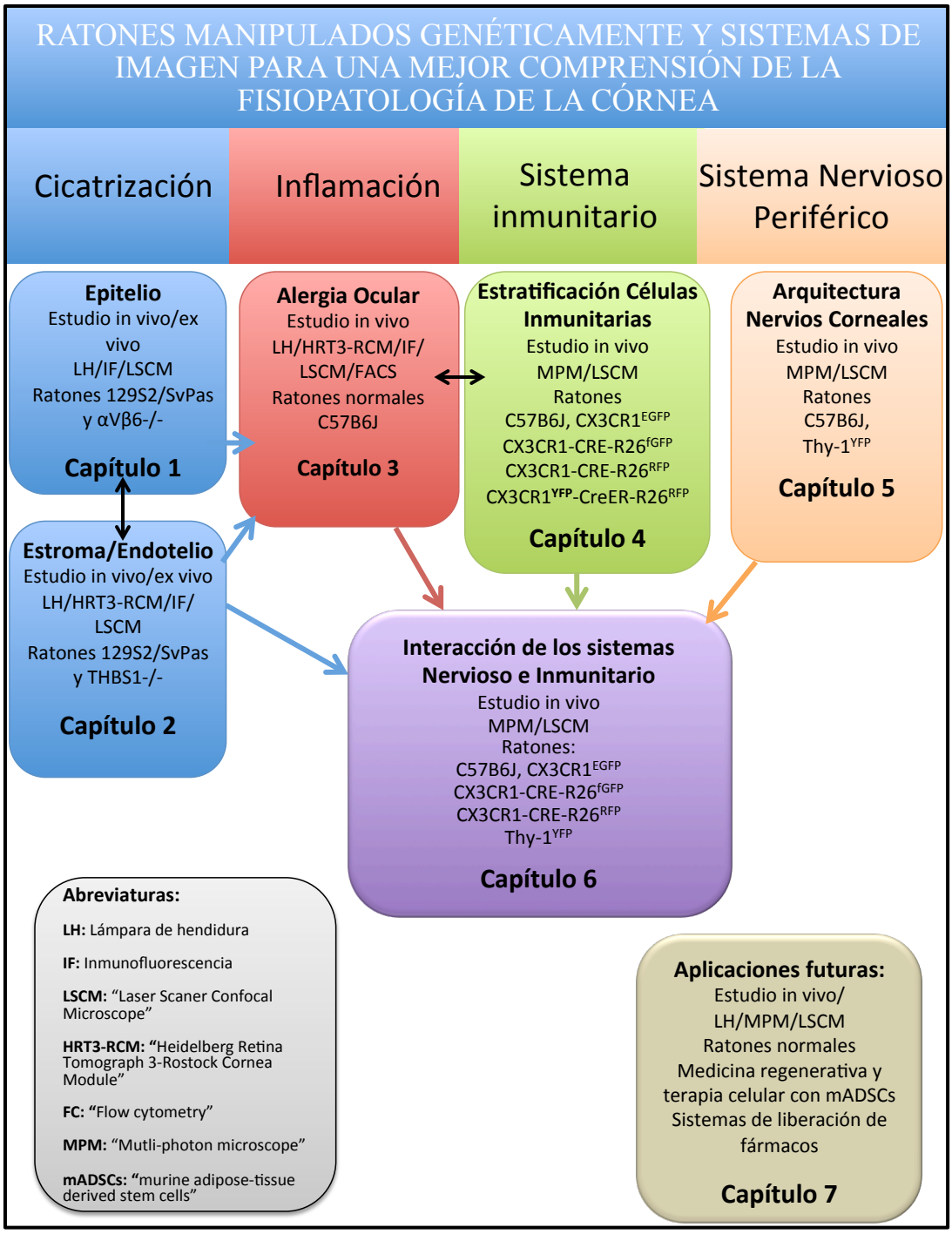

Organización de la tesis. Esquema sintetizado

LISTA DE ABREVIATURAS

AC “allergic conjunctivitis”: conjuntivitis alérgica

ACAID “anterior chamber-associated immune deviation”

AED “allergic eye disease”: alergia ocular

AKC “atopic keratoconjunctivitis”: queratoconjuntivitis atópica

APCs “antigen presenting cells”: células presentadoras de antígeno

BGR “blue-green-red cube”: cubo azul-verde-naranja

BM “Bowman’s layer”: capa de Bowman

BMZ “basement membrane zone”: membrana basal

BSA “bovine serum albumin”

CCL2 “chemokine (C-C motif) ligand 2”

CCL20 “chemokine (C-C motif) ligand 20”

CCL21 “chemokine (C-C motif) ligand 21”

CCR1, “CCR2, CCR5, CCR7 chemokine (C-C motif) receptors: 1,2,5,7”

CGRP “calcitonin gene related peptide”

CX3CR1 “CX3C chemokine receptor 1”

Cx3cr1 “chemokine receptor 1 gene”

Cre “causes recombination”

CXL “collagen crosslinking”: entrecruzamiento del colágeno

CYR “cian-yellow-red cube”: cubo cian-verde-naranja

DAPI “4',6-diamidino-2-phenylindole”

DCs “dendritic cells”: células dendríticas

DM “Descemet’s membrane”: membrana de Descemet

ECM “extracelular matrix”: matriz extracelular

EGFP “enhanced green fluorescent protein”

FAS-L “fas ligand (CD95L)”

GFP “green fluorescent protein”: proteína fluorescente verde

H&E “hematoxylin and eosin”: hematoxilina y eosina

HLA-DR “human leukocyte antigen DR”: antígeno leucocitario humano

HRT3 “Heidelberg Retina Tomograph III”

HSV “*Herpes virus simplex*”

ICAM1 “intercellular adhesion molecule 1”: molécula de adhesión intercelular tipo 1

ICRS “intrastromal rings and segments”: segmentos y anillos intraestromales

ICs “inflammatory cells”: células inflamatorias

IFN-y “Interferon gamma”

IL-α1,-1β,-4,-6,-8,-10, -13 -17 “interleukins: 1alpha,1beta,4,6,8,10,13,17”

IL-1Ra “interleukin-1 receptor antagonist”

IP “intraperitoneal”: intraperitoneal

IVCM “in vivo confocal microscope”

LAP “latency-associated peptide”

LCs “Lagerhans cells”: células de Langerhans

LIVE-1 “lymphatic vessel endothelial receptor 1”

LSCM “laser scanning confocal microscope”

Ly6C “lymphocyte antigen 6C”

mADSCs “murine adipocyte-derived stem cells” células madre derivadas del tejido adiposo

MHC class I, II “major histocompatibility complex class I, II molecules”: complejo mayor de histocompatibilidad clase I y II

MMP-9 “matrix metallopeptidase 9”

MP-IVM “multiphoton intravital microscopy”: microscopio multifotónico

NGF “nerve growth factor”: factor de crecimiento nervioso

NK cells “natural killer cells”

OCT “optical coherence tomography”

OVA “ovalbumin”: ovoalbúmina

PAC “perennial allergic conjunctivitis”: conjuntivitis alérgica perineal

PDL-1 “programmed death-ligand 1”

PEDF “pigment epithelium-derived factor”

PFA “paraformaldehyde”: paraformaldehido

PMN “polimorphonuclear”: polimorfonuclear

PMTs “photomultiplier tubes”: tubos fotomultiplicadores

PNS “peripheral nervous system”: sistema nervioso periférico

PRGF “plasma rich in growth factors”: plasma rico en factores de crecimiento

PROX-1 “prospero Homeobox 1”

RFP “red fluorescent protein”: proteína fluorescente roja

SAC “seasonal allergic conjunctivitis”: conjuntivitis alérgica estacional

SERI&MEE “Schepens Eye Research Institute and Massachusetts Eye and Ear”

SHG “second harmonic generation”: generación de segundo armónico

SP “substance P”

TGF-β2 “transforming growth factor-beta”

THBS-1 “thrombospondin-1”

Thy.1-YFP “transgenic mice strain expressing yellow fluorescent protein under Thy-1 promoter”

TNF-α “tumor necrosis factor-α”

TPM “two-photon excitation microscopy”: microscopia de excitación de dos fotones

VEGF “vascular endothelial growth factor”: factor de crecimiento vasoendotelial

VEGFR “vascular endothelial growth factor receptor” receptor del VEGF

VIP “vasoactive intestinal peptide”: péptido vasoactivo intestinal

VKC “vernal keratoconjunctivitis”: queratoconjuntivitis vernal

WT “wild type”: tipo silveste o ratón normal

YFP “yellow fluorescent protein”: proteína fluorescente amarilla

αVβ6 “integrin alphaV-beta6”

Síntesis General

Estado del Arte

Versión en castellano del capítulo 0 (Chapter 0)

ESTADO DEL ARTE

La córnea

La córnea es el órgano más externo del sistema visual en contacto con el medio ambiente con dos funciones fundamentales: por un lado actúa como barrera protectora del sistema frente al medio externo y por otro es el elemento óptico primario del ojo. La córnea se caracteriza como un órgano transparente, avascular, con privilegio inmune, con gran elasticidad y resistencia mecánica [1].

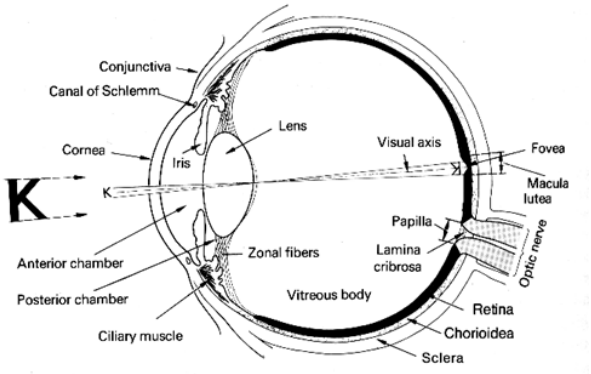

Figura 1. Estructura del sistema visual Modificada de: web.standord.edu

Figura 2. La córnea como elemento protector y refractario del ojo. Foto modificada de: "DesignPics" Don Hammond

En la parte más externa, dispone de un epitelio estratificado no queratinizado que protege a la córnea del exterior. El epitelio, en contacto con la película lagrimal, mantiene una superficie lisa e hidrofóbica, que protege a la cónrea de la invasión de patógenos y le confiere un frente raso a la entrada de la luz. Éste descansa en la lamina basal que lo ancla al estroma [2, 3]. A continuación se encuentra la capa de Bowman formada por colágeno muy organizado. Esta membrana varía en grosor según en diferentes especies y

está ausente en otras [4]. La mayor parte del órgano lo compone el estroma formado por colágeno muy organizado y queratocitos (fibroblastos en estado quiescente). El estroma supone el 90% del grosor otorgándo a la córnea su carácter refractivo [5]. En la parte posterior de la córnea se encuentra la membrana de Descemet o membrana basal sobre la que descansa el endotelio [5]. El endotelio está formado por una monocapa de células endoteliales en contacto con la cámara anterior y que mantienen el balance hídrico y la transparencia de la córnea [6].

Además de esta estructura básica, la córnea está densamente inervada [7] con dos tipos de fibras nerviosas: sensitiva con origen en la rama oftálmica del nervio trigémino [8, 9] y autónoma tanto simpática, con origen en el ganglio cervical superior [10], como parasimpática con origen en el ganglio ciliar [11-13].

La córnea contiene una población residente de células inmunitarias de origen mieloide. Éstas juegan un papel primordial en la defensa y en la respuesta inmunitaria ante situaciones de peligro pero su función está muy poco descrita [14].

Recientemente se ha propuesto que los sistemas nervioso e inmunitario podrían intercomunicarse en la córnea, ya que se ha descrito que ambos sistemas se intercomunican entre si en las vías respiratorias [15, 16]. Este tipo de conexiones tienen gran importancia en el rechazo inmunológico al trasplante [17] y en el ojo seco, pero su función no se conoce bien [18, 19].

En este escenario, la córnea se muestra como un órgano extremadamente complejo compuesto por diferentes tipos de tejidos cuya homeostasis está dirigida a mantener la integridad del sistema visual, la refracción y la transparencia. Al final de este trabajo se mostrará una visión más evolucionada de la córnea, donde además de los ya conocidos tejidos conjuntivo y epitelial, se pone de relieve como los "supersistemas" (del inglés "supersystem") [20] nervioso e inmunitario interaccionan de forma estocástica y entre si, es decir, son capaces de adaptarse uno al otro en función del medio ambiente para ejercer sus funciones.

Patologías corneales

Como órgano externo, la córnea está continuamente sometida a todo tipo de agresiones que afectan a la visión. El sistema visual ha desarrollado un mecanismo único de defensa basado en una rápida respuesta (parpadeo, lagrimeo y secreciones enzimáticas conjuntivales) ante la agresión sufrida, protegiendo así, la integridad y la transparencia [21]. Cuando la agresión afecta a la integridad de la córnea, ésta responde con un rápido mecanismo de cicatrización destinado a reparar su estructura y función y que en la mayoría de los casos no tiene consecuencias negativas [22]. Sin embargo, otras situaciones causadas por agresiones mayores como quemaduras, causticaciones, alergias, infecciones, traumas, etc., causan lesiones irreparables que necesitan de un trasplante de córnea [23].

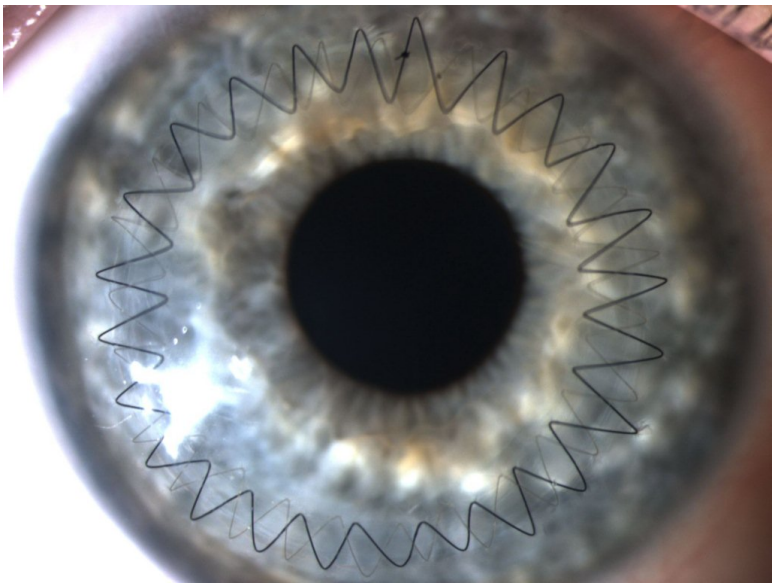

Figura 3. Trasplante lamelar de córnea. Fotografía modificada de: "Corneal Associates of New Jersey", Fairfield, NJ, EE.UU.

Por otro lado, la existencia de patologías como el queratocono, las distrofias de la membrana basal del epitelio, las ulceras neurotróficas, las distrofias basales del endotelio,

el ojo seco, la queratoconjuntivitis alérgica etc., cursan con una etiología poco conocida que en muchos casos hacen que el trasplante del órgano sea la única opción para estos pacientes [24].

La córnea a su vez es diana para diferentes patógenos que provocan diferentes tipos de inflamaciones o queratitis. Unas son causadas por amebas como la Acantamoeba y afectan sobre todo a usuarios de lentes de contacto. Otras son causadas por infecciones bacterianas como *Staphylococcus aureus* o *Pseudomonas aeruginosa*, de origen fúngico causadas por Fusarium, y otras de origen vírico causadas *Herpes simplex* o *Herpes zoster* [25, 26]. Por otro lado, la superficie ocular sufre el ataque continuo de alérgenos. En la mayor parte de los casos sólo la conjuntiva o tejido mucoso, que rodea a la córnea, sufre un proceso inflamatorio o conjuntivitis alérgica; pero en otros casos la inflamación afecta a la córnea causando queratoconjuntivitis [27]. Debido a la cirugía refractiva corneal, la incidencia de patologías post-quirúrgicas, como la pérdida de agudeza visual, halos, destellos, reflejos, sensación de cuerpos extraños y falta de lubricación ha incrementado notablemente. Otras complicaciones relacionadas con el proceso de cicatrización después de la cirugía, como los procesos fibróticos, las ectasias o la autodigestión, requieren a veces del trasplante para recuperar la visión del paciente. Además estas mismas complicaciones, con menor incidencia, pueden aparecer después de una cirugía de cataratas [28, 29].

El trasplante de córnea es la técnica quirúrgica más frecuente en el mundo, con una experiencia de más de 100 años, desde que en 1905, se realizó el primer trasplante de córnea finalizado con éxito [30]. Desde que se fundó la Organización Nacional de Trasplantes (ONT) en el año 1989 en España, se han realizado aproximadamente 60.000 trasplantes de córnea (3.477 en el año 2013 según datos publicados por dicha organización). A pesar del gran número de queratoplastias realizadas cada año en todo el mundo, el trasplante es todavía una opción terapéutica compleja. Si bien el porcentaje de rechazo inmunológico es muy bajo, son muchos los pacientes considerados de alto riesgo

de rechazo y por tanto excluidos del trasplante [31]. Además, el trasplante es una opción de los países desarrollados no disponible en la mayoría de los países en vías de desarrollo.

Debido a su inervación, son varias las patologías corneales derivadas de una incorrecta función de los nervios como las ulceras neurotróficas, el dolor crónico, el ojo seco, el queratocono o el rechazo al trasplante de córnea [7, 32-36].

La córnea goza de privilegio inmune y por ello no reacciona ante la presencia de antígenos externos. Por este motivo, y debido a la baja incidencia de rechazo inmunológico, se estableció el dogma de que la córnea estaba desprovista de células presentadoras de antígeno. Este dogma permaneció por un siglo hasta que se describió que la córnea contiene una población residente de células inmunitarias [37]. A pesar de los trabajos realizados en modelos animales durante las dos últimas décadas, la primera descripción detallada de la estratificación de la población residente de células inmunitarias de la córnea humana, se realizó recientemente (2104) [14]. La investigación de la función de las células inmunitarias de la córnea así como su origen embrionario es uno de los campos de investigación de más actualidad debido a que cada vez existen más evidencias de su implicación, tanto en la homeostasis corneal como en sus patologías. Otro descubrimiento reciente ha sido el hallazgo de vasos linfáticos periféricos y que en ciertas condiciones pueden invadir la córnea [38]. Estos vasos linfáticos tienen un papel fundamental en los procesos inflamatorios y aumentan el riesgo de rechazo al trasplante, pero su mecanismo no se conoce bien [39].

Por la complejidad y origen poco conocido de la mayoría de sus patologías como el ojo seco, las distrofias, el queratocono o las queraconjuntivitis; la córnea, como órgano, merece atención prioritaria desde el punto de vista de la investigación. Desde el punto de vista clínico, y según la Organización Nacional de Trasplantes, la córnea no se considera un verdadero órgano sino un tejido, conjuntivo y epitelial, en el cual, la presencia de otros sistemas como el nervioso periférico y el inmunitario, siguen sin tener la relevancia que las investigaciones más recientes apuntan.

Actualización privilegio inmune

De todos los sitios con privilegio inmune, la córnea es el único en contacto con el medio ambiente externo capaz de tolerar el contacto de aloantígenos sin provocar una respuesta inflamatoria [37]. En general, los injertos de tejido son reconocidos como antígenos extraños por el cuerpo y rechazados por el sistema inmunitario. Por el contrario en los órganos con privilegio inmune, los injertos pueden sobrevivir sin rechazo [40]. Desde el punto de vista evolutivo, el privilegio inmune es una adaptación para proteger las estructuras vitales del cuerpo (cerebro, ojo, placenta, feto y testículos) evitando así los efectos letales de una respuesta inflamatoria [41, 42]. La córnea es por tanto un sitio único que al no tener vasos sanguíneos ni linfáticos limita la presentación de antígeno manteniendo así su privilegio inmune [39].

Las células inmunitarias residentes de la córnea (células de Langerhans, células dendríticas, macrófagos y monocitos) expresan bajos niveles de MHC clase II y de moléculas coestimuladoras CD80 y CD86, evitando de esta manera iniciar una respuesta inmunitaria adaptativa innecesaria [43-49]. En la córnea sana, las ramas aferente y eferente de la respuesta inmunitaria están cerradas el tráfico de células inflamatorias. La rama aferente bloquea el tránsito de células presentadoras de antígeno desde la córnea hacia los nódulos linfáticos y rama eferente boquea la invasión de células inflamatorias en la córnea [39, 50].

El mantenimiento avascular de la córnea está controlado por la disponibilidad de receptores y ligandos de VEGF ("vascular endothelial growth factor"). El epitelio expresa formas solubles de VEGF-3 y VEGFR1 que actúan como receptores señuelo para VEGF-A, VEGF-C, VEGF-D y VEGFR-2, evitando la proliferación de vasos en la córnea [51, 52]. Por otro lado en la córnea se expresa trombospondina-1 (THBS-1) que regula la expresión de VEGF-C en monocitos y macrófagos a través del receptor CD36 [53]. El epitelio a su vez libera PEDF ("pigment epithelium-derived factor"), angioestatina y endostatina como potentes anti-angiogénicos [54, 55]. El TGF-β2 regula la maduración de

las células dendríticas y el ligando de FAS (FAS-L) induce apoptosis en células inmunitarias que expresan FAS [56]. El PDL-1 (programmed death-ligand 1) induce apoptosis de los linfocitos T disminuyendo así su respuesta [56, 57]. Otros factores antiinflamatorios como la IL10 y la IL-1Ra previenen el reclutamiento y la proliferación de neutrófilos, macrófagos y linfocitos T evitando de esta manera la liberación masiva de VEGF [58].

Cuando se pierde el privilegio, los vasos sanguíneos que rodean circunferencialmente al limbo y los vasos linfáticos de la periferia, invaden la córnea. La activación del receptor de VEGF tipo 3 (VEGFR-3) por sus ligandos, como el VEGF-C, promueve proliferación de células endoteliales y la formación de tubos linfáticos [59]. Por otro lado, durante la inflamación, los macrófagos CD11b expresan receptor endotelial de los vasos linfáticos tipo 1 (LIVE-1) y "prospero homeobox 1" (PROX-1) [60]. Algunas patológicas como el trauma, las infecciones, el rechazo al trasplante de córnea y el ojo seco hacen que cambie el balance entre los factores antiangiogénicos y proangiogénicos. En estos casos la proliferación de vasos linfáticos permite el tráfico de células presentadoras de antígeno a los tejidos linfáticos cercanos donde se dispara una respuesta linfocitaria adaptativa [61]. A su vez los linfocitos T CD8 liberan VEGF-C promoviendo linfangiogénesis [62]. El privilegio inmune se puede perder también como consecuencia de una herida. La córnea dispara una respuesta inflamatoria innata no específica liberando factores pro-inflamatorios como el TNFα, IL1, CCL2, CCL20 e ICAM1 [63]. Estos factores contribuyen al reclutamiento de neutrófilos y monocitos que a su vez liberan VEGF-C y VEGF-D [64]. El virus del herpes (HSV), causante de la queratitis herpética, causa infiltración de linfocitos T CD8 que a su vez estimulan el proceso de linfangiogénesis [65].

En patologías específicas, como el rechazo al trasplante de córnea o el síndrome ojo seco, el privilegio inmune se pierde debido a la proliferación de vasos linfáticos. Las células presentadoras de antígeno residentes en la córnea presnetan a los linfocitos T en nódulos linfáticos generando una respuesta efectora en la córnea que contribuye al rechazo o a mantener la inflamación crónica [34, 39]. Estos son dos ejmplos de pérdida del

privilegio inmune por una repuesta inmunitaria adaptativa que conlleva a una enfermedad autoinmune en el ojo seco o al rechazo aloreactivo en el trasplante de córnea. En el caso del ojo seco además la continua activación e infiltración de células inmunitarias patológicas, como los linfocitos T17 colabores, mantienen de forma crónica la patología no recuperándose el privilegio inmune. En el ojo seco, la proliferación de vasos linfáticos ocurre sin proliferación de vasos sanguíneos, debido al aumento en VEGF-C, VEGF-D y VEGFR-3 [66] debido a que los linfocitos Th17 liberan IL-17 que induce formación y crecimiento selectivo de vasos linfáticos pero no sanguíneos [67].

En resumen, el privilegio inmune está basado en seis importantes mecanismos los cuales por un lado bloquean la inducción de una respuesta inflamatoria y por otro se desvía la respuesta hacia una vía tolerogénica que ayuda a escapar del ataque inmunitario [68]:

1. Ausencia de vasos linfáticos y vasos sanguíneos y bloqueo de las vías aferente y eferente de la respuesta inflamatoria [69]. Además el humor acuso transporta los antígenos al bazo en lugar de los nódulos linfáticos [70].
2. Activación de linfocitos T reguladores por el alotrasplante, lo cual inhibe la activación y función de los linfocitos T aloinmunoreactivos [71].
3. Protección de la citólisis mediada por el sistema del complemento [72]
4. Inducción de apoptosis de los neutrófilos y linfocitos T en la interfase receptor-donante en el caso del trasplante [73]
5. Disminución de la proliferación de linfocitos T corneales [74]
6. Disminución de la activación de las células "natural killer" [75]

Por tanto, la inmunosupresión no es un proceso pasivo basado sólo en la ausencia de reconocimiento de antígeno, como se pensó originalmente, sino que consiste en un proceso activo de interacciones inmunológicas con múltiples posibilidades. El efecto combinado de estos mecanismos activos que inhiben la respuesta inmunológica después de introducir un antígeno en la cámara anterior, se conoce como desviación inmunológica asociada a la cámara anterior (ACAID) [76, 77].

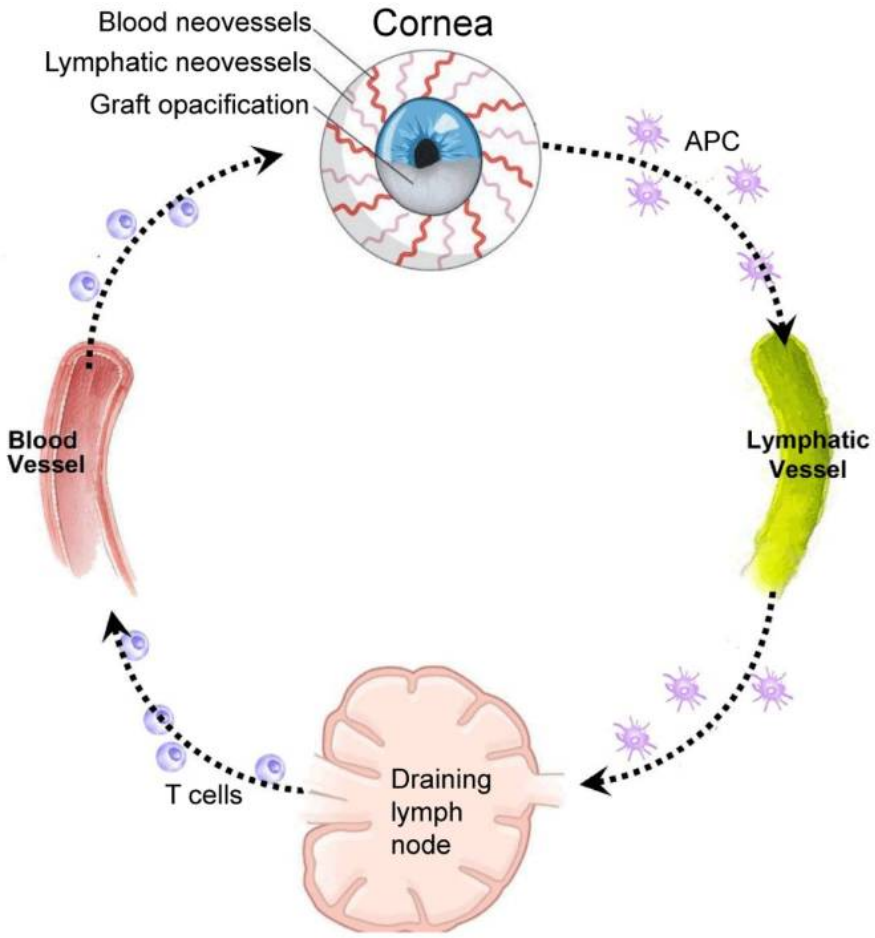

Figura 4: Función de los vasos linfáticos y sanguíneos en la aloinmunidad de la córnea. La rama aferente transporta antígenos y células presentadoras de antígeno desde el injerto hasta los nódulos linfáticos, donde los linfocitos T son cebados y proliferan. Los linfocitos T aloreactivos invaden la córnea a través de los vasos sanguíneos (vía eferente) y median el rechazo del trasplante.
Adaptada de "*Corneal Lymphatics: Role in Ocular Inflammation as Inducer and Responder of Adaptive Immunity*", Chauhan et al. [39]

Sistema inmunitario de la córnea

Al ser la córnea el único sitio con privilegio inmune en contacto con el medio externo, el estudio de su población residente de células inmunitarias es fundamental para entender su particular respuesta inflamatoria [37, 78]. Recientemente se ha puesto fin al dogma de que la transparencia de la córnea se debía, en parte, a la ausencia de células presentadoras de antígeno capaces de iniciar una respuesta inflamatoria [37]. Durante los últimos años, se ha ido confirmando la presencia de una población de células inmunitarias en la córnea sana, que si bien no está claro su origen ontogenético, se cree que pudieran tener origen en la médula ósea [45, 47]. De esta menera, el dogma establecio, se ha sido sustituido por un modelo nuevo en el cual se describe una población inmunitaria de células presentadoras de antígeno, perfectamente organizada y estratificada, en los diferentes compartimentos corneales [14]. La función de las células presentadoras de antígeno corneales no se conoce en detalle, pero cada vez hay más trabajos que ponen de relevancia su estudio para comprender su contribución a la homeostasis corneal, su respuesta inmunitaria y su función en las diferentes patologías [18, 79-81].

En la córnea del ratón se han descrito dos subpoblaciones fenotípicas diferentes de células presentadoras de antígeno: células dendríticas y macrófagos [47]. La mayoría de las células dendríticas residen en la membrana basal del epitelio. Las células dendríticas proyectan dendritas a través de las interdigitaciones del epitelio, desde el estrato basal hasta la superficie. La densidad de la distribución de las células dendríticas es mayor en la periferia disminuyendo hacia el centro. Éstas son células dendríticas clásicas que expresan CD11c, de las cuales la mayoría coexpresan MHC ("major histocompatibility complex") clase II con la misma frecuencia y distribución topográfica [82]. Además en el epitelio corneal se encuentra otro subtipo de células dendríticas CD11c o células de Langerhans que expresan languerina o CD207 [80]. La principal función de las células dendríticas de la córnea es iniciar la respuesta inmunitaria adaptativa pero no se conoce

bien el mecanismo [39, 79, 80, 83]. En el epitelio se ha observado además la presencia de linfocitos T γδ que confieren tolerancia inmunitaria a la córnea [84]

Los macrófagos residen en el estroma corneal divididos en dos subtipos diferentes. En el estroma anterior se encuentra un población de macrófagos $CD11b^+$ $CD11c^-$ MHC clase II^+ distribuidos de forma uniforme desde la periferia hasta el centro. Estos son considerados macrófagos putativos que pueden actuar como células presentadoras de antígeno de apoyo a las células dendríticas del epitelio [47]. En el estroma posterior reside otro subtipo de macrófagos $CD11b^+$ $CD11c^-$ MHC clase II^- distribuidos de forma homogénea desde el centro hasta la periferia. Estos macrófagos disparan la respuesta inmunitaria innata corneal [47]. Además se ha observado presencia de células dendríticas $CD11c^+$ y monocitos en el estroma.

Recientemente se ha descrito un patrón de estratificación similar en la córnea humana (**figura 5**) [14]. La zona basal del epitelio se encuentra poblada por células dendríticas $CD45^+$ $CD11c^+$ de las cuales la mayoría expresan HLA-DR ("human leukocyte antigen"). Al igual que en el ratón, estas células dendríticas extienden sus procesos dendríticos desde la zona basal del epitelio hasta la superficie. La mayoría de estas células se encuentra en la periferia con número decreciente hacia el centro de la córnea donde no se observan. Las células de Langerhans ($CD207^+$) se localizan también mayoritariamente en la periferia de la córnea [14]. En la parte anterior del estroma se encuentran los macrófagos $CD45^+$ $CD68^+$ de forma uniforme desde la periferia hasta el centro. La población mayoritaria en el centro es $CD45^+$ $HLA\text{-}DR^+$. No se ha observado presencia de células de Langerhans ($CD207^+$) en el centro del estroma corneal aunque se encuentran en pequeño número en la periferia [14]. Este patrón de estratificación es similar al mostrado anteriormente en el ratón, lo cual valida la córnea del ratón como un buen modelo para el estudio de la población inmunitaria de la córnea humana (**Figura 5**) [47].

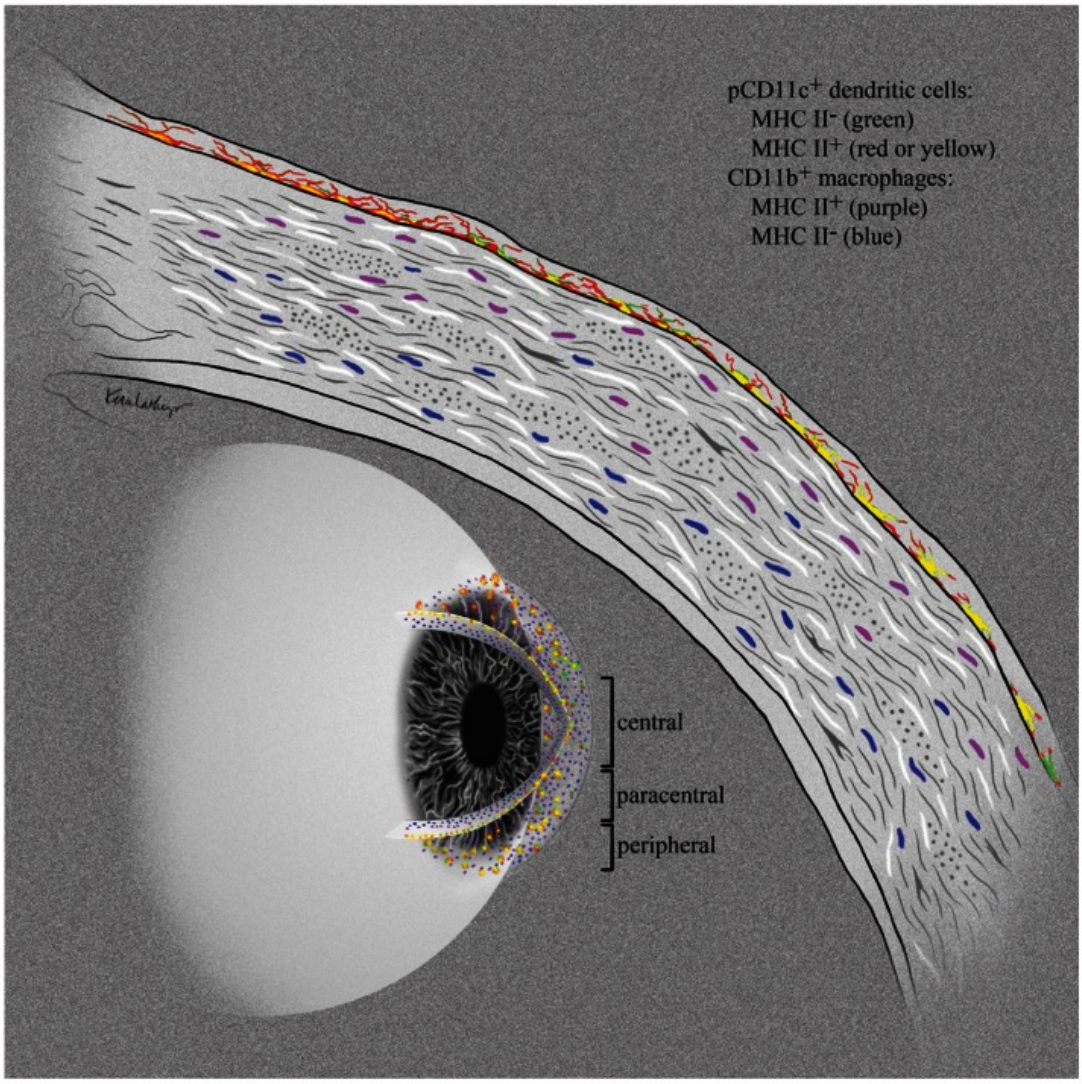

Figura 5: Estratificación de las células presentadoras de antígeno en la córnea sana. "*Stratification of Antigen-presenting Cells within the Normal Córnea*", Knickelbein et al. [47]

Actualización en inervación corneal

La córnea es uno de los órganos más inervados y por tanto sensoriales del cuerpo con inervación sensitiva con origen en la rama oftálmica del nervio trigémino y con alta densidad en el epitelio corneal [8, 9]; y autónoma tanto simpática, con origen en el ganglio cervical superior [10], como parasimpática con origen en el ganglio ciliar [11-13]. Las fibras nerviosas penetran en el tercio anterior del estroma por la periferia en una distribución radial paralela a la superficie del epitelio. Una vez en el estroma, pierden el perineuro y la envoltura de mielina de las células de Schwann para preservar la transparencia [85, 86]. En el estroma se subdividen en numerosas ramificaciones laterales que giran 90º desplazándose anteriormente hacia la membrana basal del epitelio a través de la capa de Bowman donde giran de nuevo 90º dirigiéndose radialmente hacia el centro de la córnea y en posición paralela a la superficie del epitelio formando una estructura denominada plexo basal subepitelial [7, 87]. De nuevo se subdividen en terminaciones más simples que giran perpendicularmente 90º hacia la superficie del epitelio donde ejercen sus funciones neurotróficas o sensoriales [88-90].

El correcto mantenimiento y función de estas terminaciones nerviosas es vital ya que el mal funcionamiento de las terminaciones sensoriales es, junto con otro tipo de etiologías, causante del síndrome de ojo seco [87]. Las úlceras neurotróficas, que cursan con queratitis severas, tienen también un origen en el mal funcionamiento de las terminaciones nerviosas causadas por neurismas o traumas [91-93]. Las queratitis infecciosas, como la queratitis herpética, causan destrucción y mal funcionamiento de las terminaciones nerviosas [25, 93, 94]. El queratocono [95], caracterizado por una disminución del grosor en el centro de la córnea, se cree asociado con problemas neurotróficos ya que se observa una disfunción en el intercambio de señales entre los nervios y las células epiteliales y/o estromales [95-98].

Los mecanismos, por los cuales las fibras nerviosas corneales mantienen la córnea saludable e inducen cicatrización en respuesta a una lesión, se encuentran en la actualidad

bajo creciente investigación. Las neuronas aportan soporte trófico a las células epiteliales mediante la liberación de sustancias solubles. Las neuronas del ganglio trigémino liberan neurotransmisores y neuropéptidos que dan soporte trófico en el epitelio. Este tipo de moléculas activas estimulan a las células epiteliales como parte del proceso normal de mantenimiento y renovado fisiológico para mantener la homeostasis y promover la cicatrización [92, 99]

Diferentes factores como el parpadeo, la desecación de la superficie ocular, el frío o las corrientes de aire, estimulan la liberación de substancias neuroquímicas por parte de los nervios corneales. De esta manera, pequeños cambios en la superficie ocular son rápidamente subsanados con un continuo aporte trófico [33, 100]. Sin embargo, el proceso de cicatrización corneal se muestra alterado en pacientes con ojo seco, diabetes, queratitis herpética, uso continuado de lentes de contacto, o después de un proceso de cirugía refractiva [32, 101, 102]. Estos pacientes sufren anomalías en la inervación corneal que alteran el proceso de cicatrización [103]. Las queratitis neurotróficas a su vez son causadas por daños en ganglio trigémino, traumas craneales, aneurismas o patologías neurológicas intracraneales [104, 105]. Además en las cirugías de catarata y retina, se produce también daño en los nervios corneales [106, 107]. La cirugía refractiva produce un daño masivo en los nervios estromales, en el plexo sub-basal añadiendo por tanto alteraciones epiteliales severas [35, 108].

Durante los últimos años, se ha incrementado notablemente la investigación en la inervación corneal (homeostasis y patología), sin embargo muchos aspectos relacionados con los nervios, especialmente los relacionados con las patologías como el ojo seco, las distrofias de la membrana basal, el queratocono o el rechazo al trasplante de córnea no se conocen bien.

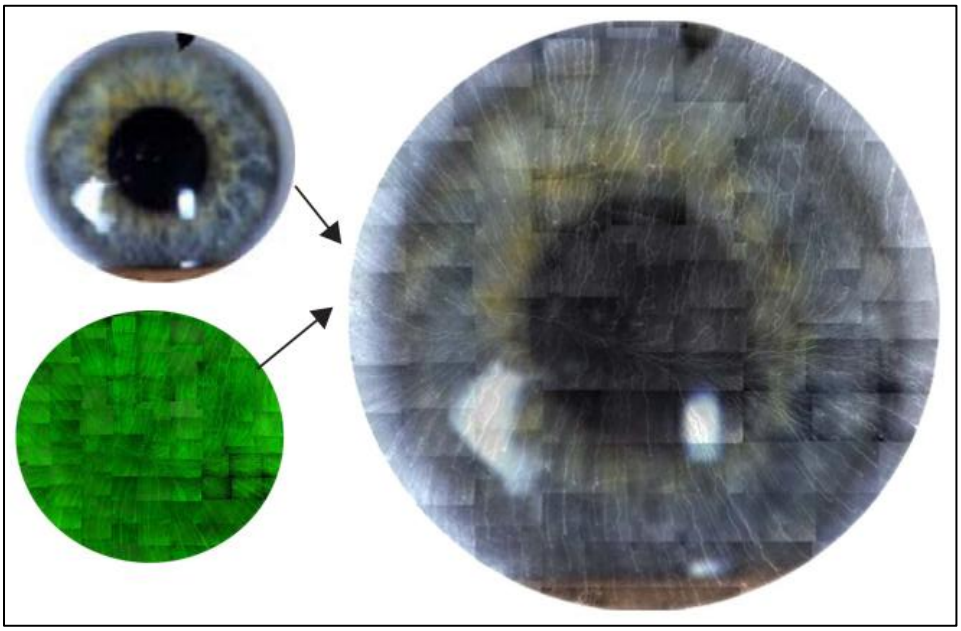

Figura 6. Distribución radial de los nervios corneales. Modificada de Kenchegowda et al. [109]

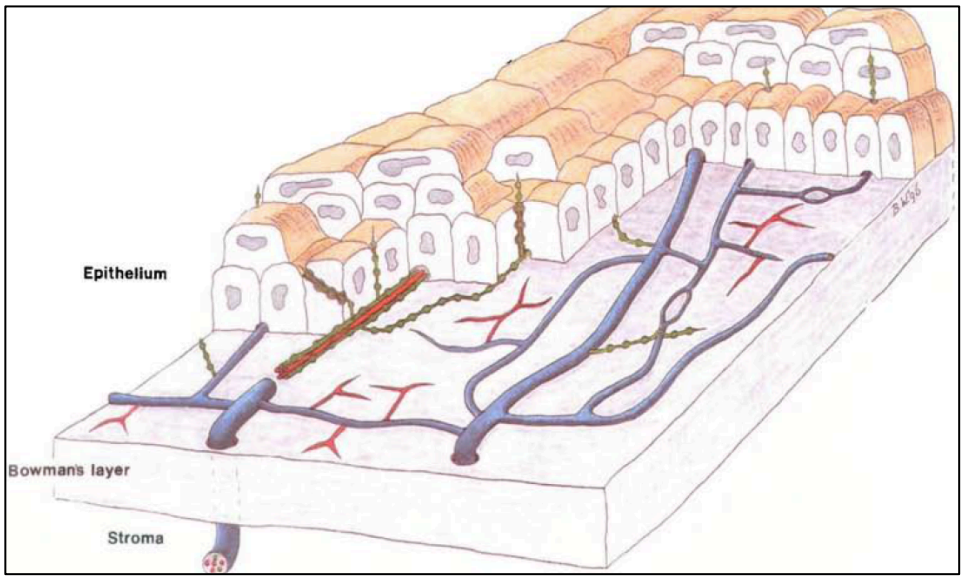

Figura 7. Anatomía de los nervios corneales. Figura modificada de Müller et al. [7]

Conceptos básicos de la inflamación corneal

Como órgano avascular con privilegio inmune, la córnea tolera la introducción de antígenos sin provocar una respuesta inflamatoria [37]. Los injertos de tejido así como los alérgenos son reconocidos como antígenos extraños y rechazados. El privilegio inmune, en si, es una adaptación para proteger las estructuras vitales del cuerpo evitando así los efectos letales de una respuesta inflamatoria [41, 42] y por esta razón, los antígenos son tolerados o los injertos sobreviven sin rechazo [40]. La córnea es por tanto un sitio único que al no tener vasos sanguíneos ni linfáticos limita la presentación de antígeno y mantiene su privilegio inmune [39]. Sin embargo éste puede perderse, por diferentes causas como la rotura de la barrería epitelial, la penetración de vasos sanguíneos y linfáticos o respuestas autoinmunes que provocan un proceso inflamatorio.

La inflamación es un proceso fundamental para la protección de los tejidos y la erradicación de infección, sin embargo es antagonista para la córnea donde mantener la trasparencia es esencial para una correcta visión y para la propia supervivencia [21, 110-112]. Durante el proceso evolutivo, la córnea ha desarrollado un complejo mecanismo fisiológico destinado a mantener su transparencia. La córnea tiene la capacidad de repararse a si misma después de una herida sin provocar cambios en su claridad, en la biomecánica y en la refracción [21, 110-112]. La inflamación de la córnea o queratitis, es causante de diferentes patologías oculares caracterizadas por los síntomas de la inflamación en general: presencia de citoquinas, vasodilatación, edema y eritema [113]. En la córnea además causa dolor, enrojecimiento del polo anterior, lagrimeo y fotofobia. En ocasiones se forman úlceras que pueden llegar a ser graves u ocasionar disminución en la agudeza visual por alteración en la transparencia [114].

Las células epiteliales contribuyen a la defensa formando una barrera a los patógenos o mediadores inflamatorios. Las células epiteliales tanto de la conjuntiva como de la córnea son las encargadas de comenzar el proceso inflamatorio expresando moléculas de adhesión y moléculas coestimuladoras en respuesta a diferentes citoquinas. Además el

epitelio por si mismo contribuye de forma activa a la inflamación mediante la libración de citoquinas como la IL-1 y el TNF-α ("tumor necrosis factor-α") [115]. La rotura de la barrera epitelial produce un aumento en la infiltración de eosinófilos en la conjuntiva estimulado por la exposición de los fibroblastos a las citoquinas de la lágrima [116]. Recientemente se ha descrito que las células epiteliales contribuyen al proceso inflamatorio liberando alarminas después de una lesión [117]. Éstas contribuyen a las respuestas inmunitaria innata y adquirida, aunque se desconoce como interaccionan con las células presentadoras de antígeno corneales [118].

Los fibroblastos son los principales moduladores de la respuesta inmune ya que liberan citoquinas y expresan moléculas de adhesión por ejemplo en los procesos de inflamación alérgica [119, 120]. Los fibroblastos expresan receptores para la IL-4 y la IL-13, VCAM-1 y liberan CCL11 en respuesta a una estimulación tipo Th2 (IL-1, IL-4 y IL-13 y otras citoquinas pro-inflamatorias como el TNF-α) [119-121]

Los componentes de la inflamación ocular varían según el tipo de agente causante. El queratocono, las distrofias de la membrana basal, las úlceras neurotróficas, la cicatrización después de cirugía refractiva o de cataratas, el trasplante de córnea son algunas de las patologías que cursan con inflamación de la córnea. Sin embargo el tipo de inflamaciones más frecuentes son las infecciónes bacterianas o víricas así como las alergias. La inflamación puede ser leve, como la conjuntivitis alérgica estacional o la conjuntivitis infecciosa transitoria, o crónica como la queratoconjuntivitis atópica, la queratoconjuntivitis vernal o el síndrome de ojo seco [33, 122, 123] que conllevan daño corneal y pueden ocasionar pérdida de la visión e incluso del órgano. En ambos tipos, se produce un reclutamiento de células inflamatorias, y una síntesis y secreción de citoquinas y otros mediadores inflamatorios como IL-1, IL-6, factor de necrosis tumoral-α (TNF-α) e interferón gamma (IFN-γ) en el epitelio conjuntival y en la película lagrimal [124].

Respuesta inmunitaria

Las células de Langerhans, células dendríticas, macrófagos y monocitos residen en la córnea normal junto a precursores inmaduros de la médula ósea que maduran en respuesta a inflamación [14, 45, 47, 79, 81, 82]. Ante una agresión física que comprometa la integridad corneal, se dispara un mecanismo de respuesta inmunitaria innata y los macrófagos invaden la zona fagocitando los restos celulares y patógenos [47]. Por otro lado las células presentadoras de antígeno como las células dendríticas y los macrófagos pueden disparar un mecanismo de respuesta inmunitaria adquirida [47]. Además durante la inflamación ocular, las células epiteliales y los queratocitos expresan HLA-DR, actuando por tanto, como células presentadoras de antígeno [125, 126]. Durante la respuesta adquirida, las células dendríticas estimulan los linfocitos T. Su capacidad de sensibilizar los linfocitos T se atribuye a la elevada expresión de MHC clase II y de moléculas coestimuladoras como CD80 y CD86 [113, 126, 127]. Las células dendríticas residentes en los tejidos no linfoides como las mucosas, migran a los órganos linfoides donde presentan de forma efectiva los antígenos a los linfocitos T. Si bien éste es un mecanismo bien conocido en la conjuntiva, no está claro como sucede en la córnea [47, 80, 81].

La expresión de varios factores inmunoregulatorios controlan el sistema de comunicación entre las células inmunitarias y las células endoteliales vasculares. El TGF-β2 regula la maduración de las células dendríticas y el ligando de FAS induce apoptosis en células inmunitarias que expresan FAS [56]. El PDL-1 induce apoptosis de los linfocitos T [57]. Otros factores antiinflamatorios como la IL10 y la IL-1Ra previenen el reclutamiento y la proliferación de neutrófilos, macrófagos y células T [58]

Ciertas condiciones patológicas como el trauma, infecciones, el rechazo al trasplante de córnea y el ojo seco hacen que cambie el balance entre los factores antiangiogénicos y proangiogénicos. En respuesta a una herida, la córnea genera una respuesta inflamatoria no específica a través del sistema inmunitario innato [61]. Se liberan factores pro-inflamatorios como el TNFα, IL1, CCL2, CCL20 e ICAM1 [63]. Estos factores contribuyen

al reclutamiento de neutrófilos y macrófagos que a su vez inducen linfangiogénesis a través de VEGF-C y VEGF-D. Otros agentes como el HSV, causante de la queratitis herpética, estimulan el proceso de linfangiogénesis [62] así como los linfocitos T $CD8^+$ generados por la respuesta adaptativa [65]. En el rechazo del trasplante de córnea y en el síndrome de ojo seco la linfangiogénesis permite a las células presentadoras de antígeno alcanzar los nódulos linfáticos cercanos, cebar los linfocitos T y generar una respuesta efectora en la córnea que contribuye al rechazo o a mantener la inflamación crónica de la superficie ocular en el ojo seco [34].

Debido a la inflamación, las células presentadoras de antígeno adquieren un fenotipo maduro que incluye aumento en la expresión de MHC clase II y de las moléculas co-estimulatorias CD80 y CD86. Por otro lado disminuyen la expresión de CCR1, CCR2, CCR5 y CX3CR1 y se aumenta la expresión de CCR7. La proliferación de los vasos linfáticos facilita la entrada de las células presentadoras de antígeno en los vasos linfáticos mediada por la expresión de CCR7 siguiendo un gradiente de CCL21 a través de un proceso mediado por ICAM-1 y VCAM-1 y sus correspondientes ligandos (**Figura 8**) [113].

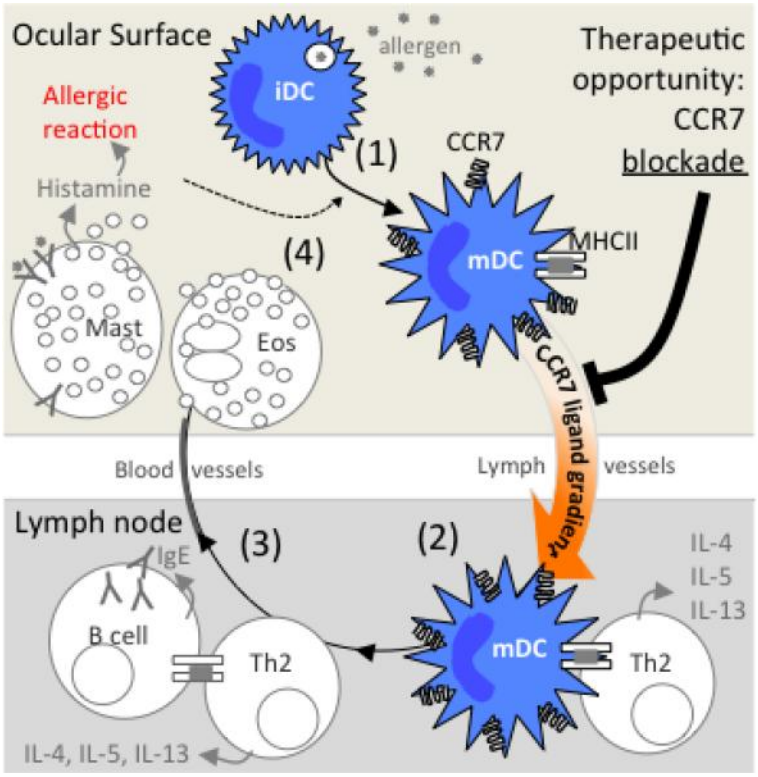

Figura 8. Modelo propuesto simplificado de un mecanismo de general de inflamación ocular y del posible efecto terapéutico mediante el bloqueo de la alergia ocular mediante el uso de anticuerpos anti CCR7. Modificada de: "*New twists to an old story: novel concepts in the pathogenesis of allergic eye disease",* Saban et al. [113]

Los pacientes con vasos linfáticos preexistentes son denominados receptores de alto riesgo para el trasplante de córnea, ya que el tráfico de células presentadoras de antígeno y la alosensibilización, aumentan con respecto a los pacientes de bajo riesgo, indicando la relevancia de la linfangiogénesis en la aloinmunidad [66, 128, 129]. La respuesta inmunitaria innata es, en si, la mayor responsable de la formación *"de novo"* de vasos en la mayor parte de las patologías de la córnea, como el rechazo o la infección, facilitando la migración de las células presentadoras de antígeno a los nódulos linfáticos [63]. Por otro

lado la respuesta adquirida puede generar en si linfangiogénesis como ocurre en los pacientes con ojo seco [61].

Las células presentadoras de antígeno presentan a los linfocitos T que liberan IL-1, IL-6, IL-8 y el TNF-α desencadenando la respuesta inflamatoria. La IL-1 es la principal molécula liberada en las primeras fases del proceso inflamatorio tanto por las células inflamatorias no residentes como por el epitelio [130]. La IL-1 tiene un amplio rango de actividades y media en la repuesta de fase aguda, actuando como molécula quimiotáctica, activando las células inflamatorias y células presentadoras de antígeno, como las células de Langerhans y los macrófagos, y estimulando neovascularización. La IL-6 es también una citoquina multifuncional liberada por macrófagos, y que comparte funciones similares a la IL-1. La IL-8 es una quimiocina liberada por macrófagos y fibroblastos y que actúa como quimioatrayente para macrófagos y polimorfonucleares [131]. El TNF-α es una citoquina proinflamatoria liberada por los macrófagos e interviene tanto en la respuesta inflamatoria, induciendo citotoxicidad, como en el proceso de cicatrización inhibiendo el TGF-beta [130].

Ejemplo de inflamación ocular: el ojo seco

Si bien considerado a veces como un problema menor, la queratoconjuntivitis sicca o el síndrome de ojo seco es un problema de inflamación ocular que afecta entre un 11%-17% de la población en los países desarrollados [132]. El ojo seco se define como "un desorden multifactorial de la lágrima y de la superficie ocular que resulta en síntomas de malestar, perturbación visual e inestabilidad de la película lagrimal que potencialmente daña la superficie ocular la cual está acompañada por un incremento en la osmolaridad de la lágrima e inflamación de la superficie ocular" [133]. En el ojo seco, la proliferación de vasos linfáticos ocurre sin proliferación de vasos sanguíneos, al contrario que en la infección y el rechazo, donde ambos ocurren paralelamente o los vasos sanguíneos preceden a los linfáticos. En el ojo seco la linfangiogénesis es debido al aumento en VEGF-C, VEGF-D y VEGFR-3 [66]. A su vez los linfocitos Th17 liberan IL-17 inducen la formación y crecimiento selectivo de vasos linfáticos [67].

El ojo seco asociado a la inflamación de la superficie ocular esta mediado por una respuesta linfocitaria anormal y crónica en la córnea con activación e infiltración de células inmunitarias patológicas como los linfocitos T17 [134]. La inflamación conjuntival se manifestada por infiltración y aumento en la expresión de CD3, CD4 y CD8 así como activación de los marcadores CD11a y HLA-DR indicando una respuesta inflamatoria autoinmune con presencia de citoquinas pro-inflamatorias y metaloproteinasas. La IL-1 es la interleuquina más abundante en el ojo seco liberada por el epitelio conjuntival [135] así como la IL-6, IL-8 y el TNF-α ("tumor necrosis factor") [136]

La respuesta de las células al estímulo extracelular como los cambios en la composición de la lágrima, la hiperosmolaridad y la radiación ultravioleta, es mediada por enzimas quinasas intracelulares (MAP) [137]. Las MAP quinasas son activadas en respuesta a citoquinas inflamatorias (IL-1 y TNF α), proteínas de choque térmico, endotoxinas bacterianas e isquemia. Esta activación media señalización necesaria para la regulación de eventos de trascripción que determinan el resultado funcional y la respuesta

al estrés causado. La activación de estas vías resulta en la expresión de MMP-9 [138] y citoquinas pro-inflamatorias (IL-1, TNF-α,) que causan daño de la superficie ocular [139]

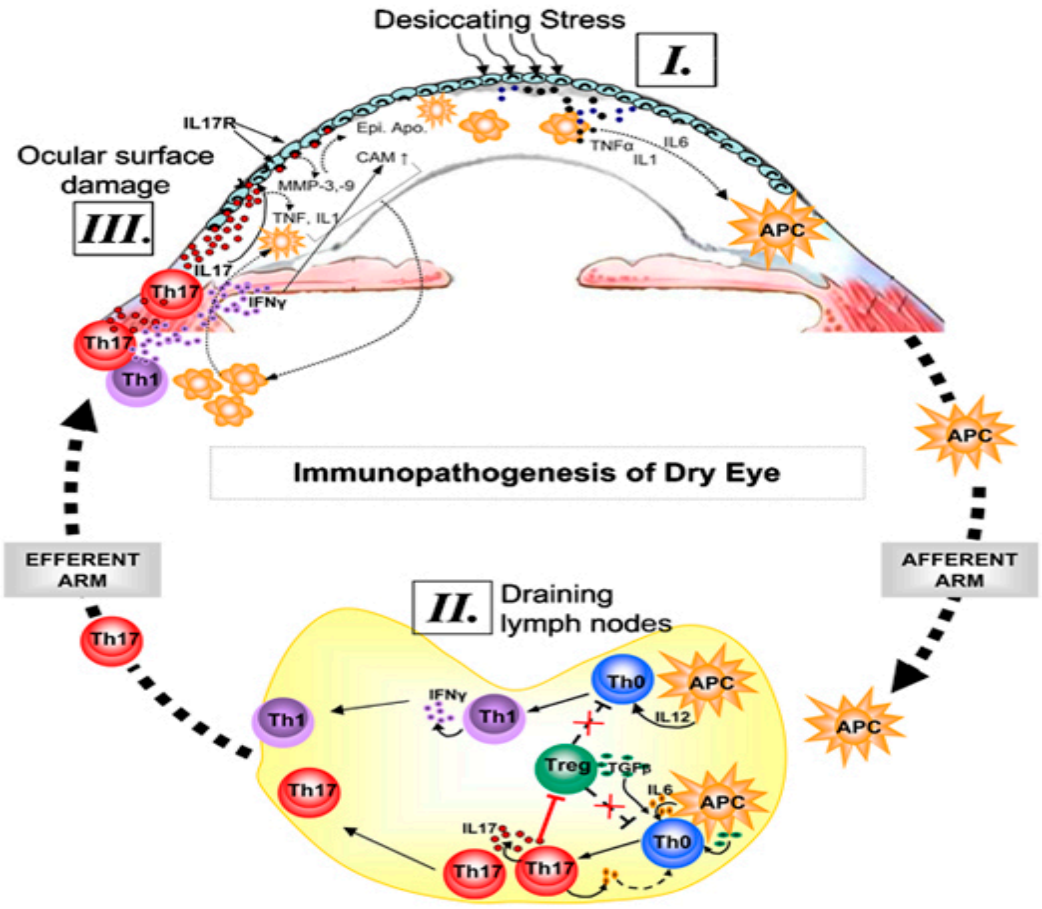

Figura 9. Diagrama de la patología del ojo seco. (**I**) La desecación de la película lacrimal induce liberación de citoquinas pro-inflamatorias por el epitelio facilitando la activación y migración de las células presentadoras de antígeno residentes hacia los nódulos linfáticos (**II**) donde generan una respuesta Th17 hacia la córnea (**III**) produciendo daño epitelial por la liberación de MMPs y citoquinas inflamatorias.

Relación entre la inflamación y la inervación corneal

La inflamación de la córnea además tiene efectos negativos en el sistema nervioso periférico que la inerva [141]. El sistema nervioso y el inmunitario están interconectados bioquímicamente. Las neuronas expresan receptores para las citoquinas a la vez que las células inmunitarias reconocen y son moduladas por neuropéptidos [142]. Por ejemplo SP y VIP confieren resistencia a la infección ya que actúan como potentes agentes pro-infamatorios y por otro lado la liberación de GCRP se cree asociada a la inmunosupresión y el mantenimiento del estado basal de la córnea [143].

Respecto a la regeneración nerviosa, la inflamación tiene un papel ambivalente [141]. Los linfocitos γδ T estimulan el proceso de regeneración nerviosa en un proceso que engloba a la IL-17, neutrófilos, plaquetas y VEGF-A [144]. Por otro lado, en los procesos infecciosos se observa una disminución de los nervios sub-basales con un aumento de células dendríticas en el centro de la córnea [145] e incluso la pérdida del plexo sub-basal durante otro tipo de inflamaciones no infecciosas [146, 147]. Esto indica que un grado moderado de inflamación facilita el crecimiento de los nervios en la córnea y por el contrario un exceso conlleva a la pérdida de los nervios en el plexo sub-basal y por tanto a neuropatías. Se ha descrito la molécula Sema7A como con link común entre la regeneración nerviosa y el proceso inflamatorio de la córnea [148]. Esta molécula promueve crecimiento axonal en el sistema nervioso periférico y a su vez es expresada en linfocitos T y juega un papel en la inflamación mediada por los linfocitos T. En la córnea Sema7A se expresa de forma constitutiva en el epitelio y en el estroma. Durante el proceso de cicatrización posterior a una herida, Sema7A estimula la regeneración nerviosa asociada con la llegada de células infamatorias. Esto ha sugerido evitar tratamientos inmunomoduladores o antiinflamatorios prolongados como estrategia para mejorar el proceso de reinervación en la córnea [148].

Además cuando se produce un daño significativo en los nervios, la córnea pierde el privilegio inmune lo cual induce un aumento en rechazo al trasplante de córnea [17]. Si bien

no se conoce el mecanismo de acción, se ha propuesto que en la interacción de los nervios con las células inmunitarias de la córnea podría estar la respuesta [149]

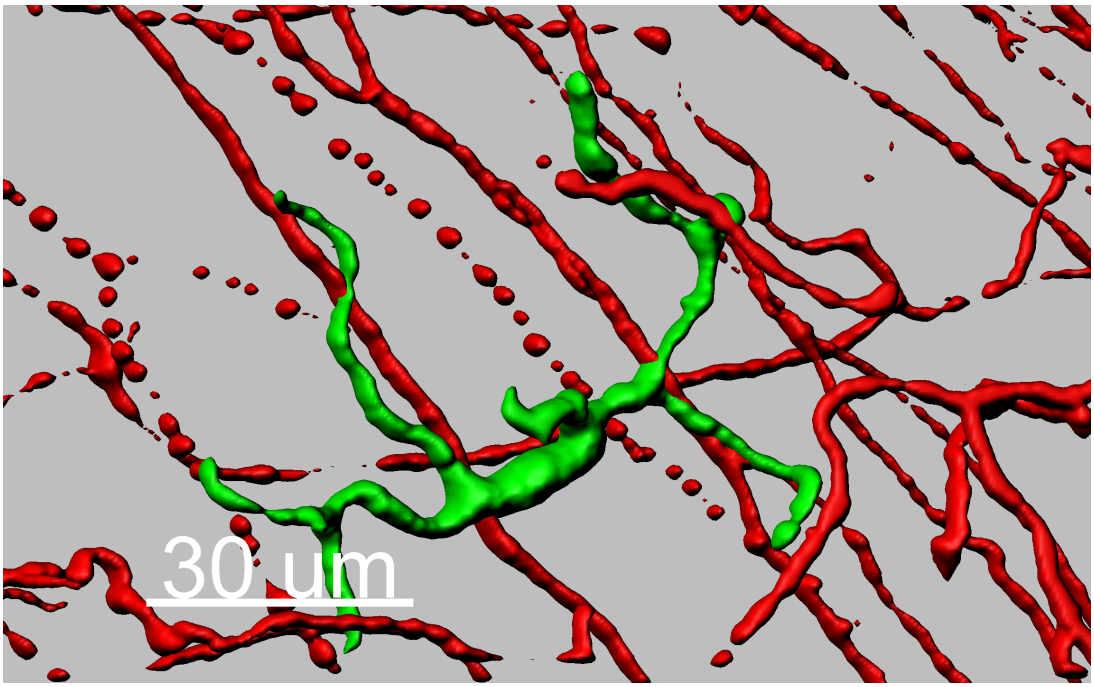

Figure 10. Célula dendrítica en contacto con los nervios del plexo sub-basal. Adaptada: "*The Cornea Has "the Nerve" to Encourage Immune Rejection*", Blanco et al. [149]

Respuesta de la córnea a la lesión y modelos animales utilizados

La cicatrización es el proceso biológico por el cual un tejido dañado o destruido se sustituye por tejido nuevo [150]. Esta sustitución del tejido puede ser total o parcial distinguiéndose dos procesos conceptualmente diferentes:

- Regeneración: Se trata de la recuperación "*ad integrum*" (morfológica y funcional) de un tejido u órgano después de que éste haya padecido una agresión o noxa, física, química, mecánica, etc. Este proceso está ligado a los tejidos epiteliales y tejidos jóvenes que aun conservan células mesenquimales.

- Reparación: Consiste en la respuesta que da un órgano o un tejido a una agresión, igual que en la reparación, pero este tejido u órgano no tiene capacidad suficiente para autodevolverse a su estado original, bien porque la lesión ha sido muy intensa o extensa o bien porque no tiene células madre totipotenciales o mesenquimales que le permiten recuperar su morfología y función primitiva. Este proceso está vinculado a tejidos muy bien diferenciados en los cuales desaparecen las células que les pueden dar esa capacidad de recuperarse como el tejido nervioso. Cuando esto ocurre, el tejido conjuntivo en general, o en el sistema nervioso central la glía, sustituyen al tejido original generando una cicatriz.

En general la respuesta de la cicatrización se divide en tres fases fundamentales [150]:

Fase inflamatoria y/o exudativa. Se inicia en el momento mismo de la herida y consiste en la hemostasis, limpieza de la zona dañada y liberación de los mediadores bioquímicos para la siguiente fase.

Fase de proliferación. Se caracteriza por la reepitelización o revestimiento de la superficie de la herida. Migración o proliferación de células del epitelio circundante y por la aparición de tejido conjuntivo.

Fase de diferenciación. Se produce proliferación, migración y diferenciación de las células del tejido conjuntivo, la maduración de las fibras de colágeno y la contracción de la herida.

El proceso de cicatrización toma matices especiales en un órgano avascular y transparente como la córnea. Este proceso consiste en una secuencia de eventos celulares (apoptosis, proliferación, migración y diferenciación) que contribuyen al cierre de la herida y al restablecimiento de las funciones [22, 98, 151, 152]. Tras la lesión, el estado basal se ve alterado desencadenándose una rápida respuesta modulada por citoquinas, factores de crecimiento, proteasas y neurotransmisores. Las interacciones entre epitelio, estroma, terminaciones nerviosas, células inflamatorias, glándula lacrimal y lágrima están interconectadas y acopladas en la respuesta final de la córnea [22, 28].

Ante una agresión, la córnea responde reparando y/o regenerado el tejido eliminado. Las variaciones tanto en eventos celulares como en la intensidad de la respuesta son tan diferentes como tipos y variantes sean las agresiones. Es por esto que no es posible describir un mecanismo común de cicatrización. Sin embargo, en general, la córnea de forma evolutiva está programada para desencadenar una serie de acontecimientos celulares que en diferente medida tienen como resultado final la regeneración del tejido dañado [22, 151, 152].

Durante los últimos años se han utilizado diferentes modelos animales para el estudio de la cicatrización corneal como conejos [22, 153], ratas [154], gallinas [155-157], primates [158] o perros [159, 160]. Sin embargo el uso de ratones se está asentando como modelo más usado en el estudio de la cicatrización corneal [161, 162]. La introducción de diferentes cepas de ratones transgénicos ha supuesto un gran avance en el conocimiento de las patologías corneales. El uso de ratones knock-out ha permitido estudiar las patologías del epitelio, del estroma y del endotelio [163-165].

Integrinas y Cicatrización Corneal

La relevancia de las integrinas de membrana, en el proceso de cicatrización, se ha puesto de manifiesto recientemente [166, 167]. Las integrinas son una familia de receptores que median las adhesiones entre células y entre células y matriz [168-170] además contribuyen a respuestas como supervivencia, proliferación y diferenciación [168]. La integrina αVβ6 se expresa a un nivel basal muy bajo en el epitelio de mamíferos adultos, pero su expresión aumenta significativamente en respuesta a un herida o inflamación [171, 172]. La ausencia de la integrina αVβ6 está vinculada a la progresión de enfermedades periodontales [173], inflamación en el pulmón y la piel [174], retraso en la cicatrización de la piel [175] y supresión de la fibrosis pulmonar [176]. En la córnea su expresión se limita al epitelio corneal, sin embargo en la queratopatía bullosa [177] y durante la cicatrización [178, 179] aumenta la expresión de la integrina αVβ6. Esta integrina es un receptor para muchos componentes de la membrana basal como la fibronectina, la vitronectina, la tenascina y las E-Cadherinas [167, 180]. Además esta integrina sirve de receptor para la secuencia Arg-Gly-Asp (RGD) del "latency-associated peptide" (LAP)-TGF-β1 y del LAP-TGF-β3 [176, 181, 182]. La asociación de αVβ6 con LAP está implicada en la activación de TGF-β [183-186], de hecho los ratones carentes de esta integrina muestran un fenotipo similar a los ratones carentes de TGF-β1 [187]. Por ello, en este trabajo, se planteó la hipótesis de que la αVβ6 juega un papel fundamental en la reparación de la córnea cuando la membrana basal del epitelio rompe como consecuencia de una lesión. Para ello se utilizaron ratones deficientes en la subunidad β6 (β6-/-) y se comparó el proceso de cicatrización con la correspondiente estirpe de ratón normal (**figura 11**) [188].

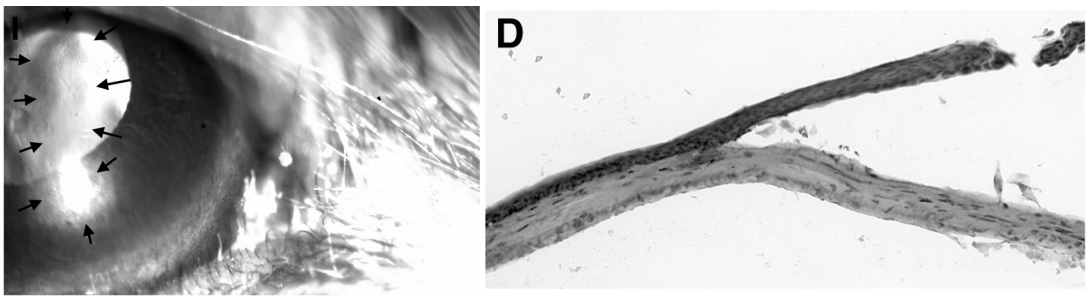

Figura 11 . Ampolla sub-epitelial en la córnea causada por la falta de la integrina αVβ6. Modificada de: "*AlphaVbeta6 integrin promotes corneal wound healing*" Blanco-Mezquita et al. [188]

Trombospondina-1 y cicatrización corneal

Recientemente se ha visto la relevancia de la trombospondina-1 (THBS1; también denominada como TSP-1) en el proceso de cicatrización corneal. La THBS1 es una glicoproteína trimérica [189, 190] de localización extracelular liberada por las plaquetas, las células epiteliales y las células mesenquimales en respuesta a una variedad de procesos fisiológicos incluyendo el desarrollo, la cicatrización, la angiogénesis, la migración tumoral, la agregación plaquetaria y la adhesión celular [191-196]. La THBS1 juega un papel poco relevante en la homeostasis, sin embargo está presente durante el desarrollo embrionario de muchos tejidos y su expresión se incrementa significativamente durante los procesos de cicatrización [197-200]. La THBS1 induce inflamación crónica, retraso en la cicatrización y pérdida de la pústula [201, 202]. En la córnea sana, la THBS1 está localizada en la zona de la membrana basal, en la membrana de Descemet y en el endotelio, pero no se encuentra en el estroma [203, 204]. La THBS1 se expresa en el limbo y en el epitelio corneal [205] y su expresión aumenta en respuesta a la cicatrización posterior a una herida [204, 206-208] sin embargo los mecanismos de acción no se conocen bien. Se ha sugerido que los defectos epiteliales en la córnea estimulan la expresión de THBS1 en el área de la

herida resultando en una aceleración del cierre del epitelio y que la falta de vitamina A reduce la expresión de la THBS1 y por tanto de la reepitelización [208, 209]. También se ha visto que la THBS1 interviene en el proceso de diferenciación de los queratocitos a miofibroblastos durante el proceso de cicatrización en un modelo de ratas [204]. Además la falta de THBS1 en ratones Thbs1$^{-/-}$ limita la migración y adhesión del endotelio [210]. Todo ello indica que la THBS1 tiene una gran relevancia en el proceso de cicatrización de la córnea [211].

La THBS1 es uno de los activadores más potentes del TGF-β1 [194, 212, 213] que induce proliferación de los queratocitos, diferenciación de los miofibroblastos y síntesis de matriz extracelular [214-216]. El TGF-β1 se libera a la matriz extracelular donde permanece anclado de forma latente y donde es activado en respuesta a una herida [217].

En el presente trabajo se propuso la hipótesis de que la THBS1 tiene un papel fundamental en el proceso de cicatrización corneal cuando la integridad total de la córnea se ve comprometida. Para demostrar esta hipótesis se realizó un corte penetrante en el centro de la córnea de ratones adultos carentes de THBS1 (Thbs1$^{-/-}$) y se comparó el proceso de cicatrización con ratones normales (**Figuras 12 y 13**) [218].

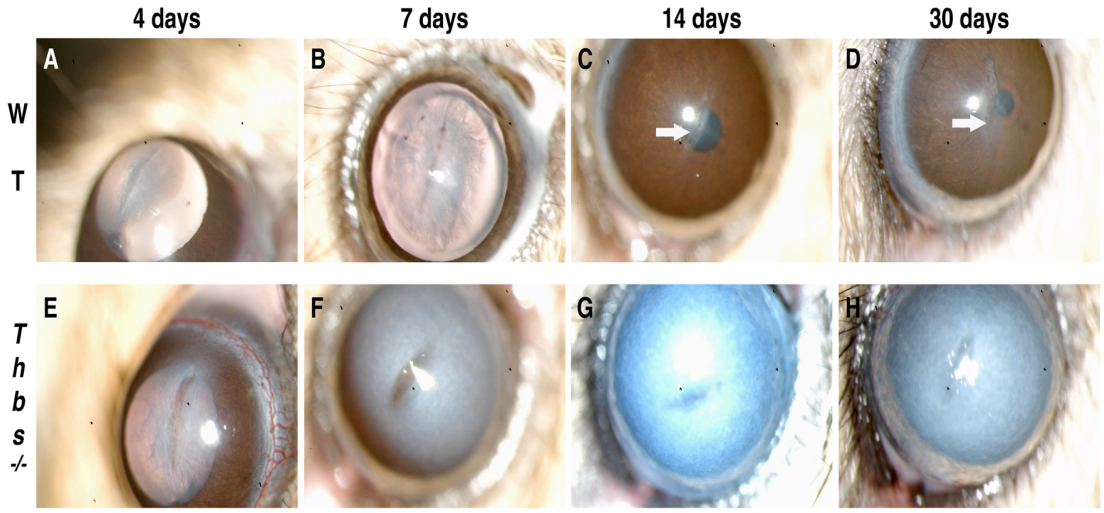

Figura 12: Comparación de la cicatrización corneal en ratones carentes de THBS-1 y ratones normales. Modificado de Blanco-Mezquita et al. [218]

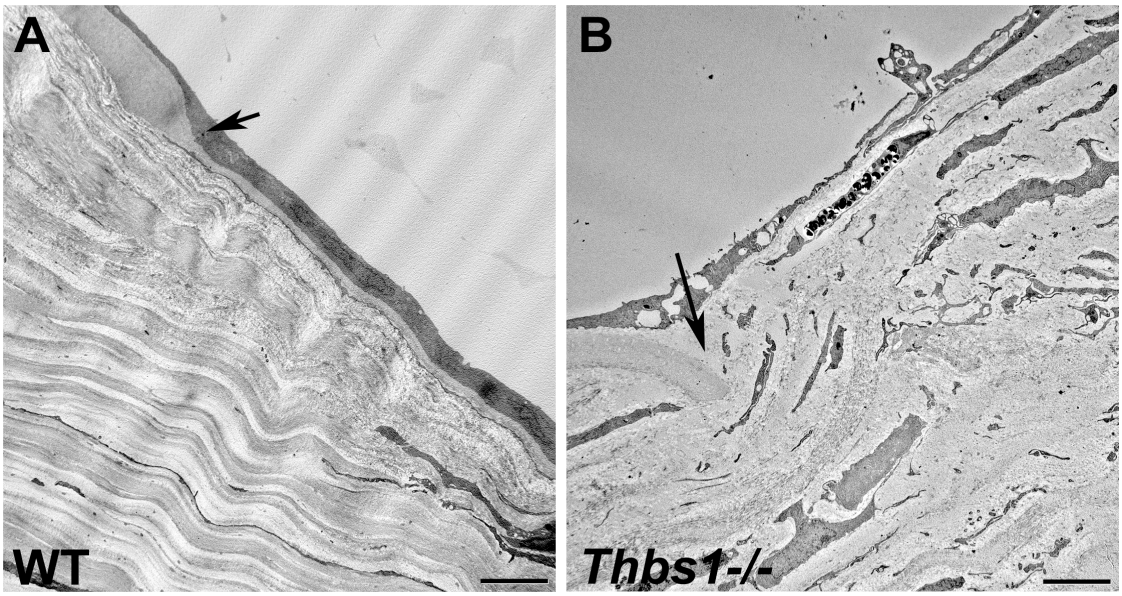

Figura 13: Comparación de la cicatrización endotelial en ratones carentes de THBS-1 y ratones normales. Modificado de Blanco-Mezquita et al. [218]

Uso de ratones y microscopía *"intravital"* para el estudio de la córnea

Los sistemas de imagen "*intravital*" están tomando gran relevancia en la investigación. De la misma manera el uso creciente de ratones que expresan fluorescencia ante la expresión de una secuencia determinada (promotor, locus, etc.), permite conocer "*in situ"* y de forma inmediata la implicación de ese gen en una patología. Los sistemas de imagen "*in vivo*" facilitan la observación del comportamiento de las células y de los tejidos así como sus mecanismos moleculares básicos. Las cepas de ratones genéticamente modificados que expresan proteínas fluorescentes se han convertido en parte esencial en la investigación actual. Esas cepas modificadas pueden ser diseñadas introduciendo en secuencias en "cis" para expresar fluorescencia en el gen de interés. Si estas secuencias introducidas en "cis" son localizadas en el sentido de lectura del gen ("downstream"), expresan la proteína fluorescente que podrá ser detectada informando del estado de la célula o población celular (**Figura 14**) [219]. El uso de los ratones con marcadores fluorescentes está muy extendido para el estudio "*ex vivo*" (microscopía confocal o citometría de flujo), extracción de células para su uso "*in vitro*" o trasplante en otros animales. Sin embargo, el análisis "*intravital*", si bien en auge no es una técnica todavía desarrollada. En el estudio de la córnea, se ha usado diferentes modelos de ratones transgénicos para determinar el origen de las células inflamatorias o la presentación de antígeno en los nódulos linfáticos [80]. Se han utilizado ratones Cx3cr1-GFP para confirmar el origen mieloide de la población inmunitaria residente en la córnea. También se ha demostrado que la expresión de Cx3cr1 juega un papel fundamental en el reclutamiento de las células dendríticas y de los macrófagos en el epitelio y estroma en córneas normales [44]. De la misma manera se han usado diferentes marcadores fluorescentes endógenos para el estudio "*ex vivo*" de los nervios corneales [221]. Este tipo de metodología está siendo de enorme relevancia en el estudio del sistema nervioso y el sistema inmunitario. En diferentes modelos se ha mostrado "*in vivo*" la captura de

antígeno por la células dendríticas intestinales y su presentación "*in situ*" a los linfocitos [222].

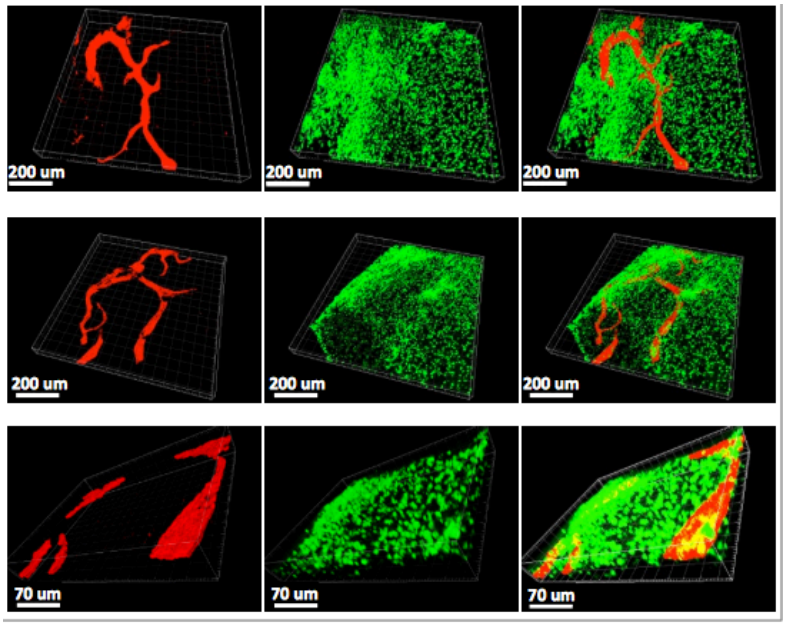

Figura 14. Células derivadas de la médula ósea de ratones CD45.1 inyectadas en el estroma córneas de ratones CD45.2 interaccionan con los vasos linfáticos. Modificada de "*Involvement of corneal lymphangiogenesis in a mouse model of allergic eye disease*" by Hyun-Soo Lee; Deniz Hos; Tomas Blanco et al. [220]

La microscopía "*intravital*" es relativamente fácil de llevar a cabo en embriones, pero presenta varios inconvenientes en los ratones adultos. Los órganos internos deden ser quirúrgicamente expuestos, la presencia de sangre, grasa y células pigmentadas causa fenómenos de autofluorescencia, reflexión y absorción de la luz y además en la mayoría de los casos los animales tienen que ser sacrificados después del procedimiento. Al ser la córnea un órgano externo, transparente, sin vasos ni células pigmentadas, se convierte en un órgano ideal para el estudio con microscopía "*intravital*". La córnea se puede explorar de forma no invasiva y sin necesidad de sacrificar al animal.

El uso de cepas de ratones que expresan GFP "green fluorescence protein" bajo el control del promotor del gen Cx3cr1 ha facilitado enormemente el estudio de la población inmunitaria de la córnea. CX3CR1 o receptor de la quimioquina-1, también denominado receptor de la fractalquina o neurotactina (CX3CL1), es una proteína expresada bajo el control del promotor del gen Cx3cr1 ("myeloid progenitor derived marker"). Insertando de forma homocigótica o heterocigótica la secuencia de la GFP, ésta puede ser observada en monocitos, células dendríticas, "natural killers", macrófagos y microglía. De esta manera se han podido realizar estudios de la función de los leucocitos en la migración, tráfico de señales, origen ontogénetico y estudios en trasplantes [223]. La interacción de CX3CR1-fractalquina, media la adhesión celular y la migración de las células que expresan dicho receptor [44, 224, 225]. El desarrollo de ratones en los cuales se ha insertado el gen de la EGFP ("enhanced" GFP) en una o en las dos copias del locus del Cx3cr1, ha permitido investigar "*in vivo*" el origen de las células mieloides en los diferentes tejidos [48, 226]. La transferencia adoptiva de monocitos marcados de ratones Cx3cr1-GFP en ratones receptores normales, ha abierto una nueva línea de investigación para estudiar la heterogeneidad de los monocitos y de los factores que regulan su diferenciación en los diferentes tejidos. De la misma manera se puede investigar la acumulación de células dendríticas y macrófagos residentes derivados de los monocitos en una gran cantidad de tejidos [48, 226].

En la superficie ocular, se ha podido evaluar el origen mieloide de la población inmunitaria residente en la córnea en ratones Cx3cr1-GFP mediante el uso de video-microscopía "*intravital*" de epifluorescencia de campo amplio. También se ha demostrado que la expresión de Cx3cr1 juega un papel fundamental en el reclutamiento de las células dendríticas y de los macrófagos en el epitelio y estroma en córneas normales [227]. Con esta misma técnica se ha observado que las células de Langerhans de la córnea se comportan de forma similar a las de la piel y ante un estímulo o irritación éstas migran desde la periferia hasta el centro [228]. Además existen otras dos técnicas de microscopía "*intravital*" que se han utilizado para estratificar las células presentadoras de

antígeno corneales. Por un lado el microscopio de fluorescencia de mano "Optiscan FIVE-1" y por otro un sistema mi microscopía multifotónica de amplio espectro (construido manualmente). Con esos dos sistemas se ha fotografiado las células dendríticas que expresan EGFP bajo el promotor de CD11c. Sin embargo los autores autocriticaron estas técnicas ya que no ofrecen un posicionamiento seguro del objetivo en el ojo del ratón [47]. Recientemente, se ha utilizado el microscopio multifotónico para el estudio "*in vivo*" de la dinámica de las células inmunitarias en contacto con los vasos linfáticos (**figura 15**) [229].

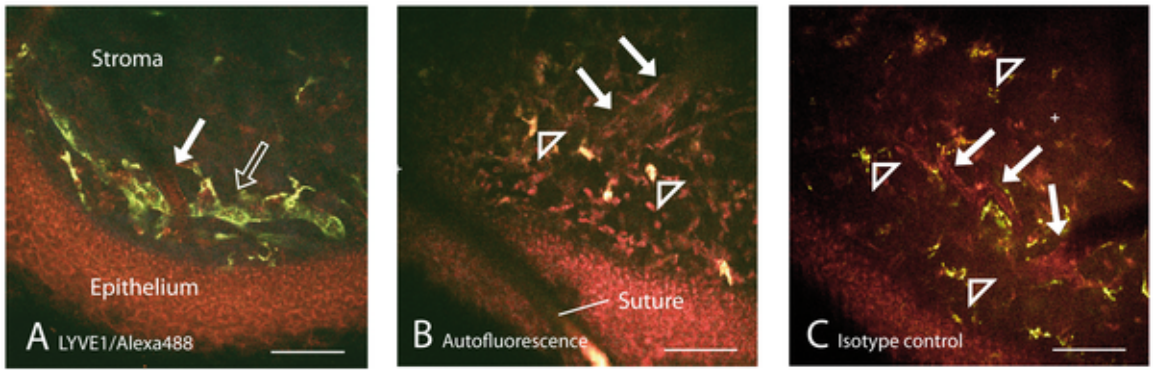

Figura 15. Microscopía "*intravital"* de los vasos linfáticos en el estroma sub-epitelial de la córnea. Adaptada de: "*Intravital two-photon microscopy of immune cell dynamics in corneal lymphatic vessels",* Steven, P. et al. [229]

En el presente trabajo se exploró de forma "*intravital*" la córnea entera del ratón usando para ello un modelo de microscopio multifotónico comercial. De esta forma se muestra la estructura de la córnea en una dimensión y resolución no descrita anteriormente, en la cual la población residente de células mieloides y los nervios son detectados "*in vivo*" usando para ello ratones transgénicos que expresan fluorescencia endógena (**Figura 16**). La combinación de microscopía multifotónica y de ratones transgénicos, nos muestra una visión de la córnea totalmente diferente y cuyas

aplicaciones en el entendimiento de éste órgano, tanto en condiciones normales como en patológicas, abre un campo sin explorar

Además en este trabajo se utilizó un sistema "Cre" en los ratones que induce expresión constitutiva, en este caso, de una proteína fluorescente por toda la vida de la célula. De esta manera las córneas de ratones transgénicos Cx3cr1^{cre} muestran fluorescencia por toda la vida de en las células de origen mieloide, independientemente de la activación del promotor.

El sistema de recombinación "Cre/loxP" es un tipo especial de recombinación específica [230]. Éste es un sistema genérico "Cre-transgene" y un alelo marcado con "Rosa26-loxP-stop-codon-loxP-fGFP/tdTomato" y un codón de stop intacto [231]. La escisión de el codón de stop mediada por "Cre" induce expresión constitutiva de la proteína fluorescente, u otro tipo de molécula como el receptor de la toxina diftérica, durante toda la vida de la célula y su descendencia (**figura 16**).

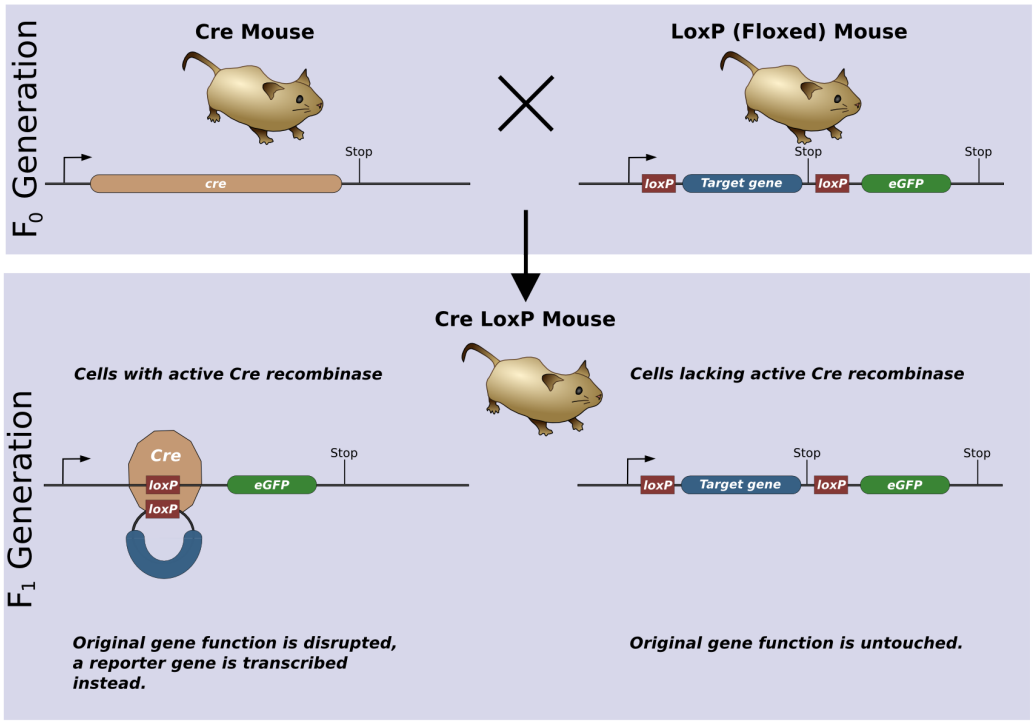

Figura 16. Ilustración de un modelo utilizando el sistema "Cre-loxP". La función del gen determinado (EGFP) se ve interrumpida por un codón de stop. La encima "Cre" reconoce los sitios "LoxP" y escinde la secuencia de stop permitiendo a la polimerasa transcribir el gen de la EGFP que es expresada de forma constitutiva durante toda la vida de la célula.
Figura creada por **Matthias Zepper** y de libre uso a través de "The Wikimedia Foundation"

Microscopía multifotónica

La microscopía de fluorescencia por excitación multifotónica es una técnica no lineal de imagen con resolución espacial micrométrica, penetración profunda y capacidad de seccionado óptico excepcional descrita por primera vez por Maria Göppert-Mayer en 1931 [232]. Este tipo de microscopía presenta una gran ventaja para experimentos "*in vivo*" a tiempo real tanto en células como en tejidos intactos. Esta técnica permite realizar experimentos en los cuales los sistemas de imagen convencional no pueden ser realizados o no darían la información deseada [233]. El sistema se basa en un modo de iluminación de láser pulsado que produce una densidad de fotones suficiente en el punto focal. De esta manera se puede localizar la excitación en una región focal muy fina permitiendo un seccionado sin el uso de "pinhole" (sistema de control de entrada de la luz procedente de una región focal en un microscopio confocal convencional). Además la excitación limitada en una región específica reduce la fototoxicidad [234].

La microscopía de fluorescencia por excitación multifotónica no produce imágenes con mayor resolución que la microscopía confocal, sin embargo incrementa significativamente la profundidad de penetración en muestras de gruesas. Esto se consigue por la ausencia de "pinhole", la ausencia de absorción de la excitación fuera de la focal y la disminución de la dispersión de la luz excitada. Para aumentar la eficiencia de la captura de la fluorescencia emitida, esta microscopía utiliza sistemas geométricos de detección de amplio espectro [233, 235-237].

La microscopía de excitación de dos fotones sucede por la absorción de dos fotones en un único evento cuántico. La energía de un fotón es inversamente proporcional a su longitud de onda por tanto los dos fotones absorbidos tienen una longitud de onda de el doble de la requerida para la excitación con un solo fotón. Por ejemplo, un fluorocromo que normalmente absorbe la luz en el ultravioleta (350 nm) puede también ser excitado

por dos fotones en la región cercana al infrarojo (700 nm) si ambos alcanzan la focal al mismo tiempo (mismo tiempo significa con un intervalo de $10xE^{(-18)}$ segundos [238].

Para producir un número significativo de eventos de absorción de dos fotones, la densidad de fotones debe ser aproximadamente un millón de veces mayor que la requerida para generar el mismo número absorciones de un solo fotón. Para ello se necesita un láser de gran potencia que genere fluorescencia generada por dos fotones. Esto se consigue focalizando un láser pulsado en el cual la energía en el pico del pulso es suficiente para generar una excitación significativa de dos fotones mientras la media de la energía del laser permanece muy baja. El resultado de dos fotones excitados, es el mismo singlete que ocurre durante experimentos con fluorescencia convencional. Por tanto, la emisión seguida de la excitación de dos fotones es exactamente la misma que la emisión generada en la excitación normal de un solo fotón.

La microscopía multifotónica usa múltiples fotones de baja energía para crear la misma excitación que es normalmente producida por la absorción de un solo fotón de alta energía [239]. La **figura 17** [240] representa el diagrama de Jablonski simplificado que ilustra la absorción de un solo fotón (ultravioleta) (izquierda) y la absorción simultánea de dos fotones en el infrarojo cercano (derecha), produciendo un estado excitado idéntico

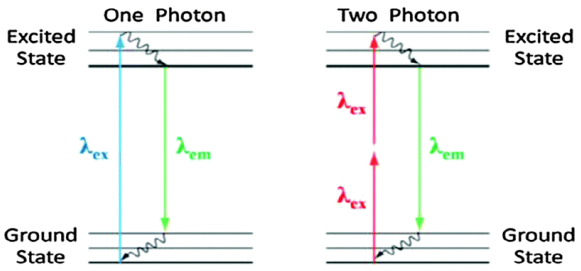

Figura 17. Diagrama de Jablonski simplificado. Absorción de un solo fotón (confocal, izquierda) y la absorción simultánea de dos fotones ("two-photon", derecha).

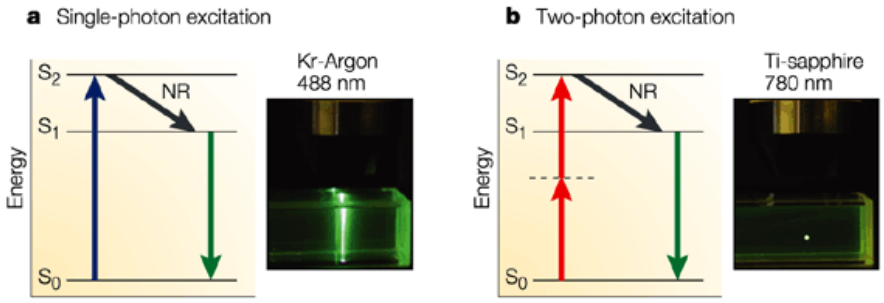

Figura 18. Diferencias en el plano de excitación del plano focal en microscopía de excitación de un solo fotón confocal (a) y microscopía de excitación de dos fotones (b) [241]

En un microscopio confocal** (**Figura 19**), la excitación (azul) es focalizada en la muestra (a), y la fluorescencia (verde) emitida por la focal es capturada por la lente del objetivo, y filtrada a través del "pinhole" y alcanza el detector (b). Esta señal fluorescente es la deseada, pero parte puede ser dispersada al atravesar al muestra (c). Esta luz dispersada no pasa a través del "pinhole" siendo por tanto perdida y no detectada. Estas pérdidas reducen la señal de fluorescencia emitida. Cuando la luz excitada pasa a través de la muestra puede ser absorbida (d) o dispersada antes de alcanzar la focal (e) perdiendo así su eficiencia de ser detectada. A su vez parte de la luz dispersada puede entrar a través del "pinhole" y ser erróneamente detectada creando un fondo indeseable (e, f).

En el método de excitación de dos fotones (**Figura 19**), la excitación de los fotones (rojo) puede ser dispersada (g) como en el sistema confocal. Sin embargo, la probabilidad de que dos fotones sean excitados a la vez en la misma muestra es nula y por tanto el ruido de fondo no se genera en este sistema. Además la mayoría de la luz excitada

alcanza el plano focal (h, i) por dos factores fundamentales: la reducida absorción fuera de foco y la escasa dispersión de la luz de mayor longitud de onda de la excitación de los dos fotones. Por otro lado, la luz generada (verde), incluso si es dispersada, tiene una gran probabilidad de ser detectada en el tubo fotomultiplicador (j) debido a la ausencia de "pinhole" que la bloquee (k). La baja sensibilidad a los efectos de dispersión y la ausencia de señal fuera de foco permite la conservación de un contraste de imagen total desde partes considerablemente profundas de la muestra [240].

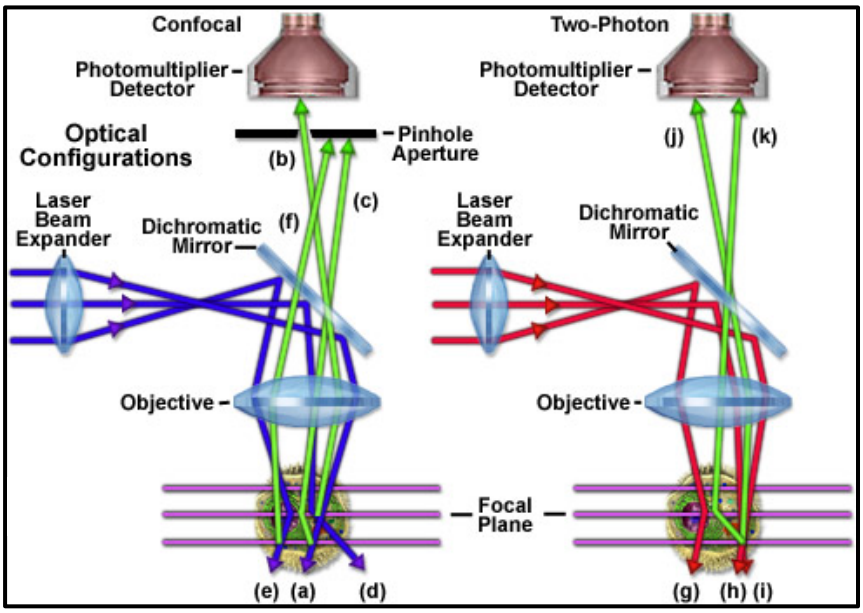

Figura 19. Diferencias entre un sistema de microscopía de excitación de un solo fotón (confocal) y microscopía de excitación de dos fotones.

****Nota**: Esta parte ha sido tomada de:

"Fundamentals and Applications in Multiphoton Excitation Microscopy, https://www.microscopyu.com/index.html

Autores: David W. Piston - Department of Molecular Physiology and Biophysics, Vanderbilt University, Nashville, Tennessee. Thomas J. Fellers and Michael W. Davidson - National High Magnetic Field Laboratory, The Florida State University, Tallahassee, Florida,

Generación del segundo armónico:

La generación del segundo armónico (SHG, "second harmonic generation") o doblado de la frecuencia es un proceso no linear en el cual los fotones con la misma frecuencia interactuando con un material no linear se combinan para generar nuevos fotones con el doble de energía y por tanto el doble de frecuencia y la mitad de la longitud de onda de los fotones iniciales [243]. Los materiales transparentes se comportan como transmisores no lineales (**figura 20**). La luz monocromática de baja intensidad pasa a través de ellos proporcionalmente a la intensidad. Si la intensidad de la luz es alta, por ejemplo un láser, el material muestra un comportamiento óptico no lineal generando un segundo harmónico [244]

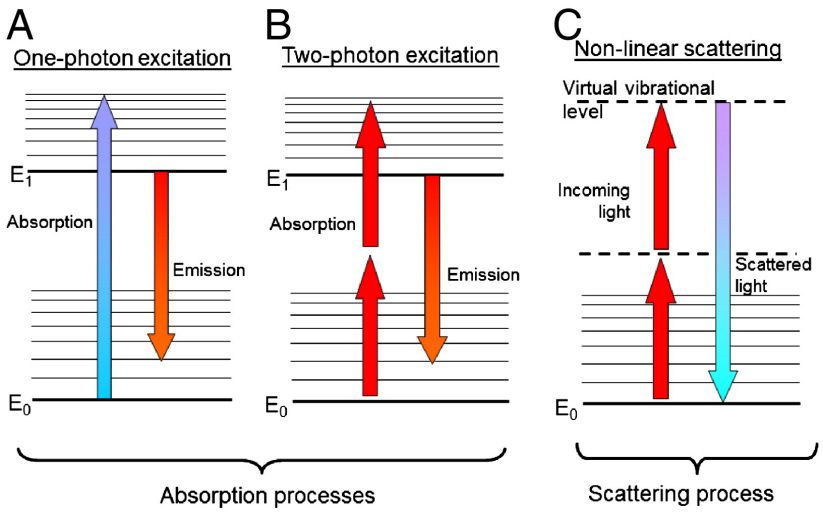

Figura 20. Diagrama de Jablonski simplificado. Absorción de un solo fotón (confocal) (A), absorción simultánea de dos fotones (B) y generación de un proceso no linear de reflexión o generación de un segundo armónico (SHG) (C).

El efecto de la generación del segundo armónico se puede detectar de forma fácil en córneas de ratón usando un microscopio multifotónico. De esta manera se puede

demarcar la córnea usando la señal emitida por el colágeno organizado del estroma (**Figura 21**)

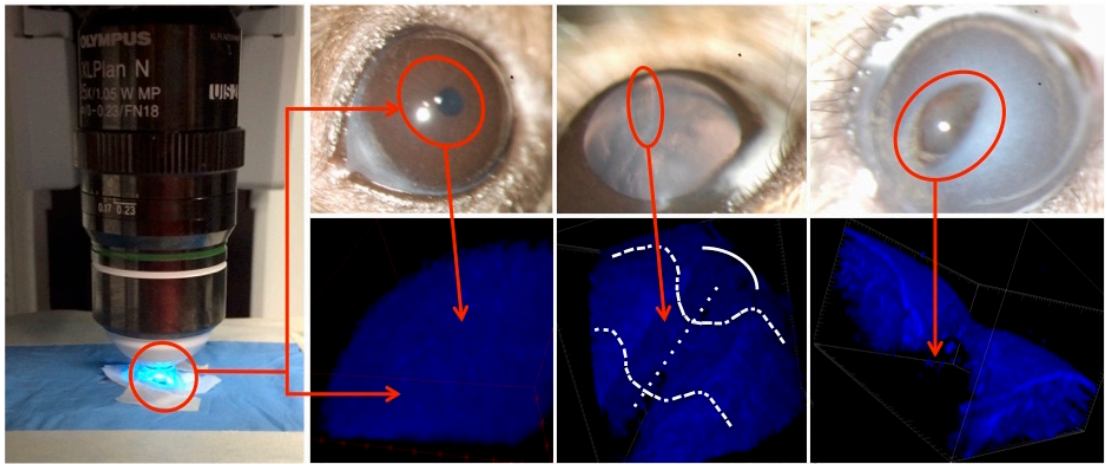

Figura 21. La estructura organizada del estroma corneal genera una señal de segundo harmónico excitable a 890-950 nm y detectable en el canal azul (420-460 nm). La falta de colágeno en la herida estromal deja un vacío en la señal que puede ser posteriormente mostrada de forma tridimensional. Fotografías propias no publicadas anteriormente, "Duke University".

Con la excepción de este trabajo, el microscopio multifotónico apenas ha sido usado en el estudio del ojo. En una tesis anterior, Tom Yu Chia Lai comparó el sistema OCT ("Optical coherence tomography") con el sistema multifotónico para la obtención de imágenes de la córnea. De esta manera se evaluó "*ex vivo*" la estructura de la córnea de cinco especies diferentes (humana, íctica, porcina, bovina y murina) [245]. Además se ha utilizado el microscopio multifotónico para el estudio "*in vivo*" de la dinámica de las células inflamatorias de la córnea en contacto con los vasos linfáticos en el ratón [229].

En el presente trabajo se exploró de forma "*intravital*" la córnea entera del ratón, usando para ello un modelo de microscopio multifotónico comercial. De esta forma se

muestra la estructura de la córnea con una resolución no descrita anteriormente en la cual la población residente de células inmunitarias y los nervios son detectados "*in vivo*" usando para ello ratones transgénicos que expresan fluorescencia endógena (**Figura 22**). La combinación de microscopía multifotónica y de ratones transgénicos, nos muestra una visión de la córnea totalmente diferente y cuyas aplicaciones en el entendimiento de éste órgano tanto en condiciones normales como en patológicas, abre un campo sin explorar.

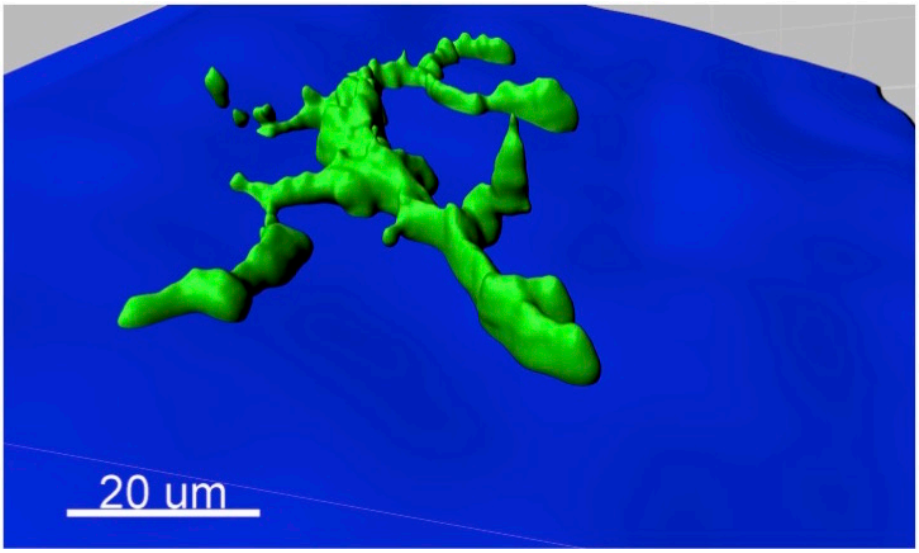

Figura 22. Fotografía de gran resolución de una célula dendrítica (verde) situada sobre el estroma (azul) en la membrana basal del epitelio. La fotografía se realizó de forma "*intravital*" con un microscopio multifotónico en un ratón vivo que expresa GFP en el promotor del receptor de la fractalquina o Cx3cr1. Fotografía propia no publicada anteriormente. "Duke University"

Bibliografía

1. C. Stephen Foster, D.T.A., Claes H. Dolman, *Smolin and Thoft's The Cornea, Scientific Foundation & Clinical Practice.* 2005.
2. Beebe, D.C. and B.R. Masters, *Cell lineage and the differentiation of corneal epithelial cells.* Invest Ophthalmol Vis Sci, 1996. **37**(9): p. 1815-25.
3. Hanna, C. and J.E. O'Brien, *Cell production and migration in the epithelial layer of the cornea.* Arch Ophthalmol, 1960. **64**: p. 536-9.
4. Wilson, S.E. and J.W. Hong, *Bowman's layer structure and function: critical or dispensable to corneal function? A hypothesis.* Cornea, 2000. **19**(4): p. 417-20.
5. Rodrigues MM, W.G.I., Hackett J, Donohoo P *Ocular Anatomy, Embryology, and Teratology.* 1982.
6. Waring, G.O., 3rd, W.M. Bourne, H.F. Edelhauser and K.R. Kenyon, *The corneal endothelium. Normal and pathologic structure and function.* Ophthalmology, 1982. **89**(6): p. 531-90.
7. Muller, L.J., G.F. Vrensen, L. Pels, B.N. Cardozo and B. Willekens, *Architecture of human corneal nerves.* Invest Ophthalmol Vis Sci, 1997. **38**(5): p. 985-94.
8. Ruskell, G.L., *Ocular fibers of the maxillary nerves in monkey.* J. Anat. Lond., 1974. **118**: p. 195–203.
9. Vonderahe, A.R., *Corneal and scleral anethesia of the lower half of the eye in a case of trauma of the superior maxillary nerve.* Arch. Neurol. Psychiatr., 1928. **20**: p. 836–837.
10. Marfurt, C.F., L.C. Ellis and M.A. Jones, *Sensory and sympathetic nerve sprouting in the rat cornea following neonatal administration of capsaicin.* Somatosens Mot Res, 1993. **10**(4): p. 377-98.
11. Marfurt, C.F., M.A. Jones and K. Thrasher, *Parasympathetic innervation of the rat cornea.* Exp Eye Res, 1998. **66**(4): p. 437-48.
12. Morgan, C., W.C. DeGroat and P.J. Jannetta, *Sympathetic innervation of the cornea from the superior cervical ganglion. An HRP study in the cat.* J Auton Nerv Syst, 1987. **20**(2): p. 179-83.
13. Tervo, T., F. Joo, K.T. Huikuri, I. Toth and A. Palkama, *Fine structure of sensory nerves in the rat cornea: an experimental nerve degeneration study.* Pain, 1979. **6**(1): p. 57-70.
14. Knickelbein, J.E., K.A. Buela and R.L. Hendricks, *Antigen-presenting cells are stratified within normal human corneas and are rapidly mobilized during ex vivo viral infection.* Invest Ophthalmol Vis Sci, 2014. **55**(2): p. 1118-23.
15. Veres, T.Z., S. Rochlitzer, M. Shevchenko, B. Fuchs, F. Prenzler, C. Nassenstein, A. Fischer, L. Welker, O. Holz, M. Muller, N. Krug and A. Braun, *Spatial*

interactions between dendritic cells and sensory nerves in allergic airway inflammation. Am J Respir Cell Mol Biol, 2007. **37**(5): p. 553-61.
16. Veres, T.Z., S. Rochlitzer and A. Braun, *The role of neuro-immune cross-talk in the regulation of inflammation and remodelling in asthma.* Pharmacol Ther, 2009. **122**(2): p. 203-14.
17. Paunicka, K.J., J. Mellon, D. Robertson, M. Petroll, J.R. Brown and J.Y. Niederkorn, *Severing corneal nerves in one eye induces sympathetic loss of immune privilege and promotes rejection of future corneal allografts placed in either eye.* Am J Transplant, 2015. **15**(6): p. 1490-501.
18. Seyed-Razavi, Y., H.R. Chinnery and P.G. McMenamin, *A novel association between resident tissue macrophages and nerves in the peripheral stroma of the murine cornea.* Invest Ophthalmol Vis Sci, 2014. **55**(3): p. 1313-20.
19. Blanco, T. and D.R. Saban, *The Cornea Has "the Nerve" to Encourage Immune Rejection.* Am J Transplant, 2015.
20. Tada, T., *The immune system as a supersystem.* Annu Rev Immunol, 1997. **15**: p. 1-13.
21. Maurice, D.M., *The structure and transparency of the cornea.* J Physiol, 1957. **136**(2): p. 263-86.
22. Wilson, S.E., *Analysis of the keratocyte apoptosis, keratocyte proliferation, and myofibroblast transformation responses after photorefractive keratectomy and laser in situ keratomileusis.* Trans Am Ophthalmol Soc, 2002. **100**: p. 411-33.
23. Hanada, K., S. Igarashi, O. Muramatsu and A. Yoshida, *Therapeutic keratoplasty for corneal perforation: clinical results and complications.* Cornea, 2008. **27**(2): p. 156-60.
24. Rabinowitz, Y.S., *Keratoconus.* Surv Ophthalmol, 1998. **42**(4): p. 297-319.
25. Kaye, S. and A. Choudhary, *Herpes simplex keratitis.* Prog Retin Eye Res, 2006. **25**(4): p. 355-80.
26. Wilson, S.E., L. Pedroza, R. Beuerman and J.M. Hill, *Herpes simplex virus type-1 infection of corneal epithelial cells induces apoptosis of the underlying keratocytes.* Exp Eye Res, 1997. **64**(5): p. 775-9.
27. Leonardi, A., L. Motterle and M. Bortolotti, *Allergy and the eye.* Clin Exp Immunol, 2008. **153 Suppl 1**: p. 17-21.
28. Netto, M.V., R.R. Mohan, R. Ambrosio, Jr., A.E. Hutcheon, J.D. Zieske and S.E. Wilson, *Wound healing in the cornea: a review of refractive surgery complications and new prospects for therapy.* Cornea, 2005. **24**(5): p. 509-22.
29. Randleman, J.B., M. Woodward, M.J. Lynn and R.D. Stulting, *Risk assessment for ectasia after corneal refractive surgery.* Ophthalmology, 2008. **115**(1): p. 37-50.
30. Zirm, E.K., *Eine erfolgreiche totale Keratoplastik (A successful total keratoplasty). 1906.* Refract Corneal Surg, 1989. **5**(4): p. 258-61.

31. van Essen, T.H., D.L. Roelen, K.A. Williams and M.J. Jager, *Matching for Human Leukocyte Antigens (HLA) in corneal transplantation - To do or not to do.* Prog Retin Eye Res, 2015. **46**: p. 84-110.
32. Benitez del Castillo, J.M., M.A. Wasfy, C. Fernandez and J. Garcia-Sanchez, *An in vivo confocal masked study on corneal epithelium and subbasal nerves in patients with dry eye.* Invest Ophthalmol Vis Sci, 2004. **45**(9): p. 3030-5.
33. Stern, M.E., R.W. Beuerman, R.I. Fox, J. Gao, A.K. Mircheff and S.C. Pflugfelder, *The pathology of dry eye: the interaction between the ocular surface and lacrimal glands.* Cornea, 1998. **17**(6): p. 584-9.
34. Stevenson, W., S.K. Chauhan and R. Dana, *Dry eye disease: an immune-mediated ocular surface disorder.* Arch Ophthalmol, 2012. **130**(1): p. 90-100.
35. Wilson, S.E. and R. Ambrosio, *Laser in situ keratomileusis-induced neurotrophic epitheliopathy.* Am J Ophthalmol, 2001. **132**(3): p. 405-6.
36. Paunicka, K.J., J. Mellon, D. Robertson, M. Petroll, J.R. Brown and J.Y. Niederkorn, *Severing Corneal Nerves in One Eye Induces Sympathetic Loss of Immune Privilege and Promotes Rejection of Future Corneal Allografts Placed in Either Eye.* Am J Transplant, 2015.
37. Streilein, J.W., *New thoughts on the immunology of corneal transplantation.* Eye (Lond), 2003. **17**(8): p. 943-8.
38. Maruyama, K., T. Nakazawa, C. Cursiefen, Y. Maruyama, N. Van Rooijen, P.A. D'Amore and S. Kinoshita, *The maintenance of lymphatic vessels in the cornea is dependent on the presence of macrophages.* Invest Ophthalmol Vis Sci, 2012. **53**(6): p. 3145-53.
39. Chauhan, S.K., T.H. Dohlman and R. Dana, *Corneal Lymphatics: Role in Ocular Inflammation as Inducer and Responder of Adaptive Immunity.* J Clin Cell Immunol, 2014. **5**.
40. Hong, S. and L. Van Kaer, *Immune privilege: keeping an eye on natural killer T cells.* J Exp Med, 1999. **190**(9): p. 1197-200.
41. Galea I, Beckmann I and P. V.H, *What is Immune Privilege (not)?* Trends in Immunology, 2007. **28**(1): p. 12-18.
42. Zenclussen, A.C., A. Schumacher, M.L. Zenclussen, P. Wafula and H.D. Volk, *Immunology of pregnancy: cellular mechanisms allowing fetal survival within the maternal uterus.* Expert Rev Mol Med, 2007. **9**(10): p. 1-14.
43. Chinnery, H.R., E. Pearlman and P.G. McMenamin, *Cutting edge: Membrane nanotubes in vivo: a feature of MHC class II+ cells in the mouse cornea.* J Immunol, 2008. **180**(9): p. 5779-83.
44. Chinnery, H.R., M.J. Ruitenberg, G.W. Plant, E. Pearlman, S. Jung and P.G. McMenamin, *The chemokine receptor CX3CR1 mediates homing of MHC class II-positive cells to the normal mouse corneal epithelium.* Invest Ophthalmol Vis Sci, 2007. **48**(4): p. 1568-74.

45. Hamrah, P., Y. Liu, Q. Zhang and M.R. Dana, *The corneal stroma is endowed with a significant number of resident dendritic cells.* Invest Ophthalmol Vis Sci, 2003. **44**(2): p. 581-9.
46. Hamrah, P., Y. Liu, Q. Zhang and M.R. Dana, *Alterations in corneal stromal dendritic cell phenotype and distribution in inflammation.* Arch Ophthalmol, 2003. **121**(8): p. 1132-40.
47. Knickelbein, J.E., S.C. Watkins, P.G. McMenamin and R.L. Hendricks, *Stratification of Antigen-presenting Cells within the Normal Cornea.* Ophthalmol Eye Dis, 2009. **1**: p. 45-54.
48. Liu, Y., P. Hamrah, Q. Zhang, A.W. Taylor and M.R. Dana, *Draining lymph nodes of corneal transplant hosts exhibit evidence for donor major histocompatibility complex (MHC) class II-positive dendritic cells derived from MHC class II-negative grafts.* J Exp Med, 2002. **195**(2): p. 259-68.
49. Sosnova, M., M. Bradl and J.V. Forrester, *CD34+ corneal stromal cells are bone marrow-derived and express hemopoietic stem cell markers.* Stem Cells, 2005. **23**(4): p. 507-15.
50. Hori, J., J.L. Vega and S. Masli, *Review of ocular immune privilege in the year 2010: modifying the immune privilege of the eye.* Ocul Immunol Inflamm, 2010. **18**(5): p. 325-33.
51. Emami-Naeini, P., T.H. Dohlman, M. Omoto, T. Hattori, Y. Chen, H.S. Lee, S.K. Chauhan and R. Dana, *Soluble vascular endothelial growth factor receptor-3 suppresses allosensitization and promotes corneal allograft survival.* Graefes Arch Clin Exp Ophthalmol, 2014. **252**(11): p. 1755-62.
52. Hajrasouliha, A.R., T. Funaki, Z. Sadrai, T. Hattori, S.K. Chauhan and R. Dana, *Vascular endothelial growth factor-C promotes alloimmunity by amplifying antigen-presenting cell maturation and lymphangiogenesis.* Invest Ophthalmol Vis Sci, 2012. **53**(3): p. 1244-50.
53. Cursiefen, C., K. Maruyama, F. Bock, D. Saban, Z. Sadrai, J. Lawler, R. Dana and S. Masli, *Thrombospondin 1 inhibits inflammatory lymphangiogenesis by CD36 ligation on monocytes.* J Exp Med, 2011. **208**(5): p. 1083-92.
54. Dawson, D.W., O.V. Volpert, P. Gillis, S.E. Crawford, H. Xu, W. Benedict and N.P. Bouck, *Pigment epithelium-derived factor: a potent inhibitor of angiogenesis.* Science, 1999. **285**(5425): p. 245-8.
55. Gabison, E., J.H. Chang, E. Hernandez-Quintela, J. Javier, P.C. Lu, H. Ye, T. Kure, T. Kato and D.T. Azar, *Anti-angiogenic role of angiostatin during corneal wound healing.* Exp Eye Res, 2004. **78**(3): p. 579-89.
56. Griffith, T.S., T. Brunner, S.M. Fletcher, D.R. Green and T.A. Ferguson, *Fas ligand-induced apoptosis as a mechanism of immune privilege.* Science, 1995. **270**(5239): p. 1189-92.

57. Jin, Y., S.K. Chauhan, J. El Annan, P.T. Sage, A.H. Sharpe and R. Dana, *A novel function for programmed death ligand-1 regulation of angiogenesis.* Am J Pathol, 2011. **178**(4): p. 1922-9.
58. Ghasemi, H., T. Ghazanfari, R. Yaraee, P. Owlia, Z.M. Hassan and S. Faghihzadeh, *Roles of IL-10 in ocular inflammations: a review.* Ocul Immunol Inflamm, 2012. **20**(6): p. 406-18.
59. Makinen, T., T. Veikkola, S. Mustjoki, T. Karpanen, B. Catimel, E.C. Nice, L. Wise, A. Mercer, H. Kowalski, D. Kerjaschki, S.A. Stacker, M.G. Achen and K. Alitalo, *Isolated lymphatic endothelial cells transduce growth, survival and migratory signals via the VEGF-C/D receptor VEGFR-3.* EMBO J, 2001. **20**(17): p. 4762-73.
60. Wigle, J.T., N. Harvey, M. Detmar, I. Lagutina, G. Grosveld, M.D. Gunn, D.G. Jackson and G. Oliver, *An essential role for Prox1 in the induction of the lymphatic endothelial cell phenotype.* EMBO J, 2002. **21**(7): p. 1505-13.
61. Chauhan, S.K., J. El Annan, T. Ecoiffier, S. Goyal, Q. Zhang, D.R. Saban and R. Dana, *Autoimmunity in dry eye is due to resistance of Th17 to Treg suppression.* J Immunol, 2009. **182**(3): p. 1247-52.
62. Conrady, C.D., M. Zheng, D.U. Stone and D.J. Carr, *CD8+ T cells suppress viral replication in the cornea but contribute to VEGF-C-induced lymphatic vessel genesis.* J Immunol, 2012. **189**(1): p. 425-32.
63. Zhu, S.N. and M.R. Dana, *Expression of cell adhesion molecules on limbal and neovascular endothelium in corneal inflammatory neovascularization.* Invest Ophthalmol Vis Sci, 1999. **40**(7): p. 1427-34.
64. Tan, K.W., S.Z. Chong, F.H. Wong, M. Evrard, S.M. Tan, J. Keeble, D.M. Kemeny, L.G. Ng, J.P. Abastado and V. Angeli, *Neutrophils contribute to inflammatory lymphangiogenesis by increasing VEGF-A bioavailability and secreting VEGF-D.* Blood, 2013. **122**(22): p. 3666-77.
65. Wuest, T.R. and D.J. Carr, *VEGF-A expression by HSV-1-infected cells drives corneal lymphangiogenesis.* J Exp Med, 2010. **207**(1): p. 101-15.
66. Dietrich, T., F. Bock, D. Yuen, D. Hos, B.O. Bachmann, G. Zahn, S. Wiegand, L. Chen and C. Cursiefen, *Cutting edge: lymphatic vessels, not blood vessels, primarily mediate immune rejections after transplantation.* J Immunol, 2010. **184**(2): p. 535-9.
67. Goyal, S., S.K. Chauhan, J. El Annan, N. Nallasamy, Q. Zhang and R. Dana, *Evidence of corneal lymphangiogenesis in dry eye disease: a potential link to adaptive immunity?* Arch Ophthalmol, 2010. **128**(7): p. 819-24.
68. Niederkorn, J.Y. and D.F. Larkin, *Immune privilege of corneal allografts.* Ocul Immunol Inflamm, 2010. **18**(3): p. 162-71.
69. Albuquerque, R.J., T. Hayashi, W.G. Cho, M.E. Kleinman, S. Dridi, A. Takeda, J.Z. Baffi, K. Yamada, H. Kaneko, M.G. Green, J. Chappell, J. Wilting, H.A. Weich, S.

Yamagami, S. Amano, N. Mizuki, J.S. Alexander, M.L. Peterson, R.A. Brekken, M. Hirashima, S. Capoor, T. Usui, B.K. Ambati and J. Ambati, *Alternatively spliced vascular endothelial growth factor receptor-2 is an essential endogenous inhibitor of lymphatic vessel growth.* Nat Med, 2009. **15**(9): p. 1023-30.

70. Streilein, J.W., *Immunological non-responsiveness and acquisition of tolerance in relation to immune privilege in the eye.* Eye (Lond), 1995. **9 (Pt 2)**: p. 236-40.
71. Chauhan, S.K., D.R. Saban, H.K. Lee and R. Dana, *Levels of Foxp3 in regulatory T cells reflect their functional status in transplantation.* J Immunol, 2009. **182**(1): p. 148-53.
72. Hargrave, S.L., E. Mayhew, S. Hegde and J. Niederkorn, *Are corneal cells susceptible to antibody-mediated killing in corneal allograft rejection?* Transpl Immunol, 2003. **11**(1): p. 79-89.
73. Yamagami, S., H. Kawashima, T. Tsuru, H. Yamagami, N. Kayagaki, H. Yagita, K. Okumura and D.S. Gregerson, *Role of Fas-Fas ligand interactions in the immunorejection of allogeneic mouse corneal transplants.* Transplantation, 1997. **64**(8): p. 1107-11.
74. Shen, L., Y. Jin, G.J. Freeman, A.H. Sharpe and M.R. Dana, *The function of donor versus recipient programmed death-ligand 1 in corneal allograft survival.* J Immunol, 2007. **179**(6): p. 3672-9.
75. Apte, R.S., D. Sinha, E. Mayhew, G.J. Wistow and J.Y. Niederkorn, *Cutting edge: role of macrophage migration inhibitory factor in inhibiting NK cell activity and preserving immune privilege.* J Immunol, 1998. **160**(12): p. 5693-6.
76. Streilein, J.W., *Ocular immune privilege: therapeutic opportunities from an experiment of nature.* Nat Rev Immunol, 2003. **3**(11): p. 879-89.
77. Streilein, J.W. and J.Y. Niederkorn, *Induction of anterior chamber-associated immune deviation requires an intact, functional spleen. 1981.* Ocul Immunol Inflamm, 2007. **15**(3): p. 187-94.
78. Billingham, R.E. and T. Boswell, *Studies on the problem of corneal homografts.* Proc R Soc Lond B Biol Sci, 1953. **141**(904): p. 392-406.
79. Hajrasouliha, A.R., Z. Sadrai, H.K. Lee, S.K. Chauhan and R. Dana, *Expression of the chemokine decoy receptor D6 mediates dendritic cell function and promotes corneal allograft rejection.* Mol Vis, 2013. **19**: p. 2517-25.
80. Hattori, T., S.K. Chauhan, H. Lee, H. Ueno, R. Dana, D.H. Kaplan and D.R. Saban, *Characterization of Langerin-expressing dendritic cell subsets in the normal cornea.* Invest Ophthalmol Vis Sci, 2011. **52**(7): p. 4598-604.
81. Khan, A., H. Fu, L.A. Tan, J.E. Harper, S.C. Beutelspacher, D.F. Larkin, G. Lombardi, M.O. McClure and A.J. George, *Dendritic cell modification as a route*

to inhibiting corneal graft rejection by the indirect pathway of allorecognition. Eur J Immunol, 2013. **43**(3): p. 734-46.
82. Forrester, J.V., H. Xu, L. Kuffova, A.D. Dick and P.G. McMenamin, *Dendritic cell physiology and function in the eye.* Immunol Rev, 2010. **234**(1): p. 282-304.
83. Hattori, T., D.R. Saban, P. Emami-Naeini, S.K. Chauhan, T. Funaki, H. Ueno and R. Dana, *Donor-derived, tolerogenic dendritic cells suppress immune rejection in the indirect allosensitization-dominant setting of corneal transplantation.* J Leukoc Biol, 2012. **91**(4): p. 621-7.
84. Heyborne, K.D., R.L. Cranfill, S.R. Carding, W.K. Born and R.L. O'Brien, *Characterization of gamma delta T lymphocytes at the maternal-fetal interface.* J Immunol, 1992. **149**(9): p. 2872-8.
85. Muller, L.J., E. Pels and G.F. Vrensen, *The specific architecture of the anterior stroma accounts for maintenance of corneal curvature.* Br J Ophthalmol, 2001. **85**(4): p. 437-43.
86. Radner, W. and R. Mallinger, *Interlacing of collagen lamellae in the midstroma of the human cornea.* Cornea, 2002. **21**(6): p. 598-601.
87. Muller, L.J., C.F. Marfurt, F. Kruse and T.M. Tervo, *Corneal nerves: structure, contents and function.* Exp Eye Res, 2003. **76**(5): p. 521-42.
88. Lim, C.H. and G.L. Ruskell, *Corneal nerve access in monkeys.* Albrecht Von Graefes Arch Klin Exp Ophthalmol, 1978. **208**(1-3): p. 15-23.
89. Moilanen, J.A., M.H. Vesaluoma, L.J. Muller and T.M. Tervo, *Long-term corneal morphology after PRK by in vivo confocal microscopy.* Invest Ophthalmol Vis Sci, 2003. **44**(3): p. 1064-9.
90. Muller, L.J., L. Pels and G.F. Vrensen, *Ultrastructural organization of human corneal nerves.* Invest Ophthalmol Vis Sci, 1996. **37**(4): p. 476-88.
91. Bonini, S., A. Lambiase, P. Rama, G. Caprioglio and L. Aloe, *Topical treatment with nerve growth factor for neurotrophic keratitis.* Ophthalmology, 2000. **107**(7): p. 1347-51; discussion 1351-2.
92. Garcia-Hirschfeld, J., L.G. Lopez-Briones and C. Belmonte, *Neurotrophic influences on corneal epithelial cells.* Exp Eye Res, 1994. **59**(5): p. 597-605.
93. Tan, M.H., J. Bryars and J. Moore, *Use of nerve growth factor to treat congenital neurotrophic corneal ulceration.* Cornea, 2006. **25**(3): p. 352-5.
94. Laycock, K.A., R.H. Brady, S.F. Lee, P.A. Osborne, E.M. Johnson and J.S. Pepose, *The role of nerve growth factor in modulating herpes simplex virus reactivation in vivo.* Graefes Arch Clin Exp Ophthalmol, 1994. **232**(7): p. 421-5.
95. Lambiase, A., D. Merlo, C. Mollinari, P. Bonini, A.M. Rinaldi, D.A. M, A. Micera, M. Coassin, P. Rama, S. Bonini and E. Garaci, *Molecular basis for keratoconus: lack of TrkA expression and its transcriptional repression by Sp3.* Proc Natl Acad Sci U S A, 2005. **102**(46): p. 16795-800.

96. Meek, K.M., S.J. Tuft, Y. Huang, P.S. Gill, S. Hayes, R.H. Newton and A.J. Bron, *Changes in collagen orientation and distribution in keratoconus corneas.* Invest Ophthalmol Vis Sci, 2005. **46**(6): p. 1948-56.
97. Wilson, S.E., *Everett Kinsey Lecture. Keratocyte apoptosis in refractive surgery.* CLAO J, 1998. **24**(3): p. 181-5.
98. Wilson, S.E., Y.G. He, J. Weng, Q. Li, A.W. McDowall, M. Vital and E.L. Chwang, *Epithelial injury induces keratocyte apoptosis: hypothesized role for the interleukin-1 system in the modulation of corneal tissue organization and wound healing.* Exp Eye Res, 1996. **62**(4): p. 325-7.
99. Baker, K.S., S.C. Anderson, E.G. Romanowski, R.A. Thoft and N. SundarRaj, *Trigeminal ganglion neurons affect corneal epithelial phenotype. Influence on type VII collagen expression in vitro.* Invest Ophthalmol Vis Sci, 1993. **34**(1): p. 137-44.
100. Mathers, W.D., *Why the eye becomes dry: a cornea and lacrimal gland feedback model.* CLAO J, 2000. **26**(3): p. 159-65.
101. Efron, N., *The Glenn A. Fry award lecture 2010: Ophthalmic markers of diabetic neuropathy.* Optom Vis Sci, 2011. **88**(6): p. 661-83.
102. Linna, T.U., M.H. Vesaluoma, J.J. Perez-Santonja, W.M. Petroll, J.L. Alio and T.M. Tervo, *Effect of myopic LASIK on corneal sensitivity and morphology of subbasal nerves.* Invest Ophthalmol Vis Sci, 2000. **41**(2): p. 393-7.
103. Yamada, M., M. Ogata, M. Kawai and Y. Mashima, *Decreased substance P concentrations in tears from patients with corneal hypesthesia.* Am J Ophthalmol, 2000. **129**(5): p. 671-2.
104. Davis, E.A. and C.H. Dohlman, *Neurotrophic keratitis.* Int Ophthalmol Clin, 2001. **41**(1): p. 1-11.
105. Paton, L., *The Trigeminal and Its Ocular Lesions.* Br J Ophthalmol, 1926. **10**(6): p. 305-42.
106. Menchini, U., A. Scialdone, C. Pietroni, F. Carones and R. Brancato, *Argon versus krypton panretinal photocoagulation side effects on the anterior segment.* Ophthalmologica, 1990. **201**(2): p. 66-70.
107. Weigt, A.K., I.P. Herring, C.F. Marfurt, J.P. Pickett, R.B. Duncan, Jr. and D.L. Ward, *Effects of cyclophotocoagulation with a neodymium:yttrium-aluminum-garnet laser on corneal sensitivity, intraocular pressure, aqueous tear production, and corneal nerve morphology in eyes of dogs.* Am J Vet Res, 2002. **63**(6): p. 906-15.
108. Tervo, T. and J. Moilanen, *In vivo confocal microscopy for evaluation of wound healing following corneal refractive surgery.* Prog Retin Eye Res, 2003. **22**(3): p. 339-58.
109. Kenchegowda, S., J. He and H.E. Bazan, *Involvement of pigment epithelium-derived factor, docosahexaenoic acid and neuroprotectin D1 in corneal*

inflammation and nerve integrity after refractive surgery. Prostaglandins Leukot Essent Fatty Acids, 2013. **88**(1): p. 27-31.
110. Dupps, W.J., Jr. and S.E. Wilson, *Biomechanics and wound healing in the cornea.* Exp Eye Res, 2006. **83**(4): p. 709-20.
111. Maurice, D.M. and A.A. Giardini, *Swelling of the cornea in vivo after the destruction of its limiting layers.* Br J Ophthalmol, 1951. **35**(12): p. 791-7.
112. Meek, K.M., D.W. Leonard, C.J. Connon, S. Dennis and S. Khan, *Transparency, swelling and scarring in the corneal stroma.* Eye (Lond), 2003. **17**(8): p. 927-36.
113. Saban, D.R., V. Calder, C.H. Kuo, N.J. Reyes, D.A. Dartt, S.J. Ono and J.Y. Niederkorn, *New twists to an old story: novel concepts in the pathogenesis of allergic eye disease.* Curr Eye Res, 2013. **38**(3): p. 317-30.
114. Pearlman, E., Y. Sun, S. Roy, M. Karmakar, A.G. Hise, L. Szczotka-Flynn, M. Ghannoum, H.R. Chinnery, P.G. McMenamin and A. Rietsch, *Host defense at the ocular surface.* Int Rev Immunol, 2013. **32**(1): p. 4-18.
115. Kumagai, N., K. Fukuda, Y. Ishimura and T. Nishida, *Synergistic induction of eotaxin expression in human keratocytes by TNF-alpha and IL-4 or IL-13.* Invest Ophthalmol Vis Sci, 2000. **41**(6): p. 1448-53.
116. Fukuda, K. and T. Nishida, *Reciprocal interaction of the conjunctiva and cornea in ocular allergy.* J Allergy Clin Immunol, 2010. **125**(2): p. 493-496 e2.
117. Fukuda, K., W. Ishida, H. Tanaka, Y. Harada, A. Matsuda, N. Ebihara and A. Fukushima, *Alarmins from corneal epithelial cells upregulate CCL11 and VCAM-1 in corneal fibroblasts.* Invest Ophthalmol Vis Sci, 2013. **54**(8): p. 5817-23.
118. Yang, D., Y.V. Postnikov, Y. Li, P. Tewary, G. de la Rosa, F. Wei, D. Klinman, T. Gioannini, J.P. Weiss, T. Furusawa, M. Bustin and J.J. Oppenheim, *High-mobility group nucleosome-binding protein 1 acts as an alarmin and is critical for lipopolysaccharide-induced immune responses.* J Exp Med, 2012. **209**(1): p. 157-71.
119. Fukuda, K., N. Kumagai, Y. Fujitsu and T. Nishida, *Fibroblasts as local immune modulators in ocular allergic disease.* Allergol Int, 2006. **55**(2): p. 121-9.
120. Kumagai, N., K. Fukuda, Y. Fujitsu, K. Yamamoto and T. Nishida, *Role of structural cells of the cornea and conjunctiva in the pathogenesis of vernal keratoconjunctivitis.* Prog Retin Eye Res, 2006. **25**(2): p. 165-87.
121. Fukuda, K., T. Nishida and A. Fukushima, *Synergistic induction of eotaxin and VCAM-1 expression in human corneal fibroblasts by staphylococcal peptidoglycan and either IL-4 or IL-13.* Allergol Int, 2011. **60**(3): p. 355-63.
122. Calonge, M., *Classification of ocular atopic/allergic disorders and conditions: an unsolved problem.* Acta Ophthalmol Scand Suppl, 1999(228): p. 10-3.

123. Pflugfelder, S.C., *Anti-inflammatory therapy of dry eye.* Ocul Surf, 2003. **1**(1): p. 31-6.
124. Enriquez-de-Salamanca, A. and M. Calonge, *Cytokines and chemokines in immune-based ocular surface inflammation.* Expert Rev Clin Immunol, 2008. **4**(4): p. 457-67.
125. Ohbayashi, M., B. Manzouri, T. Flynn, M. Toda, Y. Ikeda, T. Nakamura and S.J. Ono, *Dynamic changes in conjunctival dendritic cell numbers, anatomical position and phenotype during experimental allergic conjunctivitis.* Exp Mol Pathol, 2007. **83**(2): p. 216-23.
126. Schlereth, S., H.S. Lee, P. Khandelwal and D.R. Saban, *Blocking CCR7 at the ocular surface impairs the pathogenic contribution of dendritic cells in allergic conjunctivitis.* Am J Pathol, 2012. **180**(6): p. 2351-60.
127. Saban, D.R., F. Bock, S.K. Chauhan, S. Masli and R. Dana, *Thrombospondin-1 derived from APCs regulates their capacity for allosensitization.* J Immunol, 2010. **185**(8): p. 4691-7.
128. Bachmann, B.O., F. Bock, S.J. Wiegand, K. Maruyama, M.R. Dana, F.E. Kruse, E. Luetjen-Drecoll and C. Cursiefen, *Promotion of graft survival by vascular endothelial growth factor a neutralization after high-risk corneal transplantation.* Arch Ophthalmol, 2008. **126**(1): p. 71-7.
129. Chong, E.M. and M.R. Dana, *Graft failure IV. Immunologic mechanisms of corneal transplant rejection.* Int Ophthalmol, 2008. **28**(3): p. 209-22.
130. Wilson, S.E., Q. Li, J. Weng, P.A. Barry-Lane, J.V. Jester, Q. Liang and R.J. Wordinger, *The Fas-Fas ligand system and other modulators of apoptosis in the cornea.* Invest Ophthalmol Vis Sci, 1996. **37**(8): p. 1582-92.
131. Mo, J.S., A. Matsukawa, S. Ohkawara and M. Yoshinaga, *Role and regulation of IL-8 and MCP-1 in LPS-induced uveitis in rabbits.* Exp Eye Res, 1999. **68**(3): p. 333-40.
132. Moss, S.E., R. Klein and B.E. Klein, *Prevalence of and risk factors for dry eye syndrome.* Arch Ophthalmol, 2000. **118**(9): p. 1264-8.
133. *The definition and classification of dry eye disease: report of the Definition and Classification Subcommittee of the International Dry Eye WorkShop (2007).* Ocul Surf, 2007. **5**(2): p. 75-92.
134. Kunert, K.S., A.S. Tisdale, M.E. Stern, J.A. Smith and I.K. Gipson, *Analysis of topical cyclosporine treatment of patients with dry eye syndrome: effect on conjunctival lymphocytes.* Arch Ophthalmol, 2000. **118**(11): p. 1489-96.
135. Stern, M.E., J. Gao, T.A. Schwalb, M. Ngo, D.D. Tieu, C.C. Chan, B.L. Reis, S.M. Whitcup, D. Thompson and J.A. Smith, *Conjunctival T-cell subpopulations in Sjogren's and non-Sjogren's patients with dry eye.* Invest Ophthalmol Vis Sci, 2002. **43**(8): p. 2609-14.

136. Cejkova, J., T. Ardan, Z. Simonova, C. Cejka, J. Malec, K. Jirsova, M. Filipec, D. Dotrelova and B. Brunova, *Nitric oxide synthase induction and cytotoxic nitrogen-related oxidant formation in conjunctival epithelium of dry eye (Sjogren's syndrome).* Nitric Oxide, 2007. **17**(1): p. 10-7.
137. Paul, A., S. Wilson, C.M. Belham, C.J. Robinson, P.H. Scott, G.W. Gould and R. Plevin, *Stress-activated protein kinases: activation, regulation and function.* Cell Signal, 1997. **9**(6): p. 403-10.
138. Pflugfelder, S.C., C.S. de Paiva, L. Tong, L. Luo, M.E. Stern and D.Q. Li, *Stress-activated protein kinase signaling pathways in dry eye and ocular surface disease.* Ocul Surf, 2005. **3**(4 Suppl): p. S154-7.
139. Luo, L., D.Q. Li, A. Doshi, W. Farley, R.M. Corrales and S.C. Pflugfelder, *Experimental dry eye stimulates production of inflammatory cytokines and MMP-9 and activates MAPK signaling pathways on the ocular surface.* Invest Ophthalmol Vis Sci, 2004. **45**(12): p. 4293-301.
140. Chauhan, S.K. and R. Dana, *Role of Th17 cells in the immunopathogenesis of dry eye disease.* Mucosal Immunol, 2009. **2**(4): p. 375-6.
141. Benitez-Del-Castillo, J.M., M.C. Acosta, M.A. Wassfi, D. Diaz-Valle, J.A. Gegundez, C. Fernandez and J. Garcia-Sanchez, *Relation between corneal innervation with confocal microscopy and corneal sensitivity with noncontact esthesiometry in patients with dry eye.* Invest Ophthalmol Vis Sci, 2007. **48**(1): p. 173-81.
142. Leiper, L.J., J. Ou, P. Walczysko, R. Kucerova, D.N. Lavery, J.D. West and J.M. Collinson, *Control of patterns of corneal innervation by Pax6.* Invest Ophthalmol Vis Sci, 2009. **50**(3): p. 1122-8.
143. Bonini, S., P. Rama, D. Olzi and A. Lambiase, *Neurotrophic keratitis.* Eye (Lond), 2003. **17**(8): p. 989-95.
144. Li, H., W. Xie, J.A. Strong and J.M. Zhang, *Systemic antiinflammatory corticosteroid reduces mechanical pain behavior, sympathetic sprouting, and elevation of proinflammatory cytokines in a rat model of neuropathic pain.* Anesthesiology, 2007. **107**(3): p. 469-77.
145. Cosar, C.B., E.J. Cohen, C.J. Rapuano, M. Maus, R.P. Penne, J.C. Flanagan and P.R. Laibson, *Tarsorrhaphy: clinical experience from a cornea practice.* Cornea, 2001. **20**(8): p. 787-91.
146. Belmonte, C., A. Aracil, M.C. Acosta, C. Luna and J. Gallar, *Nerves and sensations from the eye surface.* Ocul Surf, 2004. **2**(4): p. 248-53.
147. Ueno, H., G. Ferrari, T. Hattori, D.R. Saban, K.R. Katikireddy, S.K. Chauhan and R. Dana, *Dependence of corneal stem/progenitor cells on ocular surface innervation.* Invest Ophthalmol Vis Sci, 2012. **53**(2): p. 867-72.

148. Nakamura, M., T. Nishida, K. Ofuji, T.W. Reid, M.J. Mannis and C.J. Murphy, *Synergistic effect of substance P with epidermal growth factor on epithelial migration in rabbit cornea.* Exp Eye Res, 1997. **65**(3): p. 321-9.
149. Blanco, T. and D.R. Saban, *The Cornea Has "the Nerve" to Encourage Immune Rejection.* Am J Transplant, 2015. **15**(6): p. 1453-4.
150. Nguyen, D.T., O. D.P. and M. G.F., *The Pathophysiologic Basis for Wound Healing and Cutaneous Regeneration.* Biomaterials For Treating Skin Loss, 2009. **Chapter 4**: p. 25-57.
151. Wilson, S.E., R.R. Mohan, J.W. Hong, J.S. Lee, R. Choi and R.R. Mohan, *The wound healing response after laser in situ keratomileusis and photorefractive keratectomy: elusive control of biological variability and effect on custom laser vision correction.* Arch Ophthalmol, 2001. **119**(6): p. 889-96.
152. Wilson, S.E., R.R. Mohan, R.R. Mohan, R. Ambrosio, Jr., J. Hong and J. Lee, *The corneal wound healing response: cytokine-mediated interaction of the epithelium, stroma, and inflammatory cells.* Prog Retin Eye Res, 2001. **20**(5): p. 625-37.
153. Wilson, S.E., R.R. Mohan, A.E. Hutcheon, R.R. Mohan, R. Ambrosio, J.D. Zieske, J. Hong and J. Lee, *Effect of ectopic epithelial tissue within the stroma on keratocyte apoptosis, mitosis, and myofibroblast transformation.* Exp Eye Res, 2003. **76**(2): p. 193-201.
154. Power, W.J., A.H. Kaufman, J. Merayo-Lloves, V. Arrunategui-Correa and C.S. Foster, *Expression of collagens I, III, IV and V mRNA in excimer wounded rat cornea: analysis by semi-quantitative PCR.* Curr Eye Res, 1995. **14**(10): p. 879-86.
155. Blanco-Mezquita, T., L. Espandar, R. Torres, A. Alvarez-Barcia, R. Cantalapiedra-Rodriguez, C. Martinez-Garcia and J. Merayo-Lloves, *Does mitomycin C cause toxicity in the cornea after photorefractive keratectomy? A comparative wound-healing study in a refractive surgery animal model.* Cornea, 2014. **33**(11): p. 1225-31.
156. Blanco-Mezquita, T., C. Martinez-Garcia, R. Proenca, J.D. Zieske, S. Bonini, A. Lambiase and J. Merayo-Lloves, *Nerve growth factor promotes corneal epithelial migration by enhancing expression of matrix metalloprotease-9.* Invest Ophthalmol Vis Sci, 2013. **54**(6): p. 3880-90.
157. Martinez-Garcia, M.C., J. Merayo-Lloves, T. Blanco-Mezquita and S. Mar-Sardana, *Wound healing following refractive surgery in hens.* Exp Eye Res, 2006. **83**(4): p. 728-35.
158. Del Pero, R.A., J.E. Gigstad, A.D. Roberts, G.K. Klintworth, C.A. Martin, F.A. L'Esperance, Jr. and D.M. Taylor, *A refractive and histopathologic study of excimer laser keratectomy in primates.* Am J Ophthalmol, 1990. **109**(4): p. 419-29.

159. Coassin, M., A. Lambiase, N. Costa, A. De Gregorio, R. Sgrulletta, M. Sacchetti, L. Aloe and S. Bonini, *Efficacy of topical nerve growth factor treatment in dogs affected by dry eye.* Graefes Arch Clin Exp Ophthalmol, 2005. **243**(2): p. 151-5.
160. Woo, H.M., E. Bentley, S.F. Campbell, C.F. Marfurt and C.J. Murphy, *Nerve growth factor and corneal wound healing in dogs.* Exp Eye Res, 2005. **80**(5): p. 633-42.
161. Mohan, R.R., W.M. Stapleton, S. Sinha, M.V. Netto and S.E. Wilson, *A novel method for generating corneal haze in anterior stroma of the mouse eye with the excimer laser.* Exp Eye Res, 2008. **86**(2): p. 235-40.
162. Stapleton, W.M., S.S. Chaurasia, F.W. Medeiros, R.R. Mohan, S. Sinha and S.E. Wilson, *Topical interleukin-1 receptor antagonist inhibits inflammatory cell infiltration into the cornea.* Exp Eye Res, 2008. **86**(5): p. 753-7.
163. Gibson, D.J., L. Pi, S. Sriram, C. Mao, B.E. Petersen, E.W. Scott, A. Leask and G.S. Schultz, *Conditional knockout of CTGF affects corneal wound healing.* Invest Ophthalmol Vis Sci, 2014. **55**(4): p. 2062-70.
164. Ksander, B.R., P.E. Kolovou, B.J. Wilson, K.R. Saab, Q. Guo, J. Ma, S.P. McGuire, M.S. Gregory, W.J. Vincent, V.L. Perez, F. Cruz-Guilloty, W.W. Kao, M.K. Call, B.A. Tucker, Q. Zhan, G.F. Murphy, K.L. Lathrop, C. Alt, L.J. Mortensen, C.P. Lin, J.D. Zieske, M.H. Frank and N.Y. Frank, *ABCB5 is a limbal stem cell gene required for corneal development and repair.* Nature, 2014. **511**(7509): p. 353-7.
165. Okada, Y., K. Shirai, P.S. Reinach, A. Kitano-Izutani, M. Miyajima, K.C. Flanders, J.V. Jester, M. Tominaga and S. Saika, *TRPA1 is required for TGF-beta signaling and its loss blocks inflammatory fibrosis in mouse corneal stroma.* Lab Invest, 2014. **94**(9): p. 1030-41.
166. Pajoohesh-Ganji, A., S. Pal-Ghosh, S.J. Simmens and M.A. Stepp, *Integrins in slow-cycling corneal epithelial cells at the limbus in the mouse.* Stem Cells, 2006. **24**(4): p. 1075-86.
167. Stepp, M.A., *Corneal integrins and their functions.* Exp Eye Res, 2006. **83**(1): p. 3-15.
168. Clark, E.A. and J.S. Brugge, *Integrins and signal transduction pathways: the road taken.* Science, 1995. **268**(5208): p. 233-9.
169. Hynes, R.O., *Integrins: a family of cell surface receptors.* Cell, 1987. **48**(4): p. 549-54.
170. Ruoslahti, E. and M.D. Pierschbacher, *New perspectives in cell adhesion: RGD and integrins.* Science, 1987. **238**(4826): p. 491-7.
171. Breuss, J.M., J. Gallo, H.M. DeLisser, I.V. Klimanskaya, H.G. Folkesson, J.F. Pittet, S.L. Nishimura, K. Aldape, D.V. Landers, W. Carpenter and et al., *Expression of the beta 6 integrin subunit in development, neoplasia and tissue*

repair suggests a role in epithelial remodeling. J Cell Sci, 1995. **108 (Pt 6)**: p. 2241-51.
172. Breuss, J.M., N. Gillett, L. Lu, D. Sheppard and R. Pytela, *Restricted distribution of integrin beta 6 mRNA in primate epithelial tissues.* J Histochem Cytochem, 1993. **41**(10): p. 1521-7.
173. Ghannad, F., D. Nica, M.I. Fulle, D. Grenier, E.E. Putnins, S. Johnston, A. Eslami, L. Koivisto, G. Jiang, M.D. McKee, L. Hakkinen and H. Larjava, *Absence of alphavbeta6 integrin is linked to initiation and progression of periodontal disease.* Am J Pathol, 2008. **172**(5): p. 1271-86.
174. Huang, X.Z., J.F. Wu, D. Cass, D.J. Erle, D. Corry, S.G. Young, R.V. Farese, Jr. and D. Sheppard, *Inactivation of the integrin beta 6 subunit gene reveals a role of epithelial integrins in regulating inflammation in the lung and skin.* J Cell Biol, 1996. **133**(4): p. 921-8.
175. AlDahlawi, S., A. Eslami, L. Hakkinen and H.S. Larjava, *The alphavbeta6 integrin plays a role in compromised epidermal wound healing.* Wound Repair Regen, 2006. **14**(3): p. 289-97.
176. Munger, J.S., X. Huang, H. Kawakatsu, M.J. Griffiths, S.L. Dalton, J. Wu, J.F. Pittet, N. Kaminski, C. Garat, M.A. Matthay, D.B. Rifkin and D. Sheppard, *The integrin alpha v beta 6 binds and activates latent TGF beta 1: a mechanism for regulating pulmonary inflammation and fibrosis.* Cell, 1999. **96**(3): p. 319-28.
177. Ljubimov, A.V., M. Saghizadeh, R. Pytela, D. Sheppard and M.C. Kenney, *Increased expression of tenascin-C-binding epithelial integrins in human bullous keratopathy corneas.* J Histochem Cytochem, 2001. **49**(11): p. 1341-50.
178. Hutcheon, A.E., X.Q. Guo, M.A. Stepp, K.J. Simon, P.H. Weinreb, S.M. Violette and J.D. Zieske, *Effect of wound type on Smad 2 and 4 translocation.* Invest Ophthalmol Vis Sci, 2005. **46**(7): p. 2362-8.
179. Stepp, M.A. and L. Zhu, *Upregulation of alpha 9 integrin and tenascin during epithelial regeneration after debridement in the cornea.* J Histochem Cytochem, 1997. **45**(2): p. 189-201.
180. Prieto, A.L., G.M. Edelman and K.L. Crossin, *Multiple integrins mediate cell attachment to cytotactin/tenascin.* Proc Natl Acad Sci U S A, 1993. **90**(21): p. 10154-8.
181. Annes, J.P., D.B. Rifkin and J.S. Munger, *The integrin alphaVbeta6 binds and activates latent TGFbeta3.* FEBS Lett, 2002. **511**(1-3): p. 65-8.
182. Munger, J.S., J.G. Harpel, F.G. Giancotti and D.B. Rifkin, *Interactions between growth factors and integrins: latent forms of transforming growth factor-beta are ligands for the integrin alphavbeta1.* Mol Biol Cell, 1998. **9**(9): p. 2627-38.
183. Aluwihare, P. and J.S. Munger, *What the lung has taught us about latent TGF-beta activation.* Am J Respir Cell Mol Biol, 2008. **39**(5): p. 499-502.

184. Sheppard, D., *Integrin-mediated activation of latent transforming growth factor beta.* Cancer Metastasis Rev, 2005. **24**(3): p. 395-402.
185. Shi, M., J. Zhu, R. Wang, X. Chen, L. Mi, T. Walz and T.A. Springer, *Latent TGF-beta structure and activation.* Nature, 2011. **474**(7351): p. 343-9.
186. Wipff, P.J. and B. Hinz, *Integrins and the activation of latent transforming growth factor beta1 - an intimate relationship.* Eur J Cell Biol, 2008. **87**(8-9): p. 601-15.
187. Aluwihare, P., Z. Mu, Z. Zhao, D. Yu, P.H. Weinreb, G.S. Horan, S.M. Violette and J.S. Munger, *Mice that lack activity of alphavbeta6- and alphavbeta8-integrins reproduce the abnormalities of Tgfb1- and Tgfb3-null mice.* J Cell Sci, 2009. **122**(Pt 2): p. 227-32.
188. Blanco-Mezquita, J.T., A.E. Hutcheon, M.A. Stepp and J.D. Zieske, *alphaVbeta6 integrin promotes corneal wound healing.* Invest Ophthalmol Vis Sci, 2011. **52**(11): p. 8505-13.
189. Bornstein, P., *Thrombospondins as matricellular modulators of cell function.* J Clin Invest, 2001. **107**(8): p. 929-34.
190. Carlson, C.B., J. Lawler and D.F. Mosher, *Structures of thrombospondins.* Cell Mol Life Sci, 2008. **65**(5): p. 672-86.
191. Baenziger, N.L., G.N. Brodie and P.W. Majerus, *A thrombin-sensitive protein of human platelet membranes.* Proc Natl Acad Sci U S A, 1971. **68**(1): p. 240-3.
192. Lawler, J., *The functions of thrombospondin-1 and-2.* Curr Opin Cell Biol, 2000. **12**(5): p. 634-40.
193. Leung, L.L., *Role of thrombospondin in platelet aggregation.* J Clin Invest, 1984. **74**(5): p. 1764-72.
194. Murphy-Ullrich, J.E., S. Gurusiddappa, W.A. Frazier and M. Hook, *Heparin-binding peptides from thrombospondins 1 and 2 contain focal adhesion-labilizing activity.* J Biol Chem, 1993. **268**(35): p. 26784-9.
195. Sheibani, N. and W.A. Frazier, *Thrombospondin-1, PECAM-1, and regulation of angiogenesis.* Histol Histopathol, 1999. **14**(1): p. 285-94.
196. Taraboletti, G., D.D. Roberts and L.A. Liotta, *Thrombospondin-induced tumor cell migration: haptotaxis and chemotaxis are mediated by different molecular domains.* J Cell Biol, 1987. **105**(5): p. 2409-15.
197. Darby, I., O. Skalli and G. Gabbiani, *Alpha-smooth muscle actin is transiently expressed by myofibroblasts during experimental wound healing.* Lab Invest, 1990. **63**(1): p. 21-9.
198. Desmouliere, A., A. Geinoz, F. Gabbiani and G. Gabbiani, *Transforming growth factor-beta 1 induces alpha-smooth muscle actin expression in granulation tissue myofibroblasts and in quiescent and growing cultured fibroblasts.* J Cell Biol, 1993. **122**(1): p. 103-11.

199. Friedman, S.L., *Seminars in medicine of the Beth Israel Hospital, Boston. The cellular basis of hepatic fibrosis. Mechanisms and treatment strategies.* N Engl J Med, 1993. **328**(25): p. 1828-35.
200. Murphy-Ullrich, J.E., S. Schultz-Cherry and M. Hook, *Transforming growth factor-beta complexes with thrombospondin.* Mol Biol Cell, 1992. **3**(2): p. 181-8.
201. Agah, A., T.R. Kyriakides, J. Lawler and P. Bornstein, *The lack of thrombospondin-1 (TSP1) dictates the course of wound healing in double-TSP1/TSP2-null mice.* Am J Pathol, 2002. **161**(3): p. 831-9.
202. Streit, M., P. Velasco, L. Riccardi, L. Spencer, L.F. Brown, L. Janes, B. Lange-Asschenfeldt, K. Yano, T. Hawighorst, L. Iruela-Arispe and M. Detmar, *Thrombospondin-1 suppresses wound healing and granulation tissue formation in the skin of transgenic mice.* EMBO J, 2000. **19**(13): p. 3272-82.
203. Hiscott, P., B. Seitz, U. Schlotzer-Schrehardt and G.O. Naumann, *Immunolocalisation of thrombospondin 1 in human, bovine and rabbit cornea.* Cell Tissue Res, 1997. **289**(2): p. 307-10.
204. Matsuba, M., A.E. Hutcheon and J.D. Zieske, *Localization of thrombospondin-1 and myofibroblasts during corneal wound repair.* Exp Eye Res, 2011. **93**(4): p. 534-40.
205. Sekiyama, E., T. Nakamura, L.J. Cooper, S. Kawasaki, J. Hamuro, N.J. Fullwood and S. Kinoshita, *Unique distribution of thrombospondin-1 in human ocular surface epithelium.* Invest Ophthalmol Vis Sci, 2006. **47**(4): p. 1352-8.
206. Cao, Z., H.K. Wu, A. Bruce, K. Wollenberg and N. Panjwani, *Detection of differentially expressed genes in healing mouse corneas, using cDNA microarrays.* Invest Ophthalmol Vis Sci, 2002. **43**(9): p. 2897-904.
207. Hiscott, P., D. Armstrong, M. Batterbury and S. Kaye, *Repair in avascular tissues: fibrosis in the transparent structures of the eye and thrombospondin 1.* Histol Histopathol, 1999. **14**(4): p. 1309-20.
208. Uno, K., H. Hayashi, M. Kuroki, H. Uchida, Y. Yamauchi, M. Kuroki and K. Oshima, *Thrombospondin-1 accelerates wound healing of corneal epithelia.* Biochem Biophys Res Commun, 2004. **315**(4): p. 928-34.
209. Uno, K., M. Kuroki, H. Hayashi, H. Uchida, M. Kuroki and K. Oshima, *Impairment of thrombospondin-1 expression during epithelial wound healing in corneas of vitamin A-deficient mice.* Histol Histopathol, 2005. **20**(2): p. 493-9.
210. Scheef, E.A., Q. Huang, S. Wang, C.M. Sorenson and N. Sheibani, *Isolation and characterization of corneal endothelial cells from wild type and thrombospondin-1 deficient mice.* Mol Vis, 2007. **13**: p. 1483-95.

211. Munjal, I.D., D.R. Crawford, D.A. Blake, M.D. Sabet and S.R. Gordon, *Thrombospondin: biosynthesis, distribution, and changes associated with wound repair in corneal endothelium.* Eur J Cell Biol, 1990. **52**(2): p. 252-63.
212. Bornstein, P., *Thrombospondins function as regulators of angiogenesis.* J Cell Commun Signal, 2009. **3**(3-4): p. 189-200.
213. Young, G.D. and J.E. Murphy-Ullrich, *Molecular interactions that confer latency to transforming growth factor-beta.* J Biol Chem, 2004. **279**(36): p. 38032-9.
214. Jester, J.V., P.A. Barry-Lane, W.M. Petroll, D.R. Olsen and H.D. Cavanagh, *Inhibition of corneal fibrosis by topical application of blocking antibodies to TGF beta in the rabbit.* Cornea, 1997. **16**(2): p. 177-87.
215. Jester, J.V., W.M. Petroll and H.D. Cavanagh, *Corneal stromal wound healing in refractive surgery: the role of myofibroblasts.* Prog Retin Eye Res, 1999. **18**(3): p. 311-56.
216. Moller-Pedersen, T., H.D. Cavanagh, W.M. Petroll and J.V. Jester, *Corneal haze development after PRK is regulated by volume of stromal tissue removal.* Cornea, 1998. **17**(6): p. 627-39.
217. Barcellos-Hoff, M.H., *Latency and activation in the control of TGF-beta.* J Mammary Gland Biol Neoplasia, 1996. **1**(4): p. 353-63.
218. Blanco-Mezquita, J.T., A.E. Hutcheon and J.D. Zieske, *Role of thrombospondin-1 in repair of penetrating corneal wounds.* Invest Ophthalmol Vis Sci, 2013. **54**(9): p. 6262-8.
219. Nowotschin, S., P. Xenopoulos, N. Schrode and A.K. Hadjantonakis, *A bright single-cell resolution live imaging reporter of Notch signaling in the mouse.* BMC Dev Biol, 2013. **13**: p. 15.
220. Lee, H.-S., D. Hos, T. Blanco, F. Bock, N.J. Reyes, R. Mathew, C. Cursiefen, R. Dana and D.R. Saban, *Involvement of corneal lymphangiogenesis in a mouse model of allergic eye disease.* IOVS, 2015.
221. Parra, A., R. Madrid, D. Echevarria, S. del Olmo, C. Morenilla-Palao, M.C. Acosta, J. Gallar, A. Dhaka, F. Viana and C. Belmonte, *Ocular surface wetness is regulated by TRPM8-dependent cold thermoreceptors of the cornea.* Nat Med, 2010. **16**(12): p. 1396-9.
222. Chang, S.Y., H.J. Ko and M.N. Kweon, *Mucosal dendritic cells shape mucosal immunity.* Exp Mol Med, 2014. **46**: p. e84.
223. Limatola, C. and R.M. Ransohoff, *Modulating neurotoxicity through CX3CL1/CX3CR1 signaling.* Front Cell Neurosci, 2014. **8**: p. 229.
224. Kezic, J., H. Xu, H.R. Chinnery, C.C. Murphy and P.G. McMenamin, *Retinal microglia and uveal tract dendritic cells and macrophages are not CX3CR1 dependent in their recruitment and distribution in the young mouse eye.* Invest Ophthalmol Vis Sci, 2008. **49**(4): p. 1599-608.

225. Soos, T.J., T.N. Sims, L. Barisoni, K. Lin, D.R. Littman, M.L. Dustin and P.J. Nelson, *CX3CR1+ interstitial dendritic cells form a contiguous network throughout the entire kidney.* Kidney Int, 2006. **70**(3): p. 591-6.
226. Chen, W., K. Hara, Q. Tian, K. Zhao and T. Yoshitomi, *Existence of small slow-cycling Langerhans cells in the limbal basal epithelium that express ABCG2.* Exp Eye Res, 2007. **84**(4): p. 626-34.
227. Lee, E.J., J.T. Rosenbaum and S.R. Planck, *Epifluorescence intravital microscopy of murine corneal dendritic cells.* Invest Ophthalmol Vis Sci, 2010. **51**(4): p. 2101-8.
228. Niederkorn, J.Y., J.S. Peeler and J. Mellon, *Phagocytosis of particulate antigens by corneal epithelial cells stimulates interleukin-1 secretion and migration of Langerhans cells into the central cornea.* Reg Immunol, 1989. **2**(2): p. 83-90.
229. Steven, P., F. Bock, G. Huttmann and C. Cursiefen, *Intravital two-photon microscopy of immune cell dynamics in corneal lymphatic vessels.* PLoS One, 2011. **6**(10): p. e26253.
230. Sauer, B., *Functional expression of the cre-lox site-specific recombination system in the yeast Saccharomyces cerevisiae.* Mol Cell Biol, 1987. **7**(6): p. 2087-96.
231. Miller, R.L., *Transgenic mice: beyond the knockout.* Am J Physiol Renal Physiol, 2011. **300**(2): p. F291-300.
232. M., G.-M., *Über Elementarakte mit zwei Quantensprüngen.* Annals of Physics 1931. **9**(3): p. 273–95.
233. Zipfel, W.R., R.M. Williams and W.W. Webb, *Nonlinear magic: multiphoton microscopy in the biosciences.* Nat Biotechnol, 2003. **21**(11): p. 1369-77.
234. Kaminer, I., J. Nemirovsky and M. Segev, *Optimizing 3D multiphoton fluorescence microscopy.* Opt Lett, 2013. **38**(19): p. 3945-8.
235. Williams, R.M., W.R. Zipfel and W.W. Webb, *Multiphoton microscopy in biological research.* Curr Opin Chem Biol, 2001. **5**(5): p. 603-8.
236. Xu, C., W. Zipfel, J.B. Shear, R.M. Williams and W.W. Webb, *Multiphoton fluorescence excitation: new spectral windows for biological nonlinear microscopy.* Proc Natl Acad Sci U S A, 1996. **93**(20): p. 10763-8.
237. Zipfel, W.R., R.M. Williams, R. Christie, A.Y. Nikitin, B.T. Hyman and W.W. Webb, *Live tissue intrinsic emission microscopy using multiphoton-excited native fluorescence and second harmonic generation.* Proc Natl Acad Sci U S A, 2003. **100**(12): p. 7075-80.
238. Abella, I.D., *Optical Double-Photon Absorption in Cesium Vapor.* Physical Review Letters 1962. **9**(11): p. 453–455.
239. Tang, S., Y. Zhou, K.K. Chan and T. Lai, *Multiscale multimodal imaging with multiphoton microscopy and optical coherence tomography.* Opt Lett, 2011. **36**(24): p. 4800-2.

240. Helmchen, F. and W. Denk, *Deep tissue two-photon microscopy.* Nat Methods, 2005. **2**(12): p. 932-40.
241. Cahalan, M.D., I. Parker, S.H. Wei and M.J. Miller, *Two-photon tissue imaging: seeing the immune system in a fresh light.* Nat Rev Immunol, 2002. **2**(11): p. 872-80.
242. Piston, D.W., T.J. Fellers and M.W. Davidson, *Fundamentals and Applications in Multiphoton Excitation Microscopy.* 2013.
243. Ishii, N., S. Adachi, Y. Nomura, A. Kosuge, Y. Kobayashi, T. Kanai, J. Itatani and S. Watanabe, *Generation of soft x-ray and water window harmonics using a few-cycle, phase-locked, optical parametric chirped-pulse amplifier.* Opt Lett, 2012. **37**(1): p. 97-9.
244. Eisenthal, K.B., *Second harmonic spectroscopy of aqueous nano- and microparticle interfaces.* Chem Rev, 2006. **106**(4): p. 1462-77.
245. Lai, T.Y.C., *Corneal visualization and characterization for applications in ophthalmology using optical imaging* Doctoral Thesis, 2014.
246. Masihzadeh, O., T.C. Lei, D.A. Ammar, M.Y. Kahook and E.A. Gibson, *A multiphoton microscope platform for imaging the mouse eye.* Mol Vis, 2012. **18**: p. 1840-8.

Síntesis General

JUSTIFICACIÓN

La córnea es el órgano más externo del sistema visual en contacto con el medio ambiente con dos funciones fundamentales: por un lado actúa como barrera protectora del sistema frente al medio externo, y por otro, es el elemento óptico primario del ojo. La córnea se define como un órgano transparente, avascular y con privilegio inmune. Además, la córnea se caracteriza por su elasticidad y resistencia mecánica [1]. En la parte más externa, dispone de un epitelio estratificado no queratinizado que sirve de barrera primaria del medio exterior. El epitelio está en contacto con la película lagrimal que le confiere una superficie lisa e hidrofóbica que por un lado la protege frente a la invasión de patógenos y por otro forma un frente raso a la entrada de la luz. El epitelio descansa en una lamina basal que lo ancla al estroma [2, 3]. A continuación se encuentra la capa de Bowman formada por colágeno muy organizado. Esta membrana varía en grosor en diferentes especies y está ausente en otras [4]. La mayor parte del órgano lo conforma el estroma formado por queratocitos (fibroblastos en estado quiescente) y colágeno perfectamente organizado. El estroma compone el 90% del grosor corneal otorgándole a la córnea su carácter refractivo [5]. En la parte posterior de la córnea se encuentra la membrana de Descemet o membrana basal sobre la que descansa el endotelio [5]. El endotelio está formado por una monocapa de células endoteliales que en contacto con la cámara anterior mantienen el balance hídrico y por tanto la transparencia de la córnea [6].

Además de esta estructura básica, la córnea está densamente inervada con fibras procedentes de la rama oftálmica del trigémino [7]. La córnea a su vez alberga una población residente de células inmunitarias de origen mieloide, que si bien juegan un

papel primordial en la defensa y en la respuesta inmunitaria ante situaciones de peligro, su función esta muy poco descrita [8]. En este escenario la córnea se entiende como un órgano extremadamente complejo compuesto por diferentes tipos de tejidos cuya homeostasis está dirigida a mantener en la integridad del sistema visual, la refracción y la transparencia.

Por ser un órgano externo, la córnea está continuamente sometida a todo tipo de agresiones que pueden afectar a la visión. El sistema visual ha desarrollado un mecanismo único de defensa externa basado en una rápida respuesta (parpadeo, lagrimeo, secreciones enzimáticas conjuntivales) ante la agresión sufrida protegiendo la integridad y la transparencia [9]. Cuando la agresión afecta a la integridad de la córnea, ésta responde con un rápido mecanismo de cicatrización destinado a reparar su estructura y función que en la mayoría de los casos no tiene consecuencias negativas [10]. Sin embargo, otras situaciones causadas por agresiones mayores como quemaduras, causticaciones, alergias, traumas, etc., causan lesiones irreparables que necesitan de un trasplante de córnea [11]. Por otro lado, la existencia de patologías como el queratocono, las distrofias de la membrana basal del epitelio, las ulceras neurotróficas, las distrofias basales del endotelio, las queratoconjuntivitis alérgicas o el ojo seco, cursan con una etiología poco conocida que en muchos casos hacen que el trasplante del órgano sea la única opción para estos pacientes [12].

El hecho de ser un órgano expuesto al medio exterior, hace que la córnea sea diana para diferentes patógenos que provocan diferentes tipos de queratitis o inflamaciones. Unas son causadas por amebas como la Acantamoeba y afectan sobre todo a usuarios de lentes de contacto. Otras son de origen bacteriano como *Staphylococcus aureus* o *Pseudomonas aeruginosa*, de origen fúngico causadas por Fusarium o de origen vírico como *Herpes simplex* o *Herpes zoster* [13, 14]. A la vez la superficie ocular se ve sometida a un ataque continuo de alérgenos. En la mayor parte de los casos sólo la conjuntiva o tejido mucoso que rodea a la córnea sufre el proceso inflamatorio o conjuntivitis alérgica,

pero en otros casos la inflamación compromete a la córnea causando queratoconjuntivitis alérgica [15].

Debido a la cirugía refractiva corneal así como el uso de lentes de contacto, la investigación en la patologías corneales se ha visto impulsada durante las últimas décadas. A su vez la cirugía refractiva ha aumentado la incidencia de patologías post-quirúrgicas como la pérdida de agudeza visual, halos, destellos, reflejos, sensación de cuerpos extraños y falta de lubricación. Otras complicaciones relacionadas con el proceso de cicatrización después de la cirugía, como los procesos fibróticos o la autodigestión, requieren frecuentemente del trasplante para recuperar la visión del paciente. Además estas mismas complicaciones, con menor incidencia, pueden aparecer después de una cirugía de cataratas [16, 17].

El trasplante de córnea es la técnica quirúrgica más frecuente en el mundo con una experiencia de más de 100 años desde que en 1905 se realizó el primer trasplante de córnea finalizado con éxito [18]. Desde que se fundó la Organización Nacional de Trasplantes (ONT) en el año 1989 en España, se han realizado unos 60.000 trasplantes de córnea (3.477 en el año 2013 según datos publicados por dicha organización). A pesar del gran número de queratoplastias realizadas cada año en todo el mundo, el trasplante sigue siendo una opción terapéutica compleja. Si bien el porcentaje de rechazo inmunológico es muy bajo, el número en si, es muy alto y además en muchos casos los pacientes son considerados de alto riesgo de rechazo y son excluidos del trasplante [19]. Así mismo, el trasplante es una opción de los países desarrollados no disponible en la mayoría de los países en vías de desarrollo.

En la actualidad no existen tratamientos que permitan la recuperación funcional de la córnea inflamada de forma crónica [20]. Los tratamientos disponibles sólo son paliativos de la sintomatología de las enfermedades. Por un lado las lágrimas artificiales, suplen la lágrima humana pero distan mucho de tener todas sus propiedades. Los inmunosupresores, que si bien se utilizan únicamente en casos muy sintomáticos, presentan graves efectos secundarios adversos asociados a su uso continuado [21].

En los últimos años se ha avanzado mucho en la búsqueda de alternativas terapéuticas que permitan la recuperación funcional de la córnea enferma, como el uso de materiales biopoliméricos y nanopartículas como sistemas de liberación controlada de fármacos [22, 23]. Sin embargo el trasplante de córnea [12] o técnicas alternativas como los segmentos intracorneales o el "cross-linking" del colágeno corneal (CXL), que frenan el avance de ectasias como el queratocono, son las técnicas más requeridas [24, 25]

Por otro lado, la medicina regenerativa se presenta como otra alternativa en las patologías corneales. Su uso se ha consolidado como paliativo de patologías como las úlceras neurotróficas, las disfunciones del limbo y otro tipo de alteraciones que causan una pérdida del epitelio corneal. Nuevos fármacos basados en derivados biológicos del organismo como el factor de crecimiento nervioso (NGF, "nerve growth factor") o el plasma rico en factores de crecimiento (PRGF, "plasma rich in growth factors") están dando buenos resultados [26, 27], sin embargo estos fármacos además del coste elevado suponen un uso prolongado paliativo que no resuelve, en si, la patología originaria.

Por este motivo, está justificado prestarle una atención prioritaria a la investigación de la córnea. Por ejemplo, el hecho de que la córnea sea un órgano con privilegio inmune que no reacciona ante la presencia de antígenos externos, así como debido a la baja incidencia de rechazo inmunológico, hizo creer por más de un siglo que la córnea estaba desprovista de células presentadoras de antígeno [28]. A pesar de los trabajos realizados en ratones durante la última década, fue el pasado año (2104) cuando se describió por primera vez una estratificación detallada de la población de células inmunitarias residentes en la córnea humana [8]. La presencia de vasos linfáticos en la parte periférica externa de la córnea ha sido otro hallazgo muy reciente [29]. Estos vasos linfáticos tienen un papel fundamental en los procesos inflamatorios pero su función no se conoce bien [30].

Por otro lado la córnea es el órgano periférico más inervado del cuerpo y a pesar de que la anatomía de los nervios corneales ha sido extensamente estudiada así como su fisiología, es todavía desconocida su función en la mayoría de las patologías [7]. Es por ello que la córnea, a día de hoy, es todavía considerada como un órgano compuesto por tejido

conjuntivo y epitelial, en el cual la mayoría de sus patologías permanecen sin resolverse. Esto indica que el funcionamiento de la córnea es todavía una incógnita en muchas de sus funciones.

El conocimiento básico de la etiología de las dolencias es fundamental para su tratamiento o desarrollo de nuevas estrategias tanto quirúrgicas como farmacológicas [31, 32]. La búsqueda de modelos animales que reproduzcan tanto las condiciones normales como anómalas de la córnea humana es imprescindible [31]. Si bien se ha usado varios modelos animales para el estudio de la córnea como el conejo [33], la gallina [34], la rata [35] o los primates [36]; es el ratón, en la actualidad, el modelo más aceptado. Además de presentar procesos de cicatrización similares [37] y patrones de inervación parecidos al humano [38], presentan una respuesta inflamatoria que se asemeja a la de la córnea humana [39, 40]. Por ejemplo, se ha observado recientemente en el ratón, que la pérdida del privilegio inmune que explica el rechazo del trasplante de córnea y el ojo seco, es debido a la proliferación de vasos linfáticos en la córnea y esto se comprobó en pacientes [29]. También, basándose en la estratificación de la población inmunitaria de la córnea del ratón, se ha descrito en la córnea normal [8]. Gracias al ratón, se ha ido describiendo durante la última década, la implicación las células inmunitarias en las diferentes patologías como el ojo seco, las infecciones o el rechazo al trasplante de córnea.

En esta necesidad de conocer el estado tanto normal como patológico de la córnea, el uso de ratones manipulados genéticamente es la mejor herramienta en la actualidad. Conociendo la patología, tanto en presencia como en ausencia de la proteína que codifica el gen insertado, mutado o eliminado, es posible definir el mecanismo desencadenante [41]. De esta manera es posible hacer un diagnóstico más preciso y una terapia dirigida más adecuada. Por otro lado con el uso creciente de ratones que expresan fluorescencia ante la expresión de una secuencia determinada (promotor, un locus etc.), permite conocer in situ y de forma inmediata la implicación de ese gen en una patología [41].

Por ser la córnea un órgano transparente, es posible estudiarla de forma no invasiva mediante el uso de microscopía *"intravital"* tanto confocal como de laser pulsado de

fentosegundos o multifotónico, sin necesidad de sacrificar al ratón y permitiendo un seguimiento continuado del mismo animal.

La experiencia adquirida en nuestro grupo, apoya la idea de usar ratones modificados genéticamente para el estudio de las patología corneales. A su vez, la implementación de nuevos sistemas de imagen *"intravital"*, como el microscopio confocal *"in vivo"* o el sistema de microscopía multifotónica, abren una vía totalmente nueva, no sólo en la forma de investigar, sino de como interpretar la córnea [42].

Al final de este trabajo se mostrará una visión de la córnea más evolucionada, donde además de los ya conocidos tejidos conjuntivo y epitelial, se pone de relieve como dos "supersistemas" (del inglés "supersystem") [43] nervioso e inmunitario interaccionan estocásticamente entre si. De esta manera, se presenta un modelo descriptivo de la córnea, como un órgano extremadamente complejo, que deberá tenerse en cuenta en el futuro para la comprensión de las diferentes patologías.

HIPOTESIS

1. Es posible estudiar la evolución de la cicatrización corneal y la aparición de patologías corneales derivadas mediante el uso de ratones modificados genéticamente.

2. Es posible introducir nuevas cepas de ratones modificados genéticamente que expresan fluorescencia y a su vez implementar nuevos sistemas de imagen *"intravital"* que permitan observar la córnea

3. Redefinir la córnea como un órgano en el que dos "supersistemas" (nervioso e inmunitario) interactúan de forma estocástica para mantener su homeostasis.

OBJETIVOS

Objetivo General:

Usar ratones modificados genéticamente e implementar nuevos sistemas de imagen como el microscopio confocal *"in vivo"* o el sistema de microscopía multifotónica *"intravital"* para el estudio de la fisiopatología de la córnea.

Objeticos específicos:

1. Estudiar la función de la integrina αVβ6 en el proceso de cicatrización del epitelio tras una lesión en la córnea en ratones carentes de la integrina β6 ($\beta6^{-/-}$) (**Capítulo 1**)

2. Investigar la función de la trombospondina-1 (THBS1) en el proceso de reparación corneal después de una lesión integral de todas las capas de la córnea (**Capítulo 2**)

3. Evaluar mediante el uso de microscopía confocal "*in vivo*" los cambios que se producen en la dinámica de las células inflamatorias de la superficie ocular, en un modelo de conjuntivitis alérgica (**Capítulo 3**)

4. Mediante el uso de un microscopio multifotónico, visualizar, mapear y estratificar de forma no invasiva la población residente de células de origen mieloide de la córnea, en ratones que expresan fluorescencia en el gen Cx3cr1 (**Capítulo 4**)

5. Mediante el uso de un microscopio multifotónico, redefinir la anatomía de los nervios corneales de forma no invasiva e "*in vivo*" en ratones que expresan fluorescencia en el gen Thy1(**Capítulo 5**)

6. Estudiar la relación entre el sistema nervioso periférico y el inmunitario en la córnea de ratón. Diseñar un ratón quimera que permita estudiar "*in vivo*", la interacción de ambos sistemas. (**Capítulo 6**)

7. Buscar nuevas aplicaciones del uso de la microscopía multifotónica no invasiva para el seguimiento *"in vivo"* de la regeneración corneal con células mesenquimales del tejido adiposo, para el seguimiento a tiempo real de sistemas de liberación de fármacos, observar agentes infecciosos o estudiar la repuesta a agentes tóxicos (**Capítulo 7**)

METODOLOGÍA

A continuación se describe la parte metodológica de forma general para todos los estudios realizados. Para una descripción más detallada del material, método y animales utilizados es necesario revisar los consecutivos capítulos en inglés de esta memoria. El detallado de la metodología no sigue un patrón cronológico de los capítulos, sino una descripción general.

1. Animales

1.1 Los siguientes ratones (*Mus musculus*) fueron alojados en un ambiente limpio de patógenos, en jaulas ventiladas en el animalario del "Schepens Eye Research Institute & Mass Eye and Ear Infirmary" (SERI&MEEI) en la Universidad de Harvard. Los ratones recibieron comida y agua "*ad libitum"*, permaneciendo al menos 3 días de cuarentena antes de la realización de cualquier experimento. La supervisión y cuidado de los ratones de realizó por el veterinario y el personal de dicho animalario. El estudio de los ratones se hizo de acuerdo con la normativa sobre el uso de animales de experimentación en investigación ocular de la "Association for Research in Vision and Ophthalmology" (ARVO). Todos los protocolos fuse aprobaron previamente por el Consejo para el uso de animales de investigación en el SERI&MEEI.

. Ratones normales adultos 129S2/SvPas (12-18 semanas de vida) (Taconic; Albany, NY) y **ratones 129S2/SvPas-β6$^{-/-}$** (generosamente ofrecidos por Jack Lawler, BIDMC/Harvard Medical School, Boston, MA) (***Capítulo 1***)

. Ratones adultos S129S2/SvPas (12-18 semanas de vida) (Jackson Laboratory; Bar Harbor, ME) y ratones y **129S2/SvPas-Thbs1^{tm1Hyn}/Thbs1^{tm1Hyn}** (Thbs1$^{-/-}$,

generosamente ofrecidos por el Dr. Jack Lawler, Beth Israel Deaconess Medical Center, Harvard Medical School, Boston, MA). Los ratones deficientes en THBS1 se generaron en células D3ES derivadas de la línea 129S2/SvPas. El alelo "knockout" es el Thbs1tm1Hyn (***Capítulo 2***)

. **Ratones** hembras adultas **C57BL/6** (8 semanas de vida) (Charles River Laboratories, Wilmington, MA) (***Capítulo 3***)

1.2 Los siguientes ratones fueron alojados en un ambiente limpio de patógenos, en jaulas ventiladas en el animalario del "Duke Eye Center" en la Universidad de Duke. Los ratones recibieron comida y agua "*ad libitum"*, permaneciendo al menos 3 días de cuarentena antes de la realización de cualquier experimento. La supervisión y cuidado de los ratones se realizó por el veterinario y el personal de dicho animalario. El estudio de los ratones se hizo de acuerdo con la normativa sobre el uso de animales de experimentación en investigación ocular de la "Association for Research in Vision and Ophthalmology" (ARVO). Todos los protocolos se aprobaron previamente por el Consejo para el uso de animales de investigación en el "Duke Eye Center " y la "Division of Laboratory Animal Resources" (DLAR) en la Universidad de Duke.

. **Ratones Cx3cr1^{EGFP}** "knockin" en el gen que expresa el receptor-1 de la quimiocina CX3C por EGFP (Cx3cr1^{EGFP} "knock-in mice"). Estos ratones Cx3cr1^{EGFP} expresan EGFP en monocitos, células dendríticias, "Natural Killers", macrófagos y microglía bajo el control del locus Cx3cr1. Los parentales (Jackson): machos y hembras Cx3cr1^{tm1Litt}/Cx3cr1^{+} (B6.129P2-Cx3cr1^{tm1Litt}) se cruzaron para generar homocigóticos Cx3cr1$^{EGFP/EGFP}$. Homocigóticos Cx3cr1$^{EGFP/EGFP}$ a su vez se cruzaron ratones C57BL/6 WT (Jackson) para general el homocigótico definitivo Cx3cr1$^{EGFP/WT}$, denominado aquí Cx3cr1^{EGFP} (***Capítulo 4 y 6***)

. Ratones CX3CR1^{Cre}. La actividad fluorescente enzimática de la proteína **Cre** se analizó usando ratones machos CX3CR1-Cre generados a partir de un cruce de 129/B6 ("Gene Expression Nervous System Atlas Project"), y cruzados de nuevo durante 12 generaciones por M.D. Gunn ("Departments of Immunology and Medicine, Duke University Medical Center") [44, 45]. Ratones hembras B6.Cg-Gt(ROSA)26Sor$^{tm14(CAG-tdTomato)Hze}$/J (denominados aquí RFP) ("Jackson Laboratories") o donados por M. D. Gunn; y ratones Rosa26R-CAG-fGFP (denominados aquí fGFP) [46], donados generosamente por B. L. Hogan ("Department of Cell Biology, Duke University Medical Center") se usaron como hembras. Posteriormente todos los ratones se mantuvieron y cruzaron en el laboratorio propio. Los ratones macho CX3CR1-Cre se cruzaron con ratones hembra fGFP, y en la progenie se verificó el genotipo CX3CR1$^{Cre/fGFP}$. De la misma manera ratones macho CX3CR1-Cre se cruzaron con hembras RFP y se verificó el genotipo CX3CR1$^{Cre\ RFP}$ (***Capítulo 4 y 6***)

. Ratones CX3CR1-YFP-CreER-RFP. Estos ratones fueron generados de la siguiente manera:

Los ratones macho (B6.129P2(Cg)-Cx3cr1tm2.1(cre/ERT)Litt/WganJ) codifican de forma inducible YFP y el dímero CreER bajo el control del promotor Cx3cr1. Los ratones Rosa-tdTomato (B6.Cg-Gt(ROSA)26Sortm14(CAG-tdTomato)Hze/J) contienen una secuencia insertada "loxP-flanked STOP" que previene la transcripción de la proteína fluorescente RFP (tdTomato) hasta que la secuencia de STOP sea removida en presencia de la enzima recombinasa Cre. Cuanto esto sucede la proteína RFP es expresada constitutivamente durante toda la vida de la célula independientemente de la expresión del promotor de Cx3cr1. Ambos líneas de ratones CX3CR1-YFP-CreER y Rosa-tdTomato poseen un "background C57BL/6" y se adquirieron de "Jackson Laboratories". El cruce de estas dos líneas homocigóticas resulta en una primera generación que contiene la secuencia Cx3cr1-YFP-CreER-tdTomato (CX3CR1-YFP-

CreER-RFP). El dímero CreER se puede escindir en presencia de tamoxifeno (ver más adelante) (***Capítulo 4***)

. Ratones B6.Cg-Tg(Thy1-YFP)16Jrs/J denominados aquí como Thy1.1-eYFP (Thy1-YFP) fueron generosamente donados por el Dr. Tseng (Tseng Lab, Duke Eye Center, Duke University). Estos ratones fueron generados siguiendo el protocolo descrito anteriormente [47] (***Capítulo 5 y 6***)

. Ratones C57BL/6J WT o BALB/c de 8 semanas se usaron como controles (Jackson laboratorios) (***Capítulo 4, 5 y 6***)

2. Anestesia y Eutanasia

Los ratones fueron anestesiados con una inyección intraperitoneal (IP) de ketamina (120mg/kg de peso) y xilacina (20 mg/kg de peso). Como anestesia tópica se utilizó una gota de anestésico doble clorhidrato de tetracaina (0´5%) y oxibuprocaina (1 mg). Después de cada cirugía ambos ojos fueron tratados con pomada triple antibiótica (vetropolicin). En los experimentos realizados '*in vivo*" con periodos largos de anestesia, se inyectó un flujo constante de 0.2-0.3 ml/h de una solución de 1ml of ketamina (120 mg/kg), 1 ml of xylacina (20 mg/kg), y 10 ml de cloruro sódico mediante un catéter intraperitoneal.

Los ratones fueron sacrificados por exposición en cámara de dióxido de carbono (CO_2) o por sobredosis de ketamina (120 mg/kg), 1 ml of xylacina (20 mg/kg), dependiendo del estado final del experimento.

3. Lesiones corneales:

3.1 Queratectomía y desbridamiento epitelial (*Capítulo 1*)

De forma breve: usando un trépano de 2 mm de diámetro se demarcó concéntricamente la córnea. Con una micropinza quirúrgica se retiró de forma manual un colgajo de tejido epitelio-estromal de 2 mm de diámetro y de aproximadamente 40μm de grosor.

El desbridamiento epitelial se realizó retirando el epitelio en la zona delimitada de 2 mm de diámetro con la ayuda de una espátula "Crescent" manteniendo la lámina basal del epitelio intacta.

3.2 Incisión penetrante (*Capítulo 2*)

Previo a la incisión, se aplicó una gota de atropina para dilatar la pupila. Con un cuchillo quirúrgico y en orientación nasal-temporal, se penetró el centro de la córnea con un corte de 1.5 mm de longitud.

4. Seguimiento

La evaluación clínica se realizó con la lámpara de hendidura con cámara digital incorporada. El seguimiento se realizó antes de la lesión, inmediatamente después, diariamente durante la primera semana y una vez cada 7 días hasta el final dependiendo de los estudios. Además el seguimiento con la lámpara de hendidura se hizo a todos y cada uno de los ratones utilizados en todos los estudios incorporados en la presente memoria.

4.1 Tiempo de cierre de la herida epitelial

El tiempo de cierre se evaluó con fluoresceína sódica cada 8 horas hasta que el epitelio estuvo completamente cerrado (***Capítulo 1***). La fluoresceína sódica es un colorante vital que es capaz de captar la luz en el espectro del azul y emitirla en el verde y así cuando es iluminada con luz azul, puede apreciarse un color verde intenso. Éste es un procedimiento colorimétrico sencillo e inocuo que permite poner en evidencia la mayoría de las erosiones corneales y visualizarlas fácilmente. Además la fluoresceína tiene la capacidad de unirse a las zonas de la córnea donde no hay epitelio y por tanto al teñir la córnea con fluoresceína e iluminar el ojo con luz azul, se pueden observar tanto las erosiones como las zonas desbridadas. Las fotografías se procesaron con el programa Image J de acceso universal (http://rsb.info.nih.gov/ij). El superficie se calculó acorde con la fórmula del área de una circunferencia: $A = \pi.r2$; donde A es el área y r es el radio (r = 1 en el ratón).

5. Modelo de Alergia Ocular (*Capítulo 3*)

5.1 Alosensibilización

La alergia ocular (conjuntivitis) se indujo en el ratón mediante inmunización activa con ovoalbúmina (OVA) (Sigma-Aldrich, St. Louis, MO). A los ratones se les administró una dosis intraperitoneal de 100 µg de OVA, 300 ng toxina pertussis (Sigma-Aldrich) y 1 mg de hidróxido de aluminio (Sigma-Aldrich) en PBS. Después de 14 días, se instiló una gota diaria de OVA (250 µg en PBS) en el ojo derecho de los ratones inmunizados durante 7 días. De la misa manera se instilo una gota de OVA en ratones sin inmunizar (**Figure A**)

5.2 Evaluación Clínica de la Alergia Ocular (*Capítulo 3*)

La evaluación de los signos clínicos de la alergia ocular se realizó a doble ciego por dos observadores independientes siguiendo el modelo descrito anteriormente [48], De forma breve: la evaluación se realizó diariamente después de 20 minutos, 6 y 24 horas posteriores a la instilación de OVA. Con la lámpara de hendidura se examinó los ratones midiendo cuatro parámetros independientes (edema palpebral, lagrimeo, quemosis y vasodilatación conjuntival o enrojecimiento (**Figure 1 B**). Cada parámetro se estimó en una escala de 0-3 (0 = ausencia; 3 = máximo) para alcanzar una suma total máxima de 12.

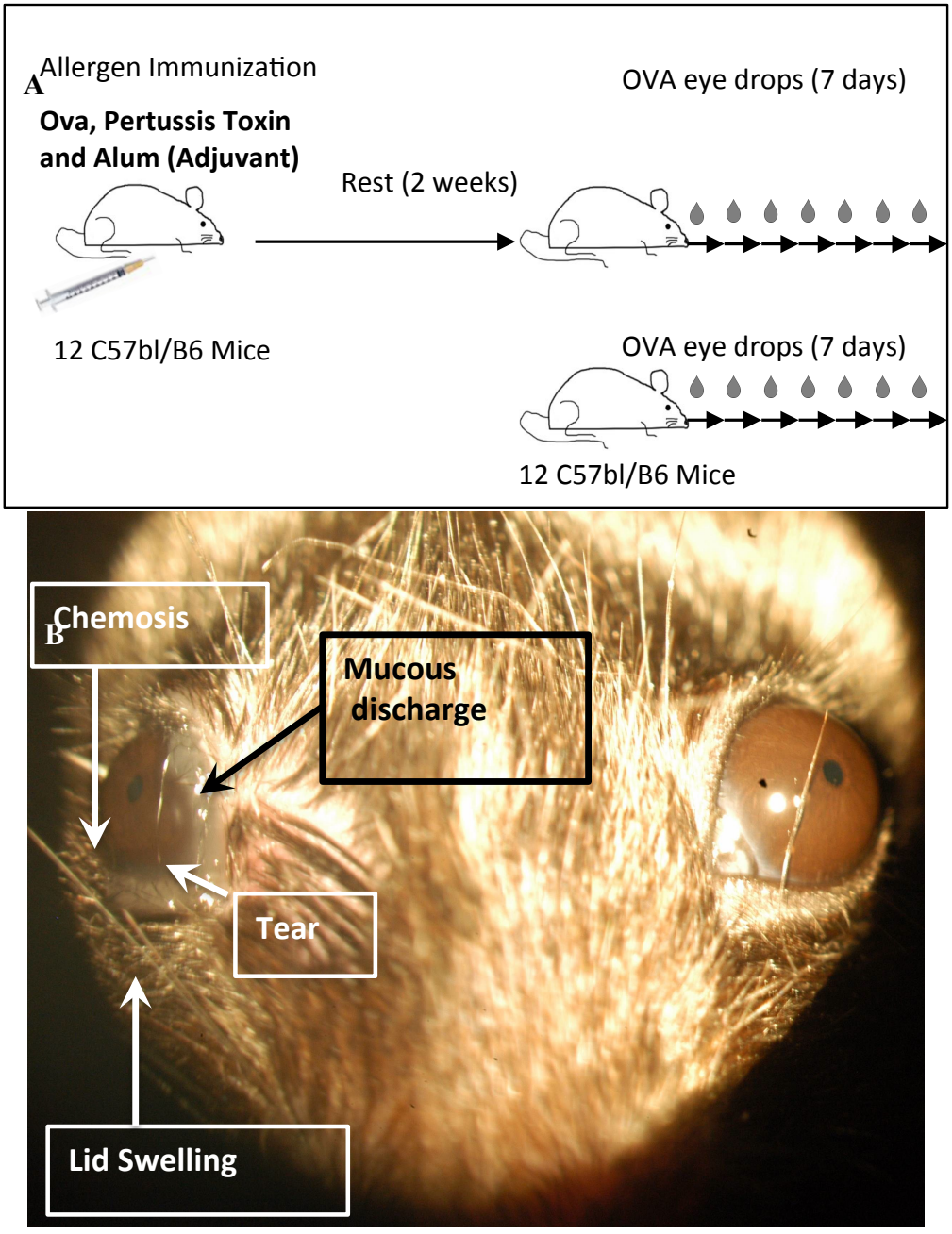

Figura 1: esquema de inmunización de los ratones (A) y síntomas clínicos (B)

6. Generación de ratones quimera (*Capítulos 5 y 6*)

6.1 Proceso de Irradiación

El proceso de irradiación se llevó a cabo en ratones receptores Cx3cr1$^{cre/RFP}$, Cx3cr1$^{cre/fGFP}$, Thy-1-YFP y C57BL/6 WT. Los ratones fueron letalmente irradiados en toda la superficie corporal (1050 cGy) en un irradiador modelo Mark I 68A Cs 137 (JL Shepherd and Associates in San Fernando, CA). La cabina del irradiador tiene unas medidas de 37cm x 30cm x 45cm. El gradiente de Cesio se elevó 15 cm desde la base de la cabina por medio de aire comprimido. En cada ciclo se introdujeron cinco ratones dentro de una caja cilíndrica de acrilato de 20 cm de diámetro. La caja se situó a 7.6 cm de altura sobre una plataforma giratoria (12 rpm) para asegurar el 100% de la irradiación a todos los animales. El tiempo de cada ciclo fue de 2 minutos y 13 segundos.

6.2 Trasplante de médula ósea y generación de quimeras (*Capítulos 5 y 6*)

La siguiente tabla muestra todas las combinaciones de ratones quiméricos generados para este trabajo. En los ratones donantes se recolectó los fémures y las tibias. Tras retirar las cabezas proximales y distales del hueso, la médula ósea fue extraída inyectando medio RPMI (LONZA) mediante una cánula de 27G. El extracto se fragmentó hasta la suspensión celular y se tamizó con un filtro de 70μm seguido de agitado con pipeta. Después de centrifugar (200g, 5 minutos, 4C), se procedió al contado celular con el método del azul tripán y el precipitado se diluyó en medio RPMI ($3x10^7$ células/mL).

Inmediatamente después de la irradiación, los ratones receptores recibieron ~$1x10^7$ células no purificadas del extracto de la médula ósea (300μL) a través de in inyección en el seno venoso retro-orbital. Posteriormente se administró tratamiento antibiótico ("Sulfamethoxazole and trimethoprim antibiotics"; SEPTRA, Hi-Tech Pharmacal Co., Amityville, NY) en el agua de bebida durante 4 semanas después de la irradiación.

Además los ratones recibieron comida suplementaria de alto contenido energético ("SuppliCal caloric supplement"; Henry Schein, Dublin, Ohio) hasta el final de los experimentos. Antes de ser examinados, los ratones se recuperaron de la irradiación al menos 4 semanas. El mismo animal fue examinado varias veces con intervalos de tiempo de una semana.

Receptor	Donante	Fenotipo transitorio	Fenotipo proyectado
Cx3cr1$^{cre/RFP}$	**Cx3cr1$^{cre/fGFP}$**	**Cx3cr1$^{cre/RFP}$/Cx3cr1$^{cre/fGFP}$**	**Cx3cr1$^{cre/fGFP}$**
Cx3cr1$^{cre/fGFP}$	**Cx3cr1$^{cre/RFP}$**	**Cx3cr1$^{cre/fGFP}$/Cx3cr1$^{cre/RFP}$**	**Cx3cr1$^{cre/RFP}$**
C57BL/6 WT	**Cx3cr1$^{cre/fGFP}$**	**Cx3cr1$^{cre/fGFP}$**	**Cx3cr1$^{cre/fGFP}$**
C57BL/6 WT	**Cx3cr1$^{cre/RFP}$**	**Cx3cr1$^{cre/RFP}$**	**C57BL6WT/Cx3cr1$^{cre/RFP}$**
Thy-1^{YFP}	**Cx3cr1$^{cre/RFP}$**	**Thy-1^{YFP}/Cx3cr1$^{cre/RFP}$**	**Thy-1^{YFP} /Cx3cr1$^{cre/RFP}$**

Tabla 1: combinaciones de ratones quimera generados en este trabajo

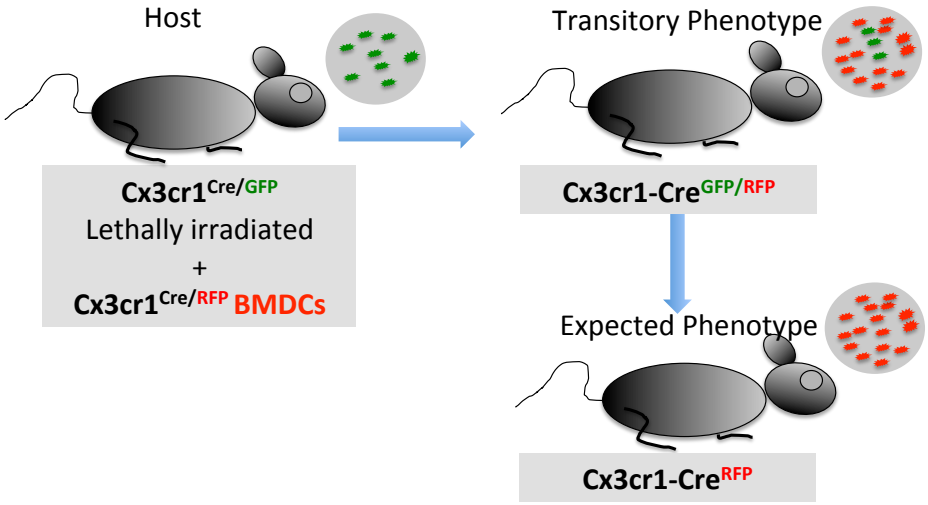

Figura 2: Generación de quimeras mediante irradiación de ratones receptores CX3CR1^{GFP} a los que se les trasplantó médula ósea de ratones CX3CR1$^{Cre/RFP}$

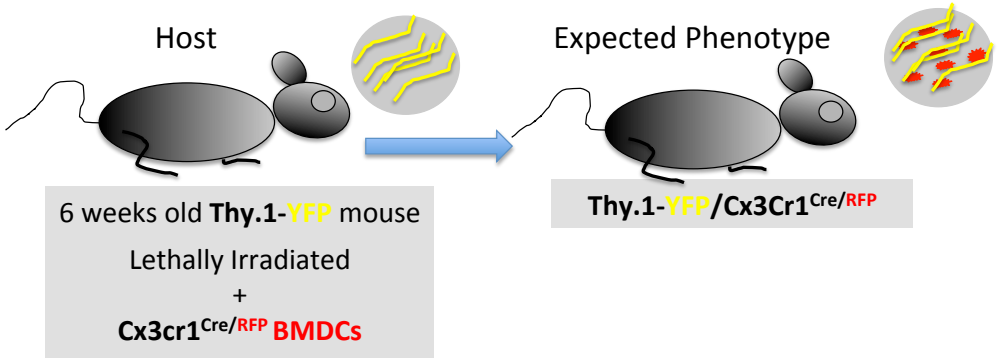

Figura 3: Generación de quimeras mediante irradiación de ratones receptores Thy-1^{YFP} a los que se les trasplantó médula ósea de ratones CX3CR1$^{Cre/RFP}$

7. "Fate mapping" de la población inmunitaria residente en córnea (*Capítulo 4*)

Para el estudio del origen de la población de las células residentes de la córnea, se utilizaron ratones CX3CR1-YFP-CreER-RFP. Estos ratones expresan YFP inducible bajo el promotor de Cx3cr1, así como el dímero formado por la enzima recombinasa Cre y el receptor de estrógeno (ER) en el citoplasma de la célula. En presencia de tamoxifeno, el dímero se disocia y la enzima Cre entra en el núcleo donde lleva a cabo su acción recombinasa induciendo la expresión constitutiva del gen reportero, en este caso "tdTomato" (RFP), durante el resto de la vida de la célula (**Ver capítulo 0**). En condiciones normales, estos ratones sólo expresan YFP inducible bajo el promotor de Cx3cr1, pero en presencia de tamoxifeno coexpresan además RFP de forma constitutiva independientemente de la expresión del promotor de Cx3cr1

Para este estudio se usaron ratones CX3CR1-YFP-CreER-RFP de 6 semanas que fueron evaluados previamente mediante microscopio multifotónico (ver más adelante). Posteriormente se inyectó de forma intraperitoneal 150ul de tamoxifeno (20mg/ml) en dos dosis consecutivas con 24 horas de separación. En los 6 meses posteriores los ratones fueron examinados "*in vivo*" dicho microscopio.

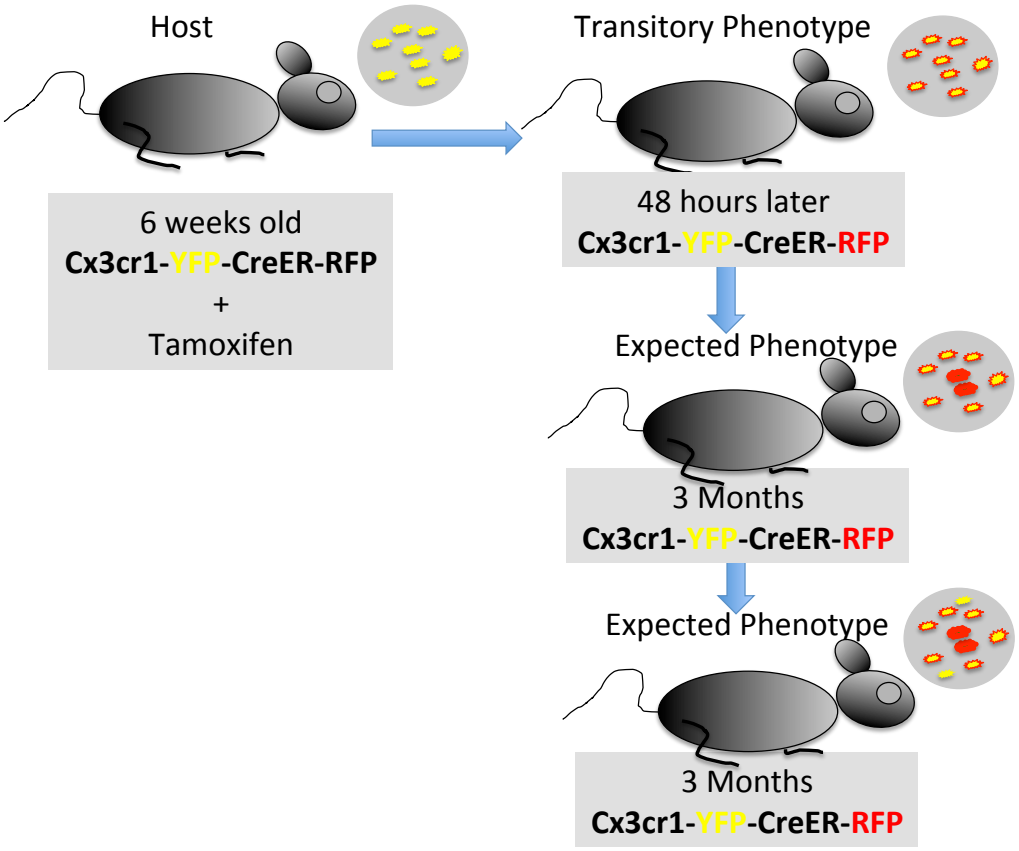

Figura 4: Inducción de expresión de RFP mediante inyección intraperitoneal de tamoxifeno en ratones CX3CR1-YFP-CreER-RFP. En condiciones normales los ratones sólo expresan YFP. Después de la inyección los ratones expresan RFP de forma constitutiva y puede observarse *"in vivo"* colocalizando con YFP

8. Microscopía

8.1 Microscopía confocal "*in vivo*" (IVCM) (***Capítulos 2 y 3***)

Esta técnica se utilizó para estudiar "*in vivo*" y a tiempo real el proceso de cicatrización en córneas de ratones (**Capítulo 2**) y para estudiar la infiltración de células inflamatorias en la superficie ocular (**Capítulo 3**). Bajo anestesia general, se examinó de forma "*intravital*" con un microscopio de escaneo con láser confocal equipado con un modulo especial para córnea HRT3-RCM (Heidelberg Retina Tomograph III, Rostock Corneal Module) (IVCM "*in vivo* confocal microscope"). Durante el exámen, se mantuvo al ratón en una tempertura constante de 37-39°C usando una placa térmica (ATC 1000 DD, LKC Technologies, Gaithersburg, MD). Se aplicó una gota de gel lubricante ocular (Genteal® Novartis Pharmaceuticals Corp, East Han- over, New Jersey) en ambos ojos. Además de lubricar el gel forma una interfaz de acoplamiento de inmersión con un índice de refracción (n=1.339) similar al agua (n=1.333 at 20C).

En diferentes tiempos se escaneó la conjuntiva bulbar (superior e inferior) y la córnea (nasal, temporal y central). El microscopio está equipado con un láser de diodo con una longitud de onda de 670nm como fuente de energía. El módulo RCM está equipado con una lente de 400µm de diámetro y un objetivo de 60X de inmersión en agua con una apertura numérica de 0.90 (Olympus, Hamburg, Germany). Las imágenes se tomaron con una resolución de 1µm/pixel. El láser refleja cambios en la trayectoria de la luz y estos son capturados por el microscopio. El HRT3/RCM viene equipado con una opción para el conteo semiautomático de células endoteliales. Esta opción se utilizó para el contado de estructuras celulares reflectantes. El número se contabilizó de forma manual en un área predeterminada y el ordenador automáticamente estimó el número total en células/mm^2. Los resultados se expresan en media y desviación estándar.

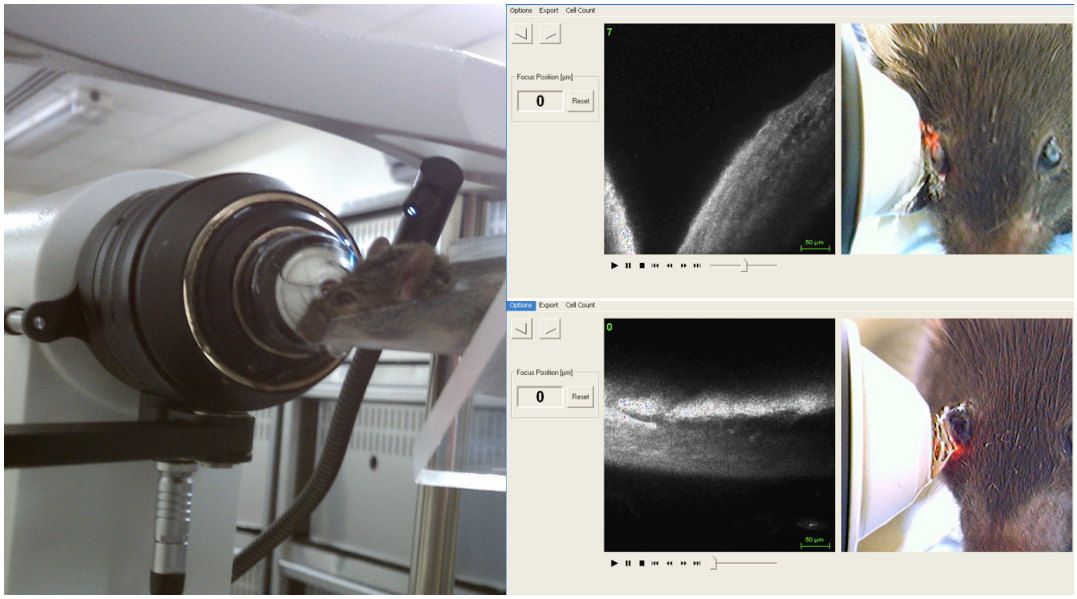

Figura 5: Examinado *"intravital"* no invasivo de la superficie ocular del ratón usando un modelo comercial de microscopio confocal HRT3-RCM
Nota: el sistema HRT3-RCM es un modelo diseñado para la superficie ocular de pacientes.

8.2 Microscopía multifotónica *"intravital"* (*Capítulos 4, 5, 6 y 7)*

De la forma descrita anteriormente, se anestesió el ratón y se colocó en un soporte diseñado para el efecto (**Figura 6**). Un flujo constante de 0.2-0.3 ml/h de una solución de 1ml of ketamina (120 mg/kg), 1 ml of xylacina (20 mg/kg), y 10 ml de cloruro sódico se administró mediante un catéter por vía intraperitoneal. Después del proceso los ratones se recuperaron y descansaron para exámenes posteriores.

Las fotografías se tomaron con un objetivo de inmersión en agua de 25x/1.05 NA ("numerical aperture") (optimizado para MPE XLPL25XWMP, WD 2.0 mm, 0-0.23 micras de corrección) en un microscopio fijo vertical Olympus BX61WI (Olimpus). El microscopio está equipado con un láser de fentosegundos Titanio:Zafiro modelo "Chamaleon Vision II". El láser permite una compensación pulsada en un rango sintonizable de 680-1080 nm (40 nm/seg, 80 MHz, 140 fseg de anchura de pulso, 0-47,000 $fsec^2$ unidades de compensación de la dispersión).

El microscopio esta equipado con dos cubos estándar de fluorescencia intercambiables en el azul, verde/amarillo y rojo. Las bandas de emisión disponibles son: DAPI, CFP, GFP, YFP y RFP. Los canales azul o cian se usaron para la detección de la generación del segundo armónico (SGH, "second harmonic generation"). El láser se sintonizó a 910 nm para el cubo BGR ("Blue, Green and Red") o 950 nm para el cubo CYR ("Cyan, Yellow and Red"). Un espejo dicroico (DM570) separa la luz emitida para los canales 1 (azul) y 2 (verde y amarillo) y el canal 4 (rojo). Un segundo espejo dicroico (DM485) divide la luz emitida para los canales 1 y 2. El cubo BGR está compuesto por filtros de paso de banda de 450-460 nm (azul y SGH), 495-540 (verde) y 575-630nm (rojo). El cubo CYR está compuesto por filtros de paso de banda de 460-500 nm (azul and SGH), 520-560 (amarillo) y 575-630nm (rojo). El sistema tiene cuatro detectores de alta eficiencia en posición de epifluorescencia que pueden ser combinados en diferentes configuraciones alternando los cubos de forma manual.

Para los exámenes "*in vivo*" de la cornea, el ratón se colocó de forma dorsal permitiendo la exposición perpendicular al ápex corneal con el objetivo del microscopio. El espacio entre el objetivo y la superficie corneal se rellenó con gel oftálmico (GenTeal, Novartis Ophthalmics, East Hanover) para crear una interfaz de acoplamiento de inmersión con un índice de refracción (n=1.339) similar al agua (n=1.333 at 20C) así como proveer lubricación a la superficie ocular (**Figura 6**).

8.2.1 Adquisición en mosaico para imágenes en 3D (*Capítulos 4, 5, 6 y 7*)

Bajo anestesia, el ratón fue colocado en un pletina motorizada situada debajo del objetivo del microscopio. El software "multi-area time-lapse" (Olympus) automatiza el proceso para la adquisición de imágenes en un mosaico predefinido ("tiling") y posterior unión ("stitching") para crear una archivo final sujeto de ser analizado y convertido en una imagen en 3D. El software registra las áreas escaneadas, y la imagen final que se muestra ofrece una vista de todas la imágenes adquiridas durante todo el proceso de captura en el mosaico preestablecido (**Figura 7**).

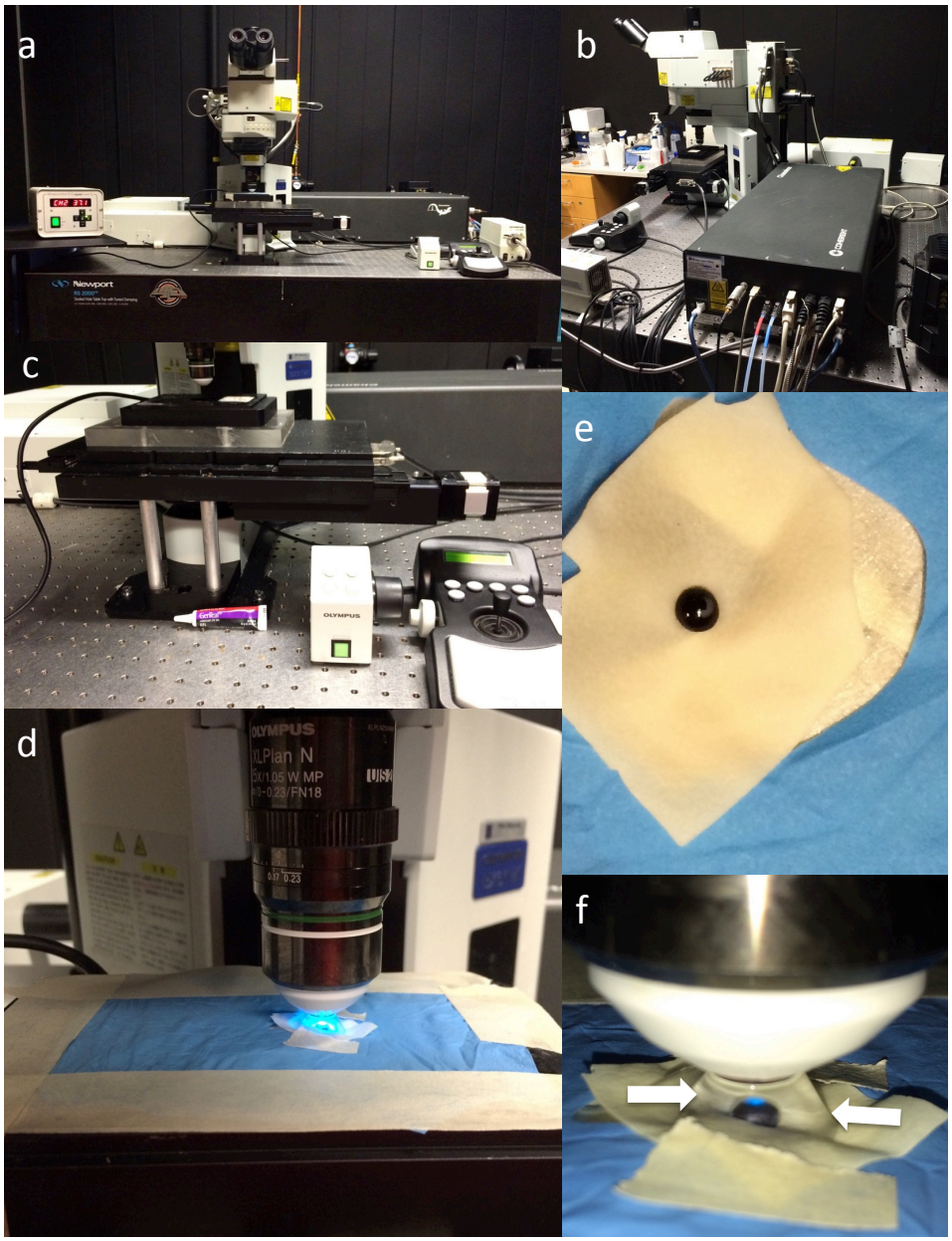

Figura 6: Sistema multifotónico de escaneo *"intravital"* no invasivo utilizado (A). El sistema está equipado con un láser de fentosegundos (B), una plataforma motorizada (C) y un objetivo de inmersión en agua (D). La cámara térmica en la que se sitúa al ratón anestesiado (D) con la córnea expuesta (E) y la interfaz creada por el gel oftálmico entre la córnea y el objetivo (F)

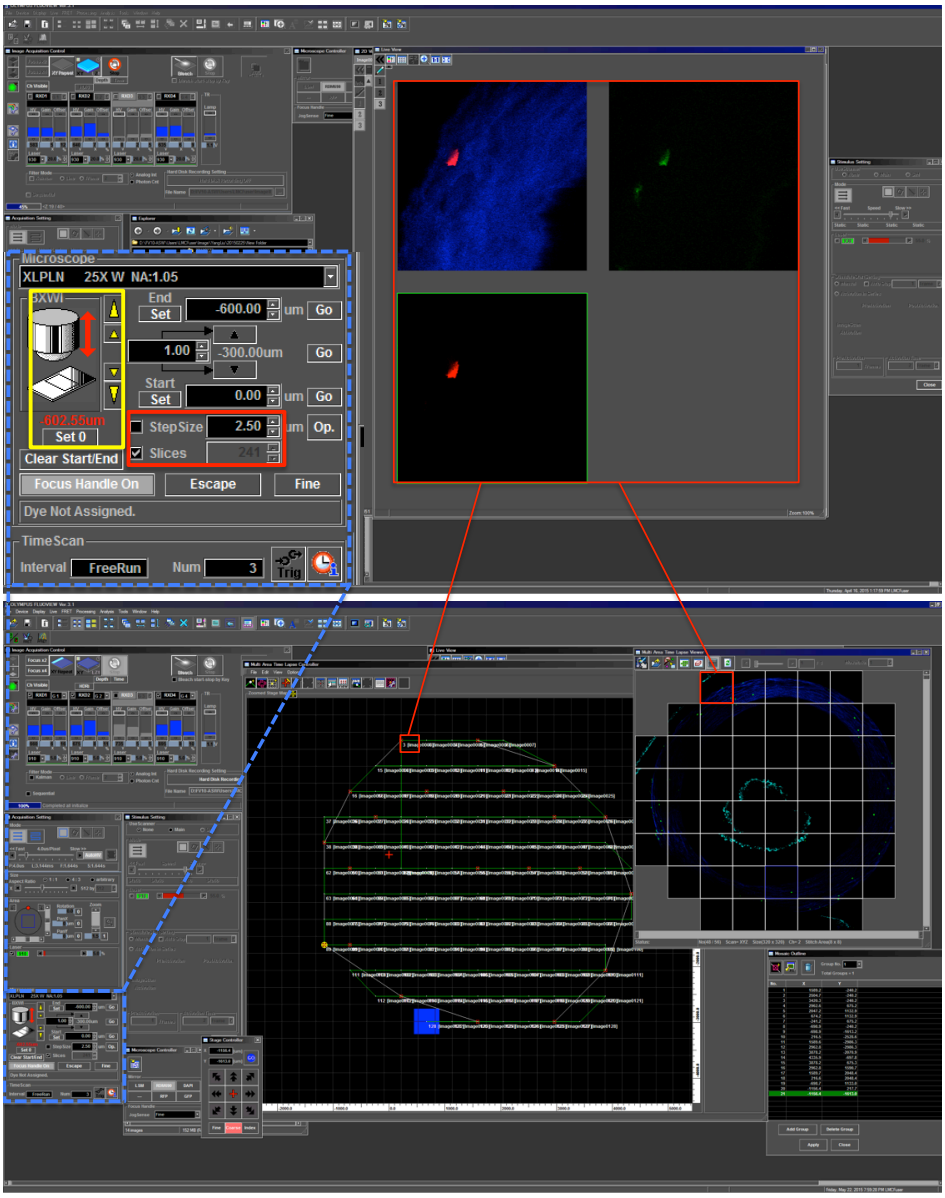

Figura 7: Sistema de adquisición en mosaico para imágenes en 3D. El microscopio fotografía la córnea siguiendo un patrón predefinido de forma manual. En este esquema el microscopio escaneó un total de 602.55 micras (distancia vertical entre el ápex corneal y el ángulo) en pasos de 2.5 micras en un total de 128 posiciones diferentes. El tiempo empleado para el escaneo total de la córnea varía en función de la resolución, pudiendo ir de varios minutos a unas pocas horas.

8.2.2 Post-procesado de las imágenes (*Capítulos 4, 5, 6 y 7*)

Los archivos de imágenes compiladas se post-procesaron con FIJI software (http://fiji.sc/Fiji) y posteriormente con Imaris ("Imaris updated versión", Bit- plane, Zurich, Switzerland). En primer lugar las archivos originales se abrieron en Imaris y se vincularon a FIJI para sustracción del grano de fondo, ajuste del control y brillo, reducción del ruido, compensación múltiple y re-ajustamiento del tamaño. A continuación la imagen se importó de nuevo en Imaris mostrando una proyección de máxima intensidad, para posteriormente proyectar una imagen real en 3D en una pantalla plana. El realismo adicional de las imágenes en 3D se consiguió con la opción "real-time shadow rendering" (Una opción del software que proyecta sombras en los tres planos del objeto)

Un objeto de superficie es una ilustración generada de forma computada de una región detallada en un área de interés. El objeto de superficie se muestra como un objeto sólido simulado. La precisión de la segmentación con la imagen original se puede verificar de forma interactiva. Para más detalles visitar: http://www.bitplane.com/imaris/imaris. El uso de Imaris permitió cuantificar células, mostrar las imágenes de forma interactiva y tridimensional, generar animaciones, realzados artísticos etc.

Nota: El hecho de que las barras de calibración no sean homogéneas en todas las imágenes es debido a la configuración del software que no permite calibraciones manuales estandarizadas.

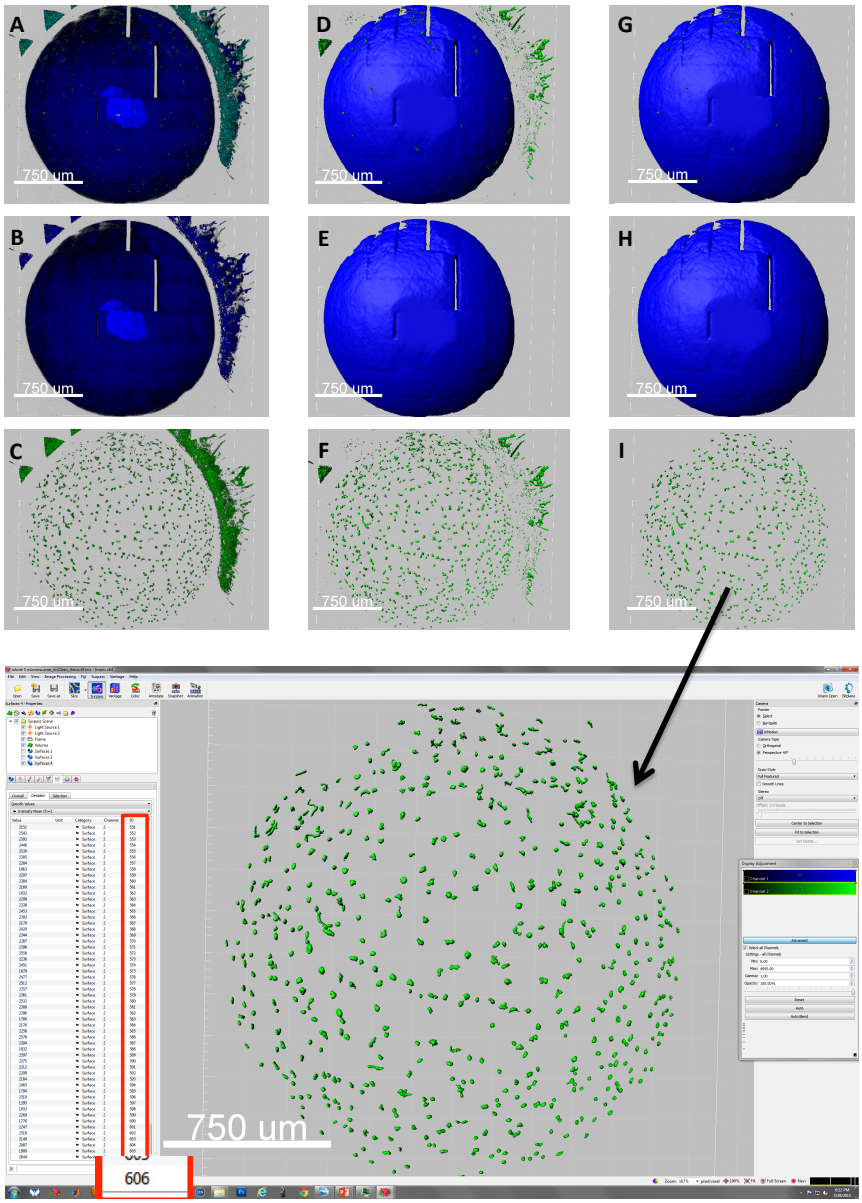

Figura 8: Procesado de las imágenes. La imagen en 3D es cargada en el programa (A, B y C), donde se elimina el fondo y se montan y se delinean las superficies (D, E y F). Por último se elimina los elementos no deseados (en este caso el párpado, G, H e I) dejando la imagen limpia para el procesado final, en este caso conteo celular automático. En la imagen, el programa muestra un total de 606 células

8.3 Microscopía confocal (*Capítulos 1, 2, 3, 4, 5 y 6*)

Para el estudio del tejido *"ex vivo"* ("whole flat mounts") se utilizó un microscopio confocal de escaneado con láser (LSCM) (Leica TCS 4D; Leica, Heidelberg, Germany). Las proyecciones tridimensionales de las imágenes se realizarón con "LAS AF software" de Leica, con FIJI (desarrollado por Wayne Rasband, National Institutes of Health; y de dominio público http://rsb.info.nih.gov/ij) e "Imaris software" (Bit-plane, Zurich, Switzerland).

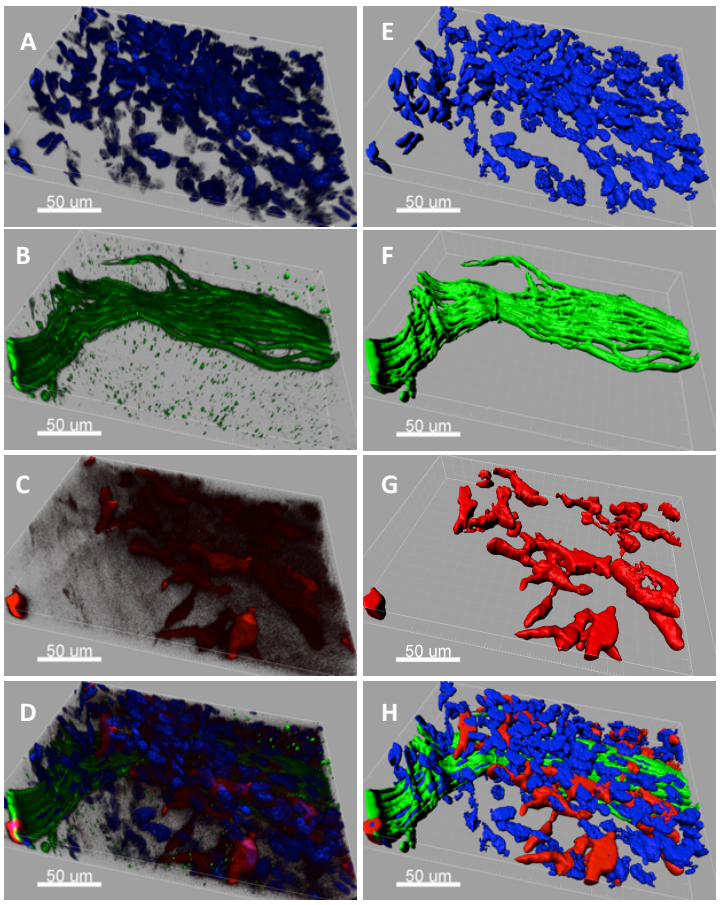

Figura: Procesado de las imágenes obtenidas con microscopio confocal. La imagen en 3D es cargada en el programa (A, B, C y D), donde se elimina el fondo y se delinean las superficies (E, F, G y H).

8.4 Microscopía Electrónica (*Capítulos 1 y 2*)

El tejido corneal se fijó en paraformaldehido 2% y glutaraldehido 2.5% en tampón cacodilato (0.1M) durante 1 hora y post-fijado en OsO4 2% en tampón cacodilato (0.1M). Posteriormente el tejido en acetato de uranilo 0.5% acuoso se deshidrató en gradiente de acetona, seguido de oxido de propileno y por último embebido en Epon-araldita. Los cortes semifinos (1µm) se tiñeron con azul de toluidina y se determinó el área a examinar. Posteriormente con un ultramicrotomo se seccionó en piezas finas (60-90Å) y se tiñeron con acetato de uranilo 2% y citrato de plomo para ser fotografiadas con un microscopio de transmisión electrónica Philips 410 (Philips Electronics N.V., Eindhoven, The Netherlands).

8.5 Microscopía óptica (*Capítulos 1, 2 y 3*)

Se procedió a la tinción histológica con: hematoxilina-eosina (H&E), tricrómico de Masson (TM) y ácido peryódico de Schiff (PAS).

9. Otras técnicas:

9.1 Estudio histopatológico (*Capítulos 1, 2 y 3*)

Previa eutanasia del animal (descrito anteriormente), se procedió a la extracción de las córneas y se dividieron en dos mitades:

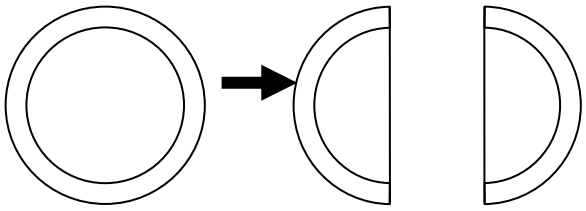

La primera de las mitades se incluyó en medio de inclusión Tissue-Tek OCT y posterior congelado a -30°C. Posteriormente se seccionaron en cortes de 6 μm. Además se tomaron secciones adicionales y se fijaron con fijador Karnovsky para microscopía electrónica. En la segunda de las mitades, se separó el epitelio del estroma y en contenedores diferentes se congelaron en nitrógeno líquido para posterior análisis con Western Blot. Además, se tomaron córneas enteras y se fijaron en paraformaldehido 4%. Posteriormente se utilizaron para inmunofluorescencia en montaje plano o "flat mount".

9.2. Inmunofluorescencia (*Capítulos 1, 2, 3, 4, 5 y 6*)

Si bien el protocolo utilizado se modificó puntualmente dependiendo de los diferentes estudios (ver capítulos), en general: en primer lugar se bloqueó el tejido con el suero de cabra, burro o conejo. Posteriormente el tejido se incubó 1 hora a temperatura ambiente o toda la noche a 4ºC con anticuerpos monoclonales o policlonales purificados o conjugados con fluorescencia. Además en el caso de los purificados, se utilizó un anticuerpo secundario conjugado con fluorescencia para amplificar la señal.
Además se realizaron controles negativos en los cuales o bien se omitió el anticuerpo primario o bien el anticuerpo primario fue sustituido por anticuerpos isotópicos.

9.3 Western Blot (*Capítulos 1 y 2*)

El tejido se homogenizó en búfer de lisis para purificar las proteínas en presencia de inhibidores de proteasas. A continuación las diferentes muestras se resolvieron en condiciones de desnaturalización en gel SDS-poliacrilamida al 10% y posteriormente se trasfirieron a una membrana de nitrocelulosa. Las membranas se bloquearon con leche en polvo al 5% en TBS y posteriormente se incubaron con anticuerpos primarios a 4ºC toda la noches y anticuerpos secundarios conjugados con peroxidasa de rábano. Por último las bandas se visualizaron mediante por método quimioluminiscente usando un lector de

rayos X (Biospectrum AC imaging system; UVP, LLC, Upland, CA). Las bandas se evaluaron con "software Image J" de acceso universal (http://rsb.info.nih.gov/ij).

9.4 Procesado del tejido y inmuno-tinción de los botones corneales (*Capítulos 1, 2, 3, 4, 5 y 6*)

Los ratones anestesiados se perfundieron con solución salina balanceada seguido de PFA 2% y finalmente PFA 4%. Posteriormente los globos oculares se post-fijaron con solución de Zamboni (24 horas en cámara fría) preservando la fluorescencia interna. El tejido se lavó varias veces durante 24 horas con PBS. Las córneas se separaron del resto del globo ocular y se escindieron en un patrón de pétalos de flor para montado plano. A continuación se permeabilizaron con Tween (0.5% en PBS) y se marcaron para epifluorescencia, microscopía confocal y multifotónica. Todos los anticuerpos se diluyeron en PBS, BSA 2% y suero normal de cabra 5%. El tejido se incubó con anticuerpo primario durante 3 días a 4C en agitación suave. Posteriormente se incubó con anticuerpos secundario durante toda la noche a 4C y agitación suave. Después de varios lavados el tejido se montó con medio de montaje con DAPI.

Los botones corneales y los cortes se fotografiaron con un microscopio de fluorescencia (Axio Observer, Zeiss, Oberkochen, Germany) y un microscopio confocal de escaneado con láser (LSCM) (Leica TCS 4D; Leica, Heidelberg, Germany Zeiss). Además algunos botones corneales se escanearon al completo siguiendo un modelo de mosaico con un en con el microscopio multifotónico descrito anteriormente.

9.5 Citometría de Flujo (*Capítulo 3*)

Los ratones se sacrificaron en los días 3 y 7 del seguimiento. La conjuntiva se separó en superior e inferior. La córnea se dividió en tres partes: nasal, temporal y un botón central de 1.5 mm de diámetro. A continuación el tejido se disoció en fragmentos y se

procedió a la digestión enzimática con 2mg/ml de colagenasa tipo IV y 0.5mg/ml de "DNAasa I" (Roche, Basel, Switzerland) durante 2-3 horas a 37°C. La suspensión se tamizó y se filtró por un filtro de a 70µm de poro. Las células se lavaron y se suspendieron en suero de albúmina bovina (BSA "bovine serum albumin", 0.5%) y posteriormente se bloquearon con una mezcla de anticuerpos CD16/CD32 ("blocking of FcγRIII/II", BD Pharmingen, San Diego, CA).

De forma breve,

Las células se marcaron con DAPI seguido de los siguiente anticuerpos: anti-CCR2-Alexa 488, anti-CD45-Cy5, anti-Ly6C-Alexa 700, anti-CD11b-PE y anti-CD11c-PE-Cy5 (Biolegend). A continuación, las células se resuspendieron en PBS para ser analizadas con un citómetro de flujo BD LSR II (BD Biosciences, San Jose, CA). Las células fueron separadas por el método "forward and side scattering". Las células muertas se excluyeron en el canal del DAPI y las células individuales se separaron de los conglomerados dobles o triples. Las células CD45+ fueron divididas en tres subpoblaciones diferentes de $CCR2^{+}Ly6\text{-}C^{High}$, $CCR2^{-}Ly6\text{-}C^{Low}$ y $CCR2^{-}Ly6\text{-}C^{-}$. Las células CD11b+ y CD11c+ fueron separadas y las población se enumeró la población CD11b.

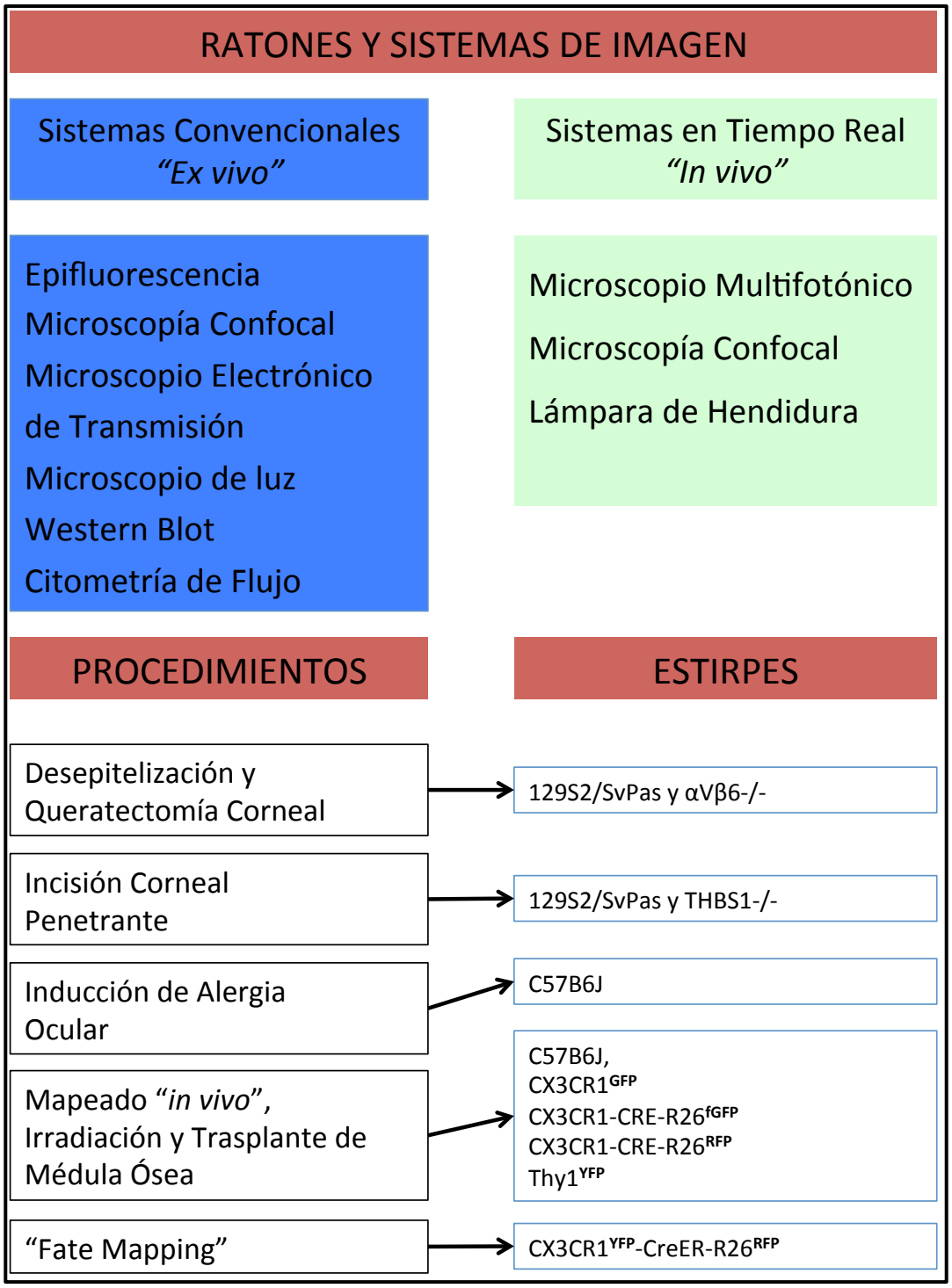

Esquema resumido: animales y método

RESULTADOS Y DISCUSION

A continuación se muestran los resultados y discusión de forma resumida, en el mismo orden que los diferentes capítulos anexos. Una presentación más detallada de los resultados y discusión se expone en los diferentes capítulos que acompañan la presente memoria.

Capítulo 1. La integrina αVβ6 estimula la cicatrización corneal.

"Chapter 1: *αVβ6 integrin promotes corneal wound healing"*

En este estudio se demuestra que la integrina αVβ6 es fundamental para la restauración de la membrana basal después una lesión. Su expresión en el epitelio durante el proceso de cicatrización corneal promueve:

1. migración epitelial,
2. síntesis de laminina
3. síntesis de integrina α6β4 y ensamblado de los hemidesmosomas
4. modulación del armazón de fibronectina

Los ratones carentes de la subunidad β6 ($\beta6^{-/-}$) no regeneran la lámina densa ni la lámina lúcida de la membrana basal ni tampoco forman hemidesmosomas maduros después de una lesión que dañe la lámina basal. Sin embargo, cuando se desepiteliza la cornea sin dañar dicha membrana, esta integrina no tiene una función relevante. Esto indica que la integrina αVβ6 es fundamental para la reparación de la membrana basal, cuando ésta haya sido dañada, pero no tiene una función relevante en el mantenimiento de las condiciones basales o si la lesión no afecta su integridad.

Durante la cicatrización, la fibronectina forma un andamio transitorio que facilita el anclaje de las células epiteliales a la matriz extracelular [49, 50]. En el presente trabajo, se observó una matriz de fibronectina transitoria que posteriormente da paso a la verdadera

membrana basal en los ratones normales. En el caso de los ratones carentes de la subunidad $\beta6^{-/-}$, dicha capa de fibronectina permanece durante todo el experimento y no es reemplazada por una nueva membrana basal. Sin embargo, esta matriz transitoria se mantiene crónica. Esto puede explicar que si bien los ratones carentes de $\beta6^{-/-}$ presentan ampollas sub-epiteliales, no llegan a desarrollar verdaderas úlceras.

Por otro lado, se ha asociado la falta de hemisdesmosomas con la carencia de la integrina α6β4 [51]. En el presente trabajo, la expresión de esta integrina disminuye significativamente en ratones $\beta6^{-/-}$ después de la lesión. De la misma manera, se observa una gran reducción en el número de hemidesmosomas en el epitelio basal. El hecho de que la integrina α6β4 se co-exprese con la laminina, sugiere que α6β4 actúa como receptor para la laminina durante el proceso de reparación de la lámina basal. Por otro lado, la presencia de laminina es necesaria para ensamblar la integrina α6β4 en hemidesmosomas maduros durante el proceso de reparación de la membrana basal.

En conclusión, con el presente estudio se demostró que la integrina αVβ6 es imprescindible para la regeneración de la membrana basal del epitelio corneal después de un lesión y su ausencia puede causar patologías como la queratopatía bullosa o distrofias de la membrana basal del epitelio.

Capítulo 2. Función de la trombospondina-1 en la reparación de heridas penetrantes en la córnea.

"Chapter 2: *Role of Thrombospondin-1 in Repair of Penetrating Corneal Wounds"*

En la córnea, la THBS1 se expresa después de una lesión en la zona dañada [52]. Durante el proceso de cicatrización los miofibroblastos se diferencian específicamente en la zona donde se expresa la THBS1 [52]. Sin embargo cuando la membrana basal se deja intacta, la THBS1 sólo se expresa en la zona apical en la zona de dicha membrana [53]. Esto sugieren que la THBS1 juega un papel primordial en el proceso de cicatrización de la córnea.

En el presente trabajo se demostró, mediante el uso de ratones Thbs1$^{-/-}$, que la THBS1 es fundamental para la cicatrización tanto del estroma como del endotelio corneal. Los ratones Thbs1$^{-/-}$ son incapaces de llevar acabo un proceso de cicatrización corneal efectivo manifestando opacidad e inflamación crónica. En este caso se realizó una incisión penetrante en la córnea con el objetivo de discernir el proceso de cicatrización en todas las capas de la córnea, en ausencia de THBS1.

La expresión de THBS1 se observó a las 24 horas en el epitelio de los ratones normales en la zona de la incisión pero no en el estroma. Más tarde, la expresión se extiende al epitelio que rodea a la incisión penetrando en el estroma en la zona dañada, con una expresión máxima a las dos semanas desde el epitelio hasta el endotelio. Por el contrario no se observó expresión de THBS1 en el epitelio ni en el estroma de la periferia adyacente a la herida. Las córneas de los ratones Thbs1$^{-/-}$ permanecen opacas durante el trascurso de todo el experimento no llevando a cabo una cicatrización efectiva. Esto indica que la THBS1 expresada en la zona de la incisión es fundamental para la reparación del estroma y del endotelio. Esto queda demostrado por el incremento de expresión de THBS1 en el endotelio de la zona lesionada en las córneas de ratones normales.

Seguido a una lesión corneal las células epiteliales rápidamente cubren el área dañada mediante un proceso de proliferación y migración [54]. En el estroma muchos de los queratocitos mueren por apoptosis mientras otros inmediatamente inician un proceso de proliferación para repoblar el área dañada y posteriormente se diferenciaran en miofibroblastos [10, 55-57]. Los miofibroblastos contraen la herida y sintetizan nueva matriz extracelular [10, 58] provocando en la córnea una opacidad en la zona de cicatrización denominada "haze" o retro-dispersión de la luz. Este fenómeno desaparece cuando la cicatrización concluye [58]. En el presente trabajo, se observó: 1) "haze" focalizado en la zona de cicatrización en el estroma y endotelio, 2) miofibroblastos y 3) nueva matriz extracelular en las córneas de los ratones normales. Sin embargo, esto no se observó en los ratones Thbs1$^{-/-}$. La presencia de miofibroblastos, junto a la expresión de THBS1, en

el área de cicatrización es evidente en el cuarto día lo cual sugiere que los queratocitos necesitan de la THBS1 para diferenciarse en miofibroblastos.

El TGF-β1 es fundamental para la transición de queratocito a miofibroblasto y la THBS1 activa el TGF-β1 [59-61]. En los trabajos anteriores no se ha especificado claramente si la THSB1 era expresada por el epitelio o por los fibroblastos/miofibroblastos [62]. En este trabajo se observa que las células epiteliales y del endotelio son las encargadas de la expresión de la THBS1. Además se detalla que muchas células epiteliales también expresan α-SMA sugiriendo una función como células mioepiteliales probablemente ayudando a contraer la herida [63]. De esta manera, se demuestra que la THBS1 juega un papel relevante en el mantenimiento de la estructura epitelial como se había sugerido anteriormente [64]. Por otro lado, no se observó expresión de THBS1 en los queratocitos ni en los miofibroblastos.

En el endotelio también se observa gran expresión de THBS1 lo cual demuestra que esta proteína es fundamental para la restauración endotelial y de la capa de Descemet. Las córneas de los ratones Thbs1$^{-/-}$ son incapaces de cerrar la barrera endotelial presentado edema y opacidad crónica. En la córnea humana, el endotelio no tiene capacidad proliferativa, sin embargo, las células endoteliales pueden migrar y por proceso de elongación restaurar una lesión [65, 66]. La importancia de la THBS1 en el proceso de reparación endotelial había sido sugerida anteriormente por Munjal et al., [67] y es corroborada en el presente trabajo. La THBS1 se une al TGF-β1 [59-61] activándolo en las células endoteliales [68] promoviendo de esta manera el mecanismo de reparación endotelial.

Por otro lado la THBS1 juega un papel primordial en el mantenimiento del privilegio inmune de la córnea ya que la THBS1 derivada de las células presentadoras de antígeno suprime el rechazo inmune [69]. No está claro si en rechazo inmune juega un papel relevante en nuestro estudio, pero es posible que la THBS1 expresada por las células inmunes de la córnea, intervenga también en el proceso de cicatrización. El hecho de que la falta de THBS1 produzca defectos en la cicatrización podría explicar defectos en la

superficie ocular causados por el ojo seco y en los cuales se ha observado una carencia de THBS1 [70].

Basado en estos resultados y trabajos previos [62, 71], la expresión de THBS1 y su persistencia en el tejido se relaciona con el tipo de la herida. Esto puede variar de unas pocas horas en una lesión epitelial, varios días en el caso de una queratectomía o hasta un mes cuando toda la integridad corneal se ve dañada.

Como conclusión, la THBS1 juega un papel primordial durante el proceso de reparación corneal. Esto incluye migración endotelial, contracción estromal y síntesis de nueva matriz extracelular.

Capítulo 3. **Detección del proceso inflamatorio corneal en un modelo de alergia ocular en ratón usando un microscopio confocal *"in vivo"***

"Chapter 3: *In vivo Confocal Microscopy Reveals Corneal Involvement in an Allergic Eye Disease Mouse Model: an in vivo Study*

En el presente estudio se evaluó el proceso inflamatorio de la superficie ocular, en un modelo de conjuntivitis alérgica en ratón, usando un microscopio confocal "*in vivo*" (IVCM, "*in vivo* confocal microscopy"). Para validar el sistema IVCM, los resultados obtenidos se compararon con los obtenidos "*ex vivo*" mediante citometría de flujo y microscopía confocal (LSCM, "Laser scanner confocal microscopy").

La principal limitación de este trabajo fue debido a que el HRT3/RCM es un dispositivo comercial diseñado originalmente para los seres humanos. La superficie ocular del ratón difiere notablemente de la humana. De esta manera sólo se evaluó la conjuntiva bulbar. Aunque la curvatura de la córnea también difiere de la humana, fue posible realizar escaneos en secciones transversales (nasales y temporales) y frontales (central). Por tanto en este trabajo, se implementó con éxito una nueva técnica no invasiva para evaluar el proceso de infiltración celular en la superficie ocular del ratón. Otros modelos anteriores exigen tediosos análisis histopatológicos "*postmortem*" [48, 72-75].

La infiltración celular se detectó midiendo la dispersión de luz con el HRT3/RCM. Se observó, que en comparación con el tejido normal, los células inflamatorias infiltradas reflejan más la luz que las normales. Inmediatamente después de la instilación del alérgeno, se observa un aumento en el número de células infamatorias en la conjuntiva. El incremento en número fue progresivo durante el experimento. El número de células inflamatorias observadas con este sistema es significativamente mayor en los ratones inmunizados comparados con los controles ($p < 0,01$). De la misma manera, usando citometría de flujo, se observó una frecuencia mayor de células CD11b positivas en la conjuntiva de los ratones inmunizados en comparación con ratones control ($p < 0,01$).

Sin embargo, lo más notable fue encontrar una reacción inflamatoria similar en la córnea. Se cree que la córnea y la conjuntiva pueden afectar una a la otra durante la inflamación alérgica ocular; sin embargo, esta interacción no está bien descrita [31, 32, 76]. La alergia severa ocular se caracterizan por diversos trastornos corneales como las úlceras persistentes en el epitelio y las placas. La pérdida de epitelio corneal aumenta la inflamación alérgica de la conjuntiva. La infiltración de eosinófilos en la conjuntiva perjudica a su vez la cicatrización del epitelio. Los eosinófilos y sus factores derivados están implicados en la patogénesis de las lesiones corneales asociadas con la alergia ocular [76]. Las proteínas citotóxicas y la metaloproteinasa 9 derivadas de los eosinófilos se acumulan en las placas de la córnea [31, 76]. De esta manera, la inflamación alérgica conjuntival y los trastornos epiteliales corneales interactúan entre si generando un círculo vicioso cuya interrupción podría proporcionar la base para nuevos tratamientos de la alergia ocular grave [31].

En el presente trabajo se observó infiltración de monocitos y neutrófilos en la parte periférica de la córnea y en menor grado en la parte central. Éstos no se observan en los ratones controles ni en los normales. Previamente estas células se habían detectado con el sistema IVCM y en correlación con el aumento de los síntomas clínicos observados con la lámpara de hendidura. El número de células inflamatorias infiltradas en la córnea es

significativamente superior en ratones inmunizados comparado con ratones normales ($p < 0,01$).

De la misma manera se vio un aumento en la frecuencia de células CD11b+ en la córnea de ratones inmunizados comparado con ratones normales y sanos ($p < 0,01$). Al final del experimento se detectó un aumento en la subpoblación CCR2+/Ly6-C$^{"high"}$/CD11b+ indicando una infiltración de monocitos en la córnea. Además se observó otra subpoblación de CCR2-/Ly6-C$^{"low"}$/CD11b+ indicando infiltración de neutrófilos. Lo más notorio fue observar que la córnea se mantuvo transparente a pesar de la gran cantidad de células inflamatorias infiltradas.

En presencia de un alérgeno, las células dendríticas inmaduras capturan el antígeno, madurando y emigrando a los nódulos linfáticos donde activan una respuesta inmune adaptativa tipo Th2. Se ha observado tráfico de células dendríticas entre la córnea y los nodos linfáticos en respuesta a un alérgeno en un modelo de alotrasplante corneal [30, 77, 78]. Sin embargo, la maduración y migración de células dendríticas de la córnea, en respuesta a un alérgeno, no está clara y se ha visto que no sucede en córneas normales [79]. Los resultados del presente estudio, sugieren un mecanismo desconocido de infiltración de células inflamatorias en la córnea, relacionado con la progresión de la respuesta inmune adaptativa de la conjuntiva.

Las células dendríticas de la conjuntiva son una población importante en la repuesta inmune adaptativa relacionada con la alergia [80]. Las células dendríticas inmaduras patrullan el tejido a la captura de antígeno [81, 82]. Cuando las células dendríticas capturan un antígeno se convierten en potentes estimuladores de las células T y en el caso de la alergia activan los linfocitos Th2. Las células dendríticas aumentan la expresión de moléculas MHC clase II y moléculas coestimuladoras CD80 y CD86. La activación Th2 induce la secreción de citoquinas IL-4, IL-5 o IL-13 que estimulan la diferenciación de células B en células plasmáticas secretoras de IgE [82-84].

Las exposiciones primarias de un alérgeno ceban las células T inmaduras quedando sensibilizadas para ese alérgeno. Exposiciones secundarias del mismo alérgeno causan

hipersensibilidad inmediata o alergia, y en casos de exposición continuada pueden causar una fase tardía posterior y crónicas [85]. Las citoquinas Th2 también desestabilizan los eosinófilos en la fase tardía de la alergia amplificando así la repuesta inflamatoria de la superficie ocular mediante el reclutamiento de monocitos, linfocitos T, eosinófilos y células dendríticas en un bucle de retroalimentación tal que mantiene la patología [84]. Sin embargo, en el presente trabajo no se ha demostrado si la respuesta infamatoria observada en la córnea juega un papel en la defensa del órgano o contribuye a un estado patológico más grave.

En conclusión, en este estudio se evaluó con éxito la reacción inflamatoria de la superficie ocular en un modelo de ratón de conjuntivitis alérgica usando un sistema IVCM. El aumento en el número de células inflamatorias está relacionado espaciotemporalmente con el aumento de la sintomatología clínica observada con la lámpara de hendidura así como con los resultados obtenidos "*ex vivo*" con citometría de flujo y microscopía confocal.

<u>Capítulo 4:</u> Innovación en sistemas de imagen *"in vivo"* I: Microscopía multifotónica *"intravital"* para visualizar la población residente de células inmunitarias en la córnea del ratón".

"Chapter 4*: Cutting Edge in vivo Imaging I: Multi-Photon intravital Microscopy to Visualize the Resident Myeloid-Derived Population in the Mouse Cornea"*

En el presente estudio se combinó microscopía multifotónica *"intravital"* (MP-IVM, "multi-photon intravital microscopy"), diferentes cepas de ratones que expresan fluorescencia bajo el promotor de Cx3cr1 y un sistema digital de tratado de imágenes para el estudio de la población inmunitaria de la córnea. Considerando los resultados, se puede extrapolar las siguientes conclusiones:

1. El sistema es adecuado para el estudio "*in vivo"* no invasivo de la población inmunitaria de la córnea tanto en condiciones normales como en patológicas.

2. El sistema de imagen es innovador desde el punto de vista de la resolución alcanzada así como desde la presentación de los resultados
3. El origen de la población inmunitaria de la córnea se intuye embrionario en lugar de la hematopoyético como se había establecido, y con una tasa de recambio muy baja.

Durante más de un siglo, prevaleció el dogma de que la córnea carecía de células presentadoras de antígeno [86], sin embargo durante los últimos años se ha establecido que la córnea está dotada de una población residente de células inmunitarias derivadas de la médula ósea [8, 39, 40, 79, 87-92] con dos fenotipos predominantes: las células dendríticas y los macrófagos [93, 94]. Las células dendríticas residen en la parte basal del epitelio y extienden sus prolongaciones dendríticas interdigitándose entre las células epiteliales, desde el lecho estromal hacia la superficie. Esta población se encuentra con mayor densidad en la periferia de la córnea disminuyendo en número centrípetamente. Por otro lado, el estroma periférico posee una pequeña población de células dendríticas. Las células dendríticas son encargadas de iniciar la respuesta inmune adaptativa en respuesta a la inflamación pero esta función no se conoce bien en la córnea [40, 90, 91].

Los macrófagos están distribuidos en estroma en dos subpoblaciones distintas. La parte anterior está habitada por macrófagos putativos que podrían servir como células presentadoras de antígeno de apoyo a las células dendríticas colaborando en una potencial respuesta inmune adaptativa. El estroma posterior está poblado por macrófagos residentes distribuidos de forma uniforme en toda la parte posterior del estroma. Estos macrófagos disparan una respuesta innata cuando se compromete la integridad corneal [8, 39, 92].

En el presente trabajo se consiguió mapear y estratificar por primera vez *"in vivo"* la población inmunitaria de la córnea del ratón. Dicha población se visualizó de forma no invasiva y sin necesidad de sacrificar el ratón como en los trabajos previos [8, 40, 95]. Se observó la presencia de células $EGFP^+$ en toda la córnea. Estas células aparecen igualmente distribuidas en el estroma, sin embargo en el epitelio el número es mayor en

la periferia, menor en la zona paracentral y ausente en el centro de la misma manera que se ha observado anteriormente en *"explantes"* [40, 95]. El tratado posterior de las imágenes mostrando una estructura tridimensional real de la córnea, facilitó la interpretación de los resultados. Las células dendríticas descansan en la zona de la membrana basal extendiendo ramificaciones dendríticas hacia la superficie ocular, como se había observado *"ex vivo"* [40, 79]. Debido a que las imágenes son tomadas *"in vivo"* y sin fijadores, los macrófagos del estroma presentan forma más real a como han sido mostrados anteriormente [40, 79].

En la actualidad existe gran discusión respecto al número total de células así como su distribución topográfica en la córnea. Algunos trabajos han publicado que la parte central del epitelio corneal está desprovista de células dendríticas, sin embargo, por otro lado se ha sugerido que una población latente de células dendríticas reside en esa zona [88, 90, 96]. Al igual que en los resultados discutidos anteriormente, en trabajos previos se han utilizado ratones "knock-in" cuya expresión de proteína fluorescente es inducible en función de la activación o desactivación del promotor, como en este caso $Cx3cr1^{GFP}$.

En el presente trabajo se introdujo un sistema de recombinación "Cre" en los ratones. El sistema "Cre" induce expresión constitutiva, en este caso, de una proteína fluorescente durante toda la vida de la célula. De esta forma se confirmó que los ratones ($Cx3cr1^{cre/FGFP}$ y $Cx3cr1^{cre/RFP}$) albergan una población de células dendríticas en el centro de la córnea. Además el número total de células mieloides en la córnea normal es significativamente mayor en los ratones $Cx3cr1^{cre}$ que en los ratones $Cx3cr1^{GFP}$ ($p<0.01$). Esto indica que la fluorescencia en el centro de la córnea desaparece al inhibirse la expresión de Cx3cr1 en esta zona. Cx3cr1 media la expresion de MHC clase II en la córnea del ratón [95]. La expresión de Cx3cr1 está inhibida en el centro de la córnea del ratón adulto y por tanto la ausencia de expresión de MHC clase II [90]. De la misma manera la expresión de GFP inducible, no se observa en el centro pero las células están presentes como se ha demostrado con el sistema "Cre".

Estos resultados indican además que la población del centro de la córnea podría no tener ni origen ni recambio de la médula ósea y que su orígen fuese difente. Durante el desarrollo embrionario, los precursores del saco vitelino emigran al embrión en formación, incluyendo la piel primordial donde dan lugar a los precursores de las células de Langerhans; al cerebro primitivo dando lugar a la microglía; y a los órganos periféricos dando lugar a los macrófagos tisulares residentes [97, 98]. Sin embargo, y al contrario que la microglía, que permanece con origen del saco vitelino durante toda la vida, los precursores en el resto de tejidos adultos son reemplazados por monocitos del hígado embrionario durante la parte final de la embriogénesis y de la médula ósea en el adulto [97, 98]. De esta manera las células de Langerhans adultas derivan predominantemente del hígado embrionario y de la médula ósea con una contribución muy baja del sado vitelino [99]. En la córnea adulta, está ampliamente aceptado que la población inmunitaria residente está originada de la médula ósea [87]. Sin embargo, los presentes resultados indican que el centro de la córnea podría estar habitado por una población diferente con origen embrionario. Como se mostró anteriormente, los ratones heterocigóticos $Cx3cr1^{GFP}$ muestran menos células fluorescentes que los ratones transgénicos $Cx3cr1^{Cre/RFP/GFP}$. De esta manera se irradió letalmente un grupo de ratones en los que posteriormente se trasplantó médula ósea de otro ratón expresando un fenotipo diferente. En primer lugar, se observó una población de células residentes del ratón receptor, resistentes a la irradiación. Por otro lado, el numero de células donantes que repoblaron la córnea 3 meses después del trasplante, es significativamente menor que en el ratón original ($p<0.01$). Además, la presencia de células donantes de la médula ósea en el centro de la córnea, es muy baja.

Para analizar la tasa de recambio de las células inmunitarias residentes de la córnea normal *"in vivo"*, se utilizaron ratones CX3CR1-YFP-CreER-RFP. Estos ratones expresan YPF inducible bajo el promotor de Cx3cr1, así como el dímero formado por la enzima recombinasa Cre y el receptor de estrógeno (ER) en el citoplasma de la célula. En presencia de tamoxifeno, el dímero se disocia y la enzima Cre pasa al núcleo donde lleva

a cabo su acción recombinasa induciendo la expresión constitutiva del gen reportero, en este caso "tdTomato" (RFP), durante el resto de la vida de la célula. En condiciones normales, estos ratones sólo expresan YFP inducible bajo la expresión del promotor de Cx3cr1, pero la YFP desparece cuando la expresión de Cx3cr1 disminuye o se detiene como en el centro de la córnea. En presencia de tamoxifeno, las mismas células expresan RFP de forma constitutiva independientemente del estado del promotor de Cx3cr1 [100].

Los ratones CX3CR1-YFP-CreER-RFP de seis semanas, expresan YFP brillante en toda la córnea pero no expresan RFP. Tras la inyección de dos dosis de tamoxifeno toda la población de células YFP coexpresa RFP. Seis meses más tarde, la expresión de YFP disminuyó drásticamente o desapareció mientras que la intensidad de RFP se mantuvo estable. En el centro se observa un gran número de células YFP- RFP+. No observó ninguna célula YFP+RFP-. Esto indica que la población mieloide de la córnea permanece estable y sin recambio de la médula ósea. Estos resultados indican que las células inmunitarias residentes en la córnea adulta sana podrían tener un origen diferente de la médula ósea y probablemente su recambio sea por división en el tejido como sucede con la microglía, las células de Kuffer o las células de Langerhans de la piel [98, 100, 101]. Esto sugiere que una población de células embrionarias, probablemente células de Langerhans y macrófagos tisulares podrían estar localizados estratégicamente en la zona óptica de la córnea. Ésta puede ser una población atenuada o quiescente con un papel fundamental en prevenir la inflamación en el zona visual de la córnea ayudando a mantener el privilegio inmune y por tanto la trasparencia. Esto se ve ratificado por la escasa expresión o ausencia de MHC clase II en el centro de la córnea [90] donde la expresión de Cx3cr1 está inhibida [95].

En conclusión, en el presente estudio se combinó microscopía multifotónica "intravital", diferentes cepas de ratones que expresan fluorescencia bajo el promotor de Cx3cr1 y un sistema digital de tratado de imágenes para el estudio de la población inmunitaria de la córnea *"in vivo"*. Este modelo es ideal para el estudio de la función de la población inmunitaria de la córnea tanto en condiciones normales como en patológicas

<u>Capítulo 5:</u> Innovación en sistemas de imagen *"in vivo"* I: Microscopía multifotónica *"intravital"* para visualizar los nervios corneales en un ratón que expresa fluorescencia en el gen de Thy-1.

"Chapter 5: *Cutting Edge in vivo Imaging II: Multi-Photon intravital Microscopy to Visualize Transgenic Neurofluorescence in a Thy1-YFP Mouse Cornea"*

En el presente estudio se combinó un sistema de microscopía multifotónica *"intravital",* ratones genéticamente modificados que emiten neurofluorescencia (Thy1-YFP), y un sistema de análisis digital para el estudio *"in vivo"* y no invasivo de los nervios de la córnea.

El estudio de los inervación corneal ha sido un gran reto durante más de un siglo [102]. Para ello se han utilizado diferentes técnicas en "*explantes*" de tejido fijado [7, 103-109]. Las técnicas de microscopía convencional requieren mucho tiempo y tan sólo muestran porciones detalladas del tejido (sub-basal, estroma anterior, periferia corneal etc.) [110-121]. Recientemente se ha descrito la anatomía nerviosa en una córnea completa [102, 122-124], sin embargo se necesitó de múltiples sesiones manuales de microscopía y un tedioso análisis de post-producción. También se ha intentado describir con sistemas IVCM pero la resolución alcanzada dista de lo deseable y sólo se ha fotografiado el plexo basal [125, 126]. Otros investigadores han usado un microscopio de fluorescencia de ancho variable ("widefield stereo fluorescent microscopy") para fotografiar "*in vivo"* los nervios de la córnea [38, 127]. A pesar de mejorar los resultados anteriores la resolución difiere mucho de ser óptima y además muchos detalles como por ejemplo las terminaciones nerviosas del epitelio, no se muestran así como falta de definición en los haces profundos [125, 126]. Por tanto, a día de hoy, este es el primer estudio en el que se muestra los nervios de la córnea utilizando una técnica no invasiva en un modelo animal *"in vivo"* para generar una imagen tridimensional de alta resolución.

La córnea es uno de los órganos más inervados del cuerpo. Su inervación es fundamentalmente de dos tipos: sensitiva con origen en la rama oftálmica del nervio trigémino y con gran densidad sensorial en el epitelio corneal [128, 129]; y autónoma, tanto simpática con origen en el ganglio cervical superior [130] como parasimpática con origen en el ganglio ciliar [131-133]. Las fibras nerviosas penetran en el tercio anterior del estroma por la periferia en una distribución radial paralela a la superficie del epitelio. Una vez en el estroma pierden el perineuro y la envoltura de mielina de las células de Schwann para mantener la transparencia corneal [134, 135]. En este punto se subdividen en numerosas ramificaciones laterales que giran 90º desplazándose anteriormente hacia la membrana basal del epitelio a través de la capa de Bowman donde giran de nuevo 90º dirigiéndose radialmente hacia el centro de la córnea y en posición paralela a la superficie del epitelio formando una estructura denominada plexo basal subepitelial [7, 136]. De nuevo se subdividen en terminaciones más simples que giran otra vez 90º dirigiéndose hacia la superficie del epitelio, a nivel de las células aladas, donde ejercen sus funciones neurotróficas o sensoriales [105, 107, 137].

De la misma manera en este trabajo se confirmó este patrón en un ratón vivo. Los haces nerviosos penetran por la periferia de la córnea para ramificarse en lecho estromal formando el plexo sub-basal paralelo a la superficie de la córnea. Los nervios están distribuidos de forma radial en su mayoría en el plexo sub-basal con el clásico patrón de horquilla, peine y espiral además de observarse las terminaciones epiteliales con gran nitidez. También fue posible localizar haces nerviosos en el tercio anterior del estroma.

Como novedad, se observó que al menos cuatro haces nerviosos penetran de forma radial, el estroma profundo cerca del endotelio, desde la periferia hasta el centro. Estos troncos nerviosos forman tres anillos concéntricos en el estroma (periférico, paracentral y central). Estos anillos interconectan varios troncos estromales radiales entre si y envían ramificaciones de horquilla desde abajo hacia el plexo basal. En la córnea humana, los nervios penetran la capa de Bowman en la periferia de la córnea y también en el centro desde el estroma anterior [107, 138]; sin embargo en otros primates los nervios sólo penetran

la capa de Bowman en la periferia y es desconocido en otras especies [105]. En el modelo aquí mostrado, una parte de los nervios penetran en la zona sub-basal del epitelio en la periferia, además de una segunda desde el estroma anterior. Sin embargo, lo novedoso es la existencia de una tercera entrada desde el estroma profundo. Las ramificaciones provenientes de esta zona se bifurcan en 180º a nivel del plexo basal. De esta manera la estructura radial del plexo sub-basal se muestra ramificada por fibras en disposición centrípeta pero también en dirección centrífuga. Estos resultados sugieren un mecanismo de protección en caso de daño del plexo basal. Esto se comprobó dañando uno de los nervios estromales profundos, observándose un proceso inflamatorio severo (perdida de la transparencia, invasión de vasos, ulceración del epitelio y placa fibrótica) en la zona especifica que inervada por ese tronco estromal. Sin embargo el centro de la córnea se mantuvo transparente. Estos resultados se confirmaron *"ex vivo"* usando "*explantes*" corneales marcados con anti tubulina beta clase III.

Por otro lado, existe todavía cierta controversia acerca del patrón de los nervios en el centro de la córnea humana. Müller et al. han propuesto un patrón arquitectónico de diferentes capas superiores e inferiores [7]. Por otro lado Patel et al., han sugerido un patrón en espiral [122]. Yu et al. han mostrado un patrón en espiral en la córnea de ratón más pronunciado en la parte central [38]. En este trabajo se ha observado que los dos modelos son válidos. Por un lado se observó un modelo arquitectónico de diferentes capas: una profunda en el estroma profundo, otra en el estroma anterior y una tercera en el plexo sub-basal y epitelio como se había sugerido por Müller et al. [7]. Por otro lado se confirmó el patrón en espiral en el plexo sub-basal similar al observado por Patel and Yu. [38, 122]. El plexo basal se observa muy bien definido en un patrón de peinado que arranca de patrones en horquilla desde el estroma. Además desde el plexo basal se subdividen terminaciones en forma de látigo hacia la superficie no detectadas *"in vivo"* en trabajos previos [38, 127].

Aunque no se cuantificó de forma objetiva la densidad de fibras nerviosas, se observó, que si bien el número de fibras es ligeramente inferior *"in vivo"* (Thy1-YFP)

comparado con tinciones con anticuerpos anti tubulina beta clase III. Sin embargo, la distribución en el tejido es similar así como sus diferentes componentes. Previamente Yu et al. cuantificaron la expresión *"in vivo"* en córneas de ratones Thy1-YFP (43 μ/mm^2) y en *"explantes"* marcados con anticuerpos anti tubulina beta clase III (94 μ/mm^2). De esta manera vieron que la expresión in vivo de YFP era la mitad que la expresión de tubulina beta clase III [38]. En el presente trabajo se utilizaron anticuerpos anti YFP conjugados con Alexa-488 para amplificar la señal de YFP *"ex vivo"* viéndose que las diferencias eran mínimas con respecto a la tinción con tubulina beta clase III. Por otro lado el hecho de se haya utilizado un microscopio multifotónico, con mayor capacidad de penetración en el tejido así como un proceso de fotoblanqueado mínimo, explica las diferencias fenotípicas respecto a los trabajos anteriores.

En este trabajo los haces estromales, el plexo basal y las terminaciones nerviosas del epitelio, desde el punto de vista estructural, se observan por igual tanto "*in vivo*" como "*ex vivo*", por ello podemos concluir que la fluorescencia emitida por YFP *"in vivo"*, es significativa y representativa de los nervios corneales.

Previamente Yu et al. concluyeron en su trabajo que su modelo permitía la observación *"in vivo"* del proceso de regeneración nerviosa en la córnea usando un microscopio motorizado de campo ancho [38]. En el presente trabajo se ha dado un avance significativo al usar un sistema de imagen que no produce daño en la córnea sino que además provee imágenes detalladas de gran resolución. La función de los nervios en patologías corneales como el ojo seco, el rechazo al trasplante, el queratocono, el dolor crónico, las queratitis o las infecciones, podrá ser estudiado de una manera más detallada con este modelo.

En conclusión, en este estudio se combinó un sistema de microscopía multifotónica *"intravital"*, ratones genéticamente modificados que emiten neuoro-fluorescencia (Thy1-YFP) y un sistema de análisis digital para el estudio *"in vivo"* no invasivo de los nervios de la córnea. Adicionalmente se muestran aspectos novedosos como los haces estromales profundos, los haces concéntricos y la particular estructura de inervación de estos troncos

estromales. El daño específico de uno de estos troncos, produce pérdida localizada del privilegio inmune en el área específica que inerva. Este modelo es ideal para el estudio de la función de los nervios corneales tanto en condiciones normales como patológicas.

<u>Capítulo 6:</u> Implicación de los nervios corneales en el rechazo al trasplante de córnea.

"Chapter 6: *The cornea has "the nerve" to encourage immune rejection"*

En el trabajo publicado se muestra la interacción de los nervios corneales con las células inmunitarias de la córnea y su posible relación con el rechazo al trasplante corneal [139]. Además se incluye material adicional, que si bien no publicado todavía, condujo a los resultados que forman parte de la publicación. Es por ello que se presenta una discusión más extendida donde además de explicar los resultados se pone de manifiesto su relevancia futura. De esta manera al final se muestra la córnea como un órgano en el cual dos "supersistemas" (nervioso e inmunitario) están físicamente interconectados. Además se creó un ratón quimera en el cual se puede estudiar "*in vivo*" la interacción de los dos "supersistemas".

La córnea, el órgano más inervado del cuerpo, contiene una población residente inmunitaria de células presentadoras de antígeno no inmunoreactivas a aloantígenos [140]. En contacto con el medio externo la córnea ha evolucionado como un órgano con privilegio inmune para mantener la transparencia y sus propiedades biomecánicas, refractivas y sensoriales [28, 141]. La córnea ha desarrollado un mecanismo de cicatrización único que le permite un proceso de auto reparación después de una lesión. Generalmente, este mecanismo ocurre con ausencia de reacción inflamatoria, en parte debido a la ausencia de vasos sanguíneos y linfáticos [9, 142-144]. La inflamación es un componente esencial para la protección de los tejidos y la erradicación de las infecciones, sin embargo en la córnea es un antagonista de la transparencia [86]. Durante los últimos años se ha estudiado el mecanismo por el cual la córnea se protege a si misma de la inflamación así

como las causas por las que ésta pierde el privilegio inmune [8, 39, 40, 88, 89, 91], sin embargo la mayoría de los aspectos permanecen todavía desconocidos.

Tomio Tada definió un "supersistema" como una sistema vivo con un alto grado de integración como por ejemplo el sistema nervioso, el sistema inmunitario y el desarrollo embrionario de los organismos superiores. Un "supersistema" se define por tres características fundamentales: 1) se genera a si mismo y a sus componentes de forma estocástica a partir de un solo progenitor, seguido de un proceso de selección y adaptación; 2) posee individualidad y es capaz de decidir su comportamiento en respuesta a un estímulo del medioambiente y 3) se genera y funciona sin un propósito dado [43].

Cada vez existen más evidencias que indican la existencia de un complejo de regulación cruzada entre los dos biosensores más importantes del cuerpo humano: el sistema inmune y el nervioso [145]. Las citoquinas controlan la temperatura corporal y disparan procesos autoinmunes en el sistema nervioso central, mientras los neuropéptidos liberados en los tejidos periféricos y órganos linfoides modulan las repuestas inmunitaria tanto adaptativa como innata. Relevancia especial está tomando este nuevo campo inexplorado en las terapias para la prevención y el tratamiento del rechazo a los trasplantes especialmente en la piel. (Para información detallada ver revisión actualizada Larregina et al. [145]).

La mayor evidencia de las interacciones celulares entre los dos sistemas viene de los estudios de las vías respiratorias [146]. La proximidad anatómica de los nervios y las células inmunitarias, predice la existencia de su interacción funcional en estado normal del tejido, además de marcar las bases de la comunicación neuro-inmunitaria, en la alergia. Las células inmunes responden a los neurotransmisores y a su vez los nervios responden a los mediadores inmunitarios. Los mastocitos y eosinófilos se asocian con las fibras nerviosas [147, 148]. Los eosinófilos rodean y se infiltran entre los haces nerviosos [149]. Las células dendríticas del tracto respiratorio regulan la respuesta inmunitaria adaptativa ante antígenos inhalados [150] y están involucradas en la patogénesis de la alergia [151]. Las células dendríticas están en contacto con fibras sensoriales positivas para CGRP en la

mucosa de los conductos respiratorios y sus interconexiones aumentan en procesos alérgicos [152]. En las vías respiratorias, las células dendríticas activan los linfocitos T mediante presentación local de antígeno [153]. En estas vías, la asociación de linfocitos T con fibras nerviosas está ampliamente descrito [146]. Por un lado los neuropéptidos liberados por las neuronas modulan directamente la actividad de las células dendríticas y linfocitos T. Por ejemplo CGRP ("Calcitonin gene related peptide") y VIP ("vasoactive intestinal peptide") tienen efectos inmunosupresores, mientras SP ("substance P") tiene efecto proinflamatorio. Las células dendríticas tienen receptores para CGRP [154],VIP [155] y SP [156]. CGRP y VIP actúan como quimioatrayentes para las células dendríticas inmaduras hacia las terminaciones nerviosas donde son arrestadas hasta un posterior maduración [157]. Además CGRP inhibe la respuesta proliferativa de los linfocitos T disminuyendo la expresión de CD86 y HLA-DR en las células dendríticas [154]. Adicionalmente CGRP inhibe la presentación de antígeno por parte de las células de Langerhans [158]. VIP induce la generación de células dendríticas tolerogénicas de la misma manera que lo hacen los linfocitos T reguladores [159]. Al contrario, la SP media el reclutamiento y la supervivencia de las células dendríticas ante un llegada secundara de un antígeno [160] potenciando así la inmunidad celular [161]. Por otro lado, la interacción bidireccional entre las células inmunitarias y los nervios también se indica a través de las neurotrofinas. Las neurotrofinas pro-inflamatorias producidas por los linfocitos, eosinófilos y macrófagos [162] durante un proceso alérgico activan la síntesis y liberación de neuropéptidos en las neuronas aferentes vagales [163].

Recientemente se ha propuesto la córnea como un órgano muy atractivo para explorar la interacción del sistema nervioso y del sistema inmunitario y como esta interacción puede tener un papel fundamental en el rechazo al trasplante corneal. Muy actual, Paunicka *et al.* ha descrito que cuando se dañan los nervios corneales durante el trasplante (inevitable durante el proceso), se inhibe el privilegio inmune incluso en el ojo contralateral [164]. La colocación de un injerto de tejido corneal incrementa el riesgo de rechazo a un alotrasplante secundario tanto en el mismo ojo como en el contralateral,

incluso cuando la causa del trasplante secundario no está relacionada con la primera. El incremento no específico del rechazo es mediado por linfocitos T ya que subsecuentes injertos singénicos sobreviven indefinidamente. Sin embargo la causa del incremento de rechazo secundario o en el ojo contralateral se ha relacionado con la respuesta al daño nervioso producido durante el primer trasplante. De esta manera, estos autores observaron resultados similares dañando los nervios corneales 360 grados alrededor de la córnea. Todos los injertos realizados fueron rechazaron inmunológicamente 60 días después del trasplante. Por otro lado, estos autores demostraron que la aplicación de SP producía el mimos efecto que dañando los propios nervios, aumentando el rechazo. La SP desestabiliza la supresión regulatoria de los linfocitos T reguladores asociada con el incremento en el rechazo [164]. Sin embargo los autores no tienen explicación de cómo los linfocitos T reguladores aumentan el rechazo inmunológico en respuesta a una liberación masiva de SP 60 días antes.

En este trabajo proponemos un papel potencial de las células dendríticas residentes y macrófagos. Ambos expresan receptores de SP, producen SP y responden a este neuropéptido [165]. Los macrófagos son células presentadoras de antígeno que migran a los órganos linfoides [166]. Se ha descrito que los macrófagos residen en la proximidad de los nervios en los periféricos [167], así como en los nervios del estroma corneal periférico [168].

En el presente artículo [139] de apoyo al trabajo de Paunicka et al. [94] mostramos que las células dendríticas epiteliales están en contacto con los nervios corneales. Además, en el trabajo suplementario se muestra la presencia de células dendríticas y macrófagos en contacto con los nervios en toda la córnea así como en el limbo. Por ejemplo, se muestra como célula dendrítica individual contacta con hasta 10 axones diferentes en el plexo sub-basal. De la misma manera lo hacen los macrófagos en el estroma tanto en el centro como en la periferia. Los nervios del estroma se ramifican en la parte basal del epitelio formando el plexo sub-basal. En cada ramificación se observa la presencia de al menos una célula mieloide. Por otro lado se ha observado la presencia de terminaciones nerviosas entrelazadas con las prolongaciones intraepiteliales de las células dendríticas.

De la misma manera se aprecia como una fibra nerviosa en su recorrido desde el centro de la córnea, hasta su salida por el limbo, está en contacto con diferentes células dendríticas y macrófagos probablemente a modo de centinelas estáticos.

Previamente, en el ***capítulo 4***, describimos la población residente inmunitaria de la córnea en un modelo *"in vivo"*. Por otro lado en el ***capítulo 5***, también se visualizó de forma "*intravital*" la anatomía de los nervios corneales en un modelo de ratón Thy1-YFP. En el presente trabajo se generó un modelo animal en ratón, idóneo para el estudio no invasivo *"in vivo"* de la interacción entre los nervios y la población inmunitaria de la córnea.

Se tomaron ratones Thy1-YFP como receptores y se irradiaron de forma letal y posteriormente se les trasplantó células derivadas de la médula ósea de ratones donantes $Cx3cr1^{Cre/}$RFP. De esta manera, fue posible visualizar *"in vivo"* en la quimera resultante, tanto los nervios como las células inmunitarias donantes.

De esta manera se comprobó que la pérdida de las células inmunitarias de la córnea, no implica pérdida del privilegio inmune. Por otro lado se comprobó que el proceso de repoblación en si tampoco hace que se pierda dicho privilegio. Pero lo más importante fue observar, como las células donantes, repueblan la córnea en contacto con los nervios, residiendo de la misma manera que se observa en el estado basal, demostrando la interacción de los dos "supersistemas" de forma estocástica en la córnea. En este caso el sistema inmunitario, sin una predeterminación establecida, interacciona con los nervios corneales para reparar a la población anterior con un origen embrionario diferente y así mantener el privilegio inmune y por tanto la trasparencia.

En conclusión y adicionalmente al artículo original titulado "The cornea has "the nerve" to encourage immune rejection" [139]; en este trabajo se muestra que el sistema nervioso periférico y el sistema inmune residente de la córnea están conectados en condiciones normales. Para el estudio de esta interconexión, se desarrolló un nuevo modelo quimérico en ratón que podrá ser útil para el estudio *"in vivo"* de las patologías corneales.

Capítulo 7: Aplicaciones futuras del uso de la microscopía multifotónica no invasiva *"in vivo*.

"Chapter 7*: Further applications of Multi-Photon Intravital Microscopy in ocular research"*

Como se ha mostrado en los capítulos anteriores, el sistema de microscopía multifotónica *"intravital"* ha sido introducido con éxito para la investigación en el ojo del ratón. Considerando la trasparencia de la córnea, en este capítulo adicional, se explotó la máxima capacidad del sistema para hacer un seguimiento *"in vivo"* de la localización y el comportamiento de:

1. Células mesenquimales del tejido adiposo inyectadas en diferentes partes de la córnea. En este estudio se observó la evolución de las células durante cuatro semanas. (Colaboración con Ladan Espandar, institución actual "Pittsburg University"). En este modelo se observó como las células se implantaban en la cámara anterior y en el estroma sin sufrir una respuesta infamatoria detectable. De la misma manera se observó las células se comportaban como del tejido propias en el caso de una lesión. Las células mesenquimales consiguieron migrar y diferenciarse en epitelio, células estromales y endotelio.

2. Diferentes sistemas de liberación de fármacos fueron inyectaron a través de la vena epiescleral y su localización se observó *"in vivo"* y a tiempo real. De esta manera se observó la presencia de los diferentes componentes en el canal de Schlemm y en la malla trabecular sin necesidad de sacrificar el ratón (Colaboración con Molly Walsh, "Duke Eye Center")

3. Inyección de adenovirus marcados en la cámara anterior. Se observó como las células endoteliales al ser infectadas por el virus emiten fluorescencia (GFP). (Colaboración con Li Quarong yDan Stramer, "Duke Eye Center")

4. Depleción de una población específica de células dendríticas CD11c-DTR con toxina diftérica. De esta manera se observó como después de la aplicación tópica de toxina diftérica, la población de células dendríticas CD11c-DTR desparecía de la córnea siendo su tiempo de retorno entre 2-3 meses (Colaboración con Sarah Dale y Virginia Calder, "University College London").

En conclusión, el sistema de microscopía multifotónica *"intravital"* permite múltiples aplicaciones *"in vivo"* que permitirá mejorar y hacer más efectivos nuevos experimentos, en los cuales, un seguimiento del animal a tiempo real, mejorará significativamente los resultados.

CONCLUSIONES

Como conclusión general, esta tesis doctoral aborda el estudio de la fisiopatología de la córnea desde el punto de vista de la cicatrización, la inflamación y el estado normal tanto de la población residente de células inmunitarias como de el sistema nervioso periférico que la inerva. Por otro lado, en esta tesis se muestra una evolución tecnológica, desde el **capítulo 1** hasta el **capítulo 7**, tanto en los sistemas de imagen como en los ratones utilizados. De esta manera se muestra la córnea como un órgano extremadamente complejo, en el que varios sistemas interaccionan entre si para mantener sus propiedades fundamentales. Entendiendo la córnea desde varios enfoques y con la posibilidad de implementar nuevos sistemas de imagen *"in vivo"* se da un avance considerable en el estudio de la patologías a tiempo real.

Teniendo en cuenta todos los resultados obtenidos en los diferentes estudios que constituyen este trabajo de tesis, se puede afinar en las siguientes conclusiones específicas:

1. La integrina α6β4 es imprescindible para la regeneración de la membrana basal del epitelio corneal después de una lesión y su ausencia puede causar patologías como la queratopatía bullosa o las distrofias de la membrana basal del epitelio.
2. La THBS1 juega un papel primordial durante el proceso de reparación corneal. Esto incluye migración endotelial, contracción estromal y síntesis de nueva matriz extracelular.
3. Se pudo evaluar la reacción inflamatoria de la superficie ocular en un modelo de conjuntivitis alérgica en ratón usando un sistema IVCM. El aumento en el número de células inflamatorias está relacionado espaciotemporalmente con el aumento de la sintomatología clínica observada con la lámpara de hendidura así

como con los resultados obtenidos "*ex vivo*" con citometría de flujo y microscopía confocal. Este incremento también afecta a la córnea.

4. Se ha podido combinar microscopía multifotónica *"intravital"*, diferentes cepas de ratones que expresan fluorescencia bajo el promotor de Cx3cr1 y un sistema digital de tratado de imágenes para el estudio de la población inmunitaria de la córnea de forma no invasiva e *"in vivo"*. Este modelo es ideal para el estudio de la función de la población inmunitaria de la córnea tanto en condiciones normales como en patológicas
5. Se ha conseguido combinar un sistema de microscopía multifotónica *"intravital"*, ratones genéticamente modificados que emiten fluorescencia bajo el control del gen Thy1 y un sistema de análisis digital para el estudio *"in vivo"* y no invasivo de los nervios de la córnea. Por otro lado se muestran aspectos novedosos como los haces estromales profundos que inervan zonas específicas de la córnea y como el daño focalizado de uno de estos troncos, produce pérdida del privilegio inmune en el área específica que inerva. Este modelo es ideal para el estudio de la función de los nervios corneales tanto en condiciones normales como patológicas.
6. Se ha podido constatar que el sistema nervioso periférico y las células inmunitarias residentes en la córnea, están conectados en condiciones normales. Para el estudio de esta interconexión, se desarrolló un nuevo ratón quimera que podrá ser útil para el estudio *"in vivo"* no invasivo de las patologías corneales. Adicionalmente se presenta la córnea como un órgano donde dos "supersistemas", nervioso e inmunitario, interactúan de forma estocástica y entre si para mantener la función corneal. Por ser la córnea un órgano transparente fácil de examinar de forma *"intravital"*, puede servir como modelo para otros órganos internos o difíciles de examinar *"in vivo"*
7. Mediante la microscopía multifotónica no invasiva se ha podido hacer el seguimiento *"in vivo"* a tiempo real de la regeneración corneal con células

mesenquimales del tejido adiposo. Además se constató a tiempo real y de forma *"intravital"* la localización de sistemas de liberación de fármacos en la cámara anterior, malla trabecular y canal de Schlemm. Se pudo observar el proceso de infección de células endoteliales por adenovirus. Por último se constató *"in vivo"* la depleción de una subpoblación específica de células dendríticas CD11c+ mediante el uso de toxina diftérica.

BIBLIOGRAFÍA

1. C. Stephen Foster, D.T.A., Claes H. Dolman, *Smolin and Thoft's The Cornea, Scientific Foundation & Clinical Practice.* 2005.
2. Beebe, D.C. and B.R. Masters, *Cell lineage and the differentiation of corneal epithelial cells.* Invest Ophthalmol Vis Sci, 1996. **37**(9): p. 1815-25.
3. Hanna, C. and J.E. O'Brien, *Cell production and migration in the epithelial layer of the cornea.* Arch Ophthalmol, 1960. **64**: p. 536-9.
4. Wilson, S.E. and J.W. Hong, *Bowman's layer structure and function: critical or dispensable to corneal function? A hypothesis.* Cornea, 2000. **19**(4): p. 417-20.
5. Rodrigues MM, W.G.I., Hackett J, Donohoo P *Ocular Anatomy, Embryology, and Teratology.* 1982.
6. Waring, G.O., 3rd, W.M. Bourne, H.F. Edelhauser and K.R. Kenyon, *The corneal endothelium. Normal and pathologic structure and function.* Ophthalmology, 1982. **89**(6): p. 531-90.
7. Muller, L.J., G.F. Vrensen, L. Pels, B.N. Cardozo and B. Willekens, *Architecture of human corneal nerves.* Invest Ophthalmol Vis Sci, 1997. **38**(5): p. 985-94.
8. Knickelbein, J.E., K.A. Buela and R.L. Hendricks, *Antigen-presenting cells are stratified within normal human corneas and are rapidly mobilized during ex vivo viral infection.* Invest Ophthalmol Vis Sci, 2014. **55**(2): p. 1118-23.
9. Maurice, D.M., *The structure and transparency of the cornea.* J Physiol, 1957. **136**(2): p. 263-86.
10. Wilson, S.E., *Analysis of the keratocyte apoptosis, keratocyte proliferation, and myofibroblast transformation responses after photorefractive keratectomy and laser in situ keratomileusis.* Trans Am Ophthalmol Soc, 2002. **100**: p. 411-33.
11. Hanada, K., S. Igarashi, O. Muramatsu and A. Yoshida, *Therapeutic keratoplasty for corneal perforation: clinical results and complications.* Cornea, 2008. **27**(2): p. 156-60.
12. Rabinowitz, Y.S., *Keratoconus.* Surv Ophthalmol, 1998. **42**(4): p. 297-319.
13. Kaye, S. and A. Choudhary, *Herpes simplex keratitis.* Prog Retin Eye Res, 2006. **25**(4): p. 355-80.
14. Wilson, S.E., L. Pedroza, R. Beuerman and J.M. Hill, *Herpes simplex virus type-1 infection of corneal epithelial cells induces apoptosis of the underlying keratocytes.* Exp Eye Res, 1997. **64**(5): p. 775-9.
15. Leonardi, A., L. Motterle and M. Bortolotti, *Allergy and the eye.* Clin Exp Immunol, 2008. **153 Suppl 1**: p. 17-21.
16. Netto, M.V., R.R. Mohan, R. Ambrosio, Jr., A.E. Hutcheon, J.D. Zieske and S.E. Wilson, *Wound healing in the cornea: a review of refractive surgery complications and new prospects for therapy.* Cornea, 2005. **24**(5): p. 509-22.

17. Randleman, J.B., M. Woodward, M.J. Lynn and R.D. Stulting, *Risk assessment for ectasia after corneal refractive surgery.* Ophthalmology, 2008. **115**(1): p. 37-50.
18. Zirm, E.K., *Eine erfolgreiche totale Keratoplastik (A successful total keratoplasty). 1906.* Refract Corneal Surg, 1989. **5**(4): p. 258-61.
19. van Essen, T.H., D.L. Roelen, K.A. Williams and M.J. Jager, *Matching for Human Leukocyte Antigens (HLA) in corneal transplantation - To do or not to do.* Prog Retin Eye Res, 2015. **46**: p. 84-110.
20. Moss, S.E., R. Klein and B.E. Klein, *Prevalence of and risk factors for dry eye syndrome.* Arch Ophthalmol, 2000. **118**(9): p. 1264-8.
21. Vichyanond, P., P. Pacharn, U. Pleyer and A. Leonardi, *Vernal keratoconjunctivitis: a severe allergic eye disease with remodeling changes.* Pediatr Allergy Immunol, 2014. **25**(4): p. 314-22.
22. Alonso, M.J., *Nanomedicines for overcoming biological barriers.* Biomed Pharmacother, 2004. **58**(3): p. 168-72.
23. Diebold, Y., M. Jarrin, V. Saez, E.L. Carvalho, M. Orea, M. Calonge, B. Seijo and M.J. Alonso, *Ocular drug delivery by liposome-chitosan nanoparticle complexes (LCS-NP).* Biomaterials, 2007. **28**(8): p. 1553-64.
24. Ertan, A. and J. Colin, *Intracorneal rings for keratoconus and keratectasia.* J Cataract Refract Surg, 2007. **33**(7): p. 1303-14.
25. Kymionis, G. and D. Portaliou, *Corneal crosslinking with riboflavin and UVA for the treatment of keratoconus.* J Cataract Refract Surg, 2007. **33**(7): p. 1143-4; author reply 1144.
26. Anitua, E., F. Muruzabal, I. Alcalde, J. Merayo-Lloves and G. Orive, *Plasma rich in growth factors (PRGF-Endoret) stimulates corneal wound healing and reduces haze formation after PRK surgery.* Exp Eye Res, 2013. **115**: p. 153-61.
27. Lambiase, A., L. Manni, P. Rama and S. Bonini, *Clinical application of nerve growth factor on human corneal ulcer.* Arch Ital Biol, 2003. **141**(2-3): p. 141-8.
28. Streilein, J.W., *New thoughts on the immunology of corneal transplantation.* Eye (Lond), 2003. **17**(8): p. 943-8.
29. Maruyama, K., T. Nakazawa, C. Cursiefen, Y. Maruyama, N. Van Rooijen, P.A. D'Amore and S. Kinoshita, *The maintenance of lymphatic vessels in the cornea is dependent on the presence of macrophages.* Invest Ophthalmol Vis Sci, 2012. **53**(6): p. 3145-53.
30. Chauhan, S.K., T.H. Dohlman and R. Dana, *Corneal Lymphatics: Role in Ocular Inflammation as Inducer and Responder of Adaptive Immunity.* J Clin Cell Immunol, 2014. **5**.
31. Fukuda, K. and T. Nishida, *Ocular allergic inflammation: interaction between the cornea and conjunctiva.* Cornea, 2010. **29 Suppl 1**: p. S62-7.

32. Fukuda, K., N. Yamada and T. Nishida, *Case report of restoration of the corneal epithelium in a patient with atopic keratoconjunctivitis resulting in amelioration of ocular allergic inflammation.* Allergol Int, 2010. **59**(3): p. 309-12.
33. Mohan, R.R., A.E. Hutcheon, R. Choi, J. Hong, J. Lee, R.R. Mohan, R. Ambrosio, Jr., J.D. Zieske and S.E. Wilson, *Apoptosis, necrosis, proliferation, and myofibroblast generation in the stroma following LASIK and PRK.* Exp Eye Res, 2003. **76**(1): p. 71-87.
34. Martinez-Garcia, M.C., J. Merayo-Lloves, T. Blanco-Mezquita and S. Mar-Sardana, *Wound healing following refractive surgery in hens.* Exp Eye Res, 2006. **83**(4): p. 728-35.
35. Power, W.J., A.H. Kaufman, J. Merayo-Lloves, V. Arrunategui-Correa and C.S. Foster, *Expression of collagens I, III, IV and V mRNA in excimer wounded rat cornea: analysis by semi-quantitative PCR.* Curr Eye Res, 1995. **14**(10): p. 879-86.
36. Del Pero, R.A., J.E. Gigstad, A.D. Roberts, G.K. Klintworth, C.A. Martin, F.A. L'Esperance, Jr. and D.M. Taylor, *A refractive and histopathologic study of excimer laser keratectomy in primates.* Am J Ophthalmol, 1990. **109**(4): p. 419-29.
37. Mohan, R.R., W.M. Stapleton, S. Sinha, M.V. Netto and S.E. Wilson, *A novel method for generating corneal haze in anterior stroma of the mouse eye with the excimer laser.* Exp Eye Res, 2008. **86**(2): p. 235-40.
38. Yu, C.Q. and M.I. Rosenblatt, *Transgenic corneal neurofluorescence in mice: a new model for in vivo investigation of nerve structure and regeneration.* Invest Ophthalmol Vis Sci, 2007. **48**(4): p. 1535-42.
39. Hamrah, P., Y. Liu, Q. Zhang and M.R. Dana, *The corneal stroma is endowed with a significant number of resident dendritic cells.* Invest Ophthalmol Vis Sci, 2003. **44**(2): p. 581-9.
40. Knickelbein, J.E., S.C. Watkins, P.G. McMenamin and R.L. Hendricks, *Stratification of Antigen-presenting Cells within the Normal Cornea.* Ophthalmol Eye Dis, 2009. **1**: p. 45-54.
41. Nowotschin, S., P. Xenopoulos, N. Schrode and A.K. Hadjantonakis, *A bright single-cell resolution live imaging reporter of Notch signaling in the mouse.* BMC Dev Biol, 2013. **13**: p. 15.
42. Steven, P., F. Bock, G. Huttmann and C. Cursiefen, *Intravital two-photon microscopy of immune cell dynamics in corneal lymphatic vessels.* PLoS One, 2011. **6**(10): p. e26253.
43. Tada, T., *The immune system as a supersystem.* Annu Rev Immunol, 1997. **15**: p. 1-13.

44. Cain, D.W., E.G. O'Koren, M.J. Kan, M. Womble, G.D. Sempowski, K. Hopper, M.D. Gunn and G. Kelsoe, *Identification of a tissue-specific, C/EBPbeta-dependent pathway of differentiation for murine peritoneal macrophages.* J Immunol, 2013. **191**(9): p. 4665-75.
45. Gong, S., C. Zheng, M.L. Doughty, K. Losos, N. Didkovsky, U.B. Schambra, N.J. Nowak, A. Joyner, G. Leblanc, M.E. Hatten and N. Heintz, *A gene expression atlas of the central nervous system based on bacterial artificial chromosomes.* Nature, 2003. **425**(6961): p. 917-25.
46. DeFalco, T., I. Bhattacharya, A.V. Williams, D.M. Sams and B. Capel, *Yolk-sac-derived macrophages regulate fetal testis vascularization and morphogenesis.* Proc Natl Acad Sci U S A, 2014. **111**(23): p. E2384-93.
47. Feng, G., R.H. Mellor, M. Bernstein, C. Keller-Peck, Q.T. Nguyen, M. Wallace, J.M. Nerbonne, J.W. Lichtman and J.R. Sanes, *Imaging neuronal subsets in transgenic mice expressing multiple spectral variants of GFP.* Neuron, 2000. **28**(1): p. 41-51.
48. Reyes, N.J., E. Mayhew, P.W. Chen and J.Y. Niederkorn, *NKT cells are necessary for maximal expression of allergic conjunctivitis.* Int Immunol. **22**(8): p. 627-36.
49. Berman, M., E. Manseau, M. Law and D. Aiken, *Ulceration is correlated with degradation of fibrin and fibronectin at the corneal surface.* Invest Ophthalmol Vis Sci, 1983. **24**(10): p. 1358-66.
50. Jester, J.V., J. Huang, P.A. Barry-Lane, W.W. Kao, W.M. Petroll and H.D. Cavanagh, *Transforming growth factor(beta)-mediated corneal myofibroblast differentiation requires actin and fibronectin assembly.* Invest Ophthalmol Vis Sci, 1999. **40**(9): p. 1959-67.
51. van der Neut, R., P. Krimpenfort, J. Calafat, C.M. Niessen and A. Sonnenberg, *Epithelial detachment due to absence of hemidesmosomes in integrin beta 4 null mice.* Nat Genet, 1996. **13**(3): p. 366-9.
52. Matsuba, M., A.E. Hutcheon and J.D. Zieske, *Localization of thrombospondin-1 and myofibroblasts during corneal wound repair.* Exp Eye Res, 2011. **93**(4): p. 534-40.
53. Uno, K., H. Hayashi, M. Kuroki, H. Uchida, Y. Yamauchi, M. Kuroki and K. Oshima, *Thrombospondin-1 accelerates wound healing of corneal epithelia.* Biochem Biophys Res Commun, 2004. **315**(4): p. 928-34.
54. Zieske, J.D., *Expression of cyclin-dependent kinase inhibitors during corneal wound repair.* Prog Retin Eye Res, 2000. **19**(3): p. 257-70.
55. Wilson, S.E., S.S. Chaurasia and F.W. Medeiros, *Apoptosis in the initiation, modulation and termination of the corneal wound healing response.* Exp Eye Res, 2007. **85**(3): p. 305-11.

56. Wilson, S.E., R.R. Mohan, J. Hong, J. Lee, R. Choi, J.J. Liu and R.R. Mohan, *Apoptosis in the cornea in response to epithelial injury: significance to wound healing and dry eye.* Adv Exp Med Biol, 2002. **506**(Pt B): p. 821-6.
57. Wilson, S.E., G.S. Schultz, N. Chegini, J. Weng and Y.G. He, *Epidermal growth factor, transforming growth factor alpha, transforming growth factor beta, acidic fibroblast growth factor, basic fibroblast growth factor, and interleukin-1 proteins in the cornea.* Exp Eye Res, 1994. **59**(1): p. 63-71.
58. Jester, J.V., W.M. Petroll and H.D. Cavanagh, *Corneal stromal wound healing in refractive surgery: the role of myofibroblasts.* Prog Retin Eye Res, 1999. **18**(3): p. 311-56.
59. Bornstein, P., *Thrombospondins as matricellular modulators of cell function.* J Clin Invest, 2001. **107**(8): p. 929-34.
60. Murphy-Ullrich, J.E., S. Gurusiddappa, W.A. Frazier and M. Hook, *Heparin-binding peptides from thrombospondins 1 and 2 contain focal adhesion-labilizing activity.* J Biol Chem, 1993. **268**(35): p. 26784-9.
61. Young, G.D. and J.E. Murphy-Ullrich, *Molecular interactions that confer latency to transforming growth factor-beta.* J Biol Chem, 2004. **279**(36): p. 38032-9.
62. Matsuba, M., A.E. Hutcheon and J.D. Zieske, *Localization of thrombospondin-1 and myofibroblasts during corneal wound repair.* Exp Eye Res, 2011.
63. Raubenheimer, E.J., *The myoepithelial cell: embryology, function, and proliferative aspects.* Crit Rev Clin Lab Sci, 1987. **25**(2): p. 161-93.
64. Hiscott, P., L. Paraoan, A. Choudhary, J.L. Ordonez, A. Al-Khaier and D.J. Armstrong, *Thrombospondin 1, thrombospondin 2 and the eye.* Prog Retin Eye Res, 2006. **25**(1): p. 1-18.
65. Bahn, C.F., R.M. Glassman, D.K. MacCallum, J.H. Lillie, R.F. Meyer, B.J. Robinson and N.M. Rich, *Postnatal development of corneal endothelium.* Invest Ophthalmol Vis Sci, 1986. **27**(1): p. 44-51.
66. Watson, S.L., G. Abiad and M.T. Coroneo, *Spontaneous resolution of corneal oedema following Descemet's detachment.* Clin Experiment Ophthalmol, 2006. **34**(8): p. 797-9.
67. Munjal, I.D., D.R. Crawford, D.A. Blake, M.D. Sabet and S.R. Gordon, *Thrombospondin: biosynthesis, distribution, and changes associated with wound repair in corneal endothelium.* Eur J Cell Biol, 1990. **52**(2): p. 252-63.
68. Sumioka, T., K. Ikeda, Y. Okada, O. Yamanaka, A. Kitano and S. Saika, *Inhibitory effect of blocking TGF-beta/Smad signal on injury-induced fibrosis of corneal endothelium.* Mol Vis, 2008. **14**: p. 2272-81.
69. Zamiri, P., S. Masli, N. Kitaichi, A.W. Taylor and J.W. Streilein, *Thrombospondin plays a vital role in the immune privilege of the eye.* Invest Ophthalmol Vis Sci, 2005. **46**(3): p. 908-19.

70. Turpie, B., T. Yoshimura, A. Gulati, J.D. Rios, D.A. Dartt and S. Masli, *Sjogren's syndrome-like ocular surface disease in thrombospondin-1 deficient mice.* Am J Pathol, 2009. **175**(3): p. 1136-47.
71. Uno, K., H. Hayashi, M. Kuroki, H. Uchida, Y. Yamauchi and K. Oshima, *Thrombospondin-1 accelerates wound healing of corneal epithelia.* Biochem Biophys Res Commun, 2004. **315**(4): p. 928-34.
72. Matsuba-Kitamura, S., T. Yoshimoto, K. Yasuda, S. Futatsugi-Yumikura, Y. Taki, T. Muto, T. Ikeda, O. Mimura and K. Nakanishi, *Contribution of IL-33 to induction and augmentation of experimental allergic conjunctivitis.* Int Immunol. **22**(6): p. 479-89.
73. Miyazaki, D., W. Ishida, T. Tominaga, T. Sumi and A. Fukushima, *Aggravation of conjunctival early-phase reaction by Staphylococcus enterotoxin B via augmentation of IgE production.* Jpn J Ophthalmol. **54**(5): p. 476-80.
74. Nakano, Y., Y. Takahashi, R. Ono, Y. Kurata, Y. Kagawa and C. Kamei, *Role of histamine H(4) receptor in allergic conjunctivitis in mice.* Eur J Pharmacol, 2009. **608**(1-3): p. 71-5.
75. Schlereth, S., H.S. Lee, P. Khandelwal and D.R. Saban, *Blocking CCR7 at the Ocular Surface Impairs the Pathogenic Contribution of Dendritic Cells in Allergic Conjunctivitis.* Am J Pathol. **180**(6): p. 2351-60.
76. Kumagai, N., K. Fukuda, Y. Fujitsu, K. Yamamoto and T. Nishida, *Role of structural cells of the cornea and conjunctiva in the pathogenesis of vernal keratoconjunctivitis.* Prog Retin Eye Res, 2006. **25**(2): p. 165-87.
77. Jin, Y., L. Shen, E.M. Chong, P. Hamrah, Q. Zhang, L. Chen and M.R. Dana, *The chemokine receptor CCR7 mediates corneal antigen-presenting cell trafficking.* Mol Vis, 2007. **13**: p. 626-34.
78. Yamagami, S. and M.R. Dana, *The critical role of lymph nodes in corneal alloimmunization and graft rejection.* Invest Ophthalmol Vis Sci, 2001. **42**(6): p. 1293-8.
79. Lee, E.J., J.T. Rosenbaum and S.R. Planck, *Epifluorescence intravital microscopy of murine corneal dendritic cells.* Invest Ophthalmol Vis Sci, 2010. **51**(4): p. 2101-8.
80. Steinman, R.M. and J. Banchereau, *Taking dendritic cells into medicine.* Nature, 2007. **449**(7161): p. 419-26.
81. Ohbayashi, M., B. Manzouri, T. Flynn, M. Toda, Y. Ikeda, T. Nakamura and S.J. Ono, *Dynamic changes in conjunctival dendritic cell numbers, anatomical position and phenotype during experimental allergic conjunctivitis.* Exp Mol Pathol, 2007. **83**(2): p. 216-23.
82. Schlereth, S., H.S. Lee, P. Khandelwal and D.R. Saban, *Blocking CCR7 at the ocular surface impairs the pathogenic contribution of dendritic cells in allergic conjunctivitis.* Am J Pathol, 2012. **180**(6): p. 2351-60.

83. Saban, D.R., F. Bock, S.K. Chauhan, S. Masli and R. Dana, *Thrombospondin-1 derived from APCs regulates their capacity for allosensitization.* J Immunol, 2010. **185**(8): p. 4691-7.
84. Saban, D.R., V. Calder, C.H. Kuo, N.J. Reyes, D.A. Dartt, S.J. Ono and J.Y. Niederkorn, *New twists to an old story: novel concepts in the pathogenesis of allergic eye disease.* Curr Eye Res, 2013. **38**(3): p. 317-30.
85. Leonardi, A., *Allergy and allergic mediators in tears.* Exp Eye Res, 2013. **117**: p. 106-17.
86. Streilein, J.W., *Immunobiology and immunopathology of corneal transplantation.* Chem Immunol, 1999. **73**: p. 186-206.
87. Chinnery, H.R., T. Humphries, A. Clare, A.E. Dixon, K. Howes, C.B. Moran, D. Scott, M. Zakrzewski, E. Pearlman and P.G. McMenamin, *Turnover of bone marrow-derived cells in the irradiated mouse cornea.* Immunology, 2008. **125**(4): p. 541-8.
88. Forrester, J.V., H. Xu, L. Kuffova, A.D. Dick and P.G. McMenamin, *Dendritic cell physiology and function in the eye.* Immunol Rev, 2010. **234**(1): p. 282-304.
89. Hajrasouliha, A.R., Z. Sadrai, H.K. Lee, S.K. Chauhan and R. Dana, *Expression of the chemokine decoy receptor D6 mediates dendritic cell function and promotes corneal allograft rejection.* Mol Vis, 2013. **19**: p. 2517-25.
90. Hattori, T., S.K. Chauhan, H. Lee, H. Ueno, R. Dana, D.H. Kaplan and D.R. Saban, *Characterization of Langerin-expressing dendritic cell subsets in the normal cornea.* Invest Ophthalmol Vis Sci, 2011. **52**(7): p. 4598-604.
91. Khan, A., H. Fu, L.A. Tan, J.E. Harper, S.C. Beutelspacher, D.F. Larkin, G. Lombardi, M.O. McClure and A.J. George, *Dendritic cell modification as a route to inhibiting corneal graft rejection by the indirect pathway of allorecognition.* Eur J Immunol, 2013. **43**(3): p. 734-46.
92. Knickelbein, J.E., R.L. Hendricks and P. Charukamnoetkanok, *Management of herpes simplex virus stromal keratitis: an evidence-based review.* Surv Ophthalmol, 2009. **54**(2): p. 226-34.
93. Limatola, C. and R.M. Ransohoff, *Modulating neurotoxicity through CX3CL1/CX3CR1 signaling.* Front Cell Neurosci, 2014. **8**: p. 229.
94. Sosnova, M., M. Bradl and J.V. Forrester, *CD34+ corneal stromal cells are bone marrow-derived and express hemopoietic stem cell markers.* Stem Cells, 2005. **23**(4): p. 507-15.
95. Chinnery, H.R., M.J. Ruitenberg, G.W. Plant, E. Pearlman, S. Jung and P.G. McMenamin, *The chemokine receptor CX3CR1 mediates homing of MHC class II-positive cells to the normal mouse corneal epithelium.* Invest Ophthalmol Vis Sci, 2007. **48**(4): p. 1568-74.
96. Steinman, R.M., *Dendritic cells: understanding immunogenicity.* Eur J Immunol, 2007. **37 Suppl 1**: p. S53-60.

97. Gomez Perdiguero, E. and F. Geissmann, *Myb-independent macrophages: a family of cells that develops with their tissue of residence and is involved in its homeostasis.* Cold Spring Harb Symp Quant Biol, 2013. **78**: p. 91-100.
98. Gomez Perdiguero, E., K. Klapproth, C. Schulz, K. Busch, E. Azzoni, L. Crozet, H. Garner, C. Trouillet, M.F. de Bruijn, F. Geissmann and H.R. Rodewald, *Tissue-resident macrophages originate from yolk-sac-derived erythro-myeloid progenitors.* Nature, 2015. **518**(7540): p. 547-51.
99. Hoeffel, G., Y. Wang, M. Greter, P. See, P. Teo, B. Malleret, M. Leboeuf, D. Low, G. Oller, F. Almeida, S.H. Choy, M. Grisotto, L. Renia, S.J. Conway, E.R. Stanley, J.K. Chan, L.G. Ng, I.M. Samokhvalov, M. Merad and F. Ginhoux, *Adult Langerhans cells derive predominantly from embryonic fetal liver monocytes with a minor contribution of yolk sac-derived macrophages.* J Exp Med, 2012. **209**(6): p. 1167-81.
100. Yona, S., K.W. Kim, Y. Wolf, A. Mildner, D. Varol, M. Breker, D. Strauss-Ayali, S. Viukov, M. Guilliams, A. Misharin, D.A. Hume, H. Perlman, B. Malissen, E. Zelzer and S. Jung, *Fate mapping reveals origins and dynamics of monocytes and tissue macrophages under homeostasis.* Immunity, 2013. **38**(1): p. 79-91.
101. Gomez Perdiguero, E., C. Schulz and F. Geissmann, *Development and homeostasis of "resident" myeloid cells: the case of the microglia.* Glia, 2013. **61**(1): p. 112-20.
102. Gray, H., *Anatomy of the human body.* 1918: p. 1003-1019.
103. Beckers, H.J., J. Klooster, G.F. Vrensen and W.P. Lamers, *Ultrastructural identification of trigeminal nerve endings in the rat cornea and iris.* Invest Ophthalmol Vis Sci, 1992. **33**(6): p. 1979-86.
104. Beckers, H.J., J. Klooster, G.F. Vrensen and W.P. Lamers, *Substance P in rat corneal and iridal nerves: an ultrastructural immunohistochemical study.* Ophthalmic Res, 1993. **25**(3): p. 192-200.
105. Lim, C.H. and G.L. Ruskell, *Corneal nerve access in monkeys.* Albrecht Von Graefes Arch Klin Exp Ophthalmol, 1978. **208**(1-3): p. 15-23.
106. Matsuda, H., *[Electron microscopic study of the corneal nerve with special reference to the nerve endings].* Nihon Ganka Gakkai Zasshi, 1968. **72**(7): p. 880-93.
107. Muller, L.J., L. Pels and G.F. Vrensen, *Ultrastructural organization of human corneal nerves.* Invest Ophthalmol Vis Sci, 1996. **37**(4): p. 476-88.
108. Tervo, T. and A. Palkama, *Ultrastructure of the corneal nerves after fixation with potassium permanganate.* Anat Rec, 1978. **190**(4): p. 851-9.
109. Tervo, T. and A. Palkama, *Innervation of the rabbit cornea. A histochemical and electron-microscopic study.* Acta Anat (Basel), 1978. **102**(2): p. 164-75.

110. Jones, M.A. and C.F. Marfurt, *Calcitonin gene-related peptide and corneal innervation: a developmental study in the rat.* J Comp Neurol, 1991. **313**(1): p. 132-50.
111. Jones, M.A. and C.F. Marfurt, *Peptidergic innervation of the rat cornea.* Exp Eye Res, 1998. **66**(4): p. 421-35.
112. Rozsa, A.J. and R.W. Beuerman, *Density and organization of free nerve endings in the corneal epithelium of the rabbit.* Pain, 1982. **14**(2): p. 105-20.
113. Schimmelpfennig, B. and R. Beuerman, *A technique for controlled sensory denervation of the rabbit cornea.* Graefes Arch Clin Exp Ophthalmol, 1982. **218**(6): p. 287-93.
114. Ueda, S., M. del Cerro, J.A. LoCascio and J.V. Aquavella, *Peptidergic and catecholaminergic fibers in the human corneal epithelium. An immunohistochemical and electron microscopic study.* Acta Ophthalmol Suppl, 1989. **192**: p. 80-90.
115. Zander, E. and G. Weddell, *Observations on the innervation of the cornea.* J Anat, 1951. **85**(1): p. 68-99.
116. Ivanusic, J.J., R.J. Wood and J.A. Brock, *Sensory and sympathetic innervation of the mouse and guinea pig corneal epithelium.* J Comp Neurol, 2013. **521**(4): p. 877-93.
117. Kubilus, J.K. and T.F. Linsenmayer, *Developmental guidance of embryonic corneal innervation: roles of Semaphorin3A and Slit2.* Dev Biol, 2010. **344**(1): p. 172-84.
118. Kubilus, J.K. and T.F. Linsenmayer, *Developmental corneal innervation: interactions between nerves and specialized apical corneal epithelial cells.* Invest Ophthalmol Vis Sci, 2010. **51**(2): p. 782-9.
119. Madrid, R., T. Donovan-Rodriguez, V. Meseguer, M.C. Acosta, C. Belmonte and F. Viana, *Contribution of TRPM8 channels to cold transduction in primary sensory neurons and peripheral nerve terminals.* J Neurosci, 2006. **26**(48): p. 12512-25.
120. Marfurt, C.F. and L.C. Ellis, *Immunohistochemical localization of tyrosine hydroxylase in corneal nerves.* J Comp Neurol, 1993. **336**(4): p. 517-31.
121. Parra, A., R. Madrid, D. Echevarria, S. del Olmo, C. Morenilla-Palao, M.C. Acosta, J. Gallar, A. Dhaka, F. Viana and C. Belmonte, *Ocular surface wetness is regulated by TRPM8-dependent cold thermoreceptors of the cornea.* Nat Med, 2010. **16**(12): p. 1396-9.
122. Patel, D.V. and C.N. McGhee, *Mapping of the normal human corneal sub-Basal nerve plexus by in vivo laser scanning confocal microscopy.* Invest Ophthalmol Vis Sci, 2005. **46**(12): p. 4485-8.
123. Esquenazi, S., J. He, N. Li, N.G. Bazan, I. Esquenazi and H.E. Bazan, *Comparative in vivo high-resolution confocal microscopy of corneal epithelium, sub-basal*

nerves and stromal cells in mice with and without dry eye after photorefractive keratectomy. Clin Experiment Ophthalmol, 2007. **35**(6): p. 545-9.
124. He, J. and H.E. Bazan, *Mapping the nerve architecture of diabetic human corneas.* Ophthalmology, 2012. **119**(5): p. 956-64.
125. Guthoff, R.F., C. Baudouin and J. Stave, *Atlas of Confocal Laser Scanning In-vivo Microscopy in Opthalmology –*
Principles and Applications in Diagnostic and Therapeutic Ophtalmology. 2007.
126. Reichard, M., M. Hovakimyan, R.F. Guthoff and O. Stachs, *In vivo visualisation of murine corneal nerve fibre regeneration in response to ciliary neurotrophic factor.* Exp Eye Res, 2014. **120**: p. 20-7.
127. Namavari, A., S. Chaudhary, J. Sarkar, L. Yco, K. Patel, K.Y. Han, B.Y. Yue, J.H. Chang and S. Jain, *In vivo serial imaging of regenerating corneal nerves after surgical transection in transgenic thy1-YFP mice.* Invest Ophthalmol Vis Sci, 2011. **52**(11): p. 8025-32.
128. Ruskell, G.L., *Ocular fibers of the maxillary nerves in monkey.* J. Anat. Lond., 1974. **118**: p. 195–203.
129. Vonderahe, A.R., *Corneal and scleral anethesia of the lower half of the eye in a case of trauma of the superior maxillary nerve.* Arch. Neurol. Psychiatr., 1928. **20**: p. 836–837.
130. Marfurt, C.F., L.C. Ellis and M.A. Jones, *Sensory and sympathetic nerve sprouting in the rat cornea following neonatal administration of capsaicin.* Somatosens Mot Res, 1993. **10**(4): p. 377-98.
131. Marfurt, C.F., M.A. Jones and K. Thrasher, *Parasympathetic innervation of the rat cornea.* Exp Eye Res, 1998. **66**(4): p. 437-48.
132. Morgan, C., W.C. DeGroat and P.J. Jannetta, *Sympathetic innervation of the cornea from the superior cervical ganglion. An HRP study in the cat.* J Auton Nerv Syst, 1987. **20**(2): p. 179-83.
133. Tervo, T., F. Joo, K.T. Huikuri, I. Toth and A. Palkama, *Fine structure of sensory nerves in the rat cornea: an experimental nerve degeneration study.* Pain, 1979. **6**(1): p. 57-70.
134. Muller, L.J., E. Pels and G.F. Vrensen, *The specific architecture of the anterior stroma accounts for maintenance of corneal curvature.* Br J Ophthalmol, 2001. **85**(4): p. 437-43.
135. Radner, W. and R. Mallinger, *Interlacing of collagen lamellae in the midstroma of the human cornea.* Cornea, 2002. **21**(6): p. 598-601.
136. Muller, L.J., C.F. Marfurt, F. Kruse and T.M. Tervo, *Corneal nerves: structure, contents and function.* Exp Eye Res, 2003. **76**(5): p. 521-42.
137. Moilanen, J.A., M.H. Vesaluoma, L.J. Muller and T.M. Tervo, *Long-term corneal morphology after PRK by in vivo confocal microscopy.* Invest Ophthalmol Vis Sci, 2003. **44**(3): p. 1064-9.

138. Martinez, R., *Etude sur l'innervation de la corne´e humaine.* 1940.
139. Blanco, T. and D.R. Saban, *The Cornea Has "the Nerve" to Encourage Immune Rejection.* Am J Transplant, 2015.
140. Streilein, J.W., *Ocular immune privilege: therapeutic opportunities from an experiment of nature.* Nat Rev Immunol, 2003. **3**(11): p. 879-89.
141. Billingham, R.E. and T. Boswell, *Studies on the problem of corneal homografts.* Proc R Soc Lond B Biol Sci, 1953. **141**(904): p. 392-406.
142. Dupps, W.J., Jr. and S.E. Wilson, *Biomechanics and wound healing in the cornea.* Exp Eye Res, 2006. **83**(4): p. 709-20.
143. Maurice, D.M. and A.A. Giardini, *Swelling of the cornea in vivo after the destruction of its limiting layers.* Br J Ophthalmol, 1951. **35**(12): p. 791-7.
144. Meek, K.M., D.W. Leonard, C.J. Connon, S. Dennis and S. Khan, *Transparency, swelling and scarring in the corneal stroma.* Eye (Lond), 2003. **17**(8): p. 927-36.
145. Larregina, A.T., S.J. Divito and A.E. Morelli, *Clinical Implications of Basic Science Discoveries: Nociceptive Neurons as Targets to Control Immunity-Potential Relevance for Transplantation.* Am J Transplant, 2015.
146. Veres, T.Z., S. Rochlitzer and A. Braun, *The role of neuro-immune cross-talk in the regulation of inflammation and remodelling in asthma.* Pharmacol Ther, 2009. **122**(2): p. 203-14.
147. Myers, A.C., B.J. Undem and D. Weinreich, *Influence of antigen on membrane properties of guinea pig bronchial ganglion neurons.* J Appl Physiol (1985), 1991. **71**(3): p. 970-6.
148. Costello, R.W., B.H. Schofield, G.M. Kephart, G.J. Gleich, D.B. Jacoby and A.D. Fryer, *Localization of eosinophils to airway nerves and effect on neuronal M2 muscarinic receptor function.* Am J Physiol, 1997. **273**(1 Pt 1): p. L93-103.
149. Jacoby, D.B., R.M. Costello and A.D. Fryer, *Eosinophil recruitment to the airway nerves.* J Allergy Clin Immunol, 2001. **107**(2): p. 211-8.
150. Hammad, H. and B.N. Lambrecht, *Dendritic cells and epithelial cells: linking innate and adaptive immunity in asthma.* Nat Rev Immunol, 2008. **8**(3): p. 193-204.
151. Upham, J.W. and P.A. Stumbles, *Why are dendritic cells important in allergic diseases of the respiratory tract?* Pharmacol Ther, 2003. **100**(1): p. 75-87.
152. Veres, T.Z., S. Rochlitzer, M. Shevchenko, B. Fuchs, F. Prenzler, C. Nassenstein, A. Fischer, L. Welker, O. Holz, M. Muller, N. Krug and A. Braun, *Spatial interactions between dendritic cells and sensory nerves in allergic airway inflammation.* Am J Respir Cell Mol Biol, 2007. **37**(5): p. 553-61.
153. Huh, J.C., D.H. Strickland, F.L. Jahnsen, D.J. Turner, J.A. Thomas, S. Napoli, I. Tobagus, P.A. Stumbles, P.D. Sly and P.G. Holt, *Bidirectional interactions between antigen-bearing respiratory tract dendritic cells (DCs) and T cells*

precede the late phase reaction in experimental asthma: DC activation occurs in the airway mucosa but not in the lung parenchyma. J Exp Med, 2003. **198**(1): p. 19-30.

154. Carucci, J.A., R. Ignatius, Y. Wei, A.M. Cypess, D.A. Schaer, M. Pope, R.M. Steinman and S. Mojsov, *Calcitonin gene-related peptide decreases expression of HLA-DR and CD86 by human dendritic cells and dampens dendritic cell-driven T cell-proliferative responses via the type I calcitonin gene-related peptide receptor.* J Immunol, 2000. **164**(7): p. 3494-9.
155. Delgado, M., A. Chorny, E. Gonzalez-Rey and D. Ganea, *Vasoactive intestinal peptide generates CD4+CD25+ regulatory T cells in vivo.* J Leukoc Biol, 2005. **78**(6): p. 1327-38.
156. Marriott, I. and K.L. Bost, *Expression of authentic substance P receptors in murine and human dendritic cells.* J Neuroimmunol, 2001. **114**(1-2): p. 131-41.
157. Dunzendorfer, S., A. Kaser, C. Meierhofer, H. Tilg and C.J. Wiedermann, *Cutting edge: peripheral neuropeptides attract immature and arrest mature blood-derived dendritic cells.* J Immunol, 2001. **166**(4): p. 2167-72.
158. Hosoi, J., G.F. Murphy, C.L. Egan, E.A. Lerner, S. Grabbe, A. Asahina and R.D. Granstein, *Regulation of Langerhans cell function by nerves containing calcitonin gene-related peptide.* Nature, 1993. **363**(6425): p. 159-63.
159. Gonzalez-Rey, E., A. Chorny, A. Fernandez-Martin, D. Ganea and M. Delgado, *Vasoactive intestinal peptide generates human tolerogenic dendritic cells that induce CD4 and CD8 regulatory T cells.* Blood, 2006. **107**(9): p. 3632-8.
160. Kradin, R., J. MacLean, S. Duckett, E.E. Schneeberger, C. Waeber and C. Pinto, *Pulmonary response to inhaled antigen: neuroimmune interactions promote the recruitment of dendritic cells to the lung and the cellular immune response to inhaled antigen.* Am J Pathol, 1997. **150**(5): p. 1735-43.
161. Janelsins, B.M., A.R. Mathers, O.A. Tkacheva, G. Erdos, W.J. Shufesky, A.E. Morelli and A.T. Larregina, *Proinflammatory tachykinins that signal through the neurokinin 1 receptor promote survival of dendritic cells and potent cellular immunity.* Blood, 2009. **113**(13): p. 3017-26.
162. Nassenstein, C., J. Kutschker, D. Tumes and A. Braun, *Neuro-immune interaction in allergic asthma: role of neurotrophins.* Biochem Soc Trans, 2006. **34**(Pt 4): p. 591-3.
163. Lindsay, R.M. and A.J. Harmar, *Nerve growth factor regulates expression of neuropeptide genes in adult sensory neurons.* Nature, 1989. **337**(6205): p. 362-4.
164. Paunicka, K.J., J. Mellon, D. Robertson, M. Petroll, J.R. Brown and J.Y. Niederkorn, *Severing corneal nerves in one eye induces sympathetic loss of*

immune privilege and promotes rejection of future corneal allografts placed in either eye. Am J Transplant, 2015. **15**(6): p. 1490-501.
165. Ho, W.Z., J.P. Lai, X.H. Zhu, M. Uvaydova and S.D. Douglas, *Human monocytes and macrophages express substance P and neurokinin-1 receptor.* J Immunol, 1997. **159**(11): p. 5654-60.
166. Saban, D.R., *The chemokine receptor CCR7 expressed by dendritic cells: a key player in corneal and ocular surface inflammation.* Ocul Surf, 2014. **12**(2): p. 87-99.
167. Perry, V.H., M.C. Brown and S. Gordon, *The macrophage response to central and peripheral nerve injury. A possible role for macrophages in regeneration.* J Exp Med, 1987. **165**(4): p. 1218-23.
168. Seyed-Razavi, Y., H.R. Chinnery and P.G. McMenamin, *A novel association between resident tissue macrophages and nerves in the peripheral stroma of the murine cornea.* Invest Ophthalmol Vis Sci, 2014. **55**(3): p. 1313-20.

SUMMARY

ABSTRACT

This doctoral thesis is presented, in part, as an evolution of the approaches used to investigate the cornea. The progress in the development of methodology can be chronologically evaluated in the successive chapters. As a main achievement, herein we present a significant improvement in the methodology compared with previous techniques currently in use.

In the first chapter, we showed that the deficiency in αVβ6 integrin impaired corneal wound healing. By using null mice in β6-integrin (β6--/--), we observed that both basement membrane and hemidesmosomes are not recovered in β6--/--. These mice show subepitelial blisters such as those observed in patients with bullous keratopathy.

In the Chapter 2 we used a mouse deficient in thrombospondin-1 (THSB1) to study the process of corneal repair after a penetrating incision. THBS1 is crucial for both stromal repair and endothelial regeneration. The corneas of mice lacking THBS1 show a complete failure in the process of healing and tissue repair. THBS1 deficient mice developed chronic corneal edema. In this work, for the first time, we used an in vivo confocal microscopy (IVCM) to evaluate the healing process in a living mouse.

Using the IVCM system, we studied the inflammation of the ocular surface in an allergic conjunctivitis mouse model (chapter 3). The cell infiltration into the ocular surface was observed in vivo at real time. The novelty of this study was to observe a corneal involvement (cellular infiltration) during the inflammatory process long before it was detected with the slit lamp. In sum,

our observation indicated that the number of infiltrated cells and their spatiotemporal distribution in the cornea is related to the progression of clinical symptoms of the allergic conjunctivitis.

Next, we incorporated a multiphoton intravital microscope (MP-IVM) and genetically-engineered reporter expressing mice strains into studies of the resident immune cells of cornea. With this technology we were able of non-invasive examination of the cornea in a living mouse. With this methodology, we stratified the myeloid-derived population in the mouse cornea with high resolution and three-dimensional space (Chapter 4). Additionally we generated chimeric mice by lethal irradiation of the host and subsequent transplant with bone marrow-derived cells of another mouse strain. This model allows for in vivo observation of the turnover of the myeloid population of the cornea. Additionally we developed an experimental in vivo model to evaluate the myeloid fate mapping of the adult cornea. This model suggests that the myeloid population of the cornea might have an embrionary origin rather than hematopoietic as has been established before.

Furthermore, we also visualized the corneal nerves in a living mouse (Chapter 5). In this model we comprehensively mapped the corneal nerves with high-resolution and three-dimensional space. Remarkably, we observed the presence of radial distributed nerve bundles in the deep part of the stroma. These nerve fibbers supply innervation from bellow to the subbasal plexus ramifying in both directions toward the center and periphery.

The interface of both immune and peripheral nervous system (PNS) is

shown in the chapter 6. This interaction is suggested to be critical for corneal transplant immune rejection. In this chapter, we proposed the cornea as a much more complex organ than it has been described before. The stochastic interaction of both "supersystems" (PNS and immune system) seems to be critical for maintaining corneal homeostasis. A chimeric mouse model was generated by lethally irradiation of a host mouse expressing neurofluorescence. This mouse was engrafted with fluorescent myeloid-derived bone marrow cells. Three months later, we intravitally observed both "supersystems" are physically interconnected, which demonstrates the proposed neuroimmune interface.

Finally, we show the possible future applications of MP-IVM. First, we in vivo evaluated the behavior of murine adipocyte-derived stem cells (mADSCs) engrafted in different parts of the cornea. Second, we monitored the efficiency of drug delivery in the anterior chamber, trabecular meshwork and Schlemm's canal. Also we evaluated the in vivo efficiency of the viral infection in the endothelial cells by adenovirus. Finally, we evaluated the turnover of a specific CD11c dendritic cells population after earlier depletion with diphtheria toxin.

ORGANIZATION OF THE DOCTORAL THESIS REPORT

This Doctoral Thesis report, which is equivalent to a PhD thesis, is presented as a "compendium of publications" and applies for the International-awarded Doctoral Thesis title. This memory has been organized following the University of Valladolid guidelines for an International Degree. The joint requirements are as follows: (1) a short general summary in both Spanish and English, in which (2) the thematic unit of the work is justified, (3) the objectives, methodology, results, discussion, and conclusions are presented. Three articles published in scientific journals with an impact factor are included (4) (chapters 1, 2 and 6). Furthermore, two additional articles under revision (chapter 3 and 5) and one in preparation (chapter 4) have been also included. The presented report met all above requirements. Furthermore, it contains supplementary material strengthening thus the chapter 6. Besides, the part proposing the future applications of developed methodology has been included as chapter 7.

Following the summary, the report is organized in eight chapters: state of the art (chapter 0), the six chapters corresponding to the articles (published, submitted awaiting decision or in preparation) that reflect different blocks of experiments and the chapter 7 describing the future applications of methodology and technics developed during the experimental work. The chapters are not chronologically organized; however, they are structured to facilitate the understanding of the work.

The thesis is organized in the following chapters:

Chapter 0: This chapter is fully presented in both Spanish and English languages; therefore, the thesis introduction is included in this part. The state of the art of the cornea as an organ as well as some pathologies are summarized. Additionally, an update on the current methodology use in the cornea research is described. This section gives

introduction into the methodology presented in the forthcoming chapters. In this block we hypothesize about the relevance of using genetically engineered mice and imaging systems for understanding the pathophysiology of the cornea. This chapter is not a subject to be published.

Chapter 1: ***αVβ6 integrin promotes corneal wound healing***.

Within the current chapter, we demonstrated that αVβ6 is upregulated in the epithelium during the corneal wound healing process when the basement membrane (BMZ) is damaged in wild type mice. The up-regulation of αVβ6 promotes epithelial migration in wounds where the BMZ was removed, and leads to up-regulation of laminin. In addition, hemidesmosome restoration is compromised after keratectomy wounds and this correlates with the absence of laminin in the BMZ in mice lacking αVβ6. This experimental work is published in *Investigative and Ophthalmology and Visual Science* [1].

Chapter 2: ***Role of Thrombospondin-1 in Repair of Penetrating Corneal Wounds***.

In this section, we showed that Thrombospondin-1 (THBS-1) is expressed by epithelium and endothelium in the cornea. THBS-1 is critical for endothelial healing and stromal contraction when integrity of the cornea is compromised by a penetrating incision. In the current experimental block, we included an *in vivo* confocal microscope (IVCM) (HRT3-RCM) to intravitally evaluate the corneal wound healing process in a living mouse. This experimental work is published in *Investigative and Ophthalmology and Visual Science* [2].

Chapter 3: ***Intravital Confocal Microscopy Reveals Corneal Involvement in an Allergic Eye Disease Mouse Model: an in vivo Study***

In this study we successfully evaluated the inflammatory immune reaction in a mouse model of allergic eye disease using an IVCM. The rise in the number of inflammatory cells observed with the IVCM, correlated with the increase of AED clinical score, and the increase of inflammatory cell numbers assessed by flow cytometry and LSCM (laser

scanning confocal microscope) analysis. Remarkably, a significant inflammatory immune reaction was intravitally detected in the transparent cornea. This experimental block is described in a manuscript submitted to *Investigative and Ophthalmology and Visual Science* (in revision) and was presented, in part, in ARVO 2012 and 2014.

Chapter 4: ***Cutting Edge in vivo Imaging I: Multi-Photon intravital Microscopy to Visualize the Resident Myeloid-Derived Population in the Mouse Cornea***

In this section we combined genetically-engineered (Cx3cr1) reporter expressing mouse strains, multiphoton intravital microscopy (MP-IVM) and imaging analysis software to obtain an outstanding *in vivo* imaging model. In this model, the myeloid-derived population of the cornea was intravitally visualized in a living mouse. Additionally, the turnover of the myeloid population of the cornea was *in vivo* assessed after lethal irradiation and transplantation with bone marrow derived-cells. Myeloid fate mapping was also measured *in vivo* by using a CX3CR1-YFP-CreER-RFP mouse model. In general, this model is suitable for studying the function of the myeloid population of the cornea in both normal and pathological conditions in a living mouse. This chapter is presented with extended introduction and bulk description of the methodology, results and discussion as well. These results are part of the submitted manuscript: ***"Mononuclear phagocytes in vivo form vast networks of membrane nanotubes that contact and track along peripheral nerves"***) (Nature Medicine). The mentioned manuscript is not included in this thesis since the cornea is not the main subject; however, the presenting of the developed *in vivo* imaging model is significantly strengthening this thesis dissertation (This part is in preparation for an independent article subjected to be submitted for publication; Also it has been presented as an oral presentation in ARVO 2013 and 2014).

Chapter 5: ***Cutting Edge in vivo Imaging II: Multi-Photon intravital Microscopy to Visualize Transgenic Neurofluorescence in a Thy1-YFP Mouse Cornea***.

In this study we combined a genetically-engineered reporter expressing mouse (Thy1-YFP), MP-IVM and imaging analysis to obtain an outstanding imaging model to study the corneal nerves. Using this model we performed the high resolution intravitally mapping of the architecture of the corneal nerves in a living mouse. This model has potential applications in the implication of the corneal nerves in pathologies such dry eye, keratoconus, corneal transplantation, chronic pain, refractive surgery complications, dystrophies, allergy, keratitis etc. This experimental block is described in a manuscript submitted to *Investigative and Ophthalmology and Visual Science* (in revision awaiting for decision) (Presented as an oral presentation in ARVO 2013 and 2014).

Chapter 6: ***"The cornea has "the nerve" to encourage immune rejection"***

This chapter contains an article as an editorial contribution to a previous work entitled "*Severing Corneal Nerves in One Eye Induces Sympathetic Loss of Immune Privilege and Promotes Rejection of Future Corneal Allografts Placed in Either Eye*" Paunicka et al., [3]. In this article we point out the relevance of the interface of both peripheral nervous system (PNS) and immune system, to maintain corneal immune privilege. This block presents the study published in *American Journal of Transplantion* [4]. Additionally, the supplementary materials, that were not included in the publication but are essential for understanding the whole block, have been added. In the supplemental results, we show that the interface of both systems is extended to the entire cornea. Moreover, we present the development of a new chimeric Thy1-YFP mouse, which was irradiated and engrafted with bone marrow derived-cells from a $CX3CR1^{Cre/RFP}$ donor mouse. In this chimera we were able to intravitally evaluate the interconnection of both corneal nerves and myeloid-derived cells *in vivo*. Finally we present the cornea as a multifaceted organ where two "supersystems" (PNS and immune system) interact with each other to keep the immune privilege and preserve transparency.

Chapter 7: ***Further Applications of Multiphoton Intravital Microscopy in Ocular Research***

In this chapter we show some potential applications of MP-IVM. First, we engrafted murine adipocyte-derived stem cells (mADSCs) in different parts of the cornea. The behavior of the cells *in vivo* was observed with the MP-IVM system up to 4 weeks. Second, we injected drug delivery carriers such as nanoparticles, liposomes and collagen binding proteins. These carriers were detected in the anterior chamber, trabecular meshwork and Schlemm's canal of a living mouse using MP-IVM. We have also injected the adenovirus, which induces expression of the GFP in the endothelial cells. Finally, we evaluated the turnover of a specific CD11c dendritic cell population, after earlier depletion with diphtheria toxin. The brief of applied methodology and the summary of the obtained results are shown. This chapter is not subject of publication as such; however, the results, observation and developed methodology are relevant for the further publications. Introduction and discussion sections are not included though.

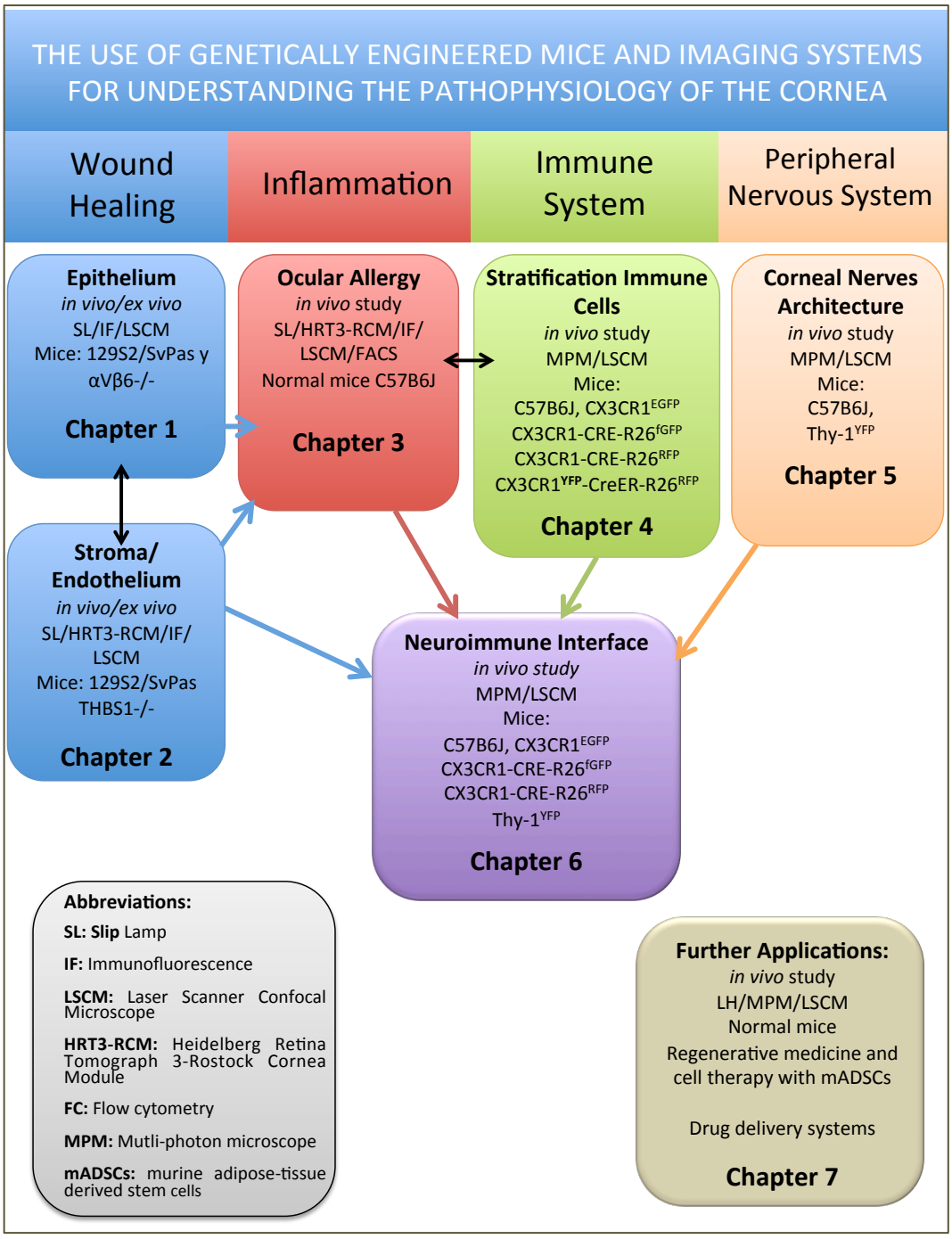
THE USE OF GENETICALLY ENGINEERED MICE AND IMAGING SYSTEMS FOR UNDERSTANDING THE PATHOPHYSIOLOGY OF THE CORNEA
Wound Healing
Inflammation
Immune System
Peripheral Nervous System
Epithelium
in vivo/ex vivo
SL/IF/LSCM
Mice: 129S2/SvPas y αVβ6-/-
Chapter 1
Ocular Allergy
in vivo study
SL/HRT3-RCM/IF/ LSCM/FACS
Normal mice C57B6J
Chapter 3
Stratification Immune Cells
in vivo study
MPM/LSCM
Mice:
C57B6J, CX3CR1EGFP
CX3CR1-CRE-R26fGFP
CX3CR1-CRE-R26RFP
CX3CR1YFP-CreER-R26RFP
Chapter 4
Corneal Nerves Architecture
in vivo study
MPM/LSCM
Mice:
C57B6J,
Thy-1YFP
Chapter 5
Stroma/ Endothelium
in vivo/ex vivo
SL/HRT3-RCM/IF/ LSCM
Mice: 129S2/SvPas THBS1-/-
Chapter 2
Neuroimmune Interface
in vivo study
MPM/LSCM
Mice:
C57B6J, CX3CR1EGFP
CX3CR1-CRE-R26fGFP
CX3CR1-CRE-R26RFP
Thy-1YFP
Chapter 6
Abbreviations:
SL: Slip Lamp
IF: Immunofluorescence
LSCM: Laser Scanner Confocal Microscope
HRT3-RCM: Heidelberg Retina Tomograph 3-Rostock Cornea Module
FC: Flow cytometry
MPM: Mutli-photon microscope
mADSCs: murine adipose-tissue derived stem cells
Further Applications:
in vivo study
LH/MPM/LSCM
Normal mice
Regenerative medicine and cell therapy with mADSCs
Drug delivery systems
Chapter 7

MOTIVATION

The cornea is the transparent part of the visual system, which refracts the light and protects the inner parts of the eye. The major and unique features of cornea are: transparency, avascularity and immune privilege. Additionally, cornea exhibits relatively high elasticity and resistance to mechanical damages[5]. In the external part, in contact with the tear film, the cornea has a stratified squamous non-keratinized epithelium. The epithelium acts as protective barrier from the external environment. In the external part, the cornea presents a hydrophobic smooth surface, which protects from pathogens and offers a flat front to the light. The epithelium rests in basement membrane [6, 7]. Underneath, the Bowman's layer is located, which is composed of very well organized collagen. This membrane is not present in all species [8]. The stroma of the cornea is composed of collagen and keratocytes and consists up to 90% of the corneal thickness. The stroma provides the main refractive power to the cornea [9]. In the posterior part of the cornea, the Descemet' membrane is located, which serves as basement membrane for the endothelium [9]. The endothelium is constituted of a monolayer of endothelial cells in contact with the anterior chamber. The endothelium maintains the transparency and is controlling the hydration of the cornea [10].

The cornea is densely innervated with fibres from the ophthalmic branch of the trigeminal ganglion [11]. The cornea is also endowed with a resident population of myeloid-derived cells that play a main role in the immune response; however, their function is not yet well described [12]. In this context, the cornea is a high-specialized organ composed of different tissues to kept homeostasis, protect the integrity of the visual system and maintain the transparency.

The cornea is constantly exposed to injuries and infections. The visual system has developed a unique defense mechanism based on quick external response (blinking, tearing, conjunctival enzymatic secretions) [13]. However, it is necessary to consider the evolutionary aspect to recognize the importance of the wound-healing response in the

cornea. Adequate vision is essential for the survival, resulting in selective pressure to develop the ability to recover from a variety of corneal injuries. Infectious agents such as viruses have posed a threat because of the potential expansion into an eye and through the eye to the brain. The wound healing response to these injuries would likely have evolved to restore the protective epithelial surface, maintain the integrity of the cornea, and restore the corneal clarity [14]. Systems designed to rapidly restore the integrity and clarity of the cornea, impeding the spread of pathogens until the immune responses eradicate the intruders, probably have provided selective advantages to organisms, dependent on sight for survival [15]. The cornea is also target for many pathogens that cause keratitis or corneal inflammation. Some keratitis caused by Acantamoeba affect contact lenses users. Bacterial keratitis caused by *Staphylococcus aureus* or *Pseudomonas aeruginosa*, fungal caused by Fusarium or viral origin as *Herpes simplex* or *Herpes zoster* cause strong inflammatory response in the cornea [15, 16].

The ocular surface often is exposed to pathogens, cosmetics and environment agents (e.g. pollen, dust mites, dander, smoke or pollution) that cause inflammation of the conjunctiva. Conjunctivitis diagnosis varies depending on etiology (viral, bacterial, chemical); however, allergic conjunctivitis (AC) is the most common ophthalmologic incidence in developed countries [17]. AC represents a spectrum of disorders that affect the lid, conjunctiva, and in more severe forms, the cornea [18]. Mild forms of AC include seasonal allergic conjunctivitis (SAC) and perennial allergic conjunctivitis (PAC) that are induced by environmental agents such as grass, pollens, or cat dander [19-21]. Together SAC and PAC comprise 95% of AC cases [19-21]. More severe forms include atopic keratoconjunctivitis (AKC) and vernal keratoconjunctivitis (VKC) [22-24]. SAC and PAC remain self-limited and present no corneal damage. By contrast, AKC and VKC progress with corneal involvement, producing discomfort, pain and may lead to impaired vision and corneal transplantation [20, 22].

Because of the refractive surgery and the massive use of contact lenses, the research in corneal pathologies has been increased during the last couple of decades. The

refractive surgery has increased the incidence of side effects such as loss of visual acuity, halos, glare, reflections, foreign body sensation, lack of lubrication and dry eye. More aggressive complications such as melting, fibrosis after surgery very often required corneal transplantation to restore the vision of the patient. Additionally some of these complications might appear after cataract surgery [25, 26].

The cornea is the most frequently transplanted tissue in humans with a success rate that exceeds all other forms of solid organ transplantation since the first successful transplant had been performed in 1905 [27]. Since the National Transplant Organization (ONT, Organizacíon Nacional de Transplantes) has been established in 1989, in Spain, 60,000 transplants were successfully performed. Although less than 10% of them undergo rejection, the total number of successful transplants is still high. Rejection is increased significantly in hosts receiving second corneal transplants [28] due to the loss of ocular immune privilege during the first transplant. Additionally patients, who are considered to be under the high risk of rejection, are excluded for transplantation [29]. Moreover, corneal transplantation is an option only available in developed countries and not accessible in many developing and undeveloped countries.

Nowadays, there is not an effective remedy that revokes chronic corneal inflammation [30].Available treatments, such as artificial tears, aid the symptoms of the disease; however, they can only be use as a palliative. Immunosuppressive treatments are used only in highly symptomatic cases but they have adverse side effects associated with its continued use [31].

During the last decade, the search of therapeutic alternatives such as biopolymers and nanoparticles as drug delivering systems is a promising option [32, 33]. Recent therapeutic options are both intrastromal rings and segments (ICRS) and collagen crosslinking (CXL) that effectively stop the progression of keratoconus [34, 35]; however, graft transplantation is still the only solution for many of the cases [28, 36].

The regenerative medicine has been recently established as an alternative in pathologies like neurothropfic ulcerations, limbal stem cell deficiency and other

alterations that provoke loss of the corneal epithelium. New biologic-based drugs such as nerve growth factor (NGF) or plasma rich in growth factors (PRGF) have good outcomes in patients [37, 38]; however, these drugs are expensive and only show palliative properties and do not revoke the primary pathology.

For all the reasons aforementioned, it is mandatory to give priority to the corneal research. For more than a century, it was believed that the cornea was devoid of APCs [39]; however, during the last few years it has been established that the cornea is endowed with a resident myeloid cell population [12, 40-48]. Two different phenotypic populations of APCs such as DCs and macrophages populate the cornea [49, 50]. DCs reside in the basal layer of the epithelium. DCs extend dendrites to interdigitate between epithelial cells from the basal toward the ocular surface. Classical $CD11c^+$ DCs are typically located in the periphery of the cornea and they are decreasing in number towards the center [51-54]. Although majority of $CD11c^+$ DCs are present in the basal layer of the epithelium, merely a small population resides in the very peripheral regions of the stroma, some of them as immature precursors [43]. The majority of the $CD11c^+$ DCs also co-express MHC class II, highest in the periphery and lesser toward the center. An additional subpopulation of CD11c-DCs that expresses langerin CD207, or Lagerhans cells (LCs), is also located in the basal epithelium [44]. DCs are potent APCs capable to initiate adaptive immune response; however, this property is still controversial in the normal cornea.

Macrophages reside in the stroma divided in two distinct subpopulations [43, 47]. The anterior stroma is populated by $CD11b^+$ $CD11c^-$ MHC class II^+ macrophages distributed relatively uniform from the periphery to the center of the stroma. These are considered putative macrophages that can serve as APCs backup for epithelial DCs in an adaptive immune response [47]. The posterior stroma is endowed of $CD11b^+$ MHC class II^- classical macrophages quietly uniform distributed from the periphery to the center. These macrophages initiate the innate immune response in the murine cornea [47]. Additionally CD11c-expressing cells as well as a different population of monocyte-derived cells also reside in the corneal stroma [40, 43, 44]. A similar APC stratification in the human cornea has

also been described [12]. $CD45^+$ $CD11c^+$ DCs, the majority expressing HLA-DR, reside in the basal layer of the epithelium extending cellular processes toward the ocular surface. Mostly of these DCs populate the periphery of the cornea and their number is decreasing centripetally toward the center. Langerin positive cells ($CD207^+$), likely LCs, are fundamentally located in the periphery of the cornea. In the stoma $CD45^+$ $CD68^+$ macrophages reside in the anterior part of the stroma distributed relatively uniformly from the periphery to the center [12]. While $CD45^+$ HLA-DR^+ population is higher in the center of the stoma, compared to paracentral and periphery, no $CD207^+$ LCs are observed in the center and only a few of them in the periphery [12]. The presence of lymphatic vessels in the peripheral cornea has been another recent finding [55]. Lymphatic vessels play a crucial role in the corneal inflammatory processes but its complete function has not been yet described [56].

The human cornea is the most innervated structure in the body. This organ is densely supplied with both sensory and autonomic nerve fibres [57]. Sensory nerves are derived from the ophthalmic division of the trigeminal nerve [58-62] and have a diversity of sensory and efferent functions [63]. The autonomic nerves consist of sympathetic fibres that are derived from the superior cervical ganglion and parasympathetic fibres that originate from the ciliary ganglion [64-66].

The proper innervation is critical for keeping the wellness and transparency of the cornea. The mechanisms by which corneal nerve fibres maintain a healthy cornea and promote wound healing after injuries is currently under active research. Neurons give trophic support to corneal epithelial cells by releasing soluble substances through. Trigeminal ganglion neurons release neurotransmitters and neuropeptides that contribute to trophism and regulatory processes such as homeostasis. Molecules released by nerves participate actively in corneal wound healing process after injuries [67, 68]

Many factors such as blinking, desiccation of the ocular surface, cooling or air currents induce release of neurochemicals by corneal nerves that in consequence aid to heal small damages in the ocular surface [69-71]. Conversely, patients who suffer from

diminished corneal innervation, caused by diabetes, herpetic keratitis, contact lens wearing and aging, show impaired wound healing [72-76]. Corneal nerves can be also damaged after cataract and retinal surgery or laser procedures (e.g. pan-retinal photocoagulation, cycloablation) [77-79]. During the last two decades, it has been shown that refractive surgery produces strong damage of corneal nerves and transient mild to severe epithelial alterations [80-82]. However, nowadays, dry eye is the most common neuropathological dysfunctional syndrome [72, 83, 84]. Despite mostly of the corneal pathologies present a neurological component, the physiological basis remains completely unknown.

Therefore, to understand the etiology of the corneal diseases is essential for developing new surgical procedures and pharmacological strategies [85, 86]. The search of new animal models that mimic the normal and pathologic conditions of the human cornea is vital [85]. Many models have been used before for the study of the cornea such as rabbit [87], chicken [88], rat [89] or primates [90]; however, the mouse is the most accepted model currently. Mice show similar process of wound healing as humans [91], parallel reinnervation process [92], and display comparable inflammatory response.[43, 47]. For example, it has recently been observed that loss of the immune privilege in mice (what causes graft immune rejection and dry eye), is caused by the proliferation of lymphatic vessels in the stromal bed. This finding was later confirmed in patients [55].Similarly, the primary discovery of immune cell population in cornea of mice, helped to describe the homologous population in human [12]. The implication of the corneal immune cells in different pathologies such as dry eye, infections and graft rejection, has also been primary elucidated in mice and helped to understand the impact of those cells on pathologies developed in humans.

Nowadays, live imaging facilitates the understanding of both tissue and cell behaviors as well as to dissect the molecular mechanisms that drive the biological processes. Genetically engineered reporter expressing mouse strains are an important tool in live imaging experiments. Such reporter strains can be engineered by placing cis-regulatory

elements of interest to direct the expression of desired reporter genes. If these cis-regulatory elements are downstream targets, and thus activated as a consequence of signaling pathway activation, such reporters can provide read-outs of the signaling status of a cell [93]. Transgenic mice, expressing either CD11c or langerin, have been recently used to describe the lineage of myeloid population in the mouse cornea [44]. The recent arrival of new strains of Cx3cr1-GFP mice expressing EGFP in monocytes, dendritic cells, NK cells and brain microglia, under control of the endogenous Cx3cr1 locus (myeloid progenitor derived marker) has made useful studies of leukocyte function in migration, trafficking and transplantation [49].

The development of mice in which a green fluorescent protein (EGFP)-encoding gene is inserted in one or both copies of the Cx3cr1 locus has permitted to investigate the fate of leukocytes in vivo [94, 95]. In the ocular surface, Cx3cr1-GFP transgenic mice have been used to confirm the presence of myeloid derived cells as a resident population of the normal murine cornea. Also, it has been demonstrated that Cx3cr1 expression plays a role in DC and macrophage recruitment in the normal corneal epithelium and stroma [96].

Intravital widefield epifluorescence videomicroscopy has been performed in corneas of anesthetized mice to probe that corneal DCs behavior bear similarities to that of skin DCs [48]. It has been shown that irritation of the cornea results in a centripetal migration of DCs from periphery and limbus [97].

The multiphoton *intravital* microscope (MP-IVM) has been recently introduced to study the eye. The composition of the different corneal layers of five different species (human, piscine, porcini, bovine and murine) has been described [98]. Additionally, the immune cell dynamic in corneal lymphatic vessels has been imaged [99] as well as the anterior chamber of the mouse eye [100].

Considering its transparency we hypothesized to intravitally study the cornea, with the slip lamp, IVMC and MP-IVM in a living mouse. Our experience justify the use of genetically engineered mice expressing fluorescence to study *in situ* the corneal pathologies in a different way as it has been shown before [99].

At the end of this work we will show a new interpretation of the cornea as an organ. In addition to the well-described presentation of the cornea as composition of the connective and epithelial tissues, we will point out how two "supersystems" (PNS and immune system) [101] stochastically interact to keep immune privilege and to maintain the transparency of this organ.

HYPOTHESIS

1. It is possible to evaluate the evolution of the corneal wound healing process and the clinical symptoms of corneal pathologies using genetically modified mice

2. It is possible to introduce both genetically-engineered fluorescent reporter mice and *in vivo* imaging systems for *intravital* visualization of cornea

3. It is possible to redefine the cornea as an organ where two "supersystems" (nervous and immune systems) stochastically interact to maintain the homeostasis (immune privilege and transparency)

OBJETIVES

General objective:

To use genetically engineered mice strains and to implement new imaging systems such as *in vivo* confocal microscope (IVCM) and multiphoton *intravital* microscope (MP-IVM) system to study the corneal pathophysiology

Specific objectives:

1. To evaluate the role of αVβ6 integrin in the wound healing process after an injury in null mice for β6 integrin ($\beta6^{-/-}$) (**Chapter 1**)

2. To study the function of trombospondin-1 (THBS1) in the wound repair process after full penetration injury in the mouse cornea (**Chapter 2**)

3. To evaluate the inflammatory process in the ocular surface in an allergic conjunctivitis mouse model using an IVCM system (**Chapter 3**)

4. To visualize, map and stratify the corneal resident population of myeloid cells using a MV-IVM system and a model mice expressing fluorescence under the promoter of Cx3cr1 (**Chapter 4**)

5. To redefine the corneal nerve anatomy using a MP-IVM system, in mice expressing neuro-fluorescence (**Chapter 5**)

6. To describe the physical interaction between the peripheral nervous system and the immune population of the cornea (**Chapter 6**)

7. To search for new applications of MP-IVM such as: *in vivo* following up of the behavior of mesenchymal adipocyte-derived stem cells engrafted in the cornea; real time visualization of drug delivery systems; studies on cytotoxicity of diphtheria toxin (**Chapter 7**)

BRIEF METHODS

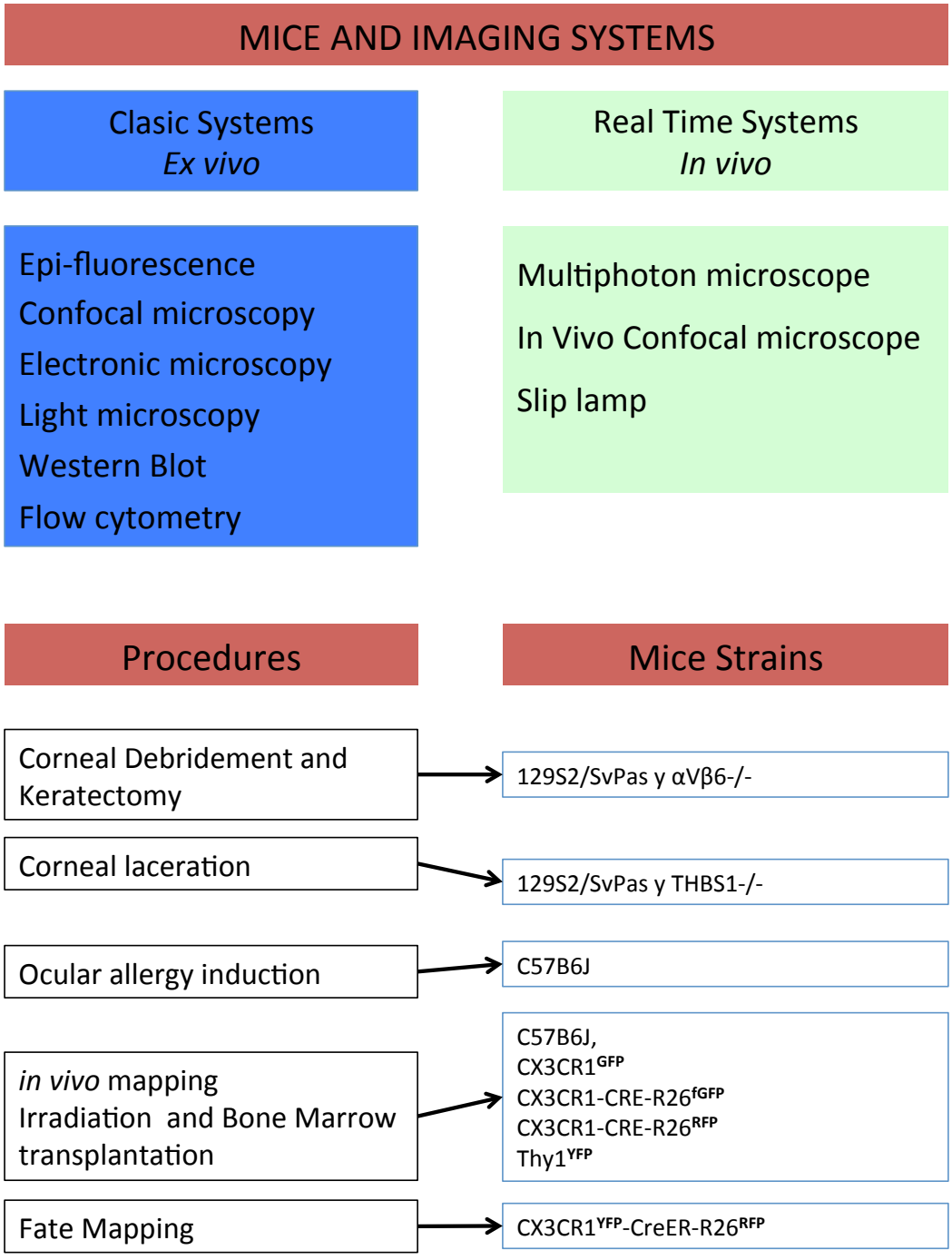

BRIEF RESULTS

The overall result of this thesis is the combinational application of genetically engineered mouse strains, MP-IVM and imaging analysis software to significantly improve the understanding of the cornea

The most specific results are summarized as follows:

1. The lack of α6β4 integrin after an injury causes pathology in the mouse cornea that might reproduce bullous keratopathy or BMZ dystrophies win humans.

2. The deficiency in THBS1 provokes failure in the corneal wound repair process. This includes endothelial migration and healing, stromal contraction and ECM synthesis.

3. The cell infiltration into the ocular surface was intravitally evaluated by using an IVCM in a mouse model of ocular allergy.

4. The resident myeloid-derived population of the cornea was *in vivo* visualized and its ontogeny described

5. The anatomy of the corneal nerves was *in vivo* visualized and the anatomy redefined

6. Corneal nerves and immune myeloid-cells interface in the cornea

7. The behavior or mADSCs engrafted in the cornea, the presence of drug delivering systems in the meshwork and Schlemm's canal, the infection of endothelial cells with adenovirus and the depletion of CD11c-DCs were *in vivo* visualized with the MP-IVM

CONCLUSIONS

The overall conclusion of this thesis is: a new strategies to study the pathophysiology of the cornea, in aspects of wound healing, inflammation, resident immune population and peripheral nervous system, were developed. Additionally, the evolvement and innovation in the methodology (described: **chapter 1** to **chapter 7**), confirm that new systems can be implemented. This methodology allowed to show the cornea as much more complex organ than it has been described before, in which different systems and "supersystems" (nervous and immune systems) interact between each other to maintain the specific properties of the cornea. Thereby, the research on the cornea undergoes a significant improvement.

Based on all the results obtained in our study and presented in this doctoral thesis, the specific conclusions are following:

1. α6β4 integrin is critical to regenerate de epithelial BMZ after an injury. The lack of this integrin causes pathologies such as bullous keratopathy or BMZ dystrophies.
2. THBS1 plays a main role during the corneal wound repair. It induces endothelial migration and healing, stromal contraction and ECM synthesis.
3. The inflammatory response of the ocular surface was evaluated using an IVCM in a mouse model of ocular allergy.
4. The use of genetically engineered reporter expressing mouse strains, MP-IVM and imaging analysis software allowed obtaining an outstanding in vivo imaging model. This model is suitable for studying the function of the corenal myeloid population such as cell ontogeny in a living mouse.
5. The combination of genetically engineered reporter expressing mouse (Thy1-YFP), MP-IVM and image analysis allowed to obtain an outstanding imaging

model to study the corneal nerves in a living mouse. This model is suitable for understanding both anatomy and function of the corneal nerves

6. It was possible to show that both peripheral nervous system and resident immune population maintain a neuroimmune interface in the healthy cornea.
7. It was possible to search for new applications for the use of the MP-IVM. This imaging system was used for: (1) following up the behavior of murine adipocyte-derived stem cells engrafted in the cornea, (2) real time visualization of drug delivering systems in the anterior chamber, trabecular meshwork and Schlemm's canal, (3) intravital detection of GFP-reporter expression by endothelial cells after adenovirus infection, (4) *in vivo* following up the depletion of a specific population of CD11c-DC after topical instillation of diphtheria toxin.

REFERENCES

1. Blanco-Mezquita, J.T., A.E. Hutcheon, M.A. Stepp and J.D. Zieske, *αVβ6 integrin promotes corneal wound healing.* Investigative ophthalmology & visual science, 2011. **52**(11): p. 8505-8513.
2. Blanco-Mezquita, J.T., A.E. Hutcheon and J.D. Zieske, *Role of thrombospondin-1 in repair of penetrating corneal wounds.* Invest Ophthalmol Vis Sci, 2013. **54**(9): p. 6262-8.
3. Paunicka, K.J., J. Mellon, D. Robertson, M. Petroll, J.R. Brown and J.Y. Niederkorn, *Severing corneal nerves in one eye induces sympathetic loss of immune privilege and promotes rejection of future corneal allografts placed in either eye.* Am J Transplant, 2015. **15**(6): p. 1490-501.
4. Blanco, T. and D.R. Saban, *The Cornea Has "the Nerve" to Encourage Immune Rejection.* Am J Transplant, 2015.
5. C. Stephen Foster, D.T.A., Claes H. Dolman, *Smolin and Thoft's The Cornea, Scientific Foundation & Clinical Practice.* 2005.
6. Beebe, D.C. and B.R. Masters, *Cell lineage and the differentiation of corneal epithelial cells.* Invest Ophthalmol Vis Sci, 1996. **37**(9): p. 1815-25.
7. Hanna, C. and J.E. O'Brien, *Cell production and migration in the epithelial layer of the cornea.* Arch Ophthalmol, 1960. **64**: p. 536-9.
8. Wilson, S.E. and J.W. Hong, *Bowman's layer structure and function: critical or dispensable to corneal function? A hypothesis.* Cornea, 2000. **19**(4): p. 417-20.
9. Rodrigues MM, W.G.I., Hackett J, Donohoo P *Ocular Anatomy, Embryology, and Teratology.* 1982.
10. Waring, G.O., 3rd, W.M. Bourne, H.F. Edelhauser and K.R. Kenyon, *The corneal endothelium. Normal and pathologic structure and function.* Ophthalmology, 1982. **89**(6): p. 531-90.
11. Muller, L.J., G.F. Vrensen, L. Pels, B.N. Cardozo and B. Willekens, *Architecture of human corneal nerves.* Invest Ophthalmol Vis Sci, 1997. **38**(5): p. 985-94.
12. Knickelbein, J.E., K.A. Buela and R.L. Hendricks, *Antigen-presenting cells are stratified within normal human corneas and are rapidly mobilized during ex vivo viral infection.* Invest Ophthalmol Vis Sci, 2014. **55**(2): p. 1118-23.
13. Maurice, D.M., *The structure and transparency of the cornea.* J Physiol, 1957. **136**(2): p. 263-86.
14. Wilson, S.E., *Analysis of the keratocyte apoptosis, keratocyte proliferation, and myofibroblast transformation responses after photorefractive keratectomy and laser in situ keratomileusis.* Trans Am Ophthalmol Soc, 2002. **100**: p. 411-33.
15. Wilson, S.E., L. Pedroza, R. Beuerman and J.M. Hill, *Herpes simplex virus type-1 infection of corneal epithelial cells induces apoptosis of the underlying keratocytes.* Exp Eye Res, 1997. **64**(5): p. 775-9.

16. Kaye, S. and A. Choudhary, *Herpes simplex keratitis.* Prog Retin Eye Res, 2006. **25**(4): p. 355-80.
17. Blaiss, M.S., *Allergic rhinoconjunctivitis: burden of disease.* Allergy Asthma Proc, 2007. **28**(4): p. 393-7.
18. Ono, S.J. and M.B. Abelson, *Allergic conjunctivitis: update on pathophysiology and prospects for future treatment.* J Allergy Clin Immunol, 2005. **115**(1): p. 118-22.
19. Bonini, S., S. Bonini, A. Lambiase, S. Marchi, P. Pasqualetti, O. Zuccaro, P. Rama, L. Magrini, T. Juhas and M.G. Bucci, *Vernal keratoconjunctivitis revisited: a case series of 195 patients with long-term followup.* Ophthalmology, 2000. **107**(6): p. 1157-63.
20. Leonardi, A., *Vernal keratoconjunctivitis: pathogenesis and treatment.* Prog Retin Eye Res, 2002. **21**(3): p. 319-39.
21. Pucci, N., E. Novembre, E. Lombardi, A. Cianferoni, R. Bernardini, C. Massai, R. Caputo, L. Campa and A. Vierucci, *Atopy and serum eosinophil cationic protein in 110 white children with vernal keratoconjunctivitis: differences between tarsal and limbal forms.* Clin Exp Allergy, 2003. **33**(3): p. 325-30.
22. Leonardi, A., L. Motterle and M. Bortolotti, *Allergy and the eye.* Clin Exp Immunol, 2008. **153 Suppl 1**: p. 17-21.
23. Leonardi, A., *The central role of conjunctival mast cells in the pathogenesis of ocular allergy.* Curr Allergy Asthma Rep, 2002. **2**(4): p. 325-31.
24. Bielory, L., *Ocular allergy guidelines: a practical treatment algorithm.* Drugs, 2002. **62**(11): p. 1611-34.
25. Netto, M.V., R.R. Mohan, R. Ambrosio, Jr., A.E. Hutcheon, J.D. Zieske and S.E. Wilson, *Wound healing in the cornea: a review of refractive surgery complications and new prospects for therapy.* Cornea, 2005. **24**(5): p. 509-22.
26. Randleman, J.B., M. Woodward, M.J. Lynn and R.D. Stulting, *Risk assessment for ectasia after corneal refractive surgery.* Ophthalmology, 2008. **115**(1): p. 37-50.
27. Zirm, E.K., *Eine erfolgreiche totale Keratoplastik (A successful total keratoplasty). 1906.* Refract Corneal Surg, 1989. **5**(4): p. 258-61.
28. Coster, D.J. and K.A. Williams, *The impact of corneal allograft rejection on the long-term outcome of corneal transplantation.* Am J Ophthalmol, 2005. **140**(6): p. 1112-22.
29. van Essen, T.H., D.L. Roelen, K.A. Williams and M.J. Jager, *Matching for Human Leukocyte Antigens (HLA) in corneal transplantation - To do or not to do.* Prog Retin Eye Res, 2015. **46**: p. 84-110.
30. Moss, S.E., R. Klein and B.E. Klein, *Prevalence of and risk factors for dry eye syndrome.* Arch Ophthalmol, 2000. **118**(9): p. 1264-8.

31. Vichyanond, P., P. Pacharn, U. Pleyer and A. Leonardi, *Vernal keratoconjunctivitis: a severe allergic eye disease with remodeling changes.* Pediatr Allergy Immunol, 2014. **25**(4): p. 314-22.
32. Alonso, M.J., *Nanomedicines for overcoming biological barriers.* Biomed Pharmacother, 2004. **58**(3): p. 168-72.
33. Diebold, Y., M. Jarrin, V. Saez, E.L. Carvalho, M. Orea, M. Calonge, B. Seijo and M.J. Alonso, *Ocular drug delivery by liposome-chitosan nanoparticle complexes (LCS-NP).* Biomaterials, 2007. **28**(8): p. 1553-64.
34. Ertan, A. and J. Colin, *Intracorneal rings for keratoconus and keratectasia.* J Cataract Refract Surg, 2007. **33**(7): p. 1303-14.
35. Kymionis, G. and D. Portaliou, *Corneal crosslinking with riboflavin and UVA for the treatment of keratoconus.* J Cataract Refract Surg, 2007. **33**(7): p. 1143-4; author reply 1144.
36. Rabinowitz, Y.S., *Keratoconus.* Surv Ophthalmol, 1998. **42**(4): p. 297-319.
37. Anitua, E., F. Muruzabal, I. Alcalde, J. Merayo-Lloves and G. Orive, *Plasma rich in growth factors (PRGF-Endoret) stimulates corneal wound healing and reduces haze formation after PRK surgery.* Exp Eye Res, 2013. **115**: p. 153-61.
38. Lambiase, A., L. Manni, P. Rama and S. Bonini, *Clinical application of nerve growth factor on human corneal ulcer.* Arch Ital Biol, 2003. **141**(2-3): p. 141-8.
39. Streilein, J.W., *Immunobiology and immunopathology of corneal transplantation.* Chem Immunol, 1999. **73**: p. 186-206.
40. Chinnery, H.R., T. Humphries, A. Clare, A.E. Dixon, K. Howes, C.B. Moran, D. Scott, M. Zakrzewski, E. Pearlman and P.G. McMenamin, *Turnover of bone marrow-derived cells in the irradiated mouse cornea.* Immunology, 2008. **125**(4): p. 541-8.
41. Forrester, J.V., H. Xu, L. Kuffova, A.D. Dick and P.G. McMenamin, *Dendritic cell physiology and function in the eye.* Immunol Rev, 2010. **234**(1): p. 282-304.
42. Hajrasouliha, A.R., Z. Sadrai, H.K. Lee, S.K. Chauhan and R. Dana, *Expression of the chemokine decoy receptor D6 mediates dendritic cell function and promotes corneal allograft rejection.* Mol Vis, 2013. **19**: p. 2517-25.
43. Hamrah, P., Y. Liu, Q. Zhang and M.R. Dana, *The corneal stroma is endowed with a significant number of resident dendritic cells.* Invest Ophthalmol Vis Sci, 2003. **44**(2): p. 581-9.
44. Hattori, T., S.K. Chauhan, H. Lee, H. Ueno, R. Dana, D.H. Kaplan and D.R. Saban, *Characterization of Langerin-expressing dendritic cell subsets in the normal cornea.* Invest Ophthalmol Vis Sci, 2011. **52**(7): p. 4598-604.
45. Khan, A., H. Fu, L.A. Tan, J.E. Harper, S.C. Beutelspacher, D.F. Larkin, G. Lombardi, M.O. McClure and A.J. George, *Dendritic cell modification as a route*

to inhibiting corneal graft rejection by the indirect pathway of allorecognition. Eur J Immunol, 2013. **43**(3): p. 734-46.
46. Knickelbein, J.E., R.L. Hendricks and P. Charukamnoetkanok, *Management of herpes simplex virus stromal keratitis: an evidence-based review.* Surv Ophthalmol, 2009. **54**(2): p. 226-34.
47. Knickelbein, J.E., S.C. Watkins, P.G. McMenamin and R.L. Hendricks, *Stratification of Antigen-presenting Cells within the Normal Cornea.* Ophthalmol Eye Dis, 2009. **1**: p. 45-54.
48. Lee, E.J., J.T. Rosenbaum and S.R. Planck, *Epifluorescence intravital microscopy of murine corneal dendritic cells.* Invest Ophthalmol Vis Sci, 2010. **51**(4): p. 2101-8.
49. Limatola, C. and R.M. Ransohoff, *Modulating neurotoxicity through CX3CL1/CX3CR1 signaling.* Front Cell Neurosci, 2014. **8**: p. 229.
50. Sosnova, M., M. Bradl and J.V. Forrester, *CD34+ corneal stromal cells are bone marrow-derived and express hemopoietic stem cell markers.* Stem Cells, 2005. **23**(4): p. 507-15.
51. Chinnery, H.R., E. Pearlman and P.G. McMenamin, *Cutting edge: Membrane nanotubes in vivo: a feature of MHC class II+ cells in the mouse cornea.* J Immunol, 2008. **180**(9): p. 5779-83.
52. Hamrah, P., Y. Liu, Q. Zhang and M.R. Dana, *Alterations in corneal stromal dendritic cell phenotype and distribution in inflammation.* Arch Ophthalmol, 2003. **121**(8): p. 1132-40.
53. Nakamura, T., F. Ishikawa, K.H. Sonoda, T. Hisatomi, H. Qiao, J. Yamada, M. Fukata, T. Ishibashi, M. Harada and S. Kinoshita, *Characterization and distribution of bone marrow-derived cells in mouse cornea.* Invest Ophthalmol Vis Sci, 2005. **46**(2): p. 497-503.
54. Shen, L., S. Barabino, A.W. Taylor and M.R. Dana, *Effect of the ocular microenvironment in regulating corneal dendritic cell maturation.* Arch Ophthalmol, 2007. **125**(7): p. 908-15.
55. Maruyama, K., T. Nakazawa, C. Cursiefen, Y. Maruyama, N. Van Rooijen, P.A. D'Amore and S. Kinoshita, *The maintenance of lymphatic vessels in the cornea is dependent on the presence of macrophages.* Invest Ophthalmol Vis Sci, 2012. **53**(6): p. 3145-53.
56. Chauhan, S.K., T.H. Dohlman and R. Dana, *Corneal Lymphatics: Role in Ocular Inflammation as Inducer and Responder of Adaptive Immunity.* J Clin Cell Immunol, 2014. **5**.
57. Muller, L.J., C.F. Marfurt, F. Kruse and T.M. Tervo, *Corneal nerves: structure, contents and function.* Exp Eye Res, 2003. **76**(5): p. 521-42.
58. Arvidson, B., *Retrograde axonal transport of horseradish peroxidase from cornea to trigeminal ganglion.* Acta Neuropathol, 1977. **38**(1): p. 49-52.

59. Marfurt, C.F. and D.R. Del Toro, *Corneal sensory pathway in the rat: a horseradish peroxidase tracing study.* J Comp Neurol, 1987. **261**(3): p. 450-9.
60. Marfurt, C.F., R.E. Kingsley and S.E. Echtenkamp, *Sensory and sympathetic innervation of the mammalian cornea. A retrograde tracing study.* Invest Ophthalmol Vis Sci, 1989. **30**(3): p. 461-72.
61. Morgan, C.W., I. Nadelhaft and W.C. de Groat, *Anatomical localization of corneal afferent cells in the trigeminal ganglion.* Neurosurgery, 1978. **2**(3): p. 252-8.
62. ten Tusscher, M.P., J. Klooster and G.F. Vrensen, *The innervation of the rabbit's anterior eye segment: a retrograde tracing study.* Exp Eye Res, 1988. **46**(5): p. 717-30.
63. Lele, P.P. and G. Weddell, *Sensory nerves of the cornea and cutaneous sensibility.* Exp Neurol, 1959. **1**: p. 334-59.
64. Marfurt, C.F., M.A. Jones and K. Thrasher, *Parasympathetic innervation of the rat cornea.* Exp Eye Res, 1998. **66**(4): p. 437-48.
65. Morgan, C., W.C. DeGroat and P.J. Jannetta, *Sympathetic innervation of the cornea from the superior cervical ganglion. An HRP study in the cat.* J Auton Nerv Syst, 1987. **20**(2): p. 179-83.
66. Tervo, T., F. Joo, K.T. Huikuri, I. Toth and A. Palkama, *Fine structure of sensory nerves in the rat cornea: an experimental nerve degeneration study.* Pain, 1979. **6**(1): p. 57-70.
67. Baker, K.S., S.C. Anderson, E.G. Romanowski, R.A. Thoft and N. SundarRaj, *Trigeminal ganglion neurons affect corneal epithelial phenotype. Influence on type VII collagen expression in vitro.* Invest Ophthalmol Vis Sci, 1993. **34**(1): p. 137-44.
68. Garcia-Hirschfeld, J., L.G. Lopez-Briones and C. Belmonte, *Neurotrophic influences on corneal epithelial cells.* Exp Eye Res, 1994. **59**(5): p. 597-605.
69. Mathers, W.D., *Why the eye becomes dry: a cornea and lacrimal gland feedback model.* CLAO J, 2000. **26**(3): p. 159-65.
70. Stern, M.E., R.W. Beuerman, R.I. Fox, J. Gao, A.K. Mircheff and S.C. Pflugfelder, *The pathology of dry eye: the interaction between the ocular surface and lacrimal glands.* Cornea, 1998. **17**(6): p. 584-9.
71. Stern, M.E., R.W. Beuerman, R.I. Fox, J. Gao, A.K. Mircheff and S.C. Pflugfelder, *A unified theory of the role of the ocular surface in dry eye.* Adv Exp Med Biol, 1998. **438**: p. 643-51.
72. Benitez del Castillo, J.M., M.A. Wasfy, C. Fernandez and J. Garcia-Sanchez, *An in vivo confocal masked study on corneal epithelium and subbasal nerves in patients with dry eye.* Invest Ophthalmol Vis Sci, 2004. **45**(9): p. 3030-5.
73. Benitez-Del-Castillo, J.M., M.C. Acosta, M.A. Wassfi, D. Diaz-Valle, J.A. Gegundez, C. Fernandez and J. Garcia-Sanchez, *Relation between corneal*

innervation with confocal microscopy and corneal sensitivity with noncontact esthesiometry in patients with dry eye. Invest Ophthalmol Vis Sci, 2007. **48**(1): p. 173-81.

74. Hamrah, P., A. Cruzat, M.H. Dastjerdi, L. Zheng, B.M. Shahatit, H.A. Bayhan, R. Dana and D. Pavan-Langston, *Corneal sensation and subbasal nerve alterations in patients with herpes simplex keratitis: an in vivo confocal microscopy study.* Ophthalmology, 2010. **117**(10): p. 1930-6.
75. Rosenberg, M.E., T.M. Tervo, I.J. Immonen, L.J. Muller, C. Gronhagen-Riska and M.H. Vesaluoma, *Corneal structure and sensitivity in type 1 diabetes mellitus.* Invest Ophthalmol Vis Sci, 2000. **41**(10): p. 2915-21.
76. Yamada, M., M. Ogata, M. Kawai and Y. Mashima, *Decreased substance P concentrations in tears from patients with corneal hypesthesia.* Am J Ophthalmol, 2000. **129**(5): p. 671-2.
77. Johnson, S.M., *Neurotrophic corneal defects after diode laser cycloablation.* Am J Ophthalmol, 1998. **126**(5): p. 725-7.
78. Menchini, U., A. Scialdone, C. Pietroni, F. Carones and R. Brancato, *Argon versus krypton panretinal photocoagulation side effects on the anterior segment.* Ophthalmologica, 1990. **201**(2): p. 66-70.
79. Weigt, A.K., I.P. Herring, C.F. Marfurt, J.P. Pickett, R.B. Duncan, Jr. and D.L. Ward, *Effects of cyclophotocoagulation with a neodymium:yttrium-aluminum-garnet laser on corneal sensitivity, intraocular pressure, aqueous tear production, and corneal nerve morphology in eyes of dogs.* Am J Vet Res, 2002. **63**(6): p. 906-15.
80. Tervo, T. and J. Moilanen, *In vivo confocal microscopy for evaluation of wound healing following corneal refractive surgery.* Prog Retin Eye Res, 2003. **22**(3): p. 339-58.
81. Wilson, S.E., *Laser in situ keratomileusis-induced (presumed) neurotrophic epitheliopathy.* Ophthalmology, 2001. **108**(6): p. 1082-7.
82. Wilson, S.E. and R. Ambrosio, *Laser in situ keratomileusis-induced neurotrophic epitheliopathy.* Am J Ophthalmol, 2001. **132**(3): p. 405-6.
83. Efron, N., *The Glenn A. Fry award lecture 2010: Ophthalmic markers of diabetic neuropathy.* Optom Vis Sci, 2011. **88**(6): p. 661-83.
84. Linna, T.U., M.H. Vesaluoma, J.J. Perez-Santonja, W.M. Petroll, J.L. Alio and T.M. Tervo, *Effect of myopic LASIK on corneal sensitivity and morphology of subbasal nerves.* Invest Ophthalmol Vis Sci, 2000. **41**(2): p. 393-7.
85. Fukuda, K. and T. Nishida, *Ocular allergic inflammation: interaction between the cornea and conjunctiva.* Cornea, 2010. **29 Suppl 1**: p. S62-7.
86. Fukuda, K., N. Yamada and T. Nishida, *Case report of restoration of the corneal epithelium in a patient with atopic keratoconjunctivitis resulting in*

amelioration of ocular allergic inflammation. Allergol Int, 2010. **59**(3): p. 309-12.

87. Mohan, R.R., A.E. Hutcheon, R. Choi, J. Hong, J. Lee, R.R. Mohan, R. Ambrosio, Jr., J.D. Zieske and S.E. Wilson, *Apoptosis, necrosis, proliferation, and myofibroblast generation in the stroma following LASIK and PRK.* Exp Eye Res, 2003. **76**(1): p. 71-87.
88. Martinez-Garcia, M.C., J. Merayo-Lloves, T. Blanco-Mezquita and S. Mar-Sardana, *Wound healing following refractive surgery in hens.* Exp Eye Res, 2006. **83**(4): p. 728-35.
89. Power, W.J., A.H. Kaufman, J. Merayo-Lloves, V. Arrunategui-Correa and C.S. Foster, *Expression of collagens I, III, IV and V mRNA in excimer wounded rat cornea: analysis by semi-quantitative PCR.* Curr Eye Res, 1995. **14**(10): p. 879-86.
90. Del Pero, R.A., J.E. Gigstad, A.D. Roberts, G.K. Klintworth, C.A. Martin, F.A. L'Esperance, Jr. and D.M. Taylor, *A refractive and histopathologic study of excimer laser keratectomy in primates.* Am J Ophthalmol, 1990. **109**(4): p. 419-29.
91. Mohan, R.R., W.M. Stapleton, S. Sinha, M.V. Netto and S.E. Wilson, *A novel method for generating corneal haze in anterior stroma of the mouse eye with the excimer laser.* Exp Eye Res, 2008. **86**(2): p. 235-40.
92. Yu, C.Q. and M.I. Rosenblatt, *Transgenic corneal neurofluorescence in mice: a new model for in vivo investigation of nerve structure and regeneration.* Invest Ophthalmol Vis Sci, 2007. **48**(4): p. 1535-42.
93. Nowotschin, S., P. Xenopoulos, N. Schrode and A.K. Hadjantonakis, *A bright single-cell resolution live imaging reporter of Notch signaling in the mouse.* BMC Dev Biol, 2013. **13**: p. 15.
94. Chen, W., K. Hara, Q. Tian, K. Zhao and T. Yoshitomi, *Existence of small slow-cycling Langerhans cells in the limbal basal epithelium that express ABCG2.* Exp Eye Res, 2007. **84**(4): p. 626-34.
95. Liu, Y., P. Hamrah, Q. Zhang, A.W. Taylor and M.R. Dana, *Draining lymph nodes of corneal transplant hosts exhibit evidence for donor major histocompatibility complex (MHC) class II-positive dendritic cells derived from MHC class II-negative grafts.* J Exp Med, 2002. **195**(2): p. 259-68.
96. Chinnery, H.R., M.J. Ruitenberg, G.W. Plant, E. Pearlman, S. Jung and P.G. McMenamin, *The chemokine receptor CX3CR1 mediates homing of MHC class II-positive cells to the normal mouse corneal epithelium.* Invest Ophthalmol Vis Sci, 2007. **48**(4): p. 1568-74.
97. Niederkorn, J.Y., J.S. Peeler and J. Mellon, *Phagocytosis of particulate antigens by corneal epithelial cells stimulates interleukin-1 secretion and migration of Langerhans cells into the central cornea.* Reg Immunol, 1989. **2**(2): p. 83-90.

98. Lai, T.Y.C., *Corneal visualization and characterization for applications in ophthalmology using optical imaging* Doctoral Thesis, 2014.
99. Steven, P., F. Bock, G. Huttmann and C. Cursiefen, *Intravital two-photon microscopy of immune cell dynamics in corneal lymphatic vessels.* PLoS One, 2011. **6**(10): p. e26253.
100. Masihzadeh, O., T.C. Lei, D.A. Ammar, M.Y. Kahook and E.A. Gibson, *A multiphoton microscope platform for imaging the mouse eye.* Mol Vis, 2012. **18**: p. 1840-8.
101. Tada, T., *The immune system as a supersystem.* Annu Rev Immunol, 1997. **15**: p. 1-13.

CHAPTER 0

State of the Art

The Cornea

The cornea is the external organ of the visual system with two main functions: refract the light and protect the eye. The specific features of the cornea are: transparency, avascularity and immune privilege. The cornea is also characterized by its elasticity and resistance to mechanical damage.

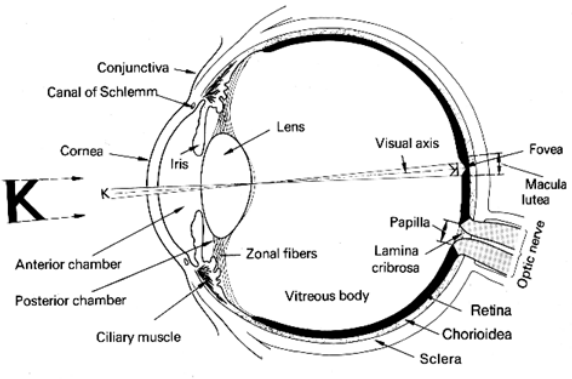

Figure 1. Structure of the ocular system Modified: web.standord.edu

Figure 2. The cornea: protective barrier and primary refractive system of the eye. Modified from: "DesignPics" Don Hammond

In the external part, the cornea has a stratified squamous non-keratinized epithelium in contact with the tear film, which acts as protective barrier form the external environment. The outside epithelial cell layer has a hydrophobic smooth surface to offer a flat front to the light and prevent from pathogens. The epithelium rests in basement membrane [3, 4]. Underneath, the Bowman's layer is located, composed of very well organized collagen. This membrane is not present in all the species [5]. The stroma of the cornea is composed of collagen and keratocytes and consists up to 90% of the corneal thickness. The stroma provides the main refractive power to the cornea [6]. In the posterior part of the cornea, the Descemet' membrane is located, which is considered as the

basement membrane for the endothelium[6]. The endothelium is composed with a monolayer of endothelial cells in contact with the anterior chamber. The endothelium maintains the transparency controlling the hydration of the cornea [7].

Furthermore, the cornea is densely innervated with fibres from the ophthalmic branch of the trigeminal ganglion [8].The cornea is also endowed with a resident population of myeloid-derived cells that play a main role in the immune response; however, the function of these cells is not yet well understood [9]. Therefore, the cornea is a high-specialized organ composed of different tissues in order to protect the integrity of the visual system and maintain its transparency.

Corneal pathologies

The cornea is constantly exposed to injuries and infections. The visual system has developed a unique defense mechanism based in quick external response (blinking, tearing, conjunctival enzymatic secretions) [10]It is necessary to consider the evolutionary aspect to recognize the importance of the wound-healing response in the cornea, though. Adequate vision is essential for the survival resulting in selective pressure to develop the ability to recover from a variety of corneal injuries. Infectious agents such as viruses have posed a threat because of the potential expansion into an eye and through the eye to the brain. The wound healing response to these injuries would likely have evolved to restore the protective epithelial surface, maintain the integrity of the cornea, and restore the corneal clarity [11]. Systems designed to rapidly restore the integrity and clarity of the cornea, impeding the spread of pathogens until the immune response eradicate the intruders, probably have provided selective advantages to organisms, dependent on sight for survival [12].

The cornea is also target for many pathogens that cause keratitis or inflammation of the cornea. Some types of keratitis caused by Acantamoeba affect contact lens users. Bacterial keratitis caused by *Staphylococcus aureus* o *Pseudomonas aeruginosa*, fungal caused by Fusarium or viral origin as *Herpes simplex* o *Herpes zoster* cause strong inflammatory response in the cornea[12, 13].

The ocular surface often is exposed to pathogens, cosmetics and environment agents (e.g. pollen, dust mites, dander, smoke or pollution) that cause inflammation of the conjunctiva. Conjunctivitis diagnosis varies depending on etiology (viral, bacterial, chemical); however, allergic conjunctivitis (AC) is the most common ophthalmologic incidence in developed countries [14]. AC represents a spectrum of disorders that affect the lid, conjunctiva, and in more severe forms, the cornea [15]. Mild forms of AC include seasonal allergic conjunctivitis (SAC) and perennial allergic conjunctivitis (PAC) that are induced by environmental agents such as grass, pollens, or cat dander [16-18]. Together SAC

and PAC comprise 95% of AC cases [16-18]. More severe forms include atopic keratoconjunctivitis (AKC) and vernal keratoconjunctivitis (VKC) [19-21]. SAC and PAC remain self-limited and present no corneal damage. By contrast, AKC and VKC progress with corneal involvement, producing discomfort, pain and may lead to impaired vision and corneal transplantation [17, 19].

Both refractive surgery and use of contact lenses have an impact on the research in corneal pathologies during the last couple of decades. The refractive surgery has increased the incidence of side effects such as loss of visual acuity, halos, glare, reflections, foreign body sensation, lack of lubrication and dry eye. More aggressive complications such as melting, fibrosis after surgery often required corneal transplantation to restore the vision of the patient. Additionally some of these complications might appear after cataract surgery [22, 23].

The cornea is the most frequently transplanted tissue in humans with a success rate that exceeds all other forms of solid organ transplantation since the first successful transplant had been performed in 1905 [24]. Since the National Transplant Organization (ONT, "Organizacíon Nacional de Transplantes") has been established in 1989 in Spain, the 60, 000 transplants were successfully performed (according with published data for this organization). Although less than 10% of them undergo rejection, the total number of successful transplants is still high and topical corticosteroids are the only immunosuppressive agents used. However, rejection increases significantly in hosts receiving second corneal graft [25] due to the loss of ocular immune privilege in the first transplant. Additionally patients, who are considered to be under high risk of rejection are excluded for transplantation [26]. Moreover, corneal transplantation is an option only available in developed countries and not accessible in many developing and undeveloped countries.

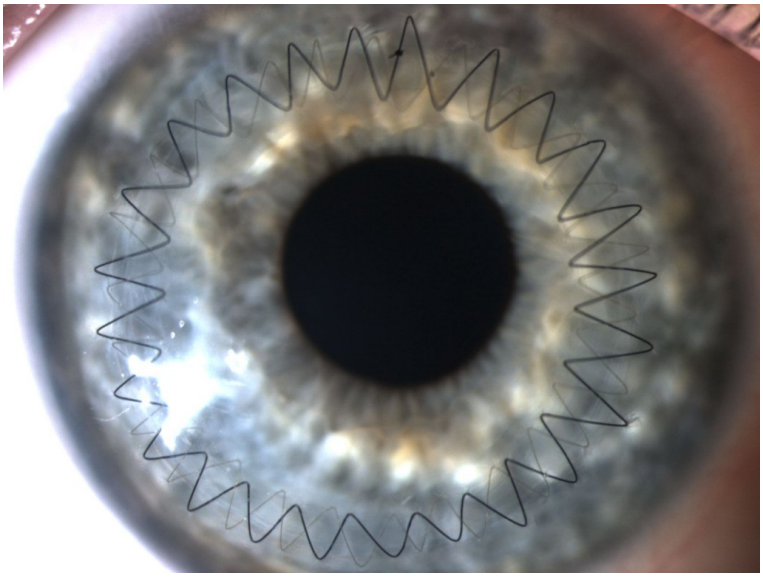

Figure 3. Corneal transplant. Modifies form "Corneal Associates of New Jersey", Fairfield, NJ, EE.UU.

The human cornea is the most innervated structure in the body densely supplied by both sensory and autonomic nerve fibres [27]. Sensory nerves are derived from the ophthalmic division of the trigeminal nerve [28-32] and have a diversity of sensory and efferent functions [33]. The autonomic nerves consist of sympathetic fibres that are derived from the superior cervical ganglion and parasympathetic fibres that originate from the ciliary ganglion [34-36]. The proper innervation is critical for keeping the wellness and transparency of the cornea. The mechanisms by which corneal nerve fibres maintain a healthy cornea and promote wound healing after injuries is currently under active research. Neurons give trophic support to corneal epithelial cells by releasing soluble substances through. Trigeminal ganglion neurons release neurotransmitters and

neuropeptides that contribute to trophism and regulatory processes such as homeostasis. Molecules released by nerves participate actively in corneal wound healing process after injuries [37, 38].

Many factors such as blinking, desiccation of the ocular surface, cooling or air currents induce release neurochemicals by corneal nerves that in consequence aid to heal small damages in the ocular surface [39-41]. Conversely, patients who suffer from diminished corneal innervation, caused by diabetes, herpetic keratitis, contact lens wearing and aging, show impaired wound healing [42-46]. Corneal nerves can be also damaged after cataract and retinal surgery or laser procedures (e.g. pan-retinal photocoagulation, cycloablation) [47-49]. During the last two decades, it has been shown that refractive surgery produces strong damage of corneal nerves and transient mild to severe epithelial alterations [50-52]. Nevertheless, dry eye is nowadays the most common neuropathological dysfunctional syndrome [42, 53, 54]. Mostly of the corneal pathologies present a neurological component; however, the physiological bases remain in many cases still unknown.

The cornea is an immune privileged place, with no lymphatic and blood vessels, which antigen presenting cells (APCs) are not immunoreactive to alloantigens in normal conditions [55-58]. For more than a century, it was believed that the cornea was devoid of APCs [59]; however, during the last few years it has been established that the cornea is endowed with a resident myeloid cell population [9, 60-68] composed of two different phenotypic populations of APCs such as DCs and macrophages[67, 69, 70]. DCs reside in the basal layer of the epithelium and are capable to initiate adaptive immune response [57, 71-73].

Macrophages reside in the stroma [63, 67]. The anterior stroma is populated by putative macrophages that can serve as APCs backup for epithelial DCs in an adaptive immune response [67]. The posterior stroma is endowed of classical macrophages capable to initiate an innate immune response [67].

Immune privilege

Inflammation is an essential component of tissue protection and eradication of infection but also a major antagonist of corneal clarity where maintaining the transparency is essential for unaltered vision and survival. During its evolution, the cornea has developed a complex mechanism to keep the unaltered transparency. The cornea has the unique capability to repair itself after an injury with minimal changes in transparency, biomechanical, refractive and sensory properties [10, 74-76]. The cornea is an immune privileged place, with no lymphatic and blood vessels, which antigen presenting cells (APCs) are not immunoreactive to alloantigens in normal conditions [55-58]. In a healthy cornea, both afferent (lymphatic) and efferent (vascular) arms of the immune response are suppressed [72, 77]. Lymphatic vessels mediate the afferent arm of the immune system by facilitating migration of APCs and alloantigens to the draining lymph nodes, where alloreactive effector T cells are primed, which then return to the ocular surface via blood vessels (efferent arm). To prevent lymphangiogenesis, corneal epithelium expresses soluble forms of VEGF-3 and VEGFR1 acting as trap receptors for VEGF-A, VEGF-C, VEGF-D and VEGFR-2 [78, 79]. In addition, the epithelial cells release PEDF (Pigment Epithelium-Derived Factor), angiostatin and endostatin that prevent lymphangiogenesis [80, 81]. Corneal endothelium also expresses both TGF-β2, which regulates DCs maturation, and FAS-L and PDL-1 (Programmed Death-Ligand 1) driving T cells to apoptosis [82]. Additionally IL10 and IL-1Ra suppress recruitment and proliferation or neutrophils, macrophages and T lymphocytes preventing thus massive release of VEGF [83].

Inflammation revokes this unique immune and angiogenic privilege of the cornea; however, the mechanism has been not well-investigated [84]. The relevance of lymphatic vessels in alloimmunity is illustrated by the high rate of rejection seen in those transplants performed in corneal beds with pre-existing lymphatics, so called ‘high-risk’ hosts [85-87]. Unusual growth of lymphatic vessels into the cornea allows APCs travel to the draining

lymphatic nodes and therefore presenting antigens. This causes an atypical infiltration of T helper cells into the cornea causing an exacerbated inflammatory allorejection [88].

The VEGF family mediates lymphangiogenesis. Activation of by VEGFR-3 by VEGF-C, promotes formation of lymphatic vessels and proliferation of endothelial cells [89]. Macrophages CD11b express LIVE-1 (lymphatic vessel endothelial receptor 1) and PROX-1 (Prospero Homeobox 1) [90]. The balance between antiangiogenic or proangiogenic factors can be modified by corneal pathologies. The proliferation of lymphatic vessels allows APC traffic to the lymphatic nodes triggering and adaptive immune response by T cells [88]. T CD8 cells release VEGF-C promoting linfangiogenesis [91]. As a consequence of an injury, TNFα, IL1, CCL2, CCL20 and ICAM1 expression induces also loss of the immune privilege leading to an unspecific innate immune response [92]. These factors promote recruitment of neutrophils and monocytes that release VEGF-C and VEGF-D [93]. *Herpes virus simplex* (HSV) causes herpetic keratitis by inducing infiltration of lymphocytes that also promote lymphangiogenesis [94].

The proliferation of lymphatic vessels causes also corneal transplantation immune-rejection and dry eye. Corneal APCs can travel to the lymphatic nodes triggering an adaptive immune response by T cells [88] that contribute to maintain a chronic inflammation or rejection [77, 95]. Both examples of losing immune privilege are caused by an adaptive immune response. In dry eye, continuous activation and infiltration of Th17 cells, maintain a chronic state and immune privilege is never restored. VEGF-C, VEGF-D and VEGFR-3 promote lymphangiogenesis [87] and Th17 cells release IL-17 inducing selective formation and growing of lymphatic but not blood vessels [96].

In conclusion, the immune privilege is maintained by different mechanisms that block the induction of an inflammatory reaction but also deviate the immune response into a tolerogenic pathway [97]:

1. Absence of lymphatic vessels in the cornea [98].
2. Induction of T regs in corneal allografts, which inhibits induction and function of alloimmune T lymphocytes [99].

3. Protection of corneal cells from complement-mediated cytolysis by complement-fixing alloantibodies [100].
4. Induction of apoptosis of neutrophils and T cells at graft–host interface by FasL [101].
5. PD-L1 Inhibition of T-lymphocyte proliferation and induction of apoptosis of T cells at graft-host interface PD-L1 [102].
6. Inhibition of NK cells preventing cytolysis of MHC class I-negative corneal endothelial cells [103].

Therefore, immunosuppression in not only a passive process based in the recognition of the antigen, as it has thought for many years; however, this is an active process involving multiple immunologic variations. The combined result of these active mechanisms that effectively inhibit the immune response after introducing an external antigen in the anterior chamber, is named anterior chamber-associated immune deviation (ACAID) [104, 105]

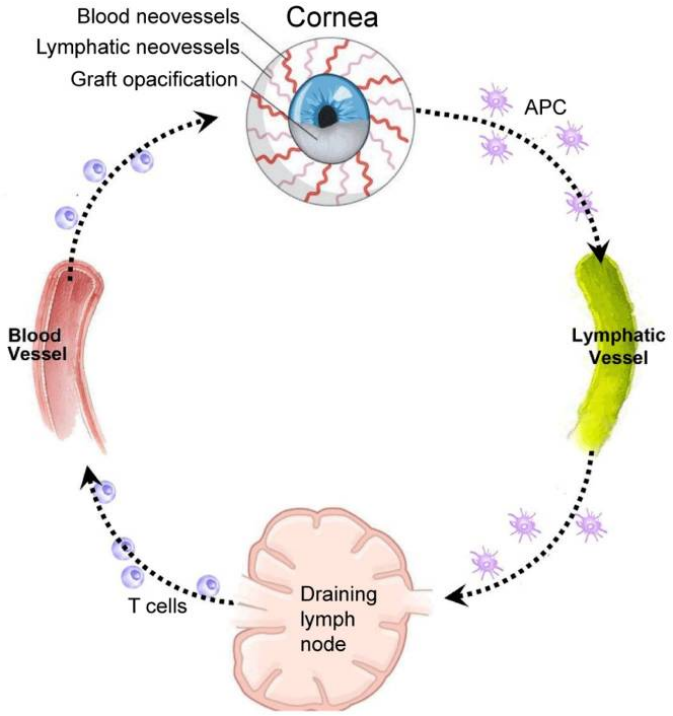

Figure 4: Role of lymphathic and blood vessels in corneal alloimmunity. The afferent arm transports antigens and APCs from the graft site to the draining lymph nodes. Alloreactive T cells go to the cornea through the efferent arm and mediate rejection. Adapted from:
"Corneal Lymphatics: Role in Ocular Inflammation as Inducer and Responder of Adaptive Immunity", Chauhan et al.[77]

Corneal immune population

For more than one hundred years ago, it has been believed that the cornea was devoid of resident APCs capable to initiate an inflammatory response; therefore, maintenance of corneal transparency was attributed, in part, to a lack of such cells [106]. During the last decade, it has been confirmed the cornea is endowed with a particular stratified population of resident myeloid-derived APCs [9, 61-63, 65, 67]. Two main different phenotypic subpopulations, such as DCs and macrophages, compose corneal myeloid population [67]. The majority of DCs reside in the basal layer of the epithelium. DCs extend dendrites to interdigitate between epithelial cells from the basal toward the ocular surface. Classical $CD11c^+$ DCs are typically located in the periphery of the cornea and decreasing in number towards the center [57, 71-73]. Although majority of $CD11c^+$ DCs are present in the basal layer of the epithelium, merely a small population resides in the very peripheral regions of the stroma, some of them as immature precursors [63]. The majority of the $CD11c^+$ DCs also co-express MHC class II, highest in the periphery and lesser toward the center. An additional subpopulation of CD11c-DCs that expresses langerin CD207, or Lagerhans cells (LCs), is also located in the basal epithelium [64]. DCs are potent APCs capable to initiate adaptive immune response; however, this property is still controversial in the normal cornea.

Macrophages that reside in the stroma are divided in two distinct subpopulations [63, 67]. The anterior stroma is populated by $CD11b^+$ $CD11c^-$ MHC class II^+ macrophages, distributed relatively uniformly from the periphery to the center of the stroma. These cells are considered putative macrophages that can serve as APCs backup for epithelial DCs in an adaptive immune response [67]. The posterior stroma is endowed of $CD11b^+$ MHC class II^- classical macrophages, uniformly distributed from the periphery to the center. These macrophages initiate the innate immune response in the murine cornea [67]. Additionally CD11c-expressing cells as well as a different population of monocyte-derived cells also reside in the corneal stroma [60, 63, 64].

Recently Knickelbein et al. have proposed a similar model of APC stratification in the human cornea [9]. $CD45^+$ $CD11c^+$ DCs, the majority expressing HLA-DR, reside in the basal layer of the epithelium extending cellular processes toward the ocular surface. Mostly of these DCs populate the periphery of the cornea and their number is decreasing centripetally toward the center. Langerin positive cells ($CD207^+$), likely LCs, are fundamentally located in the periphery of the cornea. In the stoma $CD45^+$ $CD68^+$ macrophages reside in the anterior part of the stroma distributed relatively uniformly from the periphery to the center [9]. While $CD45^+$ HLA-DR^+ population is higher in the center of the stoma, compared to paracentral and periphery, no $CD207^+$ LCs are observed in the center and only a few of them in the periphery [9].

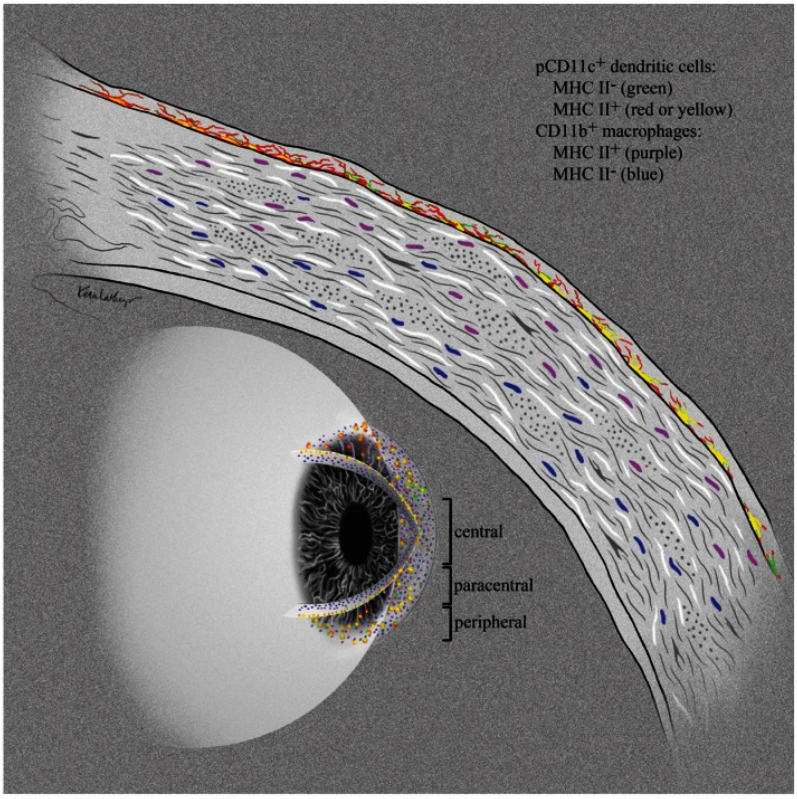

Figure 5: *"Stratification of Antigen-presenting Cells within the Normal Cornea"*. Knickelbein et al.[67]

Corneal innervation

The human cornea is the most densely innervated structure in the body supplied by both sensory and autonomic nerve fibres [27]. Sensory nerves are derived from the ophthalmic division of the trigeminal nerve [28-32] and have a diversity of sensory and efferent functions [33]. The autonomic nerves consist of sympathetic fibres that are derived from the superior cervical ganglion and parasympathetic fibres that originate from the ciliary ganglion [34-36].

The proper innervation is critical for keeping both wellness and transparency. The mechanisms by which corneal nerve fibres maintain a healthy cornea and promote wound healing after injuries is currently under active research. Neurons give trophic support to corneal epithelial cells by releasing soluble substances through. Trigeminal ganglion neurons release neurotransmitters and neuropeptides that contribute to maintain regulatory processes such as corneal trophism and homeostasis. Molecules released by nerves participate actively in corneal wound healing process after injuries [37, 38]

Many factors such as blinking, desiccation of the ocular surface, cooling or air currents induce release neurochemicals by corneal nerves that in consequence aid to heal small damages in the ocular surface [39-41]. Conversely, patients who suffer from diminished corneal innervation, caused by diabetes, herpetic keratitis, contact lens wearing and aging, show impaired wound healing [42-46]. Corneal nerves can be also damaged after cataract and retinal surgery or laser procedures (e.g. pan-retinal photocoagulation, cycloablation) [47-49]. During the last two decades, it has been shown that refractive surgery produces strong damage of corneal nerves and transient mild to severe epithelial alterations [50-52]. Nowadays, dry eye is the most common neuropathological dysfunctional syndrome [42, 53, 54]. Despite mostly of the corneal pathologies present a neurological component, the physiological basis remains still unknown.

The corneal nerve anatomy is briefly described [27]: nerve bundles enter radially through the sclera into of the cornea, paralleled to the surface. In the limbus, nerve bundles lose the perineurium and myelin sheaths. Inside of the peripheral cornea, bundles subdivide into smaller side branches. The majority of the stromal nerve fibres are located in the anterior third of the stroma; however, some stromal nerve trunks can be located below in the peripheral cornea [107, 108]. Bundles contain variable number of axons, and occasionally, keratocytes enwrap adjacent nerve fibres with cytoplasmic extensions. The stromal nerve fibres turn abruptly 90° progressing toward the surface. After penetrating Bowman's layer, large nerve bundles divide into several smaller bundles [109, 110]. Afterward, small nerve axons turn suddenly 90° forming an epithelial leash parallel to the corneal surface in the sub-basal plexus, between Bowman's layer and the basal epithelial cell layer. Epithelial leashes consist of mixtures of straight and beaded nerve fibres that project in separated units toward more superficial layers where release or take up cellular or extracellular substances from adjacent epithelial cells [109, 111-114]. Corneal nerve density is approximately 5400–7200 nerve bundles in the human plexus [45, 115, 116]. Each nerve bundle arises 3–7 individual axons sprouting roughly to a total of 19000–44000 axons [8]. The total number of free nerve endings are between 315000 and 630000, (approximately 7000/mm^2), homogeneously distributed across the cornea [8].

Different methods have been used to describe the anatomy of the corneal nerves. The first understanding of corneal nerve architecture and morphology was established by using acetylcholinesterase (gold chloride), and immunohistochemistry [117-122]. Posteriorly, corneal nerve ultrastructure has been described by electron microscopy [8, 109, 111-114, 123, 124]. Later, with the use of monoclonal and polyclonal antibodies, corneas of different species were compared [125-130]. Retrograde labeling methods allowed backward label of TG sensory cell bodies whose axons innervate the cornea [27, 30]. With the use of electrophysiology techniques, the sensorial nature of the different terminal endings has been demonstrated [130]. In vivo Confocal Microscopy (IVCM), widely used to visualize

corneal nerves in patients, has notably increased the understanding of nerve anatomy in healthy and pathologic corneas, [45, 50, 54, 116, 131-135]

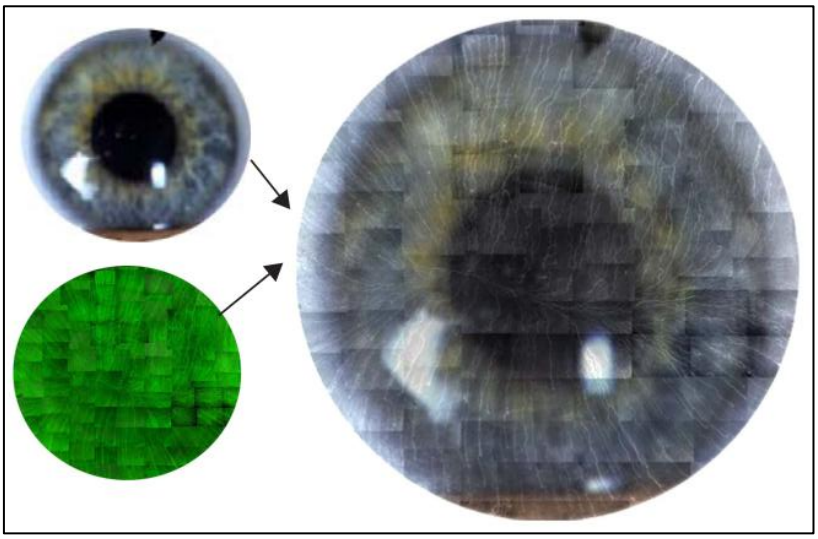

Figure 6. Radial distribution of the corneal nerves Modified from Kenchegowda et al. [136]

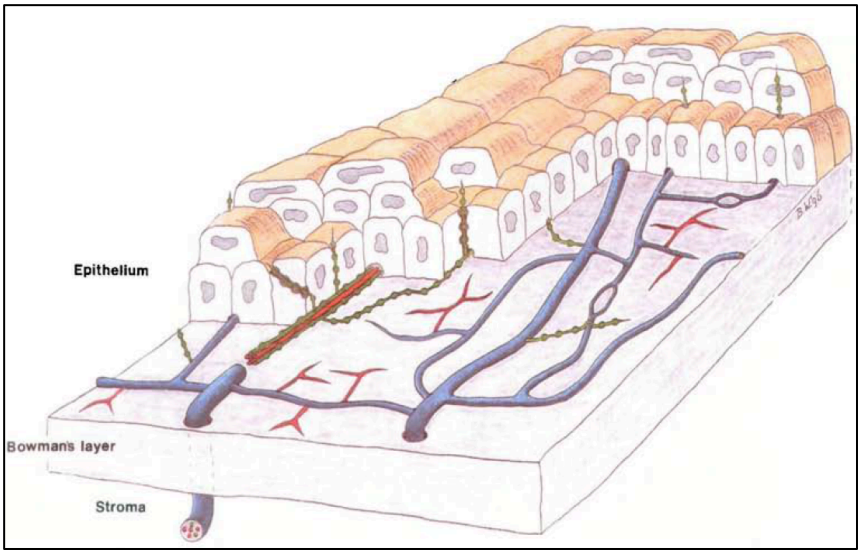

Figure 7. Anatomy of the corneal nerves. Modified from de Müller et al. [8]

Corneal inflammation

In addition to cornea's primary functions: refraction and transmission of light, this organ acts as a primary protective barrier for the inner structures of the eye. The basic structure of the cornea is composed of three different tissues: epithelium, connective tissue or stroma, and endothelium. These tissues are well-organized layers separated by three additional structures; both the basement membrane (BMZ) and Bowman's layer (BM) separate epithelium from stroma and Descemet's membrane (DM) acts as a barrier between the deep stroma and endothelium. The correct organization of these components is essential for keeping the health of the cornea as well as to maintain transparency. Disruption of any of these components leads into an inflammation [11, 12, 72, 77, 83, 94, 137, 138].

Inflammation is an essential component of tissue protection and eradication of infection but also a major antagonist of corneal clarity where to maintain the transparency is essential for unaltered vision and survival. During its evolution, the cornea has developed a complex mechanism to keep the unaltered transparency. The cornea has the unique capability to repair itself after an injury with minimal changes in transparency, biomechanical, refractive and sensory properties [10, 74-76]. The cornea is an immune privileged place, with no lymphatic and blood vessels, which antigen presenting cells (APCs) are not immunoreactive to alloantigens in normal conditions [55-58]. For many years it was believed that the cornea was devoid of resident APCs capable to initiate an inflammatory response [106]. As showed above, the cornea is endowed with a particular stratified population of resident myeloid-derived APCs [9, 61-63, 65, 67] such as DCs and macrophages [67]. The majority of DCs reside in the basal layer of the epithelium DCs are potent APCs capable to initiate adaptive immune response [67]. Macrophages reside in the stroma [63, 67]. The anterior stroma is populated by putative macrophages that can serve as APCs backup for epithelial DCs in an adaptive immune response [67]. The posterior stroma is endowed of classical macrophages that initiate the innate immune response in the murine cornea [67].

In a healthy cornea, both afferent (lymphatic) and efferent (vascular) arms of the immune response are suppressed [72, 77]. Lymphatic vessels mediate the afferent arm of the immune system by facilitating migration of APCs and alloantigens to the draining lymph nodes, where alloreactive effector T cells are primed, which then return to the ocular surface via blood vessels (efferent arm). To prevent lymphangiogenesis, corneal epithelium expresses soluble forms of VEGF-3 and VEGFR1 acting as decoy receptors for VEGF-A, VEGF-C, VEGF-D y VEGFR-2 [78, 79]. In addition, the epithelial cells release PEDF (Pigment Epithelium-Derived Factor), angiostatin and endostatin that prevent lymphangiogenesis [80, 81]. Corneal endothelium also expresses both FAS ligand (FAS-L) and PDL-1 (Programmed Death-Ligand 1) driving T cells to apoptosis [82].

Inflammation revokes this unique immune and angiogenic privilege of the cornea; however, the mechanism is not well-understood [84]. Corneal inflammation or keratitis causes different pathologies that course with the classic symptoms of inflammation such as cytokines release, vasodilatation, edema and erythema [139]. Additionally, in the cornea, inflammation causes pain, tearing, photophobia, ocular surface redness but also ulcerations that affect transparency [140].

LCs, DCs and macrophages that reside in the normal cornea as immature resident myeloid population, are undergoing maturation in response to corneal inflammation. However keratocytes also play key roles in the recruitment of inflammatory cells into the cornea during acquired or innate immune responses. The corneal epithelium serves as a barrier to protect the eye from external agents such as antigens, dust, inflammatory mediators, and microbes. When the barrier is compromised, epithelial cells initiate the inflammatory response. Epithelial cells express adhesion and co-stimulatory molecules in response to several cytokines. The epithelium also releases IL-1 and TNF-α (tumor necrosis factor-α) [141]. The rupture of the epithelial barrier increases eosinophil infiltration in the conjunctiva. However this mechanism is mediated by fibroblast exposition to the tear cytokines [142]. Recently it has been also described that epithelial cells release alarmins in response to an injury [143]. Alarmins contribute to both innate and adaptive immune

response; but how alarmins interact with APCs in the cornea, remains unknown [144]. Nevertheless, corneal fibroblasts are the main modulators of the inflammatory response since they release cytokines and express adhesion molecules for example in allergic inflammatory reaction [145, 146]. Fibroblasts express receptors for IL-4, IL-13, VCAM-1 but also release CCL11 in response to a Th2 stimulation (IL-1, IL-4, IL-13 y TNF-α). CCL11 is a chemokine for eosinophils which infiltration increases after corneal damage in patients with atopic keratoconjunctivitis [145-147]

Ocular inflammation varies depending on the triggering agent. Keratoconus, basement membrane dystrophies, neurotrophic ulcerations, wound healing after refractive surgery or cataracts and corneal transplantation are some pathologies that courses with corneal inflammation. Ocular surface inflammatory diseases are acute and mild, such as seasonal allergic conjunctivitis and transient infectious conjunctivitis. Alternatively, ocular surface inflammatory diseases can be chronic and/or severe, such as atopic keratoconjunctivitis, vernal keratoconjunctivitis, dry eye syndrome, and healing autoimmune conjunctivitis, all of which usually involve corneal damage and may lead to vision loss [40, 148, 149]. In both types, inflammatory cell recruitment occurs by the synthesis and secretion of cytokines and other inflammatory mediators. For instance, significant increase of interleukin IL-1, IL-6, TNF-α and IFN-y occur in the conjunctival epithelium and tear film of dry eye syndrome patients [150].

Immune response

LCs, DCs, macrophages, monocytes and bone marrow immature precursors reside in the normal cornea but undergo maturation in response to inflammation [9, 61-63, 65, 67]. When the corneal integrity is compromised, an innate immune response is activated. Macrophages invade the damage area, cleaning cellular debris and pathogens [67]. On the other hand DCs and macrophages start an adaptive immune response [67]. Epithelial cells and keratocytes also express HLA-DR acting thus as APCs [151, 152]. In an adaptive immune response, DCs prime T cell. DCs increase the expression of MHC class II and co-stimulatory molecules as CD80 and CD86 [139, 152, 153]. DCs migrate from non-lymphoid tissues to lymphatic nodes where effectively present the antigen to T cells. This general mechanism is not well known in the cornea [64, 65, 67]

In a healthy cornea, both afferent (lymphatic) and efferent (vascular) arms of the immune response are suppressed [72, 77]. Lymphatic vessels mediate the afferent arm of the immune system by facilitating migration of APCs and alloantigens to the draining lymph nodes, where alloreactive effector T cells are primed, which then return to the ocular surface via blood vessels (efferent arm) (See above). Unusual growth of lymphatic vessels into the cornea allows APCs travel to the draining lymphatic nodes and therefore presenting antigens. This causes an atypical infiltration of T helper cells into the cornea causing an exacerbated inflammatory allorejection [88]. TGF-β2 controls DC maturation, and FAS-L and PDL-1 drive T cells to apoptosis [82]. Other anti-inflammatory factors such as IL10 and IL-1Ra prevent recruitment of neutrophils, macrophages and T cells preventing massive release of VEGF [83]. The loss of the corneal immune privilege leads to corneal angiogenesis. The activation of VEGF-3 by its ligands such as VEGF-C, promotes proliferation of endothelial cells and formation of lymphatic vessels [89]. Besides, macrophages CD11b express LIVE-1 (lymphatic vessel endothelial hyaluronan receptor 1) and PROX-1 (Prospero Homeobox 1) [90].

Corneal inflammation revokes the balance between pro-inflammatory and anti-inflammatory factors. In this situation corneal APCs travel to the near lymphatic nodes where will present antigens to T cells [88]. Additionally recruited T CD8 lymphocytes release VEGF-C promoting lymphangiogenesis [91]. The immune privilege can be also revoked as a consequence of an injury, being pro-inflammatory factors released such as TNFα, IL1, CCL2, CCL20 or ICAM1 [92]. These factors contribute to the recruitment of neutrophils and monocytes but also induce lymphangiogenesis thought VEGF-C and VEGF-D [93]. Other agents such as Herpes virus cause herpetic keratitis that causes loss of the immune privilege by stimulating lymphangiogenesis through T CD8 stimulation [94].
During inflammation, APCs undergo maturation increasing the expression of MHC class II and co-stimulatory molecules as CD80 and CD86 [151, 152]. Besides APCs decrease the expression of CCR1, CCR2, CCR5 and CX3CR1 but increase expression of CCR7. The proliferation of lymphatic vessel into the cornea, allows APCs enter by expression of CCR7 in a gradient of CCL21. This process is mediated by ICAM-1 and VCAM-1 (**Figure 8**) [139].

The relevance of lymphatic vessels in alloimmunity is illustrated by the high rate of rejection seen in those transplants performed in corneal beds with pre-existing lymphatics, so called 'high-risk' hosts [85-87]. Unusual growth of lymphatic vessels into the cornea allows APCs travel to the draining lymphatic nodes and therefore presenting antigens. This results in an atypical infiltration of T helper cells into the cornea causing an exacerbated inflammatory reaction following the graft immune rejection or dry eye [88].
In the lymph nodes, APCs present antigens to T lymphocytes that release IL-1, IL-6, IL-8 and TNF-α triggering the inflammatory response. IL-1 is the most important cytokine released in the early stages of the inflammatory process [154]. IL-1 mediates the acute response, acts as chemoattractant, activates inflammatory cells and APCs and stimulates neovascularization. IL-6released by macrophages has similar functions as IL-1. IL-8 is released by macrophages and fibroblasts and acts as chemoattractant for

polymorphonuclears and macrophages [155]. TNF-α is released by macrophages and induces cytotoxicity but also inhibits TGF-ß during the wound healing process [154].

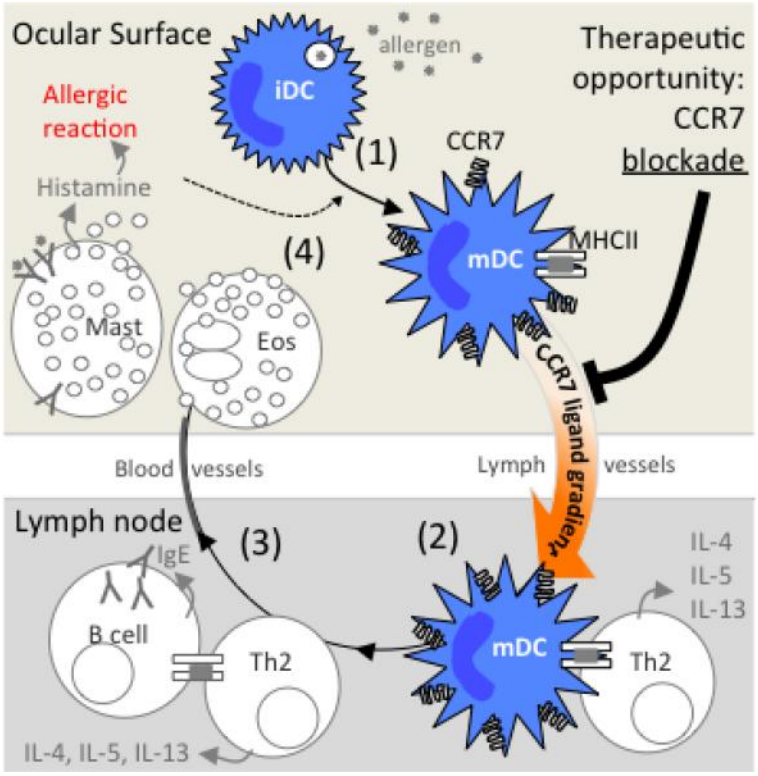

Figure 8. Ocular surface inflammation proposed model and potential therapeutic effect of blocking ocular allergy by using CCR7 antibodies. Adapted form: "*New twists to an old story: novel concepts in the pathogenesis of allergic eye disease"*, Saban et al. [139]

Dry Eye, an example of ocular inflammation

Often considered as a minor problem, *keratoconjunctivitis sicca* or dry eye syndrome is an ocular inflammatory disorder that affects 11-17% of the population of developed countries [156]. Dry eye is a multifactorial disease of the tears and ocular surface that results in symptoms of discomfort, visual disturbance, and tear film instability with potential damage to the ocular surface. It is accompanied by increased osmolarity of the tear film and inflammation of the ocular surface [157]. In Dry Eye syndrome, the proliferation of lymphatic vessels happens without neovascularization in response to infection and graft rejection, where both lymphatic and blood vessels proliferate at the time. Lymphatic vessels proliferation is induced by release of VEGF-C, VEGF-D and VEGFR-3 [87,] while formation of specific lymphatic vessels is promoted by IL-17 [96].

Dry eye associated with ocular surface inflammation is mediated by a chronic lymphocytic response in the cornea with activation and infiltration of pathologic immune cells such as T17 lymphocytes [158]. Conjunctival inflammation is manifested by infiltration and increase in the expression of CD3, CD4 and CD8 as well activation of CD11a and HLA-DR indicating an autoimmune inflammatory response with presence of pro-inflammatory cytokines and metalloproteinases. IL-1, released by conjunctiva epithelial cells, is the most abundant interleukin in the dry eye [159]. Moreover, IL-6, IL-8 and TNF-α are also elevated[160].

Extracellular changes such as hyperosmolarity, UV radiation and changes in the tear composition induce a cellular response mediated by intracellular kinases (MAP) [161]. MAP kinases are activated in response to pro-inflammatory cytokines (IL-1 and TNF α), heat sock proteins, endotoxins and ischemia. This activation mediates signaling to regulate transcription events that mediate a response to the stress. The activation of these pathways causes MMP-9 expression [162] and pro-inflammatory cytokines (IL-1, TNF-α,) that damage the ocular surface [163].

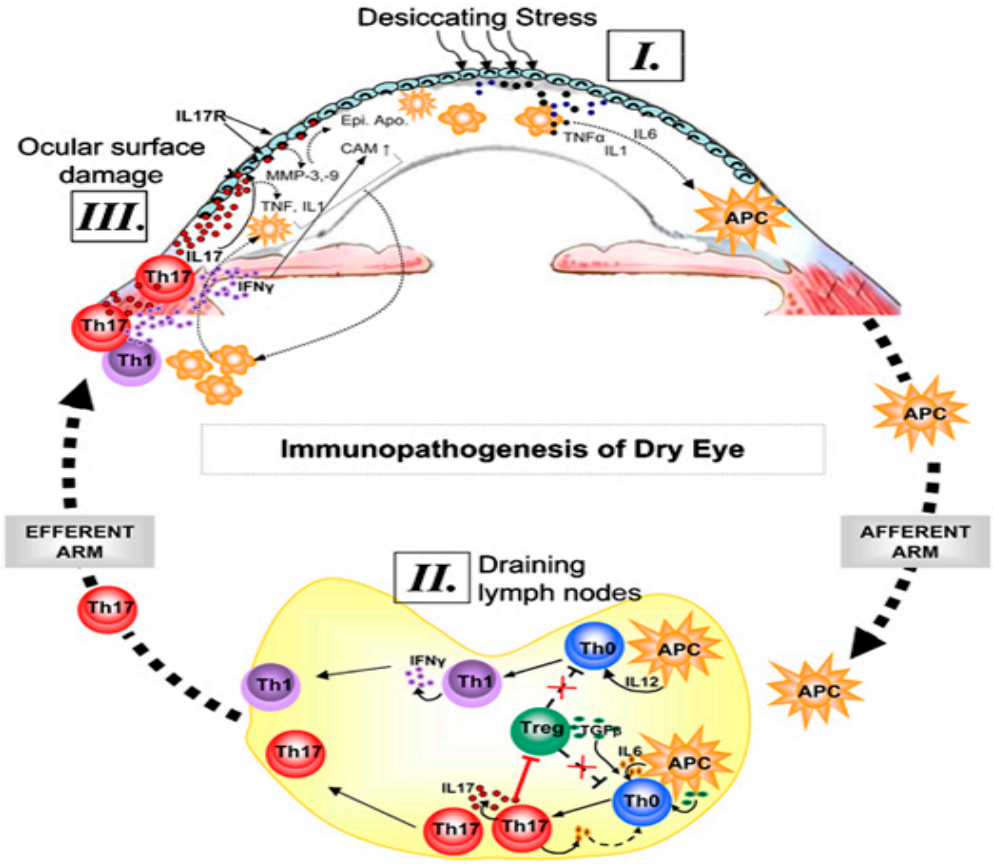

Figure 9: Diagram of dry eye sindrome (**I**) Dessicating stress induces secretion of inflammatory cytokines by ocular surface tissues, which facilitate activation and migration of resident antigen presenting cells (APC) toward draining lymph nodes (**II**) where generate and Th17 immune response directed to the cornea (**III**) releasing MMPs can inflammatory cytokines damaging the epithelium.
"Role of Th17 cells in the immunopathogenesis of dry eye disease". Chauhan et al. [164]

Corneal innervation and inflammation

Inflammation has negative consequences on the PNS of the cornea [43]. Both nervous and immune systems are biochemically interconnected. Neurons express cytokine receptors and immune cells are recognized and modulated by neuropeptides [165]. For example SP and VIP confer resistance to infection by acting as potent pro-inflammatory factors. On the other hand GCRP is associated with immunosuppression and maintaining cornea homeostasis [166].

Regarding nerve regeneration, the role of inflammation is inconclusive [43]. The γδ T cells stimulate nerve regeneration in a process that involves IL-17, neutrophils, platelets and VEGF-A [167]. During infection, sub-basal nerves are observed diminished in the center of the cornea. In contrast, DCs are seen augmented, indicating an interaction between both: nerves and DCs [168].In other non-infectious pathologies, the loss of the sub-basal nerve plexus has been observed [169, 170]. It has been suggested that a moderate inflammation promotes nerve regeneration in the cornea; however, a strong inflammatory reaction implicates loss of the sub-basal nerve plexus and neuropathies. The Sema7A protein function is proposed to link nerve regeneration and inflammatory process in the cornea [171]. This molecule, expressed by T cells, promotes axonal growing and plays a role in the T cell-mediated inflammatory reaction. In the cornea, Sema7 is constitutively expressed in the epithelium and stroma. During the wound healing process, Sema7A-induced nerve regeneration is associated with inflammatory cell income. Therefore, it has been suggested that evading the long-term immunosuppressive or anti-inflammatory treatments, might benefit in improvement of the nerve regeneration in the cornea [171].

Recently it has been shown that severing corneal nerves in one eye induces sympathetic loss of immune privilege and promotes rejection of future corneal allografts placed in either eye [172]. Although the mechanism is not well described, a potential role of the interactions between the nerves and the corneal resident myeloid population has been suggested [173].

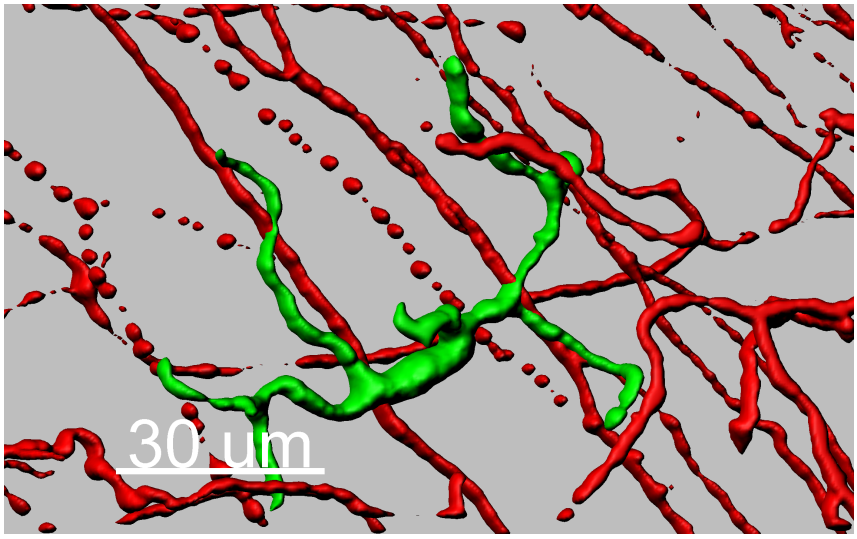

Figure 10: Myeloid cells are in contact with corneal nerves. Adapted from: *"The Cornea Has "the Nerve" to Encourage Immune Rejection"*, Blanco et al. [173]

Corneal wound healing and animal models

Wound healing is a biological process restoring a damage tissue [174]. The tissue replacement can be total or partial, thus the two distinct processes leading to wound healing are differentiated.

Regeneration, is defined as full: morphological and functional recovery ("*ad integrum"*) of damaged tissue. This process is linked to epithelial tissues and sites that still contain mesenchymal stem cells.

Repair, is defined as the response of an organ and/or tissue to an aggression, but the tissue and/or organ do not have sufficient capacity to self-renew into their original state. This happens when the injury is very intense or extensive or because of the loss of totipotent or mesenchymal stem cells. This process takes place in well-differentiated tissues, where cells that potentially have the ability to recover, have disappeared (for example neural tissue). In general, connective tissue replaces the wounded area with a fibrotic collagen generating a scar. In the central nervous system, the glia replaces the original tissue generating a scar as well.

In general, the wound healing response can be divided in three different steeps [174]:

Inflammatory reaction. This phase is initiated at the moment of the injury. Inflammation is associated with hemostasis, cleaning of the wounded area and release of biochemical mediators for the nest next phase.

Proliferation phase. This step is characterized by a re-epithelialization process and coating the wounded area. This involves migration and proliferation of surrounded epithelial cells and establishment of new connective tissue.

Differentiation phase. This stage is characterized by the proliferation, migration and differentiation of connective tissue cells, collagen fibbers maturation, and wound contraction. The wound healing process has high relevance in an avascular and transparent organ such as the cornea. The wound healing process consists of a sequence of cellular events (apoptosis, proliferation, migration and differentiation) engaged to

close the wound and to reestablish the corneal functions [11, 137, 138, 175]. After an injury, the loss of the homeostasis triggers a quick response mediated by cytokines, growth factors, proteases and neurotransmitters. The interactions between the epithelium, stromal cells, corneal nerves, immune cells, lacrimal gland and tear are functionally interconnected in the final response of the cornea [11, 22].

After an injury, the cornea repairs and/or regenerates the damaged tissue. There are multiple variations regarding cellular events as well as the intensity of the response. The response varies depending of the aggression. For that reason it is not possible to describe a common mechanism of wound healing. However, in general, the cornea is evolutionary programmed to trigger a cascade of events that effectively restore the damaged tissue [11, 137, 175].

For many years different animal models have been used to study the wound healing process, including rabbits [11, 176], rats [177], chickens [178-180], primates [181] or dogs [182, 183]. However, the mouse is the most common animal model used for corneal wound healing research [184, 185]. The recent development of different transgenic mice strains allows for a dynamic progress in the investigation and understanding of the corneal pathologies. The use of knockout mice has greatly improved the study of pathologies related with the epithelium, stroma and endothelium [186-188].

Integrins and Corneal Wound Healing

The relevance of membrane integrins in the corneal wound healing process is a subject of intense recent investigation [189, 190]. Integrins are a family of receptors that mediate cell-cell and cell-matrix adhesion [191-193], as well as they contribute to a wide variety of cellular responses, including survival, proliferation, and migration [191]. These heterodimeric transmembrane glycoproteins have both alpha (α) and beta (β) subunits. The combination of these 2 subunits results in at least 22 different cell surface receptors with wide ligand binding specificities. Integrin αvβ6 is expressed at very low levels in epithelial cells of healthy adult mammals; however, its expression is considerably upregulated in response to injury or inflammation [194, 195]. Absence of αvβ6 is linked to initiation and progression of periodontal disease [196], regulation of lung and skin inflammation [197], delay in epidermal wound healing [198] and suppression of pulmonary fibrosis [199]. In the cornea, expression of αvβ6 is restricted to the epithelium. Under pathologic conditions, such as in patients with bullous keratopathy [200] and during wound healing, αvβ6 is upregulated, suggesting a role in corneal epithelial wound repair and keratinocyte migration [201, 202]. αvβ6 is a receptor for many of the components of the basement membrane zone (BMZ) including fibronectin, vitronectin, tenascin, and E-cadherins [190, 203]. It is also the receptor for the Arg-Gly-Asp (RGD) attachment site of both latency-associated peptide (LAP)-TGF-β1 and LAP-TGF-β3 [199, 204, 205]. Attachment of αvβ6 to latent TGF-β has been shown in several investigations to be involved in the activation of TGF-β [206-209]. Indeed, αvβ6-null mice recapitulate much of the phenotype of TGF- β1-null mice [210] Because αvβ6is known to be expressed in remodeling rat basal corneal epithelium and human bullous keratopathy [200] and is an activator of latent TGF-β [199, 204, 205], we hypothesized that αvβ6 plays an important role in corneal repair when the BMZ is compromised by surgery. We addressed this hypothesis by using adult β6 integrin-deficient mice (β6-/-) and comparing them with wild type (WT) mice [211].

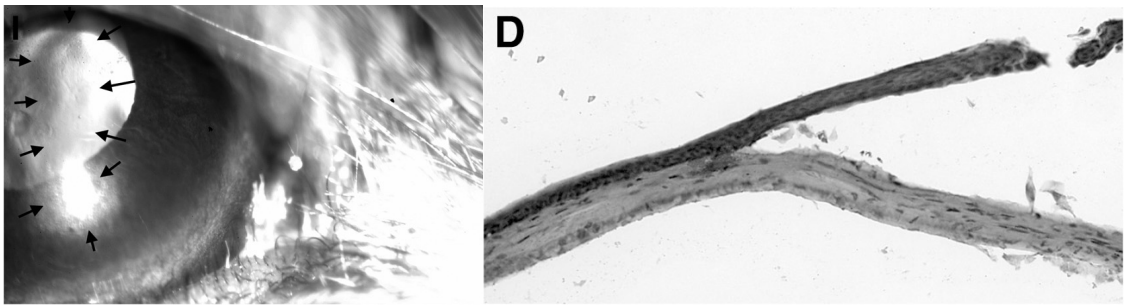

Figure 11: Corneal sub-epithelial blister caused by the lack of αvβ6. Modified form: "AlphaVbeta6 integrin promotes corneal wound healing" Blanco-Mezquita et al. [211]

Trombospondine-1 and Corneal wound Healing

Recently it has been shown that thrombospondin-1 (THBS1, also referred to as TSP-1) is essential during the corneal wound healing process [212]. THBS1 is a large (450 kDa) trimeric extracellular glycoprotein [213, 214]released by platelets, and epithelial and mesenchymal cells in response to many of the physiologic processes, including development, wound healing, angiogenesis, tumor cell migration, platelet aggregation, and cell adhesion [215-220]. It is not known if THBS1 has a significant role in normal tissue homeostasis; however, it is present during development of many embryonic tissues, and its expression is increased dramatically during the wound-healing process [221-224]. Absence of THBS1 leads to prolonged inflammation, delayed wound healing, and delayed scab loss [225, 226]. In the healthy cornea, THBS1 is localized in the basement membrane zone (BMZ), Descemet's membrane (DM), and corneal endothelium (CE), but not within the stroma of human bovine and rat corneas [212, 227]. In addition, Sekiyama et al. [228] demonstrated that limbal and corneal epithelium express Thbs1 mRNA in human corneas. THBS1 and Thbs1 mRNA expression is increased immediately during corneal wound healing after injury [212, 229-231]; however, the mechanisms of action and function remain unclear. Uno et al. suggest that epithelial defects in the cornea stimulate the expression of THBS1 in the wound area, resulting in the accelerated reepithelialization of the cornea and that lack of vitamin A reduced THBS1 expression [231, 232]. Recently, Matsuba et al. [212] proposed that THBS1 might be involved in the transformation of the keratocytes into myofibroblasts during wound healing after a corneal keratectomy in rats [212]. One of the potential roles of THBS1 is the activation of TGF-β1. THBS1 has been demonstrated to be one of the most important activators of TGF-β1 [218, 233, 234] which induces keratocyte proliferation, myofibroblast differentiation, and extracellular matrix (ECM) production [235-237]. TGF- β1 is released and suspended within the ECM in a latent form, which is activated in response to injury [238]. It also has been observed that adhesion and migration were impaired in vitro in Thbs1$^{-/-}$ mouse corneal endothelium [212] thus

showing that THBS1 has a major role during endothelial wound healing as well [239]. Since THBS1 is known to be expressed in remodeling corneal epithelium [231, 232], corneal stroma [212], and corneal endothelium, [239] and is an activator of latent TGF-β1 [218, 233, 234], we hypothesized that THBS1 has an important role in corneal wound repair when the corneal barrier's integrity is compromised.

We addressed this hypothesis by performing a full thickness incision wound in the central cornea of adult THBS1-deficient mice (Thbs1$^{-/-}$) and comparing them to wild type (WT) mice.

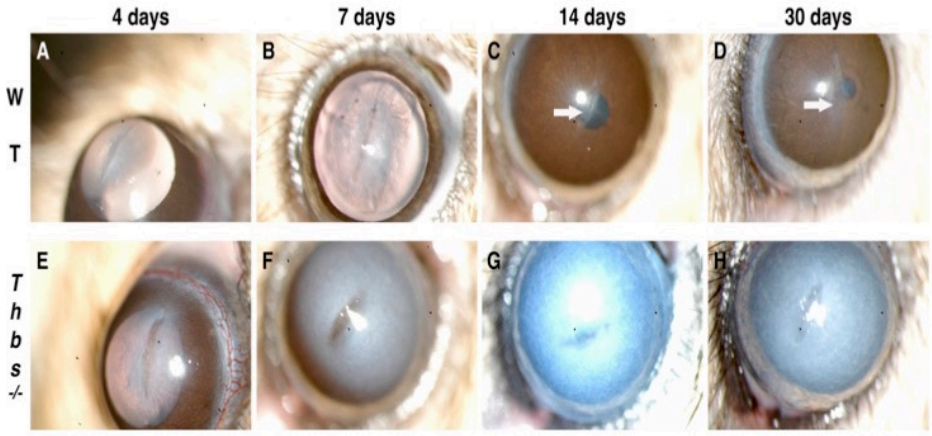

Figure 12: Corneal wound healing in THBS1 and WT mice. Modified from: *Role of thrombospondin-1 in repair of penetrating corneal wounds,* Blanco-Mezquita et al. [240]

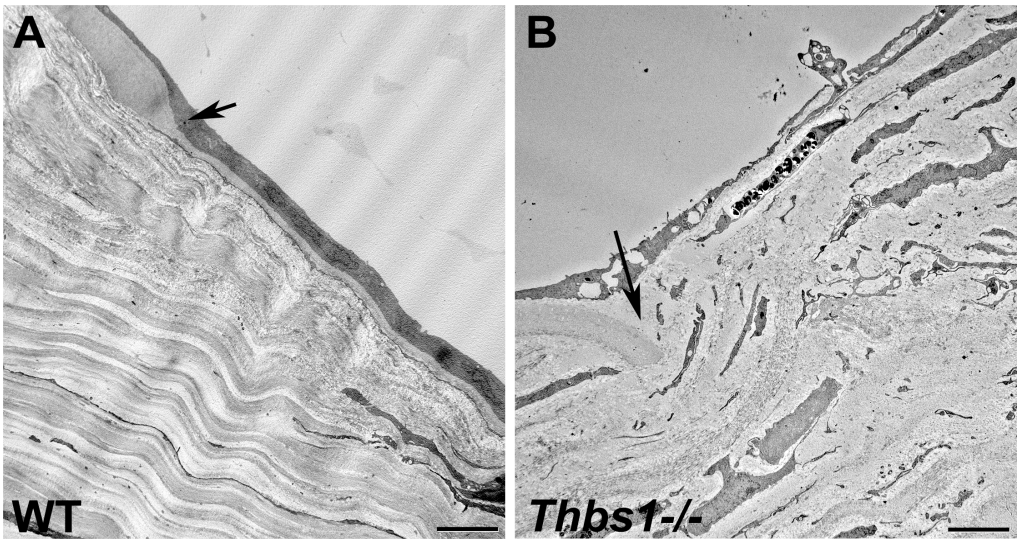

Figure 13: Corneal wound healing in THBS1 and WT mice. Endothelium chronic failure is observed in THBS1 null mice corneas. Modified from: *Role of thrombospondin-1 in repair of penetrating corneal wounds,* Blanco-Mezquita et al. [240]

The use of mice in corneal research

Nowadays, live imaging facilitates the understanding of both tissue and cell behaviors as well as it allows to dissect the molecular mechanisms that drive the biological processes. Genetically-modified reporter expressing mouse strains are an important tool for use in live imaging experiments. Such reporter strains can be engineered by placing cis-regulatory elements of interest to direct the expression of desired reporter genes. If these cis-regulatory elements are downstream targets, and thus activated as a consequence of signaling pathway activation, such reporters can provide read-outs of the signaling status of a cell [241]

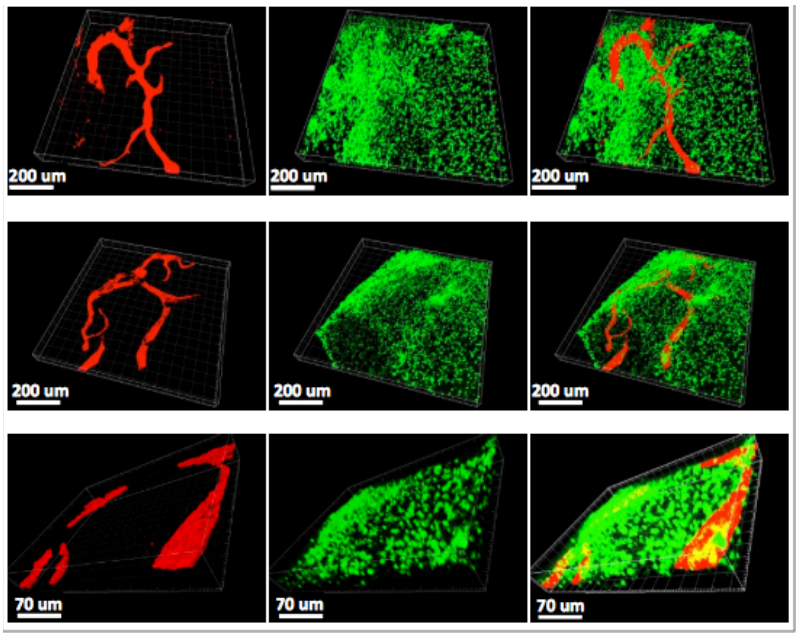

Figure 14: Bone marrow derived-cells form CD45.1 mice engrafted in the stroma of CD45.2 mice. Modified from *"Involvement of corneal lymphangiogenesis in a mouse model of allergic eye disease"* by Hyun-Soo Lee; Deniz Hos; Tomas Blanco et al. [242]

Transgenic mice expressing either CD11c or langerin have been recently used to describe the lineage of corneal APCs [64]. The development of new strains of Cx3cr1-GFP mice expressing EGFP in monocytes, dendritic cells, NK cells and brain microglia, under control of the endogenous Cx3cr1 locus (myeloid progenitor derived marker) facilitated the studies of leukocyte function in migration, trafficking and transplantation [69].

CX3CR1 (Chemokine receptor1), also known as fractalkine receptor, is a protein encoded by the Cx3cr1 gene. CX3CR1 binds the chemokine CX3CL1, also known as fractalkine or neurotactin, a transmembrane protein and chemokine involved in the adhesion and migration of leukocytes. CX3CR1 fractalkine interaction mediates cell-cell adhesion, and migration of CX3CR1-bearing cells predominantly myeloid origin such as monocytes, NK cells, T-cells, DCs, and macrophages including microglia [243-245]

The development of mice in which a green fluorescent protein (EGFP)-encoding gene is inserted in one or both copies of the Cx3cr1 locus has permitted to investigate the fate of leukocytes in vivo [246, 247]. The adoptive transfer of labeled monocytes, from Cx3cr1-GFP mice into wild-type (WT) recipients, has created a new line of research to study monocyte heterogeneity and the factors regulating their differentiation within different tissues. Additionally, it can be investigated the accumulation of normal resident monocyte-derived DCs and macrophages in a diverse range of tissues [246, 247].

In the ocular surface, Cx3cr1-GFP transgenic mice have been used to confirm the presence of myeloid derived cells as a resident population of the normal murine cornea. Also, it has been demonstrated that Cx3cr1 expression plays a role in DC and macrophage recruitment in the normal corneal epithelium and stroma [243]. Heterozygous $Cx3cr1^{+/GFP}$ transgenic mice have provided a powerful tool to investigate macrophage and DC populations by using *intravital* microscopy. *Intravital* widefield epifluorescence videomicroscopy has been performed in corneas of anesthetized mice to probe that corneal DCs behavior bear similarities to that of skin DCs [68]. It has been shown that after irritation of the cornea results in a centripetal migration of DCs from periphery and limbus [248]. Recently Knickelbein et al. have combined LSCM (laser scanning confocal

microscope) with two different *intravital* novel techniques to describe the APCs stratification in the mouse cornea [66]. By using either an Optiscan FIVE-1 handheld fluorescence microscope or a home-built non-descanned two-channel multiphoton system, these authors imaged DCs in corneas of anesthetized mice expressing eGFP driven by the CD11c promoter. However, the authors criticized this technology since a no reliable positioning of the objective on the murine eye, for precise analysis of different regions of the cornea, was possible [66]. Recently, it has been used a multiphoton *intravital* microscopy (MP-IVM) system to study *in vivo* the behavior of inflammatory cells and lymphatic vessels in a mouse cornea [249].

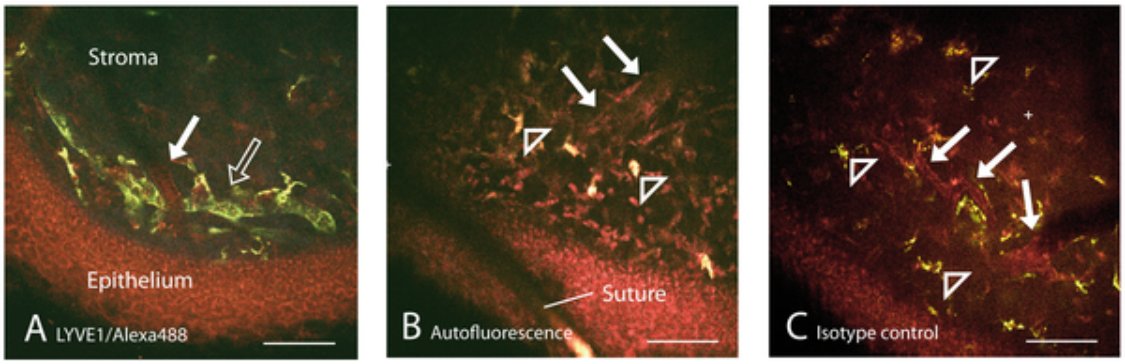

Figure 15. Intravital visualization of lymphatic vessels in the subepithelial stroma of the cornea. Modified from: "*Intravital two-photon microscopy of immune cell dynamics in corneal lymphatic vessels",* Steven, P., et al.249

In the present study, we used a real multiphoton microscope (MPM), equipped with a motorized versatile stage with spacer to give large free working distance under the objective, to visualize the resident myeloid-derived cell population in a living mouse cornea. We used Cx3cr1 transgenic mice expressing GFP (green fluorescent protein), YFP (yellow fluorescent protein) or RFP (red fluorescent protein). Furthermore, we have implemented digital post-analysis commercial software to generate a real tree-dimensional view of the cornea. Additionally we used a Cre system, which induces

constitutively expression of a fluorescent protein for the life span of the cell; therefore, Cx3cr1^{cre} transgenic mice show fluorescence for the entire life of the cell independently of the expression of the gene promoter. The Cre/loxP recombination system is a form of specific recombination [250]. The system is conformed by a generic Cre-transgene construct, one allele labeled with a sequence "Rosa26-loxP-stop-codon-loxP-fGFP/tdTomato" and one intact stop codon (**figure 16**). [251]. The excision of the stop codon Cre-mediated induces constitutive expression of a fluorescence protein or another protein such as diphtheria toxin receptor for the whole life span of the cell.

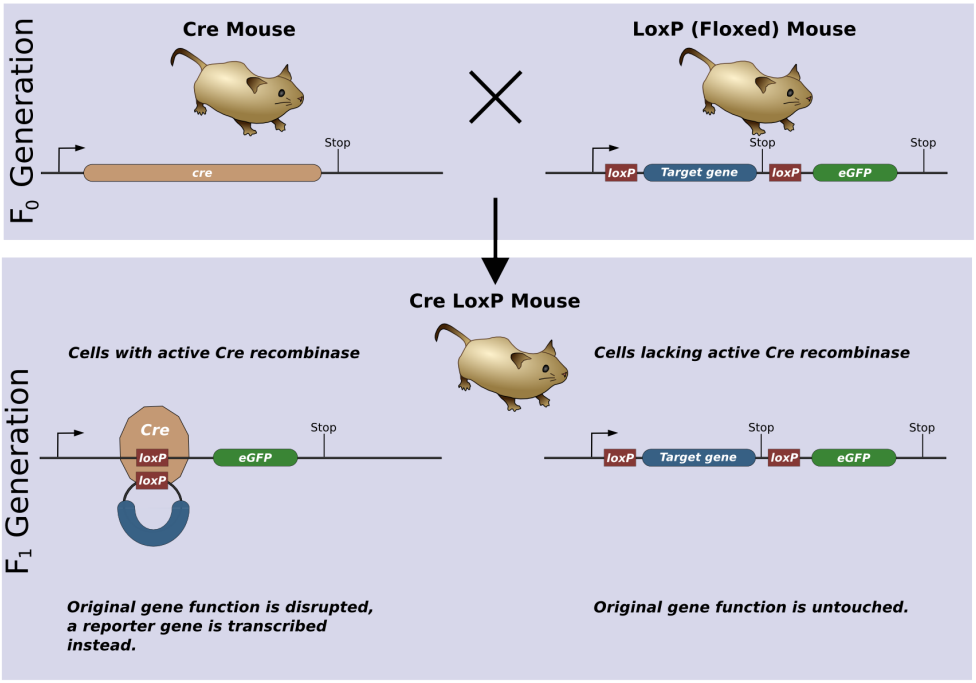

Figure 16. Illustration of a Cre-loxP system model. The function of EGFP gen is interrupted with a stop codon. The enzyme Cre recombinase recognizes the LoxP sites and exscind the stop sequence and allowing the transcription of the eGFP gene by the polymerase. The eGFP will be constitutively expressed for the entire life of the cell
Figure created by Matthias Zepper. Free domain at The Wikimedia Foundation

Microscopy

The fluorescence microscopy by muthiphton excitation was first suggested by Maria Göppert-Mayer in 1931 and applied experimentally thirty years later with the invention of the laser [252]. The singularity of two-photon excitation happens from the simultaneous absorption of two photons in a single quantized event. The energy of a photon is inversely proportional to its wavelength therefore the two absorbed photons have a wavelength about twice that required for one-photon excitation. For example, a fluorophore that normally absorbs ultraviolet light (350 nm) can also be excited by two photons of near-infrared light (700 nm) if both reach the focal at the same time. "The same time" means within an interval of about $10 \times E^{-18}$ seconds [253].

Two-photon excitation microscopy (TPM) presents a great advantage for *in vivo* real time imaging of living cells in a thick intact tissue. TPM makes possible many experiments in which conventional imaging cannot be performed, or would not provide the information desired. Relying on mode-locked (pulsed) laser illumination to produce sufficient photon density at the focal point, two-photon excitation occurs only in the focal plane. The benefit of localized excitation is that emission is restricted to the narrow focal region, providing sectioning ability without the use of a pinhole. Furthermore, the limited excitation region reduces phototoxicity because photodamage is largely confined to the focal volume [254].

Two-photon excitation microscopy does not produce images with higher resolution than confocal microscopy; however, it allows deeper penetration into thick specimens. The greater penetration is due in part by the lack of pinhole geometry, the absence of out-of-focus absorption and decreased scattering. Two-photon microscope uses non-descanned detection geometries, which increase collection efficiency of scattered fluorescence photons. Two-photon excitation allows experiments that would not be possible by using confocal microscopy.

In order to produce a significant number of two-photon absorption events, the photon density must be approximately one million times more that then required to generate the same number of one-photon absorptions [255]. The consequence is that extremely high laser power is required to generate significant two-photon-excited fluorescence. This power level is easily achieved by focusing mode-locked (pulsed) lasers, in which the power during the peak of the pulse is high enough to generate significant two-photon excitation, while the average laser power remains fairly low. In this situation, the resulting two-photon-excited state from which emission occurs is the same singlet state that is populated when carrying out a conventional fluorescence experiment. Thus, fluorescent emission following two-photon excitation is exactly the same as emission generated in normal one-photon excitation.

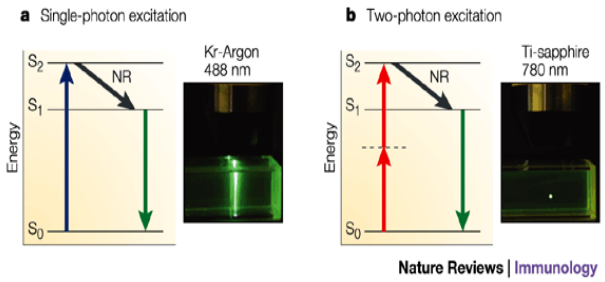

Figure 17. Jablonski diagram. Single photon absorption (confocal, left) and two photons absorption (two-photon, derecha).

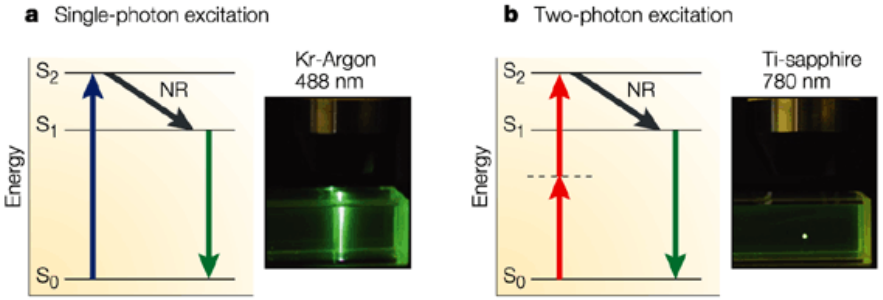

In a

Figure 18. Different excitation in the focal plane comparing single photon absorption (a) and two-photon (b) [256]

confocal microscope (**figure 19**)**, the excitation light (blue) is focused into the specimen (a), and the fluorescence (green) from that focal spot is captured by the objective lens, passes cleanly through the pinhole, and reaches the detector (b). This fluorescence light is the desired signal, but some of it can be scattered as it passes back through the specimen (c). This scattered fluorescence does not pass through the pinhole, and is therefore lost and not detected. These losses greatly reduce the detected fluorescence signal. As the excitation light passes through the specimen, it may be absorbed (d) or scattered before it reaches the focus (e). If it is absorbed, it can generate fluorescence. Since this fluorescence does not arise from the focal spot, it does not pass through the pinhole, so it is not efficiently detected. However, a small portion of out-of-focus fluorescence can be scattered into the pinhole, and then be detected. This fluorescence will create a background fog that will be roughly constant across the image. This fog reduces the dynamic range of the image, thus reducing the image contrast. Likewise, the scattered excitation can generate fluorescence (e), and this fluorescence can also contribute to the background fog (f).

In the two-photon excitation method (also referring to Figure 6), the excitation photons (red) can be scattered (g) as in the confocal system. However, the probability of two photons being scattered simultaneously to the same specimen location is essentially zero, and consequently, the background fog that plagues confocal imaging in thick specimens is not generated in two-photon excitation. In addition, a greater proportion of the excitation light reaches the focal plane (h and i) due to the first two factors discussed above: the reduced out-of-focus absorption and the decreased scattering of the longer-wavelength two-photon excitation light. Importantly, the generated fluorescence (green), even if scattered, has an increased likelihood of being detected by the photomultiplier tube (j) because no pinhole is present to block it (k). This insensitivity to scattering effects and absence of out-of-focus absorption allow for the preservation of the full image contrast from considerable depth within specimens.

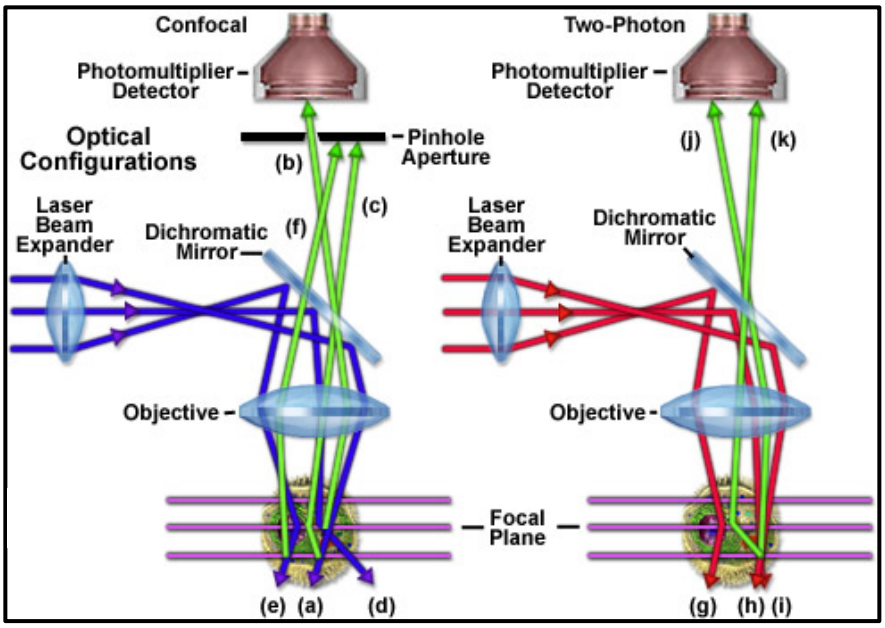

Figure 19. Differences between a single photon excitation microscopy (confocal) and two-photon excitation microscope are shown. Modify from: "Fundamentals and Applications in Multiphoton Excitation Microscopy" .

****Note**: This part has been complemented from: Fundamentals and Applications in Multiphoton Excitation Microscopy, https://www.microscopyu.com/index.html

Contributing Authors:

David W. Piston, Department of Molecular Physiology and Biophysics, Vanderbilt University, Nashville, Tennessee.

Thomas J. Fellers and Michael W. Davidson, National High Magnetic Field Laboratory, The Florida State University, Tallahassee, Florida,

Second Harmonic Generation:

The second harmonic generation (SHG) or frequency doubling is a non-linear process in witch two photons with the same frequency interacting with a non-linear material are combined to generate new photons with twice the energy and frequency and half of the wavelength of the originals [257]. Transparent materials behave as non-linear transmitters. Monochromatic light with low intensity passes through them proportionally to its original intensity. When light intensity is high, for example a laser, the material shows a non-linear optic behavior generating thus a second harmonic [258]

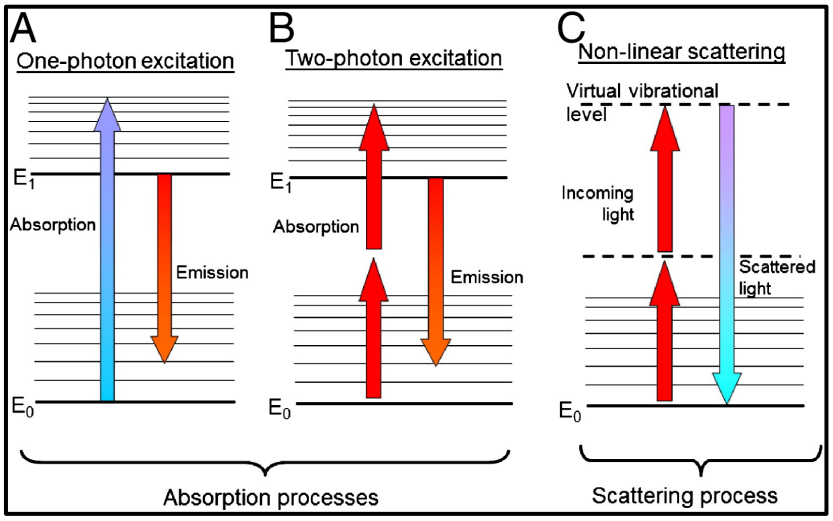

Figure 20. Jablonsky diagram. Single photon absorption (confocal) (A), simultaneous two-photon absorption (B) and generation of a non-linear process of reflection or second harmonic generation (SHG) (C).

The effect to the SHG can be easily detected in mouse corneas by using a MP-IVCM system. As can be observed in the **figure 21**, is possible to delineate the cornea collection the emission of the corneal collagen.

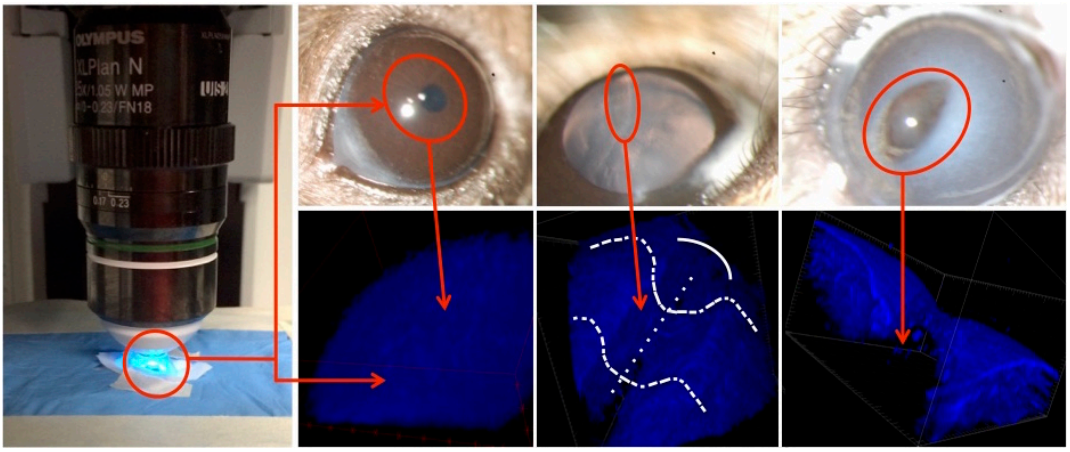

Figure 21. The organized structure of the corneal stroma generates a second harmonic signal by excitation at 890-950 nm and detectable in the blue canal (420-460 nm). The lack of collagen in the wounded area leaves a gap in the signal. After, it can be tree-dimensionally reconstructed showing a real shape of the cornea. Unpublished photographs generated in our lab. Duke University

The MP-IVM system has been barely used in ocular research. In a previous thesis dissertation, Tom Yu Chia Lai compared the OCT system (Optical coherence tomography) with the MPM system to obtain pictures of the cornea. The structure of the cornea of five different species (human, fish, porcine, bovine and murine) was evaluated *ex vivo* [259]. Additionally the MP-IVM system has been used *in vivo* in to study the dynamics of inflammatory cells and lymphatic vessels in a mouse cornea [249]. A different work showed the anterior chamber of the mouse eye [260].

Taking advantage of corneal transparency, in the present work, we explored the full potential of the MP-IVM using both: Cx3cr1 transgenic mice expressing GFP, YFP or RFP and Thy1-YFP transgenic mice models. We used a real multiphoton microscope (MPM), equipped with a motorized versatile stage with spacer to give large free working distance under the objective, to visualize the resident myeloid-derived cell population and

nerves in a living mouse cornea. Furthermore, we have implemented digital post-analysis commercial software to generate a real tree-dimensional view of the cornea with a sharp resolution and outstanding tree-dimensional post-production (**figure 22**).

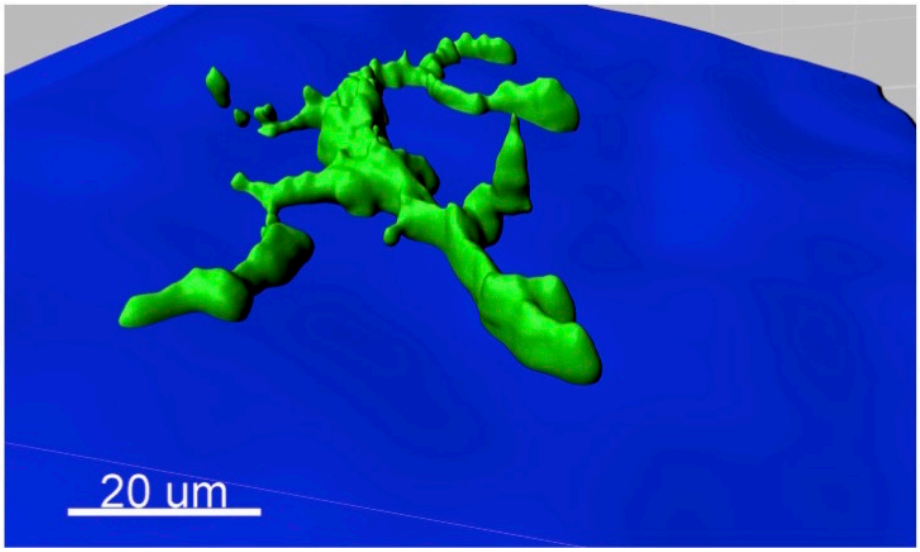

Figure 22. High-resolution photograph of a DC (green) seated in the storma (blue) in the sub-basal area of the epithelium. The picture was acquired *in vivo* by using the MP-IVM in a Cx3CR1^{GFP} knock-in mouse cornea
Unpublished photographs generated in our lab. Duke University.

References:

1. C. Stephen Foster, D.T.A., Claes H. Dolman, *Smolin and Thoft's The Cornea, Scientific Foundation & Clinical Practice.* 2005.
2. Piston, D.W., T.J. Fellers and M.W. Davidson, *Fundamentals and Applications in Multiphoton Excitation Microscopy.* 2013.
3. Beebe, D.C. and B.R. Masters, *Cell lineage and the differentiation of corneal epithelial cells.* Invest Ophthalmol Vis Sci, 1996. **37**(9): p. 1815-25.
4. Hanna, C. and J.E. O'Brien, *Cell production and migration in the epithelial layer of the cornea.* Arch Ophthalmol, 1960. **64**: p. 536-9.
5. Wilson, S.E. and J.W. Hong, *Bowman's layer structure and function: critical or dispensable to corneal function? A hypothesis.* Cornea, 2000. **19**(4): p. 417-20.
6. Rodrigues MM, W.G.I., Hackett J, Donohoo P *Ocular Anatomy, Embryology, and Teratology.* 1982.
7. Waring, G.O., 3rd, W.M. Bourne, H.F. Edelhauser and K.R. Kenyon, *The corneal endothelium. Normal and pathologic structure and function.* Ophthalmology, 1982. **89**(6): p. 531-90.
8. Muller, L.J., G.F. Vrensen, L. Pels, B.N. Cardozo and B. Willekens, *Architecture of human corneal nerves.* Invest Ophthalmol Vis Sci, 1997. **38**(5): p. 985-94.
9. Knickelbein, J.E., K.A. Buela and R.L. Hendricks, *Antigen-presenting cells are stratified within normal human corneas and are rapidly mobilized during ex vivo viral infection.* Invest Ophthalmol Vis Sci, 2014. **55**(2): p. 1118-23.
10. Maurice, D.M., *The structure and transparency of the cornea.* J Physiol, 1957. **136**(2): p. 263-86.
11. Wilson, S.E., *Analysis of the keratocyte apoptosis, keratocyte proliferation, and myofibroblast transformation responses after photorefractive keratectomy and laser in situ keratomileusis.* Trans Am Ophthalmol Soc, 2002. **100**: p. 411-33.
12. Wilson, S.E., L. Pedroza, R. Beuerman and J.M. Hill, *Herpes simplex virus type-1 infection of corneal epithelial cells induces apoptosis of the underlying keratocytes.* Exp Eye Res, 1997. **64**(5): p. 775-9.
13. Kaye, S. and A. Choudhary, *Herpes simplex keratitis.* Prog Retin Eye Res, 2006. **25**(4): p. 355-80.
14. Blaiss, M.S., *Allergic rhinoconjunctivitis: burden of disease.* Allergy Asthma Proc, 2007. **28**(4): p. 393-7.
15. Ono, S.J. and M.B. Abelson, *Allergic conjunctivitis: update on pathophysiology and prospects for future treatment.* J Allergy Clin Immunol, 2005. **115**(1): p. 118-22.
16. Bonini, S., S. Bonini, A. Lambiase, S. Marchi, P. Pasqualetti, O. Zuccaro, P. Rama, L. Magrini, T. Juhas and M.G. Bucci, *Vernal keratoconjunctivitis*

revisited: a case series of 195 patients with long-term followup. Ophthalmology, 2000. **107**(6): p. 1157-63.
17. Leonardi, A., *Vernal keratoconjunctivitis: pathogenesis and treatment.* Prog Retin Eye Res, 2002. **21**(3): p. 319-39.
18. Pucci, N., E. Novembre, E. Lombardi, A. Cianferoni, R. Bernardini, C. Massai, R. Caputo, L. Campa and A. Vierucci, *Atopy and serum eosinophil cationic protein in 110 white children with vernal keratoconjunctivitis: differences between tarsal and limbal forms.* Clin Exp Allergy, 2003. **33**(3): p. 325-30.
19. Leonardi, A., L. Motterle and M. Bortolotti, *Allergy and the eye.* Clin Exp Immunol, 2008. **153 Suppl 1**: p. 17-21.
20. Leonardi, A., *The central role of conjunctival mast cells in the pathogenesis of ocular allergy.* Curr Allergy Asthma Rep, 2002. **2**(4): p. 325-31.
21. Bielory, L., *Ocular allergy guidelines: a practical treatment algorithm.* Drugs, 2002. **62**(11): p. 1611-34.
22. Netto, M.V., R.R. Mohan, R. Ambrosio, Jr., A.E. Hutcheon, J.D. Zieske and S.E. Wilson, *Wound healing in the cornea: a review of refractive surgery complications and new prospects for therapy.* Cornea, 2005. **24**(5): p. 509-22.
23. Randleman, J.B., M. Woodward, M.J. Lynn and R.D. Stulting, *Risk assessment for ectasia after corneal refractive surgery.* Ophthalmology, 2008. **115**(1): p. 37-50.
24. Zirm, E.K., *Eine erfolgreiche totale Keratoplastik (A successful total keratoplasty). 1906.* Refract Corneal Surg, 1989. **5**(4): p. 258-61.
25. Coster, D.J. and K.A. Williams, *The impact of corneal allograft rejection on the long-term outcome of corneal transplantation.* Am J Ophthalmol, 2005. **140**(6): p. 1112-22.
26. van Essen, T.H., D.L. Roelen, K.A. Williams and M.J. Jager, *Matching for Human Leukocyte Antigens (HLA) in corneal transplantation - To do or not to do.* Prog Retin Eye Res, 2015. **46**: p. 84-110.
27. Muller, L.J., C.F. Marfurt, F. Kruse and T.M. Tervo, *Corneal nerves: structure, contents and function.* Exp Eye Res, 2003. **76**(5): p. 521-42.
28. Arvidson, B., *Retrograde axonal transport of horseradish peroxidase from cornea to trigeminal ganglion.* Acta Neuropathol, 1977. **38**(1): p. 49-52.
29. Marfurt, C.F. and D.R. Del Toro, *Corneal sensory pathway in the rat: a horseradish peroxidase tracing study.* J Comp Neurol, 1987. **261**(3): p. 450-9.
30. Marfurt, C.F., R.E. Kingsley and S.E. Echtenkamp, *Sensory and sympathetic innervation of the mammalian cornea. A retrograde tracing study.* Invest Ophthalmol Vis Sci, 1989. **30**(3): p. 461-72.
31. Morgan, C.W., I. Nadelhaft and W.C. de Groat, *Anatomical localization of corneal afferent cells in the trigeminal ganglion.* Neurosurgery, 1978. **2**(3): p. 252-8.

32. ten Tusscher, M.P., J. Klooster and G.F. Vrensen, *The innervation of the rabbit's anterior eye segment: a retrograde tracing study.* Exp Eye Res, 1988. **46**(5): p. 717-30.
33. Lele, P.P. and G. Weddell, *Sensory nerves of the cornea and cutaneous sensibility.* Exp Neurol, 1959. **1**: p. 334-59.
34. Marfurt, C.F., M.A. Jones and K. Thrasher, *Parasympathetic innervation of the rat cornea.* Exp Eye Res, 1998. **66**(4): p. 437-48.
35. Morgan, C., W.C. DeGroat and P.J. Jannetta, *Sympathetic innervation of the cornea from the superior cervical ganglion. An HRP study in the cat.* J Auton Nerv Syst, 1987. **20**(2): p. 179-83.
36. Tervo, T., F. Joo, K.T. Huikuri, I. Toth and A. Palkama, *Fine structure of sensory nerves in the rat cornea: an experimental nerve degeneration study.* Pain, 1979. **6**(1): p. 57-70.
37. Baker, K.S., S.C. Anderson, E.G. Romanowski, R.A. Thoft and N. SundarRaj, *Trigeminal ganglion neurons affect corneal epithelial phenotype. Influence on type VII collagen expression in vitro.* Invest Ophthalmol Vis Sci, 1993. **34**(1): p. 137-44.
38. Garcia-Hirschfeld, J., L.G. Lopez-Briones and C. Belmonte, *Neurotrophic influences on corneal epithelial cells.* Exp Eye Res, 1994. **59**(5): p. 597-605.
39. Mathers, W.D., *Why the eye becomes dry: a cornea and lacrimal gland feedback model.* CLAO J, 2000. **26**(3): p. 159-65.
40. Stern, M.E., R.W. Beuerman, R.I. Fox, J. Gao, A.K. Mircheff and S.C. Pflugfelder, *The pathology of dry eye: the interaction between the ocular surface and lacrimal glands.* Cornea, 1998. **17**(6): p. 584-9.
41. Stern, M.E., R.W. Beuerman, R.I. Fox, J. Gao, A.K. Mircheff and S.C. Pflugfelder, *A unified theory of the role of the ocular surface in dry eye.* Adv Exp Med Biol, 1998. **438**: p. 643-51.
42. Benitez del Castillo, J.M., M.A. Wasfy, C. Fernandez and J. Garcia-Sanchez, *An in vivo confocal masked study on corneal epithelium and subbasal nerves in patients with dry eye.* Invest Ophthalmol Vis Sci, 2004. **45**(9): p. 3030-5.
43. Benitez-Del-Castillo, J.M., M.C. Acosta, M.A. Wassfi, D. Diaz-Valle, J.A. Gegundez, C. Fernandez and J. Garcia-Sanchez, *Relation between corneal innervation with confocal microscopy and corneal sensitivity with noncontact esthesiometry in patients with dry eye.* Invest Ophthalmol Vis Sci, 2007. **48**(1): p. 173-81.
44. Hamrah, P., A. Cruzat, M.H. Dastjerdi, L. Zheng, B.M. Shahatit, H.A. Bayhan, R. Dana and D. Pavan-Langston, *Corneal sensation and subbasal nerve alterations in patients with herpes simplex keratitis: an in vivo confocal microscopy study.* Ophthalmology, 2010. **117**(10): p. 1930-6.

45. Rosenberg, M.E., T.M. Tervo, I.J. Immonen, L.J. Muller, C. Gronhagen-Riska and M.H. Vesaluoma, *Corneal structure and sensitivity in type 1 diabetes mellitus.* Invest Ophthalmol Vis Sci, 2000. **41**(10): p. 2915-21.
46. Yamada, M., M. Ogata, M. Kawai and Y. Mashima, *Decreased substance P concentrations in tears from patients with corneal hypesthesia.* Am J Ophthalmol, 2000. **129**(5): p. 671-2.
47. Johnson, S.M., *Neurotrophic corneal defects after diode laser cycloablation.* Am J Ophthalmol, 1998. **126**(5): p. 725-7.
48. Menchini, U., A. Scialdone, C. Pietroni, F. Carones and R. Brancato, *Argon versus krypton panretinal photocoagulation side effects on the anterior segment.* Ophthalmologica, 1990. **201**(2): p. 66-70.
49. Weigt, A.K., I.P. Herring, C.F. Marfurt, J.P. Pickett, R.B. Duncan, Jr. and D.L. Ward, *Effects of cyclophotocoagulation with a neodymium:yttrium-aluminum-garnet laser on corneal sensitivity, intraocular pressure, aqueous tear production, and corneal nerve morphology in eyes of dogs.* Am J Vet Res, 2002. **63**(6): p. 906-15.
50. Tervo, T. and J. Moilanen, *In vivo confocal microscopy for evaluation of wound healing following corneal refractive surgery.* Prog Retin Eye Res, 2003. **22**(3): p. 339-58.
51. Wilson, S.E., *Laser in situ keratomileusis-induced (presumed) neurotrophic epitheliopathy.* Ophthalmology, 2001. **108**(6): p. 1082-7.
52. Wilson, S.E. and R. Ambrosio, *Laser in situ keratomileusis-induced neurotrophic epitheliopathy.* Am J Ophthalmol, 2001. **132**(3): p. 405-6.
53. Efron, N., *The Glenn A. Fry award lecture 2010: Ophthalmic markers of diabetic neuropathy.* Optom Vis Sci, 2011. **88**(6): p. 661-83.
54. Linna, T.U., M.H. Vesaluoma, J.J. Perez-Santonja, W.M. Petroll, J.L. Alio and T.M. Tervo, *Effect of myopic LASIK on corneal sensitivity and morphology of subbasal nerves.* Invest Ophthalmol Vis Sci, 2000. **41**(2): p. 393-7.
55. Beebe, D.C., *Maintaining transparency: a review of the developmental physiology and pathophysiology of two avascular tissues.* Semin Cell Dev Biol, 2008. **19**(2): p. 125-33.
56. Hori, J., J.L. Vega and S. Masli, *Review of ocular immune privilege in the year 2010: modifying the immune privilege of the eye.* Ocul Immunol Inflamm, 2010. **18**(5): p. 325-33.
57. Shen, L., S. Barabino, A.W. Taylor and M.R. Dana, *Effect of the ocular microenvironment in regulating corneal dendritic cell maturation.* Arch Ophthalmol, 2007. **125**(7): p. 908-15.
58. Streilein, J.W., J. Yamada, M.R. Dana and B.R. Ksander, *Anterior chamber-associated immune deviation, ocular immune privilege, and orthotopic corneal allografts.* Transplant Proc, 1999. **31**(3): p. 1472-5.

59. Streilein, J.W., *Immunobiology and immunopathology of corneal transplantation.* Chem Immunol, 1999. **73**: p. 186-206.
60. Chinnery, H.R., T. Humphries, A. Clare, A.E. Dixon, K. Howes, C.B. Moran, D. Scott, M. Zakrzewski, E. Pearlman and P.G. McMenamin, *Turnover of bone marrow-derived cells in the irradiated mouse cornea.* Immunology, 2008. **125**(4): p. 541-8.
61. Forrester, J.V., H. Xu, L. Kuffova, A.D. Dick and P.G. McMenamin, *Dendritic cell physiology and function in the eye.* Immunol Rev, 2010. **234**(1): p. 282-304.
62. Hajrasouliha, A.R., Z. Sadrai, H.K. Lee, S.K. Chauhan and R. Dana, *Expression of the chemokine decoy receptor D6 mediates dendritic cell function and promotes corneal allograft rejection.* Mol Vis, 2013. **19**: p. 2517-25.
63. Hamrah, P., Y. Liu, Q. Zhang and M.R. Dana, *The corneal stroma is endowed with a significant number of resident dendritic cells.* Invest Ophthalmol Vis Sci, 2003. **44**(2): p. 581-9.
64. Hattori, T., S.K. Chauhan, H. Lee, H. Ueno, R. Dana, D.H. Kaplan and D.R. Saban, *Characterization of Langerin-expressing dendritic cell subsets in the normal cornea.* Invest Ophthalmol Vis Sci, 2011. **52**(7): p. 4598-604.
65. Khan, A., H. Fu, L.A. Tan, J.E. Harper, S.C. Beutelspacher, D.F. Larkin, G. Lombardi, M.O. McClure and A.J. George, *Dendritic cell modification as a route to inhibiting corneal graft rejection by the indirect pathway of allorecognition.* Eur J Immunol, 2013. **43**(3): p. 734-46.
66. Knickelbein, J.E., R.L. Hendricks and P. Charukamnoetkanok, *Management of herpes simplex virus stromal keratitis: an evidence-based review.* Surv Ophthalmol, 2009. **54**(2): p. 226-34.
67. Knickelbein, J.E., S.C. Watkins, P.G. McMenamin and R.L. Hendricks, *Stratification of Antigen-presenting Cells within the Normal Cornea.* Ophthalmol Eye Dis, 2009. **1**: p. 45-54.
68. Lee, E.J., J.T. Rosenbaum and S.R. Planck, *Epifluorescence intravital microscopy of murine corneal dendritic cells.* Invest Ophthalmol Vis Sci, 2010. **51**(4): p. 2101-8.
69. Limatola, C. and R.M. Ransohoff, *Modulating neurotoxicity through CX3CL1/CX3CR1 signaling.* Front Cell Neurosci, 2014. **8**: p. 229.
70. Sosnova, M., M. Bradl and J.V. Forrester, *CD34+ corneal stromal cells are bone marrow-derived and express hemopoietic stem cell markers.* Stem Cells, 2005. **23**(4): p. 507-15.
71. Chinnery, H.R., E. Pearlman and P.G. McMenamin, *Cutting edge: Membrane nanotubes in vivo: a feature of MHC class II+ cells in the mouse cornea.* J Immunol, 2008. **180**(9): p. 5779-83.

72. Hamrah, P., Y. Liu, Q. Zhang and M.R. Dana, *Alterations in corneal stromal dendritic cell phenotype and distribution in inflammation.* Arch Ophthalmol, 2003. **121**(8): p. 1132-40.
73. Nakamura, T., F. Ishikawa, K.H. Sonoda, T. Hisatomi, H. Qiao, J. Yamada, M. Fukata, T. Ishibashi, M. Harada and S. Kinoshita, *Characterization and distribution of bone marrow-derived cells in mouse cornea.* Invest Ophthalmol Vis Sci, 2005. **46**(2): p. 497-503.
74. Dupps, W.J., Jr. and S.E. Wilson, *Biomechanics and wound healing in the cornea.* Exp Eye Res, 2006. **83**(4): p. 709-20.
75. Maurice, D.M. and A.A. Giardini, *Swelling of the cornea in vivo after the destruction of its limiting layers.* Br J Ophthalmol, 1951. **35**(12): p. 791-7.
76. Meek, K.M., D.W. Leonard, C.J. Connon, S. Dennis and S. Khan, *Transparency, swelling and scarring in the corneal stroma.* Eye (Lond), 2003. **17**(8): p. 927-36.
77. Chauhan, S.K., T.H. Dohlman and R. Dana, *Corneal Lymphatics: Role in Ocular Inflammation as Inducer and Responder of Adaptive Immunity.* J Clin Cell Immunol, 2014. **5**.
78. Emami-Naeini, P., T.H. Dohlman, M. Omoto, T. Hattori, Y. Chen, H.S. Lee, S.K. Chauhan and R. Dana, *Soluble vascular endothelial growth factor receptor-3 suppresses allosensitization and promotes corneal allograft survival.* Graefes Arch Clin Exp Ophthalmol, 2014. **252**(11): p. 1755-62.
79. Hajrasouliha, A.R., T. Funaki, Z. Sadrai, T. Hattori, S.K. Chauhan and R. Dana, *Vascular endothelial growth factor-C promotes alloimmunity by amplifying antigen-presenting cell maturation and lymphangiogenesis.* Invest Ophthalmol Vis Sci, 2012. **53**(3): p. 1244-50.
80. Dawson, D.W., O.V. Volpert, P. Gillis, S.E. Crawford, H. Xu, W. Benedict and N.P. Bouck, *Pigment epithelium-derived factor: a potent inhibitor of angiogenesis.* Science, 1999. **285**(5425): p. 245-8.
81. Gabison, E., J.H. Chang, E. Hernandez-Quintela, J. Javier, P.C. Lu, H. Ye, T. Kure, T. Kato and D.T. Azar, *Anti-angiogenic role of angiostatin during corneal wound healing.* Exp Eye Res, 2004. **78**(3): p. 579-89.
82. Griffith, T.S., T. Brunner, S.M. Fletcher, D.R. Green and T.A. Ferguson, *Fas ligand-induced apoptosis as a mechanism of immune privilege.* Science, 1995. **270**(5239): p. 1189-92.
83. Ghasemi, H., T. Ghazanfari, R. Yaraee, P. Owlia, Z.M. Hassan and S. Faghihzadeh, *Roles of IL-10 in ocular inflammations: a review.* Ocul Immunol Inflamm, 2012. **20**(6): p. 406-18.
84. Steinman, R.M., *Dendritic cells: understanding immunogenicity.* Eur J Immunol, 2007. **37 Suppl 1**: p. S53-60.

85. Bachmann, B.O., F. Bock, S.J. Wiegand, K. Maruyama, M.R. Dana, F.E. Kruse, E. Luetjen-Drecoll and C. Cursiefen, *Promotion of graft survival by vascular endothelial growth factor a neutralization after high-risk corneal transplantation.* Arch Ophthalmol, 2008. **126**(1): p. 71-7.
86. Chong, E.M. and M.R. Dana, *Graft failure IV. Immunologic mechanisms of corneal transplant rejection.* Int Ophthalmol, 2008. **28**(3): p. 209-22.
87. Dietrich, T., F. Bock, D. Yuen, D. Hos, B.O. Bachmann, G. Zahn, S. Wiegand, L. Chen and C. Cursiefen, *Cutting edge: lymphatic vessels, not blood vessels, primarily mediate immune rejections after transplantation.* J Immunol, 2010. **184**(2): p. 535-9.
88. Chauhan, S.K., J. El Annan, T. Ecoiffier, S. Goyal, Q. Zhang, D.R. Saban and R. Dana, *Autoimmunity in dry eye is due to resistance of Th17 to Treg suppression.* J Immunol, 2009. **182**(3): p. 1247-52.
89. Makinen, T., T. Veikkola, S. Mustjoki, T. Karpanen, B. Catimel, E.C. Nice, L. Wise, A. Mercer, H. Kowalski, D. Kerjaschki, S.A. Stacker, M.G. Achen and K. Alitalo, *Isolated lymphatic endothelial cells transduce growth, survival and migratory signals via the VEGF-C/D receptor VEGFR-3.* EMBO J, 2001. **20**(17): p. 4762-73.
90. Wigle, J.T., N. Harvey, M. Detmar, I. Lagutina, G. Grosveld, M.D. Gunn, D.G. Jackson and G. Oliver, *An essential role for Prox1 in the induction of the lymphatic endothelial cell phenotype.* EMBO J, 2002. **21**(7): p. 1505-13.
91. Conrady, C.D., M. Zheng, D.U. Stone and D.J. Carr, *CD8+ T cells suppress viral replication in the cornea but contribute to VEGF-C-induced lymphatic vessel genesis.* J Immunol, 2012. **189**(1): p. 425-32.
92. Zhu, S.N. and M.R. Dana, *Expression of cell adhesion molecules on limbal and neovascular endothelium in corneal inflammatory neovascularization.* Invest Ophthalmol Vis Sci, 1999. **40**(7): p. 1427-34.
93. Tan, K.W., S.Z. Chong, F.H. Wong, M. Evrard, S.M. Tan, J. Keeble, D.M. Kemeny, L.G. Ng, J.P. Abastado and V. Angeli, *Neutrophils contribute to inflammatory lymphangiogenesis by increasing VEGF-A bioavailability and secreting VEGF-D.* Blood, 2013. **122**(22): p. 3666-77.
94. Wuest, T.R. and D.J. Carr, *VEGF-A expression by HSV-1-infected cells drives corneal lymphangiogenesis.* J Exp Med, 2010. **207**(1): p. 101-15.
95. Stevenson, W., S.K. Chauhan and R. Dana, *Dry eye disease: an immune-mediated ocular surface disorder.* Arch Ophthalmol, 2012. **130**(1): p. 90-100.
96. Goyal, S., S.K. Chauhan, J. El Annan, N. Nallasamy, Q. Zhang and R. Dana, *Evidence of corneal lymphangiogenesis in dry eye disease: a potential link to adaptive immunity?* Arch Ophthalmol, 2010. **128**(7): p. 819-24.
97. Niederkorn, J.Y. and D.F. Larkin, *Immune privilege of corneal allografts.* Ocul Immunol Inflamm, 2010. **18**(3): p. 162-71.

98. Albuquerque, R.J., T. Hayashi, W.G. Cho, M.E. Kleinman, S. Dridi, A. Takeda, J.Z. Baffi, K. Yamada, H. Kaneko, M.G. Green, J. Chappell, J. Wilting, H.A. Weich, S. Yamagami, S. Amano, N. Mizuki, J.S. Alexander, M.L. Peterson, R.A. Brekken, M. Hirashima, S. Capoor, T. Usui, B.K. Ambati and J. Ambati, *Alternatively spliced vascular endothelial growth factor receptor-2 is an essential endogenous inhibitor of lymphatic vessel growth.* Nat Med, 2009. **15**(9): p. 1023-30.
99. Chauhan, S.K., D.R. Saban, H.K. Lee and R. Dana, *Levels of Foxp3 in regulatory T cells reflect their functional status in transplantation.* J Immunol, 2009. **182**(1): p. 148-53.
100. Hargrave, S.L., E. Mayhew, S. Hegde and J. Niederkorn, *Are corneal cells susceptible to antibody-mediated killing in corneal allograft rejection?* Transpl Immunol, 2003. **11**(1): p. 79-89.
101. Yamagami, S., H. Kawashima, T. Tsuru, H. Yamagami, N. Kayagaki, H. Yagita, K. Okumura and D.S. Gregerson, *Role of Fas-Fas ligand interactions in the immunorejection of allogeneic mouse corneal transplants.* Transplantation, 1997. **64**(8): p. 1107-11.
102. Shen, L., Y. Jin, G.J. Freeman, A.H. Sharpe and M.R. Dana, *The function of donor versus recipient programmed death-ligand 1 in corneal allograft survival.* J Immunol, 2007. **179**(6): p. 3672-9.
103. Apte, R.S., D. Sinha, E. Mayhew, G.J. Wistow and J.Y. Niederkorn, *Cutting edge: role of macrophage migration inhibitory factor in inhibiting NK cell activity and preserving immune privilege.* J Immunol, 1998. **160**(12): p. 5693-6.
104. Streilein, J.W., *Ocular immune privilege: therapeutic opportunities from an experiment of nature.* Nat Rev Immunol, 2003. **3**(11): p. 879-89.
105. Streilein, J.W. and J.Y. Niederkorn, *Induction of anterior chamber-associated immune deviation requires an intact, functional spleen. 1981.* Ocul Immunol Inflamm, 2007. **15**(3): p. 187-94.
106. Streilein, J.W., *New thoughts on the immunology of corneal transplantation.* Eye (Lond), 2003. **17**(8): p. 943-8.
107. Muller, L.J., E. Pels and G.F. Vrensen, *The specific architecture of the anterior stroma accounts for maintenance of corneal curvature.* Br J Ophthalmol, 2001. **85**(4): p. 437-43.
108. Radner, W. and R. Mallinger, *Interlacing of collagen lamellae in the midstroma of the human cornea.* Cornea, 2002. **21**(6): p. 598-601.
109. Muller, L.J., L. Pels and G.F. Vrensen, *Ultrastructural organization of human corneal nerves.* Invest Ophthalmol Vis Sci, 1996. **37**(4): p. 476-88.
110. Ruskell, G.L., *Ocular fibres of the maxillary nerve in monkeys.* J Anat, 1974. **118**(Pt 2): p. 195-203.

111. Beckers, H.J., J. Klooster, G.F. Vrensen and W.P. Lamers, *Ultrastructural identification of trigeminal nerve endings in the rat cornea and iris.* Invest Ophthalmol Vis Sci, 1992. **33**(6): p. 1979-86.
112. Beckers, H.J., J. Klooster, G.F. Vrensen and W.P. Lamers, *Substance P in rat corneal and iridal nerves: an ultrastructural immunohistochemical study.* Ophthalmic Res, 1993. **25**(3): p. 192-200.
113. Tervo, T. and A. Palkama, *Ultrastructure of the corneal nerves after fixation with potassium permanganate.* Anat Rec, 1978. **190**(4): p. 851-9.
114. Tervo, T. and A. Palkama, *Innervation of the rabbit cornea. A histochemical and electron-microscopic study.* Acta Anat (Basel), 1978. **102**(2): p. 164-75.
115. Oliveira-Soto, L. and N. Efron, *Morphology of corneal nerves using confocal microscopy.* Cornea, 2001. **20**(4): p. 374-84.
116. Vesaluoma, M., J. Perez-Santonja, W.M. Petroll, T. Linna, J. Alio and T. Tervo, *Corneal stromal changes induced by myopic LASIK.* Invest Ophthalmol Vis Sci, 2000. **41**(2): p. 369-76.
117. Jones, M.A. and C.F. Marfurt, *Calcitonin gene-related peptide and corneal innervation: a developmental study in the rat.* J Comp Neurol, 1991. **313**(1): p. 132-50.
118. Jones, M.A. and C.F. Marfurt, *Peptidergic innervation of the rat cornea.* Exp Eye Res, 1998. **66**(4): p. 421-35.
119. Rozsa, A.J. and R.W. Beuerman, *Density and organization of free nerve endings in the corneal epithelium of the rabbit.* Pain, 1982. **14**(2): p. 105-20.
120. Schimmelpfennig, B. and R. Beuerman, *A technique for controlled sensory denervation of the rabbit cornea.* Graefes Arch Clin Exp Ophthalmol, 1982. **218**(6): p. 287-93.
121. Ueda, S., M. del Cerro, J.A. LoCascio and J.V. Aquavella, *Peptidergic and catecholaminergic fibers in the human corneal epithelium. An immunohistochemical and electron microscopic study.* Acta Ophthalmol Suppl, 1989. **192**: p. 80-90.
122. Zander, E. and G. Weddell, *Observations on the innervation of the cornea.* J Anat, 1951. **85**(1): p. 68-99.
123. Lim, C.H. and G.L. Ruskell, *Corneal nerve access in monkeys.* Albrecht Von Graefes Arch Klin Exp Ophthalmol, 1978. **208**(1-3): p. 15-23.
124. Matsuda, H., *[Electron microscopic study of the corneal nerve with special reference to the nerve endings].* Nihon Ganka Gakkai Zasshi, 1968. **72**(7): p. 880-93.
125. Ivanusic, J.J., R.J. Wood and J.A. Brock, *Sensory and sympathetic innervation of the mouse and guinea pig corneal epithelium.* J Comp Neurol, 2013. **521**(4): p. 877-93.

126. Kubilus, J.K. and T.F. Linsenmayer, *Developmental guidance of embryonic corneal innervation: roles of Semaphorin3A and Slit2.* Dev Biol, 2010. **344**(1): p. 172-84.
127. Kubilus, J.K. and T.F. Linsenmayer, *Developmental corneal innervation: interactions between nerves and specialized apical corneal epithelial cells.* Invest Ophthalmol Vis Sci, 2010. **51**(2): p. 782-9.
128. Madrid, R., T. Donovan-Rodriguez, V. Meseguer, M.C. Acosta, C. Belmonte and F. Viana, *Contribution of TRPM8 channels to cold transduction in primary sensory neurons and peripheral nerve terminals.* J Neurosci, 2006. **26**(48): p. 12512-25.
129. Marfurt, C.F. and L.C. Ellis, *Immunohistochemical localization of tyrosine hydroxylase in corneal nerves.* J Comp Neurol, 1993. **336**(4): p. 517-31.
130. Parra, A., R. Madrid, D. Echevarria, S. del Olmo, C. Morenilla-Palao, M.C. Acosta, J. Gallar, A. Dhaka, F. Viana and C. Belmonte, *Ocular surface wetness is regulated by TRPM8-dependent cold thermoreceptors of the cornea.* Nat Med, 2010. **16**(12): p. 1396-9.
131. Auran, J.D., C.J. Koester, N.J. Kleiman, R. Rapaport, J.S. Bomann, B.M. Wirotsko, G.J. Florakis and J.P. Koniarek, *Scanning slit confocal microscopic observation of cell morphology and movement within the normal human anterior cornea.* Ophthalmology, 1995. **102**(1): p. 33-41.
132. Linna, T.U., M.H. Vesaluoma, W.M. Petroll, A.H. Tarkkanen and T.M. Tervo, *Confocal microscopy of a patient with irregular astigmatism after LASIK reoperations and relaxation incisions.* Cornea, 2000. **19**(2): p. 163-9.
133. Rosenberg, M.E., T.M. Tervo, W.M. Petroll and M.H. Vesaluoma, *In vivo confocal microscopy of patients with corneal recurrent erosion syndrome or epithelial basement membrane dystrophy.* Ophthalmology, 2000. **107**(3): p. 565-73.
134. Vesaluoma, M., L. Muller, J. Gallar, A. Lambiase, J. Moilanen, T. Hack, C. Belmonte and T. Tervo, *Effects of oleoresin capsicum pepper spray on human corneal morphology and sensitivity.* Invest Ophthalmol Vis Sci, 2000. **41**(8): p. 2138-47.
135. Vesaluoma, M.H., W.M. Petroll, J.J. Perez-Santonja, T.U. Valle, J.L. Alio and T.M. Tervo, *Laser in situ keratomileusis flap margin: wound healing and complications imaged by in vivo confocal microscopy.* Am J Ophthalmol, 2000. **130**(5): p. 564-73.
136. Kenchegowda, S., J. He and H.E. Bazan, *Involvement of pigment epithelium-derived factor, docosahexaenoic acid and neuroprotectin D1 in corneal inflammation and nerve integrity after refractive surgery.* Prostaglandins Leukot Essent Fatty Acids, 2013. **88**(1): p. 27-31.

137. Wilson, S.E., R.R. Mohan, R.R. Mohan, R. Ambrosio, Jr., J. Hong and J. Lee, *The corneal wound healing response: cytokine-mediated interaction of the epithelium, stroma, and inflammatory cells.* Prog Retin Eye Res, 2001. **20**(5): p. 625-37.
138. Wilson, S.E., Y.G. He, J. Weng, Q. Li, A.W. McDowall, M. Vital and E.L. Chwang, *Epithelial injury induces keratocyte apoptosis: hypothesized role for the interleukin-1 system in the modulation of corneal tissue organization and wound healing.* Exp Eye Res, 1996. **62**(4): p. 325-7.
139. Saban, D.R., V. Calder, C.H. Kuo, N.J. Reyes, D.A. Dartt, S.J. Ono and J.Y. Niederkorn, *New twists to an old story: novel concepts in the pathogenesis of allergic eye disease.* Curr Eye Res, 2013. **38**(3): p. 317-30.
140. Pearlman, E., Y. Sun, S. Roy, M. Karmakar, A.G. Hise, L. Szczotka-Flynn, M. Ghannoum, H.R. Chinnery, P.G. McMenamin and A. Rietsch, *Host defense at the ocular surface.* Int Rev Immunol, 2013. **32**(1): p. 4-18.
141. Kumagai, N., K. Fukuda, Y. Ishimura and T. Nishida, *Synergistic induction of eotaxin expression in human keratocytes by TNF-alpha and IL-4 or IL-13.* Invest Ophthalmol Vis Sci, 2000. **41**(6): p. 1448-53.
142. Fukuda, K. and T. Nishida, *Reciprocal interaction of the conjunctiva and cornea in ocular allergy.* J Allergy Clin Immunol, 2010. **125**(2): p. 493-496 e2.
143. Fukuda, K., W. Ishida, H. Tanaka, Y. Harada, A. Matsuda, N. Ebihara and A. Fukushima, *Alarmins from corneal epithelial cells upregulate CCL11 and VCAM-1 in corneal fibroblasts.* Invest Ophthalmol Vis Sci, 2013. **54**(8): p. 5817-23.
144. Yang, D., Y.V. Postnikov, Y. Li, P. Tewary, G. de la Rosa, F. Wei, D. Klinman, T. Gioannini, J.P. Weiss, T. Furusawa, M. Bustin and J.J. Oppenheim, *High-mobility group nucleosome-binding protein 1 acts as an alarmin and is critical for lipopolysaccharide-induced immune responses.* J Exp Med, 2012. **209**(1): p. 157-71.
145. Fukuda, K., N. Kumagai, Y. Fujitsu and T. Nishida, *Fibroblasts as local immune modulators in ocular allergic disease.* Allergol Int, 2006. **55**(2): p. 121-9.
146. Kumagai, N., K. Fukuda, Y. Fujitsu, K. Yamamoto and T. Nishida, *Role of structural cells of the cornea and conjunctiva in the pathogenesis of vernal keratoconjunctivitis.* Prog Retin Eye Res, 2006. **25**(2): p. 165-87.
147. Fukuda, K., T. Nishida and A. Fukushima, *Synergistic induction of eotaxin and VCAM-1 expression in human corneal fibroblasts by staphylococcal peptidoglycan and either IL-4 or IL-13.* Allergol Int, 2011. **60**(3): p. 355-63.
148. Calonge, M., *Classification of ocular atopic/allergic disorders and conditions: an unsolved problem.* Acta Ophthalmol Scand Suppl, 1999(228): p. 10-3.
149. Pflugfelder, S.C., *Anti-inflammatory therapy of dry eye.* Ocul Surf, 2003. **1**(1): p. 31-6.

150. Enriquez-de-Salamanca, A. and M. Calonge, *Cytokines and chemokines in immune-based ocular surface inflammation.* Expert Rev Clin Immunol, 2008. **4**(4): p. 457-67.
151. Ohbayashi, M., B. Manzouri, T. Flynn, M. Toda, Y. Ikeda, T. Nakamura and S.J. Ono, *Dynamic changes in conjunctival dendritic cell numbers, anatomical position and phenotype during experimental allergic conjunctivitis.* Exp Mol Pathol, 2007. **83**(2): p. 216-23.
152. Schlereth, S., H.S. Lee, P. Khandelwal and D.R. Saban, *Blocking CCR7 at the ocular surface impairs the pathogenic contribution of dendritic cells in allergic conjunctivitis.* Am J Pathol, 2012. **180**(6): p. 2351-60.
153. Saban, D.R., F. Bock, S.K. Chauhan, S. Masli and R. Dana, *Thrombospondin-1 derived from APCs regulates their capacity for allosensitization.* J Immunol, 2010. **185**(8): p. 4691-7.
154. Wilson, S.E., Q. Li, J. Weng, P.A. Barry-Lane, J.V. Jester, Q. Liang and R.J. Wordinger, *The Fas-Fas ligand system and other modulators of apoptosis in the cornea.* Invest Ophthalmol Vis Sci, 1996. **37**(8): p. 1582-92.
155. Mo, J.S., A. Matsukawa, S. Ohkawara and M. Yoshinaga, *Role and regulation of IL-8 and MCP-1 in LPS-induced uveitis in rabbits.* Exp Eye Res, 1999. **68**(3): p. 333-40.
156. Moss, S.E., R. Klein and B.E. Klein, *Prevalence of and risk factors for dry eye syndrome.* Arch Ophthalmol, 2000. **118**(9): p. 1264-8.
157. *The definition and classification of dry eye disease: report of the Definition and Classification Subcommittee of the International Dry Eye WorkShop (2007).* Ocul Surf, 2007. **5**(2): p. 75-92.
158. Kunert, K.S., A.S. Tisdale, M.E. Stern, J.A. Smith and I.K. Gipson, *Analysis of topical cyclosporine treatment of patients with dry eye syndrome: effect on conjunctival lymphocytes.* Arch Ophthalmol, 2000. **118**(11): p. 1489-96.
159. Stern, M.E., J. Gao, T.A. Schwalb, M. Ngo, D.D. Tieu, C.C. Chan, B.L. Reis, S.M. Whitcup, D. Thompson and J.A. Smith, *Conjunctival T-cell subpopulations in Sjogren's and non-Sjogren's patients with dry eye.* Invest Ophthalmol Vis Sci, 2002. **43**(8): p. 2609-14.
160. Cejkova, J., T. Ardan, Z. Simonova, C. Cejka, J. Malec, K. Jirsova, M. Filipec, D. Dotrelova and B. Brunova, *Nitric oxide synthase induction and cytotoxic nitrogen-related oxidant formation in conjunctival epithelium of dry eye (Sjogren's syndrome).* Nitric Oxide, 2007. **17**(1): p. 10-7.
161. Paul, A., S. Wilson, C.M. Belham, C.J. Robinson, P.H. Scott, G.W. Gould and R. Plevin, *Stress-activated protein kinases: activation, regulation and function.* Cell Signal, 1997. **9**(6): p. 403-10.

162. Pflugfelder, S.C., C.S. de Paiva, L. Tong, L. Luo, M.E. Stern and D.Q. Li, *Stress-activated protein kinase signaling pathways in dry eye and ocular surface disease.* Ocul Surf, 2005. **3**(4 Suppl): p. S154-7.
163. Luo, L., D.Q. Li, A. Doshi, W. Farley, R.M. Corrales and S.C. Pflugfelder, *Experimental dry eye stimulates production of inflammatory cytokines and MMP-9 and activates MAPK signaling pathways on the ocular surface.* Invest Ophthalmol Vis Sci, 2004. **45**(12): p. 4293-301.
164. Chauhan, S.K. and R. Dana, *Role of Th17 cells in the immunopathogenesis of dry eye disease.* Mucosal Immunol, 2009. **2**(4): p. 375-6.
165. Leiper, L.J., J. Ou, P. Walczysko, R. Kucerova, D.N. Lavery, J.D. West and J.M. Collinson, *Control of patterns of corneal innervation by Pax6.* Invest Ophthalmol Vis Sci, 2009. **50**(3): p. 1122-8.
166. Bonini, S., P. Rama, D. Olzi and A. Lambiase, *Neurotrophic keratitis.* Eye (Lond), 2003. **17**(8): p. 989-95.
167. Li, H., W. Xie, J.A. Strong and J.M. Zhang, *Systemic antiinflammatory corticosteroid reduces mechanical pain behavior, sympathetic sprouting, and elevation of proinflammatory cytokines in a rat model of neuropathic pain.* Anesthesiology, 2007. **107**(3): p. 469-77.
168. Cosar, C.B., E.J. Cohen, C.J. Rapuano, M. Maus, R.P. Penne, J.C. Flanagan and P.R. Laibson, *Tarsorrhaphy: clinical experience from a cornea practice.* Cornea, 2001. **20**(8): p. 787-91.
169. Belmonte, C., A. Aracil, M.C. Acosta, C. Luna and J. Gallar, *Nerves and sensations from the eye surface.* Ocul Surf, 2004. **2**(4): p. 248-53.
170. Ueno, H., G. Ferrari, T. Hattori, D.R. Saban, K.R. Katikireddy, S.K. Chauhan and R. Dana, *Dependence of corneal stem/progenitor cells on ocular surface innervation.* Invest Ophthalmol Vis Sci, 2012. **53**(2): p. 867-72.
171. Nakamura, M., T. Nishida, K. Ofuji, T.W. Reid, M.J. Mannis and C.J. Murphy, *Synergistic effect of substance P with epidermal growth factor on epithelial migration in rabbit cornea.* Exp Eye Res, 1997. **65**(3): p. 321-9.
172. Paunicka, K.J., J. Mellon, D. Robertson, M. Petroll, J.R. Brown and J.Y. Niederkorn, *Severing corneal nerves in one eye induces sympathetic loss of immune privilege and promotes rejection of future corneal allografts placed in either eye.* Am J Transplant, 2015. **15**(6): p. 1490-501.
173. Blanco, T. and D.R. Saban, *The Cornea Has "the Nerve" to Encourage Immune Rejection.* Am J Transplant, 2015. **15**(6): p. 1453-4.
174. Nguyen, D.T., O. D.P. and M. G.F., *The Pathophysiologic Basis for Wound Healing and Cutaneous Regeneration.* Biomaterials For Treating Skin Loss, 2009. **Chapter 4**: p. 25-57.
175. Wilson, S.E., R.R. Mohan, J.W. Hong, J.S. Lee, R. Choi and R.R. Mohan, *The wound healing response after laser in situ keratomileusis and photorefractive*

keratectomy: elusive control of biological variability and effect on custom laser vision correction. Arch Ophthalmol, 2001. **119**(6): p. 889-96.
176. Wilson, S.E., R.R. Mohan, A.E. Hutcheon, R.R. Mohan, R. Ambrosio, J.D. Zieske, J. Hong and J. Lee, *Effect of ectopic epithelial tissue within the stroma on keratocyte apoptosis, mitosis, and myofibroblast transformation.* Exp Eye Res, 2003. **76**(2): p. 193-201.
177. Power, W.J., A.H. Kaufman, J. Merayo-Lloves, V. Arrunategui-Correa and C.S. Foster, *Expression of collagens I, III, IV and V mRNA in excimer wounded rat cornea: analysis by semi-quantitative PCR.* Curr Eye Res, 1995. **14**(10): p. 879-86.
178. Blanco-Mezquita, T., L. Espandar, R. Torres, A. Alvarez-Barcia, R. Cantalapiedra-Rodriguez, C. Martinez-Garcia and J. Merayo-Lloves, *Does mitomycin C cause toxicity in the cornea after photorefractive keratectomy? A comparative wound-healing study in a refractive surgery animal model.* Cornea, 2014. **33**(11): p. 1225-31.
179. Blanco-Mezquita, T., C. Martinez-Garcia, R. Proenca, J.D. Zieske, S. Bonini, A. Lambiase and J. Merayo-Lloves, *Nerve growth factor promotes corneal epithelial migration by enhancing expression of matrix metalloprotease-9.* Invest Ophthalmol Vis Sci, 2013. **54**(6): p. 3880-90.
180. Martinez-Garcia, M.C., J. Merayo-Lloves, T. Blanco-Mezquita and S. Mar-Sardana, *Wound healing following refractive surgery in hens.* Exp Eye Res, 2006. **83**(4): p. 728-35.
181. Del Pero, R.A., J.E. Gigstad, A.D. Roberts, G.K. Klintworth, C.A. Martin, F.A. L'Esperance, Jr. and D.M. Taylor, *A refractive and histopathologic study of excimer laser keratectomy in primates.* Am J Ophthalmol, 1990. **109**(4): p. 419-29.
182. Coassin, M., A. Lambiase, N. Costa, A. De Gregorio, R. Sgrulletta, M. Sacchetti, L. Aloe and S. Bonini, *Efficacy of topical nerve growth factor treatment in dogs affected by dry eye.* Graefes Arch Clin Exp Ophthalmol, 2005. **243**(2): p. 151-5.
183. Woo, H.M., E. Bentley, S.F. Campbell, C.F. Marfurt and C.J. Murphy, *Nerve growth factor and corneal wound healing in dogs.* Exp Eye Res, 2005. **80**(5): p. 633-42.
184. Mohan, R.R., W.M. Stapleton, S. Sinha, M.V. Netto and S.E. Wilson, *A novel method for generating corneal haze in anterior stroma of the mouse eye with the excimer laser.* Exp Eye Res, 2008. **86**(2): p. 235-40.
185. Stapleton, W.M., S.S. Chaurasia, F.W. Medeiros, R.R. Mohan, S. Sinha and S.E. Wilson, *Topical interleukin-1 receptor antagonist inhibits inflammatory cell infiltration into the cornea.* Exp Eye Res, 2008. **86**(5): p. 753-7.

186. Gibson, D.J., L. Pi, S. Sriram, C. Mao, B.E. Petersen, E.W. Scott, A. Leask and G.S. Schultz, *Conditional knockout of CTGF affects corneal wound healing.* Invest Ophthalmol Vis Sci, 2014. **55**(4): p. 2062-70.
187. Ksander, B.R., P.E. Kolovou, B.J. Wilson, K.R. Saab, Q. Guo, J. Ma, S.P. McGuire, M.S. Gregory, W.J. Vincent, V.L. Perez, F. Cruz-Guilloty, W.W. Kao, M.K. Call, B.A. Tucker, Q. Zhan, G.F. Murphy, K.L. Lathrop, C. Alt, L.J. Mortensen, C.P. Lin, J.D. Zieske, M.H. Frank and N.Y. Frank, *ABCB5 is a limbal stem cell gene required for corneal development and repair.* Nature, 2014. **511**(7509): p. 353-7.
188. Okada, Y., K. Shirai, P.S. Reinach, A. Kitano-Izutani, M. Miyajima, K.C. Flanders, J.V. Jester, M. Tominaga and S. Saika, *TRPA1 is required for TGF-beta signaling and its loss blocks inflammatory fibrosis in mouse corneal stroma.* Lab Invest, 2014. **94**(9): p. 1030-41.
189. Pajoohesh-Ganji, A., S. Pal-Ghosh, S.J. Simmens and M.A. Stepp, *Integrins in slow-cycling corneal epithelial cells at the limbus in the mouse.* Stem Cells, 2006. **24**(4): p. 1075-86.
190. Stepp, M.A., *Corneal integrins and their functions.* Exp Eye Res, 2006. **83**(1): p. 3-15.
191. Clark, E.A. and J.S. Brugge, *Integrins and signal transduction pathways: the road taken.* Science, 1995. **268**(5208): p. 233-9.
192. Hynes, R.O., *Integrins: a family of cell surface receptors.* Cell, 1987. **48**(4): p. 549-54.
193. Ruoslahti, E. and M.D. Pierschbacher, *New perspectives in cell adhesion: RGD and integrins.* Science, 1987. **238**(4826): p. 491-7.
194. Breuss, J.M., J. Gallo, H.M. DeLisser, I.V. Klimanskaya, H.G. Folkesson, J.F. Pittet, S.L. Nishimura, K. Aldape, D.V. Landers, W. Carpenter and et al., *Expression of the beta 6 integrin subunit in development, neoplasia and tissue repair suggests a role in epithelial remodeling.* J Cell Sci, 1995. **108 (Pt 6)**: p. 2241-51.
195. Breuss, J.M., N. Gillett, L. Lu, D. Sheppard and R. Pytela, *Restricted distribution of integrin beta 6 mRNA in primate epithelial tissues.* J Histochem Cytochem, 1993. **41**(10): p. 1521-7.
196. Ghannad, F., D. Nica, M.I. Fulle, D. Grenier, E.E. Putnins, S. Johnston, A. Eslami, L. Koivisto, G. Jiang, M.D. McKee, L. Hakkinen and H. Larjava, *Absence of alphavbeta6 integrin is linked to initiation and progression of periodontal disease.* Am J Pathol, 2008. **172**(5): p. 1271-86.
197. Huang, X.Z., J.F. Wu, D. Cass, D.J. Erle, D. Corry, S.G. Young, R.V. Farese, Jr. and D. Sheppard, *Inactivation of the integrin beta 6 subunit gene reveals a role of epithelial integrins in regulating inflammation in the lung and skin.* J Cell Biol, 1996. **133**(4): p. 921-8.

198. AlDahlawi, S., A. Eslami, L. Hakkinen and H.S. Larjava, *The alphavbeta6 integrin plays a role in compromised epidermal wound healing.* Wound Repair Regen, 2006. **14**(3): p. 289-97.
199. Munger, J.S., X. Huang, H. Kawakatsu, M.J. Griffiths, S.L. Dalton, J. Wu, J.F. Pittet, N. Kaminski, C. Garat, M.A. Matthay, D.B. Rifkin and D. Sheppard, *The integrin alpha v beta 6 binds and activates latent TGF beta 1: a mechanism for regulating pulmonary inflammation and fibrosis.* Cell, 1999. **96**(3): p. 319-28.
200. Ljubimov, A.V., M. Saghizadeh, R. Pytela, D. Sheppard and M.C. Kenney, *Increased expression of tenascin-C-binding epithelial integrins in human bullous keratopathy corneas.* J Histochem Cytochem, 2001. **49**(11): p. 1341-50.
201. Hutcheon, A.E., X.Q. Guo, M.A. Stepp, K.J. Simon, P.H. Weinreb, S.M. Violette and J.D. Zieske, *Effect of wound type on Smad 2 and 4 translocation.* Invest Ophthalmol Vis Sci, 2005. **46**(7): p. 2362-8.
202. Stepp, M.A. and L. Zhu, *Upregulation of alpha 9 integrin and tenascin during epithelial regeneration after debridement in the cornea.* J Histochem Cytochem, 1997. **45**(2): p. 189-201.
203. Prieto, A.L., G.M. Edelman and K.L. Crossin, *Multiple integrins mediate cell attachment to cytotactin/tenascin.* Proc Natl Acad Sci U S A, 1993. **90**(21): p. 10154-8.
204. Annes, J.P., D.B. Rifkin and J.S. Munger, *The integrin alphaVbeta6 binds and activates latent TGFbeta3.* FEBS Lett, 2002. **511**(1-3): p. 65-8.
205. Munger, J.S., J.G. Harpel, F.G. Giancotti and D.B. Rifkin, *Interactions between growth factors and integrins: latent forms of transforming growth factor-beta are ligands for the integrin alphavbeta1.* Mol Biol Cell, 1998. **9**(9): p. 2627-38.
206. Aluwihare, P. and J.S. Munger, *What the lung has taught us about latent TGF-beta activation.* Am J Respir Cell Mol Biol, 2008. **39**(5): p. 499-502.
207. Sheppard, D., *Integrin-mediated activation of latent transforming growth factor beta.* Cancer Metastasis Rev, 2005. **24**(3): p. 395-402.
208. Shi, M., J. Zhu, R. Wang, X. Chen, L. Mi, T. Walz and T.A. Springer, *Latent TGF-beta structure and activation.* Nature, 2011. **474**(7351): p. 343-9.
209. Wipff, P.J. and B. Hinz, *Integrins and the activation of latent transforming growth factor beta1 - an intimate relationship.* Eur J Cell Biol, 2008. **87**(8-9): p. 601-15.
210. Aluwihare, P., Z. Mu, Z. Zhao, D. Yu, P.H. Weinreb, G.S. Horan, S.M. Violette and J.S. Munger, *Mice that lack activity of alphavbeta6- and alphavbeta8-integrins reproduce the abnormalities of Tgfb1- and Tgfb3-null mice.* J Cell Sci, 2009. **122**(Pt 2): p. 227-32.

211. Blanco-Mezquita, J.T., A.E. Hutcheon, M.A. Stepp and J.D. Zieske, *alphaVbeta6 integrin promotes corneal wound healing.* Invest Ophthalmol Vis Sci, 2011. **52**(11): p. 8505-13.
212. Matsuba, M., A.E. Hutcheon and J.D. Zieske, *Localization of thrombospondin-1 and myofibroblasts during corneal wound repair.* Exp Eye Res, 2011. **93**(4): p. 534-40.
213. Bornstein, P., *Thrombospondins as matricellular modulators of cell function.* J Clin Invest, 2001. **107**(8): p. 929-34.
214. Carlson, C.B., J. Lawler and D.F. Mosher, *Structures of thrombospondins.* Cell Mol Life Sci, 2008. **65**(5): p. 672-86.
215. Baenziger, N.L., G.N. Brodie and P.W. Majerus, *A thrombin-sensitive protein of human platelet membranes.* Proc Natl Acad Sci U S A, 1971. **68**(1): p. 240-3.
216. Lawler, J., *The functions of thrombospondin-1 and-2.* Curr Opin Cell Biol, 2000. **12**(5): p. 634-40.
217. Leung, L.L., *Role of thrombospondin in platelet aggregation.* J Clin Invest, 1984. **74**(5): p. 1764-72.
218. Murphy-Ullrich, J.E., S. Gurusiddappa, W.A. Frazier and M. Hook, *Heparin-binding peptides from thrombospondins 1 and 2 contain focal adhesion-labilizing activity.* J Biol Chem, 1993. **268**(35): p. 26784-9.
219. Sheibani, N. and W.A. Frazier, *Thrombospondin-1, PECAM-1, and regulation of angiogenesis.* Histol Histopathol, 1999. **14**(1): p. 285-94.
220. Taraboletti, G., D.D. Roberts and L.A. Liotta, *Thrombospondin-induced tumor cell migration: haptotaxis and chemotaxis are mediated by different molecular domains.* J Cell Biol, 1987. **105**(5): p. 2409-15.
221. Darby, I., O. Skalli and G. Gabbiani, *Alpha-smooth muscle actin is transiently expressed by myofibroblasts during experimental wound healing.* Lab Invest, 1990. **63**(1): p. 21-9.
222. Desmouliere, A., A. Geinoz, F. Gabbiani and G. Gabbiani, *Transforming growth factor-beta 1 induces alpha-smooth muscle actin expression in granulation tissue myofibroblasts and in quiescent and growing cultured fibroblasts.* J Cell Biol, 1993. **122**(1): p. 103-11.
223. Friedman, S.L., *Seminars in medicine of the Beth Israel Hospital, Boston. The cellular basis of hepatic fibrosis. Mechanisms and treatment strategies.* N Engl J Med, 1993. **328**(25): p. 1828-35.
224. Murphy-Ullrich, J.E., S. Schultz-Cherry and M. Hook, *Transforming growth factor-beta complexes with thrombospondin.* Mol Biol Cell, 1992. **3**(2): p. 181-8.
225. Agah, A., T.R. Kyriakides, J. Lawler and P. Bornstein, *The lack of thrombospondin-1 (TSP1) dictates the course of wound healing in double-TSP1/TSP2-null mice.* Am J Pathol, 2002. **161**(3): p. 831-9.

226. Streit, M., P. Velasco, L. Riccardi, L. Spencer, L.F. Brown, L. Janes, B. Lange-Asschenfeldt, K. Yano, T. Hawighorst, L. Iruela-Arispe and M. Detmar, *Thrombospondin-1 suppresses wound healing and granulation tissue formation in the skin of transgenic mice.* EMBO J, 2000. **19**(13): p. 3272-82.
227. Hiscott, P., B. Seitz, U. Schlotzer-Schrehardt and G.O. Naumann, *Immunolocalisation of thrombospondin 1 in human, bovine and rabbit cornea.* Cell Tissue Res, 1997. **289**(2): p. 307-10.
228. Sekiyama, E., T. Nakamura, L.J. Cooper, S. Kawasaki, J. Hamuro, N.J. Fullwood and S. Kinoshita, *Unique distribution of thrombospondin-1 in human ocular surface epithelium.* Invest Ophthalmol Vis Sci, 2006. **47**(4): p. 1352-8.
229. Cao, Z., H.K. Wu, A. Bruce, K. Wollenberg and N. Panjwani, *Detection of differentially expressed genes in healing mouse corneas, using cDNA microarrays.* Invest Ophthalmol Vis Sci, 2002. **43**(9): p. 2897-904.
230. Hiscott, P., D. Armstrong, M. Batterbury and S. Kaye, *Repair in avascular tissues: fibrosis in the transparent structures of the eye and thrombospondin 1.* Histol Histopathol, 1999. **14**(4): p. 1309-20.
231. Uno, K., H. Hayashi, M. Kuroki, H. Uchida, Y. Yamauchi, M. Kuroki and K. Oshima, *Thrombospondin-1 accelerates wound healing of corneal epithelia.* Biochem Biophys Res Commun, 2004. **315**(4): p. 928-34.
232. Uno, K., M. Kuroki, H. Hayashi, H. Uchida, M. Kuroki and K. Oshima, *Impairment of thrombospondin-1 expression during epithelial wound healing in corneas of vitamin A-deficient mice.* Histol Histopathol, 2005. **20**(2): p. 493-9.
233. Bornstein, P., *Thrombospondins function as regulators of angiogenesis.* J Cell Commun Signal, 2009. **3**(3-4): p. 189-200.
234. Young, G.D. and J.E. Murphy-Ullrich, *Molecular interactions that confer latency to transforming growth factor-beta.* J Biol Chem, 2004. **279**(36): p. 38032-9.
235. Jester, J.V., P.A. Barry-Lane, W.M. Petroll, D.R. Olsen and H.D. Cavanagh, *Inhibition of corneal fibrosis by topical application of blocking antibodies to TGF beta in the rabbit.* Cornea, 1997. **16**(2): p. 177-87.
236. Jester, J.V., W.M. Petroll and H.D. Cavanagh, *Corneal stromal wound healing in refractive surgery: the role of myofibroblasts.* Prog Retin Eye Res, 1999. **18**(3): p. 311-56.
237. Moller-Pedersen, T., H.D. Cavanagh, W.M. Petroll and J.V. Jester, *Corneal haze development after PRK is regulated by volume of stromal tissue removal.* Cornea, 1998. **17**(6): p. 627-39.
238. Barcellos-Hoff, M.H., *Latency and activation in the control of TGF-beta.* J Mammary Gland Biol Neoplasia, 1996. **1**(4): p. 353-63.

239. Scheef, E.A., Q. Huang, S. Wang, C.M. Sorenson and N. Sheibani, *Isolation and characterization of corneal endothelial cells from wild type and thrombospondin-1 deficient mice.* Mol Vis, 2007. **13**: p. 1483-95.
240. Blanco-Mezquita, J.T., A.E. Hutcheon and J.D. Zieske, *Role of thrombospondin-1 in repair of penetrating corneal wounds.* Invest Ophthalmol Vis Sci, 2013. **54**(9): p. 6262-8.
241. Nowotschin, S., P. Xenopoulos, N. Schrode and A.K. Hadjantonakis, *A bright single-cell resolution live imaging reporter of Notch signaling in the mouse.* BMC Dev Biol, 2013. **13**: p. 15.
242. Lee, H.-S., D. Hos, T. Blanco, F. Bock, N.J. Reyes, R. Mathew, C. Cursiefen, R. Dana and D.R. Saban, *Involvement of corneal lymphangiogenesis in a mouse model of allergic eye disease.* IOVS, 2015.
243. Chinnery, H.R., M.J. Ruitenberg, G.W. Plant, E. Pearlman, S. Jung and P.G. McMenamin, *The chemokine receptor CX3CR1 mediates homing of MHC class II-positive cells to the normal mouse corneal epithelium.* Invest Ophthalmol Vis Sci, 2007. **48**(4): p. 1568-74.
244. Kezic, J., H. Xu, H.R. Chinnery, C.C. Murphy and P.G. McMenamin, *Retinal microglia and uveal tract dendritic cells and macrophages are not CX3CR1 dependent in their recruitment and distribution in the young mouse eye.* Invest Ophthalmol Vis Sci, 2008. **49**(4): p. 1599-608.
245. Soos, T.J., T.N. Sims, L. Barisoni, K. Lin, D.R. Littman, M.L. Dustin and P.J. Nelson, *CX3CR1+ interstitial dendritic cells form a contiguous network throughout the entire kidney.* Kidney Int, 2006. **70**(3): p. 591-6.
246. Chen, W., K. Hara, Q. Tian, K. Zhao and T. Yoshitomi, *Existence of small slow-cycling Langerhans cells in the limbal basal epithelium that express ABCG2.* Exp Eye Res, 2007. **84**(4): p. 626-34.
247. Liu, Y., P. Hamrah, Q. Zhang, A.W. Taylor and M.R. Dana, *Draining lymph nodes of corneal transplant hosts exhibit evidence for donor major histocompatibility complex (MHC) class II-positive dendritic cells derived from MHC class II-negative grafts.* J Exp Med, 2002. **195**(2): p. 259-68.
248. Niederkorn, J.Y., J.S. Peeler and J. Mellon, *Phagocytosis of particulate antigens by corneal epithelial cells stimulates interleukin-1 secretion and migration of Langerhans cells into the central cornea.* Reg Immunol, 1989. **2**(2): p. 83-90.
249. Steven, P., F. Bock, G. Huttmann and C. Cursiefen, *Intravital two-photon microscopy of immune cell dynamics in corneal lymphatic vessels.* PLoS One, 2011. **6**(10): p. e26253.
250. Sauer, B., *Functional expression of the cre-lox site-specific recombination system in the yeast Saccharomyces cerevisiae.* Mol Cell Biol, 1987. **7**(6): p. 2087-96.

251. Miller, R.L., *Transgenic mice: beyond the knockout.* Am J Physiol Renal Physiol, 2011. **300**(2): p. F291-300.
252. M., G.-M., *Über Elementarakte mit zwei Quantensprüngen.* Annals of Physics 1931. **9**(3): p. 273–95.
253. Abella, I.D., *Optical Double-Photon Absorption in Cesium Vapor.* Physical Review Letters 1962. **9**(11): p. 453–455.
254. Kaminer, I., J. Nemirovsky and M. Segev, *Optimizing 3D multiphoton fluorescence microscopy.* Opt Lett, 2013. **38**(19): p. 3945-8.
255. Tang, S., Y. Zhou, K.K. Chan and T. Lai, *Multiscale multimodal imaging with multiphoton microscopy and optical coherence tomography.* Opt Lett, 2011. **36**(24): p. 4800-2.
256. Cahalan, M.D., I. Parker, S.H. Wei and M.J. Miller, *Two-photon tissue imaging: seeing the immune system in a fresh light.* Nat Rev Immunol, 2002. **2**(11): p. 872-80.
257. Ishii, N., S. Adachi, Y. Nomura, A. Kosuge, Y. Kobayashi, T. Kanai, J. Itatani and S. Watanabe, *Generation of soft x-ray and water window harmonics using a few-cycle, phase-locked, optical parametric chirped-pulse amplifier.* Opt Lett, 2012. **37**(1): p. 97-9.
258. Eisenthal, K.B., *Second harmonic spectroscopy of aqueous nano- and microparticle interfaces.* Chem Rev, 2006. **106**(4): p. 1462-77.
259. Lai, T.Y.C., *Corneal visualization and characterization for applications in ophthalmology using optical imaging* Doctoral Thesis, 2014.
260. Masihzadeh, O., T.C. Lei, D.A. Ammar, M.Y. Kahook and E.A. Gibson, *A multiphoton microscope platform for imaging the mouse eye.* Mol Vis, 2012. **18**: p. 1840-8.

CHAPTER 1

αVβ6 integrin promotes corneal wound healing

Cornea

αVβ6 Integrin Promotes Corneal Wound Healing

José Tomás Blanco-Mezquita,[1,2] *Audrey E. K. Hutcheon,*[1,2] *Mary Ann Stepp,*[3,4] *and James D. Zieske*[1,2]

Purpose. To appreciate the role of the integrin αvβ6 in corneal wound repair, corneal debridement and keratectomy in β6 knockout ($\beta6^{-/-}$) mice were examined.

Methods. Either a 2-mm debridement or keratectomy was made in 129SVE wild type mice (WT) and $\beta6^{-/-}$ mice and allowed to heal for up to 4 months. The pattern of corneal restoration was studied "in vivo" by slit lamp and in tissue sections by means of both light and electron microscopy. In addition, αvβ6, α6β4, laminin, and fibronectin were evaluated by indirect immunofluorescence microscopy and/or Western blot analysis.

Results. αvβ6 expression was upregulated in migrating corneal epithelium after a keratectomy. Healing rates were unaffected in debridement wounds, but were significantly slowed in keratectomy wounds. Most dramatically, mice lacking αvβ6 had a severe defect in basement membrane zone (BMZ) regeneration. Levels of laminin were greatly reduced and no BMZ reformation was observed in transmission electron microscopy (TEM). In addition, hemidesmosome reformation was also impaired in the $\beta6^{-/-}$ mice. Analysis of the hemidesmosome component α6β4 indicated that normal amounts of this integrin were synthesized, suggesting that the defect was in reassembly of the hemidesmosomes. Finally, fibronectin persisted in the BMZ for as long as 4 months after keratectomy in the $\beta6^{-/-}$ mice.

Conclusions. It is hypothesized that the lack of αvβ6 leads to reduced laminin production during wound repair. This lack of laminin prevents reassembly of the BMZ and mature hemidesmosomes after keratectomy in $\beta6^{-/-}$ mice. (*Invest Ophthalmol Vis Sci.* 2011;52:8505–8513) DOI:10.1167/iovs.11-8194

Integrins are a family of receptors that mediate cell-cell and cell-matrix adhesion,[1–3] as well as contributing to a wide variety of cellular responses, including survival, proliferation, and migration.[3] These heterodimeric transmembrane glycoproteins have both alpha (α) and beta (β) subunits. The combination of these 2 subunits results in at least 22 different cell surface receptors with wide ligand binding specificities.

Integrin αvβ6 is expressed at very low levels in epithelial cells of healthy adult mammals; however, its expression is considerably upregulated in response to injury or inflammation.[4,5] Absence of αvβ6 is linked to initiation and progression of periodontal disease,[6] regulation of lung and skin inflammation,[7] delay in epidermal wound healing,[8] and suppression of pulmonary fibrosis.[9] In the cornea, expression of αvβ6 is restricted to the epithelium. Under pathologic conditions, such as in patients with bullous keratopathy,[10] and during wound healing, αvβ6 is upregulated, suggesting a role in corneal epithelial wound repair[11] and keratinocyte migration.[12] αvβ6 is a receptor for many of the components of the basement membrane zone (BMZ) including fibronectin, vitronectin, tenascin, and E-cadherins.[13,14] It is also the receptor for the Arg-Gly-Asp (RGD) attachment site of both latency-associated peptide (LAP)-TGF-β1 and LAP-TGF-β3.[9,15,16] Attachment of αvβ6 to latent TGF-β has been shown in several investigations to be involved in the activation of TGF-β (for review see references 17–20). Indeed, αvβ6-null mice recapitulate much of the phenotype of TGF-β1-null mice.[21]

Because αvβ6 is known to be expressed in remodeling rat basal corneal epithelium and human bullous keratopathy,[10,11] and is an activator of latent TGF-β,[9,15,16] we hypothesized that αvβ6 plays an important role in corneal repair when the BMZ is compromised by surgery. We addressed this hypothesis by using adult β6 integrin-deficient mice ($\beta6^{-/-}$) and comparing them with wild type (WT) mice.

Materials and Methods

All studies were conducted in accordance with the ARVO Statement for Use of Animals in Ophthalmic and Vision Research. Adult male 129SVE WT (Taconic; Albany, NY) and 12- to 18-week-old male and female 129SVE $\beta6^{-/-}$ mice (a kind gift from Jack Lawler, BIDMC/Harvard Medical School, Boston, MA) were anesthetized and either a 2-mm superficial keratectomy or debridement was performed, as previously described.[22,23] In total, 200 mice per strain were examined—96 mice were used for Western blot analysis, 8 for transmission electron microscopy (TEM), 36 for light microscopy, 36 for immunofluorescence, and 24 for whole mounts.

In Vivo Wound Healing Experiments

Either a 2-mm superficial keratectomy was created,[23] where the epithelium, BMZ, and anterior stroma were removed, or a 2-mm debridement was created,[22] where only the epithelium was removed. Corneas were allowed to heal for up to 4 months. At the designated time, animals were euthanized and tissue was harvested and processed for indirect immunofluorescence microscopy, light microscopy, or Western blot analysis.

Determination of Wound Healing Rates

The healing process was monitored every day for the first week and then once every week under a slit lamp (Topcon Medical Systems, Inc.; Oakland, NJ). The corneas were photographed before and after 2% fluorescein stain, and the rate of epithelial healing was evaluated by measuring the wound size with image processing software (ImageJ v.1.5;

From the [1]Schepens Eye Research Institute and [2]Department of Ophthalmology, Harvard University Medical School, Boston, Massachusetts; and the Departments of [3]Anatomy and Cell Biology and [4]Ophthalmology, The George Washington University Medical School, Washington, DC.

Supported by NIH/NEI Grant R01 EY05665 (JDZ).

Submitted for publication July 9, 2011; revised September 1, 2011; accepted September 19, 2011.

Disclosure: **J.T. Blanco-Mezquita**, None; **A.E.K. Hutcheon**, None; **M.A. Stepp**, None; **J.D. Zieske**, None

Corresponding author: James D. Zieske, Schepens Eye Research Institute, 20 Staniford Street, Boston, MA 02114; james.zieske@schepens.harvard.edu.

developed by Wayne Rasband, National Institutes of Health; Bethesda, MD; http://rsb.info.nih.gov/ij). The data were averaged and analyzed for significant variations (** $P < 0.01$ and *** $P < 0.001$). Two-way ANOVA and Bonferroni post test were applied to compare means by row, and the fold enhancement was plotted (Prism 5.0; GraphPad Software, La Jolla, CA).

Indirect Immunofluorescence Microscopy

For frozen sections, the eyes were enucleated, frozen in OCT, 6-μm sections were cut, and indirect immunofluorescence (IF) was performed.[11] For whole mount, the corneas were enucleated, fixed in prechilled 100% methanol and dimethyl sulfoxide (4:1) for 2 hours at 20°C and then stored in 100% methanol at 20°C until ready to use. The corneas were prepared for immunofluorescence as described in Pal-Ghosh et al.[24] The following primary antibodies were used on both the sections and whole mounts and incubated at 4°C overnight: αvβ6 (clone ch6.2A1: 2.36 μg/mL in TTBS + 0.1% BSA)[25]; β4 (clone 346-11A: 5μg/mL in TTBS/5% donkey serum: BD Pharmingen; San Diego, CA); laminin (0.76 μg/mL in 10% donkey serum in PBS: Dako; Carpinteria, CA); and fibronectin (C-20: 2 μg/mL in TTBS/5% donkey serum: Santa Cruz Biotechnology; Santa Cruz, CA). The following secondary antibodies from Jackson Immunoresearch (West Grove, PA) conjugated to either fluorescein or rhodamine were then used with the same blocking conditions as the primary antibody associated with it and incubated at either room temperature for 1 hour (sections) or 4°C overnight (whole mount): donkey anti-human IgG (αvβ6); donkey anti-rat IgG (β4); donkey anti-rabbit IgG (laminin); and donkey anti-goat IgG (fibronectin). Sections and whole mounts were mounted and coverslipped with mounting media containing DAPI (Vectashield; Vector Laboratories, Burlingame, CA), a marker of all cell nuclei. The sections were examined under both a fluorescence microscope (Nikon Eclipse E800; Nikon, Melville, NY) equipped with a digital camera (SPOT; Diagnostic Instruments, Sterling Heights, MI) and with a confocal microscope (TCS-SP5; Leica Microsystems, Bannockburn, IL). Negative controls where the primary antibody was omitted were run with all experiments. As an additional control, irrelevant antibodies of the same isotype were compared to ensure specificity. At least 3 corneas per condition per antibody were observed.

The images captured on the confocal microscope were further imaged with image analysis software (Image Pro Plus v.7; Media Cybernetics, Bethesda, MD). The confocal file was uploaded and an orthogonal image was created.

Light Microscopy

Corneas were enucleated and either fixed in ½ strength Karnovsky's for transmission electron microscopy (TEM) or in 4% paraformaldehyde for hematoxylin-eosin (H&E). For TEM, corneas were processed as previously published.[26] Tissues were cut on an ultramicrotome (LKB; Bromma, Sweden) at 60–90 Å thick and examined with an electron microscope (Philips 410; Philips Electronics N.V., Eindhoven, The Netherlands). For H&E, 6-μm sections were cut and stained. The sections were examined under a light microscope

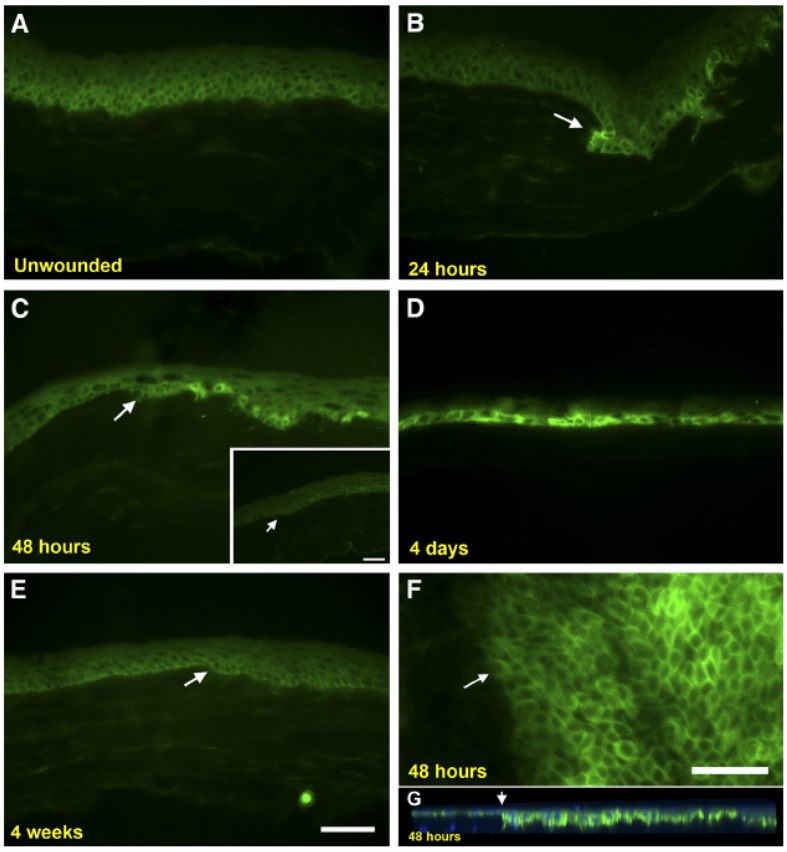

FIGURE 1. Immunolocalization of αvβ6 (*green*) in WT mouse corneas: (**A**) unwounded, (**B**) 24 hours, (**C**) 48 hours, (**D**) 4 days, and (**E**) 4 weeks after keratectomy. (**C**, *inset*) WT mouse cornea 48 hours after debridement. In (**F**) and (**G**) whole mount corneas were examined by confocal microscopy 48 hours after keratectomy. (**G**) A 3-D software reconstruction (Image Pro Plus v.7; Media Cybernetics). Note the abrupt increase of expression in the basal cells migrating to cover the wound area. *Blue* in (**G**), DAPI, a marker of cell nuclei. *Arrows* denote the original wound edge. Bar, 50 μm.

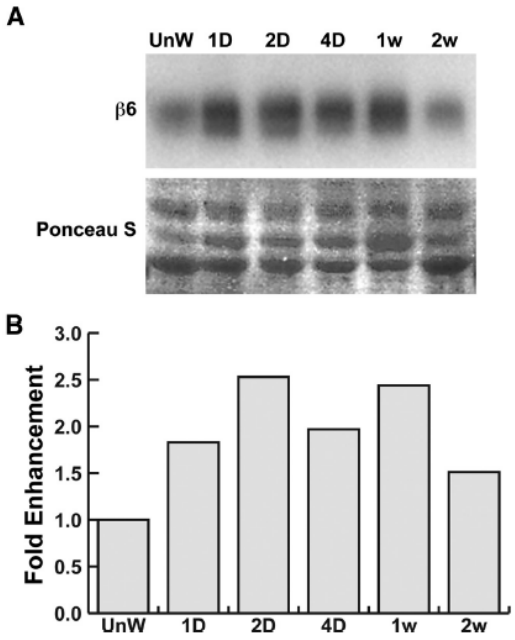

FIGURE 2. Western blot analysis of αvβ6 in WT mouse corneas after a keratectomy wound. (A) Representative Western blot images documenting the increased expression of αvβ6, and the corresponding stain (Ponceau S; Sigma) of the blot to document equal loading of samples (region from 40 to 70 kDa). Experiments were repeated three times using at least six mice per time point. (B) Density of the bands, quantitated and plotted.

(Nikon Eclipse E800; Nikon) equipped with a digital camera (Olympus DP70; Olympus America Inc.; Melville, NY).

Western Blot Analysis

Immediately after euthanizing the mice, the epithelium was scraped from limbus to limbus, flash frozen in liquid nitrogen, and processed for Western blot analysis, as previously described.[27] Eight corneas were used for each experimental condition. Tissues were homogenized and lysed, and the protein was purified and assayed (Biorad; Hercules, CA). Equal amounts of total protein were loaded on a nonreducing 4%–20% Tris-Glycine gel (Invitrogen, Carlsbad, CA). Proteins were transferred to a membrane (Immobilon-P; Millipore, Billerica, MA), which was then stained (Ponceau S; Sigma) to check for transfer efficiency. Membranes were blocked with 5% milk in TBS and then probed, as previously described[27] with the following primary antibodies and incubated at 4°C overnight: αvβ6, clone ch6.2A1 (0.5–1 μg/mL); β4 (1:500)[28]; and laminin antibody (0.76 μg/mL). The appropriate HRP-conjugated secondary antibody (Jackson Immunoresearch) was then incubated with the membranes for 1 hour at room temperature: donkey anti-human IgG (αvβ6); donkey anti-rabbit IgG (β4); and donkey anti-rabbit IgG (laminin). Immunoreactive bands were visualized (Biospectrum AC imaging system; UVP, LLC, Upland, CA) using enhanced chemiluminescence Western blot detection reagents (Millipore). Experiments were repeated two to three times. Software was used to measure intensity of the bands (ImageJ v.1.5) and plot the fold enhancement for the values (Prism 5.0; GraphPad Software).

RESULTS

Healing of Keratectomy Wounds Is Accompanied by Enhanced Expression of αvβ6 Integrin in the Basal Epithelial Cells

We have previously demonstrated that αvβ6 is upregulated in response to keratectomy and debridement wounds in rat cornea.[11] To confirm our rat experiments, we examined the spatial and temporal changes of αvβ6 in response to wounds in 129SVE WT mice. In unwounded corneas (Fig. 1A), little, if any αvβ6 was present; however, 24 hours after keratectomy (Fig. 1B), the number of cells with αvβ6 increased, localizing in the basal epithelial cells that were migrating to cover the wound area. αvβ6 continued to be present within this area at 48 hours (Figs. 1C, 1F, 1G), through 4 days (Fig. 1D) and 1 week (data not shown). It then gradually decreased and returned to baseline by 4 weeks (Fig. 1E). No upregulation of αvβ6 was observed in the peripheral epithelial cells, as can be seen in Figures 1B, 1C, 1F, and 1G. In contrast to rats, αvβ6 was not enhanced in the migrating epithelium in debridement wounds in 129SVE mice (Fig. 1C, inset).

To confirm the apparent increase in αvβ6 in the epithelial cells within the wound area after keratectomy, tissue was collected and processed for Western blot analysis. The data from the Western blot analysis agreed with that observed in immunofluorescence (Fig. 2). Low levels of αvβ6 were observed in the epithelium of unwounded (UnW) control corneas, and increased at 1, 2, and 4 days (D), and 1 week (w) post-keratectomy. The protein amount then began to decrease by 2 weeks. Stained (Ponceau S; Sigma) membrane showed equal loading (Fig. 2A).

αvβ6 Integrin Plays a Main Role in Epithelial Cell Migration after Keratectomy

Because αvβ6 was observed in the migrating basal corneal epithelial cells in WT mice, we decided to examine the wound-healing rate in WT and $\beta6^{-/-}$ mice in vivo to see if αvβ6 played a role in wound healing. As can be seen in Figure 3 (red and blue lines), 24 hours after a keratectomy, most of the corneas had recovered 25% of their surface, without differences among mouse genotypes. However, an increase in the migration rate in the WT mice was observed after 24 hours. The rate of migration was significantly delayed in the $\beta6^{-/-}$ corneas, especially at 32 and 40 hours ($P < 0.001$) (Fig. 3).

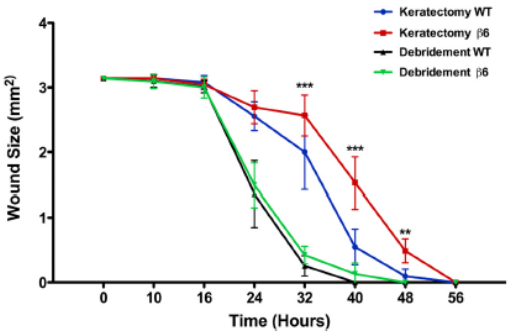

FIGURE 3. Graphical documentation of healing rates of WT and $\beta6^{-/-}$ mice after 2-mm debridement or keratectomy. At least six mice were used per time point. ** $P < 0.01$, *** $P < 0.001$.

To compare the effect of αvβ6 on wounds with or without damage to the BMZ, we also examined the wound healing rate of WT and $\beta6^{-/-}$ mice with debridement wounds. As with the keratectomy, the epithelial wound healing rates were approximately the same for both strains of mice up until 16 hours post wounding (Fig. 3, green and black lines). However, at 16 hours post debridement, whether it was WT or $\beta6^{-/-}$ mice, there was an increase in the wound healing rate. This increase occurred approximately 8 hours earlier than in the corneas with a keratectomy (Fig. 3, red and blue lines). By 24 hours post debridement, both strains of mice had resurfaced > 50% of the original wound size. No statistically significant difference was observed after debridement between WT and $\beta6^{-/-}$ mice at any time point (Fig. 3).

αvβ6 Integrin Mediates Attachment of Epithelium to Extracellular Matrix (ECM) during Wound Healing after Keratectomy

Once the defect is closed and epithelial migration is over, new cell-cell and cell-ECM adhesions need to be created for both restoration of barrier function and anchoring of the epithelium. Assembly of hemidesmosomes in the new epithelial basal layer is essential to maintain the integrity of the epithelia.[29] In both the WT and $\beta6^{-/-}$ mice, the unwounded corneas look similar (Figs. 4A, 4B). By 4 days post keratectomy, the epithelium in both strains covered the wound area (Figs. 4C, 4D). In WT mice, the epithelium appeared to be forming adhesions to the stroma (Fig. 4C), whereas in $\beta6^{-/-}$ mice, the epithelium had a large area that was not attached to the stroma (Fig. 4D). By 2 weeks post keratectomy, the WT mice appeared to have returned to normal and more adhesions appeared to have been formed (Fig. 4E). However, in the $\beta6^{-/-}$ mice, there was still a large area where the epithelium was not attached to the stroma (Fig. 4F). This detachment was observed in six of six of the $\beta6^{-/-}$ mice and in zero of six of the WT mice. By 4 weeks, the WT mouse corneas had returned to that seen in unwounded (Fig. 4G); whereas the $\beta6^{-/-}$ mouse cornea's morphology (Fig. 4H) was more similar to that seen in the WT mice at 2 weeks (Fig. 4E). On slit lamp examination, the epithelium could be seen to be loosely adherent in the $\beta6^{-/-}$ mice with blister-like structures (Fig. 4I). These blister-like structures were not present in the WT mice (data not shown).

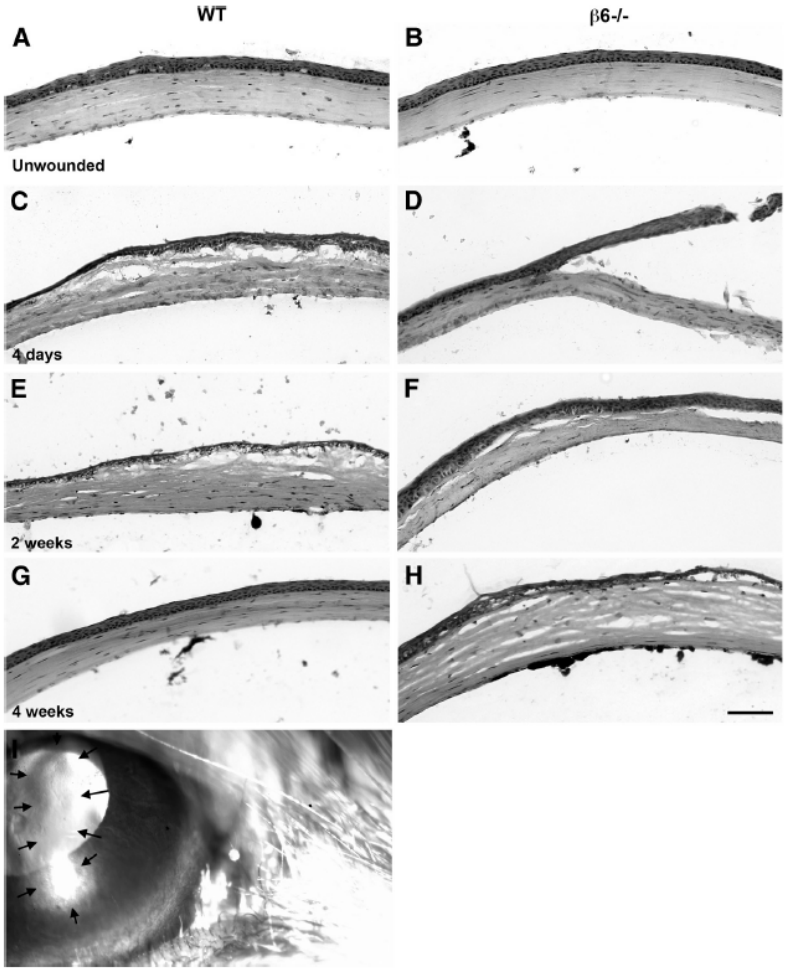

FIGURE 4. Morphologic analysis of WT (A, C, E, G) and $\beta6^{-/-}$ (B, D, F, H) in (A, B) unwounded corneas, (C, D) 4 days, (E, F) 2 weeks, and (G, H) 4 weeks post keratectomy. Note that epithelium is loosely adherent in $\beta6^{-/-}$ after wounding. Bar, 100 μm. (I) Slit lamp image (magnification, ×40) of $\beta6^{-/-}$ cornea 1 week after keratectomy. Note the blister-like structure extends across the cornea (*arrows*).

αvβ6 Integrin Helps to Restore the BMZ after Keratectomy by Upregulating New Laminin and Promoting Assembly of Hemidesmosomes

Because the wound-healing rate was slowed and the adherence of the epithelium to the stroma was defective in $\beta6^{-/-}$ mice after a keratectomy wound, we examined the structure of the BMZ by TEM. One month after debridement, in both strains of mice (Figs. 5A, 5B), the BMZ looked similar to that seen in unwounded corneas (data not shown). One month after keratectomy, the WT BMZ appeared to be reforming hemidesmosomes and a nearly continuous BMZ was observed (Fig. 5C). In contrast, the number of mature hemidesmosomes was greatly reduced in the $\beta6^{-/-}$ mouse corneas and there were no signs of BMZ reformation (Fig. 5D). By 4 months post keratectomy, the BMZ of the WT mice (Fig. 5E) looked similar to that seen in unwounded corneas; however, the amount of hemidesmosomes present in $\beta6^{-/-}$ mice was markedly reduced compared with WT, and only a faint suggestion of BMZ was observed (Fig. 5F).

This apparent lack of BMZ and reduced number of hemidesmosomes in the $\beta6^{-/-}$ mice after a keratectomy leads us to question, how is the lack of αvβ6 disrupting their reformation? To examine this question, two markers were used. A laminin antibody generated using rat yolk sac tumor laminin as an antigen, which localizes to the BMZ, but does not identify a specific laminin molecule, and α6β4, which localizes within

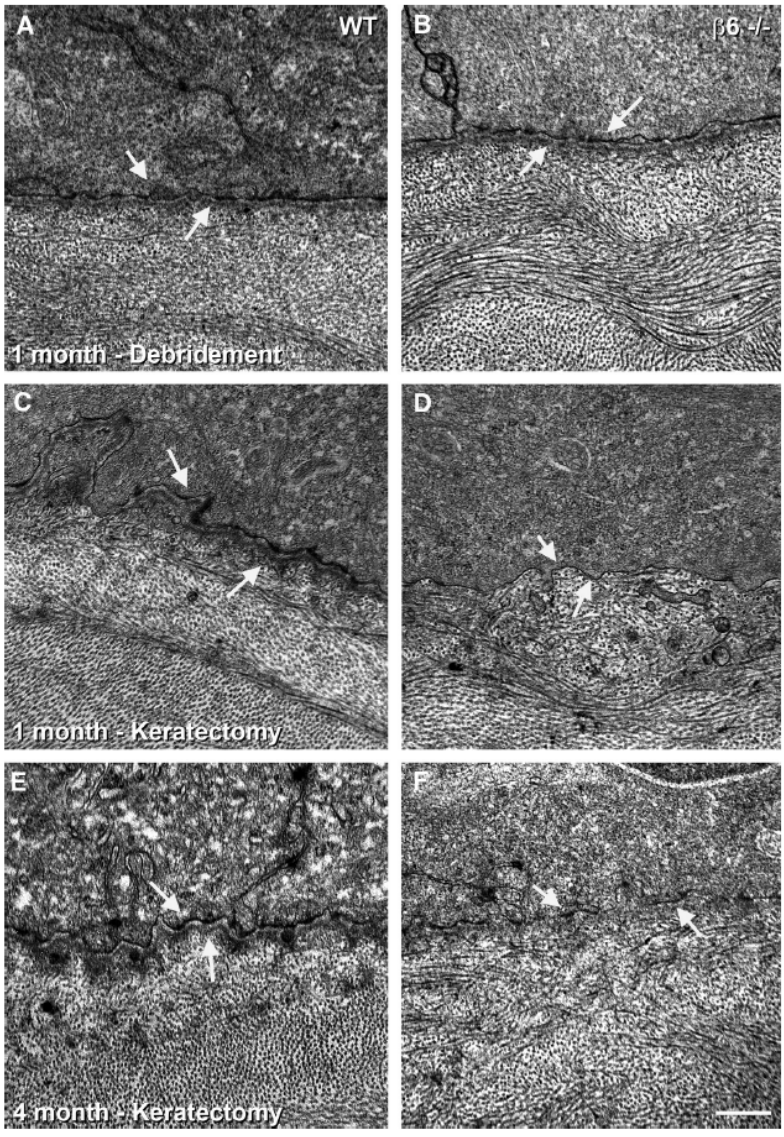

FIGURE 5. Transmission electron micrographs of WT (A, C, E) and $\beta6^{-/-}$ (B, D, F) mouse corneas 1 month after debridement (A, B), and 1 (C, D) and 4 months (E, F) post keratectomy. Note the complete absence of BMZ and the greatly reduced number of electron dense hemidesmosomes 1 month after keratectomy in the $\beta6^{-/-}$ mice. Also note the epithelial projections into the stroma that may help anchor the epithelium. Arrows indicate location of BMZ. Bar, 500 nm.

hemidesmosomes at the BMZ (Fig. 6). As with humans, rats, and chickens,[11,30–32] an uninterrupted linear pattern of laminin was observed beneath the epithelium in unwounded corneas of WT and $\beta6^{-/-}$ mice (Figs. 6A, 6E). Laminin colocalized with $\alpha6\beta4$ in both genotypes before wounding (Figs. 6A1, 6E1). After keratectomy, the BMZ was removed and therefore, there was no laminin or $\alpha6\beta4$ localization within the wound area in either strain of mice (data not shown). In WT mice 4 days post keratectomy, laminin (Fig. 6B) and $\alpha6\beta4$ (Fig. 6B1) colocalized and appeared just below the epithelium; however, they were not yet continuous, but rather, patchy and thickened. By 1 week, the patchiness of both laminin and $\alpha6\beta4$ began to disappear (Figs. 6C, 6C1). By 4 weeks, both markers continued to colocalize and the thickening was disappearing (data not shown) and by 2 months (Figs. 6D, 6D1), it was similar to unwounded (Figs. 6A, 6A1). On the other hand, 4 days after a keratectomy in $\beta6^{-/-}$ mice (Figs. 6F, 6F1), small patches of laminin and $\alpha6\beta4$ were present, but the majority of the wound area had little staining. One week post keratectomy (Figs. 6G, 6G1), there appeared to be more patches of staining. This increase in patchy localization continued at 2 (Figs. 6H, 6H1) and 4 weeks (data not shown). By 4 months, laminin (Fig. 6I) and $\alpha6\beta4$ (Fig. 6I1) colocalized where the epithelium and the stroma met; however, in the area where the epithelium did not appear to be adhering to the stroma, laminin was not present.

To confirm the amounts of laminin and $\alpha6\beta4$ in the migrating epithelium over time, we performed Western blot analysis. In Figure 7.1, it can be seen that laminin levels increased rapidly in WT mice after wounding and continued to rise for at least 1 week

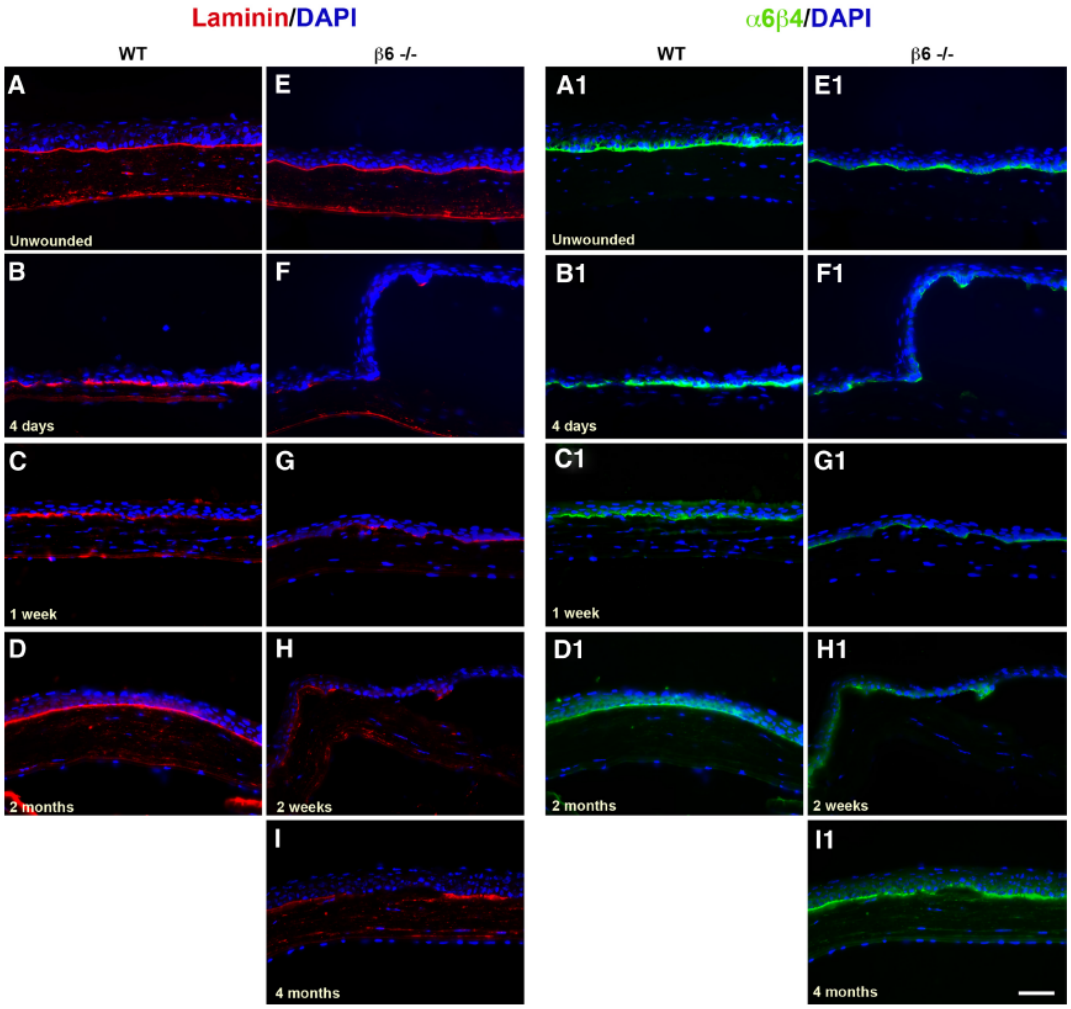

FIGURE 6. Immunolocalization of laminin (A–I, *red*) and $\alpha6\beta4$ (A1–I1, *green*) in WT (A–D, A1–D1) and $\beta6^{-/-}$ (E–I, E1–I1) mice. Proteins were localized in unwounded corneas (A, A1, E, E1) and 4 days (B, B1, F, F1), 1 week (C, C1, G, G1), 2 weeks (H, H1), 2 months (D, D1) and 4 months (I, I1) post keratectomy. Note that laminin and $\alpha6\beta4$ were analyzed on single sections that are shown separately for ease of viewing. DAPI, a marker of all cell nuclei, *blue*. Bar, 50 μm. At least four corneas per time point were analyzed.

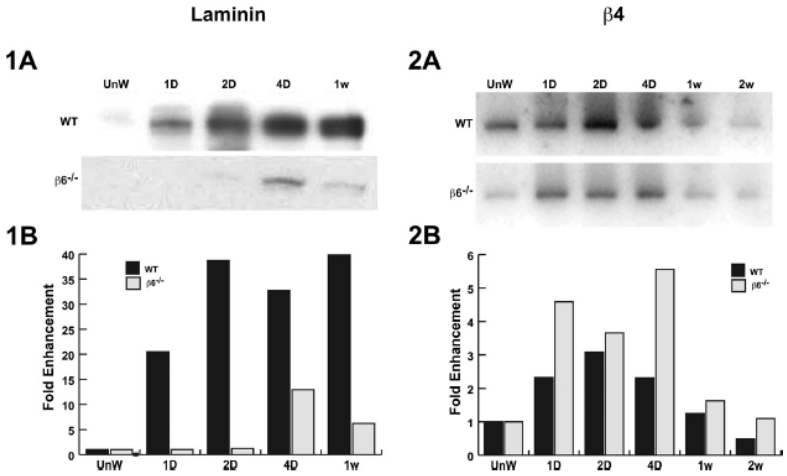

FIGURE 7. Representative Western blot images documenting the increased expression of laminin (**1A**) and $\alpha6\beta4$ (**2A**) after keratectomy wounds. Stain (Ponceau S; Sigma) of the blots was used to document equal loading of samples (data not shown). Experiments were repeated two or three times using at least six mice per time point. The density of the bands was quantitated and fold enhancement was plotted (**1B**, **2B**). Note: Only epithelium was included in these samples.

in a representative experiment. In contrast, only very low levels of laminin were present in the epithelium of $\beta6^{-/-}$ mice after a keratectomy wound. As seen in Figure 7.2, the amount of $\alpha6\beta4$ increased in both strains after keratectomy, with WT peaking by 2 days post keratectomy and $\beta6^{-/-}$ by 4 days. The levels of $\alpha6\beta4$ then decreased to unwounded by 2 weeks in both strains.

Fibronectin Persists after Keratectomy in αvβ6 Null Mice

Release of fibronectin within the injured area is critical for healing. The released fibronectin acts as a temporary matrix allowing attachment of the new migrating cells.[4] Fibronectin is also known to be a ligand for $\alpha v\beta6$.[33] We, therefore, examined the spatial and temporal changes of fibronectin in the WT and $\beta6^{-/-}$ mice after keratectomy (Fig. 8). In unwounded corneas of both strains of mice, no fibronectin was observed (data not shown). At 24 hours, fibronectin was observed from edge-to-edge in the wounded area beneath the migrating epithelium in both WT and $\beta6^{-/-}$ mice, and no fibronectin was observed in the peripheral tissue (data not shown). In both strains of mice, fibronectin peaked at 1 week (Figs. 8A, 8B). After 1 week, fibronectin decreased suddenly in WT mice, and only a little staining was observed at 2 weeks (data not shown). By 2 months, fibronectin rarely was observed in WT mice (Fig. 8C). In contrast, $\beta6^{-/-}$ mice continued to have fibronectin at 2 and 4 months (Figs. 8D and 8E, respectively).

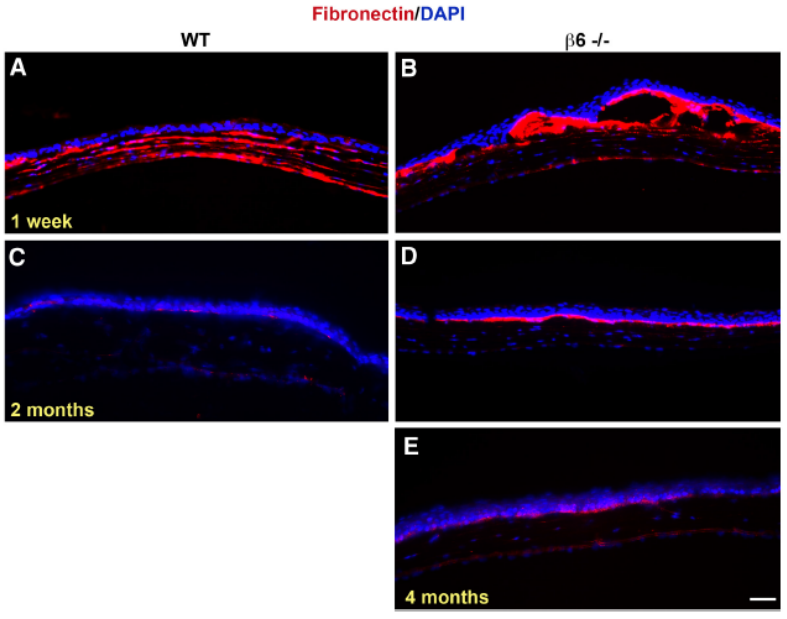

FIGURE 8. Immunolocalization of fibronectin (*red*) in WT (**A**, **C**) and $\beta6^{-/-}$ (**B**, **D**, **E**) mice: (**A**, **B**) 1 week, (**C**, **D**) 2 and (**E**) 4 months post keratectomy. Note that no fibronectin was present in unwounded corneas, or beyond 2 weeks after wounding in WT cornea. DAPI, a marker of all cell nuclei, *blue*. Bar, 50 μm.

DISCUSSION

Healthy corneal epithelium is essential for maintaining transparency, avoiding infection and maintaining corneal integrity. To preserve the structure, the epithelium anchors to the stroma ECM through the BMZ. We previously observed a spatial/time correlation between αvβ6 upregulation in basal corneal epithelial cells and laminin expression in the BMZ of rats after a keratectomy wound.[11,12] With the present study, we extended our work to demonstrate that $\beta6^{-/-}$ mice did not restore the BMZ or reform mature hemidesmosomes after a keratectomy wound. By 1 month after keratectomy, WT mice showed a nearly fully restored BMZ by TEM, with restoration of both lamina densa and lucida, as well as a high density of hemidesmosomes. Dramatically, all these components were missing in the $\beta6^{-/-}$ mice, indicating that αvβ6 is required for regeneration of the BMZ and hemidesmosomes. In contrast, after debridement, both WT and $\beta6^{-/-}$ mouse corneas showed a normal appearance in both BMZ and hemidesmosomes.

Immediately after photorefractive keratectomy, humans, rats, and chickens all deposit laminin underneath the epithelium.[11,30–32] Concordant with these works, WT mouse corneas showed a continuous laminin line limbus-to-limbus by 2 weeks after keratectomy. However, within the damaged zone in the $\beta6^{-/-}$ mice, laminin was absent, weeks and even months after a keratectomy, and when present, only present as clusters within the healing BMZ. Even by 4 months, continuous laminin localization was not observed, which is in agreement with the lack of BMZ observed by TEM. Western blot analysis and IF results demonstrated that laminin production decreased and its assembly into BMZ was impaired. One possible explanation for the lack of laminin production is that activation of TGF-β1 or -β3 may be impaired by the lack of αvβ6. This possibility is supported by studies suggesting that laminin production is increased in epithelial cells in response to autocrine TGF-β1 activation.[34,35] We hypothesize that laminin expression may be upregulated in the corneal epithelium by αvβ6-activated TGF-β.[36] This type of activation has been reported in numerous systems,[17–20] and αvβ6 expression has been frequently linked to fibrosis.[37–41]

Both loose epithelium and lack of hemidesmosomes have been observed in mice lacking α6β4 integrin.[42] Our $\beta6^{-/-}$ mouse corneas appear to have a greatly reduced number of mature hemidesmosomes after 1 and 4 months post keratectomy. An evident colocalization of α6β4 and laminin is observed in both WT and $\beta6^{-/-}$ unwounded corneas. This colocalization is also observed in healing corneas of WT mice after keratectomy; therefore, this strongly suggests that α6β4 is a receptor for laminin during BMZ repair, and that the presence of laminin is necessary to assemble α6β4 into hemidesmosomes, during corneal epithelial BMZ repair.

In addition to the defective restoration of the BMZ, we observed that wound closure in the $\beta6^{-/-}$ mice was slowed after a keratectomy. Although some studies have suggested that lack of αvβ6 compromises epidermal repair,[6,8] others have proposed that it does not,[7,21] or only the re-epithelialization is compromised in $\beta6^{-/-}$ diabetic mice, but not in $\beta6^{-/-}$ healthy mice.[43] In the current work, we observed significant differences in the rate of migration between WT and $\beta6^{-/-}$ mice when the BMZ was removed by keratectomy. Interestingly, $\beta6^{-/-}$ mice did not show any significant slowing of migration after a debridement wound, nor did αvβ6 appear to be enhanced after a debridement wound. These data suggest that αvβ6 plays a major role in migration only when the BMZ is damaged. The data also suggest that matrix might be responsible for inducing αvβ6.

Because fibronectin is observed in the wound-healing stroma after a keratectomy, and is believed to be involved in epithelial migration[4] and is known to be a substrate for αvβ6,[33] there may be an interaction between the αvβ6 in the migrating epithelium and the upregulated fibronectin in the stroma that increases the speed of epithelial migration over the wound area after a keratectomy. In the healing cornea, fibronectin is released, facilitating both epithelial migration and attachment to ECM.[44,45] When the wound defect is closed, fibronectin is lost, correlating with the appearance of laminin. As in a previous experiment in rabbits,[46] loss of fibronectin expression correlating with BMZ restoration was evident in the WT mice; however, the loss of fibronectin and appearance of laminin was not observed in the $\beta6^{-/-}$ mice. Instead, interrupted costaining of fibronectin and laminin remained in the later time points, suggesting that lack of BMZ restoration was associated with the continuing expression of fibronectin.

With the current work, we demonstrate that αvβ6 is upregulated in the epithelium during corneal wound healing when the BMZ is damaged in WT mice. The upregulation of αvβ6 promotes epithelial migration in wounds where the BMZ is removed, and leads to upregulation of laminin. In addition, in mice lacking αvβ6, hemidesmosome restoration is compromised after keratectomy wounds and this correlates with the absence of laminin in the BMZ.

Acknowledgments

The authors thank Shelia M. Violette (Stromedix, Cambridge, MA) for providing the human αvβ6 antibody, and Patricia Pearson and Bianai Fan for providing technical expertise.

References

1. Ruoslahti E, Pierschbacher MD. New perspectives in cell adhesion: RGD and integrins. *Science.* 1987;238:491–497.
2. Hynes RO. Integrins: a family of cell surface receptors. *Cell.* 1987; 48:549–554.
3. Clark EA, Brugge JS. Integrins and signal transduction pathways: the road taken. *Science.* 1995;268:233–239.
4. Breuss JM, Gillett N, Lu L, Sheppard D, Pytela R. Restricted distribution of integrin beta 6 mRNA in primate epithelial tissues. *J Histochem Cytochem.* 1993;41:1521–1527.
5. Breuss JM, Gallo J, DeLisser HM, et al. Expression of the beta 6 integrin subunit in development, neoplasia and tissue repair suggests a role in epithelial remodeling. *J Cell Sci.* 1995;108:2241–2251.
6. Ghannad F, Nica D, Fulle MI, et al. Absence of alphavbeta6 integrin is linked to initiation and progression of periodontal disease. *Am J Pathol.* 2008;172:1271–1286.
7. Huang XZ, Wu JF, Cass D, et al. Inactivation of the integrin beta 6 subunit gene reveals a role of epithelial integrins in regulating inflammation in the lung and skin. *J Cell Biol.* 1996;133:921–928.
8. AlDahlawi S, Eslami A, Hakkinen L, Larjava HS. The alphavbeta6 integrin plays a role in compromised epidermal wound healing. *Wound Repair Regen.* 2006;14:289–297.
9. Munger JS, Huang X, Kawakatsu H, et al. The integrin alpha v beta 6 binds and activates latent TGF beta 1: a mechanism for regulating pulmonary inflammation and fibrosis. *Cell.* 1999;96:319–328.
10. Ljubimov AV, Saghizadeh M, Pytela R, Sheppard D, Kenney MC. Increased expression of tenascin-C-binding epithelial integrins in human bullous keratopathy corneas. *J Histochem Cytochem.* 2001; 49:1341–1350.
11. Hutcheon AE, Guo XQ, Stepp MA, et al. Effect of wound type on Smad 2 and 4 translocation. *Invest Ophthalmol Vis Sci.* 2005;46: 2362–2368.
12. Stepp MA, Zhu L. Upregulation of alpha 9 integrin and tenascin during epithelial regeneration after debridement in the cornea. *J Histochem Cytochem.* 1997;45:189–201.
13. Stepp MA. Corneal integrins and their functions. *Exp Eye Res.* 2006;83:3–15.
14. Prieto AL, Edelman GM, Crossin KL. Multiple integrins mediate cell attachment to cytotactin/tenascin. *Proc Natl Acad Sci U S A.* 1993;90:10154–10158.

15. Munger JS, Harpel JG, Giancotti FG, Rifkin DB. Interactions between growth factors and integrins: latent forms of transforming growth factor-beta are ligands for the integrin alphavbeta1. *Mol Btol Cell.* 1998;9:2627–2638.
16. Annes JP, Rifkin DB, Munger JS. The integrin alphaVbeta6 binds and activates latent TGFbeta3. *FEBS Lett.* 2002;511:65–68.
17. Aluwihare P, Munger JS. What the lung has taught us about latent TGF-beta activation. *Am J Resptr Cell Mol Btol.* 2008;39:499–502.
18. Sheppard D. Integrin-mediated activation of latent transforming growth factor beta. *Cancer Metastasis Rev.* 2005;24:395–402.
19. Shi M, Zhu J, Wang R, et al. Latent TGF-beta structure and activation. *Nature.* 2011;474:343–349.
20. Wipff PJ, Hinz B. Integrins and the activation of latent transforming growth factor beta1 - an intimate relationship. *Eur J Cell Btol.* 2008;87:601–615.
21. Aluwihare P, Mu Z, Zhao Z, et al. Mice that lack activity of alphavbeta6- and alphavbeta8-integrins reproduce the abnormalities of Tgfb1- and Tgfb3-null mice. *J Cell Sci.* 2009;122:227–232.
22. Zieske JD, Gipson IK. Protein synthesis during corneal epithelial wound healing. *Invest Ophthalmol Vis Sci.* 1986;27:1–7.
23. Zieske JD, Higashijima SC, Spurr-Michaud SJ, Gipson IK. Biosynthetic responses of the rabbit cornea to a keratectomy wound. *Invest Ophthalmol Vis Sci.* 1987;28:1668–1677.
24. Pal-Ghosh S, Pajoohesh-Ganji A, Brown M, Stepp MA. A mouse model for the study of recurrent corneal epithelial erosions: alpha9beta1 integrin implicated in progression of the disease. *Invest Ophthalmol Vis Sci.* 2004;45:1775–1788.
25. Weinreb PH, Simon KJ, Rayhorn P, et al. Function-blocking integrin alphavbeta6 monoclonal antibodies: distinct ligand-mimetic and nonligand-mimetic classes. *J Btol Chem.* 2004;279:17875–17887.
26. Gipson IK, Grill SM, Spurr SJ, Brennan SJ. Hemidesmosome formation in vitro. *J Cell Btol.* 1983;97:849–857.
27. Zieske JD, Takahashi H, Hutcheon AE, Dalbone AC. Activation of epidermal growth factor receptor during corneal epithelial migration. *Invest Ophthalmol Vis Sci.* 2000;41:1346–1355.
28. Sta Iglesia DD, Gala PH, Qiu T, Stepp MA. Integrin expression during epithelial migration and restratification in the tenascin-C-deficient mouse cornea. *J Histochem Cytochem.* 2000;48:363–376.
29. Gipson IK. Adhesive mechanisms of the corneal epithelium. *Acta Ophthalmol Suppl.* 1992;13–17.
30. Javier JA, Lee JB, Oliveira HB, Chang JH, Azar DT. Basement membrane and collagen deposition after laser subepithelial keratomileusis and photorefractive keratectomy in the leghorn chick eye. *Arcb Ophthalmol.* 2006;124:703–709.
31. Hutcheon AE, Sippel KC, Zieske JD. Examination of the restoration of epithelial barrier function following superficial keratectomy. *Exp Eye Res.* 2007;84:32–38.
32. Bystrom B, Virtanen I, Rousselle P, Miyazaki K, Linden C, Pedrosa Domellof F. Laminins in normal, keratoconus, bullous keratopathy and scarred human corneas. *Histochem Cell Btol.* 2007;127:657–667.
33. Busk M, Pytela R, Sheppard D. Characterization of the integrin alpha v beta 6 as a fibronectin-binding protein. *J Btol Chem.* 1992;267:5790–5796.
34. Moyano JV, Greciano PG, Buschmann MM, Koch M, Matlin KS. Autocrine transforming growth factor-{beta}1 activation mediated by integrin {alpha}V{beta}3 regulates transcriptional expression of laminin-332 in Madin-Darby canine kidney epithelial cells. *Mol Btol Cell.* 2010;21:3654–3668.
35. Kumar NM, Sigurdson SL, Sheppard D, Lwebuga-Mukasa JS. Differential modulation of integrin receptors and extracellular matrix laminin by transforming growth factor-beta 1 in rat alveolar epithelial cells. *Exp Cell Res.* 1995;221:385–394.
36. Hyytiainen M, Penttinen C, Keski-Oja J. Latent TGF-beta binding proteins: extracellular matrix association and roles in TGF-beta activation. *Crit Rev Clin Lab Sci.* 2004;41:233–264.
37. Eslami A, Gallant-Behm CL, Hart DA, et al. Expression of integrin alphavbeta6 and TGF-beta in scarless vs scar-forming wound healing. *J Histochem Cytochem.* 2009;57:543–557.
38. Moutasim KA, Jenei V, Sapienza K, et al. Betel-derived alkaloid up-regulates keratinocyte alphavbeta6 integrin expression and promotes oral submucous fibrosis. *J Pathol.* 2011;223:366–377.
39. Nadler EP, Patterson D, Violette S, et al. Integrin alphavbeta6 and mediators of extracellular matrix deposition are up-regulated in experimental biliary atresia. *J Surg Res.* 2009;154:21–29.
40. Popov Y, Patsenker E, Stickel F, et al. Integrin alphavbeta6 is a marker of the progression of biliary and portal liver fibrosis and a novel target for antifibrotic therapies. *J Hepatol.* 2008;48:453–464.
41. Sullivan BP, Weinreb PH, Violette SM, Luyendyk JP. The coagulation system contributes to alphaVbeta6 integrin expression and liver fibrosis induced by cholestasis. *Am J Pathol.* 2010;177:2837–2849.
42. van der Neut R, Krimpenfort P, Calafat J, Niessen CM, Sonnenberg A. Epithelial detachment due to absence of hemidesmosomes in integrin beta 4 null mice. *Nat Genet.* 1996;13:366–369.
43. Jacobsen JN, Steffensen B, Hakkinen L, Krogfelt KA, Larjava HS. Skin wound healing in diabetic beta6 integrin-deficient mice. *Apmis.* 118:753–764.
44. Berman M, Manseau E, Law M, Aiken D. Ulceration is correlated with degradation of fibrin and fibronectin at the corneal surface. *Invest Ophthalmol Vis Sci.* 1983;24:1358–1366.
45. Jester JV, Huang J, Barry-Lane PA, Kao WW, Petroll WM, Cavanagh HD. Transforming growth factor(beta)-mediated corneal myofibroblast differentiation requires actin and fibronectin assembly. *Invest Ophthalmol Vis Sci.* 1999;40:1959–1967.
46. Kang SJ, Kim EK, Kim HB. Expression and distribution of extracellular matrices during corneal wound healing after keratomileusis in rabbits. *Ophthalmologica.* 1999;213:20–24.

CHAPTER 2

Role of Thrombospondin-1 in Repair of Penetrating Corneal Wounds

Cornea

Role of Thrombospondin-1 in Repair of Penetrating Corneal Wounds

José Tomás Blanco-Mezquita, Audrey E. K. Hutcheon, and James D. Zieske

Schepens Eye Research Institute/Massachusetts Eye and Ear and Department of Ophthalmology, Harvard Medical School, Boston, Massachusetts

Correspondence: James D. Zieske, 20 Staniford Street, Boston, MA 02114; James_Zieske@meei.harvard.edu.

Submitted: January 22, 2013
Accepted: July 28, 2013

Citation: Blanco-Mezquita JT, Hutcheon AEK, Zieske JD. Role of thrombospondin-1 in repair of penetrating corneal wounds. *Invest Ophthalmol Vis Sci.* 2013;54:6262–6268. DOI: 10.1167/iovs.13-11710

Purpose. Thrombospondin-1 (THBS1) has been suggested as a corneal wound-healing modulator. Therefore, we compromised the integrity of the cornea to elucidate the role of THBS1.

Methods. Full-thickness penetrating corneal incisions (1.5 mm) were created in wild type (WT, 129S2/SvPas) and THBS1-deficient mice (*Thbs1*$^{-/-}$, 129S2/SvPas-*Thbs1*^{tm1Hyn}/*Thbs1*^{tm1Hyn}), and allowed to heal up to 1 month, while being monitored by slit-lamp and intravital corneal examinations. Corneas also were examined by transmission electron microscopy and indirect immunofluorescence. To determine how THBS1 was involved in the healing process, we examined THBS1 and α-smooth muscle actin (SMA), a marker of myofibroblasts and myoepithelial cells.

Results. In WT mice by 1 month, corneas appeared transparent with a thin scar, and endothelium and Descemet's membrane (DM) were restored. In contrast, *Thbs1*$^{-/-}$ corneas exhibited chronic edema and persistent opacity after wounding. The DM and endothelium were not restored, and wound contraction was impaired. The THBS1 was localized in epithelial cells at early stages of the healing process, and in the stroma and endothelial cells during later stages. The SMA-positive epithelial cells and myofibroblasts were observed within the healing area at day 4, peaked at day 14, and disappeared at day 30. The SMA-positive cells were reduced greatly in *Thbs1*$^{-/-}$ mice.

Conclusions. In the current study, we demonstrated that corneal restoration is strikingly compromised by a penetrating incision in *Thbs1*$^{-/-}$ mice. The wound results in persistent edema and wound gaping. This appears to be the result of the lack of endothelial migration and DM restoration. In addition, myofibroblast formation is compromised, resulting in the lack of wound contraction.

Keywords: thrombospondin-1, corneal wound healing, penetrating wound, endothelial restoration, corneal epithelium

Thrombospondin-1 (THBS1, also referred to as TSP-1) is a large (450 kDa) trimeric extracellular glycoprotein[1,2] released by platelets, and epithelial and mesenchymal cells in response to many of the physiologic processes, including development, wound healing, angiogenesis, tumor cell migration, platelet aggregation, and cell adhesion.[3–8] It is not known if THBS1 has a significant role in normal tissue homeostasis; however, it is present during development of many embryonic tissues, and its expression is increased dramatically during the wound-healing process.[9–12] Absence of THBS1 leads to prolonged inflammation, delayed wound healing, and delayed scab loss.[13,14]

In the healthy cornea, THBS1 is localized in the basement membrane zone (BMZ), Descemet's membrane (DM), and corneal endothelium (CE), but not within the stroma of human, bovine,[15] and rat corneas.[16] In addition, Sekiyama et al.[17] demonstrated that limbal and corneal epithelium express *Thbs1* mRNA in human corneas. THBS1 and *Thbs1* mRNA expression is increased immediately during corneal wound healing after injury[16–20]; however, the mechanisms of action and function remain unclear. Uno et al. suggest that epithelial defects in the cornea stimulate the expression of THBS1 in the wound area, resulting in the accelerated reepithelialization of the cornea and that lack of vitamin A reduced THBS1 expression.[20,21] Recently, Matsuba et al.[16] proposed that THBS1 might be involved in the transformation of the keratocytes into myofibroblasts during wound healing after a corneal keratectomy in rats. One of the potential roles of THBS1 is the activation of TGF-β. THBS1 has been demonstrated to be one of the most important activators of TGF-β1,[6,22,23] which induces keratocyte proliferation, myofibroblast differentiation, and extracellular matrix (ECM) production.[24–26] TGF-β1 is released and suspended within the ECM in a latent form, which is activated in response to injury.[27] It also has been observed that adhesion and migration were impaired in vitro in *Thbs1*$^{-/-}$ mouse corneal endothelium,[28] thus showing that THBS1 has a major role during endothelial wound healing as well.[29]

Since THBS1 is known to be expressed in remodeling corneal epithelium,[20] corneal stroma,[16] and corneal endothelium,[28,29] and is an activator of latent TGF-β1,[6,22,23] we hypothesized that THBS1 has an important role in corneal wound repair when the corneal barrier's integrity is compromised. We addressed this hypothesis by performing a full-thickness incision wound in the central cornea of adult THBS1-

www.iovs.org | ISSN: 1552-5783

deficient mice (*Thbs1*$^{-/-}$) and comparing them to wild type (WT) mice.

Materials and Methods

All studies were conducted in accordance with the ARVO Statement for Use of Animals in Ophthalmic and Vision Research. A full-thickness incision was performed with a 1.5-mm blade (Fine Science Tools, Foster City, CA) in the central cornea of 12- to 18-week-old male 129S2/SvPas (WT; The Jackson Laboratory, Bar Harbor, ME), and 12- to 18-week-old male and female 129S2/SvPas- *Thbs1*^{tm1Hyn}/*Thbs1*^{tm1Hyn} mice (*Thbs1*$^{-/-}$; a kind gift from Jack Lawler, Beth Israel Deaconess Medical Center, Harvard Medical School, Boston, MA). THBS1-deficient mice were generated in D3 ES cells, which were derived from the 129S2/SvPas strain.[13,30] The knockout allele is called *Thbs1*^{tm1Hyn}. Contralateral eyes served as controls. Approximately 70 animals of WT and *Thbs1*$^{-/-}$ were examined, allowing for at least 3 corneas to be examined per condition per time point.

Full-Thickness Penetrating Incision

At 20 minutes before the procedure, one drop of 1% atropine sulfate ophthalmic solution (Bausch and Lomb, Inc., Rochester, NY) was instilled in the right eye. In a preliminary experiment without topical instillation of atropine, chronic iris incarceration into the corneal incision was observed. Under the microscope, a nasal-temporal orientated full-thickness penetrating incision (1.5 mm in length) was created in the center of the cornea with a surgical blade. Animals were monitored with a slit-lamp (Topcon Medical Systems, Inc., Oakland, NJ) everyday for a week and then weekly until the end of the experiment. Intravital corneal examination also was performed at days 14 and 30 using a Heidelberg Retina Tomograph III (HRT; Heidelberg Engineering, Heidelberg, Germany). At the appropriate time (1, 2, 4, 7, 14, and 30 days) animals were euthanized and corneas either were processed for indirect immunofluorescence (IF; frozen sections and whole mounts) or transmission electron microscopy (TEM).

IF Microscopy

For frozen sections, the eyes were enucleated, frozen in OCT, 6 μm sections were cut, and IF was performed.[16] For whole mount, the corneas were enucleated, fixed in prechilled 100% methanol and dimethyl sulfoxide (4:1) for 2 hours at 20°C, and then stored in 100% methanol at 20°C until ready to use. The corneas were prepared for immunofluorescence as described by Pal-Ghosh et al.[31] The lens, iris, and retina were removed, and the corneas were cut in half, perpendicular to the original line of incision. Two cuts were placed in each half of the cornea to allow the corneas to lie flat, and then the sections and whole mounts were incubated at 4°C overnight with the following primary antibodies: SMA-FITC (Sigma-Aldrich, St. Louis, MO) and THBS1 (Abcam, Cambridge, MA). Then, the secondary antibody, rhodamine-conjugated donkey anti-mouse IgG (Jackson ImmunoResearch Laboratories, Inc., West Grove, PA) was applied for a 1-hour incubation at room temperature (sections) or overnight at 4°C (whole mounts). Coverslips were mounted with mounting media containing 4′6-diamidino-2-phenylindole (DAPI, Vectashield; Vector Laboratories, Burlingame, CA), a marker of all cell nuclei. The sections were examined and documented with a fluorescence microscope (Nikon Eclipse E800; Nikon, Melville, NY) equipped with a digital camera (SPOT; Diagnostic Instruments, Sterling Heights, MI). Whole mounts were examined with a Leica TCS-SP5 laser confocal scanning microscope (LCSM; Leica Microsystems, Bannockburn, IL). Three-dimensional image projections were performed with LAS AF Lite software (Leica Microsystems). Negative controls, where the primary antibody was omitted, were run with all experiments. As an additional control, irrelevant antibodies of the same isotype were compared to ensure specificity.

Transmission Electron Microscopy

Corneas were fixed in half-strength Karnovsky's fixative and processed for TEM, as described previously.[32] Briefly, fixed corneas were rinsed for 24 hours with cacodylate buffer 0.1 M and postfixed in 1% osmium tetroxide for 1 to 2 hours at room temperature. The tissue then was dehydrated in ascending concentrations of acetone, infiltrated with propylene oxide, and embedded in Epon plastic. Sections 60 to 90 angstroms (Å) thick were cut on an ultramicrotome (LKB ultramicrotome; LKB, Bromma, Sweden) and examined with an electron microscope (Philips 410 electron microscope; Philips Research Laboratories, Eindhoven, The Netherlands).

Results

Pathologic Manifestations of Lack of Thbs1

In WT corneas, the incision was sealed by wound-healing epithelium within 1 day. Incipient edema was observed during the first days around the incision, but corneas became transparent after 4 to 7 days (Figs. 1A, 1B). All *Thbs1*$^{-/-}$ corneas became chronically opaque from day 4 until the end of the experiment (Figs. 1E–H). In the WT mice, the stromal wound closed rapidly (Fig. 1B), healing with a thin scar (Figs. 1C, 1D). However, in *Thbs1*$^{-/-}$ corneas the incision gaped rather than sealing shut (Figs. 1E, 1F) and never appeared to close fully (Figs. 1G, 1H).

These findings were confirmed via intravital examination with the HRT. A highly reflective stromal tissue was observed under the epithelium of WT corneas by cross-section (Figs. 2A, 2B) and enface (Figs. 2E, 2F) scanning. At 2 weeks, WT corneas recovered almost the total thickness with a newly deposited stromal tissue (appears brightly) and a hyperplasic epithelium (Fig. 2A). However, both sides of the cleft remained separated (Fig. 2E). At 4 weeks, the incision was tightly contracted with a highly reflective matrix (Figs. 2B, 2F). Minimal reflective stromal tissue or stromal healing activity was found in *Thbs1*$^{-/-}$ corneas (Figs. 2C, 2D, 2G, 2H). In the endothelial layer, WT corneas showed high healing activity at 2 (Fig. 2A) and 4 (Fig. 2B) weeks after injury, as indicated by the high level of reflectance (arrowheads). No evidence of endothelial-healing activity was observed in *Thbs1*$^{-/-}$ corneas (Figs. 2C, 2D). The lack of endothelial repair in the *Thbs1*$^{-/-}$ corneas is consistent with the persistent edema seen in Figure 1, suggesting that THBS1 has an important role in endothelial migration during wound repair.

Localization of THBS1 After Incision

In corneal[16,20] and nonocular[1] models, THBS1 is deposited within 48 hours after injury. As seen in Figure 3, THBS1 was observed only in the endothelium of unwounded WT corneas (Fig. 3A), and then in the epithelium covering the incision 24 hours after wounding (Fig. 3B). At 48 hours after wounding, THBS1 expression was extended to surrounding epithelial cells and into the cleft created by the incision (Fig. 3D). As expected, no THBS1 was observed in the *Thbs1*$^{-/-}$ mouse corneas 24 and 48 hours after incision (Figs. 3C, 3E). Expression of THBS1 gradually increased by days 4 (Fig. 4A) and 7 (Fig. 4B), and was maximal at day 14 (Fig. 4C), where an interrupted column of THBS1 localization was visualized from

Investigative Ophthalmology & Visual Science

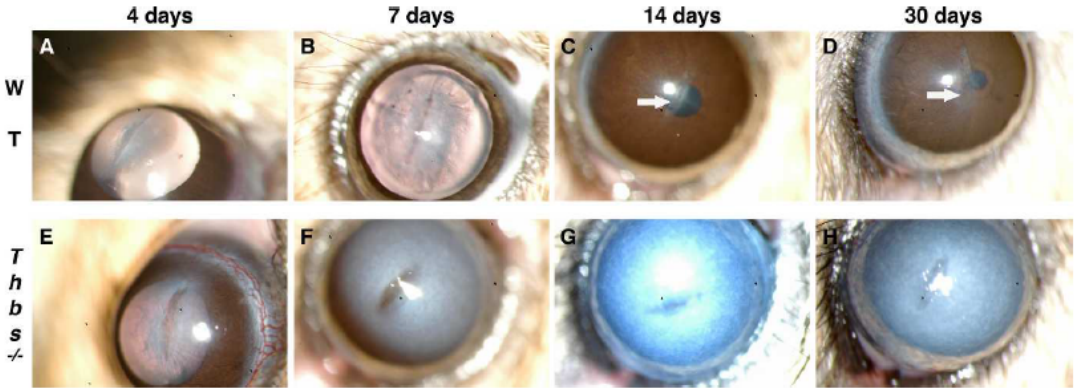

FIGURE 1. Slit-lamp evaluation of WT (A–D) and *Tbbs1*$^{-/-}$ (E–H) mouse corneas. In WT mice, stromal matrix contraction around the closed wound can be seen at 7 days (B). WT mice show transparent corneas with a thin reflective line of subepithelial haze in the incision area at 14 (C) and 30 (D) days. Scar indicated by *white arrows*. Lack of contractility with unclosed wounds can be observed at 4 (E) and 7 (F) days in *Tbbs1*$^{-/-}$. Persistent corneal edema with full opacity is observed from day 4 (E) until the end of the experiment (G, H).

the top of the epithelium to the endothelium. THBS1 levels were diminished by 30 days after injury (data not shown). Strikingly, THBS1 was elevated in the endothelium at these later time points (Figs. 4A–C). Localization of THBS1 in the epithelial cells was seen clearly in enface imaging (Figs. 4E–G). Presence of THBS1 in peripheral stroma, or epithelium of injured or unwounded corneas was not observed.

Myofibroblast Differentiation Appears to Correlate With THBS1 Expression

Cytoplasmic colocalization of THBS1 and α-smooth muscle actin (SMA) was evident in the epithelial cells of WT mice 4 days after wounding (Figs. 4E–G). In the *Tbbs1*$^{-/-}$ corneas, few, if any, SMA-positive epithelial cells were observed (Fig. 4D). The *Tbbs1*$^{-/-}$ corneas appeared to lack the ability to contract, as the wound remained open longer and appeared to gape (Fig. 1). In WT mice, myofibroblasts were observed on days 4 (Fig. 4A) and 7 (Fig. 4B) in the anterior aspect of the incision. By 14 days (Fig. 4C), as with THBS1, the presence of myofibroblasts reached its maximum, and a column of SMA-positive cells was observed connecting the epithelium with the endothelium (Fig. 4C). By 30 days after incision, no myofibroblasts or SMA-positive epithelial cells were observed, and the wound was fully sealed by new ECM (data not shown). Greatly

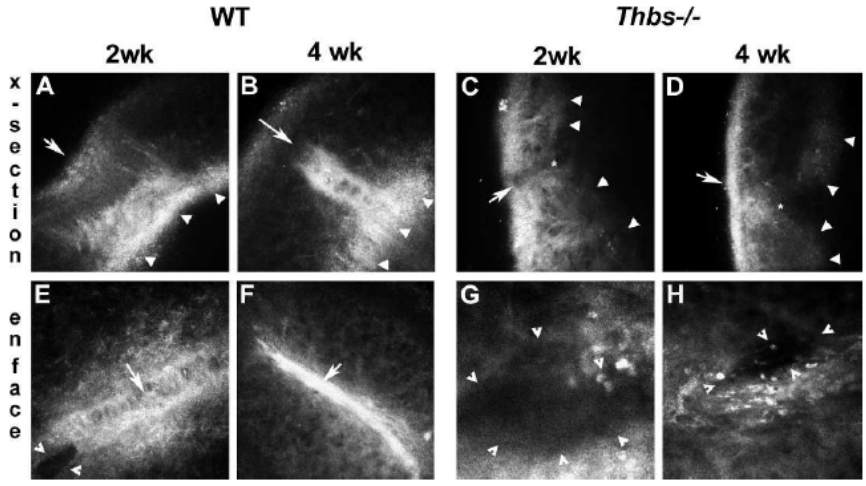

FIGURE 2. HRT intravital evaluation of WT (A, B, E, F) and *Tbbs1*$^{-/-}$ (C, D, G, H) mouse corneas 2 and 4 weeks after wounding showing cross-section (*x-section*) and enface images. A reflective fibrotic process can be observed in the WT stroma at 2 weeks (A, E) with the area of fibrosis appearing to contract at 4 weeks (B, F). Highly reflective endothelium indicating wound repair also can be observed at 2 and 4 weeks (A, B). In contrast, the absence of stromal or endothelial wound healing is evident in the *Tbbs1*$^{-/-}$ corneas (C, D, G, H). *White arrows* (A–F) indicate the incision. *Closed arrowheads* (A–D) indicate extent of posterior cornea. *Open arrowheads* (E, G, H) indicate gape in stroma, demonstrating lack of wound closure. *Asterisk* (C, D) indicates tip of cleft in *Tbbs1*$^{-/-}$ corneas. Also note highly pigmented cells in wound area of *Tbbs1*$^{-/-}$ corneas (G, H). At least three corneas per time point were examined with similar results.

Investigative Ophthalmology & Visual Science

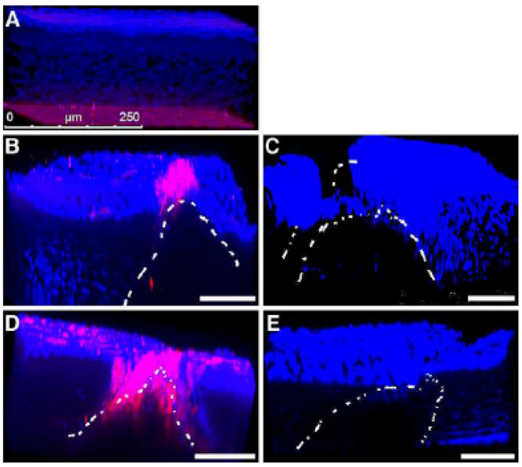

FIGURE 3. Three-dimensional projection of whole mount corneas immunolabeled with THBS1 (*pink*) in WT (A, B, D) and *Thbs1*$^{-/-}$ (C, E) mice, unwounded (A), and 24 (B, C) and 48 (D, E) hours after wounding. In unwounded cornea (A), THBS1 is present primarily in the endothelial cell layer. A *narrow line* of THBS1 is localized in the corneal epithelium of WT 24 hours after incision (B), which expanded to peripheral epithelium and stroma by 48 hours (D). As expected, no THBS1 was detected in *Thbs1*$^{-/-}$ mice (C, E). *White lines* show the borders of the incision. DAPI (*blue*) is a marker of all cell nuclei. *Scale bars*: 100 μm (B–E).

reduced numbers of myofibroblasts were observed in the *Thbs1*$^{-/-}$ corneas (Fig. 4D).

Corneal Endothelial Barrier Restoration Is Impaired Severely in Thbs1$^{-/-}$ Corneas

A proper endothelial function is essential to maintain the stroma with the appropriate hydration for keeping corneal transparency. Incipient edema in the corneas was observed around the incision in the WT mice before becoming transparent after 4 to 7 days (Figs. 1A, 1B). However, *Thbs1*$^{-/-}$ corneas remained chronically opaque until the end of the experiment (Figs. 1G, 1H). A reflective new tissue was observed at endothelial level in WT corneas, indicating a wound-healing process at 2 (Fig. 2A) and 4 (Fig. 2B) weeks, suggesting that the corneal endothelium is healing. This was confirmed in Figure 5 by TEM, where a new layer of endothelial cells was observed in the WT mice at day 15 after incision (Fig. 5A). Of interest, a new thin well-organized DM was found to be present between the stroma and the new corneal endothelial cells 2 weeks after injury (Fig. 5A). This incipient DM can be observed at the border of the wound area as a continuation of the unwounded DM. The lack of endothelial barrier in the *Thbs1*$^{-/-}$ was confirmed in vivo by slit-lamp and HRT examination (Figs. 2C, 2D). In the *Thbs1*$^{-/-}$, attenuated corneal endothelial cells were apparent in the wound area; however, no new DM was observed (Fig. 5B). The original DM appeared to be broken and curved into the stroma without continuation (Fig. 5B).

DISCUSSION

Previously, we demonstrated that THBS1 expression accompanied myofibroblast generation during the healing process after keratectomy in rats.[16] THBS1 was deposited into the stroma following a wound where the BMZ was damaged[16]; however, when the BMZ was left intact, THBS1 was expressed only in the most superficial aspect of the stroma, corresponding to the BMZ.[20] In concordance with Uno et al.,[20] we also showed previously that THBS1 expression was maximal early after wounding and gradually decreased.[16] These studies suggest that THBS1 has an important role in the healing process. In the current report, we made use of *Thbs1*$^{-/-}$ mice to examine further the role of THBS1, and we demonstrated that stromal, as well as endothelial healing, was severely impaired in mice lacking *Thbs1*. In the current model, a full-thickness corneal incision was performed. In WT mice at 24 hours, the expression of THBS1 was observed in the epithelium that covers the incision, but not in the stroma (Fig. 3B). Later, THBS1 expression extended gradually to the surrounding epithelial cells and down into the stroma around the wound, peaking at 14 days (Fig. 4C). At this time point, THBS1 was observed in an interrupted column pattern filling both sides of the incision from the epithelial surface to the endothelium (Fig. 4C); however, no THBS1 was observed in the unwounded peripheral stroma or epithelium (data not shown). One of the unexpected and most striking results of our investigation was that *Thbs1*$^{-/-}$ corneas rapidly became opaque after an incision wound and never appeared to heal. These results indicated that THBS1 is a necessary component of endothelial wound repair. This is supported further by the observation that THBS1 expression increased in the endothelial cell layer after wounding in the WT mice (Figs. 4A–C).

When the corneal integrity is compromised, epithelial cells quickly cover the damaged area by proliferation and migration.[33] In the stroma, keratocytes within the wound area undergo apoptosis, leaving the stroma devoid of cells that must be replaced, and the keratocytes surrounding the wound area proliferate and become fibroblasts.[34] These fibroblasts then migrate to fill the stromal wound area, with many of them differentiating into myofibroblasts, a cellular phenotype with contractile properties and ECM synthesis capabilities.[24,35,36] Such a healing environment, with myofibroblasts and new ECM, produces an optical phenomenon called light backscattering or subepithelial haze,[24,26] which usually disappears when the wound-healing process is done.[24] In the current work, subepithelial haze (Figs. 1A, 1B), reflective stromal and endothelial tissue (Figs. 2A, 2B, 2E, 2F), myofibroblasts (Fig. 4), and new ECM were observed in the WT mice. However, all of these processes were strikingly absent or reduced in *Thbs1*$^{-/-}$ mice. Previously, we observed that the expression of THBS1 correlated with the appearance of myofibroblasts after a corneal keratectomy in rats,[16] where THBS1 was localized in the wound area beginning at 1 day, and myofibroblasts were detected in the same area by day 4. A similar pattern was observed in the current work in mice. These data clearly suggested that keratocytes differentiate to become myofibroblasts in response to THBS1. Since it is known that THBS1 can activate TGF-β1, one possible mechanism of action would be the stimulation of keratocytes/fibroblasts by TGF-β1, which was activated by THBS1 in the wound area. One unclear aspect from our previous work[16] was whether fibroblasts, myofibroblasts, or epithelial cells were responsible for THBS1 expression. Confocal images revealed intracellular expression of THBS1 by epithelial and endothelial cells. Interestingly, many of the epithelial cells expressing THBS1 also expressed SMA, suggesting that they were myoepithelial cells. Presence of myoepithelial cells is well known in other tissues,[37,38] but is not well documented in the cornea. Hiscott et al. suggested a main role of THBS1 in the maintenance of the epithelial structure during wound repair.[39] This was confirmed by our results in the *Thbs1*$^{-/-}$ mice.

Investigative Ophthalmology & Visual Science

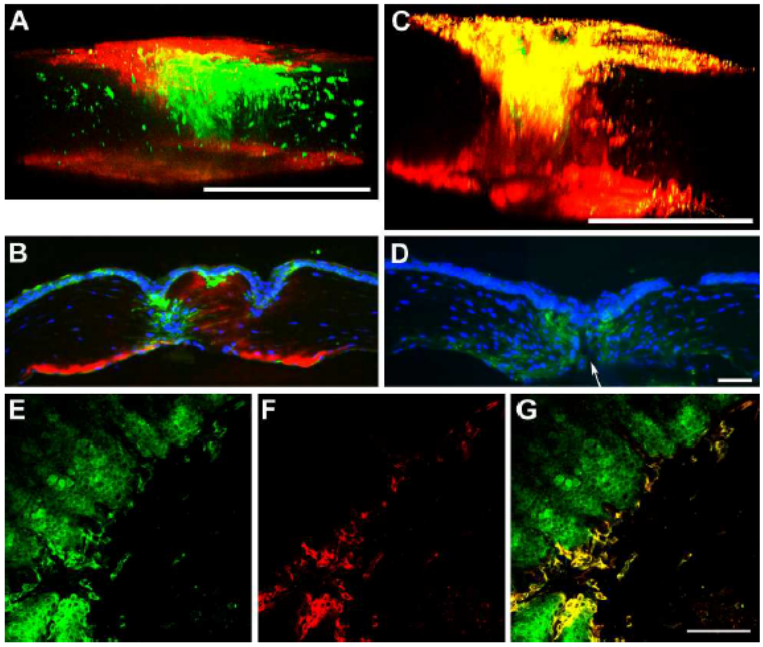

FIGURE 4. Immunolocalization of SMA (*green*) and THBS1 (*red*) in WT (A–C, E–G) and *Thbs1*$^{-/-}$ (D) mice. (A, C) Three-dimensional projection of whole mount corneas at 4 (A) and 14 (C) days after injury. (B, D) Cross-sections at 7 days after incision in WT (B) and *Thbs1*$^{-/-}$ (D) mice. (E–G) Epithelial localization in whole mount corneas 4 days after wounding: (E) SMA, (F) THBS1, and (G) SMA/THBS1 overlay. Note the expression of THBS1 in the epithelium, upper stroma, and endothelium after wounding (A–C). Colocalization of THBS1 and SMA is evident at 14 days (C), and SMA-positive cells extend further from edge of wound than THBS1-positive cells (E–G). Also, note the gape (*arrow*) in the *Thbs1*$^{-/-}$ cornea (D) and reduced level of SMA localization compared to (B). DAPI (*blue*) is a marker of all cell nuclei. *Scale bars*: 250 μm (A, C), 50 μm (D, G).

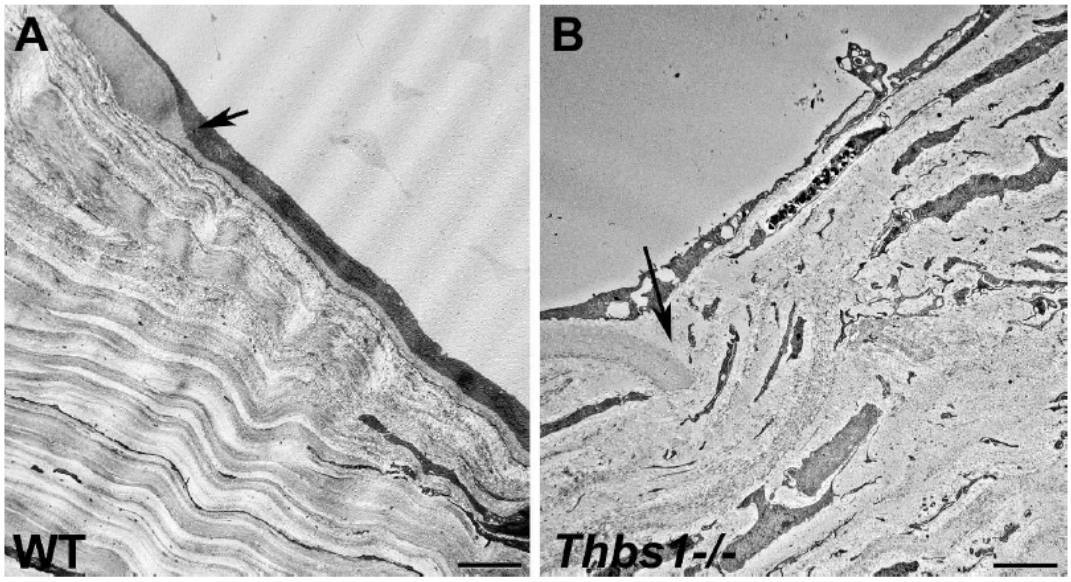

FIGURE 5. TEM micrographs of WT (A) and *Thbs1*$^{-/-}$ (B) mouse corneas 15 days after incision. In WT corneas (A), the endothelium has migrated to cover the wound area and the DM is partially restored. In contrast, only highly attenuated endothelial cells are seen in *Thbs1*$^{-/-}$ corneas (B) and no signs of DM regeneration were observed. *Arrows* indicate edge of cut DM. *Scale bars*: 5 μm.

Investigative Ophthalmology & Visual Science

In contrast to the epithelial cells, no myofibroblasts or keratocytes expressed intracellular THBS1. While this does not rule out the possibility that myofibroblasts, nerves, or inflammatory cells are producing THBS1, our data were consistent with the epithelial cells being a primary source. Interestingly, the corneal endothelium also appeared to be a source of THBS1. In our study, we extended our work to demonstrate that THBS1 is critical also for endothelial restoration, since *Thbs1*$^{-/-}$ mice develop chronic edema and persistent corneal opacification. Neither of these healing defects was observed in the WT mice. In the WT mice, THBS1 expression was observed to increase in the healing endothelium from day 4 (Fig. 4A) until the end of the experiment, reaching maximal intensity at 14 days (Fig. 4C). The new monolayer rests over a thin, but well-defined DM (Fig. 5A). Dramatically, all of these components are missing in the *Thbs1*$^{-/-}$ mouse corneas. It is well established that endothelial cell proliferation is lacking in humans[40]; however, if the endothelial barrier is damaged, a restorative process occurs by migration and/or hypertrophy of surrounding endothelial cells.[41,42] In lung microvascular endothelia, THBS1 increases tyrosine phosphorylation of components in the cell-cell adherens junctions, inducing actin reorganization and focal adhesion disassembly.[43,44] Migration, hypertrophy, and adhesion are impaired in vitro in *Thbs1*$^{-/-}$ mouse endothelial cells,[28] suggesting a major role of THBS1 during the endothelial barrier repair,[29] which is confirmed strongly by our in vivo results. In addition, previous studies have demonstrated that TGF-β1 stimulates endothelial cells to proliferate, migrate, and produce ECM.[45–47] The THBS1 binds the TGF-β–LAP,[11] leading to activation of endogenous TGF-β expressed by endothelial cells.[48] It also has been suggested that TGF-β1 has a role in maintaining the endothelial cells in a nonproliferative state.[49] Our results suggested that TGF-β1 and THBS1 have an important role in endothelial cell repair.

In our current study, we made the novel observation that penetrating wounds in *Thbs1*$^{-/-}$ corneas fail to heal, and exhibit persistent edema and prolonged wound gaping. We have demonstrated that lack of endothelial healing and wound contraction is the functional mechanism that appears to cause these defects. However, we have not uncovered the molecular mechanism of THBS1 in these processes. While THBS1 has been shown to have an important role in activation of TGF-β1, which certainly may have a role in these processes, THBS1 has been demonstrated to have multiple effects in the cornea. Haddadin et al. have demonstrated that *Thbs1*$^{-/-}$ corneas are thinner than WT by 6.5% and that intraocular pressure was reduced by 10%.[50] This could make the cornea more susceptible to healing defects. In addition, THBS1 has an important role in maintaining immune privilege, in that THBS1 derived from antigen-presenting cells is necessary to suppress immune rejection.[51] It is not clear if immune rejection has a role in our studies; however, THBS1 derived from immune cells certainly could be involved in the healing response. In addition to its role in immune suppression, lack of THBS1 also has been reported to result in ocular surface defects that mimic dry eye.[52] Again, it is not clear if this impacts our studies, but it is possible that these ocular surface defects make the cornea susceptible to wound-healing defects. Finally, Sekiyama et al.[17] suggest that THBS1 is bound or trapped by Bowman's layer in human corneas. Our data in mice and rats, which lack Bowman's layer, supported their findings in that we see minimal accumulation of THBS1 at the epithelial/stromal interface.[16] In total, there appear to be multiple potential molecular mechanisms of THBS1 that may affect corneal wound repair.

We concluded that THBS1 has critical roles during corneal restoration when its integrity is compromised by a penetrating incision, including endothelial migration and stromal contraction. Based on our results and other published reports, THBS1 expression and persistence in the tissue seem to be related to the extent of the injury, ranging from a few hours in the BMZ[20] of an epithelial wound to a few days in the upper aspect of the stroma of a superficial keratectomy[16] to one month in all the corneal layers following a penetrating wound. THBS1 also appears to be expressed by the corneal epithelium and endothelium, and has a role in epithelial, stromal, and endothelial repair. These experiments raise many questions regarding the mechanisms of THBS1 in wound repair; however, these questions will be addressed in further work.

Acknowledgments

Supported by National Institutes of Health/National Eye Institute Grants EY005665 (JDZ), EY05665-25S1 (JDZ), and EY03790 (Core-JDZ).

Disclosure: **J.T. Blanco-Mezquita**, None; **A.E.K. Hutcheon**, None; **J.D. Zieske**, None

References

1. Bornstein P. Thrombospondins as matricellular modulators of cell function. *J Clin Invest*. 2001;107:929–934.
2. Carlson CB, Lawler J, Mosher DF. Structures of thrombospondins. *Cell Mol Life Sci*. 2008;65:672–686.
3. Baenziger NL, Brodie GN, Majerus PW. A thrombin-sensitive protein of human platelet membranes. *Proc Natl Acad Sci U S A*. 1971;68:240–243.
4. Lawler J. The functions of thrombospondin-1 and-2. *Curr Opin Cell Biol*. 2000;12:634–640.
5. Leung LL. Role of thrombospondin in platelet aggregation. *J Clin Invest*. 1984;74:1764–1772.
6. Murphy-Ullrich JE, Gurusiddappa S, Frazier WA, Hook M. Heparin-binding peptides from thrombospondins 1 and 2 contain focal adhesion-labilizing activity. *J Biol Chem*. 1993; 268:26784–26789.
7. Sheibani N, Frazier WA. Thrombospondin-1, PECAM-1, and regulation of angiogenesis. *Histol Histopathol*. 1999;14:285–294.
8. Taraboletti G, Roberts DD, Liotta LA. Thrombospondin-induced tumor cell migration: haptotaxis and chemotaxis are mediated by different molecular domains. *J Cell Biol*. 1987; 105:2409–2415.
9. Darby I, Skalli O, Gabbiani G. Alpha-smooth muscle actin is transiently expressed by myofibroblasts during experimental wound healing. *Lab Invest*. 1990;63:21–29.
10. Desmouliere A, Geinoz A, Gabbiani F, Gabbiani G. Transforming growth factor-beta 1 induces alpha-smooth muscle actin expression in granulation tissue myofibroblasts and in quiescent and growing cultured fibroblasts. *J Cell Biol*. 1993; 122:103–111.
11. Murphy-Ullrich JE, Schultz-Cherry S, Hook M. Transforming growth factor-beta complexes with thrombospondin. *Mol Biol Cell*. 1992;3:181–188.
12. Friedman SL. Seminars in medicine of the Beth Israel Hospital, Boston. The cellular basis of hepatic fibrosis. Mechanisms and treatment strategies. *N Engl J Med*. 1993;328:1828–1835.
13. Agah A, Kyriakides TR, Lawler J, Bornstein P. The lack of thrombospondin-1 (TSP1) dictates the course of wound healing in double-TSP1/TSP2-null mice. *Am J Pathol*. 2002; 161:831–839.
14. Streit M, Velasco P, Riccardi L, et al. Thrombospondin-1 suppresses wound healing and granulation tissue formation in the skin of transgenic mice. *EMBO J*. 2000;19:3272–3282.

15. Hiscott P, Seitz B, Schlotzer-Schrehardt U, Naumann GO. Immunolocalisation of thrombospondin 1 in human, bovine and rabbit cornea. *Cell Tissue Res*. 1997;289:307–310.
16. Matsuba M, Hutcheon AE, Zieske JD. Localization of thrombospondin-1 and myofibroblasts during corneal wound repair. *Exp Eye Res*. 2011;93:534–540.
17. Sekiyama E, Nakamura T, Cooper LJ, et al. Unique distribution of thrombospondin-1 in human ocular surface epithelium. *Invest Ophthalmol Vis Sci*. 2006;47:1352–1358.
18. Cao Z, Wu HK, Bruce A, Wollenberg K, Panjwani N. Detection of differentially expressed genes in healing mouse corneas, using cDNA microarrays. *Invest Ophthalmol Vis Sci*. 2002;43:2897–2904.
19. Hiscott P, Armstrong D, Batterbury M, Kaye S. Repair in avascular tissues: fibrosis in the transparent structures of the eye and thrombospondin 1. *Histol Histopathol*. 1999;14:1309–1320.
20. Uno K, Hayashi H, Kuroki M, et al. Thrombospondin-1 accelerates wound healing of corneal epithelia. *Biochem Biophys Res Commun*. 2004;315:928–934.
21. Uno K, Kuroki M, Hayashi H, Uchida H, Kuroki M, Oshima K. Impairment of thrombospondin-1 expression during epithelial wound healing in corneas of vitamin A-deficient mice. *Histol Histopathol*. 2005;20:493–499.
22. Young GD, Murphy-Ullrich JE. Molecular interactions that confer latency to transforming growth factor-beta. *J Biol Chem*. 2004;279:38032–38039.
23. Bornstein P. Thrombospondins function as regulators of angiogenesis. *J Cell Commun Signal*. 2009;3:189–200.
24. Jester JV, Petroll WM, Cavanagh HD. Corneal stromal wound healing in refractive surgery: the role of myofibroblasts. *Prog Retin Eye Res*. 1999;18:311–356.
25. Jester JV, Barry-Lane PA, Petroll WM, Olsen DR, Cavanagh HD. Inhibition of corneal fibrosis by topical application of blocking antibodies to TGF beta in the rabbit. *Cornea*. 1997;16:177–187.
26. Moller-Pedersen T, Cavanagh HD, Petroll WM, Jester JV. Corneal haze development after PRK is regulated by volume of stromal tissue removal. *Cornea*. 1998;17:627–639.
27. Barcellos-Hoff MH. Latency and activation in the control of TGF-beta. *J Mammary Gland Biol Neoplasia*. 1996;1:353–363.
28. Scheef EA, Huang Q, Wang S, Sorenson CM, Sheibani N. Isolation and characterization of corneal endothelial cells from wild type and thrombospondin-1 deficient mice. *Mol Vis*. 2007;13:1483–1495.
29. Munjal ID, Crawford DR, Blake DA, Sabet MD, Gordon SR. Thrombospondin: biosynthesis, distribution, and changes associated with wound repair in corneal endothelium. *Eur J Cell Biol*. 1990;52:252–263.
30. Lawler J, Sunday M, Thibert V, et al. Thrombospondin-1 is required for normal murine pulmonary homeostasis and its absence causes pneumonia. *J Clin Invest*. 1998;101:982–992.
31. Pal-Ghosh S, Pajoohesh-Ganji A, Brown M, Stepp MA. A mouse model for the study of recurrent corneal epithelial erosions: alpha9beta1 integrin implicated in progression of the disease. *Invest Ophthalmol Vis Sci*. 2004;45:1775–1788.
32. Gipson IK, Kiorpes TC, Brennan SJ. Epithelial sheet movement: effects of tunicamycin on migration and glycoprotein synthesis. *Dev Biol*. 1984;101:212–220.
33. Zieske JD. Expression of cyclin-dependent kinase inhibitors during corneal wound repair. *Prog Retin Eye Res*. 2000;19:257–270.
34. Zieske JD, Guimaraes SR, Hutcheon AE. Kinetics of keratocyte proliferation in response to epithelial debridement. *Exp Eye Res*. 2001;72:33–39.
35. Wilson SE. Analysis of the keratocyte apoptosis, keratocyte proliferation, and myofibroblast transformation responses after photorefractive keratectomy and laser in situ keratomileusis. *Trans Am Ophthalmol Soc*. 2002;100:411–433.
36. Maltseva O, Folger P, Zekaria D, Petridou S, Masur SK. Fibroblast growth factor reversal of the corneal myofibroblast phenotype. *Invest Ophthalmol Vis Sci*. 2001;42:2490–2495.
37. Berman JJ. *Neoplasms: Principles of Development and Diversity*. Sudbury, MA: Jones and Bartlett Publishers; 2009.
38. Raubenheimer EJ. The myoepithelial cell: embryology, function, and proliferative aspects. *Crit Rev Clin Lab Sci*. 1987;25:161–193.
39. Hiscott P, Paraoan L, Choudhary A, Ordonez JL, Al-Khaier A, Armstrong DJ. Thrombospondin 1, thrombospondin 2 and the eye. *Prog Retin Eye Res*. 2006;25:1–18.
40. Bahn CF, Glassman RM, MacCallum DK, et al. Postnatal development of corneal endothelium. *Invest Ophthalmol Vis Sci*. 1986;27:44–51.
41. Jacobi C, Zhivov A, Korbmacher J, et al. Evidence of endothelial cell migration after Descemet membrane endothelial keratoplasty. *Am J Ophthalmol*. 2011;152:537–542.
42. Watson SL, Abiad G, Coroneo MT. Spontaneous resolution of corneal oedema following Descemet's detachment. *Clin Experiment Ophthalmol*. 2006;34:797–799.
43. Goldblum SE, Young BA, Wang P, Murphy-Ullrich JE. Thrombospondin-1 induces tyrosine phosphorylation of adherens junction proteins and regulates an endothelial paracellular pathway. *Mol Biol Cell*. 1999;10:1537–1551.
44. Liu A, Mosher DF, Murphy-Ullrich JE, Goldblum SE. The counteradhesive proteins, thrombospondin 1 and SPARC/osteonectin, open the tyrosine phosphorylation-responsive paracellular pathway in pulmonary vascular endothelia. *Microvasc Res*. 2009;77:13–20.
45. Grant MB, Khaw PT, Schultz GS, Adams JL, Shimizu RW. Effects of epidermal growth factor, fibroblast growth factor, and transforming growth factor-beta on corneal cell chemotaxis. *Invest Ophthalmol Vis Sci*. 1992;33:3292–3301.
46. Plouet J, Gospodarowicz D. Transforming growth factor beta-1 positively modulates the bioactivity of fibroblast growth factor on corneal endothelial cells. *J Cell Physiol*. 1989;141:392–399.
47. Usui T, Takase M, Kaji Y, et al. Extracellular matrix production regulation by TGF-beta in corneal endothelial cells. *Invest Ophthalmol Vis Sci*. 1998;39:1981–1989.
48. Sumioka T, Ikeda K, Okada Y, Yamanaka O, Kitano A, Saika S. Inhibitory effect of blocking TGF-beta/Smad signal on injury-induced fibrosis of corneal endothelium. *Mol Vis*. 2008;14:2272–2281.
49. Joyce NC, Harris DL, Mello DM. Mechanisms of mitotic inhibition in corneal endothelium: contact inhibition and TGF-beta2. *Invest Ophthalmol Vis Sci*. 2002;43:2152–2159.
50. Haddadin RI, Oh DJ, Kang MH, et al. Thrombospondin-1 (TSP1)-null and TSP2-null mice exhibit lower intraocular pressures. *Invest Ophthalmol Vis Sci*. 2012;53:6708–6717.
51. Zamiri P, Masli S, Kitaichi N, Taylor AW, Streilein JW. Thrombospondin has a vital role in the immune privilege of the eye. *Invest Ophthalmol Vis Sci*. 2005;46:908–919.
52. Turpie B, Yoshimura T, Gulati A, Rios JD, Dartt DA, Masli S. Sjögren's syndrome-like ocular surface disease in thrombospondin-1 deficient mice. *Am J Pathol*. 2009;175:1136–1147.

Investigative Ophthalmology & Visual Science

CHAPTER 3

Intravital Confocal Microscopy Reveals Corneal Involvement in an Allergic Eye Disease Mouse Model: an in vivo Study

Intravital Confocal Microscopy Reveals Corneal Involvement in an Allergic Eye Disease Mouse Model: an *in vivo* Study

Tomas Blanco[1, 2, 3], Hyun Soo Lee[3], Daniel R. Saban[1,4].

[1]Ophthalmology Department, Duke Eye Center, Duke School of Medicine, Durham, NC

[2]Ophthalmology Department, IOBA, Valladolid School of Medicine, Valladolid, Spain

[3]Ophthalmology Department, Schepens Eye Research Institute & Massachusetts Eye and Ear, Harvard Medical School, Boston, MA.

[4]Immunology Department, Duke Eye Center, Duke School of Medicine, Durham, NC

Supported by Research to Prevent Blindness, Career Development Award (Saban); R01EY021798 (Saban).

Disclosure: The authors of this manuscript have no conflicts of interest to disclose as described by the IOVS

Abstract

Purpose: Allergic eye disease (AED) occurs mostly in the conjunctiva, but is only thought to significantly involve the cornea in advance forms (e.g. allergic keratoconjunctivitis). We intravitally investigated inflammatory cell infiltration (IC) of the ocular surface in an AED experimental mouse model.

Methods: Allergic conjunctivitis (AC) was induced in C57BL/6 mice via immunization with ovalbumin (OVA; 100µg)/pertussis toxin (300ng)/alum (1mg), and challenged with OVA (250 ug) eye drops once daily for 7 days. Standardized slit lamp scoring of AED clinical signs (lid edema, tearing, chemosis and redness) was done. *In vivo* confocal microscopy (IVCM) was performed with a Heidelberg Retina Tomograph III (HRT3). Flow cytometry and immunofluorescence (laser scanning confocal microscopy, LSCM) were additionally performed. Experiments (n=4) were repeated 3 times

Results: Increased AED clinical scores began on challenge day 3 in immunized mice relative to non-immunized mice ($p<0.01$). HRT3 showed an increased number of hyper-reflective events in bulbar conjunctiva and cornea of immunized mice compared to non-immunized mice ($p<0.01$). Flow cytometry indicated a significant increment in the CD11b+ frequency in the conjunctiva and cornea of immunized mice compared non-immunized mice ($p<0.01$). LSCM showed mononuclear cells in the conjunctiva and cornea similarly included monocytes in immunized mice.

Conclusions: IVCM allows visualization and quantitation of ICs in both conjunctiva and cornea in an experimental AED mouse model. Significant IC infiltration occurs throughout the cornea and the kinetics of their recruitment is associated with progression of AED clinical signs. The detection of ICs in the transparent cornea during progression of AED may represent an important component in the pathology of this disease.

INTRODUCTION

Ocular inflammation such as allergy, dry eye, trauma or surgery involves a complex immune response in the ocular surface [1]. The ocular surface is composed of conjunctiva, a mucosal tissue, and the cornea, the transparent window of the eye. The ocular surface often is exposed to pathogens, cosmetics and environment agents (e.g. pollen, dust mites, dander, smoke or pollution) that cause inflammation of the conjunctiva. Conjunctivitis diagnosis varies depending on etiology (viral, bacterial, chemical); however, allergic conjunctivitis (AC) is the most common ophthalmologic incidence in developed countries [2]. AC represents a spectrum of disorders that affect the lid, conjunctiva, and in more severe forms, the cornea [3]. Mild forms of AC include seasonal allergic conjunctivitis (SAC) and perennial allergic conjunctivitis (PAC) that are induced by environmental agents such as grass, pollens, or cat dander [4-6]. Together SAC and PAC comprise 95% of AC cases [4-6]. More severe forms include atopic keratoconjunctivitis (AKC) and vernal keratoconjunctivitis (VKC) [7-9]. SAC and PAC remain self-limited and present no corneal damage. By contrast, AKC and VKC progress with corneal involvement, producing discomfort, pain and may lead to impaired vision and corneal transplantation [5, 7].

AC is an immediate hypersensitivity reaction that occurs in response to an allergen encountered at the ocular surface [1] . The development of AC consists of two phases: an early and a late phase reaction. The early phase occurs within minutes after antigen exposure. The allergen cross-links specific IgE antibodies bound via FcεRI receptors on the surface of ocular mast cells resulting in the release of histamine, leukotrienes, proteases, prostaglandins and cytokines [10-12]. Classic symptoms of immediate hypersensitivity are itching, lid edema, tearing, chemosis, hyperemia, and conjunctival redness [13]. The late phase occurs hours after allergen exposure and involves the infiltration of inflammatory cells, primarily eosinophils but also other granulocytes, as well as monocytes and dendritic cells (DCs) [10]. Th2 cells are critical for the development and sustenance of an allergic response. The IL-4 produced by primed Th2 cells is

involved in isotype class switching, allowing B cells to secrete IgE. IL-5 Th2-produced, activates and promotes the maturation of infiltrating eosinophils [14], while IL-13 is involved in increasing mucus production in allergic responses [15]

Severe ocular allergic diseases are characterized also by a variety of corneal disorders such as persistent epithelial defects and shield ulcer. Cornea and conjunctiva are believed to affect each other during ocular allergic inflammation; however, direct evidence for interaction between both is still drought [16]. Loss of corneal epithelium exacerbates conjunctival allergic inflammation; conversely, eosinophil infiltration into the conjunctiva impairs epithelium healing. Eosinophils and eosinophil-derived factors are implicated in the pathogenesis of corneal lesions associated with ocular allergy. Cytotoxic granule proteins derived from eosinophils such as major basic protein and matrix metalloproteinase 9 have been detected in shield ulcer. Thus, conjunctival allergic inflammation and corneal epithelial disorders influence each other to generate a vicious cycle, interruption of which might provide the basis for novel approaches to the treatment of severe ocular allergy [16, 17]. Fukuda et al., suggested that the establishment of animal models of severe ocular allergy that manifest corneal complications should also increase the understanding of the pathogenesis of such disease and provide a basis for development of novel treatments [16].

HRT3 is a laser-scanning in vivo confocal microscope system (IVMC) for imaging of anterior and posterior segments of the eye. IVCM with the HRT Rostock Cornea Module (HRT3/RCM) provides detailed views of the ocular surface [18]. Corneal module helps to differentiate bacterial, viral, parasitic and fungal infections, but also can be used for image of LASIK flaps, filtering blebs, counting endothelial cells, dystrophies diagnosis, post surgical follow-up and many other applications [19, 20]. We recently observed the presence of inflammatory cells (ICs) by using an IVCM system, in a mouse model of corneal wound healing [21]. Herein we confirmed previous studies and extended to investigate at real time the inflammatory process in an AC mouse model.

MATERIAL AND METHODS

Mice and Anesthesia

Fifty-four C57BL/6 8 weeks old female mice were purchased from Charles River Laboratories (Wilmington, MA). Mice were housed in a specific pathogen-free environment at the Schepens Eye Research Institute animal facility. All procedures were approved by the Institutional Animal Care and Use Committee following ARVO Statement for the Use of Animals in Ophthalmic and Vision Research. Anesthesia was used for all procedures with intraperitoneal (IP) administered ketamine/xylazine suspensions (120 and 20 mg/kg, respectively).

AC induction by active immunization

Following a previous protocol [22], AC was induced in mice by immunizing with ovalbumin (OVA) (Sigma-Aldrich, St. Louis, MO allergen). Briefly: mice were given an IP injection of 100 μg of OVA, 300 ng of pertussis toxin (Sigma-Aldrich) and 1 mg of aluminum hydroxide (Sigma-Aldrich) in PBS. After 14 days, immunized mice received a 250 μg of OVA in PBS instilled on the right eye daily for up to 7 days (immunized). Control mice were not immunized but received OVA instillations (naive not immunized). Additional mice not immunized nor challenged were used as a normal control.

AC Clinical Scoring

As described previously [23], clinical score was performed by two independent observers. Briefly, scoring was performed daily at 20 minutes, 6 and 24 hours after challenge. Mice were examined with the slip lamp based on four independent parameters, which include lid swelling, tearing, chemosis, and conjunctival vasodilation (redness) [23]. Each parameter was ascribed 0 (i.e., absent) to 3+ points (i.e., maximal) and was summed to yield a maximum score of 12.

Intravital HRT3 examination

For *intravital* examination, a Heidelberg Retina Tomograph equipped with a Rostock Cornea Module (HRT3/RCM, Heidelberg Engineering GmbH, Heidelberg, Germany), was used as *in vivo* confocal microscope (IVCM). Under anesthesia, mice were wrapped in a thermal cloth inside modified decapa-cones. During the procedure, mice temperature was continuously monitored with a temperature controller and maintained in a 37-39°C threshold (ATC 1000 DD, LKC Technologies, Gaithersburg, MD). Genteal® lubrican eye gel (Novartis Pharmaceuticals Corp, East Han- over, New Jersey) was applied in both eyes. Right eye was examined before first challenge, 20 minutes, 6 hours and 24 hours after. The same procedure was repeated daily for up to 7 days. Several cross-scanner sections were sequentially taken in the same area at superior and inferior conjunctiva; nasal, temporal and central cornea (***Figure 1A***). The HRT3 works with a diode laser with wavelength of 670nm as a laser source. The RCM device is equipped with a 400µm diameter lens and a 60x magnification water immersion objective with a numerical aperture 0.90 (Olympus, Hamburg, Germany). Images were taken with a 400µm lens with a transverse optical resolution of 1µm/pixel. HRT/RCM offers a semi-automatic endothelial cell counting feature. On the endothelial cell image, a region of interest is marked, then following one of several accepted counting methods, cells are marked and the system automatically calculates cell density. This application was used for counting hyper-reflective cells in an equal pre-marked area. Each cell was labeled using the interactive computer display. The number of marks was automatically counted by the computer and cellular densities expressed as cells/mm^2. The analysis was carried out in a masked fashion.

Enzymatic Digestion and Flow Cytometry

Mice were euthanized on day 3 and 7. The conjunctiva (including bulbar through palpebral regions from separated superior and inferior areas) was surgically procured. A 1.5 mm diameter corneal bottom was procured from the center of the cornea. The

remaining corneal ring was excised in both temporal and nasal regions. Single-cell suspensions were prepared using standard collagenase digestion methods as previously described [24]. Briefly, tissue pieces were minced into small fragments, followed by digestion with 2 mg/mL of collagenase type IV and 0.5 mg/mL of DNase I (Roche, Basel, Switzerland) for 2 to 3 hours at 37°C. The suspension was triturated using a syringe and filtered through a 70μm cell strainer. Cells were thoroughly washed and resuspended in 0.5% bovine serum albumin (BSA) (Invitrogen) buffer, followed (by blocking of FcγRIII/II with CD16/CD32 antibodies as per the manufacturer's instructions (BD Pharmingen, San Diego, CA). Cells were stained as per the manufacturer's instructions with DAPI and following antibodies anti-CCR2 (clone 30-F11)-Alexa 488, anti-Ly6C-Alexa 700, anti CD11b-PE and anti-CD11c-PE-Cy5 (Biolegend). After 30 minutes, cells were washed, resuspended in PBS and analyzed with BD LSR II flow cytometer (BD Biosciences, San Jose, CA). Cell population was identified by forward and side scattering. The dead cells were excluded by DAPI staining and the single cells were separated from doublets. CD45+ cells were divided in three different subpopulations of $CCR2^{+}Ly6\text{-}C^{High}$, $CCR2^{-}Ly6\text{-}C^{Low}$ and $CCR2^{-}Ly6\text{-}C^{-}$. The CD11b+ and CD11c+ cells were separated and CD11b population was enumerated.

Whole Mounts Immunofluorescence

At the day 3 and 7, conjunctiva and corneal tissue were excised as described above and fixed in 4% PFA. The conjunctiva was transversely sectioned in two equals. Corneas were sectioned into a flowered pattern to aid in flattening the tissue. The tissue was washed three times with PBS and posteriorly shocked for 30 minutes in 2% BSA buffer, following with blocking of FcγRIII/II with anti-CD16/CD32 antibodies (BD Pharmingen, San Diego, CA). Tissues were stained with mouse monoclonal anti-α-CD11b-FITC antibody (1:500 in PBS 2% BSA, Biolegend), mouse anti-Ly6C-APC (1:500 in PBS 2% BSA, Biolegend) and monoclonal rat anti-F4/80 (overnight at 4ºC, Serotec) followed by

Alexa 594 secondary antibody (Jackson) (1 hour, room temperature). To achieve the best flattening, mounting medium with DAPI (Vectashield; Vector Laboratories) was added allowing place tissue epithelial-side-up and then cover-slipped. The whole mounts were examined with a Leica TCS-SP5 laser confocal scanning microscope (LSCM) (Leica Microsystems, Bannockburn, IL). A 3-D reconstitution and orthogonal image projection were performed with LAS AF Lite software (Leica Microsystems, Bannockburn, IL). Samples stained only with secondary antibodies or with isotype control antibodies followed the secondary antibodies were included as the negative controls to ensure the specificity of the staining.

Light microscopy

After LSCM scanning, conjunctival tissue was rinsed in ice cold PBS, embedded in OCT and frozen. Cross-sections (7 μm) were performed with a cryostat. Sections were stained with hematoxylin and eosin (H&E), Giemsa, and Toloudine Blue (TB).

Statistical analysis

Statistical analyses included 1-way ANOVA and Bonferroni's Multiple Comparison Test, in addition to two-tailed Student's t-test. Standard error and standard deviation of the mean were calculated. A p-value <0.05 was considered statistically significant and p-value <0.01 high statistically significant.

RESULTS

Mice Developed Strong Symptoms of AC Following OVA Challenge

Mice were OVA challenged once daily for 7 days, and masked scoring was performed each day at 20 min post challenge (i.e. immediate hypersensitivity response), as well as 6 hours and 24 hours post challenge (i.e. late phase response).

Both Immunized and naive mice showed an immediate hypersensitivity response with increase in the tearing directly after challenge; however, no differences were observed between both groups until day 3 (***Figure 1***). At day 7 prominent lid swelling, abundant tearing, chemosis, mucous discharge, severe redness and occlusion of the Meibomian glands ducts were observed in the immunized mice (***Figure 1A***). Despite severe clinical symptoms of allergic inflammation, immunized corneas remained transparent in the central part throughout the duration of the experiment (***Figure 1A***). An incipient edema was observed in the periphery-limbal area at the end of the experiment (***Figure 1A***). Naive non-immunized mice did not show any significant increase in the clinical score after day 3 nor corneal edema (***Figure 1A***)

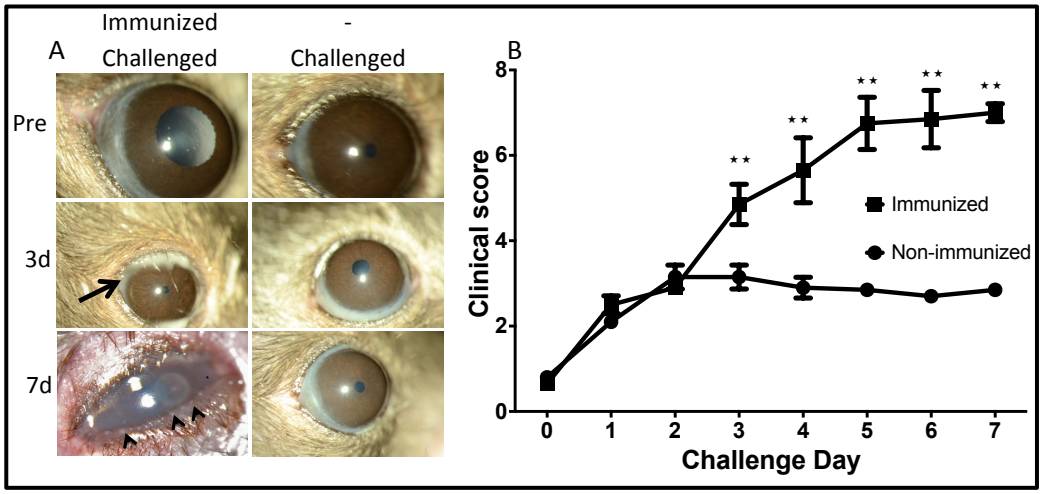

Figure 1. Clinical progression of allergic eye disease
Sensitized mice progressed with stronger symptoms of ocular allergy than non-immunized mice after topical challenge with OVA. A) Mice were scored for clinical signs (lid swelling, tearing/discharge, conjunctival chemosis and hyperemia). Corneas remained transparent by the slip lamp. Black arrow: white mucous discharge. Black arrowheads: obstruction of the Meibomian gland ducts B) Graph shows the results from one experiment (n=4/group), and is representative of 3 independent experiments.
** $p<0.01$

IVCM quantification of Cellular Infiltrates in the Conjunctiva

The process of cellular infiltration into de conjunctiva was intravitally observed utilized with an IVCM. Hyper-reflective cells were observed immediately within hours after first challenge (***Figure 2B***). The cells were located in the anterior part of the conjunctiva underneath the epithelium. The superior conjunctiva appeared visibly inflamed after few hours (***Figure 2B***). The parenchyma showed swelling collagen fibers separated from one another with bright cells located in between (***Figures 2B and C***). The inferior conjunctiva was less accessible with the microscope; therefore, swelling was not observed compared

to the superior aspect. No stromal swelling was observed in any non-immunized mice (data not showed). Six hours post-challenge the number of ICs increased (178±18 superior, 121±13 inferior) in the immunized mice compared to (142±16 superior, 0 inferior) in the naive mice (***Figure E***). Twenty-four hours later, cell infiltration happened in both superior and inferior conjunctiva. The conjunctiva burst as a blister with both, debris and cells on the surface. The number of counted cells increased at 24 hours, after the second OVA challenge, in immunized mice (323±8 superior, 97±5 inferior) compared to naive mice (116±11 superior, 48±4 inferior) (***Figure E***). The same increasing trend was observed 3 days after OVA challenge in immunized mice (364±8 superior, 149±16 inferior) (***Figure E***). By contrast, at the same time point no cells were observed in both superior and inferior conjunctiva of non-immunized mice. At the end of day seven, the number of cells was the highest in the immunized mice (596±40 superior, 447±40 inferior), while no cells were detected in the naive mice ***(Figure E***). A pattern of blowing/bursting was observed in the conjunctiva of immunized mice. Blisters were seen 3 hours after first ova challenge and bursting 24 hours later with a subsequent swelling decrease. A new blister was watched next day that burst hours later. At the day seven, the conjunctiva was completely inflamed with hyper-reflective cells in both parenchyma and epithelium.

IVCM quantification of Cellular Infiltrates in the Cornea

Hyper-reflective cells were observed immediately within hours after first challenge in the cornea (***Figure 2B***). The cells were located in the stroma underneath the epithelium. Few hours after challenge, an increase in the number of hyper-reflective cells was observed in either, temporal nasal and central (***Figure 2F***). After 3 days, the number of hyper-reflective cells was (208±17 temporal, 142±18 nasal, 33±3 central) in the immunized mice compared to (72±6 temporal, 0 nasal, 27±3 central) in the non-immunized mice (***Figure 2C and 2 F***). The trend was increasing in the immunized mice until the day

seven (340±28 temporal, 438±29 nasal, 62±5 central). By contrast, the trend was decreasing in the non-immunized mice (0 temporal, 0 nasal, 21±2 central (***Figure 2C and 2 F***). Although both nasal and temporal cornea showed a gradually increasing trend until the end of the experiment (***Figure 2D and 2 F***), the center of the cornea was showing a different pattern. The number of cells was much lesser compared with the periphery but also a reversal fluctuating pattern was seen (***Figure 2F***).

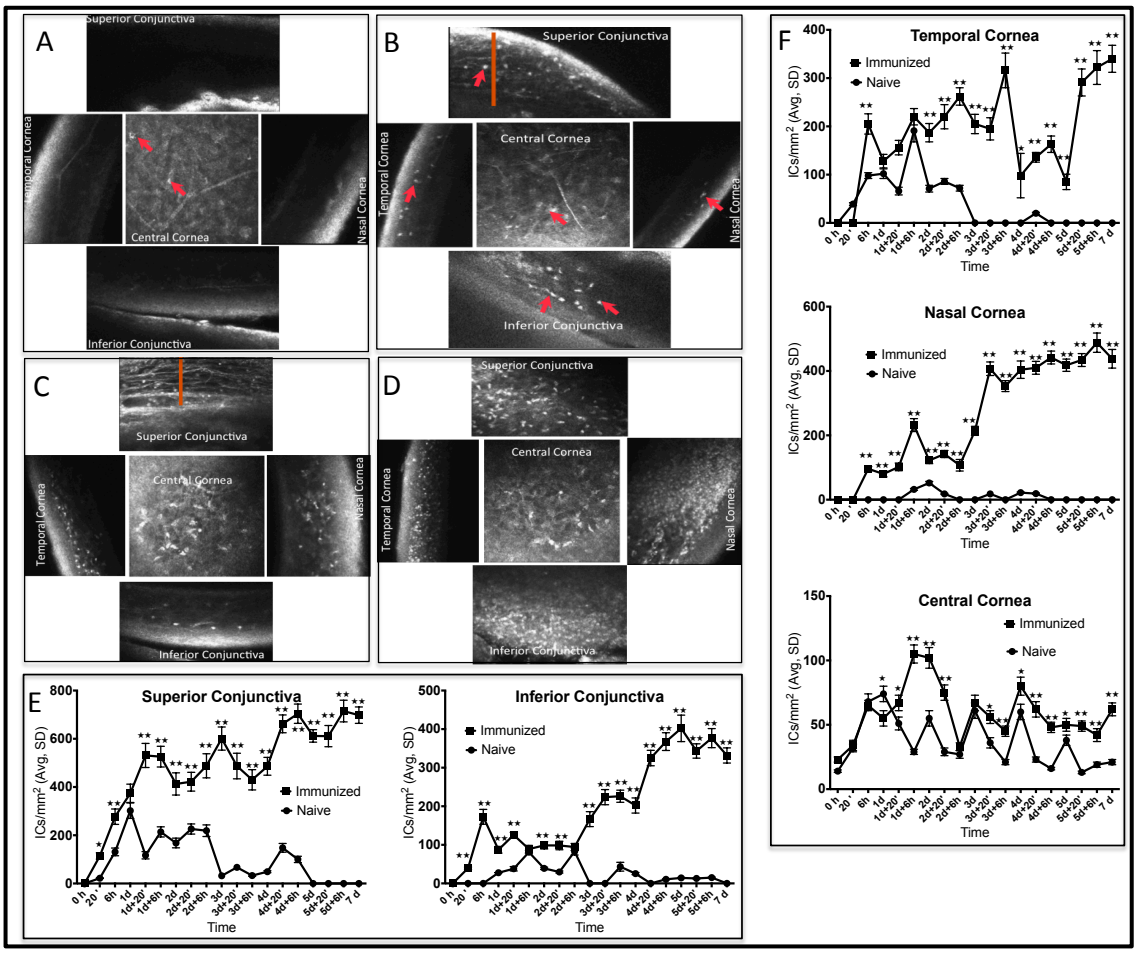

Figure 2. Intravital examination reveals immune cell recruitment to both the conjunctiva and cornea in AED

Superior and inferior conjunctiva as well as temporal, nasal and central cornea were imaged A). Compared to naïve mice, increased number of hyper-reflective events (arrow), suggestive of recruited immune cells, were observed as early as 6 hr on Challenge Day 1 (B), and increased on Day 3 (E) and Day 7 (F). Graphs show results from one experiment (n=4/group) and are representative of 3 independent experiments. Superior and inferior conjunctiva (E), nasal, temporal and central cornea (F) are displayed. Data are presented as mean and SD. Statistical significance was computed via student's t-test for immunized versus no sensitization.

Red arrows show hyper-reflective cells. Red vertical bar shows swelling in the superior conjunctiva.

$^{\star}p<0.05$, $^{\star\star}p<0.01$

Flow Cytometry Corroborated Immune Cell Infiltration in both Conjunctiva and Cornea

Conjunctiva and cornea were procured from immunized, non-immunized and normal mice. Tissues were collagenase digested into single-cell suspensions and stained with DAPI and anti-CD11b. After exclusion of dead cells (DAPI+) and exclusion of doublets we enumerated the frequency of CD11b+ cells by flow cytometry. Our findings show a CD11b+ cell population in a normal conjunctiva (1.82 % inferior, 2.17% superior) (***Figure 3A***). However, frequency of CD11b+ cells was significantly higher ($p<0.001$) in the immunized mice (23.1% inferior, 14% superior) compared to naive (3.4%, 1.94% superior) at day 3 (***Figure 3A***). At day 7, differences were much higher ($p<0.001$) and CD11b+ population was (39.7% inferior, 41.9% superior) in immunized mice compared to naive (10.9% inferior, 7.17% superior) (***Figure 3A***).

We found a CD11b+ cell population in a normal cornea (4.3 % temporal, 3.78 % nasal and 1.89 central) (***Figure 3B***). However, frequency of CD11b+ cells was significantly higher ($p<0.001$) in the immunized mice (21.3 % temporal, 30.5 % nasal and 13.5 central) compared to naive/challenged (6.55 % temporal, 4.15 % nasal and 4.52 central) at day 3 (***Figure 3B***). At day 7, CD11b+ cell frequency was significantly higher ($p<0.001$) in the immunized mice (44.4 % temporal, 37.2 % nasal and 47.4 central) compared to naive/challenged (5.67 % temporal, 6.28 % nasal and 2.07 central) (***Figure 3B***).

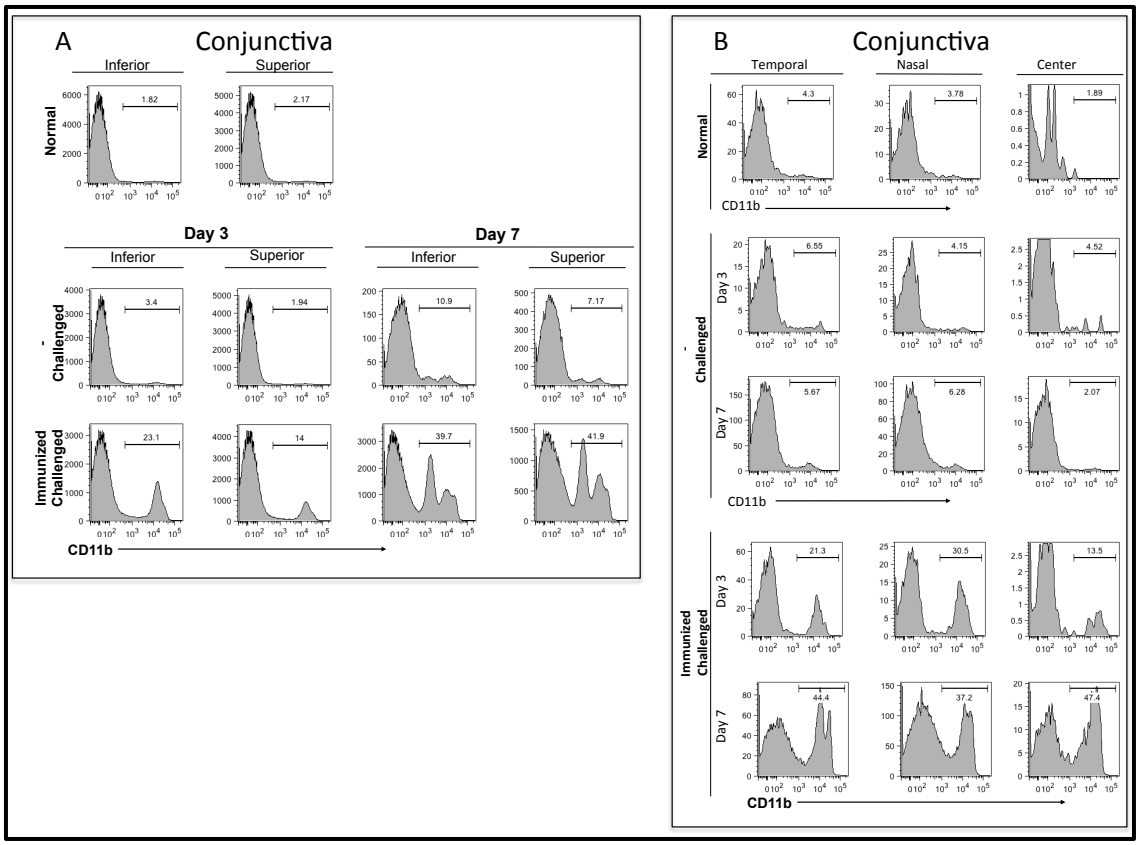

Figure 3. Flow cytometry shows the progression of myeloid cell recruitment to the ocular surface in AED. Myeloid cells (CD11b+) were analyzed by flow cytometry from superior and inferior conjunctivae (A) and from temporal, nasal, and central regions of the cornea (B). The samples were collected at baseline and on Challenge Days 3 and 7. A significant increase in myeloid cells in both superior and inferior conjunctiva of immunized mice respect to both normal and naive mice can be observed in A. Also a significant increase in myeloid cells was detected in the corneas of immunized mice respect to both normal and naive mice.

Plotted results are from one experiment (n=4/group), and is representative of 3 independent experiments

Inflammatory Cells Infiltrate the Mouse Cornea in Response to OVA

A CD11b+/CCR2^{+}/Ly6C^{hi}/ population was detected in the cornea after 3 days OVA challenge (***Figure 4***). This population is consistent with an inflammatory monocyte phenotype. Inflammatory monocytes were expressed at approximately tenfold higher levels (upon the examined areas) in immunized mice compared with both non-immunized and control mice (***Figure 4***). CD11b+/CCR2^{-}/Ly6C$^{low/neg}$ population was also found which suggests of granulocytic infiltration (likely neutrophils), but also other different subsets of monocytes (***Figure 4***)

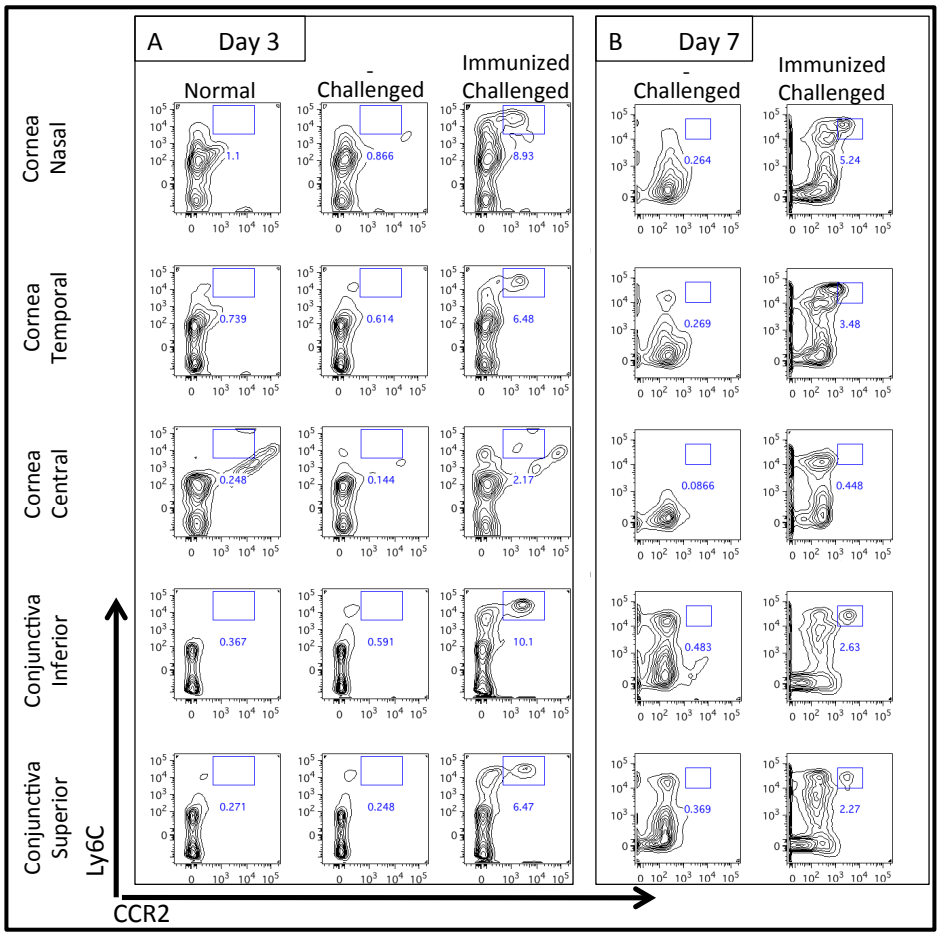

Figure 4. Characterization of recruited myeloid cells in the cornea of AED mice.

Corneas were collected on day 3 (A) and 7 (B) for flow cytometry and assessed using the indicated gating scheme. Plotted results are from one experiment (n=4/group), and is representative of 3 independent experiments. Notice the increase in the percentage $CCR2^{+}Ly6C^{hight}$ (likely monocyte infiltrated) in immunized challenged mice respect to both non-immunized and normal mice, at 3 (A) and 7 days (B).

CD11b Inflammatory Cells Were Located in the Conjunctiva in Response to OVA

Most of the hyper-reflective cells observed with the IVCM were in the substantia propia of the conjunctiva but also in the epithelium. LSCM showed CD11b+ cells in conjunctiva flat mounts. CD11b+ cells were majority observed in the stroma but also in the epithelium (***Figure 5***). Few cells were observed in the non-immunized conjunctiva (***not shown***). At day 7 the conjunctiva appeared totally occupied of CD11b+ cells in immunized mice. CD11b+ cells were observed also in naive mice but much lesser in number (***not shown***).

CD11b/Ly6C Inflammatory Monocytes Were Located in the Cornea in Response to OVA

LSCM confirmed also presence of CD11b+ in the cornea. The majority of the CD11b+ cells were present in the peripheral stroma (temporal and nasal) and also in the center colocalizing with Ly6C marker (***Figure 5***). Minor staining was observed in the non-immunized cornea (***not shown***). A drastic increase in CD11b+/Ly6C+ cells was observed in immunized mice compared to naive mice at day 7 (***Figure 5***).

Inflammatory Cells Were Confirmed with Optical Microscopy

Activated mast cells clusters in different states of granulation and de-granulation were seen with TB staining (***Figure 5D***). PMNs, eosinophils, monocytes and lymphocytes were detected by H&E staining in the conjunctiva stroma (***Figure 5E***). Infiltrated monocytes were observed in the periphery of the cornea (***Figure 5F***).

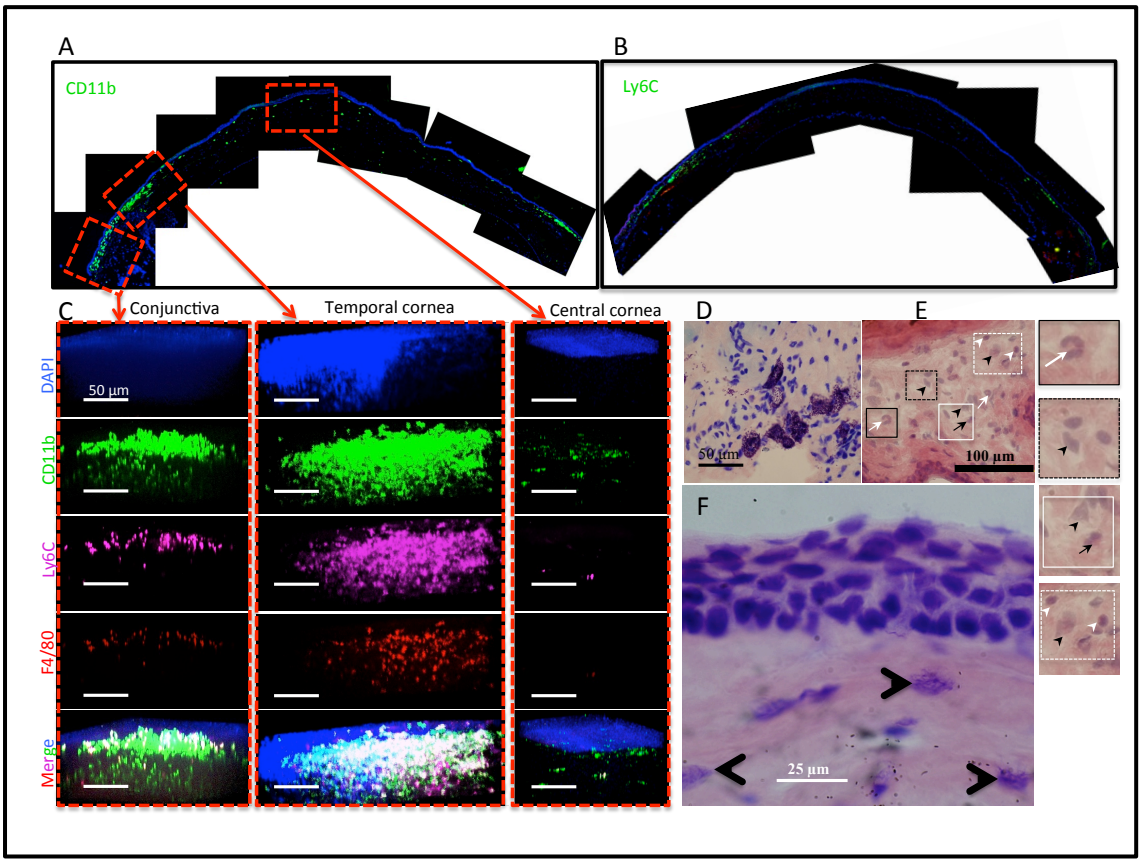

Figure 5. Distribution and characterization of recruited myeloid cells in both conjunctiva and cornea in AED.

(A) Distribution of CD11b labeled cells (green) in ocular tissue cross-sections. Location of Ly6C labeled cells (green) in ocular tissue cross-sections (B). (C) Representative 3D reconstructions of flat mounted immunostained tissue (conjunctiva, temporal and central cornea) imaged with a LSCM. (D) Toluidine blue staining shows mast cells clusters in the conjunctiva (E). H&E shows PMN (white arrows), eosinophils (black arrows), mononuclear myeloid cells (black arrowheads) and lymphocytes (white arrows heads) in the conjunctiva. (F) Giemsa staining shows infiltrated monocytes (black arrowheads) in the peripheral cornea.

DISCUSSION

In the present study, we intravitally evaluated the inflammatory process in an AC mouse model by using and IVCM. The results were accordingly compared with *ex vivo* flow cytometry and immunofluorescence analysis. Considering these results, the following conclusions can be drawn:

1. Inflammatory CI can be observed in a living mouse at real time by using an IVCM. The same mouse can be intravitally followed at multiple time points.
2. The increase in the number of inflammatory ICs observed with the IVCM correlates with the progression of AED and the increase in the frequency of CD11b+ ICs observed with both flow and LSCM.
3. An inflammatory reaction is perceived with the IVCM in the cornea long before is clinically detected with the slip lamp.

IVCM is normally used for the diagnosis of corneal pathologies such as basement membrane dystrophies, nerve degeneration, Bowman layer disruptions, stromal irregularities or endothelial dystrophies The etiology of keratitis such as bacterial, fungal, acanthamoeba or ketaconjunctivatis can be identified with the IVCM [20]. Nevertheless, IVCM has been barely used in animal models. Few experiments, for example, to quantify epithelial cells in a dry eye model [25] or brief descriptions of the corneal anatomy in different species (rabbit, rat and mice) [26, 27] have been done. In a previous work, we used an IVCM to evaluate the corneal wound healing process in a THBS1 deficient mouse model [21]. More recently Reichard et al., examined the regeneration of the murine sub-basal nerve plexus by using an IVCM system [28]. In the current work, we intravitally evaluated both bulbar conjunctiva and cornea in an AC mouse model. The main limitation in this work came up with the IVCM system. HRT3/RCM is a commercial device originally designed for humans. Mouse ocular surface differs notably from human (i.e. external exposition of the conjunctiva and corneal curvature). Therefore, the bulbar

aspect of the conjunctiva was only evaluated. In addition the cornea was also imaged in cross-sections (nasal and temporal) and on phase (central).

Clinical subjective scoring and IgG measurement are the methods often to evaluate AC. [23, 29-32]. Additionally, tedious postmortem histopathological analysis is still necessary. In the current work, we successfully implemented a non-invasive technique to evaluate the progression of the AED in a living mouse model. Cell infiltration into the ocular surface was detected by measuring light scattering with an IVCM. Compared to the normal tissue, ICs become hyper-reflective and therefore can be intravitally visualized. CI was observed in the conjunctiva within few hours after antigen challenge. Additionally, swelling of the substancia propia was detectable. A progressive increase in the number of hyper-reflective cells was seen in the superior and inferior conjunctiva. This number was statistically higher in immunized mice compared to both non- immunized and normal mice ($p<0.01$) . CD11b+ cells were identified using both flow cytometer and LSCM. The frequency of CD11b+ was statistically higher in immunized mice compared to both non-immunized and normal mice ($p<0.01$). Therefore, these findings strongly suggest that hyper-reflective cells, observed with the IVCM system, are recruited into the tissue as part of the progression of the AED.

Surprisingly, it was remarkable to find a similar inflammatory reaction in the cornea. The cornea and conjunctiva affect each other during ocular allergic inflammation; however, direct evidence of this interaction is not well described [16, 17, 33]. Severe ocular allergic diseases are characterized by various corneal disorders such as persistent epithelial defects and shield ulcer. Loss of corneal epithelium exacerbates conjunctival allergic inflammation, whereas eosinophil infiltration into the conjunctiva impairs epithelium healing. Eosinophils and eosinophil-derived factors are implicated in the pathogenesis of corneal lesions associated with ocular allergy [33]. Cytotoxic granule proteins such as major basic protein and matrix metalloproteinase 9 derived from eosinophils are present in shield ulcer [16, 33]. This indicates that conjunctiva allergic inflammation and corneal epithelial disorders interact with each other to generate a vicious cycle, interruption of

which might provide the basis for novel approaches to the treatment of severe ocular allergy [16].

We observed hyper-reflective cells in the periphery of the cornea but also in the center. The number of ICs observed by IVCM was incremented in correlation with the increase of the progression of AED. Interestingly, it was found an increase of CD11b frequency in both periphery and central cornea at days 3 and 7 with flow cytomerty. Augmented presence of CD11b+ cells was also observed in corneal explants by immunostaining. The increase in the $CD11b^{+}/CCR2^{+}Ly6\text{-}C^{high}$ subpopulation indicates a monocyte infiltration into the cornea. A second subpopulation of $CD11b^{+}/CCR2^{-}Ly6\text{-}C^{low}$ also indicates other granulocytes subsets. However, the most strikingly was to observe how transparent remained the cornea with such a significant infiltration. An incipient edema was observed in the limbus-periphery at the end of the experiment but mostly of the cornea remained fully transparent and no fluorescein staining was detected.

In the presence of an allergen steady state DCs maturate activating an adaptive Th2 immune response. It has been suggested corneal DCs trafficking between the cornea and the lymphatic nodes in response to allergen in a corneal allotransplantation model [34-36]; however, maturation and migration of corneal DCs, in response to allergen, unlikely happens in the normal cornea [37]. Collectively, our data suggests an unknown mechanism of cell infiltration into the cornea related with the progression of the adaptive immune response displayed by the conjunctiva, rather than by corneal DCs. Ocular surface DCs are an important population in adaptive immunity implicated in allergy [38]. Steady state immature DCs patrol tissues focused on antigen capture, rather than T cell activation [22, 39]. Following Ag capturing, DCs mature as potent stimulators of T cells, which in allergy activate Th2 cells. DCs up-regulate both MHC II molecules and co-stimulatory molecules such as CD80 and CD86. Mature DC-mediated activation of Th2 induces cytokines secretion such as IL-4, IL-5 or IL-13 that promote B cell differentiation into IgE-secreting plasma cells [1, 22, 40]. T cell response is key to all phases of allergic immunity. Primary exposures prime naive T cells and lead to allergen sensitization. Secondary

allergen exposures cause immediate hypersensitivity, and in some, subsequent late-phase and chronic disease [41]. Th2 cytokines also destabilize eosinophils in the late phase of allergy. This amplifies ocular surface inflammation by recruiting monocytes, memory T lymphocytes, eosinophils and dendritic cells that likewise enter into this feedback loop contributing to pathology [1]. However, in the present work whether the immune CI into the cornea plays a role in defending the tissue or leading to a pathologic state, escapes to our current knowledge and is subjected of further investigations.

In conclusion, in this study we successfully evaluated the inflammatory immune reaction in a mouse model of AED by using an IVCM. The rise in the number of inflammatory cells observed with the IVCM, correlates with the increase of AED clinical score, flow cytometer and LSCM analysis. Surprisingly, a significant inflammatory immune reaction was detected in the transparent cornea.

REFERENCES

1. Saban, D.R., V. Calder, C.H. Kuo, N.J. Reyes, D.A. Dartt, S.J. Ono and J.Y. Niederkorn, *New twists to an old story: novel concepts in the pathogenesis of allergic eye disease.* Curr Eye Res, 2013. **38**(3): p. 317-30.
2. Blaiss, M.S., *Allergic rhinoconjunctivitis: burden of disease.* Allergy Asthma Proc, 2007. **28**(4): p. 393-7.
3. Ono, S.J. and M.B. Abelson, *Allergic conjunctivitis: update on pathophysiology and prospects for future treatment.* J Allergy Clin Immunol, 2005. **115**(1): p. 118-22.
4. Bonini, S., S. Bonini, A. Lambiase, S. Marchi, P. Pasqualetti, O. Zuccaro, P. Rama, L. Magrini, T. Juhas and M.G. Bucci, *Vernal keratoconjunctivitis revisited: a case series of 195 patients with long-term followup.* Ophthalmology, 2000. **107**(6): p. 1157-63.
5. Leonardi, A., *Vernal keratoconjunctivitis: pathogenesis and treatment.* Prog Retin Eye Res, 2002. **21**(3): p. 319-39.
6. Pucci, N., E. Novembre, E. Lombardi, A. Cianferoni, R. Bernardini, C. Massai, R. Caputo, L. Campa and A. Vierucci, *Atopy and serum eosinophil cationic protein in 110 white children with vernal keratoconjunctivitis: differences between tarsal and limbal forms.* Clin Exp Allergy, 2003. **33**(3): p. 325-30.
7. Leonardi, A., L. Motterle and M. Bortolotti, *Allergy and the eye.* Clin Exp Immunol, 2008. **153 Suppl 1**: p. 17-21.
8. Leonardi, A., *The central role of conjunctival mast cells in the pathogenesis of ocular allergy.* Curr Allergy Asthma Rep, 2002. **2**(4): p. 325-31.
9. Bielory, L., *Ocular allergy guidelines: a practical treatment algorithm.* Drugs, 2002. **62**(11): p. 1611-34.
10. Dace, D.S., P.W. Chen and J.Y. Niederkorn, *CD4+ T-cell-dependent tumour rejection in an immune-privileged environment requires macrophages.* Immunology, 2008. **123**(3): p. 367-77.
11. Fukuda, K., M. Ohbayashi, K. Morohoshi, L. Zhang, F.T. Liu and S.J. Ono, *Critical role of IgE-dependent mast cell activation in a murine model of allergic conjunctivitis.* J Allergy Clin Immunol, 2009. **124**(4): p. 827-33 e2.
12. Galatowicz, G., Y. Ajayi, M.E. Stern and V.L. Calder, *Ocular anti-allergic compounds selectively inhibit human mast cell cytokines in vitro and conjunctival cell infiltration in vivo.* Clin Exp Allergy, 2007. **37**(11): p. 1648-56.
13. Abelson, M., I. Udell, M. Allansmith and M. Raizman, *Principles and practice od ophthalmology. Philadelphia: Saunders, .* In: Albert DM, Jacobiec FA, eds, 1994. **1**(Allergic and toxic reactions): p. 259-88

.

14. Hamelmann, E. and E.W. Gelfand, *IL-5-induced airway eosinophilia--the key to asthma?* Immunol Rev, 2001. **179**: p. 182-91.
15. Akbari, O., P. Stock, R.H. DeKruyff and D.T. Umetsu, *Role of regulatory T cells in allergy and asthma.* Curr Opin Immunol, 2003. **15**(6): p. 627-33.
16. Fukuda, K. and T. Nishida, *Ocular allergic inflammation: interaction between the cornea and conjunctiva.* Cornea, 2010. **29 Suppl 1**: p. S62-7.
17. Fukuda, K., N. Yamada and T. Nishida, *Case report of restoration of the corneal epithelium in a patient with atopic keratoconjunctivitis resulting in amelioration of ocular allergic inflammation.* Allergol Int, 2010. **59**(3): p. 309-12.
18. Kumar, R.L., A. Cruzat and P. Hamrah, *Current state of in vivo confocal microscopy in management of microbial keratitis.* Semin Ophthalmol. **25**(5-6): p. 166-70.
19. Cruzat, A., D. Pavan-Langston and P. Hamrah, *In vivo confocal microscopy of corneal nerves: analysis and clinical correlation.* Semin Ophthalmol. **25**(5-6): p. 171-7.
20. Guthoff, R.F., C. Baudouin and J. Stave, *Atlas of Confocal Laser Scanning In-vivo Microscopy in Opthalmology –Principles and Applications in Diagnostic and Therapeutic Ophtalmology.* 2007.
21. Blanco-Mezquita, T., A.E. Hutcheon and Z. J.D., *Role of Thrombospondin-1 in Repair of Penetrating Corneal Wounds.* IOVS, 2013.
22. Schlereth, S., H.S. Lee, P. Khandelwal and D.R. Saban, *Blocking CCR7 at the ocular surface impairs the pathogenic contribution of dendritic cells in allergic conjunctivitis.* Am J Pathol, 2012. **180**(6): p. 2351-60.
23. Reyes, N.J., E. Mayhew, P.W. Chen and J.Y. Niederkorn, *NKT cells are necessary for maximal expression of allergic conjunctivitis.* Int Immunol. **22**(8): p. 627-36.
24. Saban, D.R., S.K. Chauhan, X. Zhang, J. El Annan, Y. Jin and R. Dana, *'Chimeric' grafts assembled from multiple allodisparate donors enjoy enhanced transplant survival.* Am J Transplant, 2009. **9**(3): p. 473-82.
25. Li, N., J. He, C.E. Schwartz, P. Gjorstrup and H.E. Bazan, *Resolvin E1 improves tear production and decreases inflammation in a dry eye mouse model.* J Ocul Pharmacol Ther. **26**(5): p. 431-9.
26. Labbe, A., H. Liang, C. Martin, F. Brignole-Baudouin, J.M. Warnet and C. Baudouin, *Comparative anatomy of laboratory animal corneas with a new-generation high-resolution in vivo confocal microscope.* Curr Eye Res, 2006. **31**(6): p. 501-9.
27. Reichard, M., M. Hovakimyan, A. Wree, A. Meyer-Lindenberg, I. Nolte, C. Junghans, R. Guthoff and O. Stachs, *Comparative in vivo confocal microscopical*

study of the cornea anatomy of different laboratory animals. Curr Eye Res, 2010. **35**(12): p. 1072-80.
28. Reichard, M., M. Hovakimyan, R.F. Guthoff and O. Stachs, *In vivo visualisation of murine corneal nerve fibre regeneration in response to ciliary neurotrophic factor.* Exp Eye Res, 2014. **120**: p. 20-7.
29. Matsuba-Kitamura, S., T. Yoshimoto, K. Yasuda, S. Futatsugi-Yumikura, Y. Taki, T. Muto, T. Ikeda, O. Mimura and K. Nakanishi, *Contribution of IL-33 to induction and augmentation of experimental allergic conjunctivitis.* Int Immunol. **22**(6): p. 479-89.
30. Miyazaki, D., W. Ishida, T. Tominaga, T. Sumi and A. Fukushima, *Aggravation of conjunctival early-phase reaction by Staphylococcus enterotoxin B via augmentation of IgE production.* Jpn J Ophthalmol. **54**(5): p. 476-80.
31. Nakano, Y., Y. Takahashi, R. Ono, Y. Kurata, Y. Kagawa and C. Kamei, *Role of histamine H(4) receptor in allergic conjunctivitis in mice.* Eur J Pharmacol, 2009. **608**(1-3): p. 71-5.
32. Schlereth, S., H.S. Lee, P. Khandelwal and D.R. Saban, *Blocking CCR7 at the Ocular Surface Impairs the Pathogenic Contribution of Dendritic Cells in Allergic Conjunctivitis.* Am J Pathol. **180**(6): p. 2351-60.
33. Kumagai, N., K. Fukuda, Y. Fujitsu, K. Yamamoto and T. Nishida, *Role of structural cells of the cornea and conjunctiva in the pathogenesis of vernal keratoconjunctivitis.* Prog Retin Eye Res, 2006. **25**(2): p. 165-87.
34. Chauhan, S.K., T.H. Dohlman and R. Dana, *Corneal Lymphatics: Role in Ocular Inflammation as Inducer and Responder of Adaptive Immunity.* J Clin Cell Immunol, 2014. **5**.
35. Jin, Y., L. Shen, E.M. Chong, P. Hamrah, Q. Zhang, L. Chen and M.R. Dana, *The chemokine receptor CCR7 mediates corneal antigen-presenting cell trafficking.* Mol Vis, 2007. **13**: p. 626-34.
36. Yamagami, S. and M.R. Dana, *The critical role of lymph nodes in corneal alloimmunization and graft rejection.* Invest Ophthalmol Vis Sci, 2001. **42**(6): p. 1293-8.
37. Lee, E.J., J.T. Rosenbaum and S.R. Planck, *Epifluorescence intravital microscopy of murine corneal dendritic cells.* Invest Ophthalmol Vis Sci, 2010. **51**(4): p. 2101-8.
38. Steinman, R.M. and J. Banchereau, *Taking dendritic cells into medicine.* Nature, 2007. **449**(7161): p. 419-26.
39. Ohbayashi, M., B. Manzouri, T. Flynn, M. Toda, Y. Ikeda, T. Nakamura and S.J. Ono, *Dynamic changes in conjunctival dendritic cell numbers, anatomical position and phenotype during experimental allergic conjunctivitis.* Exp Mol Pathol, 2007. **83**(2): p. 216-23.

40. Saban, D.R., F. Bock, S.K. Chauhan, S. Masli and R. Dana, *Thrombospondin-1 derived from APCs regulates their capacity for allosensitization.* J Immunol, 2010. **185**(8): p. 4691-7.
41. Leonardi, A., *Allergy and allergic mediators in tears.* Exp Eye Res, 2013. **117**: p. 106-17.

CHAPTER 4

Cutting Edge in vivo Imaging I: Multi-Photon intravital Microscopy to Visualize the Resident Myeloid-Derived Population in the MouseCornea

Cutting Edge *in vivo* Imaging I: Multi-Photon *intravital* Microscopy to Visualize the Resident Myeloid-Derived Population in the Mouse Cornea

Tomas Blanco[1, 2], O'koren[1] E. Daniel R. Saban[1, 3].

[1]Ophthalmology Department, Duke Eye Center, Duke School of Medicine, Durham, NC

[2]Ophthalmology Department, IOBA, Valladolid School of Medicine, Valladolid, Spain

[2]Immunology Department, Duke Eye Center, Duke School of Medicine, Durham, NC

ABSTRACT

Aim: The purpose of this study was to combine genetically-engineered reporter expressing mouse strains, multi-photon intravital microscopy (MP-IVM) and digital post-analysis software to obtain a novel imaging model. This model should be suitable for studying the myeloid-derived population of the cornea in normal and pathological conditions in a living mouse.

Methods: In the present study, we used a real multiphoton microscope (MPM), equipped with a motorized versatile stage with spacer to give large free working distance under the objective, to visualize the resident myeloid-derived cell population in a living mouse cornea. We took the advantage of Cx3cr1 transgenic mice expressing GFP, YFP or RFP. Furthermore, we have implemented digital post-analysis commercial software to generate a real tree-dimensional view of the cornea.

Results: The expression of myeloid specific GFP, YFP or RFP in a transgenic mouse cornea was successfully detected *in vivo* with a MP-IVM system. The myeloid derived cells DCs where delineated by using the signal of the second harmonic generation (SGH) and digitally counted. The fate mapping indicates that resident population might have a embryonic origin rather than hematopoietic as has been thought before.

Conclusion: In this study we combined genetically-engineered reporter expressing mouse strains, MP-IVM and imaging analysis software to obtain an outstanding *in vivo* imaging model. This model is suitable for studying the function of the myeloid population of the cornea in both normal and pathological conditions in a living mouse.

INTRODUCTION

Inflammation is an essential component of tissue protection and eradication of infection but also a major antagonist of corneal clarity where to maintain the transparency is essential for unaltered vision and survival. During its evolution, the cornea has developed a complex mechanism to keep the unaltered transparency. The cornea has the unique capability to repair itself after an injury with minimal changes in transparency, biomechanical, refractive and sensory properties [1-4]. The cornea is an immune privileged place, with no lymphatic and blood vessels, which antigen presenting cells (APCs) are not immunoreactive to alloantigens in normal conditions [5-8]. In a healthy cornea, both afferent (lymphatic) and efferent (vascular) arms of the immune response are suppressed [9, 10]. Lymphatic vessels mediate the afferent arm of the immune system by facilitating migration of APCs and alloantigens to the draining lymph nodes, where alloreactive effector T cells are primed, which then return to the ocular surface via blood vessels (efferent arm). To prevent lymphangiogenesis, corneal epithelium expresses soluble forms of VEGF-3 and VEGFR1 acting as decoy receptors for VEGF-A, VEGF-C, VEGF-D y VEGFR-2 [11, 12]. In addition, the epithelial cells release PEDF (Pigment Epithelium-Derived Factor), angiostatin and endostatin that prevent lymphangiogenesis [13, 14]. Corneal endothelium also expresses both FAS ligand (FAS-L) and PDL-1 (Programmed Death-Ligand 1) driving T cells to apoptosis [15]. Inflammation revokes this unique immune and angiogenic privilege of the cornea; however, the mechanism is not well understood [16]. The relevance of lymphatic vessels in alloimmunity is illustrated by the high rate of rejection seen in those transplants performed in corneal beds with pre-existing lymphatics, so called 'high-risk' hosts [17-19]. Unusual growth of lymphatic vessels into the cornea allows APCs travel to the draining lymphatic nodes and therefore presenting antigens. This causes an atypical infiltration of T helper cells into the cornea causing an exacerbated inflammatory allorejection [20].

Until a few years ago, it was believed that the cornea was devoid of resident APCs capable to initiate an inflammatory response; therefore, maintenance of corneal transparency was attributed, in part, to a lack of such a cells [21]. During the last decade, many works have confirmed the mouse cornea is endowed with a particular stratified population of resident myeloid-derived APCs [22-27]. Two main different phenotypic subpopulations, such as DCs and macrophages, compose corneal myeloid population [27]. The majority of DCs reside in the basal layer of the epithelium. DCs extend dendrites to interdigitate between epithelial cells from the basal toward the ocular surface. Classical $CD11c^+$ DCs are typically located in the periphery of the cornea and decreasing in number towards the center [7, 10, 28, 29]. Although majority of $CD11c^+$ DCs are present in the basal layer of the epithelium, merely a small population resides in the very peripheral regions of the stroma, some of them as immature precursors [24]. The majority of the $CD11c^+$ DCs also co-express MHC class II, highest in the periphery and lesser toward the center. An additional subpopulation of CD11c-DCs that expresses langerin CD207, or Lagerhans cells (LCs), is also located in the basal epithelium [30]. DCs are potent APCs capable to initiate adaptive immune response; however, this property is still controversial in the normal cornea.

Macrophages reside in the stroma divided in two distinct subpopulations [24, 27]. The anterior stroma is populated by $CD11b^+$ $CD11c^-$ MHC class II^+ macrophages distributed relatively uniform from the periphery to the center of the stroma. These are considered putative macrophages that can serve as APCs backup for epithelial DCs in an adaptive immune response [27]. The posterior stroma is endowed of $CD11b^+$ MHC class II^- classical macrophages quietly uniform distributed from the periphery to the center. These macrophages initiate the innate immune response in the murine cornea [27]. Additionally CD11c-expressing cells as well as a different population of monocyte-derived cells also

Recently Knickelbein et al. have proposed a similar model of APC stratification in the human cornea [26]. $CD45^+$ $CD11c^+$ DCs, the majority expressing HLA-DR, reside in the

basal layer of the epithelium extending cellular processes toward the ocular surface. Mostly of these DCs populate the periphery of the cornea and the number is decreasing centripetally toward the center. Langerin positive cells ($CD207^+$), likely LCs, are fundamentally located in the periphery of the cornea. In the stoma $CD45^+$ $CD68^+$ macrophages reside in the anterior part of the stroma distributed relatively uniform from the periphery to the center [26]. While $CD45^+$ HLA-DR^+ population is higher in the center of the stoma, compared to paracentral and periphery, no $CD207^+$ LCs are observed in the center and only a few of them in the periphery [26].

Nowadays, live imaging facilitates the understanding of both tissue and cell behavior as well as their basic molecular mechanisms. Genetically-engineered reporter expressing mouse strains are an important tool for use in live imaging experiments. Such reporter strains can be engineered by placing cis-regulatory elements of interest to direct the expression of desired reporter genes. If these cis-regulatory elements are downstream targets, and thus activated as a consequence of signaling pathway activation, such reporters can provide read-outs of the signaling status of a cell [32]. Transgenic mice, expressing either CD11c or langerin, have been recently used to describe the lineage of myeloid population in the mouse cornea [30]. The recent arrival of new strains of CX3CR1-GFP mice expressing EGFP in monocytes, dendritic cells, NK cells and brain microglia, under control of the endogenous Cx3cr1 locus (myeloid progenitor derived marker) has made useful studies of leukocyte function in migration, trafficking and transplantation [33].

CX3CR1 (Chemokine receptor1), also known as fractalkine receptor, is a protein encoded by the Cx3cr1 gene. CX3CR1 binds the chemokine CX3CL1, also known as fractalkine or neurotactin, a transmembrane protein and chemokine involved in the adhesion and migration of leukocytes. CX3CR1 fractalkine interaction mediates cell-cell adhesion, and migration of CX3CR1-bearing cells predominantly myeloid origin such as monocytes, NK cells, T-cells, DCs, and macrophages including microglia [34-36]

The development of mice in which a green fluorescent protein (EGFP)-encoding gene is inserted in one or both copies of the CX3CR1 locus has permitted to investigate the

fate of leukocytes in vivo [37, 38]. The use of Cx3cr1-GFP transgenic mice has arisen to a new level of understanding myeloid population of the cornea. The adoptive transfer of labeled monocytes, from Cx3cr1-GFP mice into wild-type (WT) recipients, has created a new line of research to study monocyte heterogeneity and the factors regulating their differentiation within different tissues. Additionally, it can be investigated the accumulation of normal resident monocyte-derived DCs and macrophages in a diverse range of tissues [37, 38]. In the ocular surface, Cx3cr1-GFP transgenic mice have been used to confirm the presence of myeloid derived cells as a resident population of the normal murine cornea. Also, it has been demonstrated that Cx3cr1 expression plays a role in DC and macrophage recruitment in the normal corneal epithelium and stroma [34]. Heterozygous $Cx3cr1^{+/GFP}$ transgenic mice have provided a powerful tool to investigate macrophage and DC populations by using *intravital* microscopy. *Intravital* widefield epifluorescence videomicroscopy has been performed in corneas of anesthetized mice to probe that corneal DCs behavior bear similarities to that of skin DCs [39]. It has been shown that after irritation of the cornea results in a centripetal migration of DCs from periphery and limbus [40]. Recently Knickelbein et al. have combined LSCM (laser scanning confocal microscope) with two different *intravital* novel techniques to describe the APCs stratification in the mouse cornea [41]. By using either an Optiscan FIVE-1 handheld fluorescence microscope or a home-built non-descanned two-channel multiphoton system, these authors imaged DCs in corneas of anesthetized mice expressing eGFP driven by the CD11c promoter. However, the authors criticized this technology since a no reliable positioning of the objective on the murine eye, for precise analysis of different regions of the cornea, was possible [41].

In the present study, we used a real multiphoton microscope (MPM), equipped with a motorized versatile stage with spacer to give large free working distance under the objective, to visualize the resident myeloid-derived cell population in a living mouse cornea. We took the advantage of Cx3cr1 transgenic mice expressing GFP, YFP or RFP.

Furthermore, we have implemented digital post-analysis commercial software to generate a real tree-dimensional view of the cornea.

The purpose of this study was to combine genetically-engineered reporter expressing mouse strains, multi-photon intravital microscopy (MP-IVM) and digital post-analysis software to obtain a novel imaging model. This model should be suitable for studying the myeloid-derived population of the cornea in normal and pathological conditions in a living mouse.

METHODS

Mice and Anesthesia

Mice were housed in a specific pathogen-free environment at the Duke Eye Center animal facility. The Institutional Animal Care and Use Committee approved all procedures. All animals were treated according to the ARVO Statement for the Use of Animals in Ophthalmic and Vision Research. Anesthesia was given with intraperitoneal administered ketamine/xylazine suspensions (120 and 20 mg/kg, respectively).

Mice encoding GFP knocked into the gene encoding the chemokine receptor Cx3cr1 ($Cx3cr1^{EGFP}$ knock-in mice) were bred and maintained in our facility. Parental were purchased from Jackson: male and female $Cx3cr1^{tm1Litt}/Cx3cr1^{+}$ (B6.129P2-$Cx3cr1^{tm1Litt}$) were crossed to generate homozygous $Cx3cr1^{EGFP/EGFP}$. Homozygous $Cx3cr1^{EGFP/EGFP}$ were crossed back with C57BL/6J WT mice to generate heterozygous $Cx3cr1^{EGFP/WT}$.

Fluorescence-reporter Cre recombinase activated was analyzed by using CX3CR1-Cre mice generated on a mixed 129/B6 (Gene Expression Nervous System Atlas Project), and backcrossed for 12 generations by M.D. Gunn (Departments of Immunology and Medicine, Duke University Medical Center) [42, 43]. B6.Cg-Gt(ROSA)26Sor$^{tm14(CAG-tdTomato)Hze}$/J mice (referred to here as RFP) obtained from Jackson Laboratories, were also a kind gift from M. D. Gunn. Rosa26R-CAG-fGFP mice, referred to here as fGFP, have previously been described [44], were a kind gift from B. L. Hogan (Department of Cell Biology, Duke University Medical Center). These 3 mouse lines were subsequently maintained and bred in our lab. Male CX3CR1-Cre mice were crossed with female fGFP, and progeny were verified for a CX3CR1-Cre fGFP genotype. Likewise, progeny of male CX3CR1-Cre mice crossed with female RFP were verified for a CX3CR1-Cre RFP genotype.

CX3CR1-YFP-CreER mice (B6.129P2(Cg)-Cx3cr1tm2.1(cre/ERT)Litt/WganJ) encode a YFP and CreER under the control of the Cx3cr1 promoter. Rosa-tdTomato mice

(B6.Cg-Gt(ROSA)26Sortm14(CAG-tdTomato)Hze/J) contain a loxP-flanked STOP cassette that prevents transcription of the downstream red fluorescent protein (tdTomato) until the STOP cassette is removed in the presence of Cre. Both CX3CR1-YFP-CreER and Rosa-tdTomato mouse lines were purchased from Jackson Laboratories and are on a C57BL/6 background. Mating of these two homozygouse lines results in an F1 generation that contains the CX3CR1-YFP-CreER and Rosa-tdTomato construct, named here CX3CR1-YFP-CreER-RFP

C57BL/6J WT mice 8 week old were purchased from Jackson laboratories (Jackson, Farmington, Connecticut).

Irradiation procedure

Recipient $Cx3cr1^{cre/tdTomato}$, $Cx3cr1^{cre/fGFP}$, Thy-1 and C57BL/6 WT mice were total body lethally irradiated (1050 cGy) in a Mark I 68A Cs 137 irradiator (JL Shepherd and Associates in San Fernando, CA). The irradiator cabinet is 37cm x 30cm x 45cm and the Cesium source is air compressed raised over 15 from the bottom. Five mice at the time were introduced into a 20 cm diameter acrylic holder. The holder was placed above a 7.6 cm platform positioned over an automatic turntable (12 rpm) to ensure 100% irradiation. The time for the process was 2.21 minutes (2 minutes and 12.9 seconds).

Generation of Chimeras

Table 1 shows all the chimeras generated. Donor mice were euthanatized and femurs and tibia collected. Distal and proximal ends of the bone were removed and the marrow flushed out with fresh RPMI medium using a syringe with a 27G needle. Marrow suspension was fragmented into a single cell suspension by passing through a cell strainer (70μm) followed by vigorous pipetting. After centrifugation (200g, 5 minutes, 4C), live cells were counted by trypan blue exclusion and the pellet was resuspended in RPMI media and diluted as appropriate ($3x10^7$ cells/mL). Immediately after irradiation,

recipient mice received ~1x10^7 non-purified bone marrow cells (~300 μL) via retro-orbital injection of the venous sinus. Antibiotics were given in water to recipient mice (Sulfamethoxazole and trimethoprim antibiotics; SEPTRA, Hi-Tech Pharmacal Co., Amityville, NY) for up to 4 weeks after irradiation. In addition, supplement care food (SuppliCal caloric supplement; Henry Schein, Dublin, Ohio) was provided. Animals were rested for 6 weeks before MP-IVM examinations. The same animal was examined under general anesthesia several times at different time points with one week frame recovering in between examinations.

Host	Donor	Transition observed chimera	Final expected chimera
$Cx3cr1^{cre/RFP}$	$Cx3cr1^{cre/fGFP}$	$Cx3cr1^{cre/RFP}/Cx3cr1^{cre/fGFP}$	$Cx3cr1^{cre/fGFP}$
$Cx3cr1^{cre/fGFP}$	$Cx3cr1^{cre/RFP}$	$Cx3cr1^{cre/fGFP}/Cx3cr1^{cre/RFP}$	$Cx3cr1^{cre/RFP}$
C57BL/6 WT	$Cx3cr1^{cre/fGFP}$	$Cx3cr1^{cre/fGFP}$	$Cx3cr1^{cre/fGFP}$
C57BL/6 WT	$Cx3cr1^{cre/RFP}$	$Cx3cr1^{cre/RFP}$	C57BL6WT/$Cx3cr1^{cre/RFP}$

Tamoxifen injection and fate mapping follow up

CX3CR1-YFP-CreER-RFP mice were injected intraperitoneally with 150ul of Tamoxifen (20mg/ml). Six weeks old mice received two injections, one day apart. Mice were *intravitally* followed for up to 6 months.

Intravital Two-photon Microscopy

Anaesthetized mice were placed on a customized holder. Body temperature was controlled at 37C. The animals were constantly infusing 0.2-0.3 ml/h of a solution of 1ml of ketamine (120 mg/kg), 1 ml of xylacine (20 mg/kg), and 10 ml sodium chloride via intraperitoneal catheter. After experiments, animals were allowed to recover for several examinations or euthanized by ketamine/xylacine overdose. In vivo examinations were

performed with a 25x/1.05 NA water objective (optimized for MPE XLPL25XWMP, WD 2.0 mm, 0 to 0.23 micron coverslip correction) in an Olympus BX61WI upright microscope fixed stage (Olympus, Tokyo, Japan) (***Figure 1***)

A Chameleon Vision II single box Ti:Sapphire fsec laser was used. Laser permits pulse compensation in a tunable range 680-1080 nm @40 nm/sec, 80 MHz rep rate, 140 fsec pulse width with a 0-47,000 fsec2 units of dispersion compensation.

The microscope is equipped with a Blue, Green/Yellow and Red standard fluorecence cubes. Emission bands available: Dapi, CFP, GFP, YFP and Red in switchable cubes. The Blue or Cyan channels were used for SHG (Second Harmonic Generation).

Laser was tuned at 910 nm (BGR cube) or 950 nm (CYR cube) for two-photon excitation and second-harmonic generation. A dichroic mirror (DM570) splits the light emission through both channels 1 (blue) and 2 (green or yellow) and channel 4 (red). A second dichroic mirror (DM485) divides light emission for channel 1 and channel 2. The BGR cube is composed by a 450-460 nm (blue and SGH), 495-540 (Green) and 575-630nm (Red) band pass filters. The CYR cube is composed by a 460-500 nm (blue and SGH), 520-560 (Yellow) and 575-630nm (Red) band pass filters. The system has four high efficiency non-descanned detectors in the epi position 4 that can be combined in different configurations by manually alternating the cubes.

For corneal in vivo examinations, mouse was dorsally placed facilitating perpendicular exposure of the corneal apex to the microscope objective. Objective-cornea space was full filled with an ophthalmic gel (GenTeal, Novartis Ophthalmics, East Hanover) to create a coupling immersion interface with a refractive index (n=1.339) similar to water (n=1.333 at 20C) as well to provide eye lubrication.

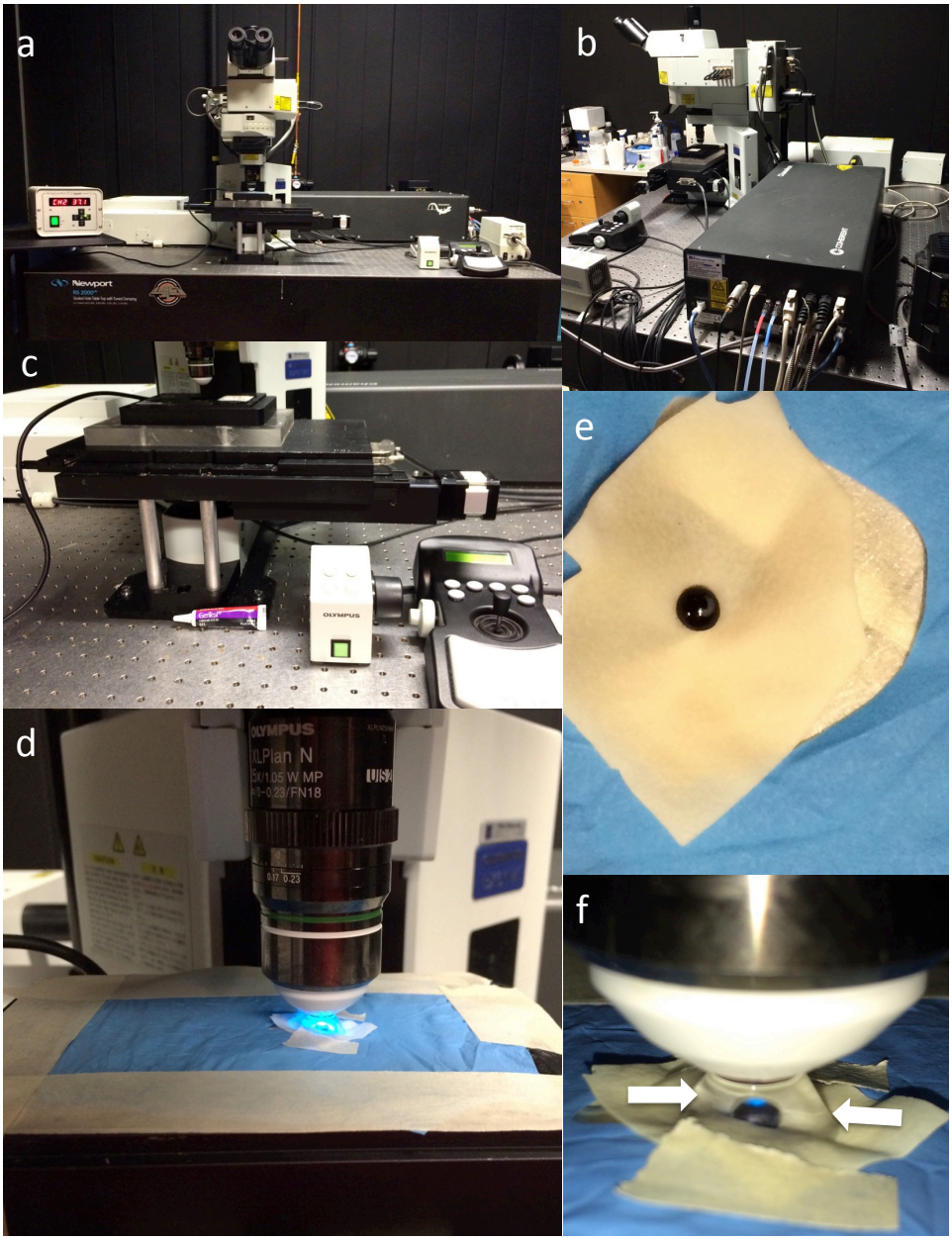

Figure 1. Two-photon *intravital* microscopy system.
Multiphoton microscope system with temperature controller (a) and Chameleon Vision II single box Ti:Sapphire fsec laser (b). A digital motorized XY stage (c) facilities tiling imaging. The mouse is placed dorsally inside of the customized warm chamber (d) with the ocular surface exposed to the objective (e). Objective-cornea space was full filled with an ophthalmic gel (f, white arrows)

Z-series images for 3D mosaic imaging.

By using a motorized XY stage (***Figure 1***), the multi-area time-lapse software (Olympus) automates the process for a 3D image acquisition and stitching. The software easily registers wide areas, and the thumbnail displayed provides a view of the entire image acquired during the mosaic imaging process. (***Figure 2***)

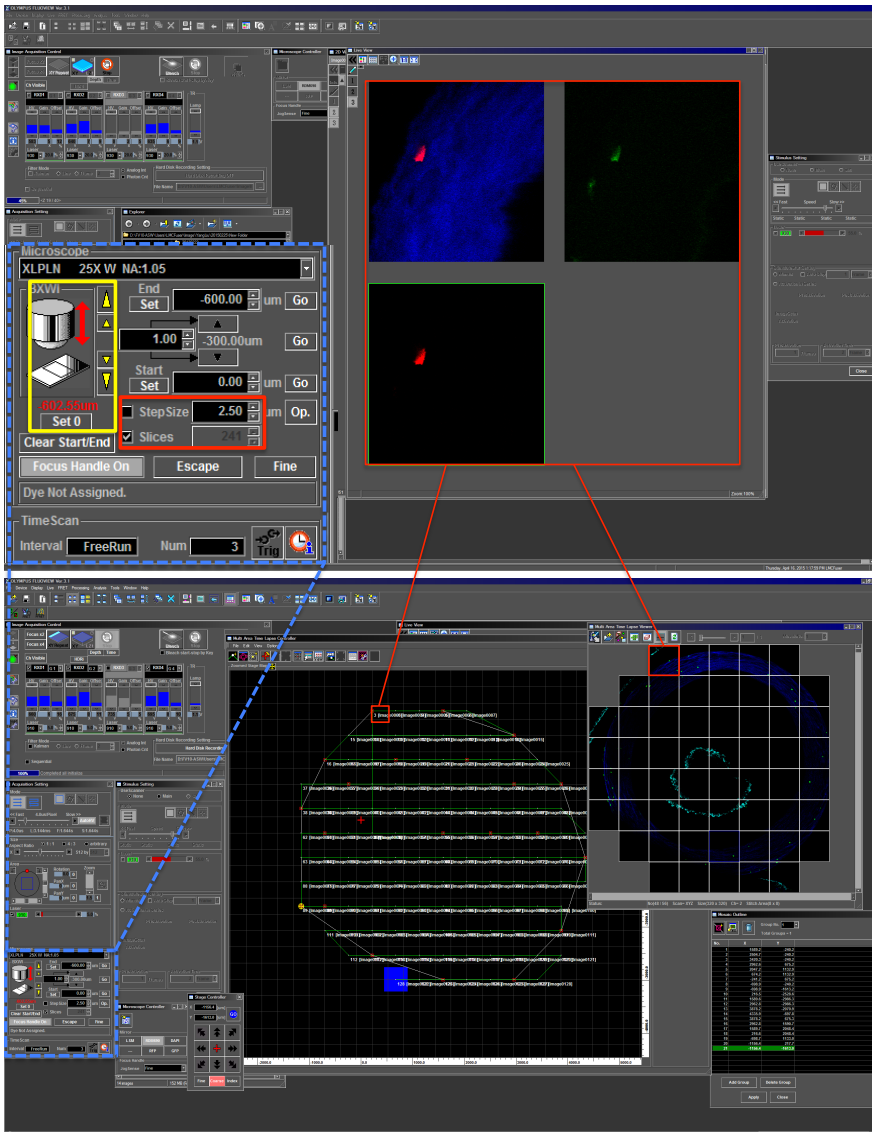

Figure 2: Imaging mosaic acquisition system.

Post-acquisition image analysis

Image stacks were analyzed using the latest version of FUJI available (developed by Wayne Rasband, National Institutes of Health; provided auto-updated by the public domain http://rsb.info.nih.gov/ij). The latest version of Imaris (Imaris, auto-updated version, Bit-plane, Zurich, Switzerland) was also used. Raw files were displayed in Imaris and linked to FIJI for background substraction, brightness/contrast adjustment, noise reduction, compression and size adjustment. After, an easy readable image was imported back from FIJI into Imaris rendering a maximum-intensity projection or blend projection providing a realistic 3D view in a 2D screen. Additional depth perception enhancing realism of the images was created with the Real-Time Shadow Rendering (a fast hardware that projects shadows on the three planes of the object). A surface object is a computer-generated illustration of a detailed region of interest in the data set. The surface object is displayed as a simulated solid object. The accuracy of segmentation against the original data can be easily verified in an interactive manner (for more details visit: http://www.bitplane.com/imaris/imaris). Surface rendering was interactively performed using optimal threshold settings for each channel in each experiment. By choosing absolute threshold, it was possible to detect large portion of the cells without picking up any noise or background with an accurate separation of touching cells. "Quality" and/or "number of voxels" filters were used for detection of seed points. It can pick up missed pixels or remove non-desirable background or noise. Filter settings were optimized comparing interactively the result with the original maximum-intensity projection. Final colors were chosen for an easy artistic visualization. In some images colors do not necessary match with the original channels. **Figure 3** shows and brief example of the procedure. All final snapshots and movies were generated with Imaris. Calibration bars were also automatically displayed.

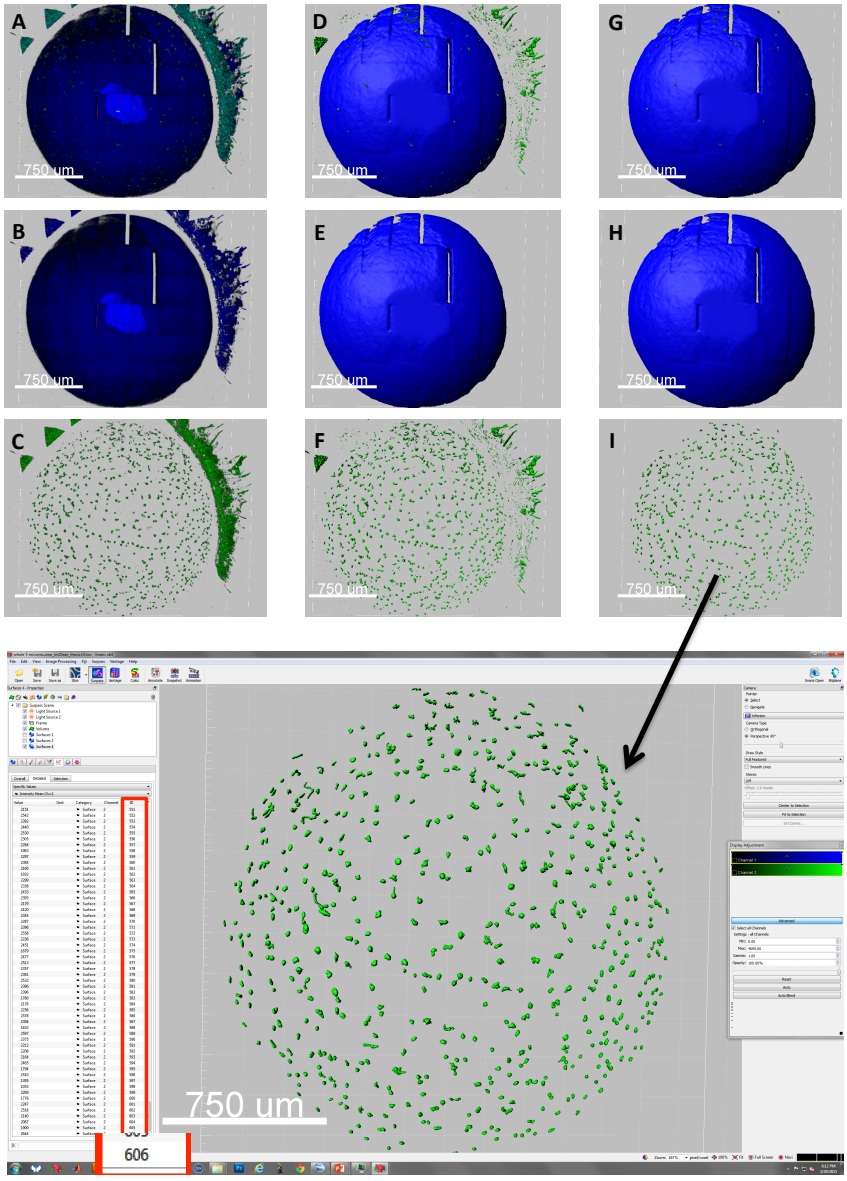

Figure 3. Post-imaging analysis process and cell counting
Files were tiled, stitched and rendered for imaging management. A 3D image was displayed for each channel (A, B and C). Surfaces were manually created. Absolute intensity thresholding was automatically calculated and a manual filter was added (D, E and F). Additional filters were applied to different channels (G and I).
The total number of cells was counted automatically with Imaris. Each cell was rendered as an individual surface. Noise was filtered and intensity mean was calculated in the channel 2.
Note: the number of surfaces computed is enclosed in the red case (606).

Tissue Processing and Whole-Mount Immunostaining

Under deep anesthesia mice were perfused with BSS, followed by 2% PFA and finally with 4% PFA. After eyeballs were post-fixed with Zamboni's solution (24 hours, cool room) allowing endogenous fluorescence preservation. The tissue was washed several times over 24 hours in PBS.

Flat mounts and cross-sections were photographed with a Zeiss Axio Observer widefield fluorescence microscope (Zeiss, Oberkochen, Germany), sequentially scanned using Leica SP5 inverted confocal microscope (Leica TCS 4D; Leica, Heidelberg, Germany) at x20 and x40 magnification.

Statistical analysis statistical analysis

The size particle was established and cell counting was digitally performed with Imaris (***Figure 3***). Statistical analyses included 1-way ANOVA and Bonferroni's Multiple Comparison Test, in addition to two-tailed Student's t-test. Standard error and standard deviation of the mean were calculated. A p-value <0.01 was considered statistically significant.

RESULTS

Intravital visualization of EGFP in the normal cornea of Cx3cr1$^{EGFP/WT}$ mice

In the current work, we used MP-IVM for imaging the resident immune population in normal corneas of genetically-engineered reporter mice expressing EGFP knocked in the Cx3cr1 promoter. The emission of EGFP in the cornea was intravitally detected (***Figure 4 and 5***). EGFP positive cells were observed in the periphery, paracentral and central areas of the cornea with similar distribution. The total number of GFP positive cells was 640±32 per cornea (***Figure 4 and Graphic 1***). However, when the stroma was delineated with the SGH signal, the distribution of EGFP positive cells differs significantly comparing stroma and epithelium (***Figure 5***).

The stroma of the cornea contains very well organized collagen matrix. Second harmonic generation (SHG), or frequency doubling, is a generation of light with a doubled frequency (half the wavelength). Two photons are destroyed creating a single photon with twice the energy. The SHG of the corneal collagen is detected with the BGR cube of the microscope by tuning the laser 880-940 nm (***Figure 2***). At 910 nm both SHG and EGFP emissions were collected in the BGR cube (***Figure 2***). Posterior digital analysis rendered an impeccable tree-dimensional view of the stroma where epithelial population can be discerned out of stromal cells (***Figure 5***). The stromal population appears equally distributed around the cornea; however, EGFP epithelial cells (likely DCs) appear with higher density in the periphery, lesser in the paracentral and vague or absent in the center (***Figure 5***).

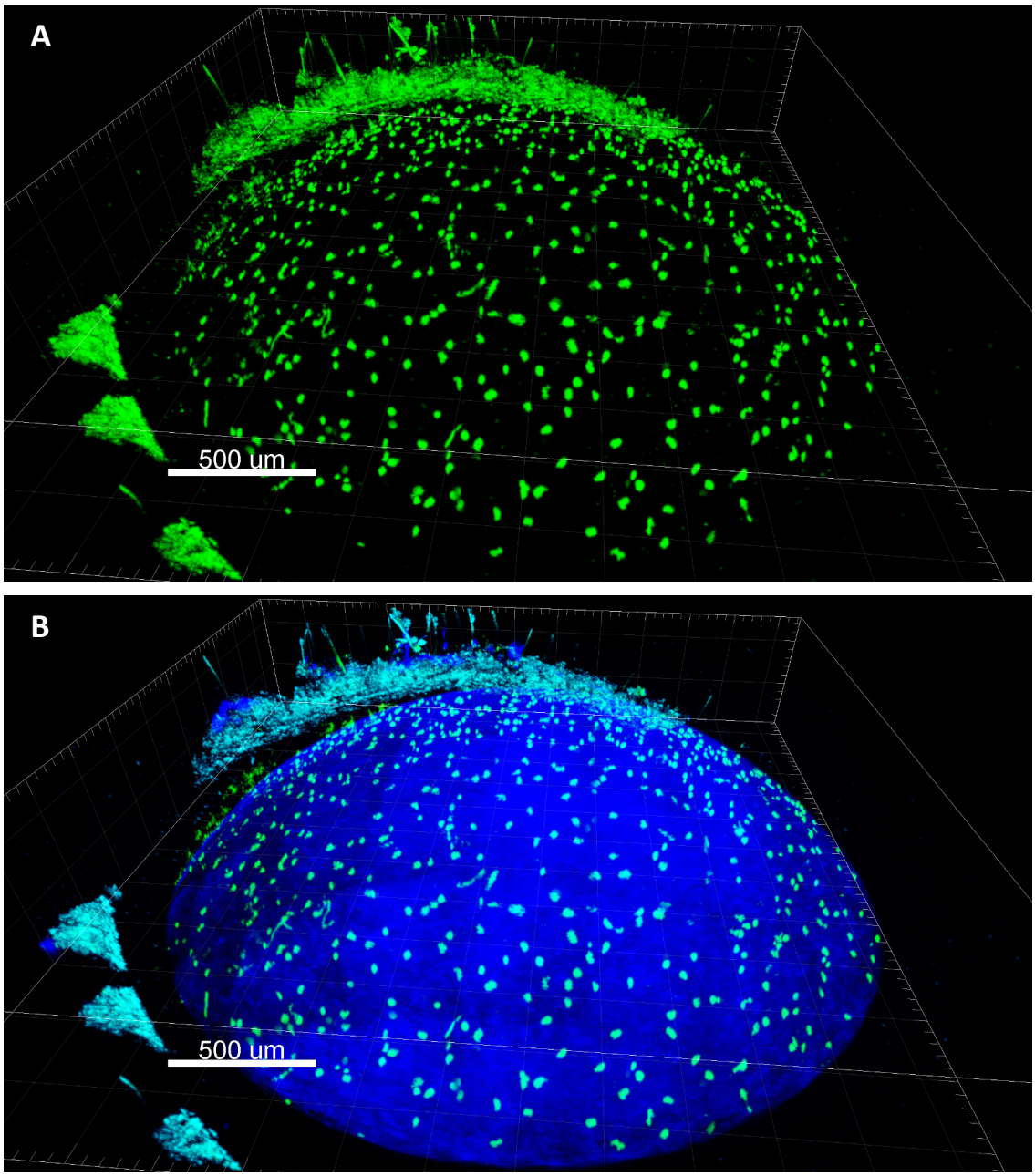

Figure 4. *Intravital* tree-dimensional view of the whole cornea.
EGFP positive cells corresponding with Cx3cr1-derived promoter are displayed in A (3D at minimum projection intensity). The combination of green channel (EGFP) and blue channel (SHG) is displayed in B. Notice the eyelid and eyelashes in the periphery of he cornea.
Myeloid population is shown in green (GFP) and stroma in blue (SGH)

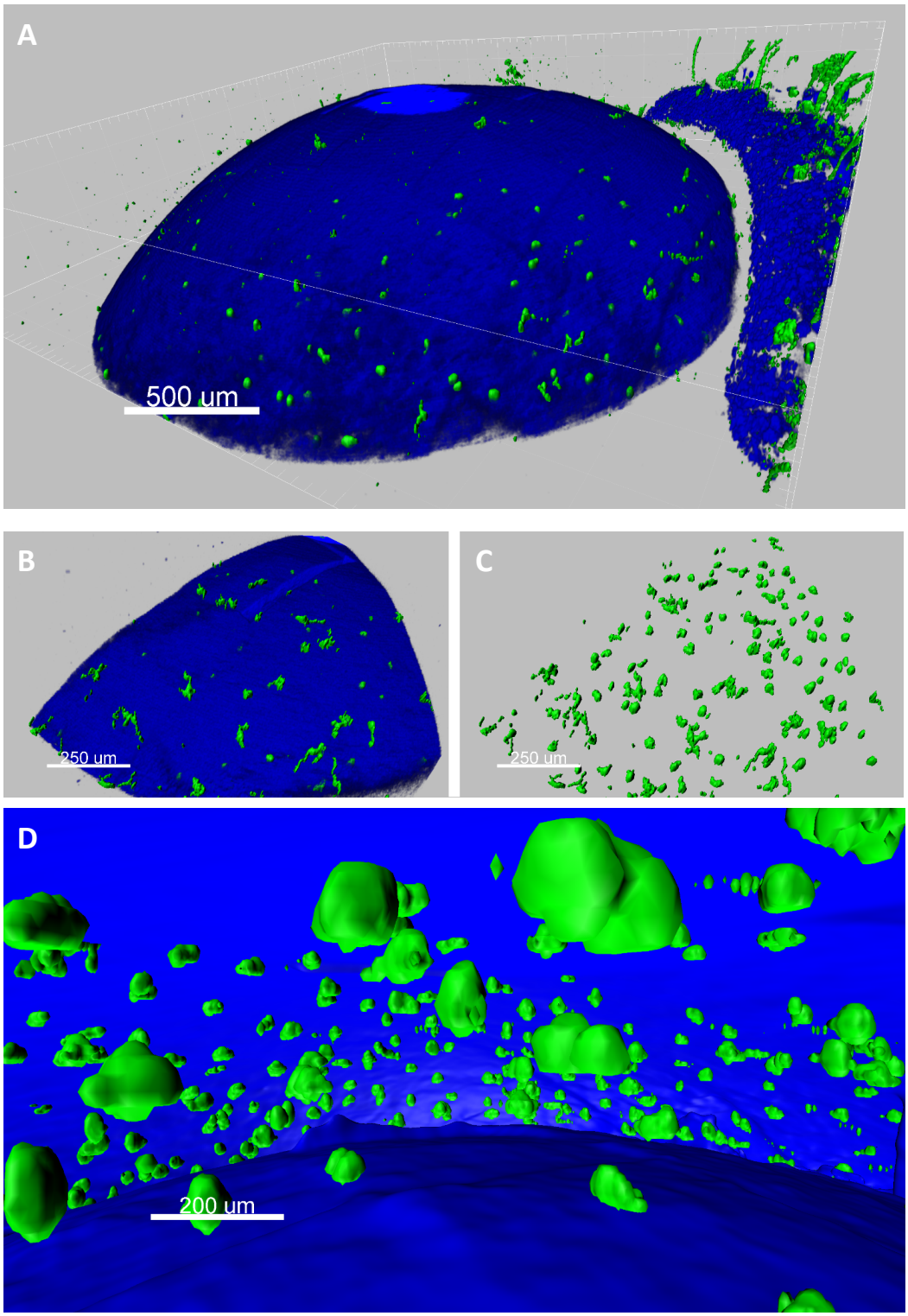
A
500 um
B
250 um
C
250 um
D
200 um

Figure 5. Stratification of Cx3cr1^{EGFP} myeloid cells in the mouse cornea
By using SHG signal the epithelial population is discerned out of the stromal population (A, B and C). Epithelial population shows dendritic morphology (B). Notice in A and B that the center is devoid of cells. Both epithelial and stromal populations can be observed in C. A 3D view inside of the stoma shows the stromal population in D. These cells have different morphology that the epithelial population. Pictures are displayed in a 3D surface view. Myeloid population is shown in green (GFP) and stroma in blue (SGH)
Notice the eyelid on the right side

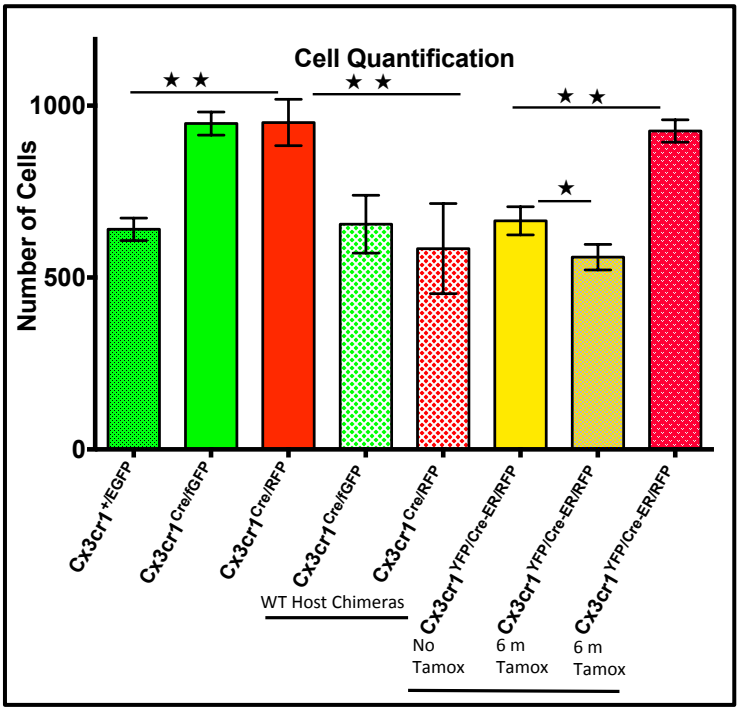

Graphic 1. Myeloid-derived cell quantification in the cornea of different mouse strains.
The number of cells was higher in both fGFP and RFP mice than EGFP mice $p<0.01$.
After transplantation (3 months), WT host chimeric mice show similar number as EGFP. Six weeks old YFP/CRE-ER/RFP mice show similar number (YFP+) than both EGFP and chimeric mice. Six months after injection with tamoxifen, YFP/CRE-ER/RFP mice show similar number of RFP+ than Cx3cr1^{Cre} mice. However YFP+ cell number is decreased respect to young mice.

In vivo visualization of either fGFP or RFP in corneas of Cx3cr1^{cre} mice

Corneas of Cx3cr1^{EGFP} mice show an EGFP^{+} population equally distributed in the stroma but with high density in the epithelium periphery, lesser in the paracentral and absent in the central (***Figure 4***).

Cre/loxP system is a generic Cre-transgene and a Rosa26-loxP-stop codon-loxP-fGFP/tdTomato targeted allele with an intact stop codon [45]. Cre-mediated excision of the stop codon induces constitutive expression of the reporter protein for the entire lifespan of the carrier cell. We examined *in vivo* corneas of either Cx3cr1$^{cre/fGFP}$ mice or Cx3cr1$^{cre/RFP}$ mice and were compared to Cx3cr1^{EGFP} mice. The total number of either fGFP or RFP cells was significantly higher than Cx3cr1^{EGFP} corneas (***Figures 5 and 6; Graphic 1***). In contrast to Cx3cr1^{EGFP} corneas (***Figure 5***), both Cx3cr1$^{cre/fGFP}$ and Cx3cr1$^{cre/RFP}$ show DCs in the central region of the epithelium (***Figures 6 and 7***).

The epithelial population shows a dendritic morphology with a cell body seating over the BMZ/stroma. Epithelial DCs extend dendrites from the stromal bed toward the ocular surface (***Figure 8***). The cells of the stromal population (likely macrophages) show spindle/round shape embedded within the collagen matrix (***Figure 8***). No EGFP signal was observed in any WT corneas.

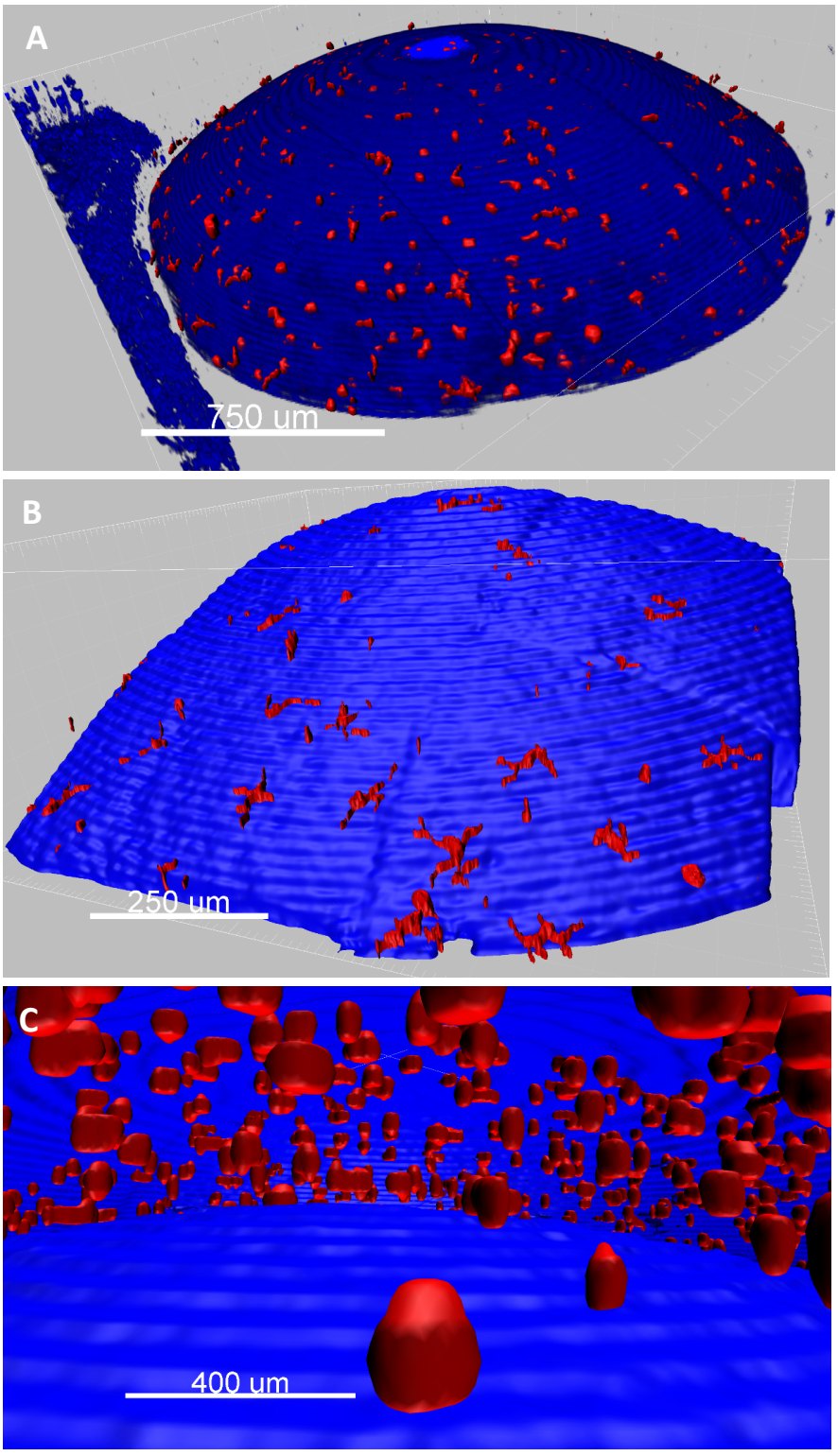
A
750 um
B
250 um
C
400 um

Figure 6. Figure 5. Stratification of Cx3cr1$^{Cre/RFP}$ myeloid cells in the mouse cornea.
The color intensity (Cre recombinase-enhanced) can be appreciated in A. Epithelial DCs appears very well defined in B. Notice in C the high density of macrophages within the stoma. Pictures as displayed in a 3D surface view. Myeloid population is shown in red (tdTomato, RFP) and stroma in blue (SGH)

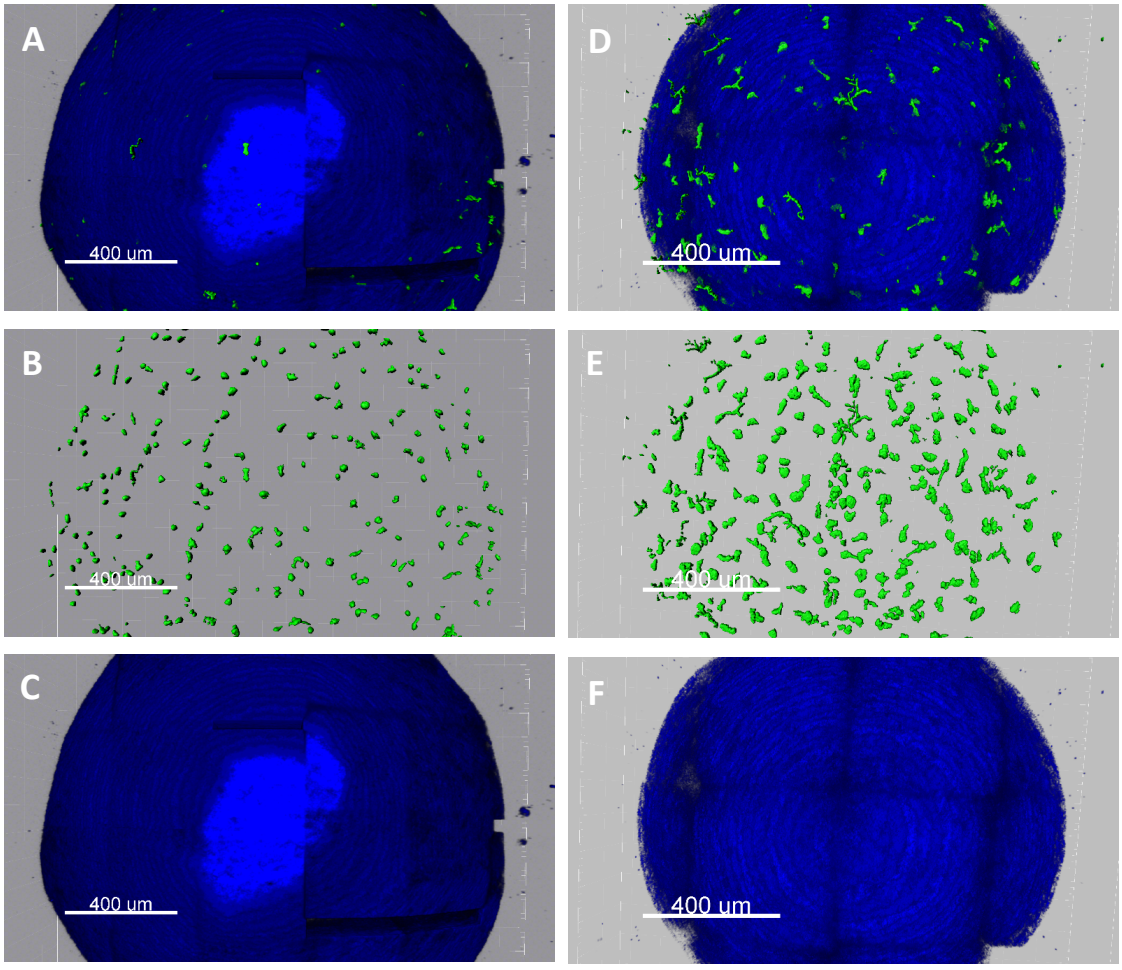

Figure 7. Cre recombinase increase the signal of the reporter
Representative pictures of Cx3cr1^{EGFP} mice (A, B and C) and Cx3cr1$^{Cre/fGFP}$ mice (D, E and F). Body shape is enhanced in E compared with B as well as cell density.
Pictures are displayed in a 3D surface view. Immune population is shown in green (EGFP: A and B, fGFP: D and E) and stroma in blue (SGH).

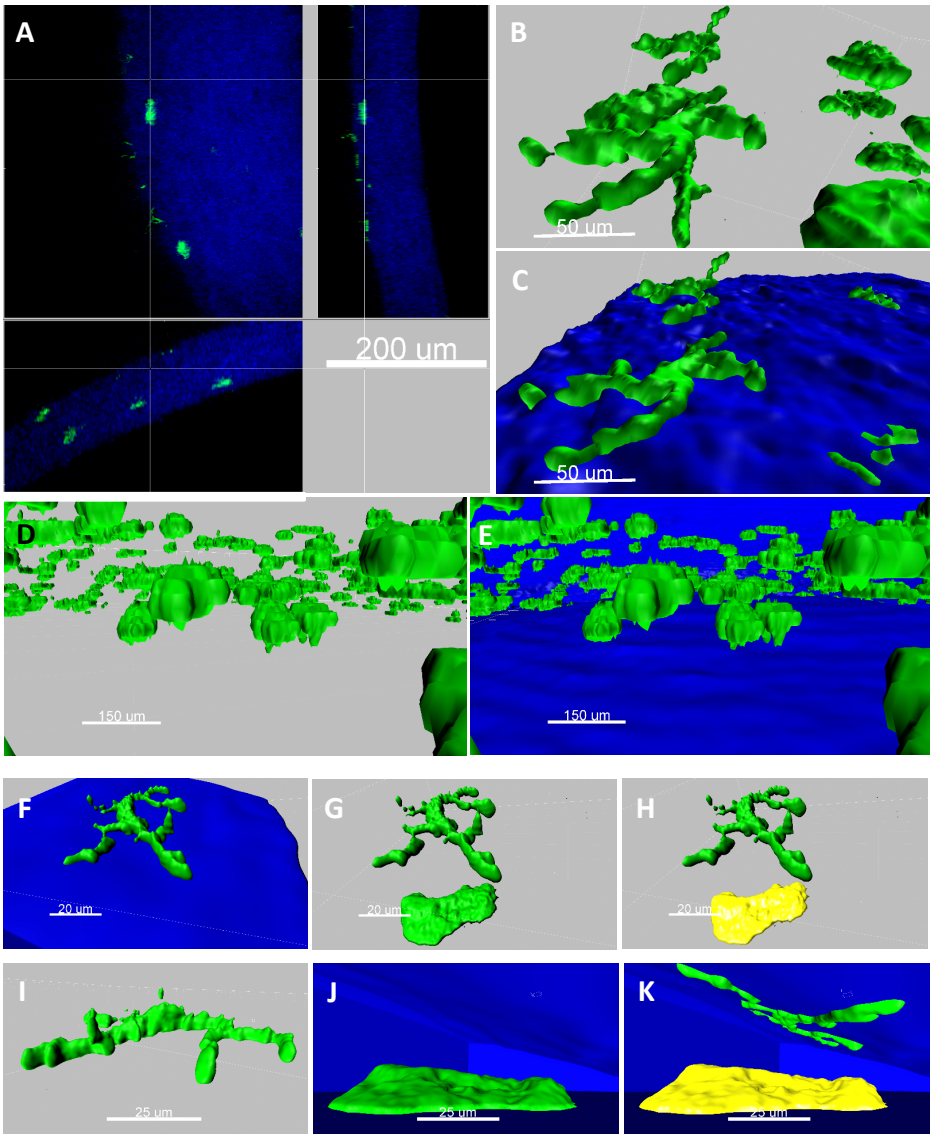

Figure 8. Post-imaging analysis:
Traditional orthogonal slicing (A) compared to 3D reconstitution of the same file. Epithelial DCs (B and C) and stromal macrophages (D and E) are displayed. High-resolution images of an individual DC (F, G, H, I and K) and macrophage (G, H, J and K) are shown.
Note: colors have been digitally picked as yellow (macrophage) and green (DC). Pictures as displayed in a 3D surface view. Immune population is shown in green/yellow and stroma in blue (SGH)

In vivo Evaluation of Corneal Myeloid Population Turnover After irradiation

The turnover of resident myeloid population of the cornea was intravitally evaluated *in vivo*. Host mice were lethally irradiated and immediately engrafted with bone marrow from donor mice as shown in ***Table 1***.

The host population was gradually diminished. The epithelial DC population disappeared within 4 weeks; however the stromal remained longer (6-8 weeks) to 3 months (end of the experiment) especially in the center (***Figures 9.1 and 9.2***).

Donor DCs were observed in the periphery and paracentral regions of the epithelium at 6 weeks after transplantation (***Figures 9.1 and 9.2***). Abundant round shape-donor cells (likely macrophages) were observed in the stroma. At 12 weeks, the cornea appears repopulated with stromal macrophages and epithelial DCs. It was observed a lack of cells in the center of the cornea (***Figures 9.1 and 9.2***). The total number of cells was significantly lesser than normal fGFP or RFP non-irradiated corneas (***Graphic 1***).

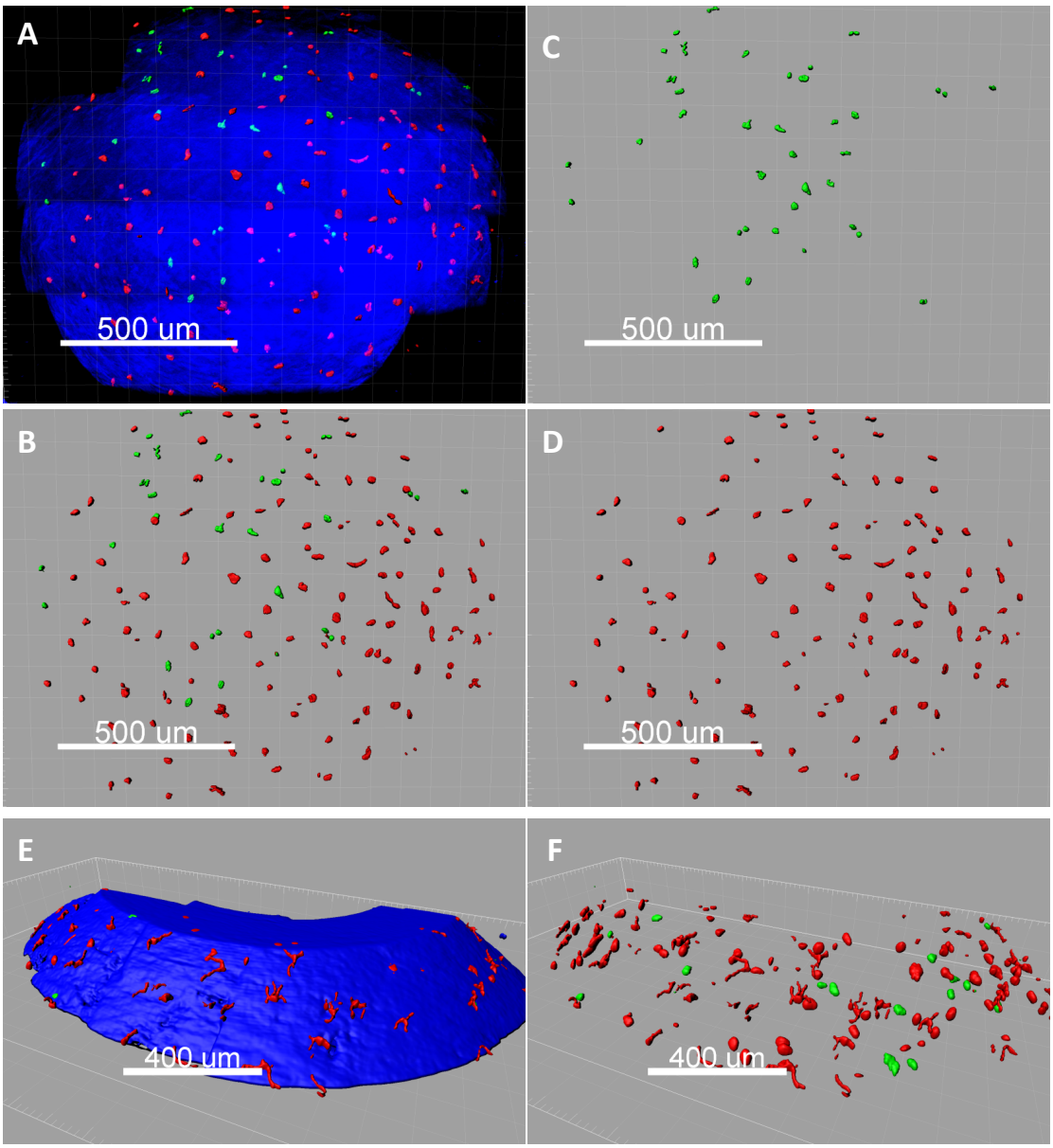

Figure 9.1. Myeloid turnover 6 weeks after irradiation
Mice chimeras were generated by irradiation of CX3CR1^{fGFP} (green) mice and engrafted with CX3CR1^{RFP} bone marrow derived-cells. RFP cells (red) were visible at 6 weeks (A, B, D, E and F). Some host fGFP positive cells (green) were still detected in the host (A, B, C and F).). A, B, C and D show the center of the cornea. E and B show the periphery. Notice the well-defined DCs (red) in the periphery (E and F). Pictures as displayed in a 3D surface view. Myeloid population is shown in green (host) or red (donor) and stroma in blue (SGH)

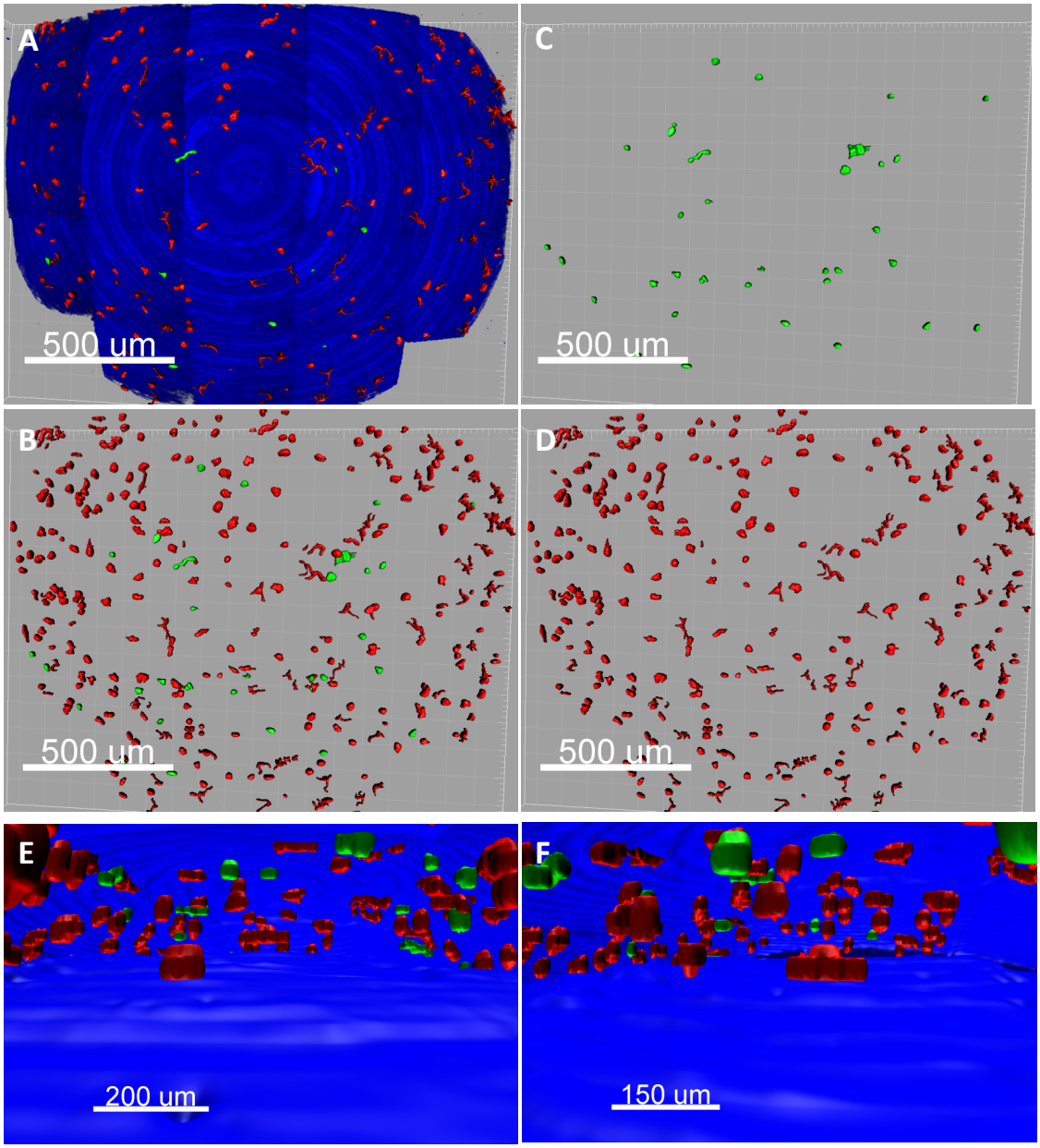

Figure 9.1 Myeloid turnover 12 weeks after irradiation
Few host fGFP cells remain in the stroma (green) (A, B, C, E and F). RFP donor cells (red) are observed (A, B, D, E and F). A, B, C and D show the center of the cornea. Notice lesser density of RFP cells the center. E and B show two different views of the stroma. Pictures as displayed in a 3D surface view. Myeloid population is shown in green (host) or red (donor) and stroma in blue (SGH)

Fate Mapping Study of Corneal Myeloid Population

Previously, we observed that Cx3cr1^{EGFP} mice lack DCs in the center of the cornea (***Figure 5***). Also, we showed that the total number of fluorescent cells is lesser in Cx3cr1^{EGFP} mice than either Cx3cr1$^{cre/fGFP}$ or Cx3cr1$^{cre/RFP}$ mice (***Graphic 1***). Here we used Cx3cr1-YFP-CreER-RFP mice. Briefly: these mice express inducible both YFP and CreER dimer under the promoter of Cx3cr1. Administration of tamoxifen dissociate the dimer and consequently Cre translocates into the nucleus inducing constitutive expression of tdTomato (RFP). The normal cornea expresses only inducible YFP similar in number as Cx3cr1^{EGFP} but no RFP myeloid cells are observed (***Figure 10 and Graphic 1***). After injection of tamoxifen, the YFP myeloid population became RFP+. In the same mice, evaluated at 3 and 6 months post injection, myeloid cells maintained strong RFP+ signal in all detectable cells; however, their YFP expression decreased or disappeared entirely in the center of the cornea and somewhat in the periphery. The total number of myeloid cells detected before and after tamoxifen injection can be observed in ***Graphic 1***. Six months after tamoxifen injection, the number of myeloid YFP+ cells was significantly lesser (559±37) than before injection (665±41) $p<0.01$). However the number of RFP+ cells was significantly higher (926±32)

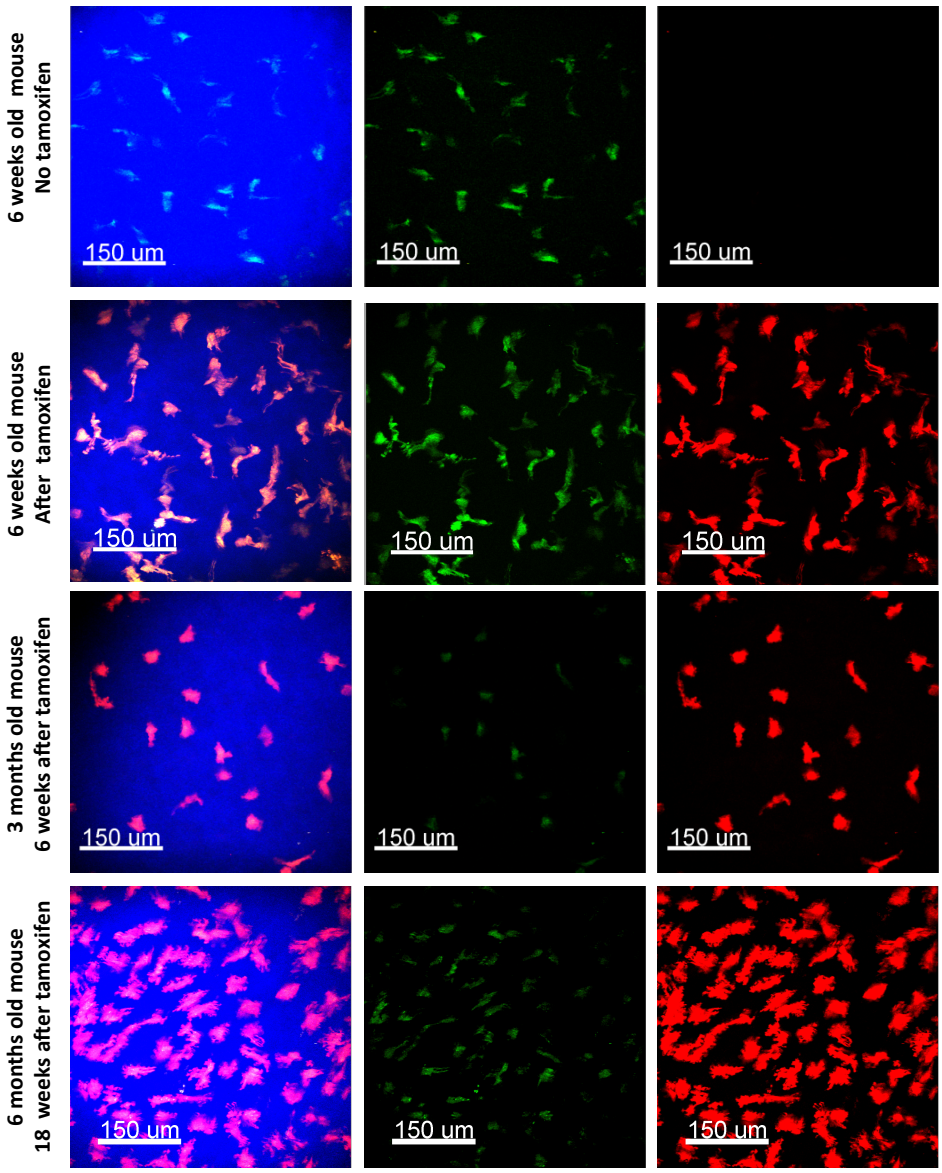

Figure 10. Corneal myeloid population fate mapping.
Six weeks young mice myeloid population expresses inducible YFP but not RFP in the cornea. After tamoxifen myeloid cells turn on RFP+. These representative images are from the same mouse, evaluated at 3 and 6 months post injection. Myeloid cells maintained strong RFP+ signal in all detectable cells; however, their YFP expression decreased or disappeared.
Note: mostly of green signal (YFP) at six months is bleed-through of the strong emission of tdTomato (constitutively expressed).

DISCUSSION

In the current study we effectively combined genetically-engineered reporter expressing mouse strains, MP-IVM and imaging analysis software to obtain an exceptional *in vivo* imaging model for studying the myeloid population of the cornea.

Considering these results, the following conclusions can be drawn:

4. The myeloid population of the cornea was successfully *intravital* visualized in a living mouse.
5. The current model is suitable to study *in vivo* the myeloid population of the cornea in both normal and pathological conditions in the same mouse.
6. Myeloid turnover and fate mapping were *in vivo* evaluated after lethal irradiation or by modulating myeloid-cell phenotype.

For more than a century, it was believed that the cornea was devoid of APCs [46]; however, during the last few years it has been established that the cornea is endowed with a resident myeloid cell population [22-27, 30, 31, 39, 41]. Two different phenotypic populations of APCs such as DCs and macrophages populate in the cornea [33, 47]. The majority of DCs reside in the basal layer of the epithelium where they extend dendrites to interdigitate between epithelial cells from the stromal bed toward the ocular surface. This population is higher in the periphery and decreasing centripetally. Additionally a small population $CD11c^+$ DCs can be found in peripheral regions of the stroma. Although it has been suggested that DCs can initiate an adoptive immune response in inflammatory conditions such as corneal transplantation, the role of DCs in the normal cornea remains not yet understood [25, 27, 30]. Macrophages occupy the stroma divided in two distinct subpopulations. The anterior stroma is populated by putative macrophages that might serve as APCs backup for DCs in an adaptive immune response. The posterior stroma is endowed by resident macrophages uniformly distributed around the cornea. These macrophages display an innate immune response when the cornea integrity is threatened [24, 26, 41].

In the current work, we describe a stratification of the resident myeloid-derived population of the normal cornea in a living mouse. Two distinct populations were visualized. One population can be distinguished in the epithelium (most likely DCS) and second population in the stroma related to macrophages. A similar stratification and distribution has been showed before in corneal explants [26, 27, 34]. $EGFP^+$ myeloid cells are located all around the cornea. $EGFP^+$ myeloid cells appear equally distributed in the stroma; however, epithelial population was observed with higher density in the periphery, lesser in the paracentral and vague or absent in the center. Similar results have been shown before in corneal explants [27, 34]. The great advantage of the current work is that we intravitally imaged the myeloid population in a living mouse, with similar resolution as showed by other authors using corneal explants [27, 34]. Additionally, we performed a post-imaging analysis to achieve a real tree-dimensional view of the cornea, which efficiently improves significantly the interpretation of the results.

Previously, it has been observed in corneal explants that DCs show a dendritic morphology with a cell body seating in the area of the BMZ and extending dendrites toward the ocular surface [27, 39]. Stromal macrophages have been shown with a round shape [27, 39]. In the current work, we intravitally photographed DCs and macrophages that additionally were enhanced with a real tree-dimensional view to confirm the same morphology and shape. Since we imaged *in vivo* (no fixatives), the morphology of the tissue was not affected, therefore more realistic shape is shown.

Previous works agree that the central part of the cornea is devoid of myeloid population; however, it has been proposed that a latent population might reside in this area [16, 22, 30]. In this work we observed lack myeloid cells in the center of the cornea in a $Cx3cr1^{GFP}$ knock-in mouse. Cx3cr1expression is down-regulated or switched off in the center of the normal cornea [34] and therefore inducible EGFP is down-regulated as well which explains the lack of signal in this zone. However, this population was confirmed in both $Cx3cr1^{cre/fGFP}$ and $Cx3cr1^{cre/RFP}$ transgenic mice. The Cre system induces constitutive expression of the reporter fluorescent protein for the lifespan of the cell. The

total number of fGFP or RFP positive cells in Cx3cr1^{cre} corneas was statistically higher than Cx3cr1 knock-in mice $p<0.01$. These results suggest that the center of the cornea might be endowed with a distinct lineage of myeloid cells than the periphery, probably embrionary LCs and tissue macrophages. During the development, yolk sac progenitors migrate to the embryo proper, including the prospective skin, where they give rise to LC precursors, the brain rudiment, where they give rise to microglial cells, and peripheral organs to give rise to tissue macrophages [48, 49]. However, in contrast to microglia, which remains of YS origin throughout life, YS-derived LC precursors are largely replaced by fetal liver monocytes during late embryogenesis and from the bone marrow in the adults [48, 49]. Consequently, adult LCs derive predominantly from fetal liver monocyte-derived cells and bone marrow with a minor contribution of YS-derived [50]. It is widely accepted that a bone marrow derived population resides in the adult cornea [31]. However, our results suggest that the center of the normal cornea might be endowed with a lineage of non-monocyte-derived DCs. First we observed that there is a population of myeloid cells resistant to irradiation indication latency. Second, bone marrow engrafted cells did not repopulate with the same density the center of the cornea. Additionally, after injection of tamoxifen to CX3CR1-YFP-CreER-RFP mice, YFP myeloid population became RFP+. The same mice, evaluated at 3 and 6 months post injection, myeloid cells maintained strong RFP+ signal in all detectable cells; however, their YFP expression decreased or disappeared entirely in the center of the cornea and somewhat in the periphery. This indicates that bone marrow turnover unlikely happen in the normal cornea. These results suggest that the adult cornea might be endowed with an embrionary myeloid population attenuated in the center to prevent inflammation in the visual axis. CX3CR1 mediates homing of MHC class II-positive cells to the normal mouse corneal epithelium [34] where MHC class II expression is particularly decreased [30].

Given that immune cell behavior can be influenced by a multitude of physical and soluble factors from structures and cells in the local environment, we propose a new method to study myeloid cell dynamics in the living mouse cornea using MP-IVM. The

advantage of transgenic mice, expressing fluorescent proteins, was taken to visualize the immune population in the murine cornea.

In conclusion, in this study we combined genetically-engineered reporter expressing mouse strains, MP-IVM and imaging analysis software to obtain an outstanding *in vivo* imaging model. This model is suitable for studying the function of the myeloid population of the cornea in both normal and pathological conditions in a living mouse.

REFERENCES

1. Dupps, W.J., Jr. and S.E. Wilson, *Biomechanics and wound healing in the cornea.* Exp Eye Res, 2006. **83**(4): p. 709-20.
2. Maurice, D.M., *The structure and transparency of the cornea.* J Physiol, 1957. **136**(2): p. 263-86.
3. Maurice, D.M. and A.A. Giardini, *Swelling of the cornea in vivo after the destruction of its limiting layers.* Br J Ophthalmol, 1951. **35**(12): p. 791-7.
4. Meek, K.M., D.W. Leonard, C.J. Connon, S. Dennis and S. Khan, *Transparency, swelling and scarring in the corneal stroma.* Eye (Lond), 2003. **17**(8): p. 927-36.
5. Beebe, D.C., *Maintaining transparency: a review of the developmental physiology and pathophysiology of two avascular tissues.* Semin Cell Dev Biol, 2008. **19**(2): p. 125-33.
6. Hori, J., J.L. Vega and S. Masli, *Review of ocular immune privilege in the year 2010: modifying the immune privilege of the eye.* Ocul Immunol Inflamm, 2010. **18**(5): p. 325-33.
7. Shen, L., S. Barabino, A.W. Taylor and M.R. Dana, *Effect of the ocular microenvironment in regulating corneal dendritic cell maturation.* Arch Ophthalmol, 2007. **125**(7): p. 908-15.
8. Streilein, J.W., J. Yamada, M.R. Dana and B.R. Ksander, *Anterior chamber-associated immune deviation, ocular immune privilege, and orthotopic corneal allografts.* Transplant Proc, 1999. **31**(3): p. 1472-5.
9. Chauhan, S.K., T.H. Dohlman and R. Dana, *Corneal Lymphatics: Role in Ocular Inflammation as Inducer and Responder of Adaptive Immunity.* J Clin Cell Immunol, 2014. **5**.
10. Hamrah, P., Y. Liu, Q. Zhang and M.R. Dana, *Alterations in corneal stromal dendritic cell phenotype and distribution in inflammation.* Arch Ophthalmol, 2003. **121**(8): p. 1132-40.
11. Emami-Naeini, P., T.H. Dohlman, M. Omoto, T. Hattori, Y. Chen, H.S. Lee, S.K. Chauhan and R. Dana, *Soluble vascular endothelial growth factor receptor-3 suppresses allosensitization and promotes corneal allograft survival.* Graefes Arch Clin Exp Ophthalmol, 2014. **252**(11): p. 1755-62.
12. Hajrasouliha, A.R., T. Funaki, Z. Sadrai, T. Hattori, S.K. Chauhan and R. Dana, *Vascular endothelial growth factor-C promotes alloimmunity by amplifying antigen-presenting cell maturation and lymphangiogenesis.* Invest Ophthalmol Vis Sci, 2012. **53**(3): p. 1244-50.
13. Dawson, D.W., O.V. Volpert, P. Gillis, S.E. Crawford, H. Xu, W. Benedict and N.P. Bouck, *Pigment epithelium-derived factor: a potent inhibitor of angiogenesis.* Science, 1999. **285**(5425): p. 245-8.

14. Gabison, E., J.H. Chang, E. Hernandez-Quintela, J. Javier, P.C. Lu, H. Ye, T. Kure, T. Kato and D.T. Azar, *Anti-angiogenic role of angiostatin during corneal wound healing.* Exp Eye Res, 2004. **78**(3): p. 579-89.
15. Griffith, T.S., T. Brunner, S.M. Fletcher, D.R. Green and T.A. Ferguson, *Fas ligand-induced apoptosis as a mechanism of immune privilege.* Science, 1995. **270**(5239): p. 1189-92.
16. Steinman, R.M., *Dendritic cells: understanding immunogenicity.* Eur J Immunol, 2007. **37 Suppl 1**: p. S53-60.
17. Bachmann, B.O., F. Bock, S.J. Wiegand, K. Maruyama, M.R. Dana, F.E. Kruse, E. Luetjen-Drecoll and C. Cursiefen, *Promotion of graft survival by vascular endothelial growth factor a neutralization after high-risk corneal transplantation.* Arch Ophthalmol, 2008. **126**(1): p. 71-7.
18. Chong, E.M. and M.R. Dana, *Graft failure IV. Immunologic mechanisms of corneal transplant rejection.* Int Ophthalmol, 2008. **28**(3): p. 209-22.
19. Dietrich, T., F. Bock, D. Yuen, D. Hos, B.O. Bachmann, G. Zahn, S. Wiegand, L. Chen and C. Cursiefen, *Cutting edge: lymphatic vessels, not blood vessels, primarily mediate immune rejections after transplantation.* J Immunol, 2010. **184**(2): p. 535-9.
20. Chauhan, S.K., J. El Annan, T. Ecoiffier, S. Goyal, Q. Zhang, D.R. Saban and R. Dana, *Autoimmunity in dry eye is due to resistance of Th17 to Treg suppression.* J Immunol, 2009. **182**(3): p. 1247-52.
21. Streilein, J.W., *New thoughts on the immunology of corneal transplantation.* Eye (Lond), 2003. **17**(8): p. 943-8.
22. Forrester, J.V., H. Xu, L. Kuffova, A.D. Dick and P.G. McMenamin, *Dendritic cell physiology and function in the eye.* Immunol Rev, 2010. **234**(1): p. 282-304.
23. Hajrasouliha, A.R., Z. Sadrai, H.K. Lee, S.K. Chauhan and R. Dana, *Expression of the chemokine decoy receptor D6 mediates dendritic cell function and promotes corneal allograft rejection.* Mol Vis, 2013. **19**: p. 2517-25.
24. Hamrah, P., Y. Liu, Q. Zhang and M.R. Dana, *The corneal stroma is endowed with a significant number of resident dendritic cells.* Invest Ophthalmol Vis Sci, 2003. **44**(2): p. 581-9.
25. Khan, A., H. Fu, L.A. Tan, J.E. Harper, S.C. Beutelspacher, D.F. Larkin, G. Lombardi, M.O. McClure and A.J. George, *Dendritic cell modification as a route to inhibiting corneal graft rejection by the indirect pathway of allorecognition.* Eur J Immunol, 2013. **43**(3): p. 734-46.
26. Knickelbein, J.E., K.A. Buela and R.L. Hendricks, *Antigen-presenting cells are stratified within normal human corneas and are rapidly mobilized during ex vivo viral infection.* Invest Ophthalmol Vis Sci, 2014. **55**(2): p. 1118-23.

27. Knickelbein, J.E., S.C. Watkins, P.G. McMenamin and R.L. Hendricks, *Stratification of Antigen-presenting Cells within the Normal Cornea.* Ophthalmol Eye Dis, 2009. **1**: p. 45-54.
28. Chinnery, H.R., E. Pearlman and P.G. McMenamin, *Cutting edge: Membrane nanotubes in vivo: a feature of MHC class II+ cells in the mouse cornea.* J Immunol, 2008. **180**(9): p. 5779-83.
29. Nakamura, T., F. Ishikawa, K.H. Sonoda, T. Hisatomi, H. Qiao, J. Yamada, M. Fukata, T. Ishibashi, M. Harada and S. Kinoshita, *Characterization and distribution of bone marrow-derived cells in mouse cornea.* Invest Ophthalmol Vis Sci, 2005. **46**(2): p. 497-503.
30. Hattori, T., S.K. Chauhan, H. Lee, H. Ueno, R. Dana, D.H. Kaplan and D.R. Saban, *Characterization of Langerin-expressing dendritic cell subsets in the normal cornea.* Invest Ophthalmol Vis Sci, 2011. **52**(7): p. 4598-604.
31. Chinnery, H.R., T. Humphries, A. Clare, A.E. Dixon, K. Howes, C.B. Moran, D. Scott, M. Zakrzewski, E. Pearlman and P.G. McMenamin, *Turnover of bone marrow-derived cells in the irradiated mouse cornea.* Immunology, 2008. **125**(4): p. 541-8.
32. Nowotschin, S., P. Xenopoulos, N. Schrode and A.K. Hadjantonakis, *A bright single-cell resolution live imaging reporter of Notch signaling in the mouse.* BMC Dev Biol, 2013. **13**: p. 15.
33. Limatola, C. and R.M. Ransohoff, *Modulating neurotoxicity through CX3CL1/CX3CR1 signaling.* Front Cell Neurosci, 2014. **8**: p. 229.
34. Chinnery, H.R., M.J. Ruitenberg, G.W. Plant, E. Pearlman, S. Jung and P.G. McMenamin, *The chemokine receptor CX3CR1 mediates homing of MHC class II-positive cells to the normal mouse corneal epithelium.* Invest Ophthalmol Vis Sci, 2007. **48**(4): p. 1568-74.
35. Kezic, J., H. Xu, H.R. Chinnery, C.C. Murphy and P.G. McMenamin, *Retinal microglia and uveal tract dendritic cells and macrophages are not CX3CR1 dependent in their recruitment and distribution in the young mouse eye.* Invest Ophthalmol Vis Sci, 2008. **49**(4): p. 1599-608.
36. Soos, T.J., T.N. Sims, L. Barisoni, K. Lin, D.R. Littman, M.L. Dustin and P.J. Nelson, *CX3CR1+ interstitial dendritic cells form a contiguous network throughout the entire kidney.* Kidney Int, 2006. **70**(3): p. 591-6.
37. Chen, W., K. Hara, Q. Tian, K. Zhao and T. Yoshitomi, *Existence of small slow-cycling Langerhans cells in the limbal basal epithelium that express ABCG2.* Exp Eye Res, 2007. **84**(4): p. 626-34.
38. Liu, Y., P. Hamrah, Q. Zhang, A.W. Taylor and M.R. Dana, *Draining lymph nodes of corneal transplant hosts exhibit evidence for donor major histocompatibility complex (MHC) class II-positive dendritic cells derived from MHC class II-negative grafts.* J Exp Med, 2002. **195**(2): p. 259-68.

39. Lee, E.J., J.T. Rosenbaum and S.R. Planck, *Epifluorescence intravital microscopy of murine corneal dendritic cells.* Invest Ophthalmol Vis Sci, 2010. **51**(4): p. 2101-8.
40. Niederkorn, J.Y., J.S. Peeler and J. Mellon, *Phagocytosis of particulate antigens by corneal epithelial cells stimulates interleukin-1 secretion and migration of Langerhans cells into the central cornea.* Reg Immunol, 1989. **2**(2): p. 83-90.
41. Knickelbein, J.E., R.L. Hendricks and P. Charukamnoetkanok, *Management of herpes simplex virus stromal keratitis: an evidence-based review.* Surv Ophthalmol, 2009. **54**(2): p. 226-34.
42. Cain, D.W., E.G. O'Koren, M.J. Kan, M. Womble, G.D. Sempowski, K. Hopper, M.D. Gunn and G. Kelsoe, *Identification of a tissue-specific, C/EBPbeta-dependent pathway of differentiation for murine peritoneal macrophages.* J Immunol, 2013. **191**(9): p. 4665-75.
43. Gong, S., C. Zheng, M.L. Doughty, K. Losos, N. Didkovsky, U.B. Schambra, N.J. Nowak, A. Joyner, G. Leblanc, M.E. Hatten and N. Heintz, *A gene expression atlas of the central nervous system based on bacterial artificial chromosomes.* Nature, 2003. **425**(6961): p. 917-25.
44. DeFalco, T., I. Bhattacharya, A.V. Williams, D.M. Sams and B. Capel, *Yolk-sac-derived macrophages regulate fetal testis vascularization and morphogenesis.* Proc Natl Acad Sci U S A, 2014. **111**(23): p. E2384-93.
45. Miller, R.L., *Transgenic mice: beyond the knockout.* Am J Physiol Renal Physiol, 2011. **300**(2): p. F291-300.
46. Streilein, J.W., *Immunobiology and immunopathology of corneal transplantation.* Chem Immunol, 1999. **73**: p. 186-206.
47. Sosnova, M., M. Bradl and J.V. Forrester, *CD34+ corneal stromal cells are bone marrow-derived and express hemopoietic stem cell markers.* Stem Cells, 2005. **23**(4): p. 507-15.
48. Gomez Perdiguero, E. and F. Geissmann, *Myb-independent macrophages: a family of cells that develops with their tissue of residence and is involved in its homeostasis.* Cold Spring Harb Symp Quant Biol, 2013. **78**: p. 91-100.
49. Gomez Perdiguero, E., K. Klapproth, C. Schulz, K. Busch, E. Azzoni, L. Crozet, H. Garner, C. Trouillet, M.F. de Bruijn, F. Geissmann and H.R. Rodewald, *Tissue-resident macrophages originate from yolk-sac-derived erythro-myeloid progenitors.* Nature, 2015. **518**(7540): p. 547-51.
50. Hoeffel, G., Y. Wang, M. Greter, P. See, P. Teo, B. Malleret, M. Leboeuf, D. Low, G. Oller, F. Almeida, S.H. Choy, M. Grisotto, L. Renia, S.J. Conway, E.R. Stanley, J.K. Chan, L.G. Ng, I.M. Samokhvalov, M. Merad and F. Ginhoux, *Adult Langerhans cells derive predominantly from embryonic fetal liver monocytes with a minor contribution of yolk sac-derived macrophages.* J Exp Med, 2012. **209**(6): p. 1167-81.

CHAPTER 5

Cutting Edge *in vivo* Imaging II: Multi-Photon *intravital* Microscopy to Visualize the Corneal Nerves in a Thy1-YFP Transgenic Mouse

Cutting Edge *in vivo* Imaging II: Multi-Photon *intravital* Microscopy to Visualize the Corneal Nerves in a Thy1-YFP Transgenic Mouse

Tomas Blanco[1], Daniel R. Saban[1,2].

[1]Ophthalmology Department, Duke Eye Center, Duke School of Medicine, Durham, NC

[2]Immunology Department, Duke Eye Center, Duke School of Medicine, Durham, NC

Supported by Research to Prevent Blindness, Career Development Award (Saban); R01EY021798 (Saban).

Disclosure: The authors of this manuscript have no conflicts of interest to disclose as described by the IOVS

ABSTRACT

Purpose:

The aim of this study was to combine a genetically-engineered reporter expressing mouse (Thy1-YFP), multiphoton *intravital* micoroscopy (MPM-IV) and digital post-production analysis, to create an exceptional model for imaging the corneal nerves. This model should be suitable for studying nerve function in normal and pathologic corneas in a living mouse.

Methods:

B6.Cg-Tg(Thy1-YFP)16Jrs/J and C57BL/6J WT mice were used. MP-IVM was used to detect neurofluorescence in the cornea of a living mouse. Additionally, corneal explants were immunelabeled with anti tubulin beta III antibody and scanned with a mutliphoton microscope (MPM) and a laser scanning confocal microscope (LSCM). Digital post-analysis was performed with image software.

Results:

The expression of neuron-specific fluorescence in a transgenic Thy1-YFP mouse cornea was successfully detected with a MP-IVM system. Stromal bundles, plexus and epithelial leashes were visualized with high resolution and acquisitions were displayed in a useful and interactive tree-dimensional image. As a novelty, tree concentric nerve rings were detected in the stroma (periphery, paracentral and central) that innervate from bellow the sub-basal plexus. Additionally, the stromal innervation of the sub-basal plexus bifurcates in opposite directions (T pattern, toward the center and toward the periphery). Although the amount of Thy1 neurofluorescence was subjectively lesser compared to tubulin beta III staining, both show a similar pattern of distribution in the mouse cornea.

Conclusions:

In this study we were able to combine a genetically-engineered reporter expressing mouse (Thy1-YFP), MP-IVM and imaging analysis to obtain an outstanding imaging model to study the corneal nerves in al living mouse. This model should be suitable for

understanding function of corneal nerves in both normal and pathologic cornea. Additionally we identified new stromal nerve bundles in the deep central part of the cornea, concentric nerve rings in the stroma and a new bifurcation pattern in the sub-basal plexus. The damage of specific nerves induce loss of the immune privilege in specific areas related with that particular nerves

INTRODUCTION

The human cornea is the most densely innervated structure in the body supplied by both sensory and autonomic nerve fibres [1]. Sensory nerves are derived from the ophthalmic division of the trigeminal nerve [2-6] and have a diversity of sensory and efferent functions [7]. The autonomic nerves consist of sympathetic fibres that are derived from the superior cervical ganglion and parasympathetic fibres that originate from the ciliary ganglion [8-10].

The proper innervation is critical for keeping both wellness and transparency. The mechanisms by which corneal nerve fibres maintain a healthy cornea and promote wound healing after injuries is currently under active research. Neurons give trophic support to corneal epithelial cells by releasing soluble substances through. Trigeminal ganglion neurons release neurotransmitters and neuropeptides that contribute to maintain regulatory processes such as corneal trophism and homeostasis. Molecules released by nerves participate actively in corneal wound healing process after injuries [11, 12]

Many factors such as blinking, desiccation of the ocular surface, cooling or air currents induce release neurochemicals by corneal nerves that in consequence aid to heal small damages in the ocular surface [13-15]. Conversely, patients who suffer from diminished corneal innervation, caused by diabetes, herpetic keratitis, contact lens wearing and aging, show impaired wound healing [16-20]. Corneal nerves can be also damaged after cataract and retinal surgery or laser procedures (e.g. pan-retinal photocoagulation, cycloablation) [21-23]. During the last two decades, it has been shown that refractive surgery produces strong damage of corneal nerves and transient mild to severe epithelial alterations [24-26]. Nowadays, dry eye is the most common neuropathological dysfunctional syndrome [16, 27, 28]. Despite mostly of the corneal pathologies present a neurological component, the physiological basis remains still unknown.

The corneal nerve anatomy briefly described [1]: nerve bundles enter radially through the sclera into of the cornea in parallel to the surface. In the limbus, nerve bundles lose

the perineurium and myelin sheaths. Inside of the peripheral cornea, bundles subdivide into smaller side branches. The majority of the stromal nerve fibres are located in the anterior third of the stroma; however, some stromal nerve trunks can be located below in the peripheral cornea [29, 30]. Bundles contain variable number of axons, and occasionally, keratocytes enwrap adjacent nerve fibres with cytoplasmic extensions. The stromal nerve fibres turn abruptly 90° progressing toward the surface. After penetrating Bowman's layer, large nerve bundles divide into several smaller [31, 32]. Afterward, small nerve axons turn suddenly 90° forming an epithelial leash parallel to the corneal surface in the sub-basal plexus, between Bowman's layer and the basal epithelial cell layer. Epithelial leashes consist of mixtures of straight and beaded nerve fibres that project in separated units toward more superficial layers where release or take up cellular or extracellular substances from adjacent epithelial cells [31, 33-36]. Corneal nerve density is approximately 5400–7200 nerve bundles in the human plexus [19, 37, 38]. Each nerve bundle arises 3–7 individual axons sprouting roughly to a total of 19000–44000 axons [39]. The total number of free nerve endings are between 315000 and 630000, (approximately 7000/mm^2), homogeneously distributed across the cornea [39].

Different methods have been used to describe the anatomy of the corneal nerves. The first understanding of corneal nerve architecture and morphology was established by using acetylcholinesterase (gold chloride), and immunohistochemistry [40-45]. Posteriorly, corneal nerve ultrastructure has been described by electron microscopic [31, 33-36, 39, 46, 47]. Later, with the use of monoclonal and polyclonal antibodies, corneas of different species were compared [48-53]. Retrograde labeling methods allowed backward label of TG sensory cell bodies whose axons innervate the cornea [1, 4]. With the use of electrophysiology techniques, it has been demonstrated the sensorial nature of the different terminal endings [53]. In vivo Confocal Microscopy (IVCM), widely used to visualize corneal nerves in patients, has notably increased the understanding of nerve anatomy in healthy and pathologic corneas, [19, 24, 28, 38, 54-58]

Very recently, the multiphoton *intravital* microscope (MP-IVM) has been introduced to study the eye. The composition of the different corneal layers of five different species (human, piscine, porcini, bovine and murine) has been described [59]. Steven et al. have recently shown the immune cell dynamic in corneal lymphatic vessels [60]. Additionally Masihzadeh et al. have imaged the anterior chamber of the eye mouse [61].

Considering the transparency of the cornea, we explored the full potential of the MP-IVM in a Thy1-YFP transgenic mouse model. In this work, we show a new model of imaging to describe the corneal nerve architecture in a living mouse, with a sharp resolution and outstanding tree-dimensional post-production.

The purpose of this study was to combine a genetically-engineered reporter expressing mouse (Thy1-YFP), MP-IVM and digital post-production analysis, to create an exceptional *in vivo* model for imaging the corneal nerves. This model should be suitable for studying nerve function in normal and pathologic corneas in a living mouse.

METHODS

Mice and Anesthesia

Mice were housed in a specific pathogen-free environment at the Duke Eye Center animal facility. The Institutional Animal Care and Use Committee approved all procedures. All animals were treated according to the ARVO Statement for the Use of Animals in Ophthalmic and Vision Research. Anesthesia was given with intraperitoneal administration of ketamine/xylazine (120 and 20 mg/kg, respectively). B6.Cg-Tg(Thy1-YFP)16Jrs/J mice, referred to here as Thy1.1-eYFP (Thy1-YFP), are commercially available and were a kind donation from H. Tseng (Department of Ophthalmology, Duke University Medical Center). Six mice were used.
Additionally six C57BL/6J 8 week old mice were purchased from Jackson laboratories (Jackson, Farmington, Connecticut).

Multiphoton Intravital Microscopy

Mice were maintained under anesthesia using constant infusion administered via IP catheter of ketamine/xylazine (120 mg/kg) at a rate of 0.2 ml/h. Body temperature was controlled at 37°C. Mice were dorsally placed, facilitating perpendicular exposure of the corneal apex to the microscope objective. Objective to cornea space was filled with an ophthalmic gel (GenTeal, Novartis Ophthalmics, East Hanover) to create a coupling immersion interface with a refractive index (n=1.339) similar to water (n=1.333 at 20° C) as well as to provide eye lubrication. A drop of propidium iodide (PI) (~50µl) was topically instilled in the cornea for 1 minute before the mouse was placed under the microscope to stain the most superficial layer of the epithelium.

A 25x/1.05 NA water objective (optimized for MPEXLPL25XWMP, WD 2.0 mm, 0 to 0.23 micron coverslip correction) of an Olympus BX61WI upright microscope fixed

stage (Olympus, Tokyo, Japan) was used (**see chapter 4**). The laser used was a ChameleonVision II single box Ti:Sapphire fsec laser, permitting pulse compensation in a tunable range of 680-1080 nm @40 nm/sec, 80 MHz rep rate, 140 fsec pulse width with a 0-47,000 fsec2 units of dispersion compensation. The microscope is equipped with a Blue, Green/Yellow and Red standard fluorescence cube. Emission bands available are DAPI, CFP, GFP, YFP and RFP in switchable cubes; the Blue or Cyan channels were used for second harmonic generation (SHG). Laser was tuned at 910 nm (BGR cube) or 950 nm (CYR cube) for two-photon excitation and second harmonic generation (SHG). A dichroic mirror (DM570) splits the light emission through both channels 1 (blue) and 2 (green or yellow) and channel 4 (red). A second dichroic mirror (DM485) divides light emission for channel 1 and channel 2. The BGR cube is composed of 450-460 nm (blue and SGH), 495-540 (Green) and 575-630 nm (Red) band pass filters. The CYR cube is composed of 460-500 nm (blue and SGH), 520-560 (Yellow) and 575-630 nm (Red) band pass filters. The system has four high efficiency non-descanned detectors in the epi position that can be combined in different configurations by manually alternating the cubes.

Z-series images for 3D mosaic imaging

By using a motorized XY stage, the multi-area time-lapse software (Olympus) automates the process for a 3D image acquisition and stitching. The software registers wide areas, and the thumbnail displayed provides a view of the entire image acquired during the mosaic imaging process (**see chapter 4**).

Post-acquisition image analysis

Image stacks were analyzed using the latest version of FUJI available (developed by Wayne Rasband, National Institutes of Health; provided auto-updated by the public domain http://rsb.info.nih.gov/ij). The latest version of Imaris (Imaris, auto-updated

version, Bit-plane, Zurich, Switzerland) was also used (**see chapter 4**). Raw files were displayed in Imaris and linked to FIJI for background substraction, brightness/contrast adjustment, noise reduction, compression and size adjustment. After, an easy readable image was imported back from FIJI into Imaris rendering a maximum-intensity projection or blend projection providing a realistic 3D view in a 2D screen. Additional depth perception enhancing realism of the images was created with the Real-Time Shadow Rendering (a fast hardware that projects shadows on the three planes of the object). A surface object is a computer-generated illustration of a detailed region of interest in the data set. The surface object is displayed as a simulated solid object. The accuracy of segmentation against the original data can be easily verified in an interactive manner (for more details visit: http://www.bitplane.com/imaris/imaris). Surface rendering was interactively performed using optimal threshold settings for each channel in each experiment. By choosing absolute threshold, it was possible to detect large portion of the cells without picking up any noise or background with an accurate separation of touching cells. "Quality" and/or "number of voxels" filters were used for detection of seed points. It can pick up missed pixels or remove non-desirable background or noise. Filter settings were optimized comparing interactively the result with the original maximum-intensity projection. Final colors were chosen for an easy artistic visualization. In some images colors do not necessary match with the original channels. Calibration bars were also automatically displayed.

Tissue Processing and Whole-Mount Immunostaining

Under deep anesthesia mice were perfused with BSS, followed by 2% PFA and finally with 4% PFA. After, eyeballs were post-fixed with Zamboni's solution (24 hours, cool room) allowing endogenous fluorescence preservation. The tissue was washed several times over 24 hours in PBS. Corneas were excised in a flowering pattern and treated with blocking buffer (2% BSA, 0.5% tween 20 and 0.2% Triton, overnight at 4C).

Posteriorly the tissue was incubated with a rabbit anti tubulin beta III antibody (1:200, overnight, 4C, Covance) and goat anti rabbit Alexa-488/594 (Vector).

Flat mounts and cross-sections were photographed with a Zeiss Axio Observer widefield fluorescence microscope (Zeiss, Oberkochen, Germany) or sequentially scanned using Leica SP5 inverted confocal microscope (Leica TCS 4D; Leica, Heidelberg, Germany) at x20 and x40 magnification. In addition whole corneal flat mounts were also scanned, tiled and stitched with the multiphoton microscope.

RESULTS

The expression of neuron-specific fluorescence and the emission of the SHG of the collagen, in a transgenic Thy1-YFP mouse cornea, are shown in ***Figure 1***. SHG, or frequency doubling, is a generation of light with double frequency (half the wavelength). Two photons are destroyed creating a single photon with twice the energy. SHG microscopy has emerged as a powerful modality for imaging fibrillar collagen in a diverse range of tissues [62]. The corneal stroma is composed of very well organized collagen matrix, which SHG can be detected by tuning the laser at 910-970 nm. Fine-tuning at 950 nm both SHG and YFP emissions were detected with the microscope CYP cube (***Figure 1)***.

At 950 nm and 2% of the laser maximum power (4mW maximum), the microscope captured individual pictures for each channel with a digital zoom of 1.5X. The resolution of each individual picture was 620 dpi with 0.25s scanning time. The start scanning was manually set up at the confluence of the iris with the sclera (600 μm deep for the corneal apex). The microscope automatically scanned, from the anterior chamber towards the apex of the cornea (2.5 μm each steep), a total of 240 acquisitions in each tile/channel (720 pictures). The microscope robotically moved to the next position to complete 120 tiles and 86.400 pictures. For each tile the microscope consumed 62 seconds and a total of 2 hours and 20 minutes for the whole cornea. Although little mouse movements were disturbing the imaging, mostly were corrected by posterior digital stitching. One important limitation was the big size of the generated files up to 50 Gigabytes (mostly empty space). Post-analysis of the files required an additional 120 GB of RAM memory in the computer (***see chapter 4***)

Herein, we present the whole acquisition of the cornea (***Figure 1***); however, specific regions can be easily observed within seconds. Higher resolution images (up to 2.400 dpi) can be already gathered (***data not shown***). In the current experiment we used 620 dpi to render the best quality at the shortest time.

The main limitations of examinations in a living mouse were:

1. Eyeball rotations. These movements were compensated by increasing xylacine concentration up to 25 mg/kg with the anesthesia.
2. Breathing movements. A mouse holder was used for long time acquisitions.
3. Additionally, a digital stitching corrects, in part, the motions. To enhance stitching process, the digital zoom was increased to 1.5x in the microscope. This option allows overlapping margins between nearest tiles; however, increases twice the acquisition time.

The entire view of the corneal nerves can be observed with a radial distribution towards the center, where a whorling pattern is appreciated in the apex (***Figure 2 and 4***). The radial nerves are located at three different levels: plexus, anterior part of the stroma and deep posterior stroma (***Figure 2, 3, 4, 5 and 7***). Nerve bundles enter radially through the periphery of the cornea in a parallel to the surface (***Figure 1, 2, 3, 4 and 7***). Some stromal nerve fibres turn abruptly 90° progressing toward the surface and divide into several smaller ones that turn again 90° forming the plexus. Epithelial leashes branch 90° from the sub-basal plexus toward the surface (***Figures 1, 2, 3, 5 and 7***).

Thick nerve bundles were found radially distributed deep in the anterior and posterior parts of the stroma (***Figures 2, 3, 4, 5 and 6***). Stromal nerve branches penetrate the basement membrane and enter the sub-basal plexus from below where bifurcate in both directions toward the center but also toward the periphery (***Figures 2 and 5***). These sub-basal nerves do not run for long distances noted in the peripherals that travel from the periphery through the center. Surprisingly, deep stromal nerves turn up in a loop connecting with superior stromal bundles thus generating tree stromal concentric nerve trunks: peripheral, paracentral and central (***Figures 3***). Different ramifications emerging form these concentric trunks enter the sub-basal plexus ramifying as described above (***Figures 2 and 3***). The central epithelium is innervated by branches coming from the

periphery through the plexus as well as many others emerging from the central ring bundle in the stroma (***Figures 2, 3 and 5***).

To probe this pattern of innervation we severed a stromal nerve deeply in the peripheral stroma (***Figures 6***). The cornea turned inflamed (opacity, epithelial erosion, neovascularization and stroma plaque) in the area innervated by this specific nerve, but the rest of the cornea remained transparent even the center.

In vivo imaging resolution of the corneal nerves (branching, sprouting, ramifications etc.) is similar to *ex vivo* explants (***Figures 4 and 7***). In this work, we did not compare objectively both; however, the number of axons stained with anti tubulin III antibody appears lightly higher than YFP gathered *in vivo*. Nevertheless, the pattern does not differ.

Additionally, we create a course-plotting mode (***Supplementary Movie***). This option allows navigation throughout the whole image. This is very useful to search for a specific region of interest without tedious staining and imaging processes.

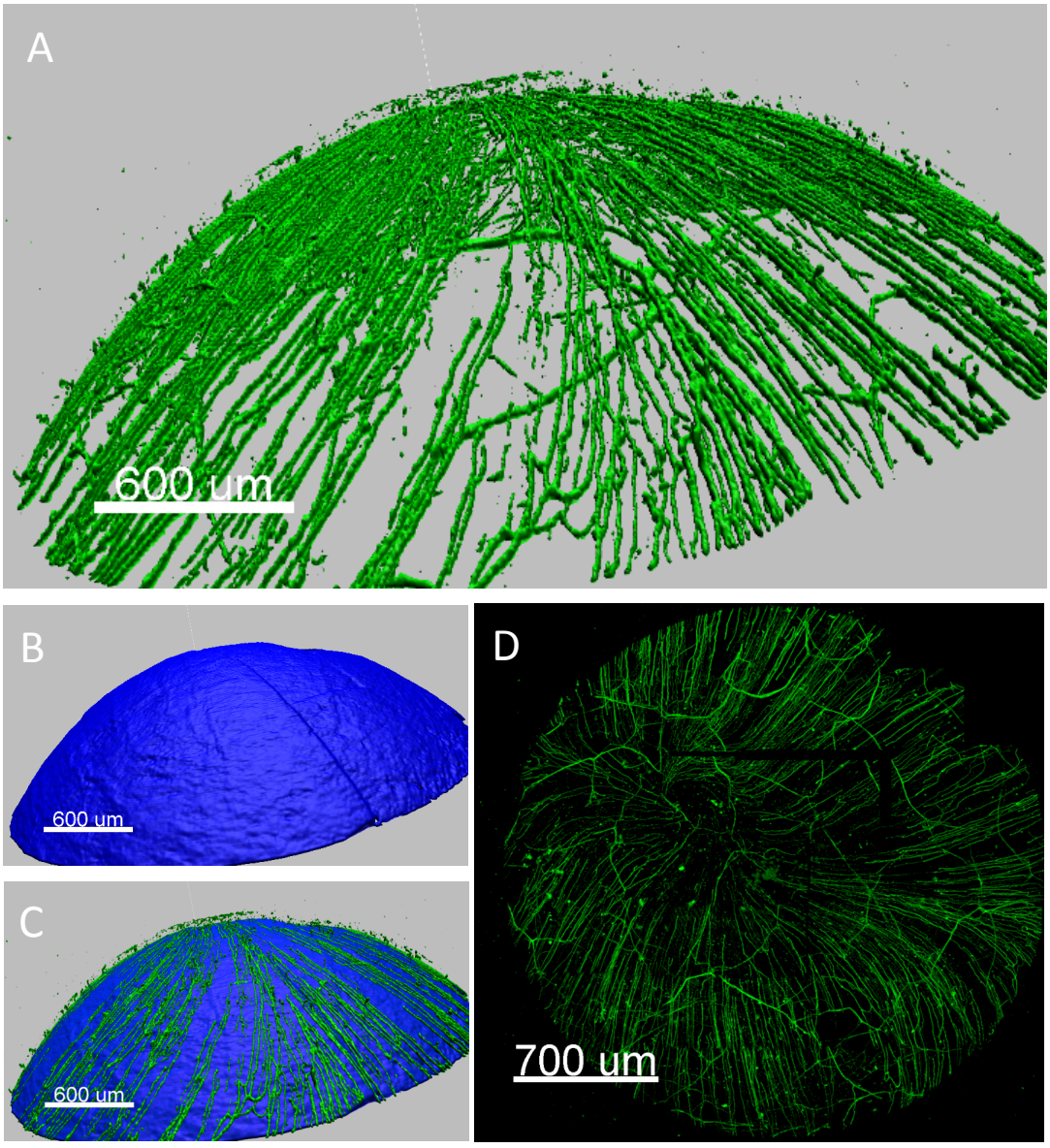
A
600 um
B
600 um
C
600 um
D
700 um

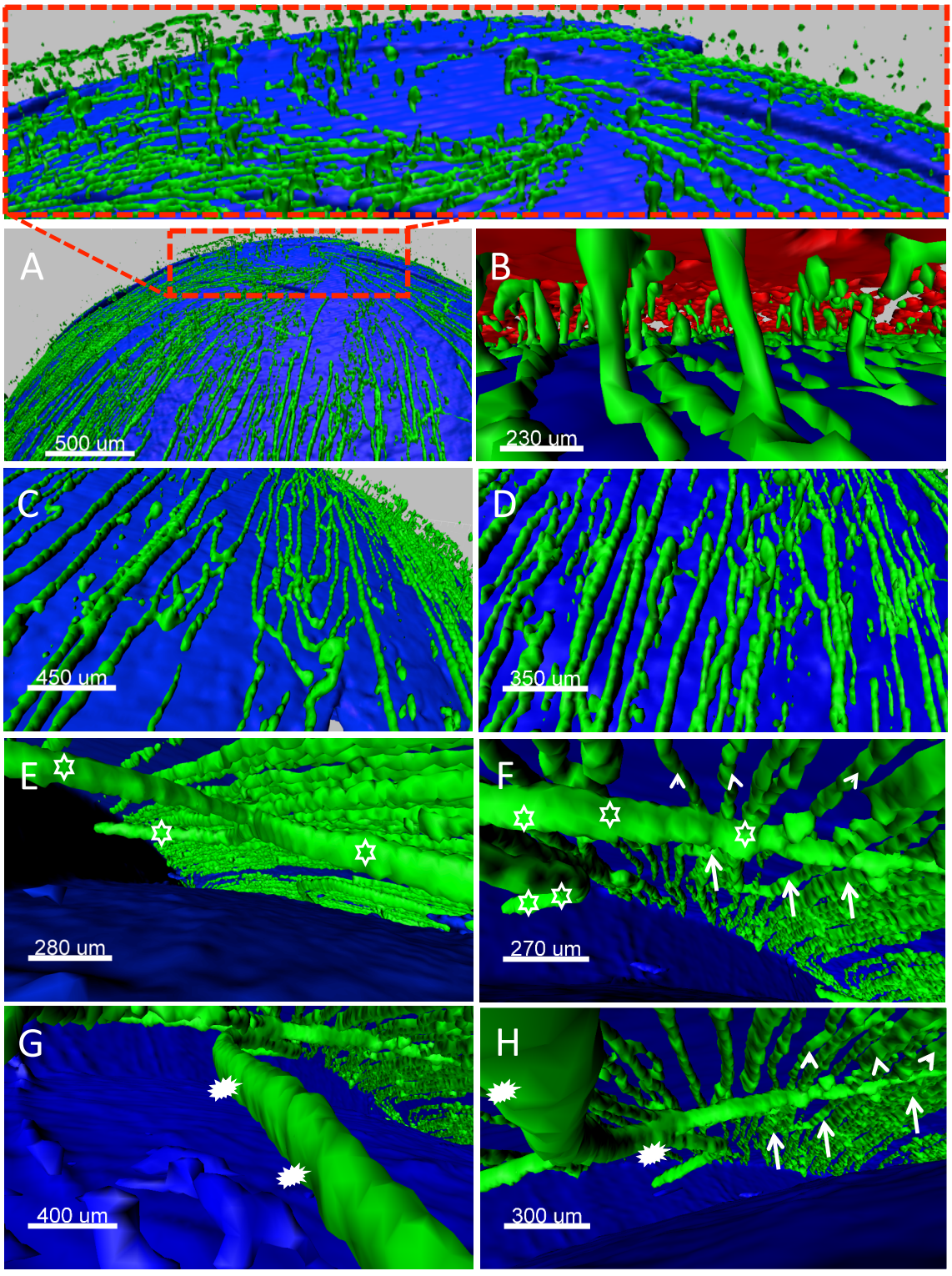
A
500 um
B
230 um
C
450 um
D
350 um
E
280 um
F
270 um
G
400 um
H
300 um

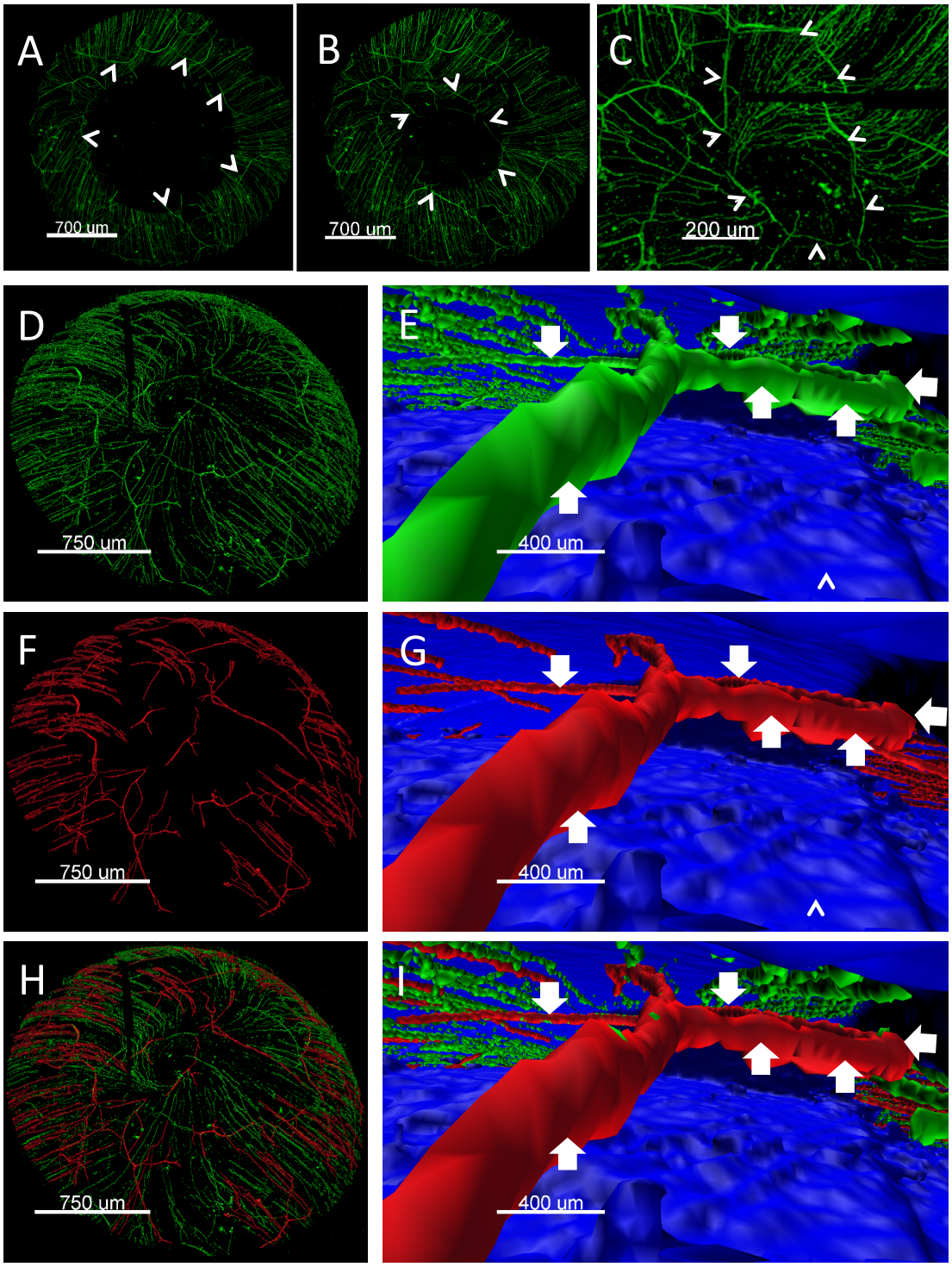
A
700 um
B
700 um
C
200 um
D
750 um
E
400 um
F
750 um
G
400 um
H
750 um
I
400 um

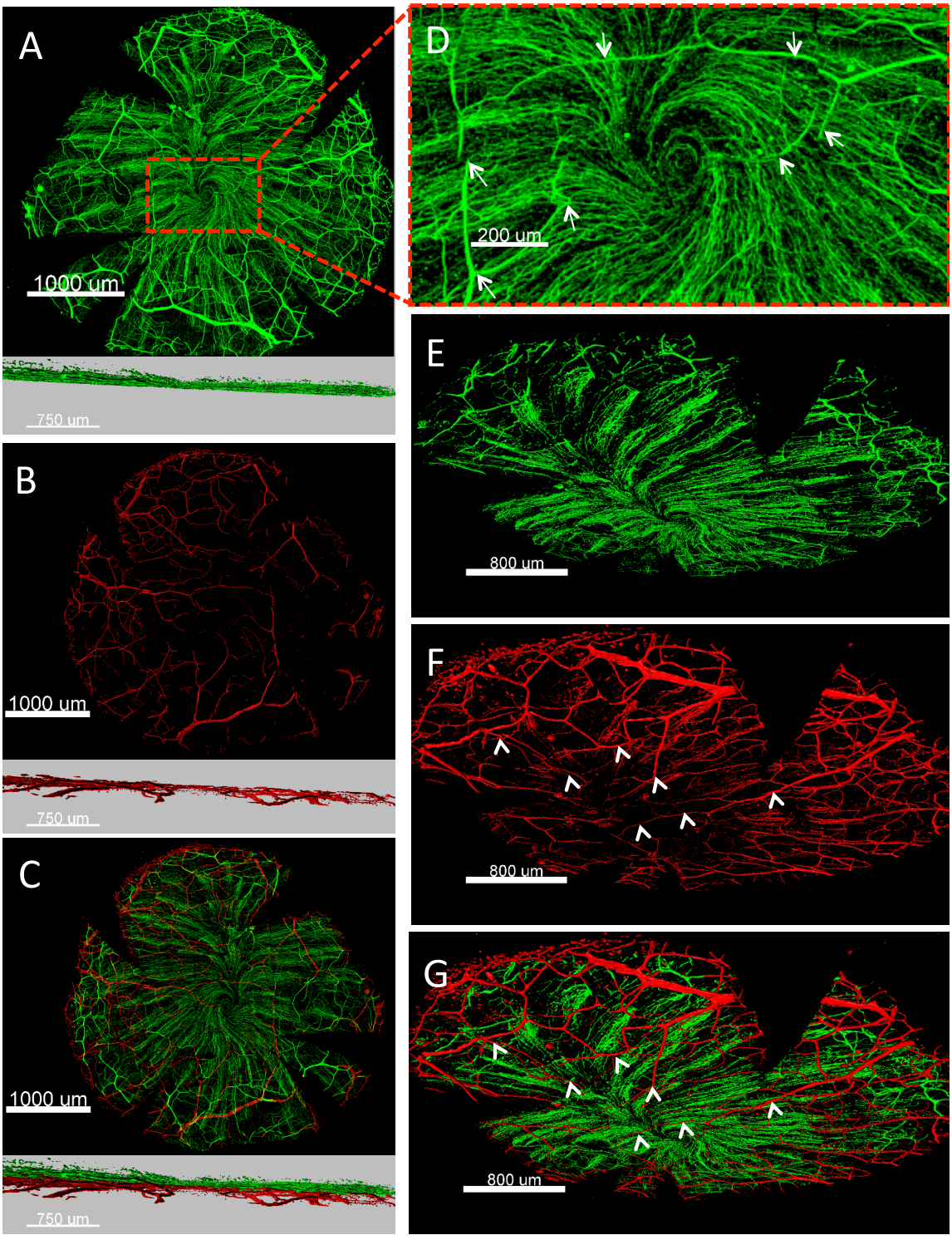
A
1000 um
750 um
B
1000 um
750 um
C
1000 um
750 um
D
200 um
E
800 um
F
800 um
G
800 um

Figure 1. *Intravital* tree-dimensional view of the whole cornea.
YFP positive nerves (green) corresponding with Thy1 derived promoter are displayed in 3D (A). The combination of yellow channel (YFP, green) (A) and blue channel (SHG) (B) is displayed in C. A maximum projection view of the nerves is displayed in D. Blue=SHG
The software automatically displayed calibration bars

Figure 2. *Intravital* tree-dimensional view of the corneal nerves
YFP positive nerves (green) are visualized with high resolution *in vivo*. The radial distribution of the subbasal plexus can be observed in A. The whorling pattern is appreciated in the apex (red box). Epithelial leashes branch 90° from the sub-basal plexus toward the surface (red: propidium iodide) (B). The hairpin pattern can be appreciated in the sub-basal plexus (C and D) with high density of fibres. Stromal view of the sub-basal plexus with nerve bundles in the anterior stroma (E and F) and posterior stroma (G and H). Posterior nerve trunks (white asterisk) ramify in thinner branches in the anterior stroma (white stars). In the sub-basal plexus nerves ramify in both directions: toward the center (white arrows) and toward the periphery (white arrow heads).
Blue=SHG

Figure 3. Corneal nerves segmentation from *in vivo* images
The deep stromal bundles interconnect each other generating tree concentric stromal rings: peripheral (A), paracentral (B), and central (C). Note the pictures were digitally cropped. Software segmentation delineates stromal nerves (F and G, red) from sub-basal (H and I, green). A thick nerve bundle located in the deep stroma loops connecting with sub-basal plexus in the center of the cornea (E, G and I). Blue=SHG

Figure 4. Corneal nerves segmentation from *ex vivo* images
The whole flat cornea was stained with anti tubulin beta III primary antibody followed by an Alexa-488 secondary antibody and then scanned with a multiphoton microscope. The high density of the corneal nerves can be observed in A and D. Whorling pattern is appreciated in the center (red box, A and D). Software segmentation delineates stromal nerves (B and F, red) from sub-basal (E, green). The stromal radial nerves are appreciated in B, C F and G. White arrow heads delineate radial stromal nerves that run form the periphery toward the center deeply in the stroma (F and G).

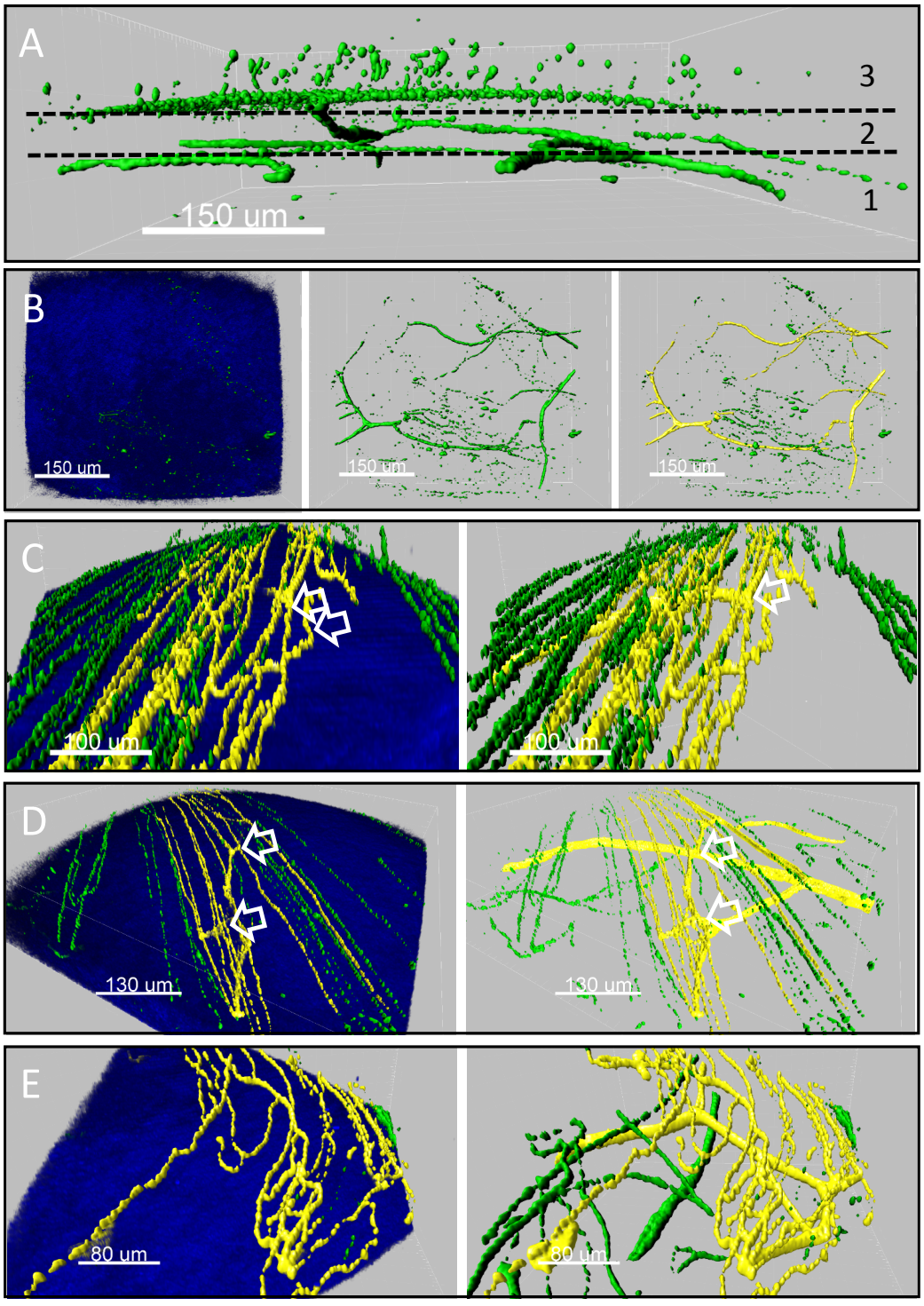
A
3
2
1
150 um
B
150 um
150 um
150 um
C
100 um
100 um
D
130 um
130 um
E
80 um
80 um

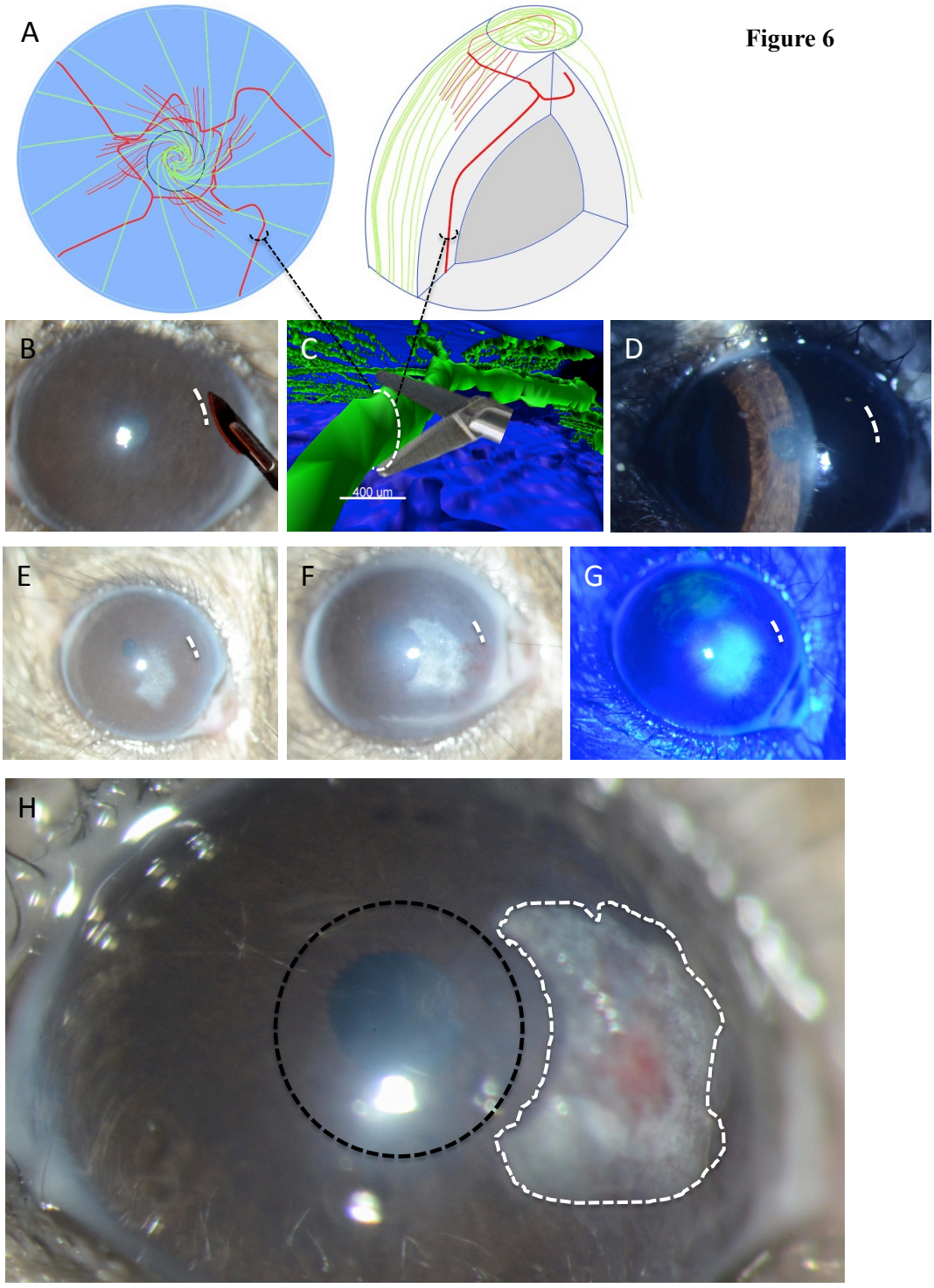

Figure 6

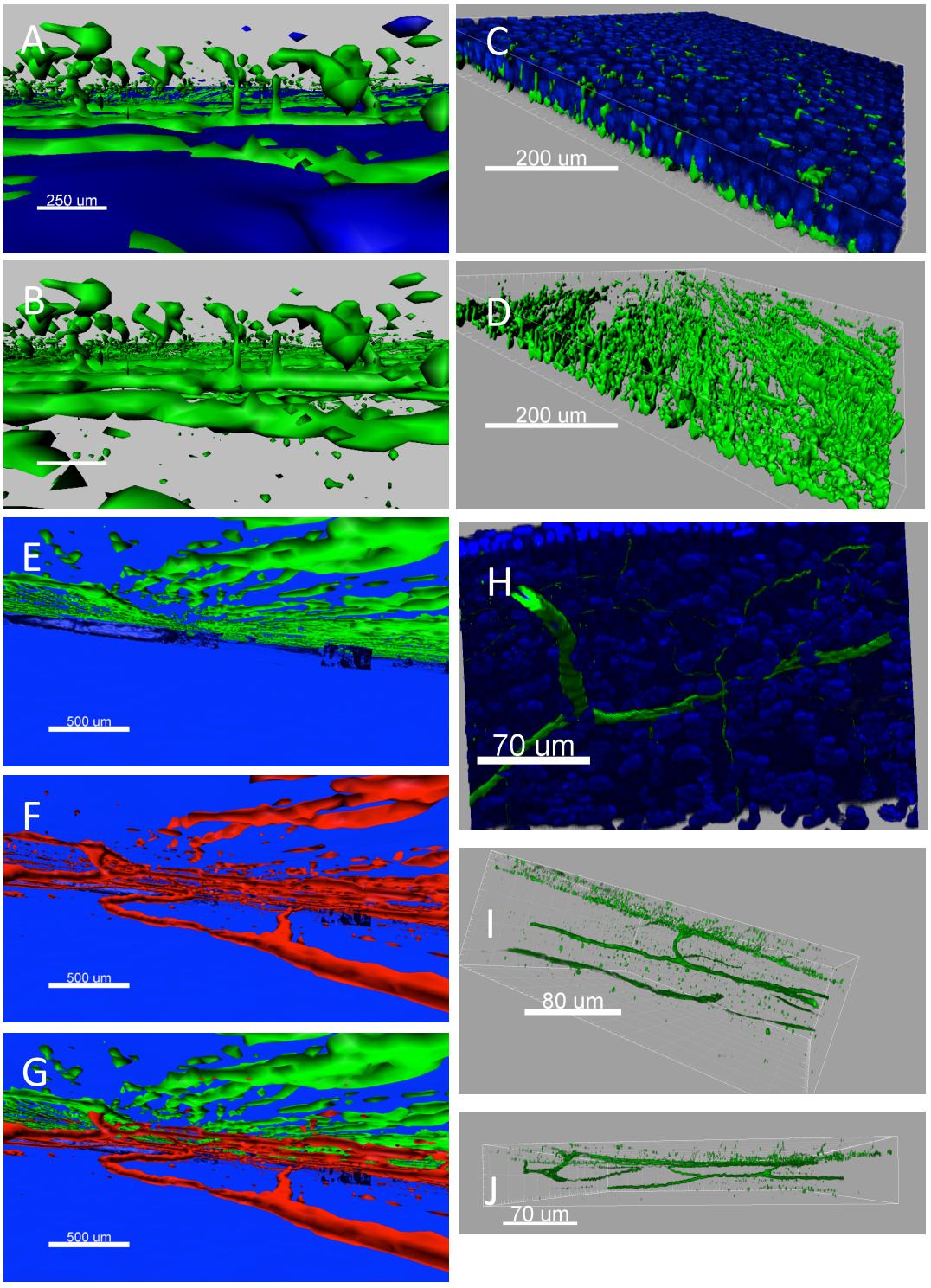
A
250 um
C
200 um
B
D
200 um
E
500 um
H
70 um
F
500 um
I
80 um
G
500 um
J
70 um

Figure 7

Figure 5. Software delineation of the corneal nerves form *in vivo* acquisitions
Tree different levels of stratification can be observed in the center of the cornea (A), deep stroma (1), anterior stroma (2) and sub-basal plexus (3). The rotation of the same figure (B) shows a concentrical ring in the central stroma (delineated in yellow). C and D show stromal nerves looping up and innervating the sub-basal plexus form bellow in near to the apex and paracentral. White arrows show bifurcations in both directions (yellow) (toward the center and periphery). The same is observed in the periphery of the cornea (E). A complete 360 ° loop is delineated in yellow.
Blue=SHG

Figure 6. Severing of deep stromal radial nerve bundle causes local corneal damage.
The innervation pattern of deep stromal nerves can be observed in A. The nerves enter from the periphery and innervate the sub-basal plexus from bellow.
Severing one of the radial stromal bundles (B and C) causes loss of transparency in paracentral area near to the incision 7 days after (D). Progression of the opacity is observed at 2 weeks (E). Ingrowth of blood vessels (F) and fluorescein staining (G) are seen at 3 weeks. At four weeks (H), the deenervated area is observed inflamed with vessels and stromal plaque. However the center of the cornea remains totally transparent

Figure 7. *In* vivo MP-IVM Vs. *ex vivo* LSCM resolution
Epithelial leashes and sub-basal plexus can be observed in vivo (A and B) and ex vivo (C and D) with similar resolution. Stromal nerves *in vivo* (F and G, red) can be compared to *ex vivo* (H, I and J).
Notice in I and J three different levels of stratification as observed *in vivo* in figure 5
Blue=SHG (A, B, E, F and G) and DAPI (C and H).

DISCUSSION

In this study, we successfully combined a genetically-engineered reporter expressing mouse strain (Thy1-YFP), MP-IVM and post-imaging analysis to obtain an outstanding high-resolution tree-dimensional imaging model for the study of the corneal innervation. Considering these results, the following conclusions can be drawn:

7. This model is suitable for a better understanding the corneal nerves in both normal and pathological conditions in a living mouse
8. Deep stromal nerve bundles have been identified as well a new bifurcation pattern in the plexus
9. The number of animals in each experiment will be significantly reduced and classic histopathology could be replaced in many studies.
10. This model has potential applications such as the study of dry eye, keratoconus, corneal transplantation, chronic pain, refractive surgery complications, dystrophies, allergy, keratitis etc.

The study of the architecture and function of the corneal nerves has been challenging during more than a century since the corneal anatomy was described [63]. To elucidate the function of the corneal nerves, different methods and techniques have been used for many decades. Corneal nerves have been studied in explants with tedious processes of fixation, staining and imaging [31, 33-36, 39, 46, 47]. Conventional microscopy requires time-consuming sessions and only small representative portions of the cornea are presented (i.e. sub-basal plexus, anterior stroma, posterior stroma, periphery, center etc.) [40-45, 48-53]. The whole anatomy of the human cornea has been recently described by using IVCM in patients as well as in *ex vivo* corneal explants [63-66]. In these works, multiple microscope acquisitions were manually taken and a tedious post-imaging analysis was required; however, gross outcomes have been presented. The anatomy of the corneal nerves has been also described in animal models by using an IVCM system; however, only sub-basal plexus

was successfully imaged with a modest resolution [67, 68]. Other authors have recently used a widefield stereo fluorescent microscopy to *in vivo* photograph corneal nerves [69, 70]. Despite the promising outcomes achieved, all previous works needed convoluted post-analysis process and images are shown with poor resolution, needless to say that epithelial leashes were not detected. Hitherto, there is not yet a satisfactory *in vivo* model that will include all aspects of the corneal nerves.

In the current work, we used a genetically-engineered reporter expressing mouse. The YFP reporter fluorescence protein is expressed under the promoter of Thy1. Thy1 or CD90 is a 25–37 kDa widely conserved cell surface protein originally discovered as a thymocyte antigen. Thy1 can be used as a marker for a variety of stem cells, murine thymocytes, T lymphocytes and axonal processes of mature neurons [71, 72]. Thy1 expression in the nervous system is predominantly neuronal, but some glial cells also express Thy1 at later stages of their differentiation [73]. Thy1 is expressed strongly in the mature axon but is also present on the soma and dendrites [74]. The absence of glial cells and the specific morphology of the nerves in the cornea, ensure neuronal specificity. In this study, the expression of YFP was imaged with a MP-IVM in a living mouse. Previously, Namavari et al., have shown expression of YFP in a model for regenerating the corneal nerves in a transgenic Thy1-YFP mice [70]. These authors used a widefield stereo fluorescent microscopy and successfully photographed the whole cornea in a single image. The sub-basal nerves and stromal nerve trunks were coarsely visualized and the intraepithelial leashes were missed. That microscope takes images off axis and consequently deconvolution and tree-dimensional reconstruction were not feasible. Additionally, the mouse pupil was constricted with carbachol to mask retinal fluorescence. Finally, the authors presented the image as maximum intensity projection in a XY dimensional view [70]. In the current work we used a MP-IVM, which effectively pulses the laser bean in the focal area. The non-descaned detectors capture exclusively the light emission from the focal avoiding residual fluorescence from the retina. PM-IVM takes images axis on, which facilitates later deconvoluion and tree-dimensional

reconstruction. The microscope has incorporated a motorized XY versatile stage, which automates the process for tiling and stitching. The final reconstruction of the imaging process allows: digital slicing, orthogonal sectioning (XYZT), gallery and maximum intensity projection. Nevertheless, the best feature is the reconstruction of real high-definition tree-dimensional image in different modes such as maximum intensity projection, normal sharing, minimum intensity projection, blending and shadow projection. Additionally, surfaces can be created in different channels to artistically enhance the final outcome.

As it has been previously described in corneal explants [1, 29, 31, 39], we observed, *in vivo,* the nerves penetrating from the periphery through the stroma and turning toward the epithelium basement membrane. In the sub-epithelial basal layer and parallel to the ocular surface, the thin fibres form the sub-basal plexus The majority of the radial nerves are located in the sub-basal plexus; however, many others appear underneath within the anterior part of the stroma as well deeper in the posterior aspect of the stroma. Interestingly, we detected three different concentric stromal nerve rings (periphery, paracentral and central). These concentric rings interconnect different radial nerve bundles in the stroma. Ramifications of these rings enter the sub-basal plexus form bellow. In human corneas, nerves penetrate Bowman's layer throughout the peripheral and central cornea [31, 75]; however, in monkey corneas, nerves penetrate Bowman's membrane only in the peripheral zone but is not well described in mice [46]. In the current work, many nerves located into the sub-basal plexus ramify from a stromal bundle in the periphery but also in the paracentral as well as center of the cornea. It has been vastly shown that nerves always extend centripetally from the periphery to the center of the cornea. We observed that stromal nerves ramify in a double hairpin pattern. Stromal nerves subdivide in both directions toward the center of the cornea but also toward the periphery. In the center stromal nerves enter from bellow the sub-basal plexus and ramify toward the periphery. This finding might suggest a backup mechanism. The cornea is continuously exposed to superficial aggressions and the sub-basal plexus is often

damaged. The radial and concentric distribution of the stromal nerves, especially in the center of the cornea, might ensure both sensorial and trophism properties when the cornea is injured.

To probe this hypothesis we severed one single stromal nerve deeply in the peripheral stroma. The cornea turned inflamed (opacity, epithelial erosion, neovascularization and stroma plaque) in the area innervated by this specific nerve, but the rest of the cornea remained transparent even the center. This is a clear indication how harming a specific nerve indices local loss of the corneal immune privilege, which remarks the increasing trend that the nerves are critical for keeping this immune privilege.

There is a controversy regarding the structure of the sub-basal plexus near the apex of the cornea. In humans, Muller et al. have indicated a superior to inferior architecture [39], whereas Patel et al. have observed a whorllike pattern [64]. Yu et al. also have shown a whorling sub-basal nerve pattern in mice, with a more pronounced spiraling of nerves in the center of cornea [69]. In the current work we observed that all the patterns described before fit in our model, but perfectly stratified. The posterior-anterior architecture observed by Müller [39] was confirmed in this work with different stratification. Stromal bundless in the posterior part of the stroma, ramified in thinner bundless in the anterior part that finally ramify through the sub-basal plexus. Also, the whorling sub-basal nerve pattern as observed by Patel et al. and Yu et al. [64, 69] was confirmed in this study. The sub-basal plexus is observed in a very well defined classic hairpin pattern with subdivided and well-demarcated epithelial leashes towards the surface. Other authors, that used a widefield stereo fluorescent microscopy to photograph *in vivo* the corneal nerves failed to image the nerve terminal endings in the epithelium [69, 70].

Previously Yu et al. have quantified the *in vivo* expression of neuron-specific fluorescence in corneas of transgenic Thy1-YFP mice [69]. These authors also compared transgenic YFP neurofluorescence with beta III tubulin immunostaining. The amount of neurofluorescence analyzed *in vivo* (43 μ/mm^2) was half than quantified *ex vivo* by immunostaining (94 μ/mm^2). In our work, the fluorescence was not objectively

quantified. Although *in vivo* expression of Th1-YFP seems to be lightly lesser than *ex vivo* staining of beta III tubulin, both show similar pattern and distribution throughout the cornea. Yu et al. fixed the tissue with PFA 4% and whole mounts were imaged with a motorized fluorescence microscope [69]. The emission of a reporter protein under epifluorescence excitation is rapidly decreased by photobleaching but also quenched after strong fixative process. In our work, YFP emission was collected *in vivo* by using a MP-IVM that indeed avoids photobleaching and increases significantly resolution in the focal. Stromal bundles, plexus and terminal endings can be observed with similar resolution *in vivo* and *ex vivo;* therefore, we can conclude that Thy1-YFP fluorescence gathered *in vivo* is representative of the corneal nerves. Yu et al. concluded that their model of Thy1-YFP mouse allows the observation of corneal neuronal growth in living animals by using a motorized epifluorescence microscope [69]. With the current work, we steep forward providing detailed resolution and tree-dimensional image with a minimal photo-damage. This model will allow examination of the corneal reinnervation after injury with more precise and detailed information. The role of the nerves in pathologies such as dry eye, corneal graft rejection, keratoconus, pain, allergy, keratitis, infection etc., could be addressed in vivo with this model.

In conclusion, in this study we were able to combine a genetically-engineered reporter expressing mouse (Thy1-YFP), MP-IVM and image analysis to obtain an outstanding imaging model to study the corneal nerves in a living mouse. This model should be suitable for understanding function of corneal nerves in both normal and pathologic conditions. Additionally we identified deep stromal nerve bundles, stromal nerve rings and new bifurcation pattern in the sub-basal plexus. The damage of specific nerves induce loss of the immune privilege in specific areas related with that particular nerves.

REFERENCES

1. Muller, L.J., C.F. Marfurt, F. Kruse and T.M. Tervo, *Corneal nerves: structure, contents and function.* Exp Eye Res, 2003. **76**(5): p. 521-42.
2. Arvidson, B., *Retrograde axonal transport of horseradish peroxidase from cornea to trigeminal ganglion.* Acta Neuropathol, 1977. **38**(1): p. 49-52.
3. Marfurt, C.F. and D.R. Del Toro, *Corneal sensory pathway in the rat: a horseradish peroxidase tracing study.* J Comp Neurol, 1987. **261**(3): p. 450-9.
4. Marfurt, C.F., R.E. Kingsley and S.E. Echtenkamp, *Sensory and sympathetic innervation of the mammalian cornea. A retrograde tracing study.* Invest Ophthalmol Vis Sci, 1989. **30**(3): p. 461-72.
5. Morgan, C.W., I. Nadelhaft and W.C. de Groat, *Anatomical localization of corneal afferent cells in the trigeminal ganglion.* Neurosurgery, 1978. **2**(3): p. 252-8.
6. ten Tusscher, M.P., J. Klooster and G.F. Vrensen, *The innervation of the rabbit's anterior eye segment: a retrograde tracing study.* Exp Eye Res, 1988. **46**(5): p. 717-30.
7. Lele, P.P. and G. Weddell, *Sensory nerves of the cornea and cutaneous sensibility.* Exp Neurol, 1959. **1**: p. 334-59.
8. Marfurt, C.F., M.A. Jones and K. Thrasher, *Parasympathetic innervation of the rat cornea.* Exp Eye Res, 1998. **66**(4): p. 437-48.
9. Morgan, C., W.C. DeGroat and P.J. Jannetta, *Sympathetic innervation of the cornea from the superior cervical ganglion. An HRP study in the cat.* J Auton Nerv Syst, 1987. **20**(2): p. 179-83.
10. Tervo, T., F. Joo, K.T. Huikuri, I. Toth and A. Palkama, *Fine structure of sensory nerves in the rat cornea: an experimental nerve degeneration study.* Pain, 1979. **6**(1): p. 57-70.
11. Baker, K.S., S.C. Anderson, E.G. Romanowski, R.A. Thoft and N. SundarRaj, *Trigeminal ganglion neurons affect corneal epithelial phenotype. Influence on type VII collagen expression in vitro.* Invest Ophthalmol Vis Sci, 1993. **34**(1): p. 137-44.
12. Garcia-Hirschfeld, J., L.G. Lopez-Briones and C. Belmonte, *Neurotrophic influences on corneal epithelial cells.* Exp Eye Res, 1994. **59**(5): p. 597-605.
13. Mathers, W.D., *Why the eye becomes dry: a cornea and lacrimal gland feedback model.* CLAO J, 2000. **26**(3): p. 159-65.

14. Stern, M.E., R.W. Beuerman, R.I. Fox, J. Gao, A.K. Mircheff and S.C. Pflugfelder, *The pathology of dry eye: the interaction between the ocular surface and lacrimal glands.* Cornea, 1998. **17**(6): p. 584-9.
15. Stern, M.E., R.W. Beuerman, R.I. Fox, J. Gao, A.K. Mircheff and S.C. Pflugfelder, *A unified theory of the role of the ocular surface in dry eye.* Adv Exp Med Biol, 1998. **438**: p. 643-51.
16. Benitez del Castillo, J.M., M.A. Wasfy, C. Fernandez and J. Garcia-Sanchez, *An in vivo confocal masked study on corneal epithelium and subbasal nerves in patients with dry eye.* Invest Ophthalmol Vis Sci, 2004. **45**(9): p. 3030-5.
17. Benitez-Del-Castillo, J.M., M.C. Acosta, M.A. Wassfi, D. Diaz-Valle, J.A. Gegundez, C. Fernandez and J. Garcia-Sanchez, *Relation between corneal innervation with confocal microscopy and corneal sensitivity with noncontact esthesiometry in patients with dry eye.* Invest Ophthalmol Vis Sci, 2007. **48**(1): p. 173-81.
18. Hamrah, P., A. Cruzat, M.H. Dastjerdi, L. Zheng, B.M. Shahatit, H.A. Bayhan, R. Dana and D. Pavan-Langston, *Corneal sensation and subbasal nerve alterations in patients with herpes simplex keratitis: an in vivo confocal microscopy study.* Ophthalmology, 2010. **117**(10): p. 1930-6.
19. Rosenberg, M.E., T.M. Tervo, I.J. Immonen, L.J. Muller, C. Gronhagen-Riska and M.H. Vesaluoma, *Corneal structure and sensitivity in type 1 diabetes mellitus.* Invest Ophthalmol Vis Sci, 2000. **41**(10): p. 2915-21.
20. Yamada, M., M. Ogata, M. Kawai and Y. Mashima, *Decreased substance P concentrations in tears from patients with corneal hypesthesia.* Am J Ophthalmol, 2000. **129**(5): p. 671-2.
21. Johnson, S.M., *Neurotrophic corneal defects after diode laser cycloablation.* Am J Ophthalmol, 1998. **126**(5): p. 725-7.
22. Menchini, U., A. Scialdone, C. Pietroni, F. Carones and R. Brancato, *Argon versus krypton panretinal photocoagulation side effects on the anterior segment.* Ophthalmologica, 1990. **201**(2): p. 66-70.
23. Weigt, A.K., I.P. Herring, C.F. Marfurt, J.P. Pickett, R.B. Duncan, Jr. and D.L. Ward, *Effects of cyclophotocoagulation with a neodymium:yttrium-aluminum-garnet laser on corneal sensitivity, intraocular pressure, aqueous tear production, and corneal nerve morphology in eyes of dogs.* Am J Vet Res, 2002. **63**(6): p. 906-15.
24. Tervo, T. and J. Moilanen, *In vivo confocal microscopy for evaluation of wound healing following corneal refractive surgery.* Prog Retin Eye Res, 2003. **22**(3): p. 339-58.
25. Wilson, S.E., *Laser in situ keratomileusis-induced (presumed) neurotrophic epitheliopathy.* Ophthalmology, 2001. **108**(6): p. 1082-7.

26. Wilson, S.E. and R. Ambrosio, *Laser in situ keratomileusis-induced neurotrophic epitheliopathy.* Am J Ophthalmol, 2001. **132**(3): p. 405-6.
27. Efron, N., *The Glenn A. Fry award lecture 2010: Ophthalmic markers of diabetic neuropathy.* Optom Vis Sci, 2011. **88**(6): p. 661-83.
28. Linna, T.U., M.H. Vesaluoma, J.J. Perez-Santonja, W.M. Petroll, J.L. Alio and T.M. Tervo, *Effect of myopic LASIK on corneal sensitivity and morphology of subbasal nerves.* Invest Ophthalmol Vis Sci, 2000. **41**(2): p. 393-7.
29. Muller, L.J., E. Pels and G.F. Vrensen, *The specific architecture of the anterior stroma accounts for maintenance of corneal curvature.* Br J Ophthalmol, 2001. **85**(4): p. 437-43.
30. Radner, W. and R. Mallinger, *Interlacing of collagen lamellae in the midstroma of the human cornea.* Cornea, 2002. **21**(6): p. 598-601.
31. Muller, L.J., L. Pels and G.F. Vrensen, *Ultrastructural organization of human corneal nerves.* Invest Ophthalmol Vis Sci, 1996. **37**(4): p. 476-88.
32. Ruskell, G.L., *Ocular fibres of the maxillary nerve in monkeys.* J Anat, 1974. **118**(Pt 2): p. 195-203.
33. Beckers, H.J., J. Klooster, G.F. Vrensen and W.P. Lamers, *Ultrastructural identification of trigeminal nerve endings in the rat cornea and iris.* Invest Ophthalmol Vis Sci, 1992. **33**(6): p. 1979-86.
34. Beckers, H.J., J. Klooster, G.F. Vrensen and W.P. Lamers, *Substance P in rat corneal and iridal nerves: an ultrastructural immunohistochemical study.* Ophthalmic Res, 1993. **25**(3): p. 192-200.
35. Tervo, T. and A. Palkama, *Ultrastructure of the corneal nerves after fixation with potassium permanganate.* Anat Rec, 1978. **190**(4): p. 851-9.
36. Tervo, T. and A. Palkama, *Innervation of the rabbit cornea. A histochemical and electron-microscopic study.* Acta Anat (Basel), 1978. **102**(2): p. 164-75.
37. Oliveira-Soto, L. and N. Efron, *Morphology of corneal nerves using confocal microscopy.* Cornea, 2001. **20**(4): p. 374-84.
38. Vesaluoma, M., J. Perez-Santonja, W.M. Petroll, T. Linna, J. Alio and T. Tervo, *Corneal stromal changes induced by myopic LASIK.* Invest Ophthalmol Vis Sci, 2000. **41**(2): p. 369-76.
39. Muller, L.J., G.F. Vrensen, L. Pels, B.N. Cardozo and B. Willekens, *Architecture of human corneal nerves.* Invest Ophthalmol Vis Sci, 1997. **38**(5): p. 985-94.
40. Jones, M.A. and C.F. Marfurt, *Calcitonin gene-related peptide and corneal innervation: a developmental study in the rat.* J Comp Neurol, 1991. **313**(1): p. 132-50.
41. Jones, M.A. and C.F. Marfurt, *Peptidergic innervation of the rat cornea.* Exp Eye Res, 1998. **66**(4): p. 421-35.
42. Rozsa, A.J. and R.W. Beuerman, *Density and organization of free nerve endings in the corneal epithelium of the rabbit.* Pain, 1982. **14**(2): p. 105-20.

43. Schimmelpfennig, B. and R. Beuerman, *A technique for controlled sensory denervation of the rabbit cornea.* Graefes Arch Clin Exp Ophthalmol, 1982. **218**(6): p. 287-93.
44. Ueda, S., M. del Cerro, J.A. LoCascio and J.V. Aquavella, *Peptidergic and catecholaminergic fibers in the human corneal epithelium. An immunohistochemical and electron microscopic study.* Acta Ophthalmol Suppl, 1989. **192**: p. 80-90.
45. Zander, E. and G. Weddell, *Observations on the innervation of the cornea.* J Anat, 1951. **85**(1): p. 68-99.
46. Lim, C.H. and G.L. Ruskell, *Corneal nerve access in monkeys.* Albrecht Von Graefes Arch Klin Exp Ophthalmol, 1978. **208**(1-3): p. 15-23.
47. Matsuda, H., *[Electron microscopic study of the corneal nerve with special reference to the nerve endings].* Nihon Ganka Gakkai Zasshi, 1968. **72**(7): p. 880-93.
48. Ivanusic, J.J., R.J. Wood and J.A. Brock, *Sensory and sympathetic innervation of the mouse and guinea pig corneal epithelium.* J Comp Neurol, 2013. **521**(4): p. 877-93.
49. Kubilus, J.K. and T.F. Linsenmayer, *Developmental guidance of embryonic corneal innervation: roles of Semaphorin3A and Slit2.* Dev Biol, 2010. **344**(1): p. 172-84.
50. Kubilus, J.K. and T.F. Linsenmayer, *Developmental corneal innervation: interactions between nerves and specialized apical corneal epithelial cells.* Invest Ophthalmol Vis Sci, 2010. **51**(2): p. 782-9.
51. Madrid, R., T. Donovan-Rodriguez, V. Meseguer, M.C. Acosta, C. Belmonte and F. Viana, *Contribution of TRPM8 channels to cold transduction in primary sensory neurons and peripheral nerve terminals.* J Neurosci, 2006. **26**(48): p. 12512-25.
52. Marfurt, C.F. and L.C. Ellis, *Immunohistochemical localization of tyrosine hydroxylase in corneal nerves.* J Comp Neurol, 1993. **336**(4): p. 517-31.
53. Parra, A., R. Madrid, D. Echevarria, S. del Olmo, C. Morenilla-Palao, M.C. Acosta, J. Gallar, A. Dhaka, F. Viana and C. Belmonte, *Ocular surface wetness is regulated by TRPM8-dependent cold thermoreceptors of the cornea.* Nat Med, 2010. **16**(12): p. 1396-9.
54. Auran, J.D., C.J. Koester, N.J. Kleiman, R. Rapaport, J.S. Bomann, B.M. Wirotsko, G.J. Florakis and J.P. Koniarek, *Scanning slit confocal microscopic observation of cell morphology and movement within the normal human anterior cornea.* Ophthalmology, 1995. **102**(1): p. 33-41.
55. Linna, T.U., M.H. Vesaluoma, W.M. Petroll, A.H. Tarkkanen and T.M. Tervo, *Confocal microscopy of a patient with irregular astigmatism after LASIK reoperations and relaxation incisions.* Cornea, 2000. **19**(2): p. 163-9.

56. Rosenberg, M.E., T.M. Tervo, W.M. Petroll and M.H. Vesaluoma, *In vivo confocal microscopy of patients with corneal recurrent erosion syndrome or epithelial basement membrane dystrophy.* Ophthalmology, 2000. **107**(3): p. 565-73.
57. Vesaluoma, M., L. Muller, J. Gallar, A. Lambiase, J. Moilanen, T. Hack, C. Belmonte and T. Tervo, *Effects of oleoresin capsicum pepper spray on human corneal morphology and sensitivity.* Invest Ophthalmol Vis Sci, 2000. **41**(8): p. 2138-47.
58. Vesaluoma, M.H., W.M. Petroll, J.J. Perez-Santonja, T.U. Valle, J.L. Alio and T.M. Tervo, *Laser in situ keratomileusis flap margin: wound healing and complications imaged by in vivo confocal microscopy.* Am J Ophthalmol, 2000. **130**(5): p. 564-73.
59. Lai, T.Y.C., *Corneal visualization and characterization for applications in ophthalmology using optical imaging* Doctoral Thesis, 2014.
60. Steven, P., F. Bock, G. Huttmann and C. Cursiefen, *Intravital two-photon microscopy of immune cell dynamics in corneal lymphatic vessels.* PLoS One, 2011. **6**(10): p. e26253.
61. Masihzadeh, O., T.C. Lei, D.A. Ammar, M.Y. Kahook and E.A. Gibson, *A multiphoton microscope platform for imaging the mouse eye.* Mol Vis, 2012. **18**: p. 1840-8.
62. Chen, X., O. Nadiarynkh, S. Plotnikov and P.J. Campagnola, *Second harmonic generation microscopy for quantitative analysis of collagen fibrillar structure.* Nat Protoc, 2012. **7**(4): p. 654-69.
63. Gray, H., *Anatomy of the human body.* 1918: p. 1003-1019.
64. Patel, D.V. and C.N. McGhee, *Mapping of the normal human corneal sub-Basal nerve plexus by in vivo laser scanning confocal microscopy.* Invest Ophthalmol Vis Sci, 2005. **46**(12): p. 4485-8.
65. Esquenazi, S., J. He, N. Li, N.G. Bazan, I. Esquenazi and H.E. Bazan, *Comparative in vivo high-resolution confocal microscopy of corneal epithelium, sub-basal nerves and stromal cells in mice with and without dry eye after photorefractive keratectomy.* Clin Experiment Ophthalmol, 2007. **35**(6): p. 545-9.
66. He, J. and H.E. Bazan, *Mapping the nerve architecture of diabetic human corneas.* Ophthalmology, 2012. **119**(5): p. 956-64.
67. Guthoff, R.F., C. Baudouin and J. Stave, *Atlas of Confocal Laser Scanning In-vivo Microscopy in Opthalmology –*
Principles and Applications in Diagnostic and Therapeutic Ophtalmology. 2007.
68. Reichard, M., M. Hovakimyan, R.F. Guthoff and O. Stachs, *In vivo visualisation of murine corneal nerve fibre regeneration in response to ciliary neurotrophic factor.* Exp Eye Res, 2014. **120**: p. 20-7.

69. Yu, C.Q. and M.I. Rosenblatt, *Transgenic corneal neurofluorescence in mice: a new model for in vivo investigation of nerve structure and regeneration.* Invest Ophthalmol Vis Sci, 2007. **48**(4): p. 1535-42.
70. Namavari, A., S. Chaudhary, J. Sarkar, L. Yco, K. Patel, K.Y. Han, B.Y. Yue, J.H. Chang and S. Jain, *In vivo serial imaging of regenerating corneal nerves after surgical transection in transgenic thy1-YFP mice.* Invest Ophthalmol Vis Sci, 2011. **52**(11): p. 8025-32.
71. Reif, A.E. and J.M. Allen, *Immunological Distinction of Akr Thymocytes.* Nature, 1964. **203**: p. 886-7.
72. Reif, A.E. and J.M. Allen, *The Akr Thymic Antigen and Its Distribution in Leukemias and Nervous Tissues.* J Exp Med, 1964. **120**: p. 413-33.
73. Kemshead, J.T., M.A. Ritter, S.F. Cotmore and M.F. Greaves, *Human Thy-1: expression on the cell surface of neuronal and glial cells.* Brain Res, 1982. **236**(2): p. 451-61.
74. Moechars, D., I. Dewachter, K. Lorent, D. Reverse, V. Baekelandt, A. Naidu, I. Tesseur, K. Spittaels, C.V. Haute, F. Checler, E. Godaux, B. Cordell and F. Van Leuven, *Early phenotypic changes in transgenic mice that overexpress different mutants of amyloid precursor protein in brain.* J Biol Chem, 1999. **274**(10): p. 6483-92.
75. Martinez, R., *Etude sur l'innervation de la corne´e humaine.* 1940.

CHAPTER 6

The cornea has “the nerve” to encourage immune rejection

American Journal of Transplantation 2015; XX: 1–2
Wiley Periodicals Inc.

doi: 10.1111/ajt.13238

Editorial

The Cornea Has "the Nerve" to Encourage Immune Rejection

T. Blanco[1] and D. R. Saban[1,2,*]

[1]*Department of Ophthalmology, Duke University School of Medicine, Durham, NC*
[2]*Department of Immunology, Duke University School of Medicine, Durham, NC*
**Corresponding author: Daniel R. Saban, daniel.saban@duke.edu*

Received 29 December 2014, revised 13 January 2015 and accepted for publication 14 January 2015

"Supersystem" is a designation given to a highly integrated life system, which was coined by the late Tomio Tada nearly a decade ago to describe both immune and nervous systems (1). Even decades earlier, however, were scientists already appreciating the level of interplay that exists between these two supersystems. Work by Paunicka et al now highlights the importance of this relationship in corneal allograft rejection (2).

The cornea is a fascinating model site to explore how the nervous and immune systems interface, as it is arguably the most densely innervated site in mammals. Furthermore, the cornea enjoys immune privilege status, which is a feature that permits spontaneous acceptance in approximately 50% of corneal allografts in certain mouse strain combinations (3). Paunicka et al now show that the severing of corneal nerves in the graft bed, an unavoidable consequence of penetrating keratoplasty, abolishes immune privilege that would otherwise be enjoyed by subsequent allografts, even in the fellow eye. This perhaps explains why a markedly increased incidence of failure of second grafts is seen in the clinic.

The authors came to this conclusion with elegant experimentation. They initially found that placement of an allograft led to the increased tempo and incidence of rejection to a subsequently placed corneal allograft in the same, or fellow eye. Importantly, this pattern was not due to a second-set rejection, as the same result was observed when the subsequent allograft was unrelated to the first. However, this antigen nonspecific increase in rejection was indeed T cell mediated, as subsequent syngeneic grafts survived indefinitely. The root cause of increased rejection turned out to be the nerve injury response, originating from the first transplantation. The same results were recapitulated by simply severing of nerves 360° around the cornea. Remarkably, an allograft placed 60 days after such injury also succumbed to increased immune rejection. Authors conclusively demonstrated that a burst of the neuropeptide substance P, produced as an effect of such nerve severing, caused this heightened state of rejection. Furthermore, they show that substance P disables T regulatory (Treg) suppression, and associated this impairment with increased rejection.

How could Tregs be impaired and augment immune rejection to a substance P burst that occurred 60 days prior? The authors are unsure, particularly given a serum half-life of only several minutes. Perhaps one could point to a role for tissue resident macrophages as a possible explanation. Indeed, these mononuclear phagocytes have a long life span of many months to even a year. Furthermore, macrophages express substance P receptors, produce substance P, and are altered by ligation of this neuropeptide (4). Additionally, macrophages are antigen-presenting cells and can migrate to lymphoid organs, likely in a CCR7-mediated fashion (5). Importantly, it has been long appreciated that many macrophages reside in close proximity to peripheral nerves (6), consistent in the cornea as well (7). One can appreciate this in Figure 1, which is an unpublished micrograph generated by our lab demonstrating the proximity of a mononuclear phagocyte with up to 10 distinct nerves in the corneal epithelium. Perhaps one plausible hypothesis to explain the fascinating findings by Paunicka et al is that the unilateral severing of corneal nerves that causes a bilateral substance P burst has a pathogenic imprinting effect on such long-lived macrophages residing proximal to nerves. Thus, upon transplantation, either immediately or long after the substance P burst, perhaps this imprint licenses macrophages to produce additional substance P. If these antigen-presenting cells, laden with alloantigen, could migrate to the lymphoid organ, their substance P may therefore subvert Treg activity and in turn may lead to increased immune rejection.

Irrespective of how substance P produces such a long-lasting ability to augment immune rejection, Paunicka et al force transplantation immunologists, particularly those studying the cornea, to now consider the interplay of both supersystems as yet another piece of the perplexing puzzle that is immune rejection.

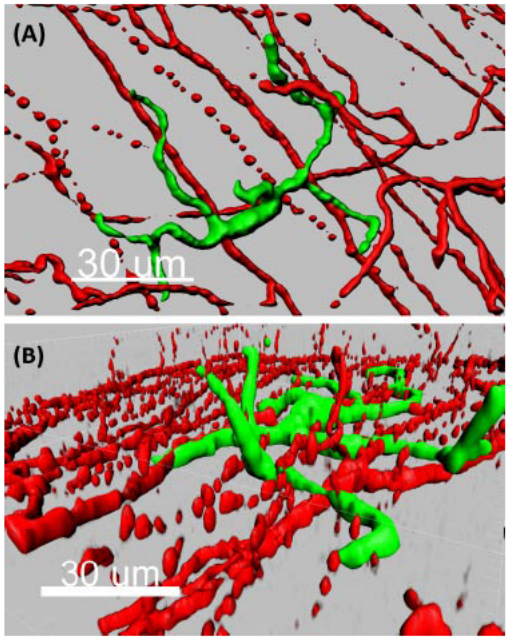

Figure 1: Mononuclear phagocytes are in contact with corneal nerves. Micrograph of normal cornea excised from CX3CR1-Cre; Rosa-fGFP mice and stained for neuron-specific class III beta-tubulin (Tuj 1). (A, B) Mononuclear phagocyte (green) and nerves (red) shown in an (A) en face and (B) side view image of the corneal epithelium.

Acknowledgments

Research to Prevent Blindness, Career Development Award (Saban); R01EY021798 (Saban).

Disclosure

The authors of this manuscript have no conflicts of interest to disclose as described by the *American Journal of Transplantation*.

References

1. Tada T. The immune system as a supersystem. Annu Rev Immunol 1997; 15: 1–13.
2. Paunicka KJ, Mellon J, Robertson D, et al. Severing corneal nerves in one eye induces sympathetic loss of immune privilege and promotes rejection of future corneal allografts placed in either eye. Am J Transplant 2015; doi: 10.1111/ajt.13240
3. Streilein JW. Ocular immune privilege: Therapeutic opportunities from an experiment of nature. Nat Rev Immunol 2003; 3: 879–889.
4. Ho WZ, Lai JP, Zhu XH, Uvaydova M, Douglas SD. Human monocytes and macrophages express substance P and neurokinin-1 receptor. J Immunol 1997; 159: 5654–5660.
5. Saban DR. The chemokine receptor CCR7 expressed by dendritic cells: A key player in corneal and ocular surface inflammation. Ocul Surf 2014; 12: 87–99.
6. Perry VH, Brown MC, Gordon S. The macrophage response to central and peripheral nerve injury. A possible role for macrophages in regeneration. J Exp Med 1987; 165: 1218–1223.
7. Seyed-Razavi Y, Chinnery HR, McMenamin PG. A novel association between resident tissue macrophages and nerves in the peripheral stroma of the murine cornea. Invest Ophthalmol Vis Sci 2014; 55: 1313–1320.

This article is an editorial contribution to a previous work entitled "*Severing Corneal Nerves in One Eye Induces Sympathetic Loss of Immune Privilege and Promotes Rejection of Future Corneal Allografts Placed in Either Eye*" Paunicka et al. [1]. In this article, we point out the relevance of the interface of both nervous and immune "supersystems" in the cornea to maintain the immune privilege [2]. Upon the article published in American Journal of Transplantation, We show supplementary material to complement the aforementioned publication in an extended version. In the additional results, we show that the interface of both "supersystems" is extended to the entire cornea. Moreover, we developed a new chimera by irradiating of a Thy1-YFP host mouse, which was engrafted with bone marrow derived-cells from a $CX3CR1^{Cre/RFP}$ donor mouse. In this chimera we were able to intravitally evaluate the physical interaction of both corneal nerves and bone marrow derived-cells *in vivo*. Finally we present the cornea as a multifaceted organ where two "supersystems" (PNS and immune systems) interact between them to keep the immune privilege and preserve transparency.

ABSTRACT

Purpose:

The cornea, the most innervated site in the body, is endowed with a myeloid resident immune population. The interface of nerves and resident immune cells is taken relevance since the cornea enjoys immune privilege status that permits spontaneous acceptance of corneal allografts. However how nerves and immune cells interplay in the cornea remains unknown. The aim of this work was to search for evidences of this interface in the mouse cornea.

Methods:

Corneal explants of $Cx3cr1^{EGFP}$ knock-in mice, $CX3CR1^{Cre/\ fGFP}$ and $CX3CR1^{Cre/\ RFP}$ mice were fixed and stained with anti tubulin beta III antibody and photographed with a confocal microsocopy. Additionally Thy1 mice were lethally irradiated and engrafted with $Cx3cr1^{cre/RFP}$ bone marrow derived-cells. Mice were examined with a mutliphoton intravital microscope (MP-IVM).

Results:

PNS and resident myeloid cells are observed in physical contact in the epithelium, sub-basal plexus and stroma of the normal cornea. Additionally a chimeric mouse was successfully generated ($Thy1^{YFP}/Cx3cr1^{cre/RFP}$). MP-IVM reveals that donor bone marrow derived-cells repopulate the host cornea in tight contact with the local nerves.

Conclusions:

Both peripheral nervous system (PNS) and resident myeloid population maintain a neuroimmune interface in the normal mouse cornea. Engrafted bone marrow derived-cells interface with the host nerves to substitute the original population maintain; therefore, the immune privilege.

METHODS

Mice and Anesthesia

Mice were housed in a specific pathogen-free environment at the Duke Eye Center animal facility. The Institutional Animal Care and Use Committee approved all procedures. All animals were treated according to the ARVO Statement for the Use of Animals in Ophthalmic and Vision Research. Anesthesia was given with intraperitoneal administered ketamine/xylazine suspensions (120 and 20 mg/kg, respectively).

C57BL/6 WT mice 8–12 wk old were purchased from Jackson laboratories (Jackson, Farmington, Connecticut).

B6.Cg-Tg(Thy1-YFP)16Jrs/J mice, referred to here as Thy1.1-eYFP (Thy1-YFP), are commercially available and were a kind donation from H. Tseng (Department of Ophthalmology, Duke University Medical Center). Six mice were used.

Mice encoding GFP knocked into the gene encoding the chemokine receptor Cx3cr1 ($Cx3cr1^{EGFP}$ knock-in mice) were bred and maintained in our facility. Parental were purchased from Jackson: male and female $Cx3cr1^{tm1Litt}/Cx3cr1^{+}$ (B6.129P2-$Cx3cr1^{tm1Litt}$) were crossed to generate homozygous $Cx3cr1^{EGFP/EGFP}$. Homozygous $Cx3cr1^{EGFP/EGFP}$ were crossed back with C57BL/6J WT mice to generate heterozygous $Cx3cr1^{EGFP/WT}$.

Fluorescence-reporter Cre recombinase activated was analyzed by using CX3CR1-Cre mice generated on a mixed 129/B6 (Gene Expression Nervous System Atlas Project), and backcrossed for 12 generations by M.D. Gunn (Departments of Immunology and Medicine, Duke University Medical Center) [14-16]. B6.Cg-Gt(ROSA)26$Sor^{tm14(CAG-tdTomato)Hze}$/J mice (referred to here as RFP) obtained from Jackson Laboratories, were also a kind gift from M. D. Gunn. Rosa26R-CAG-fGFP mice, referred to here as fGFP, have previously been described [15], were a kind gift from B. L. Hogan (Department of Cell Biology, Duke University Medical Center). These 3 mouse lines were subsequently

maintained and bred in our lab. Male CX3CR1-Cre mice were crossed with female fGFP, and progeny were verified for a CX3CR1-Cre fGFP genotype. Likewise, progeny of male CX3CR1-Cre mice crossed with female RFP were verified for a CX3CR1-Cre RFP genotype.

Irradiation procedure

As described in chapter 4, recipient Thy-1 and C57BL/6 WT mice were total body lethally irradiated (1050 cGy) in a Mark I 68A Cs 137 irradiator (JL Shepherd and Associates in San Fernando, CA). Briefly: the irradiator cabinet is 37cm x 30cm x 45cm and the Cesium source is air compressed raised over 15 from the bottom. Five mice at the time were introduced into a 20 cm diameter acrylic holder. The holder was placed above a 7.6 cm platform positioned over an automatic turntable (12 rpm) to ensure 100% irradiation. The time for the process was 2.21 minutes (2 minutes and 12.9 seconds).

Generation of Chimeras

Table1 shows all the chimeras generated. Donor mice were euthanatized and femurs and tibia collected. Distal and proximal ends of the bone were removed and the marrow flushed out with fresh RPMI medium using a syringe with a 27G needle. Marrow suspension was fragmented into a single cell suspension by passing through a cell strainer (70μm) followed by vigorous pipetting. After centrifugation (200g, 5 minutes, 4C), live cells were counted by trypan blue exclusion and the pellet was resuspended in RPMI media and diluted as appropriate ($3x10^7$ cells/mL). Immediately after irradiation, recipient mice received ~$1x10^7$ non-purified bone marrow cells (~300 μL) via retro-orbital injection of the venous sinus. Antibiotics were given in water to recipient mice (Sulfamethoxazole and trimethoprim antibiotics; SEPTRA, Hi-Tech Pharmacal Co., Amityville, NY) for up to 4 weeks after irradiation. In addition, supplement care food

(SuppliCal caloric supplement; Henry Schein, Dublin, Ohio) was provided. Animals were rested for 6 weeks before MP-IVM examinations. The same animal was examined under general anesthesia several times at different time points with one week frame recovering in between examinations.

Host	Donor	Transition observed chimera	Final expected chimera
Thy-1^{YFP}	CX3CR1$^{cre/RFP}$	Thy-1^{YFP} / CX3CR1$^{cre/RFP}$	Thy-1^{YFP} / CX3CR1$^{cre/RFP}$
C57BL/6 WT	CX3CR1$^{cre/RFP}$	C57BL6WT / CX3CR1$^{cre/RFP}$	C57BL6WT / CX3CR1$^{cre/RFP}$

Table 1

Tissue Processing and Whole-Mount Immunostaining

Under deep anesthesia mice were perfused with BSS, followed by 2% PFA and finally with 4% PFA. After, eyeballs were post-fixed with Zamboni's solution (24 hours, cool room) allowing endogenous fluorescence preservation. The tissue was washed several times over 24 hours in PBS. Corneas were excised in a flowering pattern and treated with blocking buffer (2% BSA, 0.5% tween 20 and 0.2% Triton, overnight at 4C). Posteriorly the tissue was incubated with a rabbit anti tubulin beta III antibody (1:200, overnight, 4C, Covance) and goat anti rabbit Alexa-488/594 (Vector).

Flat mounts and cross-sections were photographed with a Zeiss Axio Observer widefield fluorescence microscope (Zeiss, Oberkochen, Germany) or sequentially scanned using Leica SP5 inverted confocal microscope (Leica TCS 4D; Leica, Heidelberg, Germany) at x20 and x40 magnification.

Multiphoton Intravital Microscopy

Mice were maintained under anesthesia using constant infusion administered via IP catheter of ketamine/xylazine (120 mg/kg) at a rate of 0.2 ml/h. Body temperature was controlled at 37°C. Mice were dorsally placed, facilitating perpendicular exposure of the corneal apex to the microscope objective. Objective to cornea space was filled with an ophthalmic gel (GenTeal, Novartis Ophthalmics, East Hanover) to create a coupling immersion interface with a refractive index (n=1.339) similar to water (n=1.333 at 20° C) as well as to provide eye lubrication (**See chapter 4**)

A 25x/1.05 NA water objective (optimized for MPEXLPL25XWMP, WD 2.0 mm, 0 to 0.23 micron coverslip correction) of an Olympus BX61WI upright microscope fixed stage (Olympus, Tokyo, Japan) was used. The laser used was a ChameleonVision II single box Ti:Sapphire fsec laser, permitting pulse compensation in a tunable range of 680-1080 nm @40 nm/sec, 80 MHz rep rate, 140 fsec pulse width with a 0-47,000 fsec2 units of dispersion compensation. The microscope is equipped with a Blue, Green/Yellow and Red standard fluorescence cube. Emission bands available are DAPI, CFP, GFP, YFP and RFP in switchable cubes; the Blue or Cyan channels were used for second harmonic generation (SHG). Laser was tuned at 910 nm (BGR cube) or 950 nm (CYR cube) for two-photon excitation and second harmonic generation (SHG). A dichroic mirror (DM570) splits the light emission through both channels 1 (blue) and 2 (green or yellow) and channel 4 (red). A second dichroic mirror (DM485) divides light emission for channel 1 and channel 2. The BGR cube is composed of 450-460 nm (blue and SGH), 495-540 (Green) and 575-630 nm (Red) band pass filters. The CYR cube is composed of 460-500 nm (blue and SGH), 520-560 (Yellow) and 575-630 nm (Red) band pass filters. The system has four high efficiency non-descanned detectors in the epi position that can be combined in different configurations by manually alternating the cubes.

Z-series images for 3D mosaic imaging

By using a motorized XY stage, the multi-area time-lapse software (Olympus) automates the process for a 3D image acquisition and stitching. The software easily registers wide areas, and the thumbnail displayed provides a view of the entire image acquired during the mosaic imaging process (**See chapter 4**)

Post-acquisition image analysis

Image stacks were analyzed using the latest version of FUJI available (developed by Wayne Rasband, National Institutes of Health; provided auto-updated by the public domain http://rsb.info.nih.gov/ij). The latest version of Imaris (Imaris, auto-updated version, Bit-plane, Zurich, Switzerland) was also used. Raw files were displayed in Imaris and linked to FIJI for background substraction, brightness/contrast adjustment, noise reduction, compression and size adjustment. After, an easy readable image was imported back from FIJI into Imaris rendering a maximum-intensity projection or blend projection providing a realistic 3D view in a 2D screen. Additional depth perception enhancing realism of the images was created with the Real-Time Shadow Rendering (a fast hardware that projects shadows on the three planes of the object). A surface object is a computer-generated illustration of a detailed region of interest in the data set. The surface object is displayed as a simulated solid object. The accuracy of segmentation against the original data can be easily verified in an interactive manner (for more details visit: http://www.bitplane.com/imaris/imaris). Surface rendering was interactively performed using optimal threshold settings for each channel in each experiment. By choosing absolute threshold, it was possible to detect large portion of the cells without picking up any noise or background with an accurate separation of touching cells. "Quality" and/or "number of voxels" filters were used for detection of seed points. It can pick up missed pixels or remove non-desirable background or noise. Filter settings were optimized comparing interactively the result with the original maximum-intensity projection. Final colors were chosen for an easy artistic visualization. In some images

colors do not necessary match with the original channels. All final snapshots and movies were generated with Imaris. (**See chapter 4**)
Calibration bars were also automatically displayed.

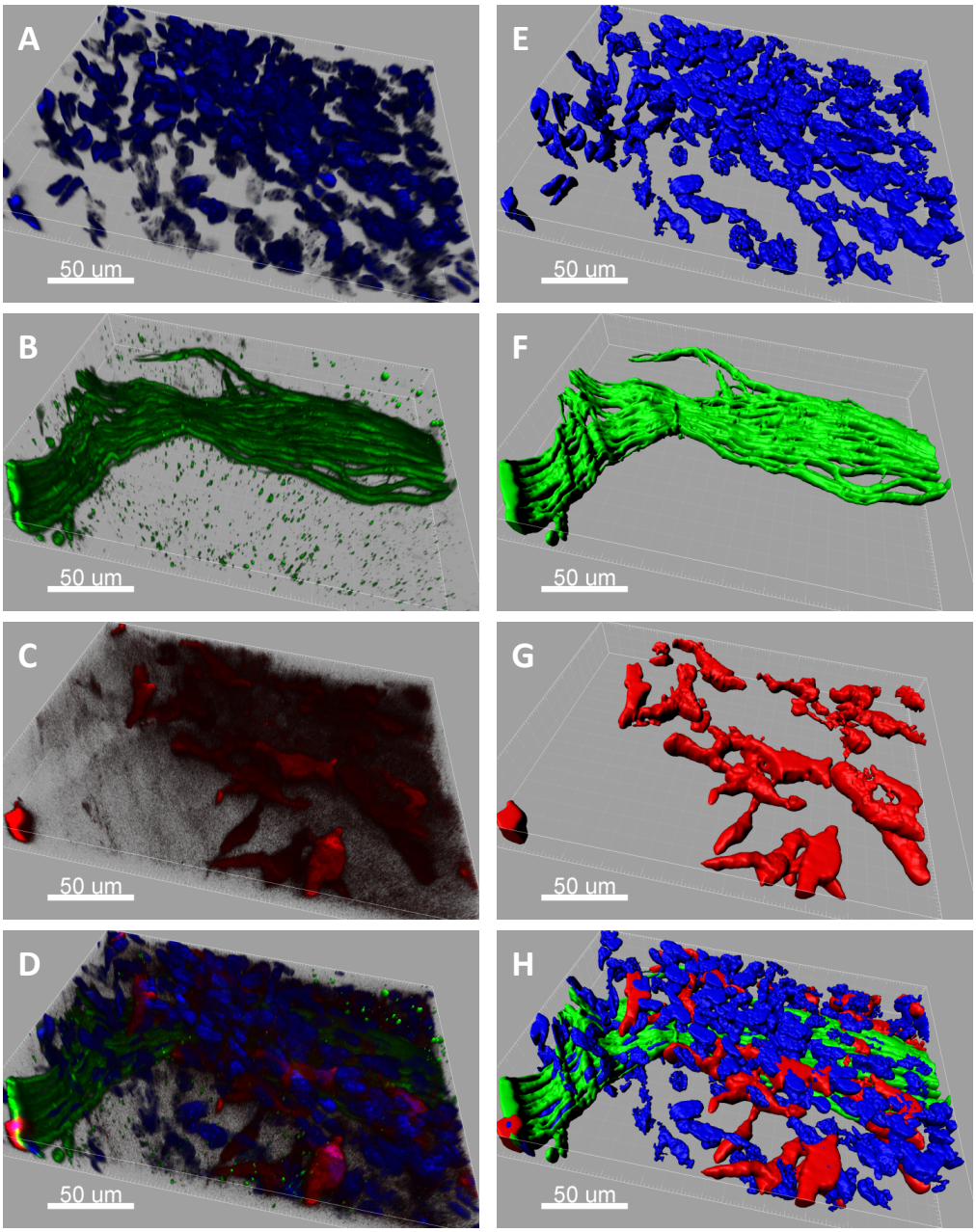

Figure 1. Post-imaging analysis process
Raw data from a LSCM acquisition was displayed in a 3D view (A, B, C and D). Surfaces were created manually with different area detail level for each channel. An absolute intensity thresholding was automatically calculated and a manual filter was added (E, F, G and H). Additional filter of number of voxels was applied to the green channel (F and G). A final color-enhanced view is observed in H.

RESULTS

Previous works have shown the interaction between immune cells and peripheral nervous system in the cornea [3-5]. This interaction has been shown in the limbus [3] and recently between stromal macrophages and stromal nerve bundles in the periphery of the cornea of CX3CR1^{EGFP} knock-in mice [5]

In addition to CX3CR1^{EGFP} mice, in the current work we used also CX3CR1$^{cre/RFP}$ and CX3CR1$^{cre/\ fGFP}$ mice. After fixation, the corneas were stained with a pan neural marker tubulin III antibody. Tubullin III is widely expressed in the whole cornea of the WT mice (***Chapter 5).*** The stratification of the corneal myeloid population of these mouse strains has been also described in the **chapter 4**. In this study, we observed myeloid cells contacting the nerves in the limbus (***Figure 3***), periphery and central stroma periphery, paracentral and central sub-basal plexus (***Figure 2, 4, 5, 6 and 7***). In limbus and stroma, macrophages enwrap nerve bundles (***Figures 3 and 4***). In the sub-basal plexus DCs are in contact with individual nerves (***Figures 5, 6 and 7***). An individual DC is contacting up to 10 distinct axons in the corneal epithelium (***See figure of above article***). A single nerve fibre is tracked by many epithelial DCs in the epithelium and macrophages in the stroma (***Figure 4 and 6***). The stromal nerve bundles enter from bellow into the sub-basal plexus where divide into small fibres that turn abruptly 90° and continues parallel to the corneal surface throughout the BMZ. Myeloid cells are located enwrapping the branch in the sub-basal plexus (***Figure 5***). A new remarkable finding was to find nerve leashes intertwining with DC dendrites (***Figure 7***)

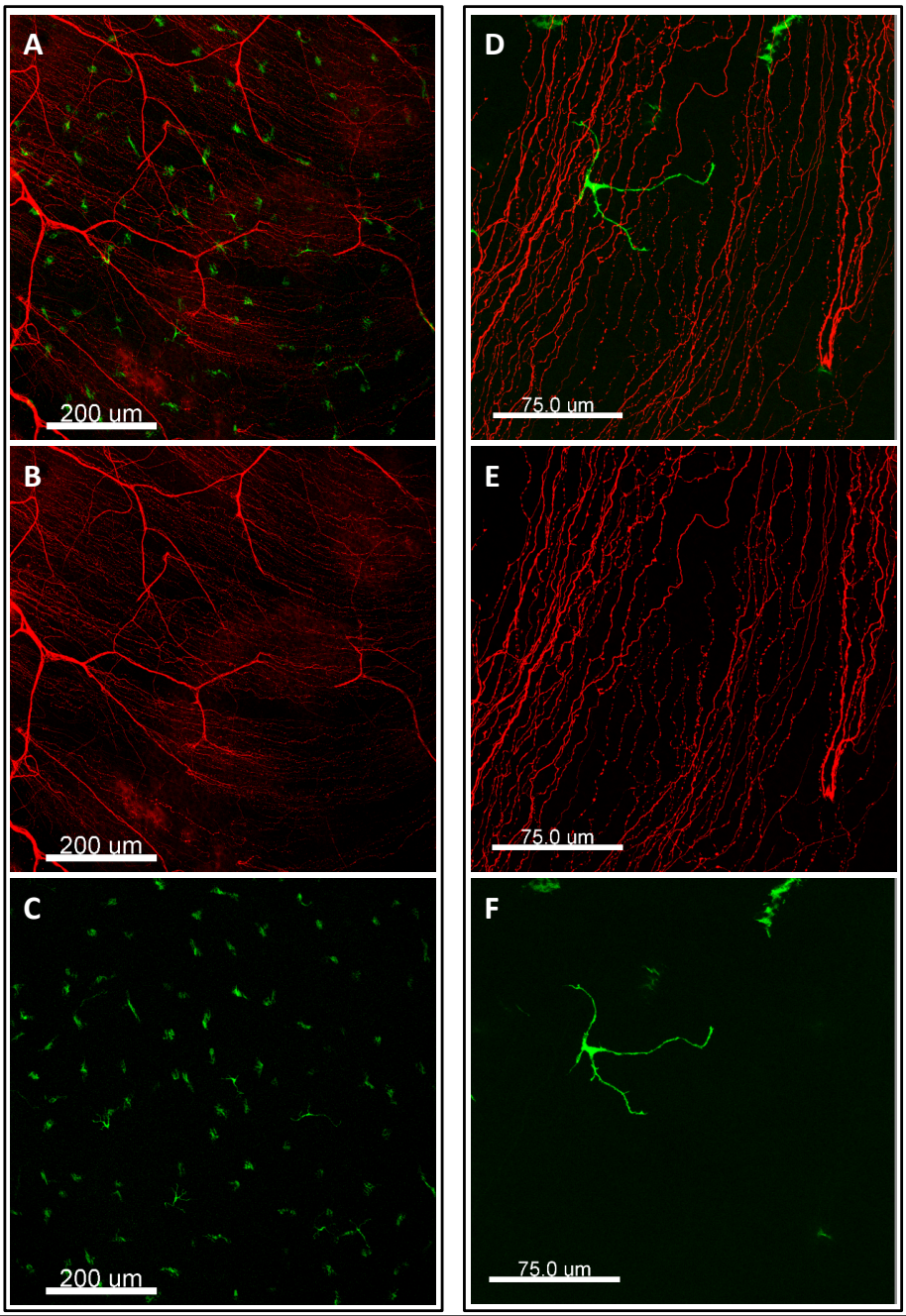

Figure 2. Flat mount cornea of a CX3CR1^{EGFP} mouse immunolabeled with anti tubulin beta III (red). Maximum projection with 10X (A, B and C) shows the proximity of the myeloid population (green) and the corneal nerves (red). With higher magnification (40X) it can be appreciated DC interdigitating with the sub-basal plexus nerves (D, E and F).

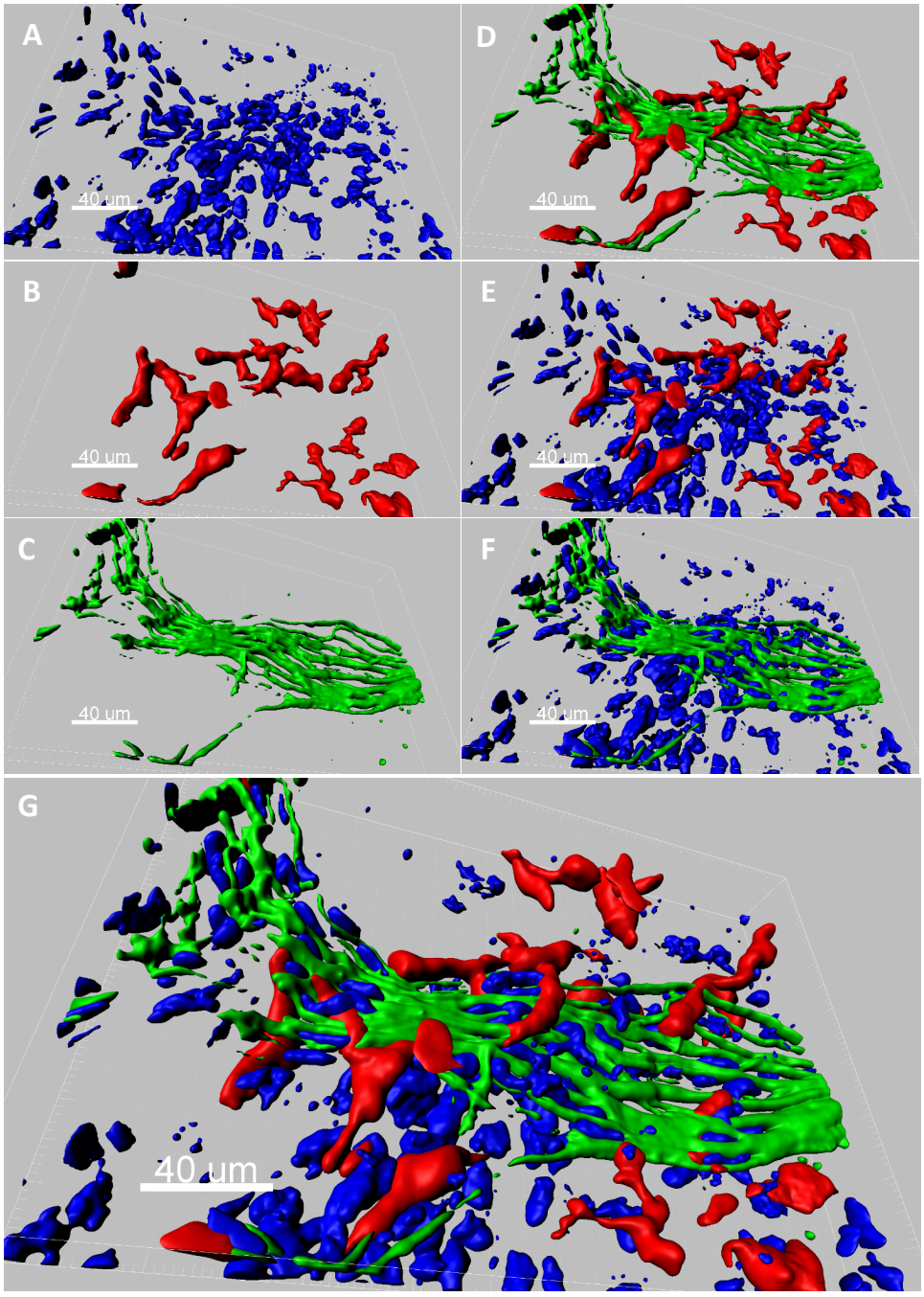

Figure 3. Perilimbal- peripheral stromal nerve trunk (green) is observed associated with macrophages (red). Nuclei were stained with DAPI (blue)

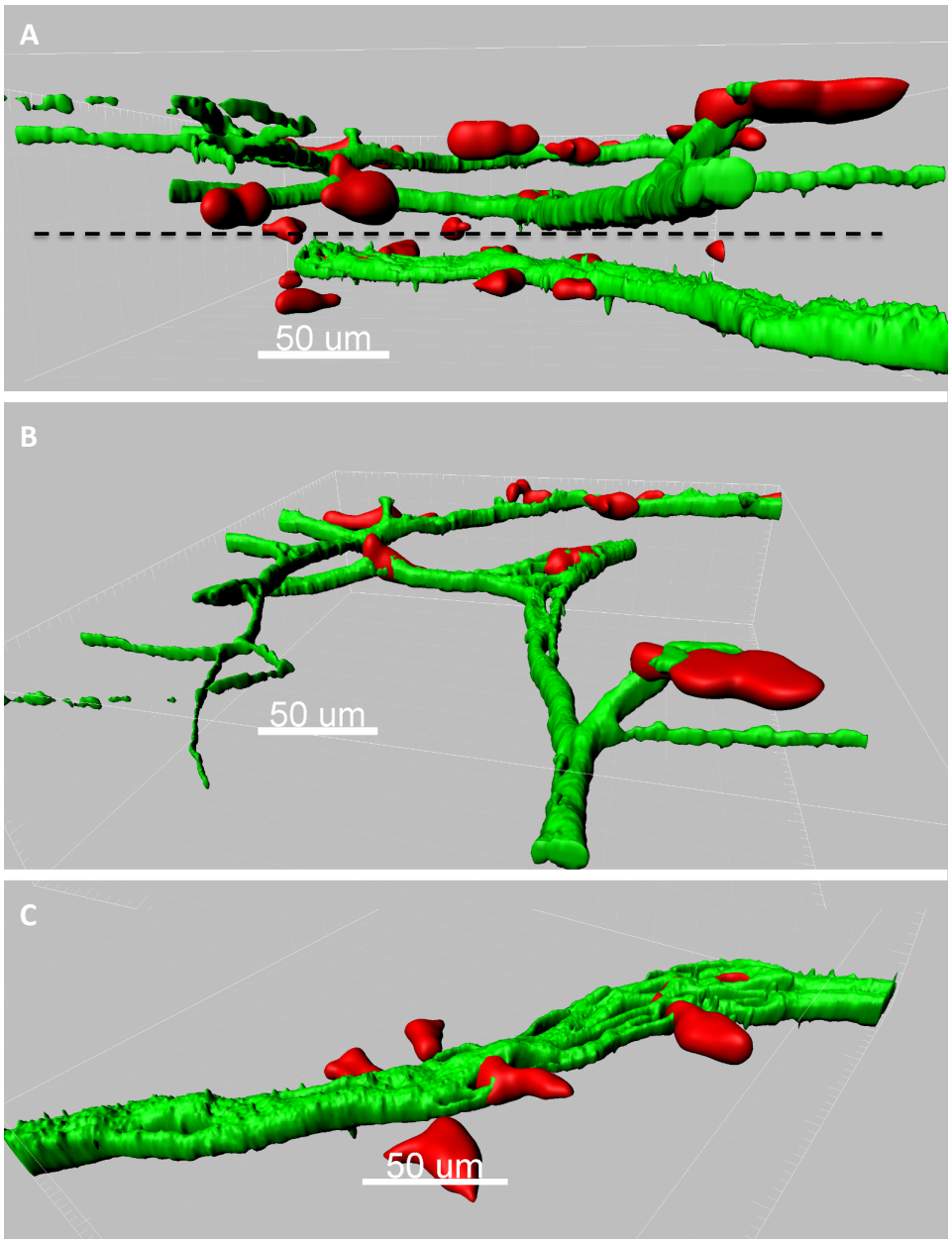

Figure 4. Central-paracental stromal nerve bundles (green) are observed associated with stromal macrophages. Dashed bar separates two independent nerve bundles (A).
The anterior bundle is observed rotated in B with a different 3D view. The tight association between nerves and macrophages can be appreciated. The same is seen in C, which shows the posterior stromal bundle in tight contact with many macrophages.

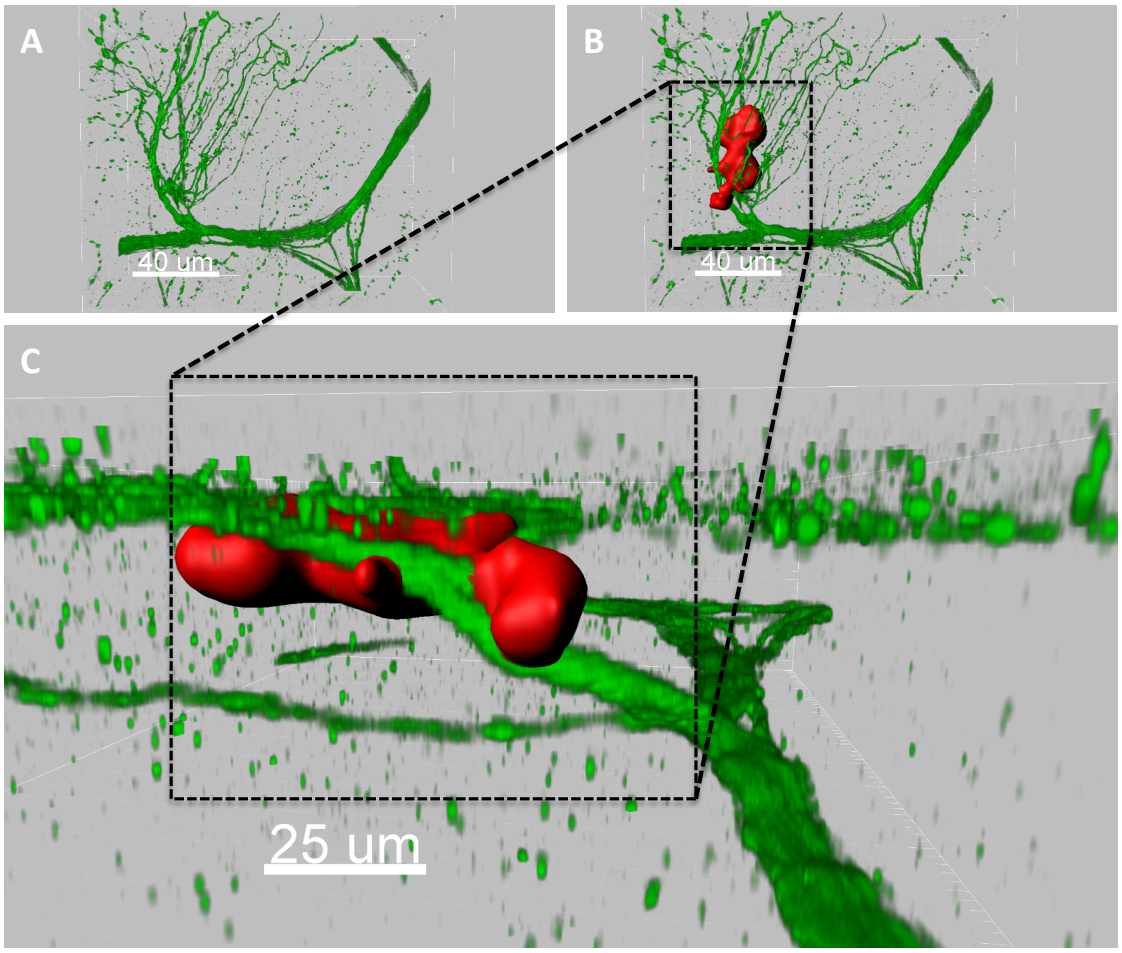

Figure 5. A stromal nerve is turning into the basement membrane and sprouting in many sub-basal axons (A, green)). A resident myeloid cell is located enwrapping the the branching (B). A more realistic 3D view can be appreciated in C.

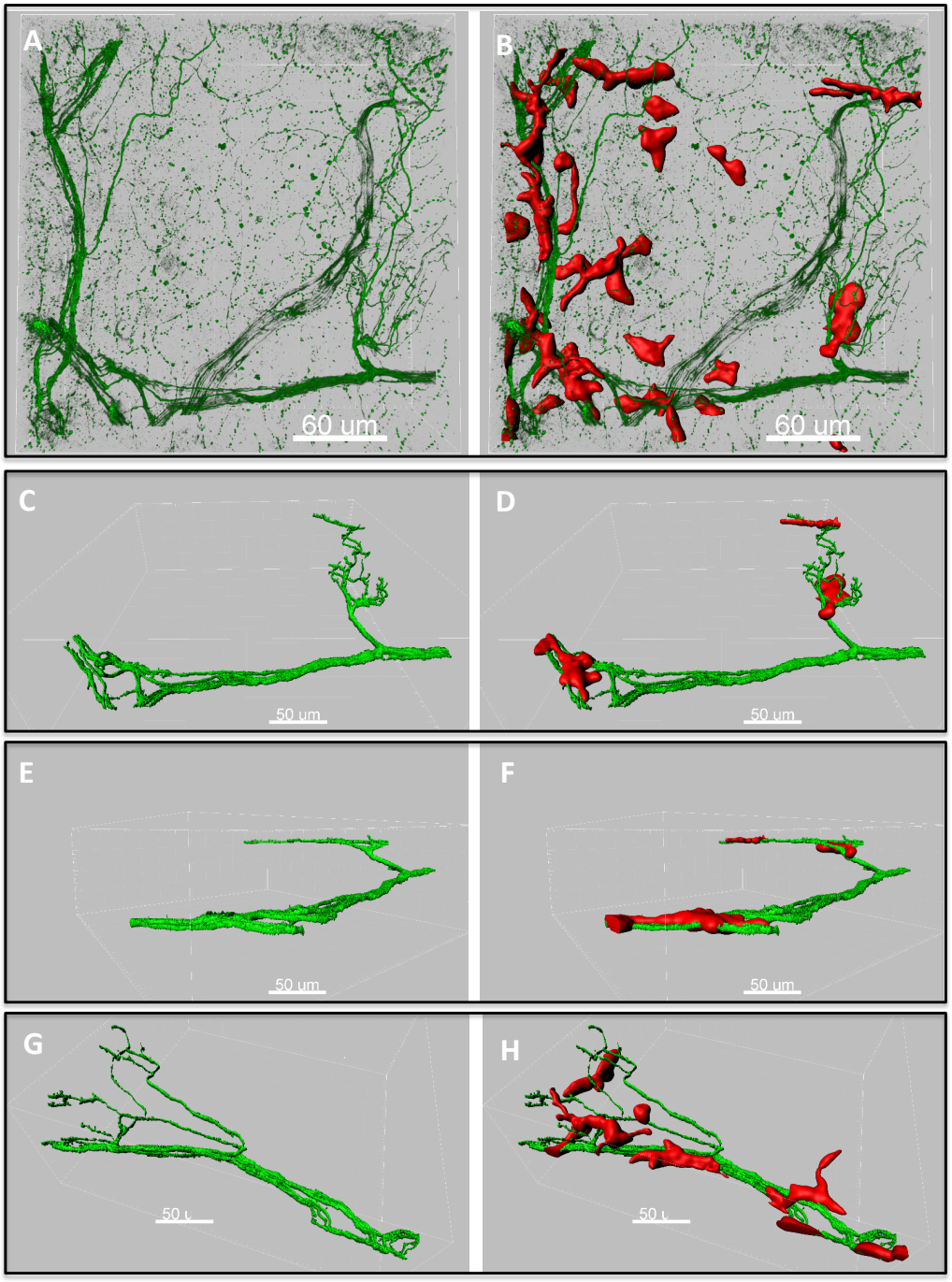

Figure 6. The corneal nerves (A) are under surveillance of many DCs and macrophages (B, green). Under microscope field (40X) it can be observed a single axon is tracked by up 3-6 different immune cells (red) from the epithelium to the stroma (D, F and H).

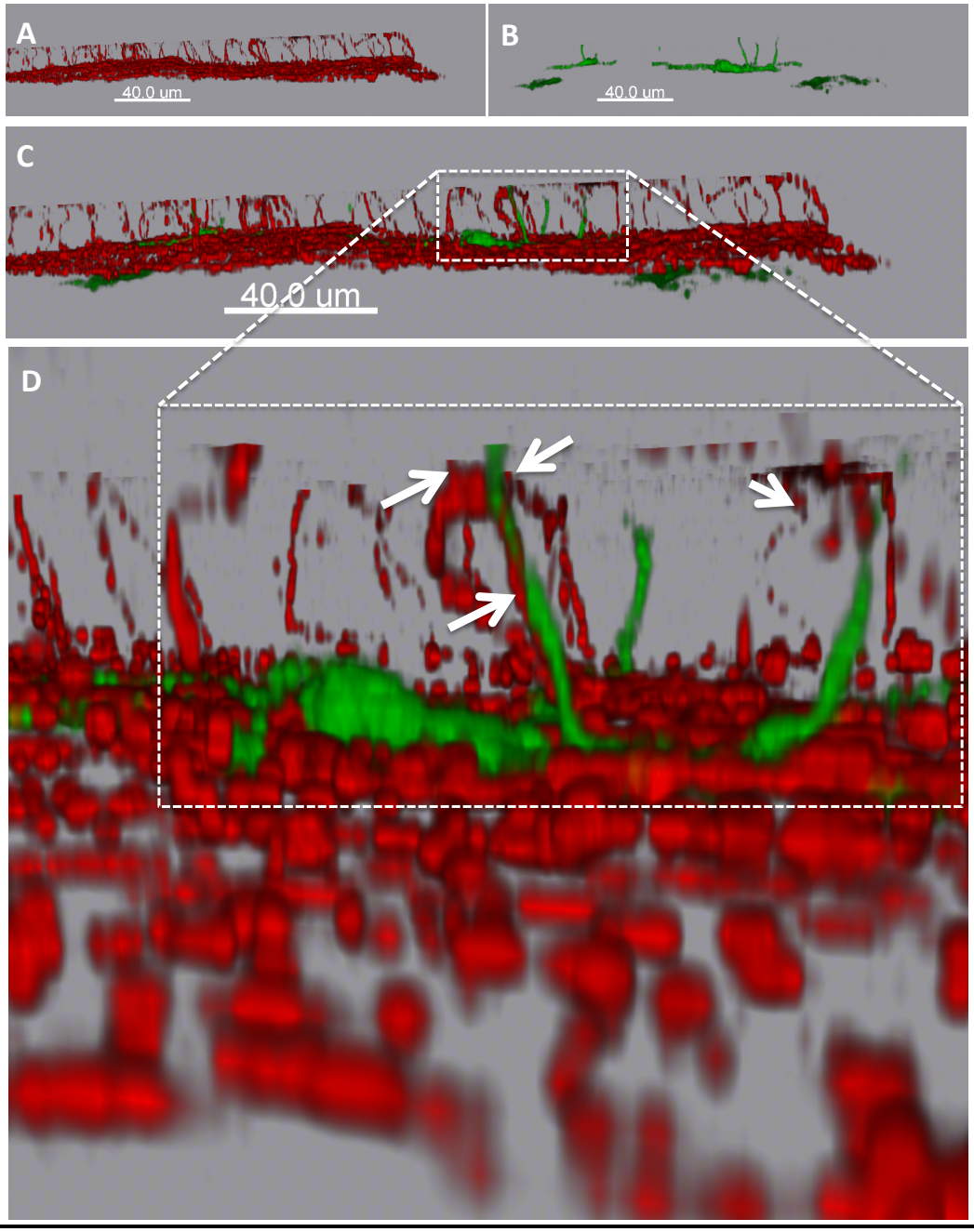

Figure 7. LSCM shows the high nerve density in the subbasal plexus (A). Subbasal DCs (B) are seen entrenched between the nerves (C). A higher magnification (D) shows nerve leashes interweaving with DC dendrites between the epithelial cells toward the ocular surface (Arrows)

Cx3cr1$^{cre/RFP}$ Bone Marrow Engrafted Cells Repopulate the Cornea in Contact with Nerves in a Thy1-YFP Irradiated Mouse Model

In the **chapter 4** we successfully engrafted either CX3CR1$^{cre/fGFP}$ or CX3CR1$^{cre/RFP}$ bone marrow derived-cells in different strains of lethally irradiated host mice, therefore multiple useful chimeras were generated. In the current work, Thy1-YFP and WT mice were lethally irradiated and posteriorly engrafted with CX3CR1$^{cre/RFP}$ bone marrow derived-cells. The mice were thereafter examined *in vivo* with a MP-IVM system

We engrafted CX3CR1$^{Cre/RFP}$ bone marrow derived-cells to maintain a bright fluorescence for the lifespan of the engrafted population (tdTomato is 10 times brighter that GFP). Equally, the emission of stable YFP neurofluorescence, under Thy1 promoter, permits the visualization of the corneal nerves. The chimera was successfully generated, but the microscope is a commercial device with only one tunable laser. Instead of photomultiplier tubes (PMTs), the microscope system collects light emission with high efficiency non-descanned detectors in the epifluorescence position. The CYR cube is composed by a 460-500 nm (blue and SGH), 520-560 (Yellow) and 575-630nm (Red) band pass filters. YFP (527nm) and tdTomato (582nm) are both nearby in their emission spectra. YFP crossovers ~16% the red channel. Conversely, tdTomato bleeds through the yellow channel ~30%. Besides, tdTomato (the brightest fluorescent protein) is ~2 fold-brighter than YFP. Maximum picks for two-photon excitation are 960 nm for YFP and 680/1052nm for tdTomato. With the CYR cube, SHG signal is only detectable in the range of 920-960 nm. Consequently, we tuned the laser at 950 nm where YFP (80% absorbance), tdTomato (20% absorbance) and SHG can be detected at the same time.

The expected chimera was successfully generated (***Figure 8 and 9***) and corneas remained transparent with no evidence of inflammation. Nerve bundles and fibres were observed in the yellow channel as well as reconstituted bone marrow population in the red channel. The stroma of the cornea was detected in the blue channel. Around 75% of

the bone marrow derived donor cells can be observed in contact with the nerves (***Figures 8 and 9***).

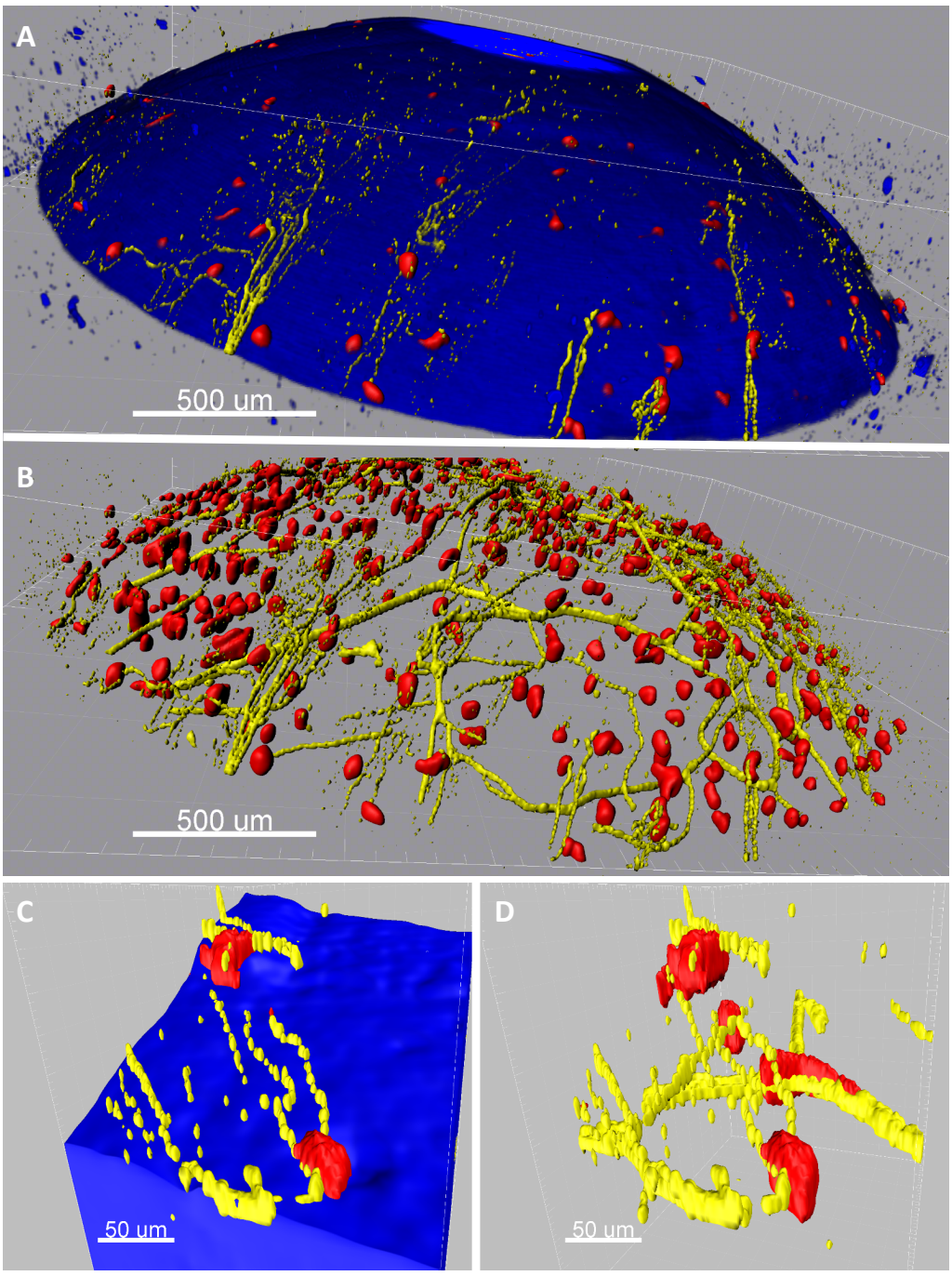

Figure 8. Neuroinmune-fluorescence chimera of Thy1-YFP irradiated mouse engrafted with Cx3cr1$^{cre/RFP}$ bone marrow derived cells.
Intravital visualization of a Thy1-YFP mouse 3 months after had been engrafted with bone marrow derived-cells. Endogenous neuro-fluorescence is observed in yellow, Cx3cr1$^{cre/RFP}$ bone marrow derived cells (red) and SHG in blue.
The majority of the cornea is successfully repopulated with the bone marrow population (A and B). The majority of the donor cells can be observed in tight-contact with the nerves in the subbasal plexus (C) as well in the stroma (D).
Pictures as displayed in a 3D surface view. Immune population is shown in red, nerves in yellow and and stroma in blue (SGH).

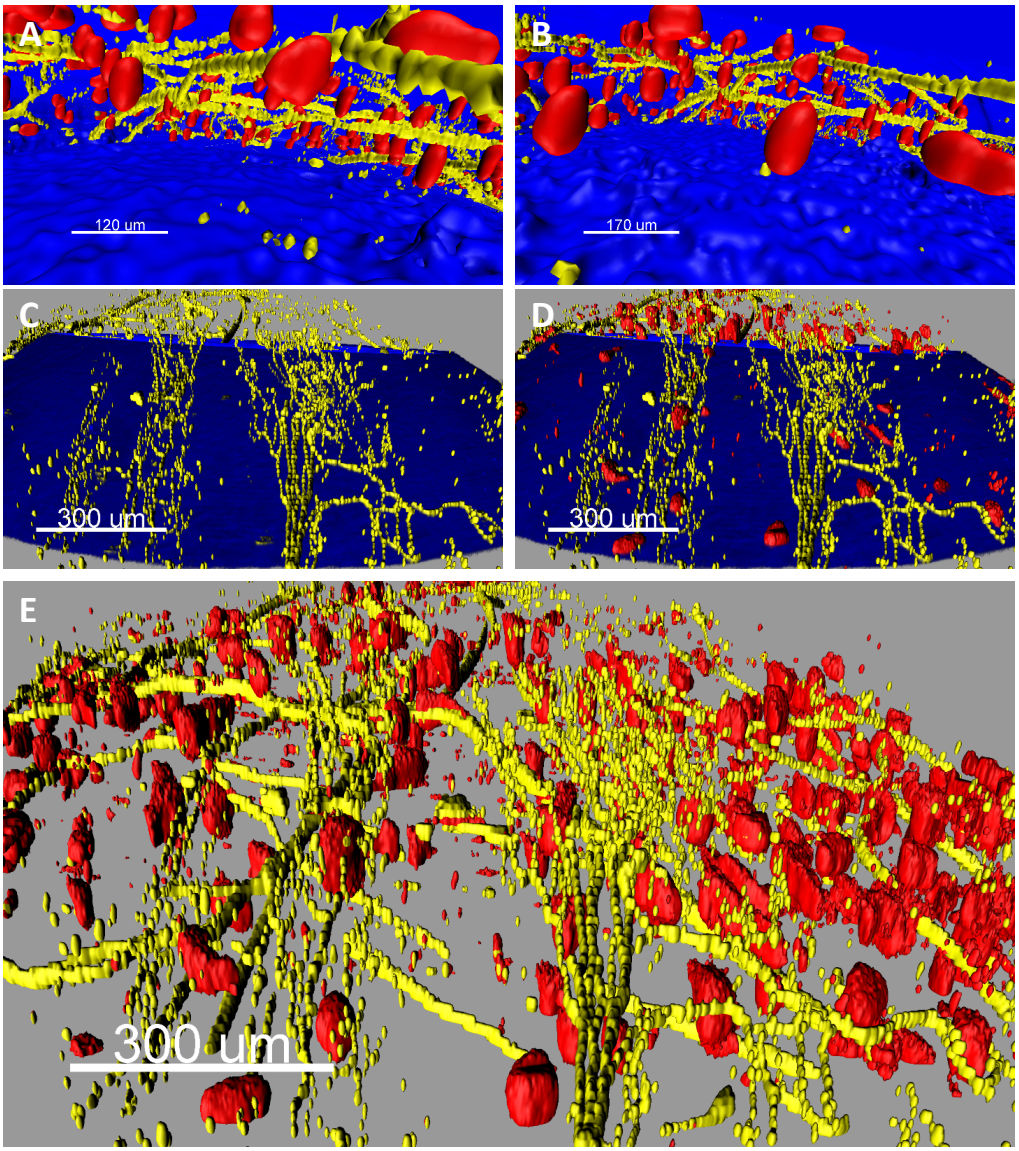

Figure 10. Neuroinmune-fluorescence chimera of Thy1-YFP irradiated mouse engrafted with Cx3cr1$^{cre/RFP}$ bone marrow derived cells.
Different 3D views of the stroma (A and B), subbasal plexus (C and D) and whole cornea (E), show that new bone marrow population of the cornea successfully engaged with the corneal nerves after transplantation
Pictures as displayed in a 3D surface view. Immune population is shown in red, nerves in yellow and and stroma in blue (SGH).

DISCUSSION

The cornea, the most densely innervated site in the body, is endowed with myeloid cells also referred as antigen presenting cells (APCs) that are not immunereactive to alloantigens [6, 7] In contact with the external environment, the cornea has evolved as an immune privileged place in order to keep transparency, biomechanical, refractive and sensory properties. The cornea has developed a unique mechanism of wound healing to repair itself after an injury with a minimal or absent inflammatory reaction due, in part, by a deprivation of lymphatic and blood vessels [8-11]. Inflammation is an essential component of tissue protection and eradication of infection but also a major antagonist of corneal clarity essential for unaltered vision and survival [12]. During the last decade, the study of the mechanisms that protect cornea from inflammation and the causes by which the cornea loss its immune privilege, has taken enormous relevance [6, 13-17]. However, mostly of the aspects involving corneal immune privilege and inflammatory reaction, remain still unknown.

Tomio Tada nearly a decade ago defined a "Supersystem" as a highly integrated life system such as the immune system, nervous system and embryonal development of higher organisms. A supersystem is defined by tree main properties: 1) engenders itself by generation of its diverse components from a single progenitor in a stochastic process followed by selection and adaptation; 2) has individuality and is capable of deciding its own behavior in response to environmental and internal stimuli by referring to its own established behavioral pattern and 3) is generated and operated without a given purpose [18].

Increasing evidence indicates the existence of a complex cross-regulation between the most important biosensors of the human body: the immune and nervous systems [19]. Cytokines control body temperature and trigger autoimmune disorders in the central nervous system, whereas neuropeptides released in peripheral tissues and lymphoid organs modulate both innate and adaptive immune responses. The effect of pro-

inflammatory neuropeptides, released by nerve fibers, in the immune system is practically unknown. It is know that nociceptive nerves regulate the pro-inflammatory function of leukocytes in peripheral tissues; however, how neuroinflammation affects immune response against allografts remains unexplored. Recent data suggest that this new area of research is worth exploring for potential development of novel complementary therapies for prevention/treatment of graft rejection (see in detail review by Larregina et al. [19].

The majority of the evidences, for direct cell-cell interactions between neural and immune cells, are derived from studies in the airway tissue. The anatomical proximity of nerves and immune cells predicts the existence of their functional interaction and might form the basis of neuro-immune communication in health and allergic disease. Immune cells respond to neurotransmitters; conversely, immune cell-derived mediators could influence the activity of nerves [20]. Mast cells and eosinophils associations with nerve fibres have been vastly observed [21, 22]. Eosinophils surround but also infiltrate into the nerve bundles [23]. DCs of the respiratory tract regulate adaptive immune responses to inhaled antigens [24] being involved in the pathogenesis of allergic airway disease [25]. DCs are extensively contacted by CGRP-positive sensory C-fibres in the mucosa of the conducting airways [26] being these interconnections increased in an allergic airway disease mice model compared to healthy mice. DCs activate T cells via local antigen presentation in the airways [27], where the association of T cells with either nerve-contacting DCs or sensory fibres has been described [20]

Neuropeptides, released by sensory neurons directly affect the activity of DCs and T cells. Whereas CGRP (calcitonin gene related peptide) and VIP (vasoactive intestinal peptide) have immunosuppressive effects, SP (substance P) acts as a pro-inflammatory factor. DCs have receptors for CGRP [28] VIP [29] and SP [30]. CGRP and VIP chemo-attract immature DCs to nerve endings where are arrested until posterior maturation [31]. Moreover, CGRP inhibits T cell proliferative response by decreasing both CD86 and HLA−DR expression in human monocyte-derived DCs [28]. Additionally, CGRP inhibits

antigen presentation by Langerhans cells [32]. VIP stimulates the generation of tolerogenic DCs induced by regulatory T cells [33]. In contrast, substance P mediates recruitment and survival of DCs upon secondary allergen [34] potentiating cellular immunity [35].

The cornea has been recently suggested as an attractive place to explore interplay of both PNS and immune supersystems. Emerging evidences suggest the relevance of corneal nerves in graft rejection. Paunicka *et al.* have shown the severing of corneal nerves in the graft bed abolishes immune privilege even in the fellow eye [1]. The placement of an allograft increases the incidence of rejection to a subsequently placed corneal allograft in the same, or fellow eye even when the subsequent allograft was unrelated to the first. The authors found that increased rejection was antigen nonspecific but T cell mediated since syngeneic grafts survived indefinitely. The cause of increased rejection was hypothesized to the nerve injury caused during the transplantation process. The same results were observed by severing of nerves 360 degrees around the cornea. Allografts placed 60 days after nerve trephination succumbed also to immune rejection. Besides, burst of substance P produced the same state of rejection. These authors show that SP disables T regulatory (Treg) suppression, and associated this impairment with increased rejection. However, the authors are unsure about how Tregs augmented immune rejection to a substance P burst that occurred 60 days prior [1].

We purposed a potential role for tissue resident DCs and macrophages as plausible explanation [36]. Mononuclear phagocytes have a long life span but also express substance P receptors, produce substance P, and are altered by ligation of this neuropeptide [37]. Additionally, macrophages are antigen-presenting cells and can migrate to lymphoid organs, likely in a CCR7 mediated fashion [38]. Macrophages reside in close proximity to peripheral nerves [39], consistent in the peripheral corneal stromal as well [5].

We appreciated the proximity of a DC with up to 10 distinct nerves in the corneal epithelium [2]. Additionally, we extended this work to observe DCs and macrophages in contact with nerves in the entire cornea. Resident myeloid-cells contact the nerves in the limbus, widely in the stroma and ubiquitously in the sub-basal plexus. Macrophages

enwrap nerve bundles in the limbus and storma. In the sub-basal plexus, DCs reside with like a "spider in the web" with the nerves. Terminal endings intertwine with the dendrites toward the corneal surface. From the apex to the limbus, a nerve fibre is extended few millimeters in length. In its path, the fibre is patrolled by many epithelial DCs along the sub-basal plexus and macrophages through the stroma and limbus.

SP and CGRP are classic sensory neuropeptides, involved in the transmission of pain. However, SP and GCRP have antagonist roles and the balance between both is critical for inflammation and wound healing. SP is a potent pro-inflammatory neuropeptide taking part in recruitment, activation and functional activity of neutrophils, monocytes/macrophages, T cells, mast cells and eosinophils, but also stimulates epithelial cell migration and wound healing [40]. Conversely, CGRP has immunosuppressive effects. Immature DCs express receptors for CGRP [28] and are chemo-attracted to nerve endings where are arrested until posterior maturation [31]. CGRP also inhibits T cell proliferative response by decreasing both CD86 and HLA−DR expression in human monocyte-derived DCs [28] and inhibits antigen presentation by Langerhans cells (LCs) [32]. As opposite to SP, CGRP is expressed during homeostasis rather than wound healing or inflammation [40].

In the normal cornea, CGRP fibers are ten times more abundant than SP fibers [41, 42]. This suggests that CGRP nerve fibres could prevent DC maturation [32] by arresting them in their proximity. Conversely, SP expression is increased in the cornea in response to an injury promoting the opposite effect [43]. Paunicka et al. have shown that either severing the corneal nerves or burst of SP induces sympathetic loss of the immune privilege and promotes rejection in either eye. DCs can be altered by ligation of SP [37]. Additionally by damaging the nerves CGRP supply will be interrupted and CGRP-chemo-attracted immature DCs might undergo maturation and probably potentiated by SP release [43]. Together, these findings suggest that CGRP fibers chemo-attract myeloid cells preventing their maturation in the normal steady state of the cornea [44].

To confirm this hypothesis, we performed an alternative experiment. Previously we have observed bone marrow transplantation, after lethally irradiation, induces slow

turnover of myeloid population without evidence of corneal inflammation (**chapter 4).** Assuming that CGRP/SP balance will remain unchanged upon irradiation, the engrafted bone marrow derived-cells will repopulate the cornea chemo-attracted by the nerves where they will remain arrested of maturation. Three months after irradiation, the cornea of Thy1-YFP irradiated chimeric host mice remained transparent and no inflammation was observed. As expected the donor bone marrow derived-cells repopulated the cornea associated with the nerves.

In conclusion, herein we show that both PNS and resident myeloid-population interface in the healthy cornea. How these two "supersystems" interplay to maintain both immune-privilege and transparency is a promising field for the coming years. This new concept should be considered in the future to undertand corneal pathologies.

REFERENCES

1. Paunicka, K.J., J. Mellon, D. Robertson, M. Petroll, J.R. Brown and J.Y. Niederkorn, *Severing corneal nerves in one eye induces sympathetic loss of immune privilege and promotes rejection of future corneal allografts placed in either eye.* Am J Transplant, 2015. **15**(6): p. 1490-501.
2. Blanco, T. and D.R. Saban, *The Cornea Has "the Nerve" to Encourage Immune Rejection.* Am J Transplant, 2015.
3. He, J., N.G. Bazan and H.E. Bazan, *Mapping the entire human corneal nerve architecture.* Exp Eye Res, 2010. **91**(4): p. 513-23.
4. Kenchegowda, S. and H.E. Bazan, *Significance of lipid mediators in corneal injury and repair.* J Lipid Res, 2010. **51**(5): p. 879-91.
5. Seyed-Razavi, Y., H.R. Chinnery and P.G. McMenamin, *A novel association between resident tissue macrophages and nerves in the peripheral stroma of the murine cornea.* Invest Ophthalmol Vis Sci, 2014. **55**(3): p. 1313-20.
6. Knickelbein, J.E., K.A. Buela and R.L. Hendricks, *Antigen-presenting cells are stratified within normal human corneas and are rapidly mobilized during ex vivo viral infection.* Invest Ophthalmol Vis Sci, 2014. **55**(2): p. 1118-23.
7. Streilein, J.W., *Ocular immune privilege: therapeutic opportunities from an experiment of nature.* Nat Rev Immunol, 2003. **3**(11): p. 879-89.
8. Dupps, W.J., Jr. and S.E. Wilson, *Biomechanics and wound healing in the cornea.* Exp Eye Res, 2006. **83**(4): p. 709-20.
9. Maurice, D.M., *The structure and transparency of the cornea.* J Physiol, 1957. **136**(2): p. 263-86.
10. Maurice, D.M. and A.A. Giardini, *Swelling of the cornea in vivo after the destruction of its limiting layers.* Br J Ophthalmol, 1951. **35**(12): p. 791-7.
11. Meek, K.M., D.W. Leonard, C.J. Connon, S. Dennis and S. Khan, *Transparency, swelling and scarring in the corneal stroma.* Eye (Lond), 2003. **17**(8): p. 927-36.
12. Streilein, J.W., *Immunobiology and immunopathology of corneal transplantation.* Chem Immunol, 1999. **73**: p. 186-206.
13. Forrester, J.V., H. Xu, L. Kuffova, A.D. Dick and P.G. McMenamin, *Dendritic cell physiology and function in the eye.* Immunol Rev, 2010. **234**(1): p. 282-304.
14. Hajrasouliha, A.R., Z. Sadrai, H.K. Lee, S.K. Chauhan and R. Dana, *Expression of the chemokine decoy receptor D6 mediates dendritic cell function and promotes corneal allograft rejection.* Mol Vis, 2013. **19**: p. 2517-25.
15. Hamrah, P., Y. Liu, Q. Zhang and M.R. Dana, *The corneal stroma is endowed with a significant number of resident dendritic cells.* Invest Ophthalmol Vis Sci, 2003. **44**(2): p. 581-9.

16. Khan, A., H. Fu, L.A. Tan, J.E. Harper, S.C. Beutelspacher, D.F. Larkin, G. Lombardi, M.O. McClure and A.J. George, *Dendritic cell modification as a route to inhibiting corneal graft rejection by the indirect pathway of allorecognition.* Eur J Immunol, 2013. **43**(3): p. 734-46.
17. Knickelbein, J.E., S.C. Watkins, P.G. McMenamin and R.L. Hendricks, *Stratification of Antigen-presenting Cells within the Normal Cornea.* Ophthalmol Eye Dis, 2009. **1**: p. 45-54.
18. Tada, T., *The immune system as a supersystem.* Annu Rev Immunol, 1997. **15**: p. 1-13.
19. Larregina, A.T., S.J. Divito and A.E. Morelli, *Clinical Implications of Basic Science Discoveries: Nociceptive Neurons as Targets to Control Immunity-Potential Relevance for Transplantation.* Am J Transplant, 2015.
20. Veres, T.Z., S. Rochlitzer and A. Braun, *The role of neuro-immune cross-talk in the regulation of inflammation and remodelling in asthma.* Pharmacol Ther, 2009. **122**(2): p. 203-14.
21. Myers, A.C., B.J. Undem and D. Weinreich, *Influence of antigen on membrane properties of guinea pig bronchial ganglion neurons.* J Appl Physiol (1985), 1991. **71**(3): p. 970-6.
22. Costello, R.W., B.H. Schofield, G.M. Kephart, G.J. Gleich, D.B. Jacoby and A.D. Fryer, *Localization of eosinophils to airway nerves and effect on neuronal M2 muscarinic receptor function.* Am J Physiol, 1997. **273**(1 Pt 1): p. L93-103.
23. Jacoby, D.B., R.M. Costello and A.D. Fryer, *Eosinophil recruitment to the airway nerves.* J Allergy Clin Immunol, 2001. **107**(2): p. 211-8.
24. Hammad, H. and B.N. Lambrecht, *Dendritic cells and epithelial cells: linking innate and adaptive immunity in asthma.* Nat Rev Immunol, 2008. **8**(3): p. 193-204.
25. Upham, J.W. and P.A. Stumbles, *Why are dendritic cells important in allergic diseases of the respiratory tract?* Pharmacol Ther, 2003. **100**(1): p. 75-87.
26. Veres, T.Z., S. Rochlitzer, M. Shevchenko, B. Fuchs, F. Prenzler, C. Nassenstein, A. Fischer, L. Welker, O. Holz, M. Muller, N. Krug and A. Braun, *Spatial interactions between dendritic cells and sensory nerves in allergic airway inflammation.* Am J Respir Cell Mol Biol, 2007. **37**(5): p. 553-61.
27. Huh, J.C., D.H. Strickland, F.L. Jahnsen, D.J. Turner, J.A. Thomas, S. Napoli, I. Tobagus, P.A. Stumbles, P.D. Sly and P.G. Holt, *Bidirectional interactions between antigen-bearing respiratory tract dendritic cells (DCs) and T cells precede the late phase reaction in experimental asthma: DC activation occurs in the airway mucosa but not in the lung parenchyma.* J Exp Med, 2003. **198**(1): p. 19-30.
28. Carucci, J.A., R. Ignatius, Y. Wei, A.M. Cypess, D.A. Schaer, M. Pope, R.M. Steinman and S. Mojsov, *Calcitonin gene-related peptide decreases expression*

of HLA-DR and CD86 by human dendritic cells and dampens dendritic cell-driven T cell-proliferative responses via the type I calcitonin gene-related peptide receptor. J Immunol, 2000. **164**(7): p. 3494-9.
29. Delgado, M., A. Chorny, E. Gonzalez-Rey and D. Ganea, *Vasoactive intestinal peptide generates CD4+CD25+ regulatory T cells in vivo.* J Leukoc Biol, 2005. **78**(6): p. 1327-38.
30. Marriott, I. and K.L. Bost, *Expression of authentic substance P receptors in murine and human dendritic cells.* J Neuroimmunol, 2001. **114**(1-2): p. 131-41.
31. Dunzendorfer, S., A. Kaser, C. Meierhofer, H. Tilg and C.J. Wiedermann, *Cutting edge: peripheral neuropeptides attract immature and arrest mature blood-derived dendritic cells.* J Immunol, 2001. **166**(4): p. 2167-72.
32. Hosoi, J., G.F. Murphy, C.L. Egan, E.A. Lerner, S. Grabbe, A. Asahina and R.D. Granstein, *Regulation of Langerhans cell function by nerves containing calcitonin gene-related peptide.* Nature, 1993. **363**(6425): p. 159-63.
33. Gonzalez-Rey, E., A. Chorny, A. Fernandez-Martin, D. Ganea and M. Delgado, *Vasoactive intestinal peptide generates human tolerogenic dendritic cells that induce CD4 and CD8 regulatory T cells.* Blood, 2006. **107**(9): p. 3632-8.
34. Kradin, R., J. MacLean, S. Duckett, E.E. Schneeberger, C. Waeber and C. Pinto, *Pulmonary response to inhaled antigen: neuroimmune interactions promote the recruitment of dendritic cells to the lung and the cellular immune response to inhaled antigen.* Am J Pathol, 1997. **150**(5): p. 1735-43.
35. Janelsins, B.M., A.R. Mathers, O.A. Tkacheva, G. Erdos, W.J. Shufesky, A.E. Morelli and A.T. Larregina, *Proinflammatory tachykinins that signal through the neurokinin 1 receptor promote survival of dendritic cells and potent cellular immunity.* Blood, 2009. **113**(13): p. 3017-26.
36. Blanco, T. and D.R. Saban, *The Cornea Has "the Nerve" to Encourage Immune Rejection.* Am J Transplant, 2015. **15**(6): p. 1453-4.
37. Ho, W.Z., J.P. Lai, X.H. Zhu, M. Uvaydova and S.D. Douglas, *Human monocytes and macrophages express substance P and neurokinin-1 receptor.* J Immunol, 1997. **159**(11): p. 5654-60.
38. Saban, D.R., *The chemokine receptor CCR7 expressed by dendritic cells: a key player in corneal and ocular surface inflammation.* Ocul Surf, 2014. **12**(2): p. 87-99.
39. Perry, V.H., M.C. Brown and S. Gordon, *The macrophage response to central and peripheral nerve injury. A possible role for macrophages in regeneration.* J Exp Med, 1987. **165**(4): p. 1218-23.
40. Micera, A., A. Lambiase and S. Bonini, *The role of neuromediators in ocular allergy.* Curr Opin Allergy Clin Immunol, 2008. **8**(5): p. 466-71.

41. Cortina, M.S., J. He, N. Li, N.G. Bazan and H.E. Bazan, *Recovery of corneal sensitivity, calcitonin gene-related peptide-positive nerves, and increased wound healing induced by pigment epithelial-derived factor plus docosahexaenoic acid after experimental surgery.* Arch Ophthalmol, 2012. **130**(1): p. 76-83.
42. Muller, L.J., C.F. Marfurt, F. Kruse and T.M. Tervo, *Corneal nerves: structure, contents and function.* Exp Eye Res, 2003. **76**(5): p. 521-42.
43. Belmonte, C., M.C. Acosta and J. Gallar, *Neural basis of sensation in intact and injured corneas.* Experimental Eye Research, 2004. **78**(3): p. 513-525.
44. Bonini, S., P. Rama, D. Olzi and A. Lambiase, *Neurotrophic keratitis.* Eye (Lond), 2003. **17**(8): p. 989-95.

CHAPTER 7

Intravital Confocal Microscopy Reveals Corneal Involvement in an Allergic Eye Disease Mouse Model: an in vivo Study

BACKGROUND

In the previous chapters, we successfully used the MP-IVM system to study both nerves and immune population in the cornea. Herein we used the MP-IVM to explore future applications and follow up *in vivo* the behavior of:

5. Engrafted GFP-labeled mADSCs (murine adipocyte-derived stem cells) in different parts of a mouse cornea. We aimed to track the distribution of the engrafted cells over a period of 4 weeks in living mice following experimental corneal injuries (collaboration with Ladan Spandar, Pittsburg University)
6. Drug delivery systems injected into the anterior chamber such as GFP-nanoparticles, collagen binding carriers Allexa-488 conjugated (collaboration with Molly Walsh, Duke Eye Center).
7. Adenovirus infection (collaboration with Li Quarong and Dan Stramer, Duke Eye Center)
8. Depletion of a specific population of CD11c dendritic cells with diphtheria toxin (Collaboration with Sarah Dale and Virginia Calder, University College London).

MATERIAL AND METHODS

GFP-mADSCs isolation and expansion

Subcutaneous white adipose tissue was collected from male enhanced green fluorescence protein (eGFP) transgenic mice (C57Bl/6-Tg(UBC-GFP)30Scha/J strain; Jackson Laboratory, Bar Harbor, ME, http://www.jax.org), ranging in age from 2 to 6 months. Cells were isolated and expanded as previously described[1]. (Data were not shown)

GFP-mADSCs engrafting

Ten female C57Bl/6 mice (2 in each group), 6–8 weeks old, were purchased from Charles River Laboratories (Wilmington, MA). After anesthesia with intraperitoneal injection of a mixture of ketamine intraperitoneal (IP) administered ketamine/xylazine suspensions (120 and 20 mg/kg, respectively), corneal injury was performed in the right eye of each mouse:

1- Anterior chamber injection: After dilatation of the pupil with 1% atropine sulfate ophthalmic solution (Bausch and Lomb Inc., Rochester, NY), 10 µL of GFP-mADSCs ($1x10^4$ cells) were injected into the anterior chamber using a 32 G Hamilton syringe (Sigma-Aldrich, St. Louis, MO).

2- Intra-stromal injection: a stromal pocket was produced by the air bubble technique using a 34 G Hamilton needle (Sigma-Aldrich, St. Louis, MO). Thereafter, 10 µL of GFP-mADSCs ($1x10^4$ cells) was injected using a 32 G Hamilton syringe.

3. Manual keratectomy: keratectomy was performed manually as described before (**chapter 1**)[2]. Briefly: the cornea was partially trephined with a 2 mm trephine. Then ~50 µm thickness of cornea was manually removed with a surgical micro forceps. Air delamination was performed in the remaining stroma using a 34 G Hamilton needle followed by injection of GFP-mADSCs ($1x10^4$ cells) with a 32 G Hamilton syringe.

4. Full-Thickness Penetrating Incision: as described previously (**chapter 2**)[3], one drop of 1% atropine sulfate ophthalmic solution (Bausch and Lomb Inc., Rochester, NY)

was instilled in the eye. A nasal-temporal orientated full-thickness penetrating incision (1.5mm length) was created in the center of the cornea with a surgical blade. GFP-mADSCs ($5x10^5$/μl) were injected intracamerally using a 30G needle.

Drug delivery systems injections

Ten male BALB/c albino mice (2 in each group), 6–8 weeks old, were purchased from Charles River Laboratories (Wilmington, MA). Mice were anesthetized and one drop of 1% atropine sulfate ophthalmic solution (Bausch and Lomb Inc., Rochester, NY) was instilled in the eye.

GFP-nanoparticles (100nm diameter), collagen binding carriers-Allexa-488-conjugated and endothelial binding carriers-Allexa-488-conjugated were injected at different concentrations (not shown) through the superior episcleral vein by using a glass microneedle (3 mm length, 30-50μm diameter).

Adenovirus infection

Adenoviruses were injected through the cornea into the anterior chamber (concentration not shown) with a 32G needle. Once the virus infects the endothelial cells, these express GFP that can be detected.

CD11c-DC depletion with diphtheria toxin

Transgene mice encoding a simian Diphtheria Toxin Receptor (DTR)-EGFP fusion protein under the control of the Itgax (or CD11c) promoter were purchase from Jackson Laboratories. These mice were generated with BALB/c background. $CD11c^{YFP\text{-}DTR}$ DCs were depleted by topical application of DT (concentration not shown).

Intravital multi-photon microscopy and post-acquisition image analysis (See chapters 4, 5 and 6)

RESULTS AND SHORT DISCUSION

The fate, dynamics, and effects of injected ADSCs in living animals are not well understood. Insight into *in vivo* stem cell biology during corneal repair could help to optimize possible therapeutic clinical strategies. Multiphoton microscopy allows for noninvasive, real-time, and serial quantitative imaging of injected labeled cells and their progeny in living animals.

After inject the cells into the anterior chamber, mADSCs were observed round and floating into the anterior chamber. Latter, mADSC attached to the endothelium showing fibroblast-shape. No anterior inflammatory reaction was observed. This indicates that the anterior chamber tolerates the presence of the cells (not shown)

Next we engrafted mADSC in an intraestromal pocket. Cells survived into the stroma for up 4 weeks. At the end of the experiment, mADSCs changed their morphology to a myofibroblast-like shape; however, they did not migrate outside of the pocket (not shown). Additionally, a manual keratectomy was performed and the cells engrafted in the remaining stromal bed. Cells migrated in different directions. Cells also change as a myofibroblast-like phenotype in the storma. Cells were observed also in the epithelium. This indicates that mADSCs might help in the process of wound healing in an open wound (**figure 1**)

Subsequent, we performed a full penetration incision in the cornea and engrafted the mADSCs into the anterior chamber. The cells were observed near to the wounded area immediately after the injury. Later cells were observed contracting the wound and making barrier in the area of the endothelium. This indicates that mADSCs might help in the process of wound repair after a lesion (**figure 1**)

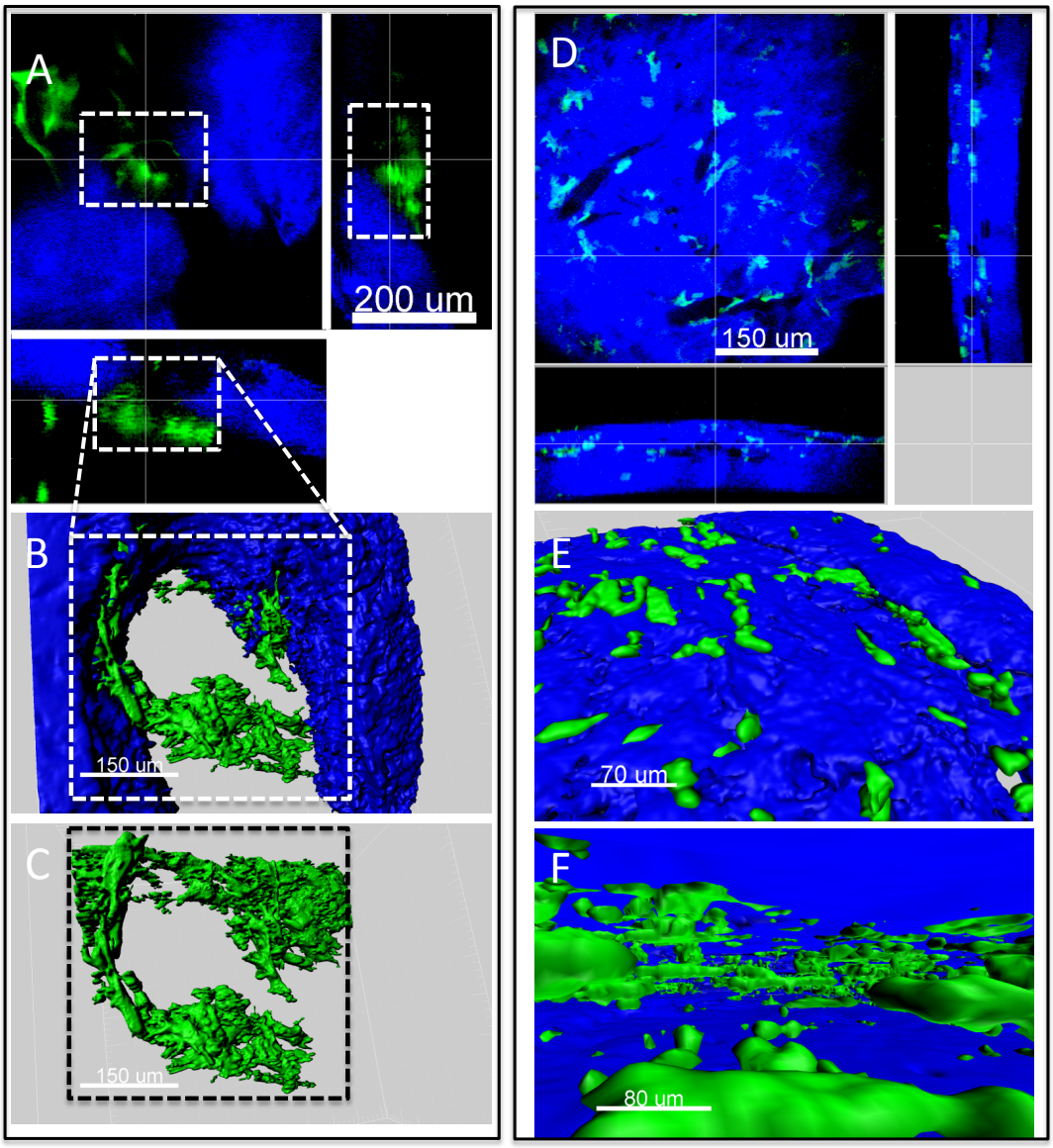

Figure 1. *In vivo* detection of mADSCs (green) in both AC and wounded area, two weeks after full penetrating incision. Orthogonal view (A) and tree-dimensional (B and C) are shown.
In vivo detection of mADSCs (green) in the wounded area four weeks after keratectomy. Orthogonal view (D) and tree-dimensional (E and F) are shown. View of the epithelium (E) and stroma (F).
Blue (SHG, second harmonic generation) delineates the stroma

GFP-nanoparticles, collagen and endothelial binding carriers-Allexa-488-conjugated were injected at different concentrations through the superior episcleral vein. The different systems were located in the trabecular meshwork and Schlemm's canal (**figure 2**). These preliminary results are promising for tracking *in vivo* at real time, the efficiency of different carriers for drug delivering in pathologies such as glaucoma.

Adenoviruses were injected through the cornea into the anterior chamber (concentration not shown) with a 32G needle. Adenoviruses infect the endothelial cells that in consequently express GFP. The success of the infection can be visualized by the expression of GFP. GFP was found in the corneal endothelium 24 hours after the injection. This is the first time that this system is visualized *in vivo* at real time using a MP-IVM (**figure 3**).

Transgene mice encoding a simian Diphtheria Toxin Receptor (DTR)-EGFP fusion protein under the control of the Itgax (or CD11c) promoter were purchase from Jackson Laboratories. These mice were generated with BALB/c background. $CD11c^{YFP\text{-}DTR}$ DCs were depleted by topical application of DT (concentration not shown). Twenty-four hours after DT application, CD11c DCs were totally depleted from the ocular surface. New CD11cYFP DCs were observed in the peripheral and paracentral by 4-12 weeks. In ongoing experiments we are studying the function of this and other specific populations (i.e. wound healing and allergy)

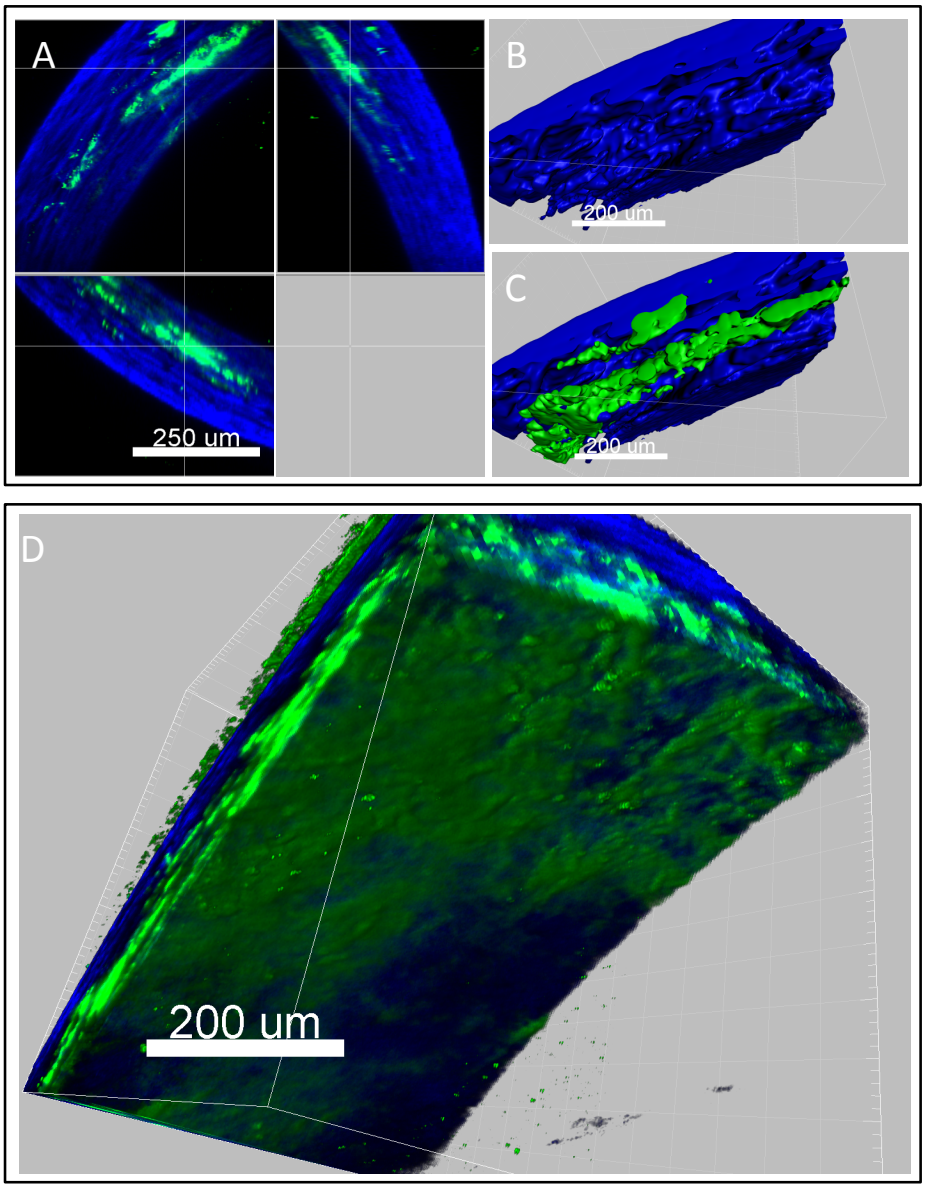

Figure 2. *In vivo* detection of nanoparticles in the trabecular meshwork and Schlemm's canal (A, B and C). Orthogonal segmentation (A) and tree-dimensional reconstructed figure (B and C) are shown. *In vivo* detection of endothelial binding carriers-Allexa-488-conjugated in the trabecular meshwork (D).

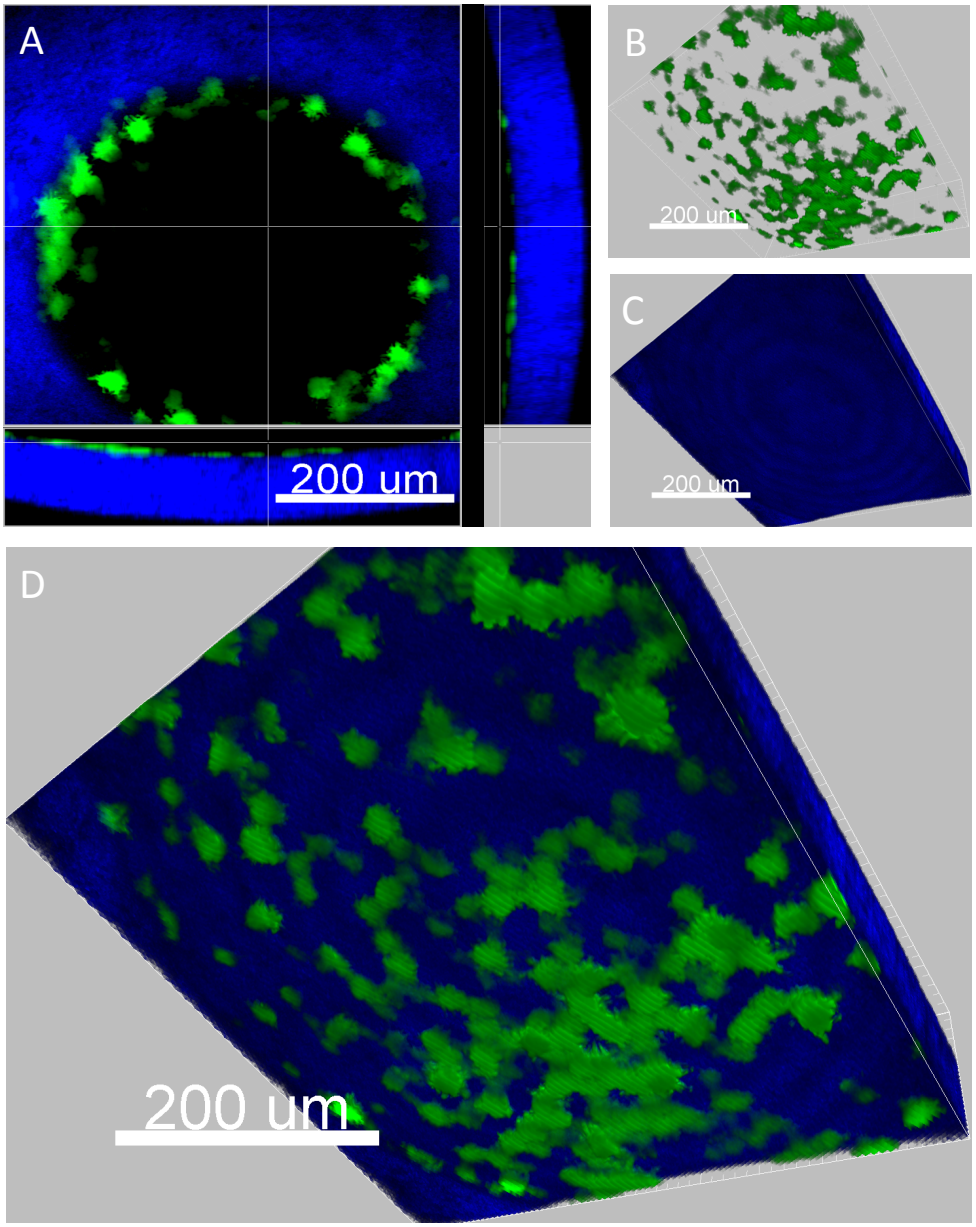

Figure 3. *In vivo* detection of GFP endothelial cells (green) in the corneal endothelium after being infected with adenovirus (A, B and D). Orthogonal segmentation (A) and tree-dimensional reconstructed figure (B, C and D) are shown. Tree-dimensional view from the AC side reflects the efficiency of the infection

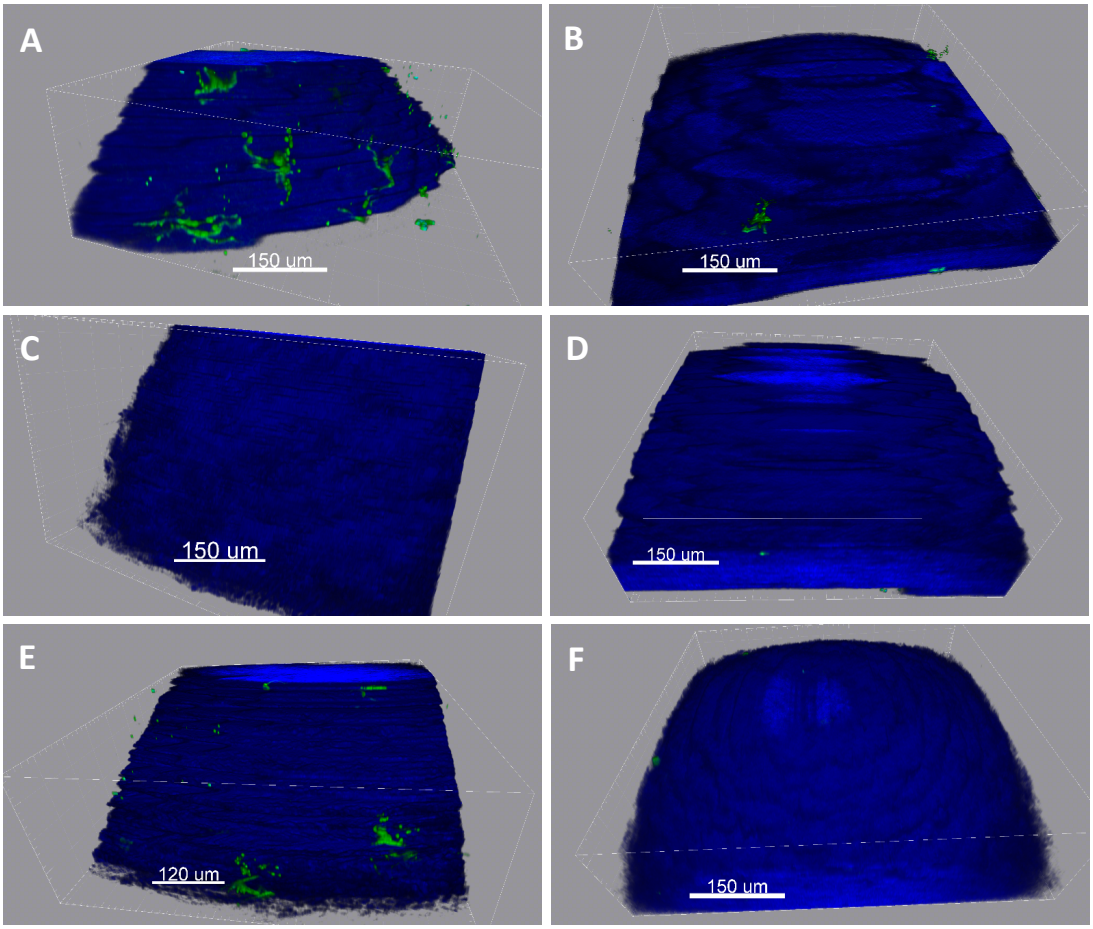

Figure 4. *In vivo* detection of CD11c-DCs (green) in the normal cornea: periphery (A) and central (B). Twenty-four hours after topical application of DT the population was completely depleted (C and D). Twelve weeks after the CD11cDCs repopulate the periphery of the cornea (E) but not the center (F).

REFERENCES

1. Semon, J.A., X. Zhang, A.C. Pandey, S.M. Alandete, C. Maness, S. Zhang, B.A. Scruggs, A.L. Strong, S.A. Sharkey, M.M. Beuttler, J.M. Gimble and B.A. Bunnell, *Administration of murine stromal vascular fraction ameliorates chronic experimental autoimmune encephalomyelitis.* Stem Cells Transl Med, 2013. **2**(10): p. 789-96.
2. Blanco-Mezquita, J.T., A.E. Hutcheon and J.D. Zieske, *Role of thrombospondin-1 in repair of penetrating corneal wounds.* Invest Ophthalmol Vis Sci, 2013. **54**(9): p. 6262-8.
3. Blanco-Mezquita, J.T., A.E. Hutcheon, M.A. Stepp and J.D. Zieske, *alphaVbeta6 integrin promotes corneal wound healing.* Invest Ophthalmol Vis Sci, 2011. **52**(11): p. 8505-13.